CHAPTER 1:

Development and implementation of Non-linear models within R framework

1.1 Introduction:

Campylobacter is considered a zoonotic pathogen and interventions focussed on preventing its access to the food chain is a necessity in order to safe guard public health. While *Campylobacter* is known to be sensitive to extreme biophysical and biochemical environments, current treatment models used by the food production industry may be deficient as they lack data that describe the biological processes relating to how the organism responds under high intensity stress. Therefore, existing treatment models do not fully take into consideration the population biology of *Campylobacter* or how the survival of *Campylobacter* may be enhanced following interactions within a particular substrate. In addition, the survival of different strains may vary according to the type and intensity of the stress encountered (Coroller *et al*., 2006). Greenacre *et al*. (2003) demonstrated that models used to describe the survival of *Listeria monocytogenes* and *Salmonella enterica* may initially take the form of concave response curves. The underlying response may then evolve to become convex or sigmoidal when biochemical or biophysical stress intensifies. Furthermore, the underlying shapes of response curves has been found to vary according to the physiological state of the cells, the current growth phase of the organism, namely stationary or exponential and the organism under study (Greenacre *et al*., 2003; Coroller *et al*., 2006; King *et al*., 2010). Similar behaviour has been recorded in *Campylobacter* where variation in the survival response of individual strains was observed under identical conditions (Hughes *et al*., 2009 and 2010).

Highly sensitive recovery and enumeration techniques will be used to determine the survival of *Campylobacter* following exposure to high intensity biophyscial and biochemical stress. A non-linear modelling framework will be used to describe variation in the underlying response of *Campylobacter* and to generate predicted response curves that provide the food production industry with an essential tool for describing survival under specific treatment conditions.

1.2 Methodology:

Experimental protocols for all simulations undertaken during the course of this study are described in detail in the appendices (A4.1 – A4.8)

1.2.1 Time-temperature Simulations:

Experimental simulations were used to determine the underlying response of *Campylobacter* to biophysical and biochemical challenges. Initial simulations examined the survival of *Campylobacter* species following exposure to increases in temperature (56^{o}C, 60^{o}C and 64^{o}C) through time (A4.2). The response of each *Campylobacter* strain at 56^{o}C was measured from 0 – 10 minutes at 2 minute intervals (Figures 1 – 14). In contrast, the overall observation period and interval between measurements was reduced at higher temperatures. At 60^{o}C observations were obtained for each strain from 0 – 7.5 minutes at intervals of 1.5 minutes (Figures 17 – 30) whereas at 64^{o}C observations were obtained from 0 – 6.0 minutes at intervals of 1 minute (Figures 31 – 44). Modifications to the duration of the observation period and the corresponding measurement intervals were designed to capture potential differences in rates of decline of viable bacteria.

1.2.2 Extended Simulations:

In an extension to the initial analyses, experimental simulations were also undertaken to examine potential differences in the underlying response of *Campylobacter* to using different experimental media and following the use of different initial inocula. Experimental simulations were undertaken to examine potential differences in the survival of sub-lethally damaged cells for two strains of *Campylobacter* 13121 (ST-45, CC-45) and 11168 (ST-43, CC-21). The numbers of cells recovered for each strain were compared using Columbia agar base (5% defibrinated blood) (CAB) plus ferrous sulphate, sodium meta-bisulphite, sodium pyruvate (FBP) or modified charcoal cefoperazone deoxycholate agar (mCCDA) (Figure 15). In addition, the impact of varying initial inocula (6 Log CFU/ml^{-1} and 8 Log CFU/ml^{-1}) on the numbers of cells recovered was examined using strains 13121 (ST-45, CC-45) and 13136 (ST-45, CC-45) (Figure 16). During each simulation, *Campylobacter* strains were exposed to 56^{o}C and observations were obtained from 0.0 – 16.0 minutes at 1 minute intervals (A4.3).

1.2.3 pH and Time-temperature Simulations

Simulations were also undertaken to examine differences in the underlying response of *Campylobacter* following exposure to the combined challenges of temperature and pH (4.5, 5.5, 6.5, 7.0 and 8.5) (A4.2). The combined effect of pH and temperature on the survival of *Campylobacter* was examined. The duration of each experimental simulation, and corresponding measurement intervals, varied according to each combination of pH and temperature. Simulations undertaken at 56^{o}C utilized an observation period of 0.0 – 12.0 minutes, while measurements were obtained at 2.0 minute intervals (Figure 45). In parallel with time-temperature simulations, the observation period and measurement intervals for combinations of pH and higher temperatures were reduced. Simulations conducted at 60^{o}C utilized an observation period of 0.0 – 9.0 minutes, while measurements were obtained at intervals of 1.5 minutes (Figure 46). The observation period for experimental simulations undertaken at 64^{o}C was reduced to 0 – 5.0 minutes, with an initial measurement interval of 0.5 minutes and subsequent measurement interval 1 minute (Figure 47).

1.2.4 Food Matrices Time-temperature Simulations

Simulations were also undertaken to assess the survival of *Campylobacter* within interiors and on exterior tissues at different temperatures and also using gradual and direct heating methods. For simulations undertaken using gradual heating of food exteriors, the survival of *Campylobacter* was determined at 56^{o}C and 70^{o}C. During direct heating, survival was assessed following exposure to 56^{o}C, 60^{o}C, 64^{o}C, 68^{o}C and 70^{o}C (A4.4). The survival of *Campylobacter* within food tissue interiors was assessed using gradual and direct heating at 64^{o}C and 68^{o}C (A4.5).

1.2.5 R Modelling Framework:

Non-linear mixed-effects models were used to determine the relationship between an observed response and a set of explanatory variables. These models are considered mechanistic insofar as they are based on a model that describes the underlying mechanism responsible for producing the observed response (Pinheiro and Bates, 2000). In addition, non-linear mixed-effects models may also be used to analyse grouped or hierarchical data in order to account for heterogeneity within and between subjects.

The analytical concept that underpins the application of non-linear mixed-effects models is that fixed-effects parameters are used to describe the underlying response at a generic or population level, whereas random-effects may be used to explain variability between individuals as a function of deviation from the mean value of the fixed-effects. Thus, the non-linear mixed-effects modelling approach accommodates individual variation though the use of random-effects but links individuals through the use of fixed-effects. Principally, a fixed-effect applies equally to all individuals in a population while a random-effect allows variability between subjects to be estimated explicitly.

An essential component of the non-linear mixed-effects modelling exercise is deciding which parameters require a random-effect to account for between subject variability and which parameters can be treated as purely fixed effects (Pinheiro and Bates, 2000). In practical terms, it is advisable to begin with a model where random-effects are assigned to all parameters and then examine the resulting model and decide which, if any of the random-effects parameters can be eliminated from subsequent iterations. However, the appropriate and combined use of random- and fixed-effects can be further complicated when attempting to incorporate covariates. The use of a covariate within a non-linear mixed-effects model allows for differences between populations to be evaluated. In addition, a covariate may be fitted to a random-effect independently of others within the model. For instance, it is possible to evaluate differences in the asymptote of a three-parameter asymptotic regression model for each subject by allowing estimates of that parameter to vary according to particular experimental factor. This can be achieved while simultaneously allowing remaining random-effects parameters to be estimated independently.

Non-linear mixed-effects models may be used with different non-linear functional forms that describe the underlying variation in a measured response variable. The variation in shape of underlying response curves of *Campylobacter* is shown in Figure A1.1. Each non-linear function may incorporate between three and five numeric input parameters. The asymptotic regression model uses three parameters to evaluate the gradient of a response that includes a horizontal asymptote (Table A1.1). The standard logistic regression is a three-parameter model and is less complex than the above in that it evaluates the response, its corresponding gradient and a single asymptote (Table A1.2). In contrast, a four-parameter logistic regression model is used to evaluate a response and its gradient. This is often used in circumstances when the shape of the response curve is sigmoidal and exhibits two horizontal asymptotes (Table A1.3). The bi-exponential model is a four-parameter regression model that evaluates the response and its gradient by forming a linear combination of two exponential terms in order to evaluating exponential decay over time (Table A1.4). Subsequently, we used variations of the Weibull model to analyse the survival of *Campylobacter* in response to biophysical and biochemical stress. The Weibull model is an analytical approach for describing linear, concave and convex curves (Coroller *et al*., 2006). The initial variant of the Weibull regression model utilises four-parameters to evaluate the response and corresponding gradient in a similar fashion to other non-linear functions (Table A1.5). And lastly, Coroller *et al*. (2006) propose a general model based on a mixture of two Weibull distributions that describe variation in the inactivation curves of *Listeria monocytogenes* and *Salmonella enterica* following exposure to acidic stress (pH 3.3). The model aims to provide researchers with a flexible means of describing the underlying response of micro-organisms following exposure to biochemical and biophysical stress.

The underlying assumption governing the use of this model is that two bacterial subpopulations exist within an organism that each differs in its ability to resist biophysical and biochemical stress. The resistance of each subpopulation is described by each Weibull distribution. The general model is fit to data using five parameters (Table A1.6) where N_0 is the initial inoculum size; δ1 and δ2 describe the time taken to achieve one logarithmic reduction in population size of each subpopulation. The parameter α determines the fraction of first subpopulation remaining within the primary population, while the shape of the inactivation curve is determined by the parameter *p*. We adopted the methodology proposed by Coroller *et al*. (2006) and incorporated the general model into the existing non-linear modelling framework in order to investigate the response of *Campylobacter* species to varying intensities of biochemical and biophysical stress. The general model devised by Coroller *et al*. (2009) was incorporated into a freely available software tool that can be used in conjunction with Microsoft EXCEL 2007 and 2010. The package, GlnaFiT (1.6) (2012) was developed by Geeraerd *et al*. (2006a and 2006b) and is maintained by the University of Leuven: http://cit.kuleuven.be/biotec/downloads.php.

1.2.6 Model Assessment:

Information Theory (IT) (Burnham and Anderson, 2002) was used to assess relative model fit and complexity simultaneously. Here, model selection was undertaken by comparing Akaike Information Criterion (AIC). AIC comprises two components; the negative log-likelihood which determines the fit of the model to the data, and a bias correction factor which increases in value as a function of the complexity of the model (Johnson and Omland 2004). As such, values of AIC will increase as a function of model complexity. Thus, when comparing candidate models, a model presenting the lowest AIC may be considered the most adequate model in describing the underlying phenomenon. However, candidate models may exhibit comparable values of AIC and the adequacy of these models must still be evaluated. Burnham and Anderson (2002) recommended calculating differences between AIC values as a means of distinguishing between such competing models;

$$\Delta_i = AIC_i - AIC_{min}$$

Burnham and Anderson (2002) proposed a threshold value of $\Delta_i \leq 2$. Where Δ_i is less than the threshold then substantial support exists for those models.

1.2.7 Model Building:

The non-linear models described above were used to examine differences in the underlying response of *Campylobacter* to each temperature profile and a combination of pH and temperature as a function of time. Each *Campylobacter* strain was modelled independently using a generalized non-linear least-squares modelling approach (Pinheiro and Bates, 2000). During the model building exercise, non-linear functions were assessed for their ability to best describe the underlying response in *Campylobacter* following exposure to variation in intensity to biochemical and biophysical stress. However, the choice of non-linear function was not always readily apparent and the identification of an optimal non-linear function may be problematic in circumstances when only general characteristics of the underlying response are known. To facilitate identifying an appropriate non-linear function, the response of *Campylobacter* to each experimental simulation was first examined visually. Models were fit to data by means of identifying optimal values for parameters that are most likely to succeed in generating and fitting a response curve. Optimisation routines are integral components to the nlme package and are specific to the non-linear function used.

However, an optimisation routine for the general model was unavailable for use in R. As such, preliminary models for each strain and simulation were generated within GInaFiT (1.6) where an optimization routine is included (Geeraerd *et al.*, 2006a and 2006b). Initial values for parameters were then exported and used within the nlme model framework in order to generate predictive models. Where it was possible to fit more than one non-linear function to data, models were generated and then compared using Information Theoretic approaches (Burnham and Anderson, 2002). Models were interrogated to ensure that underlying statistical assumptions of constant variance and identically and normally distributed within-group residual errors were obeyed. Where within-group errors are found to heteroscedastic (unequal variance) or correlated, then new models were generated by using an appropriate variance structure and/or auto-correlation function that attempted to restore underlying statistical assumptions (Pinheiro and Bates, 2000). The absolute fit of the models to the data was assessed using the goodness-of-fit statistic the concordance correlation coefficient (ρ_c) initially proposed by Lin (1989 and 2000) and Vonesh *et al*. (1996). All analyses were undertaken using the R package for statistical computing version 3.0.3 (R Core Development Team 2014) and individual models were generated using a linear and non-linear Mixed-effects Models package (nlme) (Pinheiro *et al.*, 2012).

1.3 Time-Temperature Simulations: 56°C

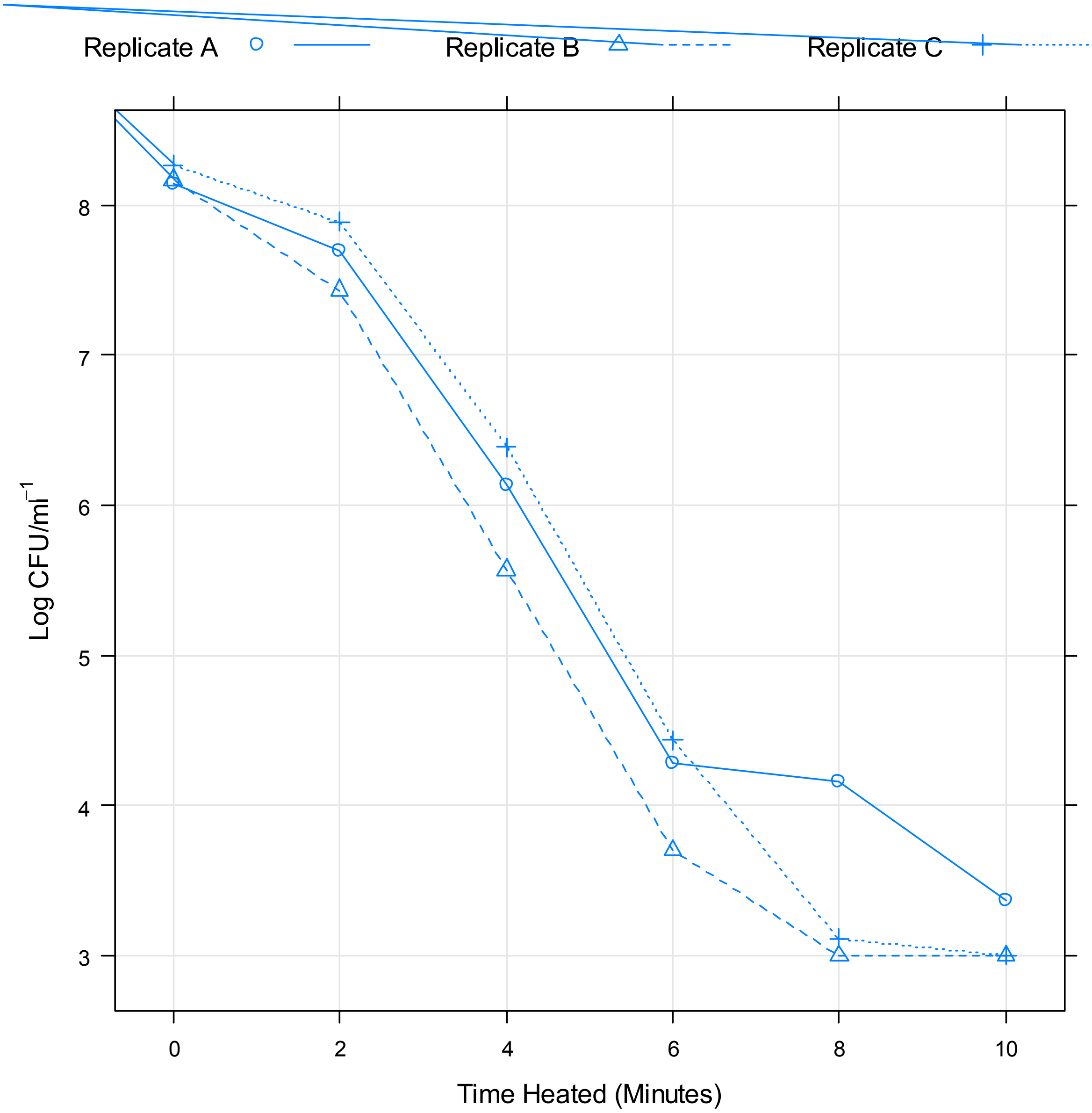

Figure 1. Plot of observed data illustrating survival of strain 11253 (ST-825, CC-828) following heating at 56°C.

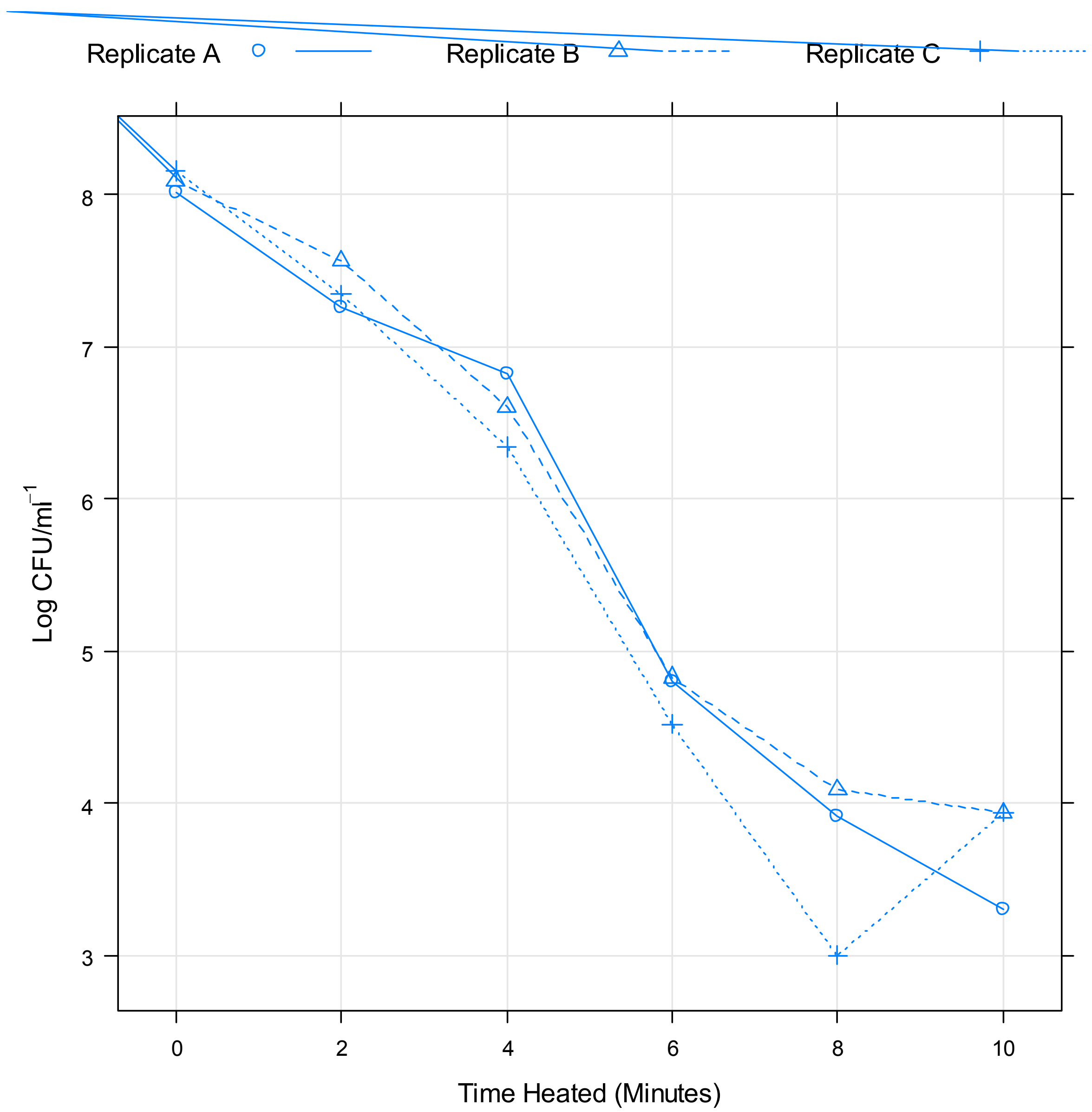

Figure 2. Plot of observed data illustrating survival of strain 11368 (ST-574, CC-574) following heating at 56°C.

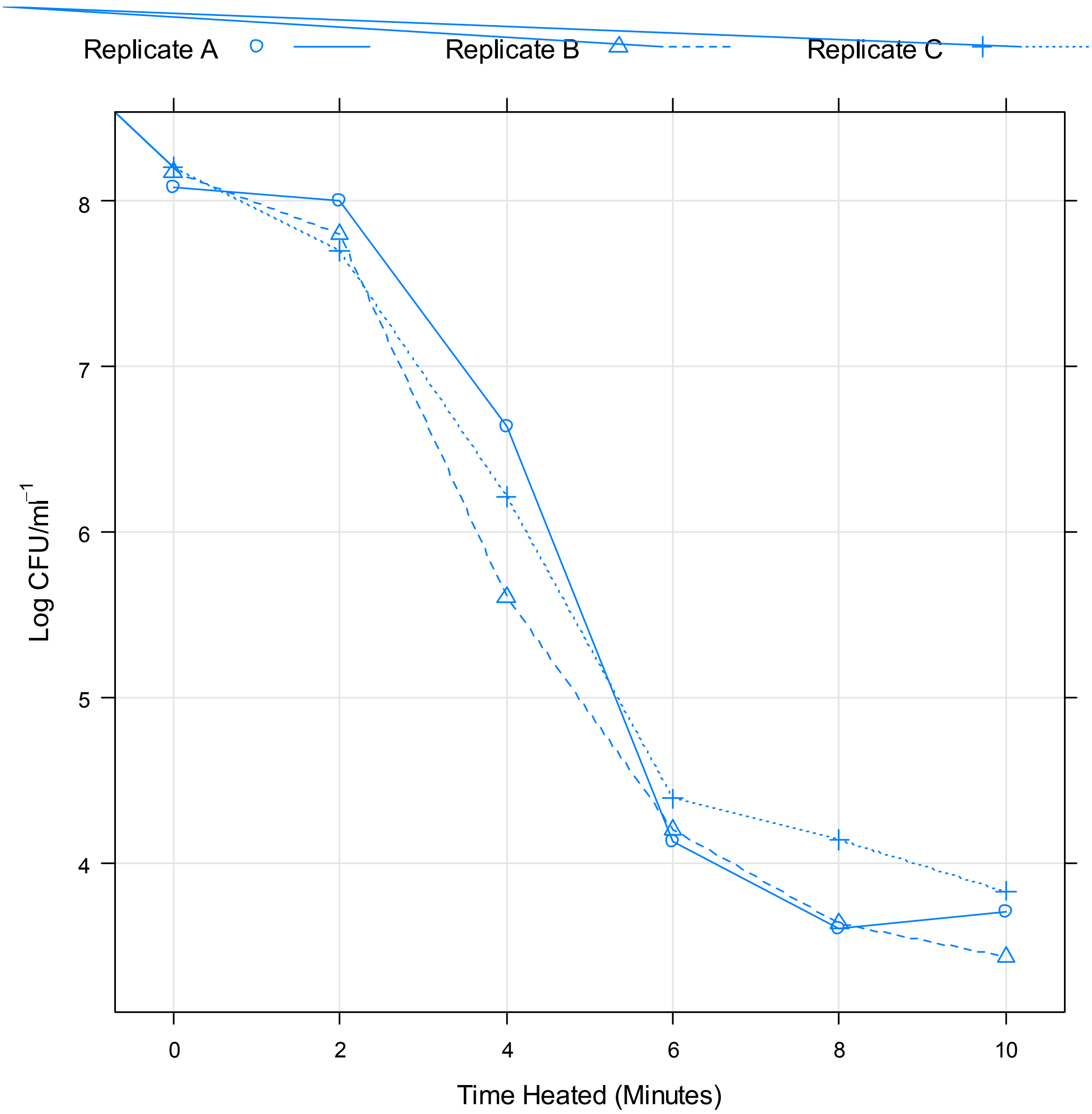

Figure 3. Plot of observed data illustrating survival of strain 11762 (ST-829, CC-828) following heating at 56°C.

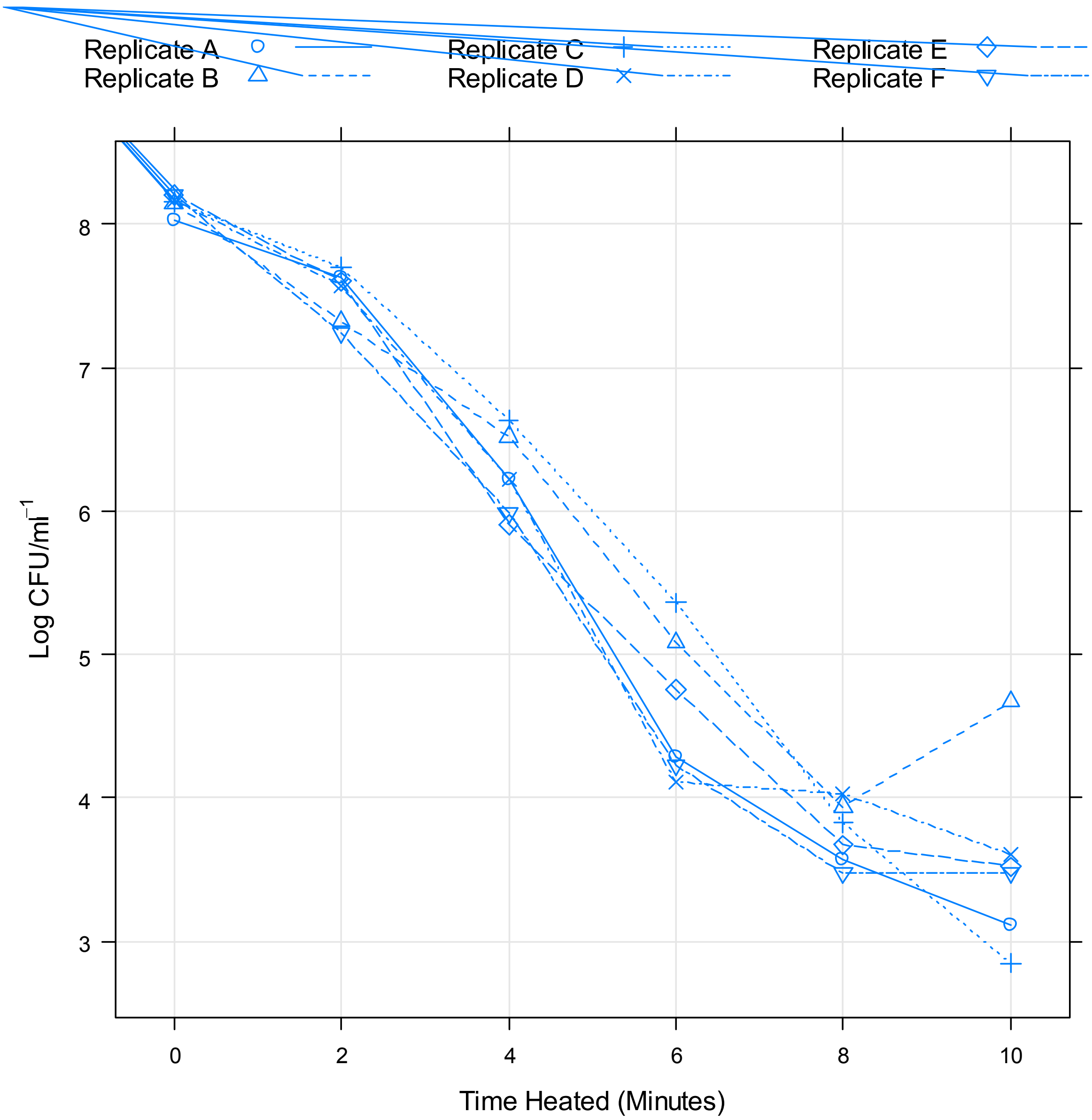

Figure 4. Plot of observed data illustrating survival of strain 12610 (ST-825, CC-828) following heating at 56°C.

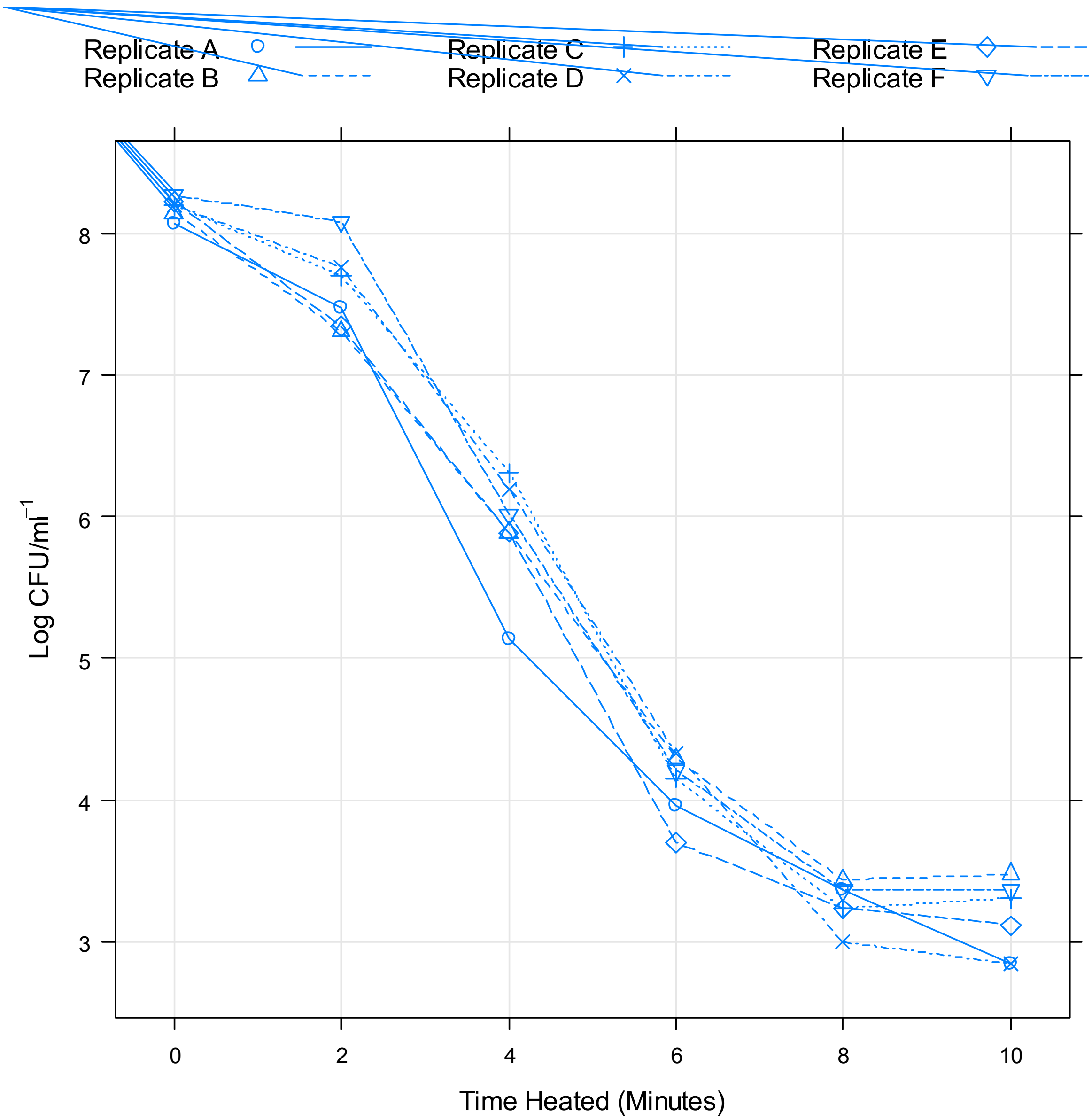

Figure 5. Plot of observed data illustrating survival of strain 12628 (ST-1773, CC-828) following heating at 56°C.

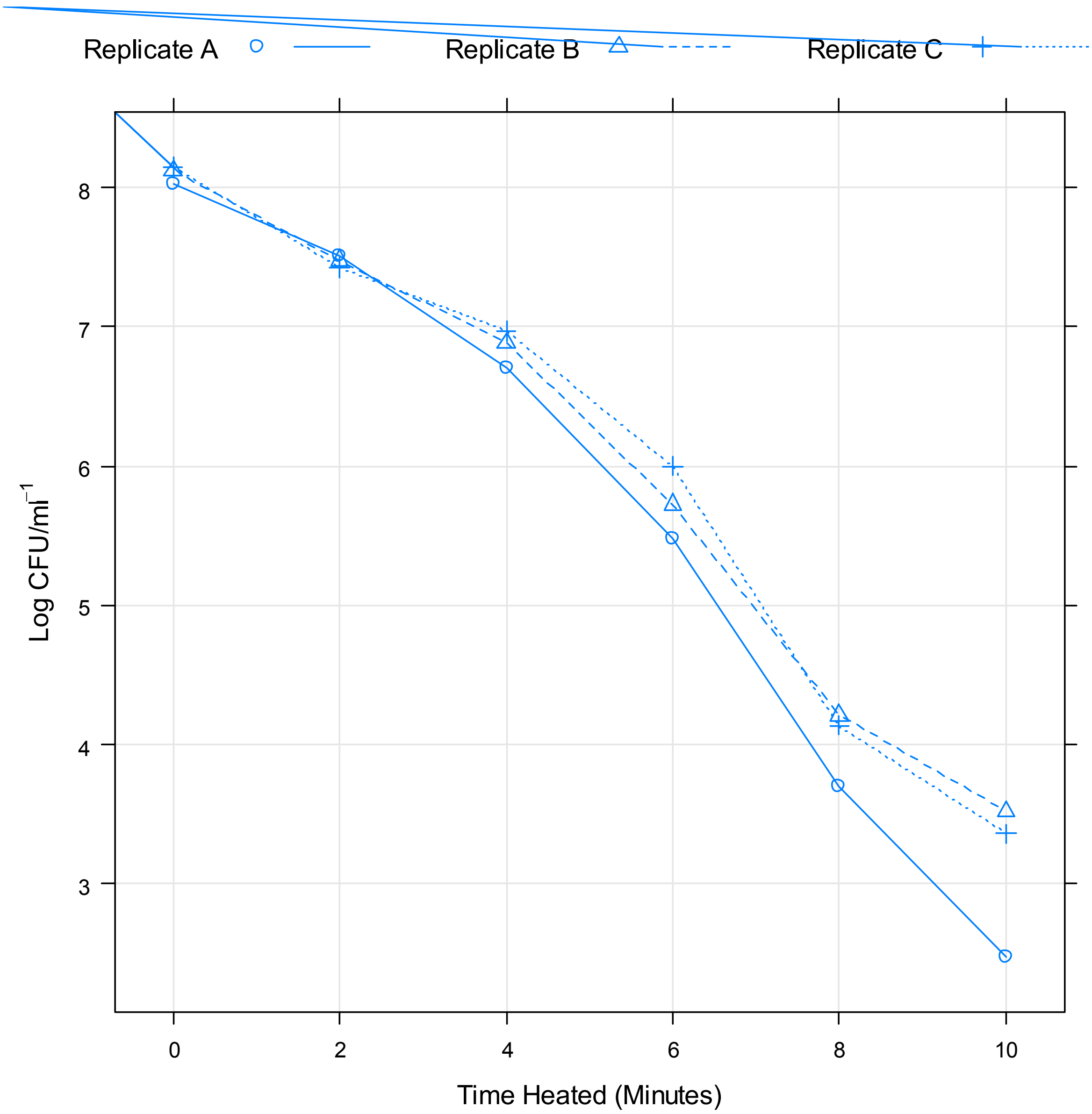

Figure 6. Plot of observed data illustrating survival of strain 12645 (ST-51, CC-43) following heating at 56°C.

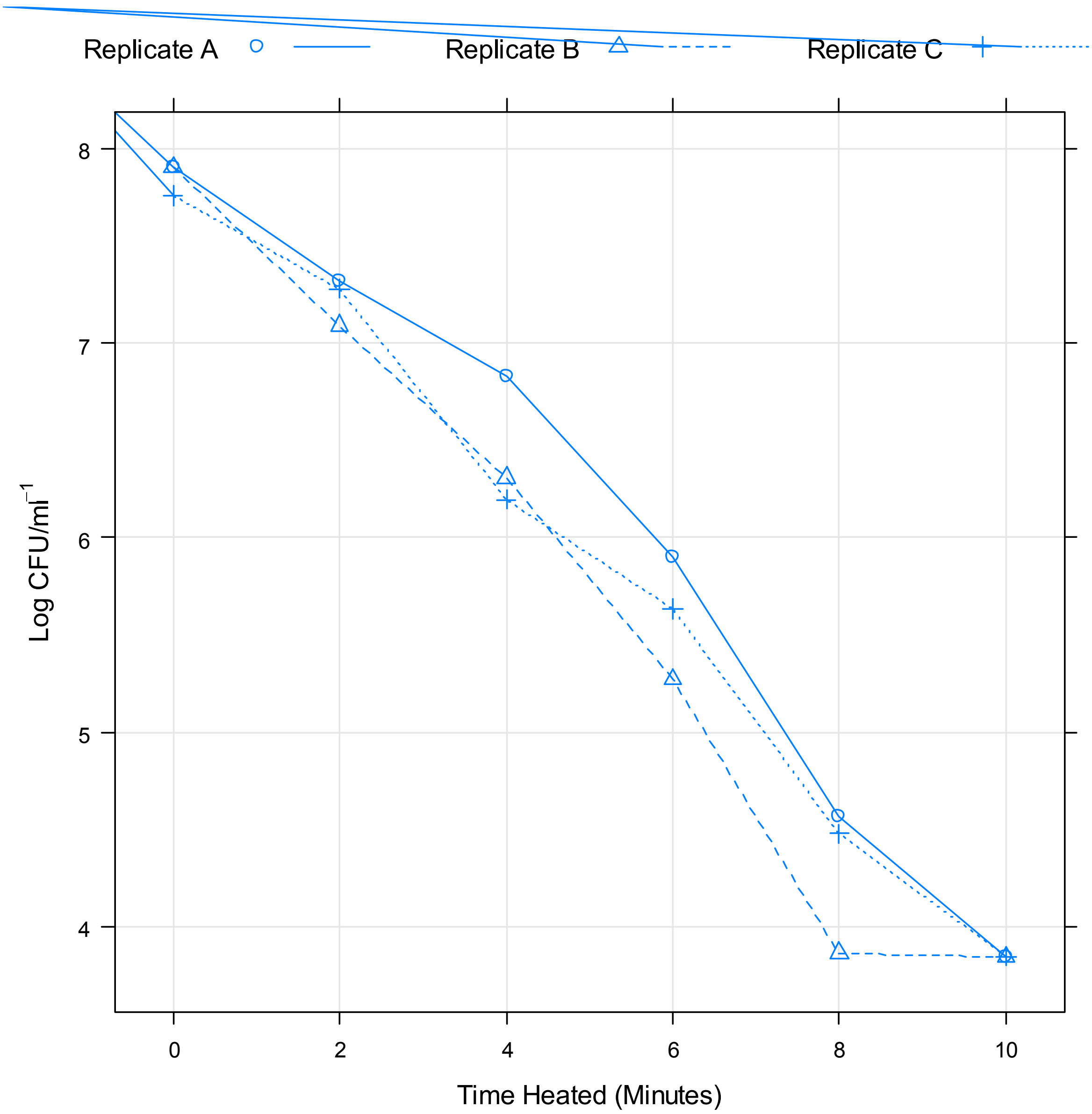

Figure 7. Plot of observed data illustrating survival of strain 12662 (ST-257, CC-257) following heating at 56°C.

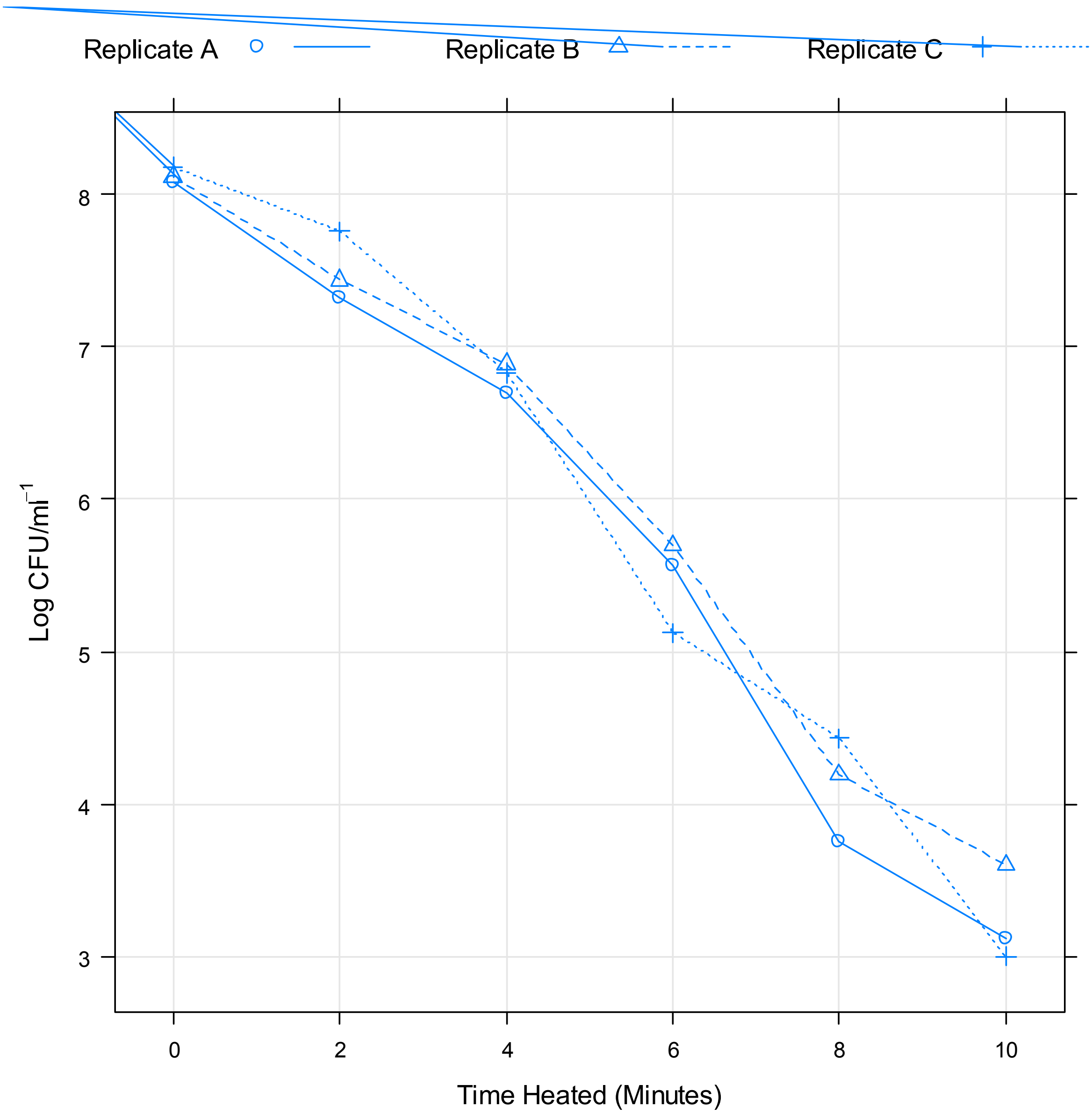

Figure 8. Plot of observed data illustrating survival of strain 12720 (ST-51, CC-443) following heating at 56°C.

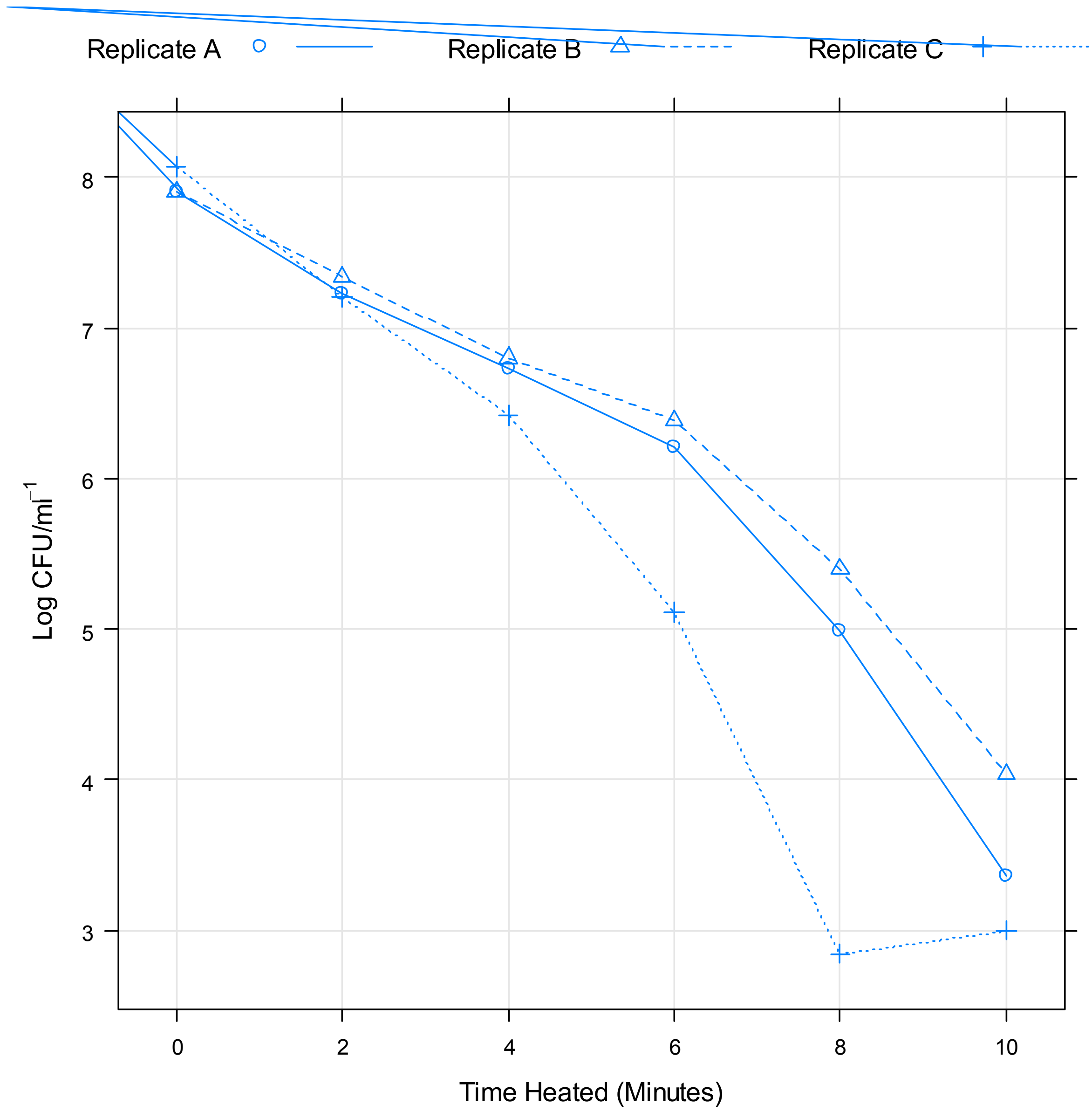

Figure 9. Plot of observed data illustrating survival of strain 12745 (ST-257, CC-257) following heating at 56°C.

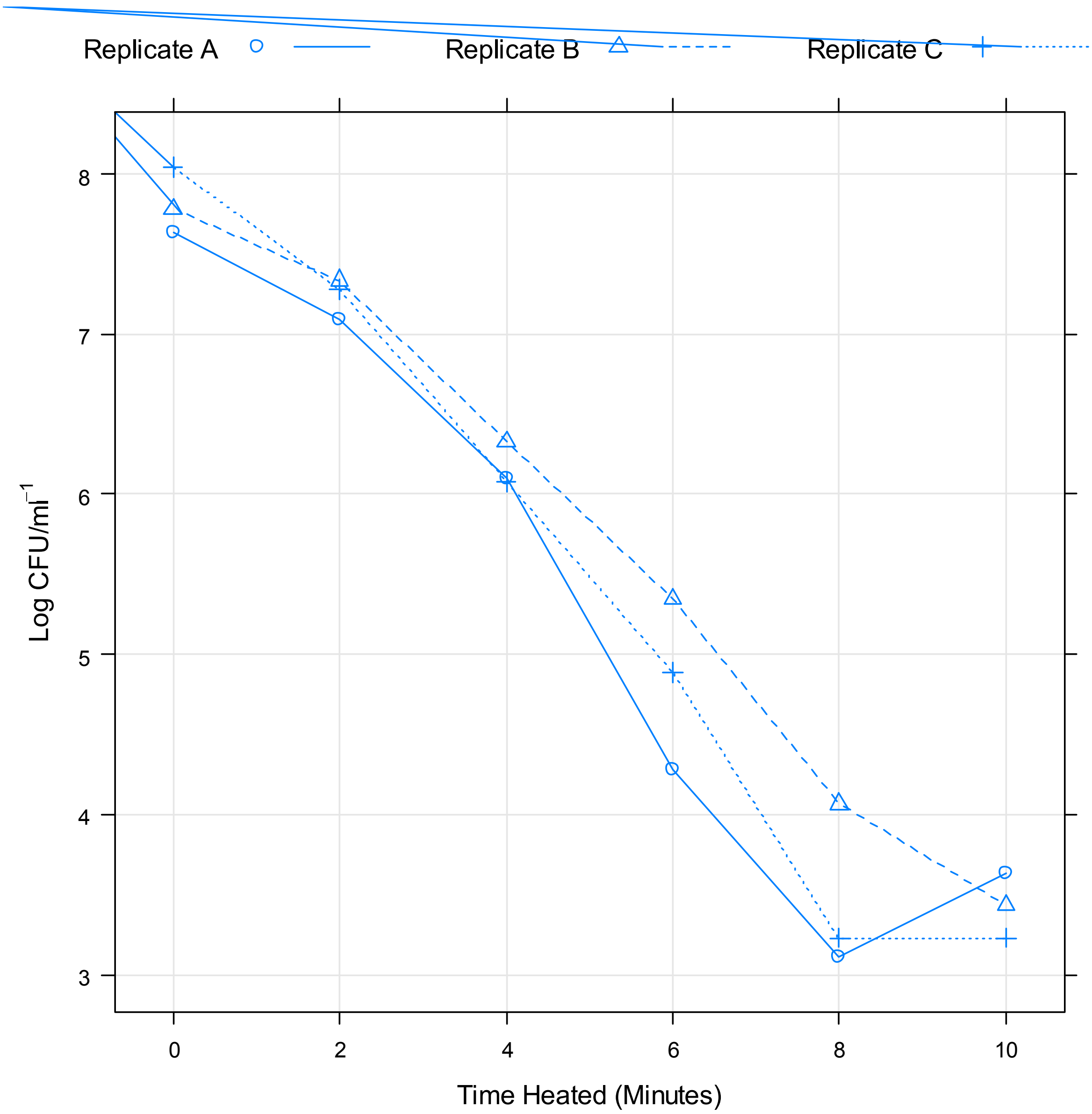

Figure 10. Plot of observed data illustrating survival of strain 12783 (ST-574, CC-574) following heating at 56°C.

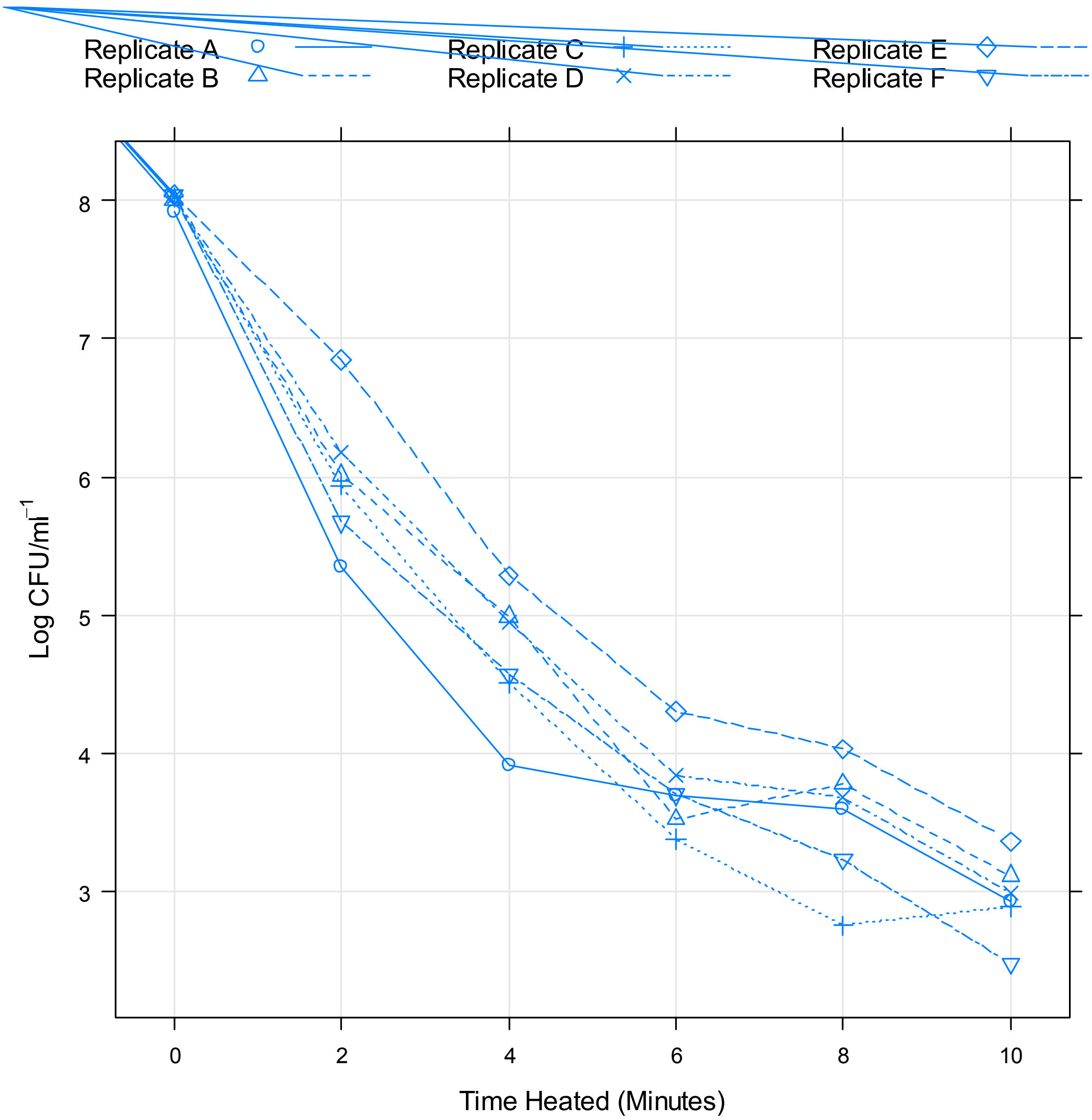

Figure 11. Plot of observed data illustrating survival of strain 13121 (ST-45, CC-45) following heating at 56°C.

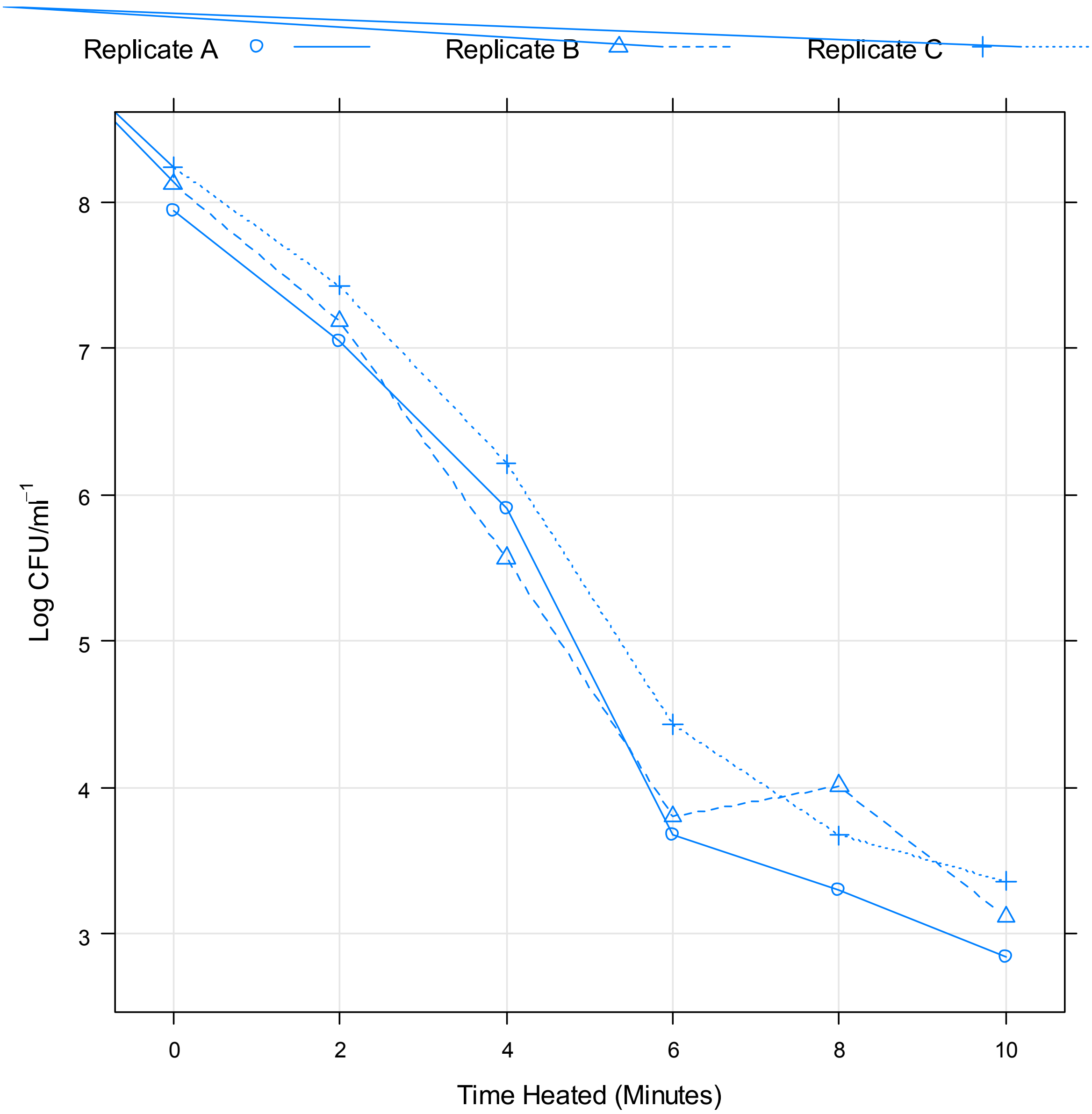

Figure 12. Plot of observed data illustrating survival of strain 13126 (ST-21, CC-21) following heating at 56°C.

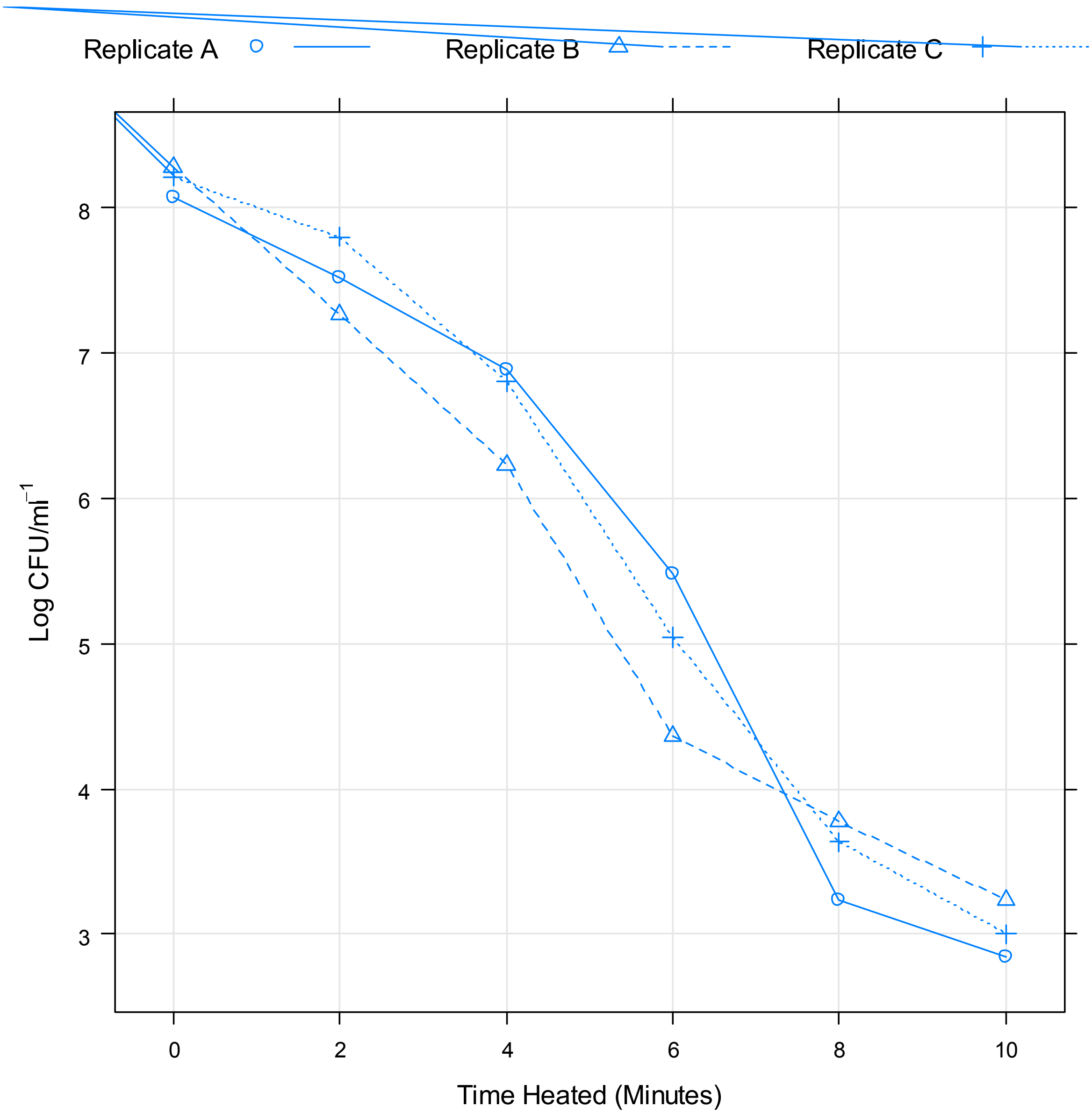

Figure 13. Plot of observed data illustrating survival of strain 13136 (ST-45, CC-45) following heating at 56°C.

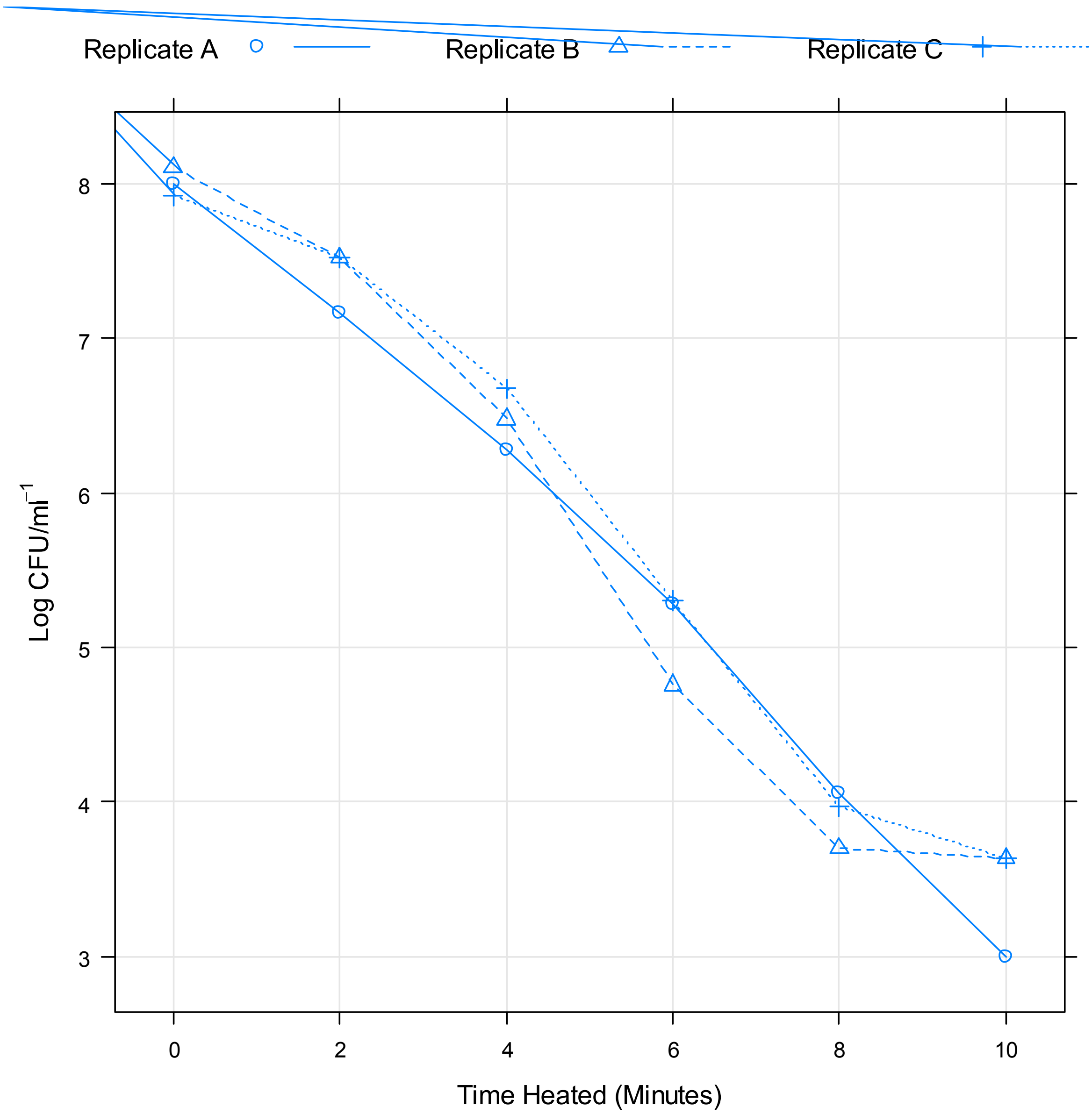

Figure 14. Plot of observed data illustrating survival of strain 13163 (ST-21, CC-21) following heating at 56°C.

1.4 Extended Analysis: Time-Temperature Profile 56°C

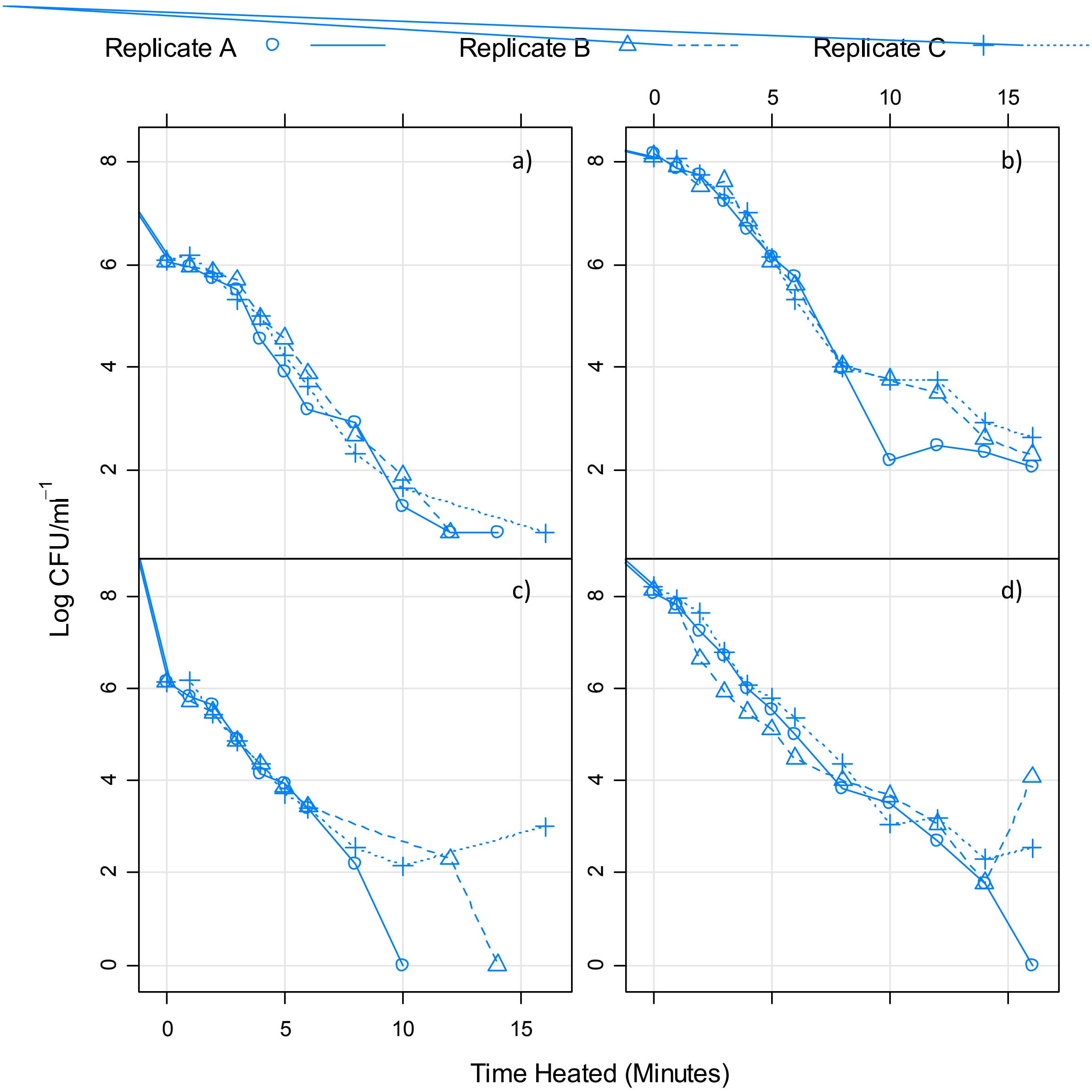

Figure 15. Plot illustrating the survival of two strains following heating at 56°C. Simulations were repeated using inoculum at 6 Log CFU/ml^{-1} and 8 Log CFU/ml^{-1}; strain 13136 (ST-45, CC-45) a) 6 Log CFU/ml^{-1}, b) 8 Log CFU/ml^{-1} and strain 13121 (ST-45, CC-45) c) 6 Log CFU/ml^{-1}, d) 8 Log CFU/ml^{-1}.

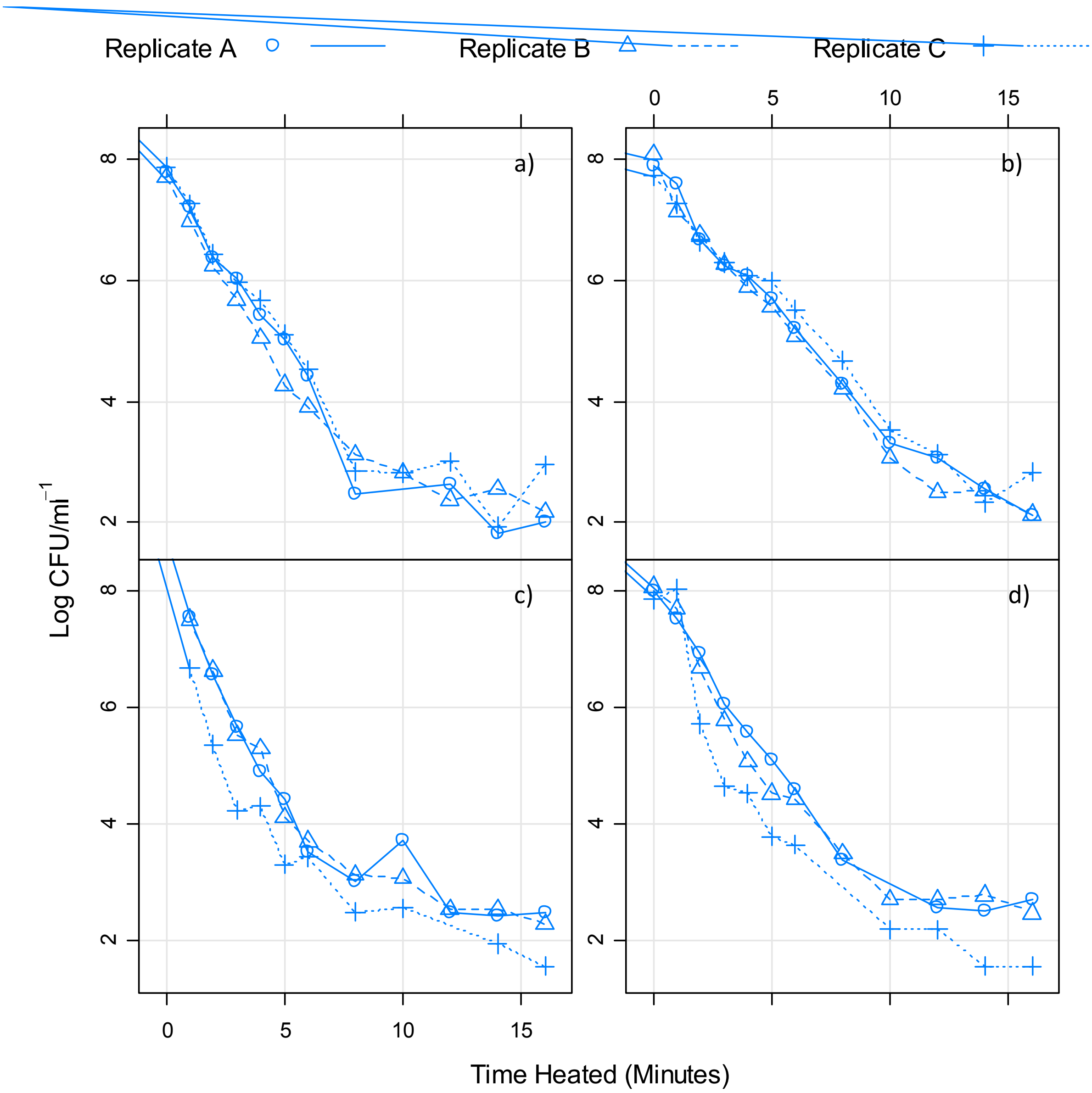

Figure 16. Plot illustrating the survival of two strains following heating at 56°C. Simulations were repeated using two media, Columbia agar base (5% defibrinated blood) (CAB) plus ferrous sulphate, sodium meta-bisulphite, sodium pyruvate (FBP) and modified charcoal cefoperazone deoxycholate agar (mCCDA); strain 11168C (ST-43, CC-21) a) mCCDA, b) CAB-FBP and strain 13121 (ST-45, CC-45) c) mCCDA, d) CAB-FBP.

1.5 Time-Temperature Simulations: 60°C

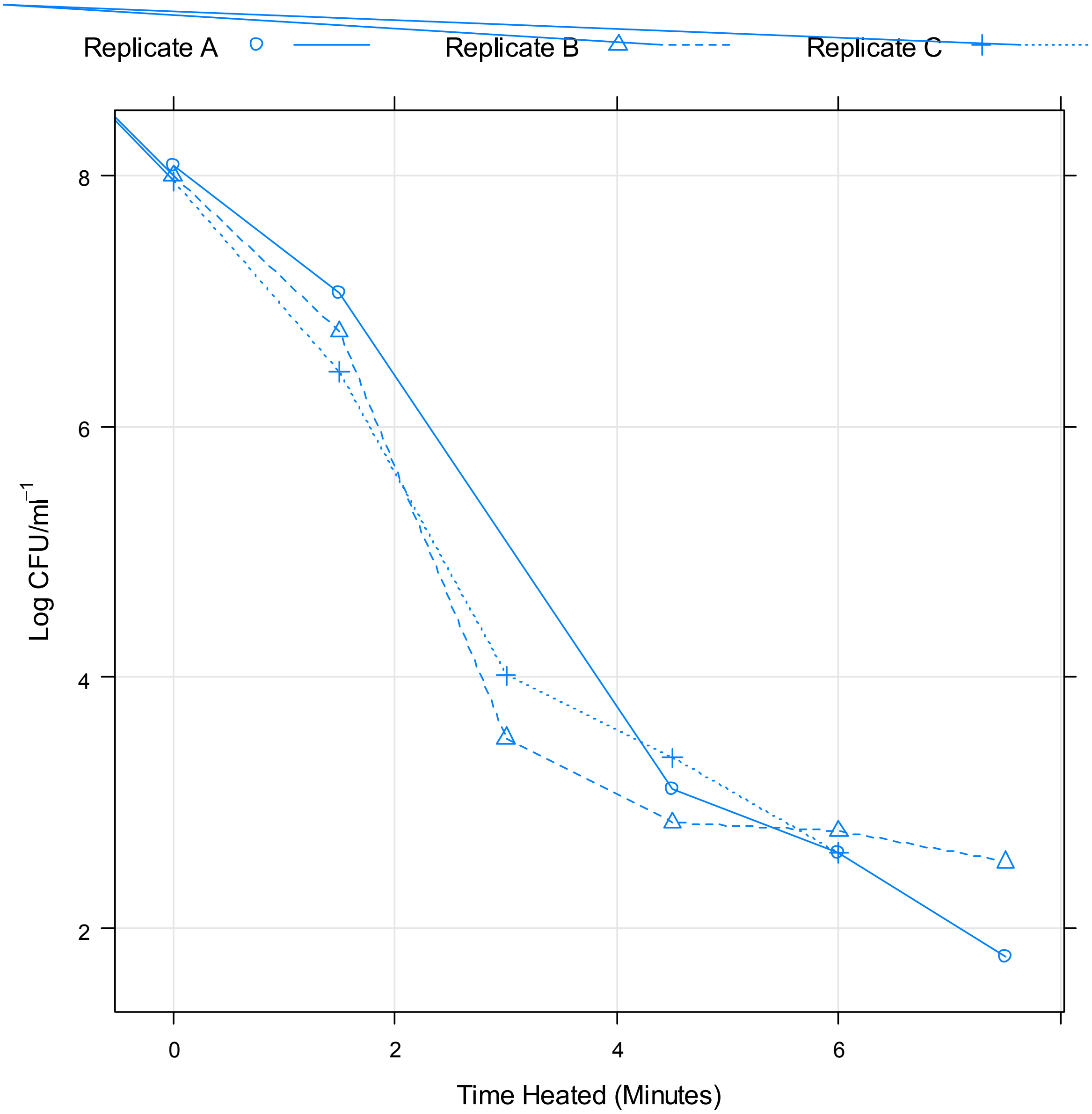

Figure 17. Plot of observed data illustrating survival of strain 11253 (ST-825, CC-828) following heating at 60°C.

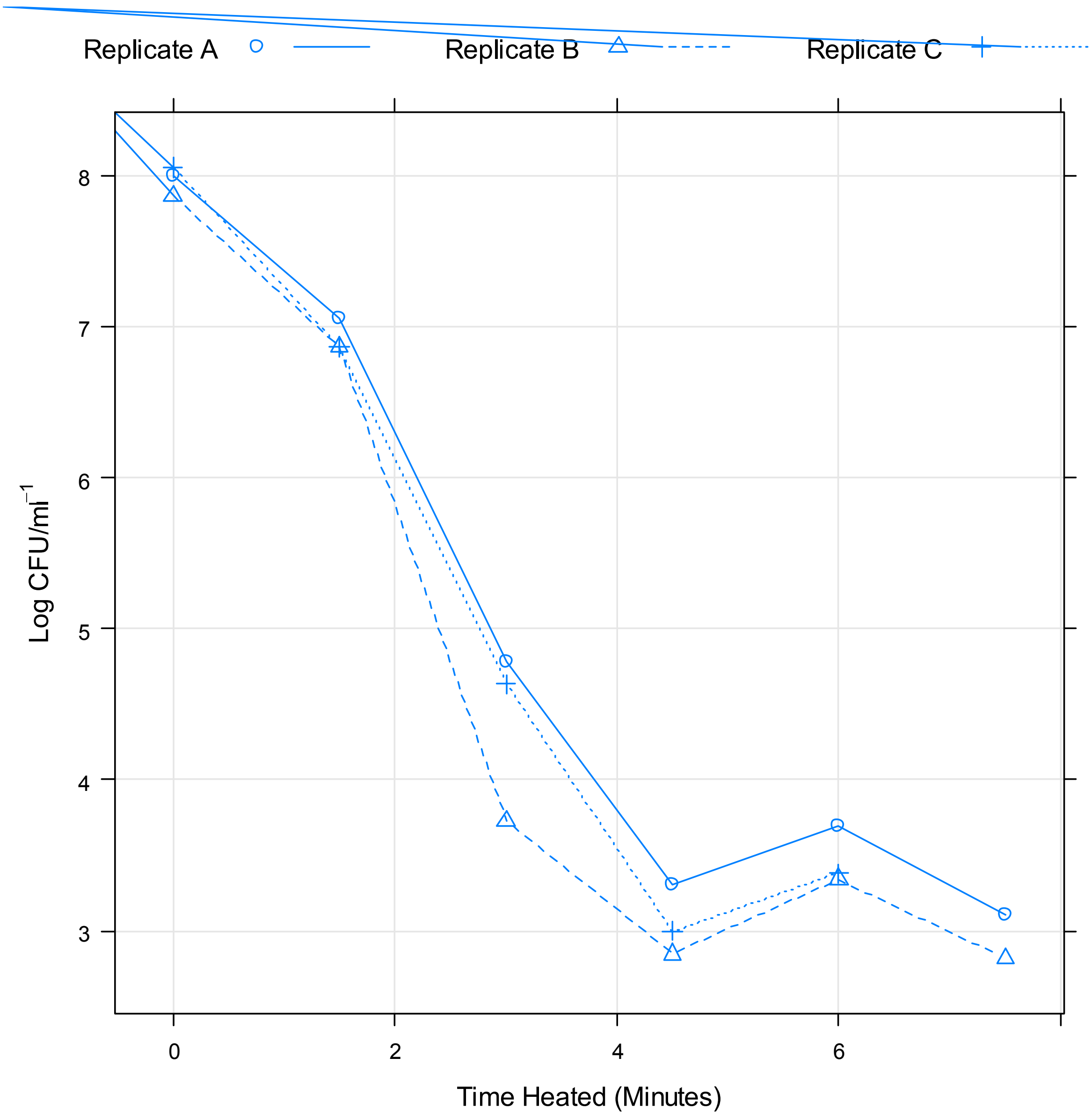

Figure 18. Plot of observed data illustrating survival of strain 11368 (ST-574, CC-574) following heating at 60°C.

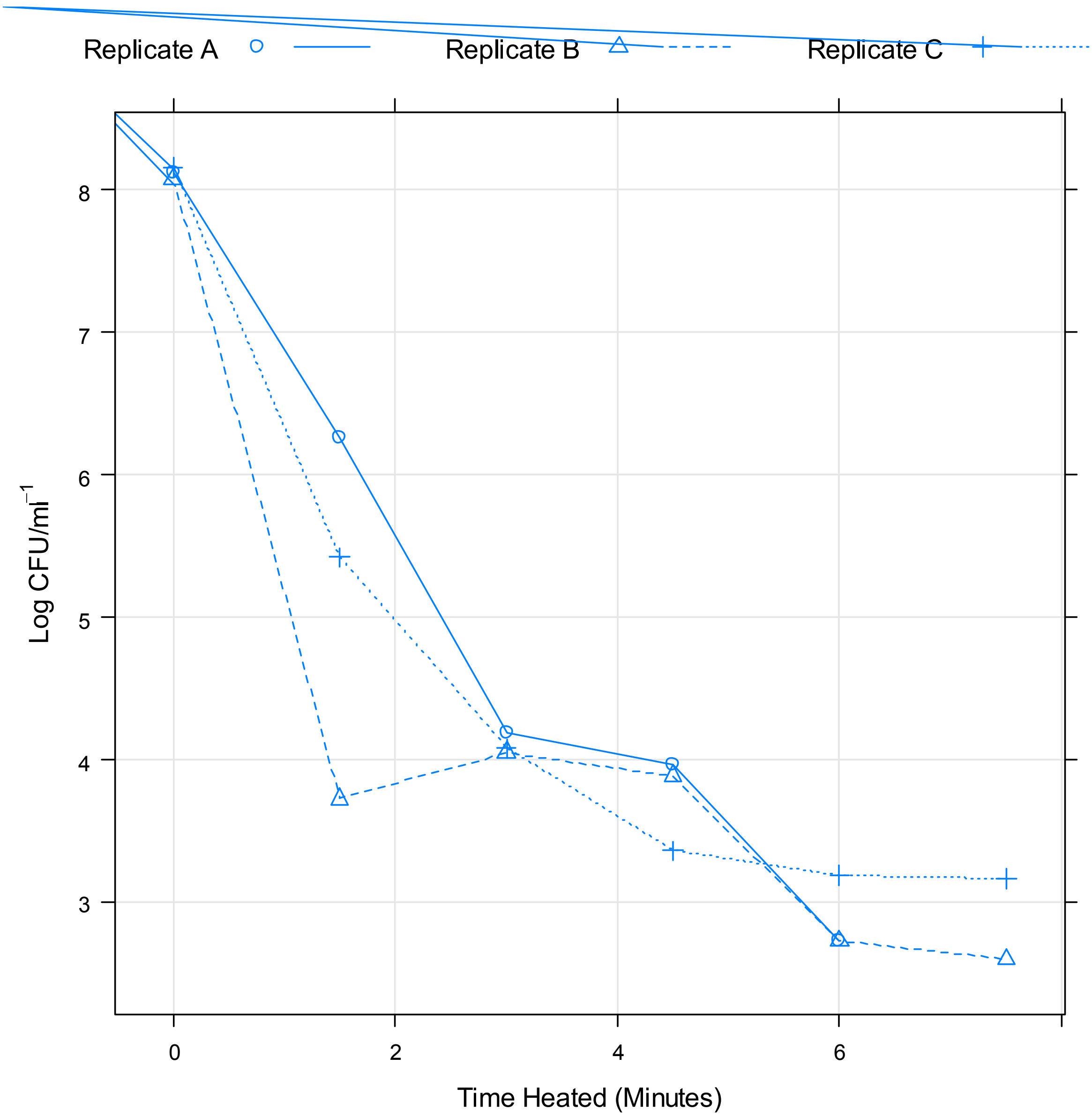

Figure 19. Plot of observed data illustrating survival of strain 11762 (ST-829, CC-828) following heating at 60°C.

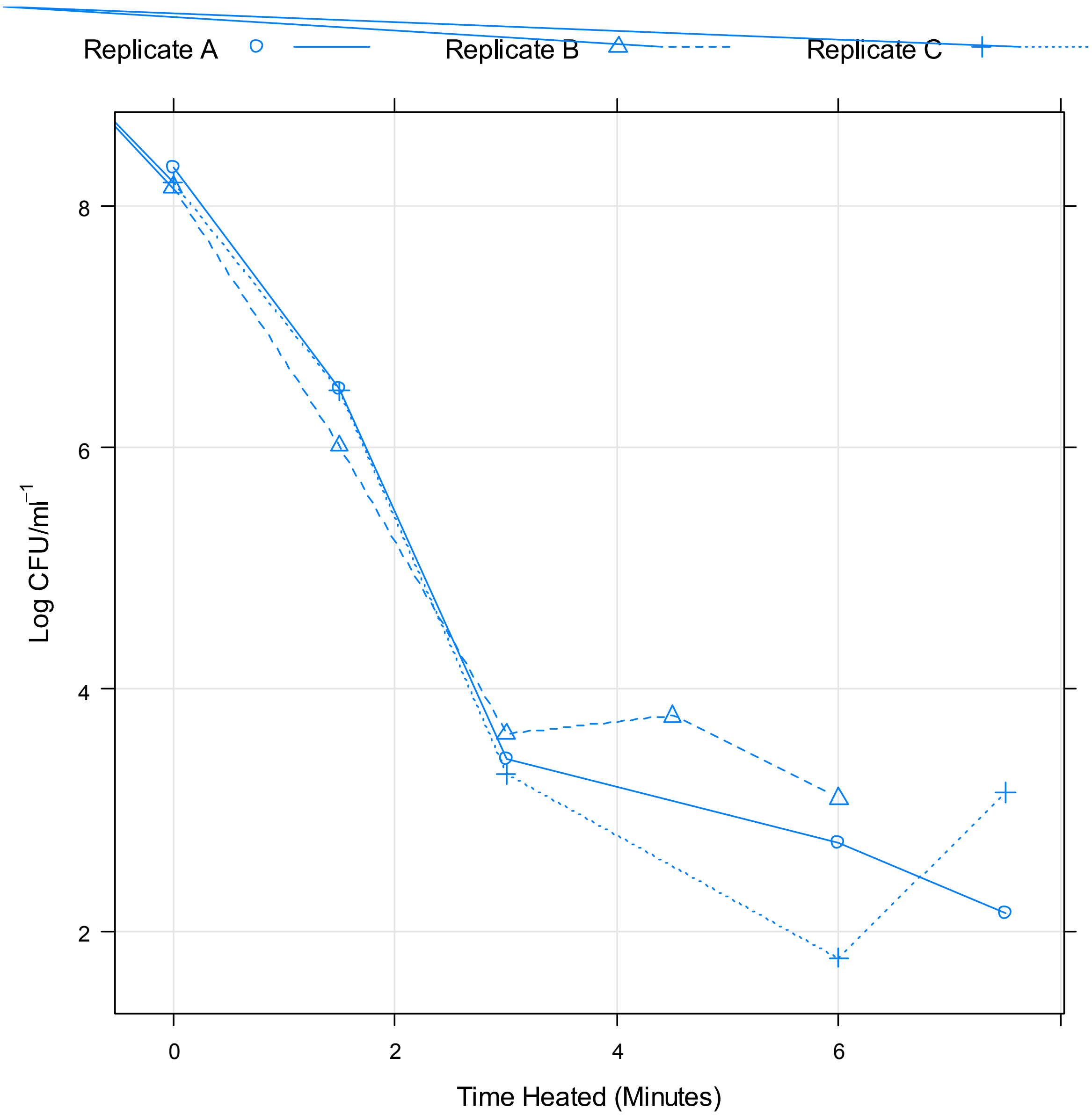

Figure 20. Plot of observed data illustrating survival of strain 12610 (ST-825, CC-828) following heating at 60°C.

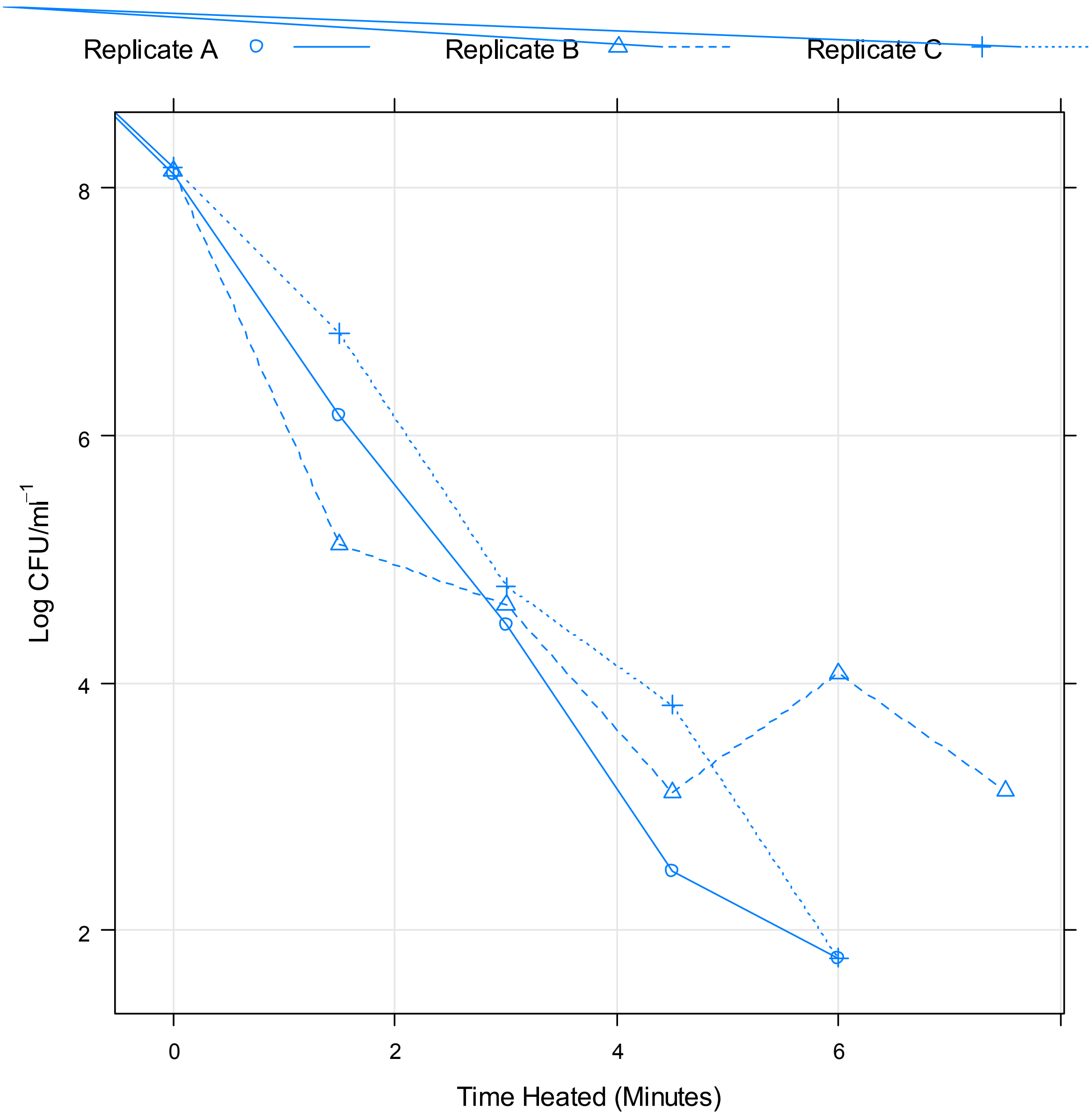

Figure 21. Plot of observed data illustrating survival of strain 12628 (ST-1773, CC-828) following heating at 60°C.

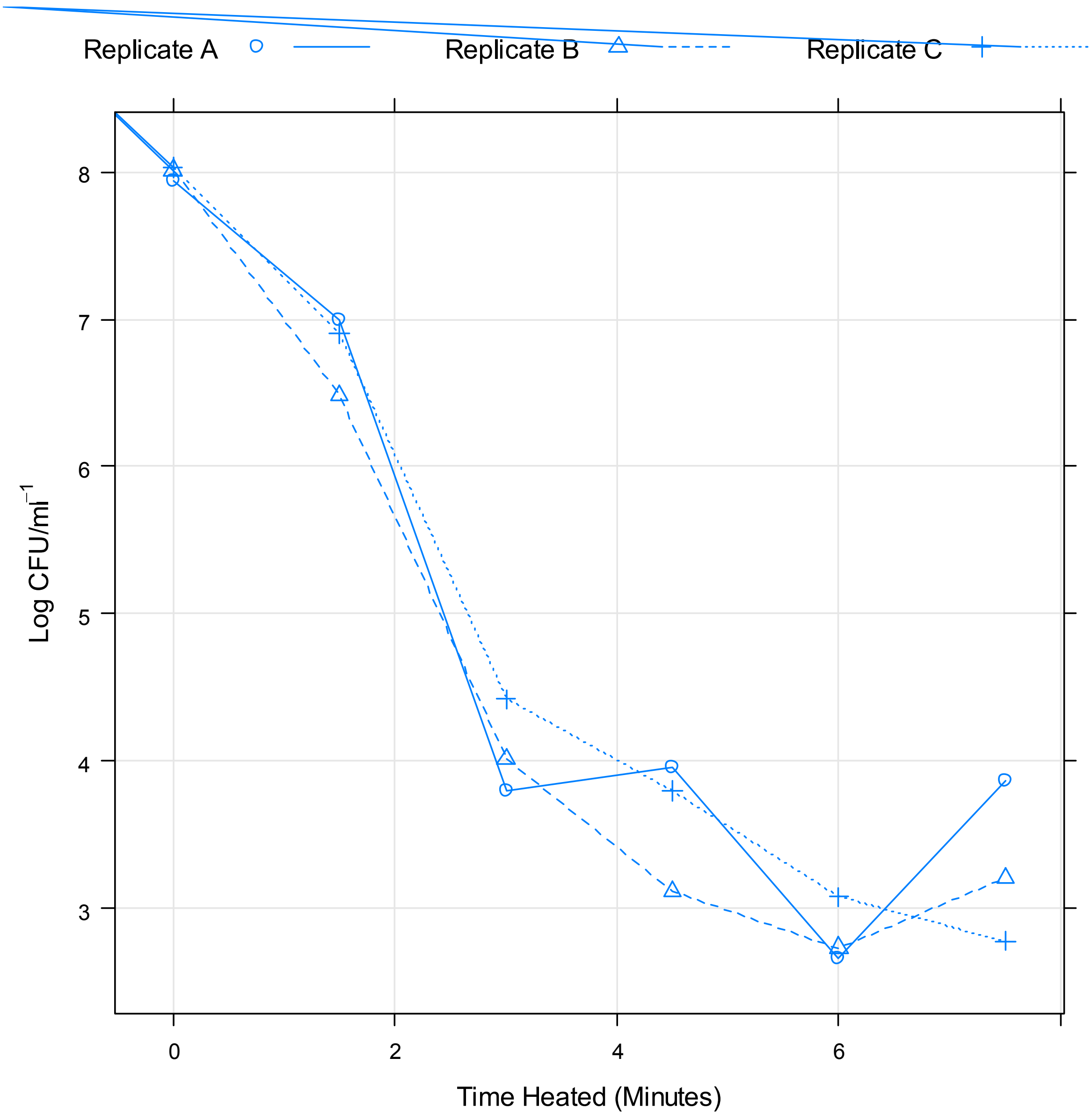

Figure 22. Plot of observed data illustrating survival of strain 12645 (ST-51, CC-443) following heating at 60°C.

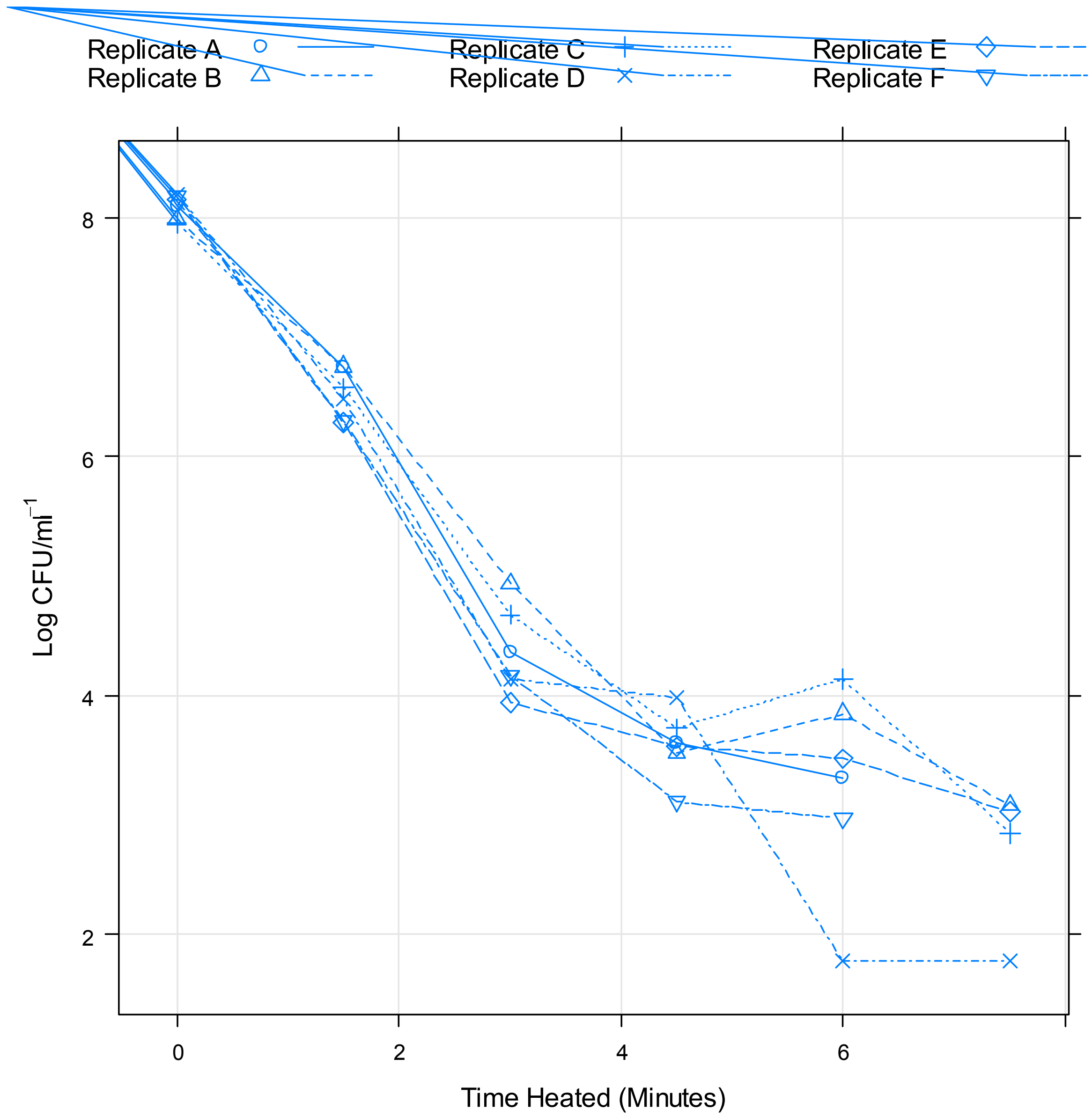

Figure 23. Plot of observed data illustrating survival of strain 12662 (ST-257, CC-257) following heating at 60°C.

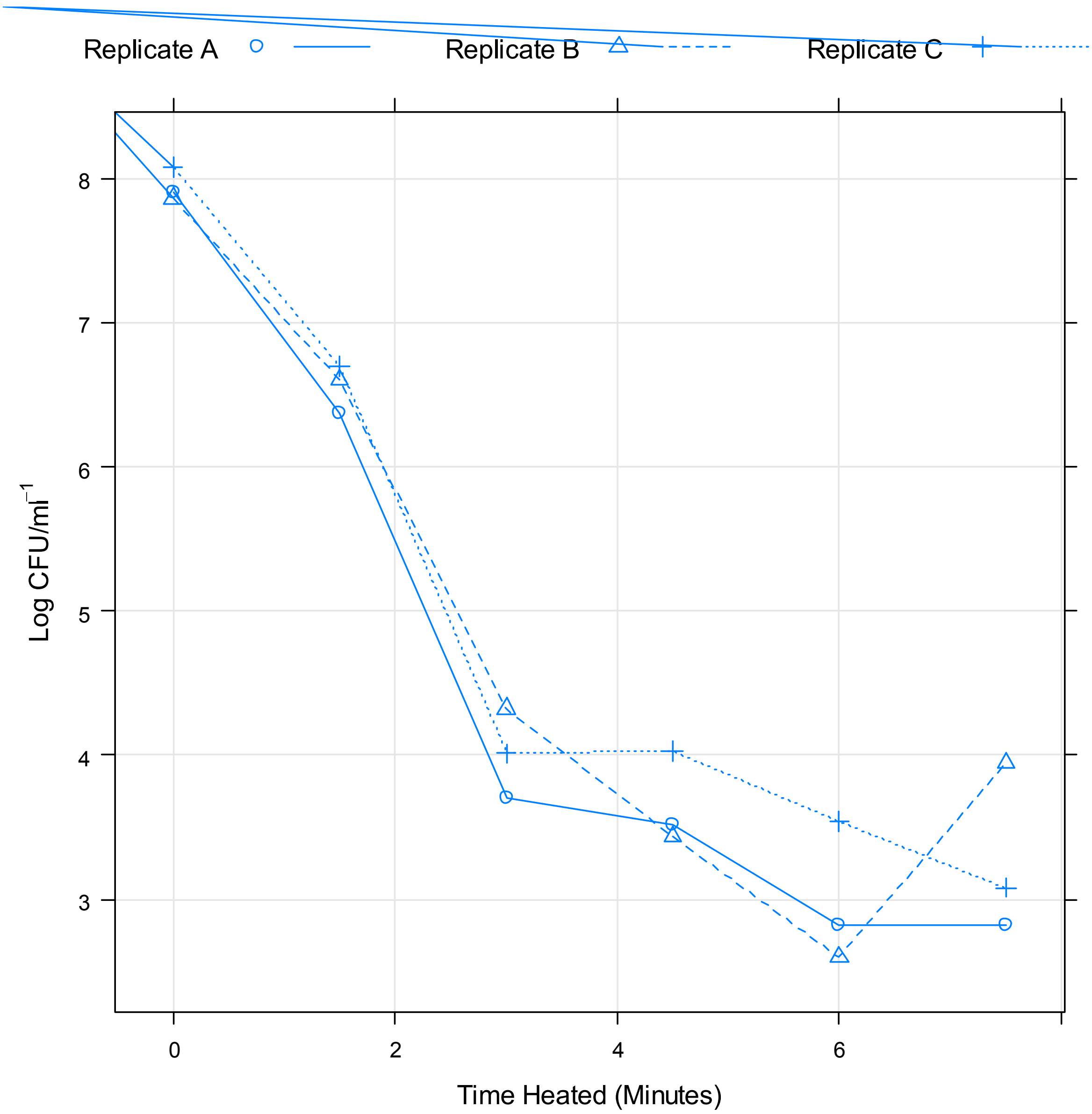

Figure 24. Plot of observed data illustrating survival of strain 12720 (ST-51, CC-443) following heating at 60°C.

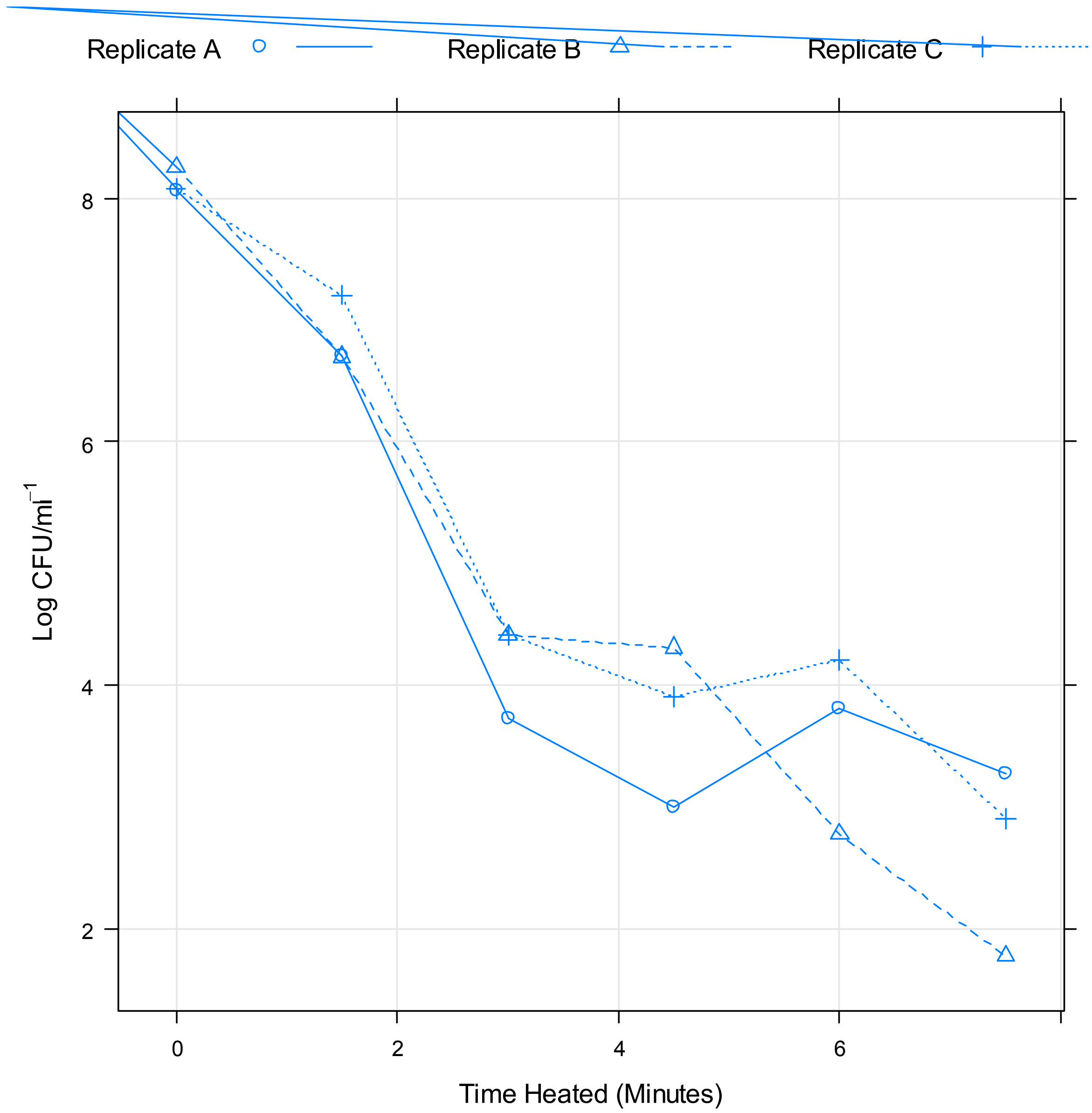

Figure 25. Plot of observed data illustrating survival of strain 12745 (ST-257, CC-257) following heating at 60°C.

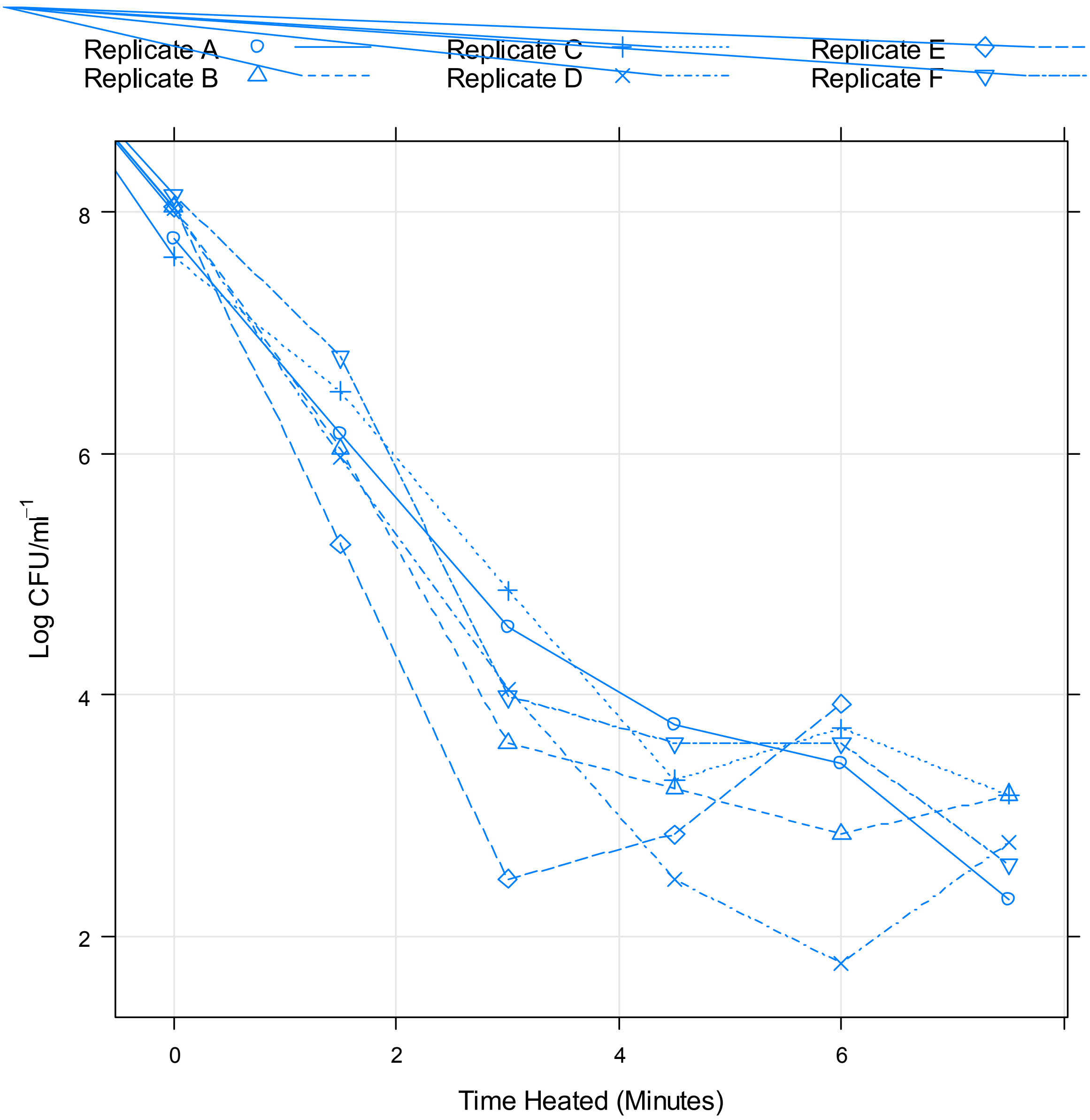

Figure 26. Plot of observed data illustrating survival of strain 12783 (ST-574, CC-574) following heating at 60°C.

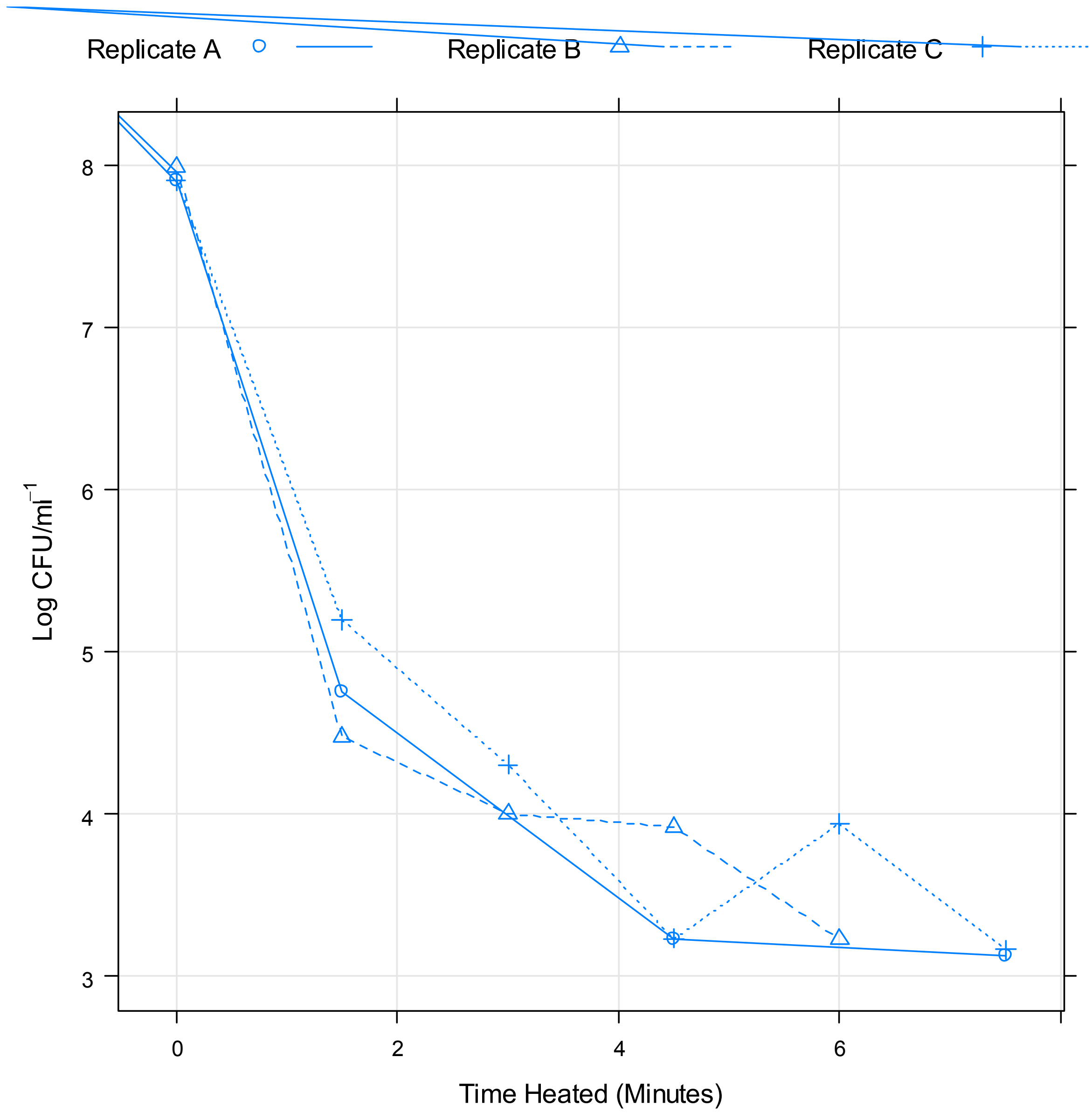

Figure 27. Plot of observed data illustrating survival of strain 13121 (ST-45, CC-45) following heating at 60°C.

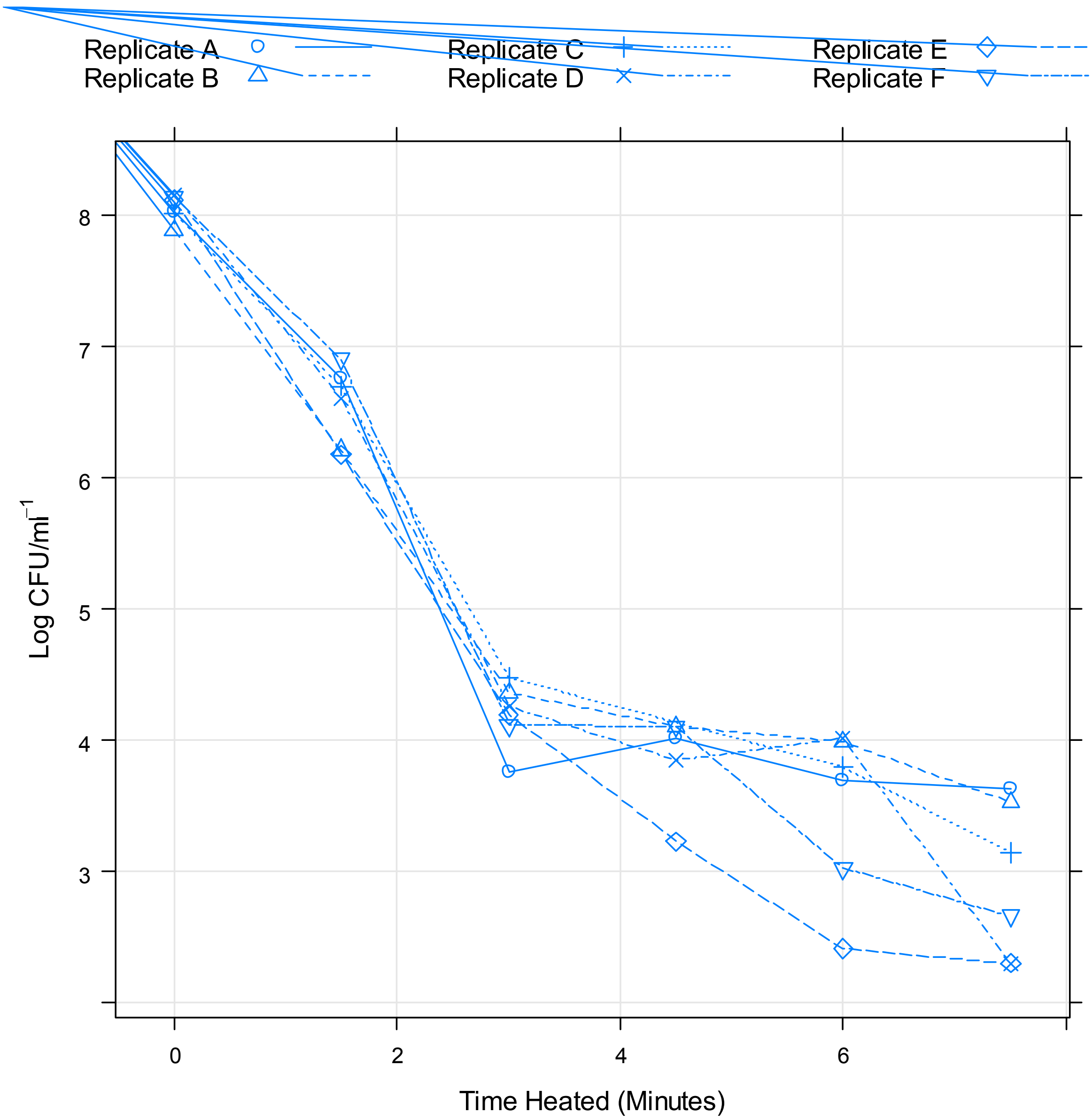

Figure 28. Plot of observed data illustrating survival of strain 13126 (ST-21, CC-21) following heating at 60°C.

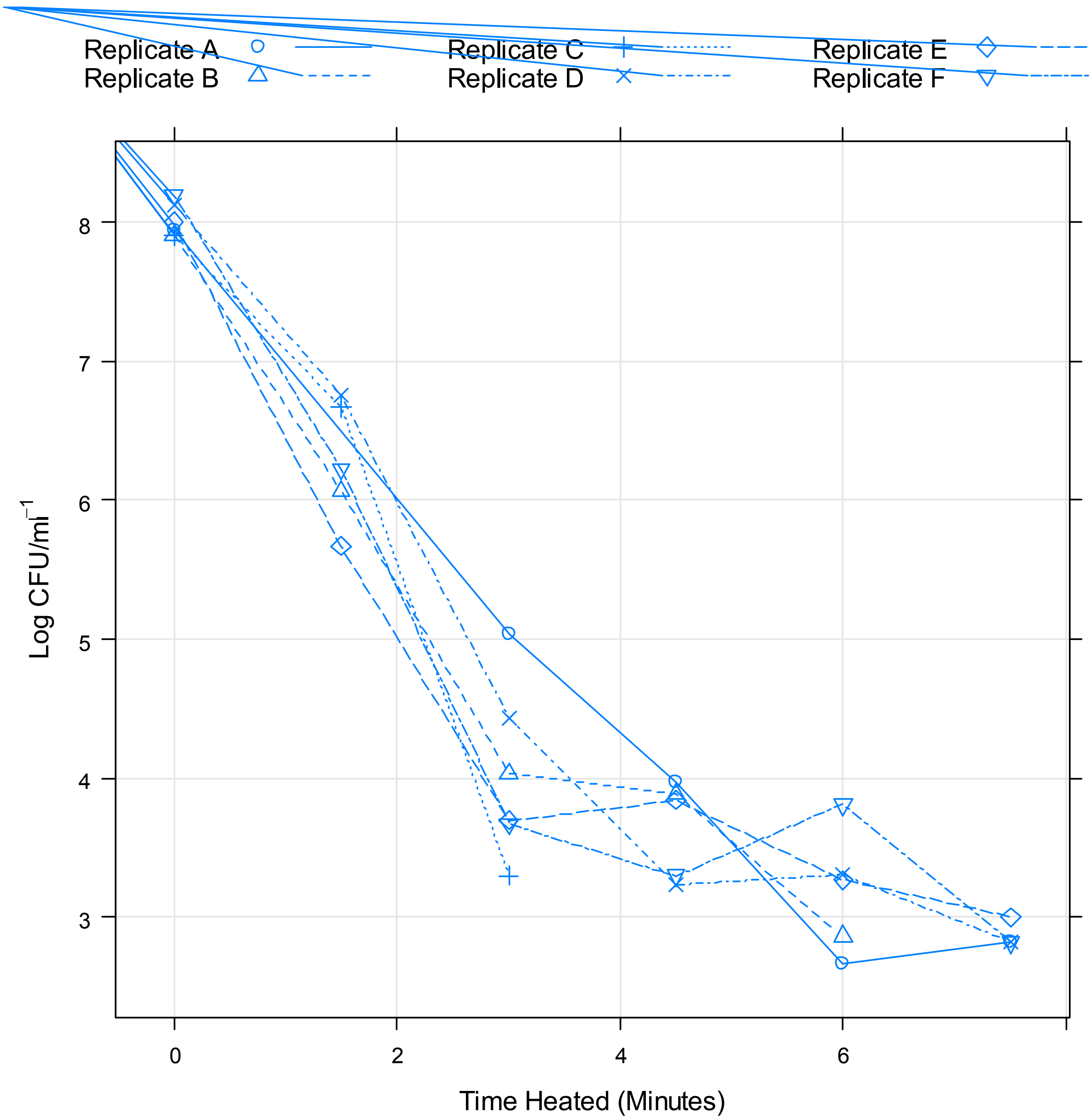

Figure 29. Plot of observed data illustrating survival of strain 13136 (ST-45, CC-45) following heating at 60°C.

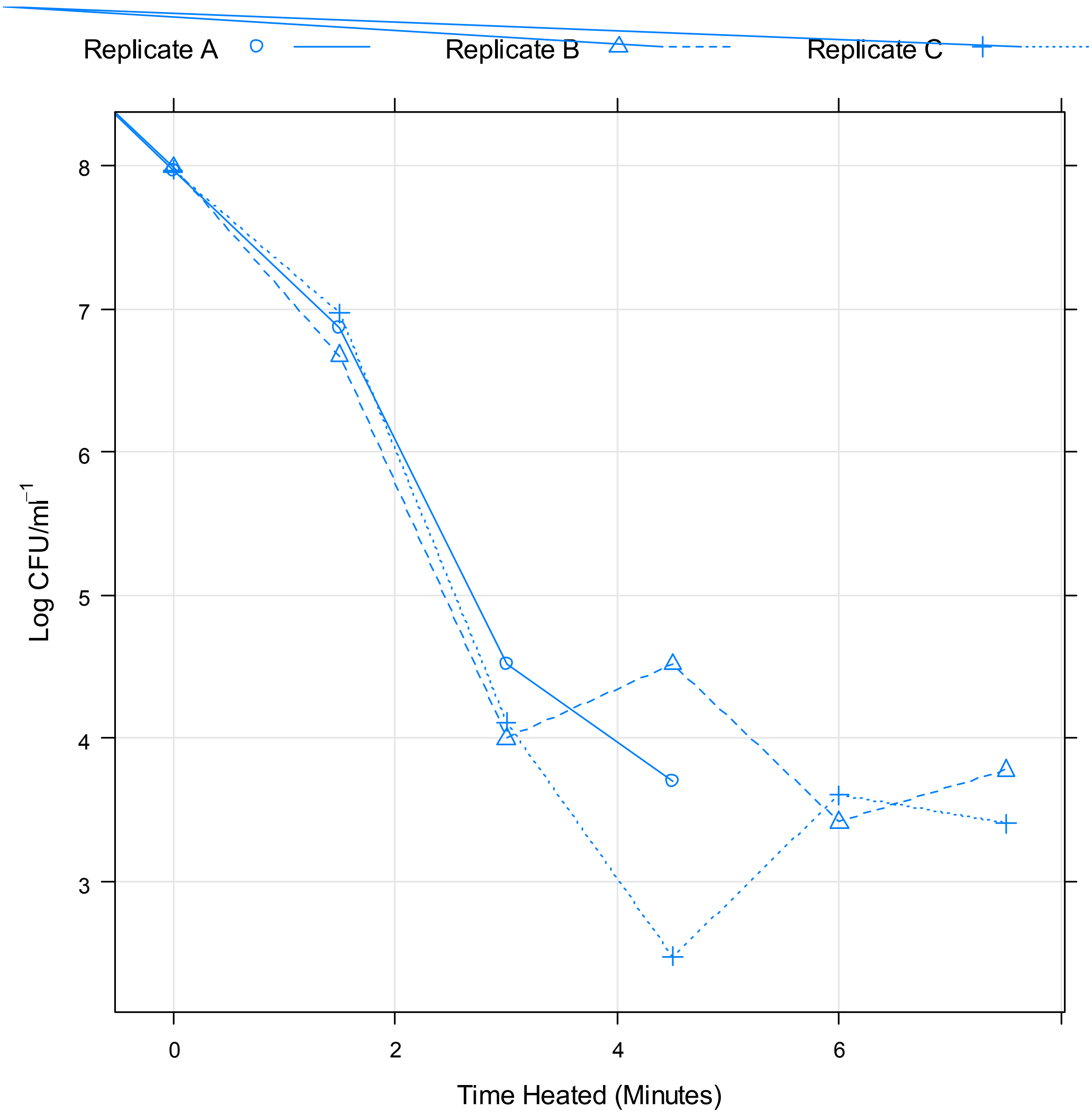

Figure 30. Plot of observed data illustrating survival of strain 13163 (ST-21, CC-21) following heating at 60°C.

1.6 Time-Temperature Simulations: 64°C

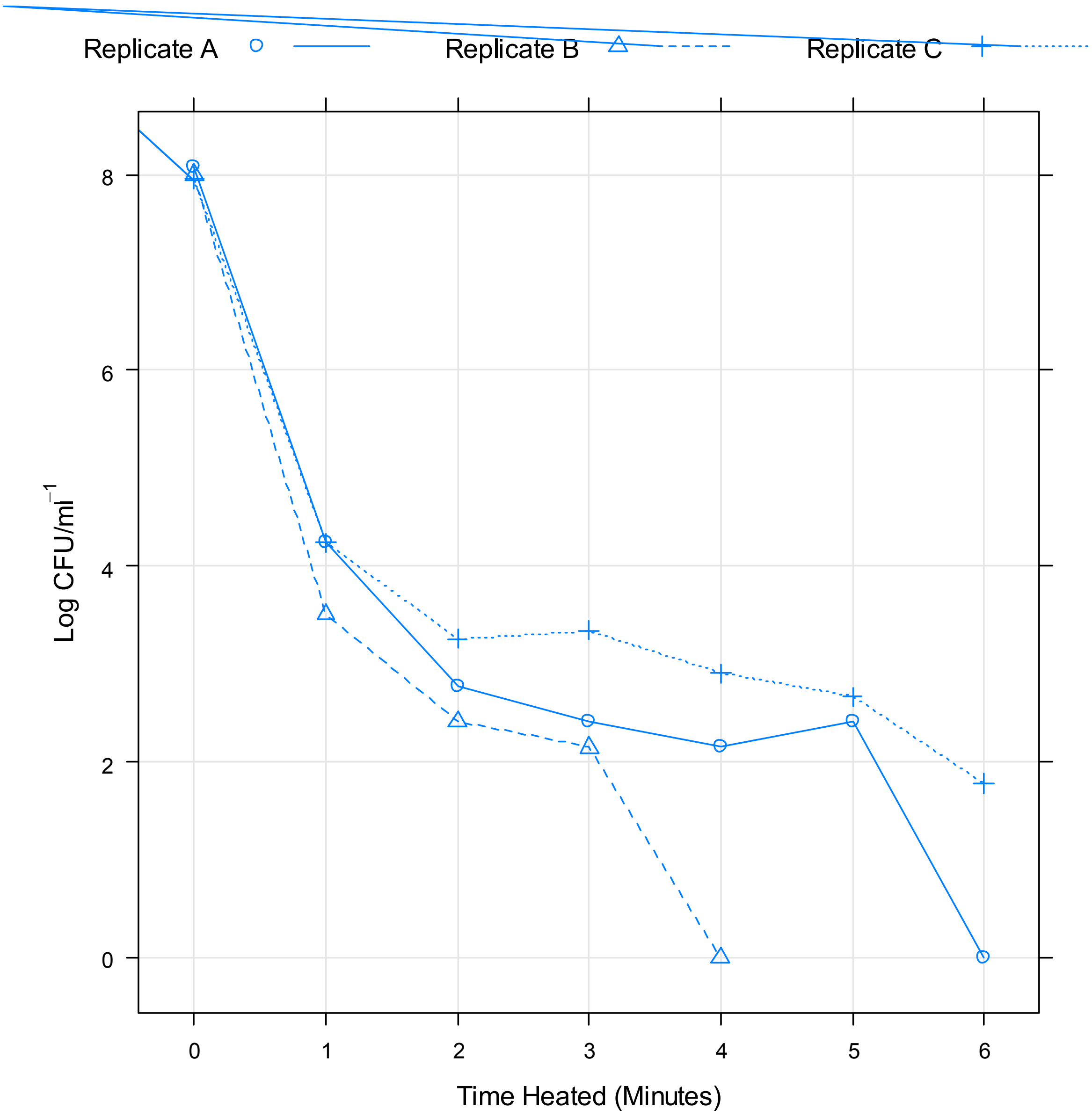

Figure 31. Plot of observed data illustrating survival of strain 11253 (ST-825, CC-828) following heating at 64°C.

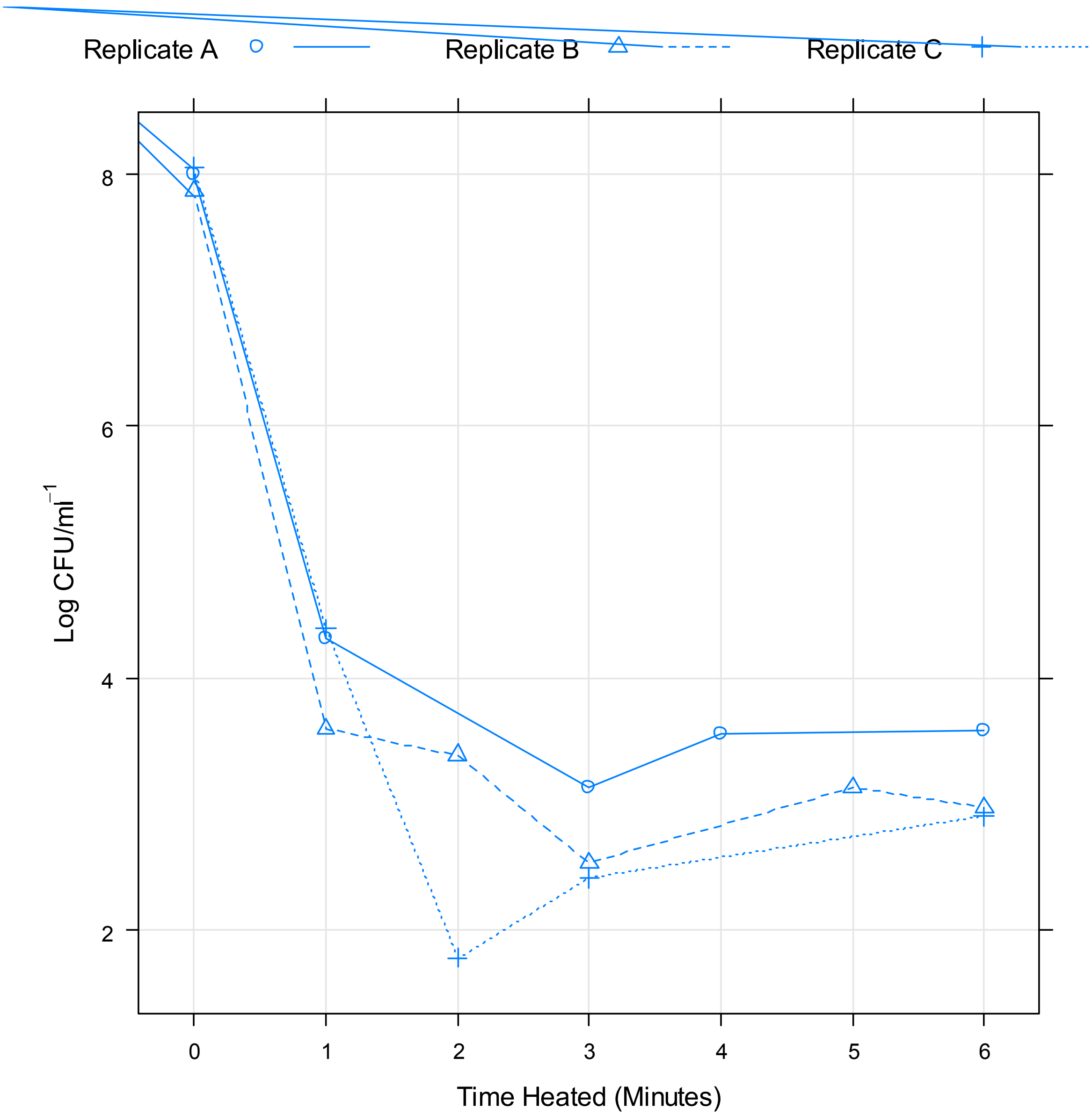

Figure 32. Plot of observed data illustrating survival of strain 11368 (ST-574, CC-574) following heating at 64°C.

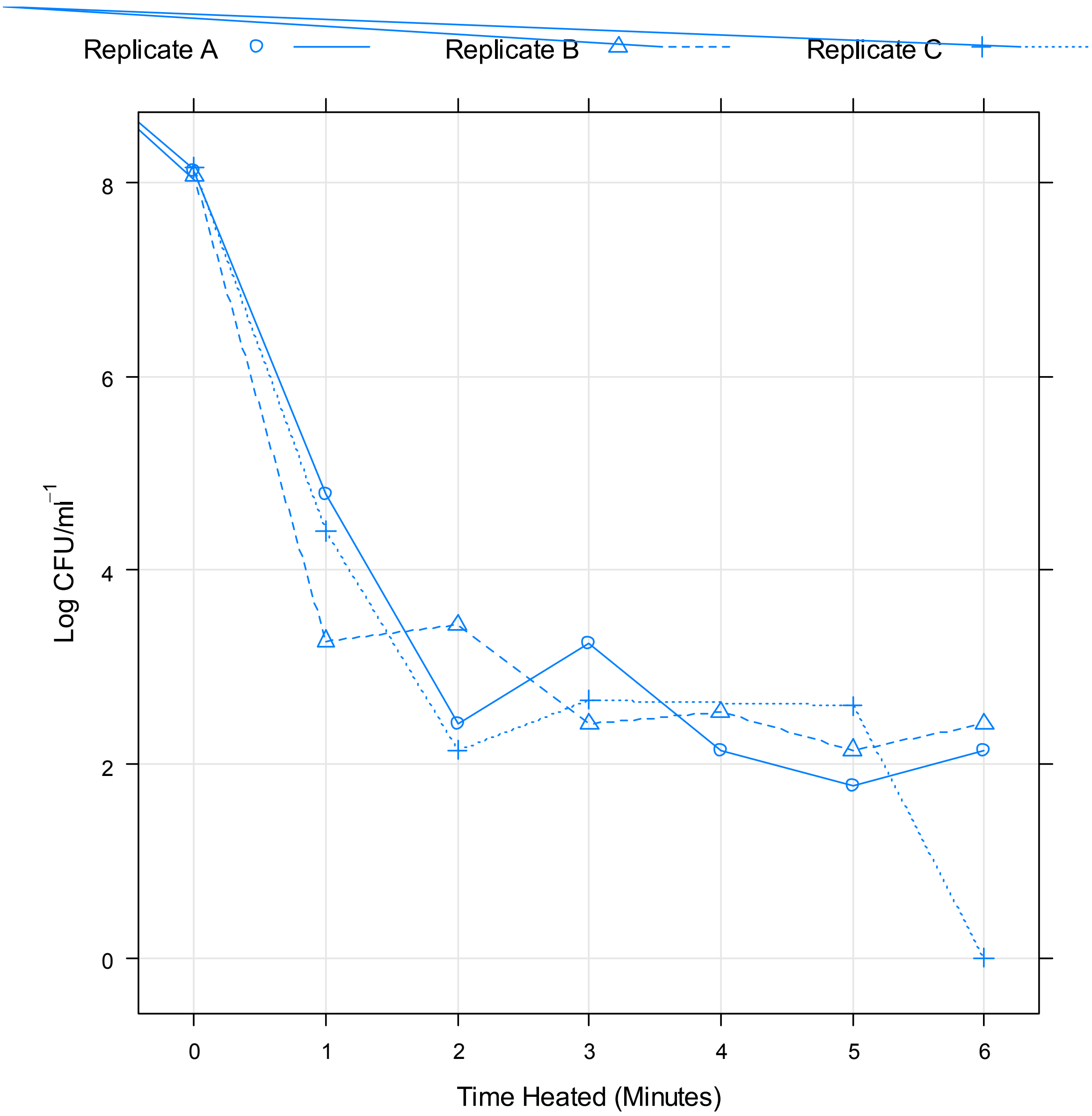

Figure 33. Plot of observed data illustrating survival of strain 11762 (ST-829, CC-828) following heating at 64°C.

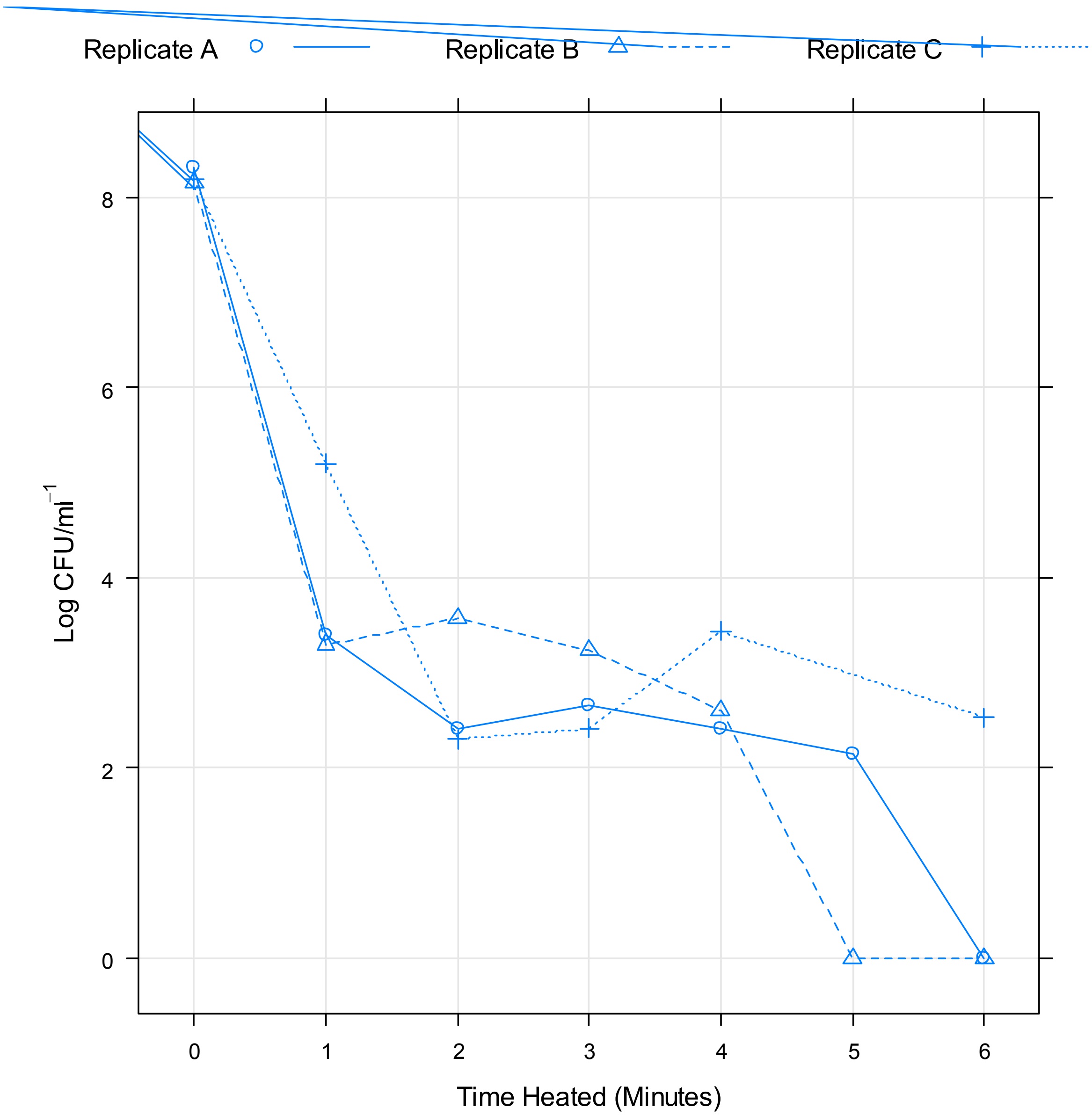

Figure 34. Plot of observed data illustrating survival of strain 12610 (ST-825, CC-828) following heating at 64°C.

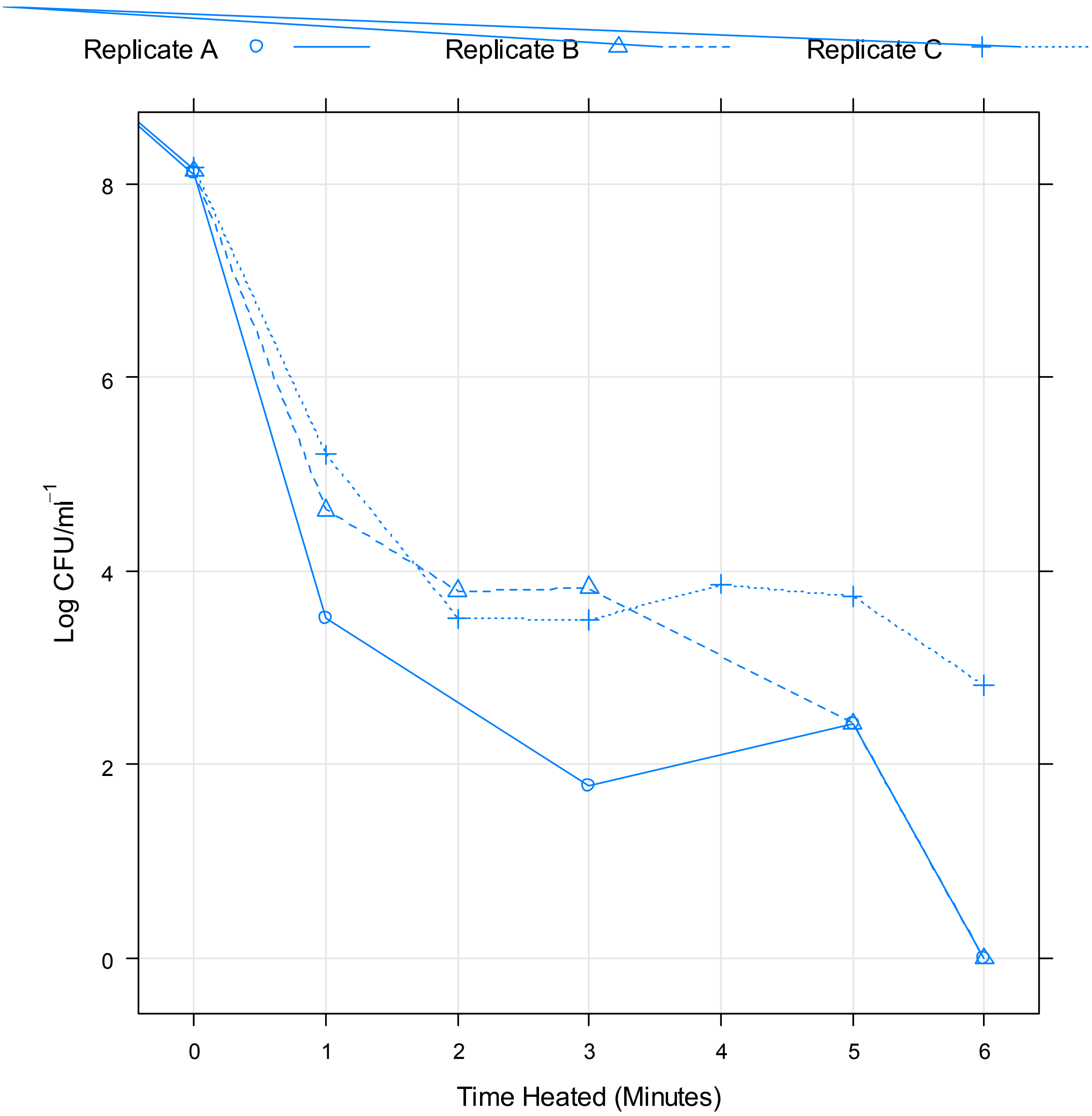

Figure 35. Plot of observed data illustrating survival of strain 12628 (ST-1773, CC-828) following heating at 64°C.

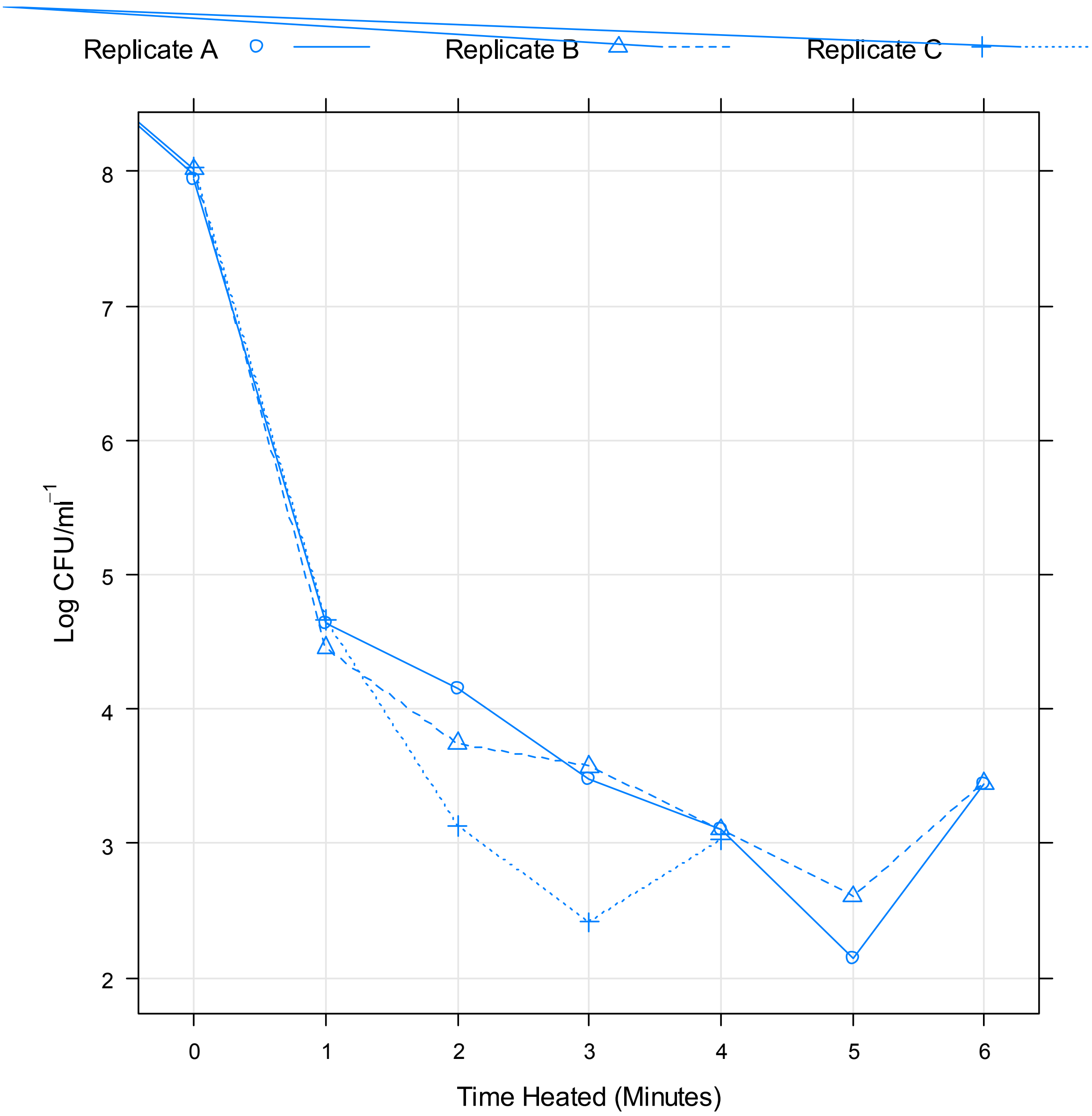

Figure 36. Plot of observed data illustrating survival of strain 12645 (ST-51, CC-443) following heating at 64°C.

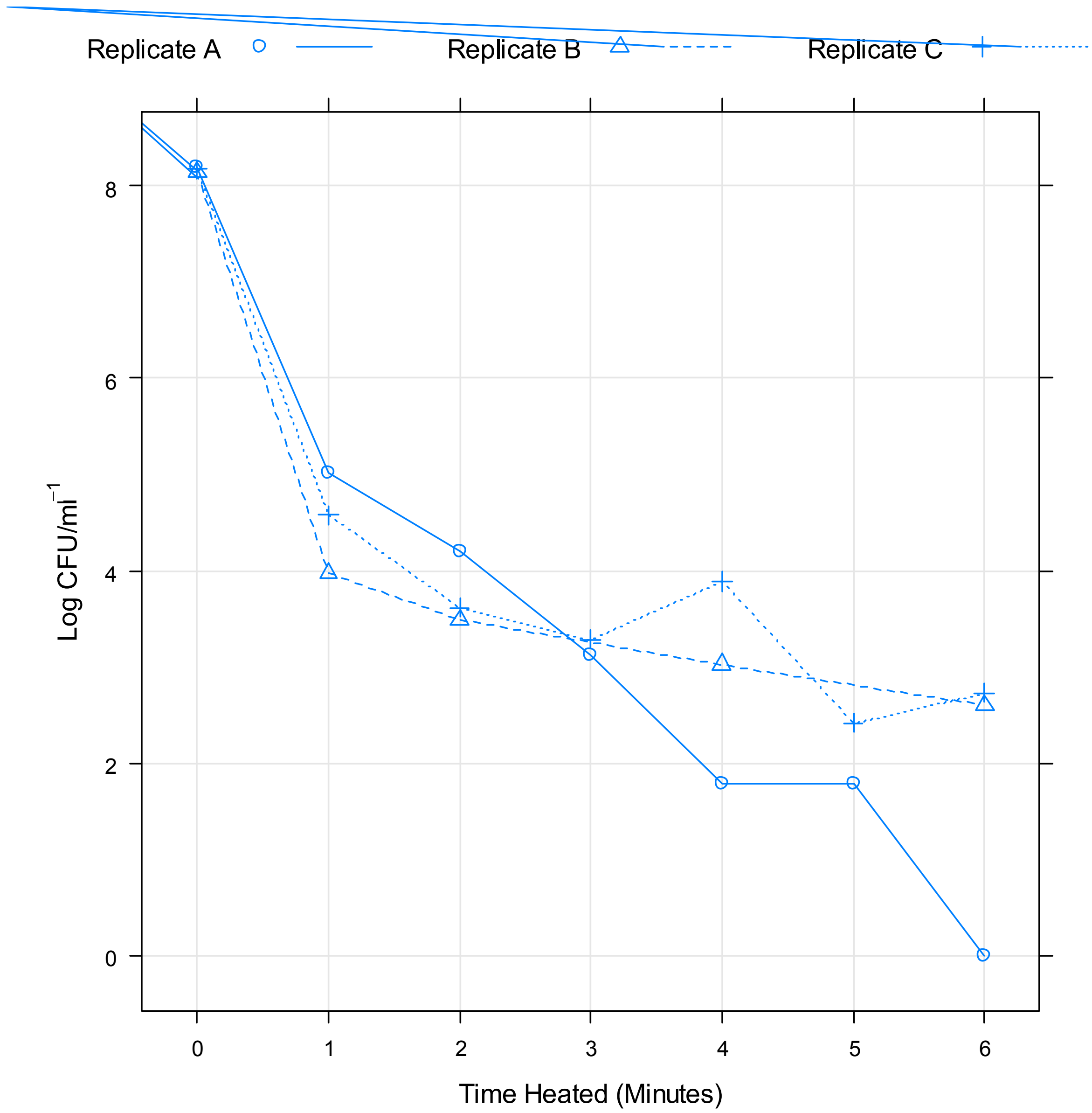

Figure 37. Plot of observed data illustrating survival of strain 12662 (ST-257, CC-257) following heating at 64°C.

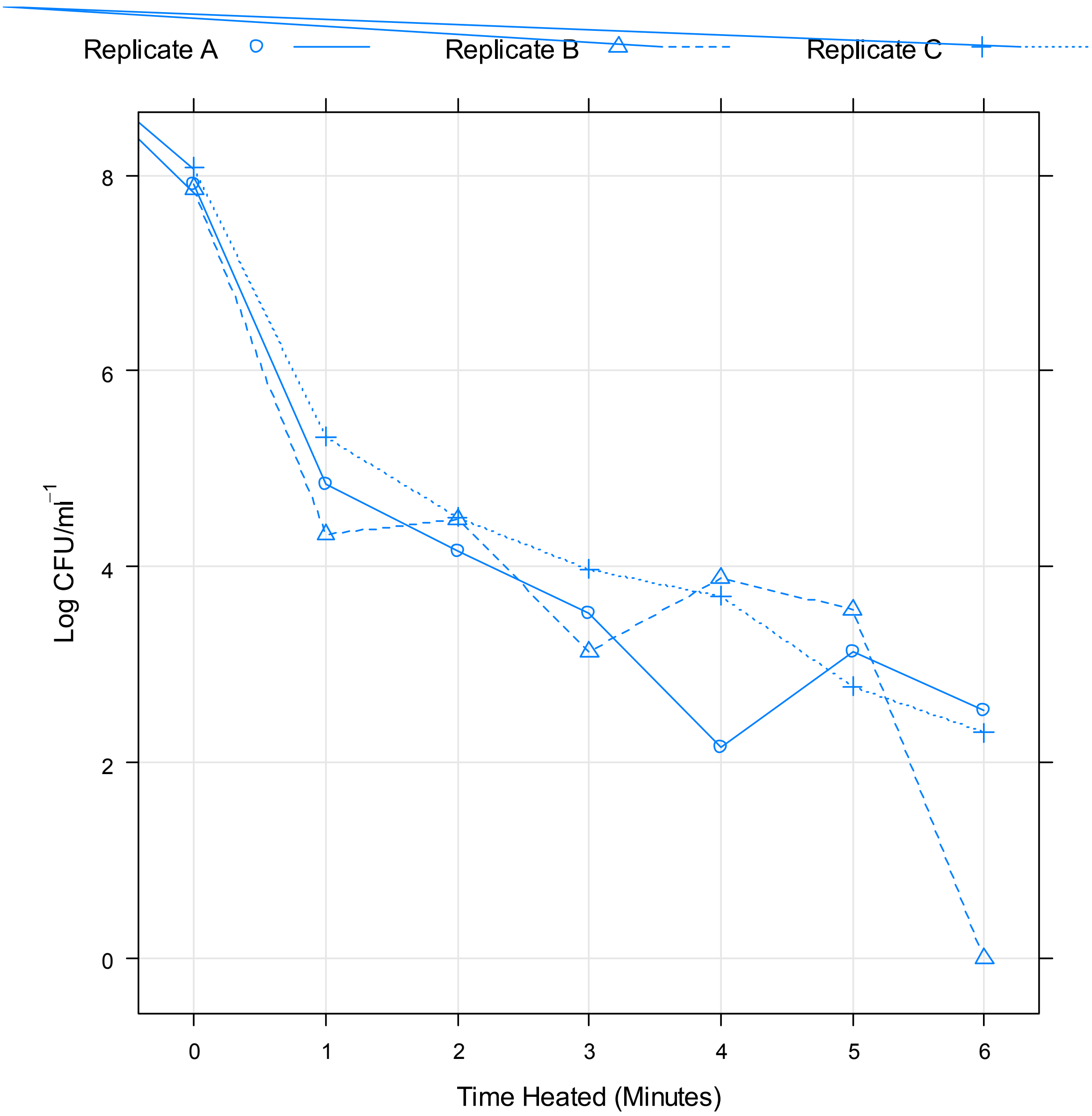

Figure 38. Plot of observed data illustrating survival of strain 12720 (ST-51, CC-443) following heating at 64°C.

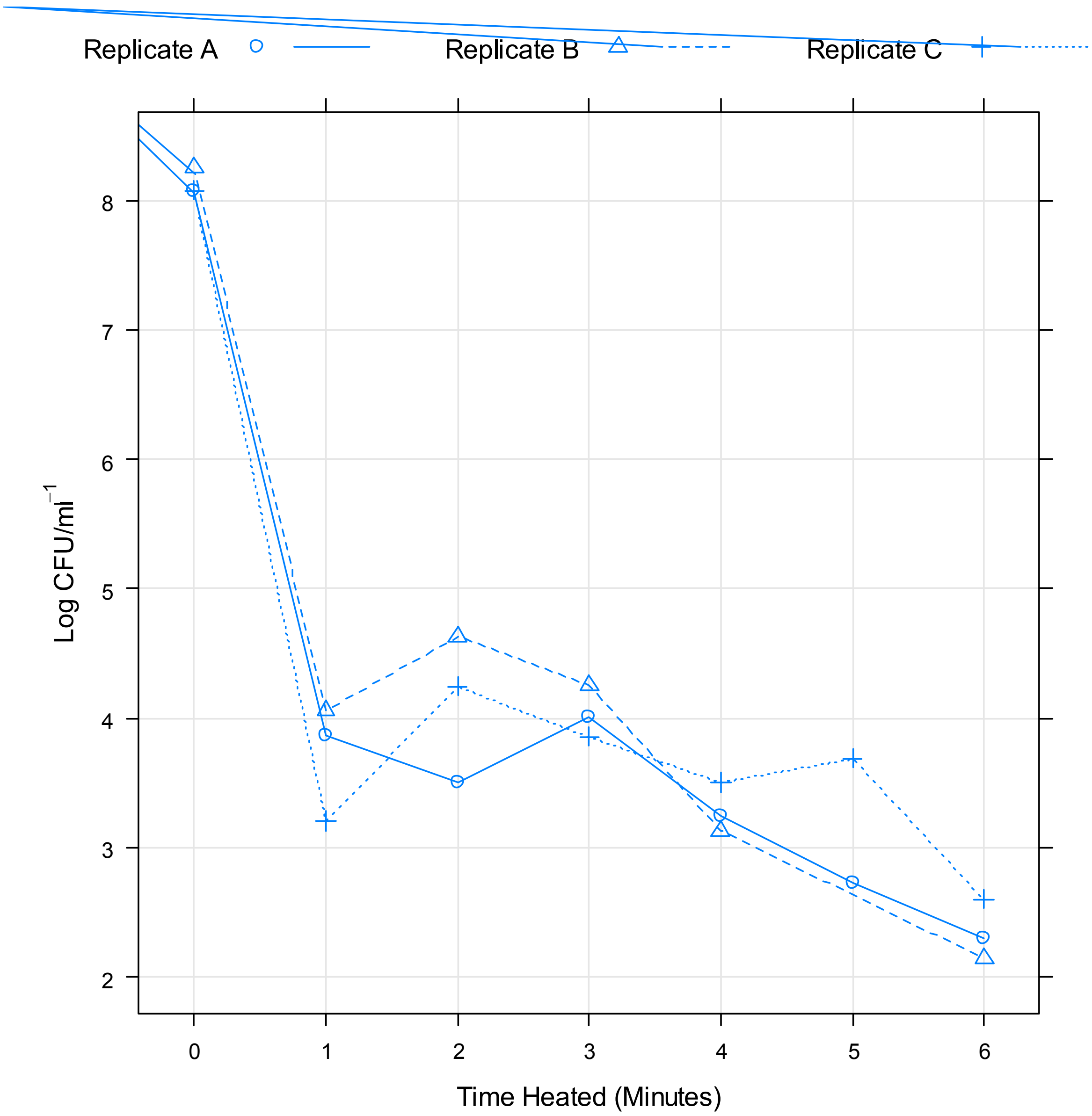

Figure 39. Plot of observed data illustrating survival of strain 12745 (ST-257, CC-257) following heating at 64°C.

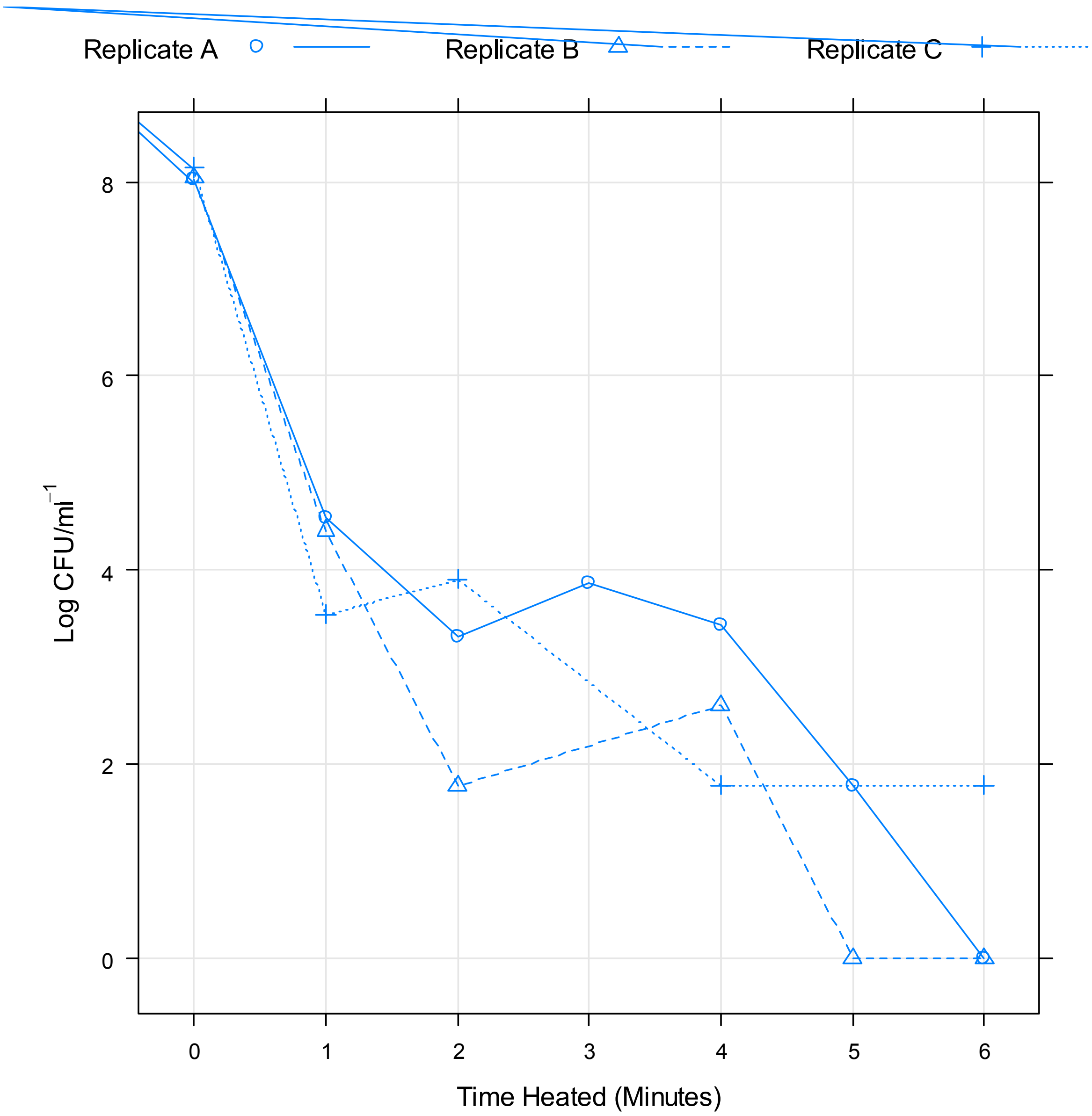

Figure 40. Plot of observed data illustrating survival of strain 12783 (ST-574, CC-574) following heating at 64°C.

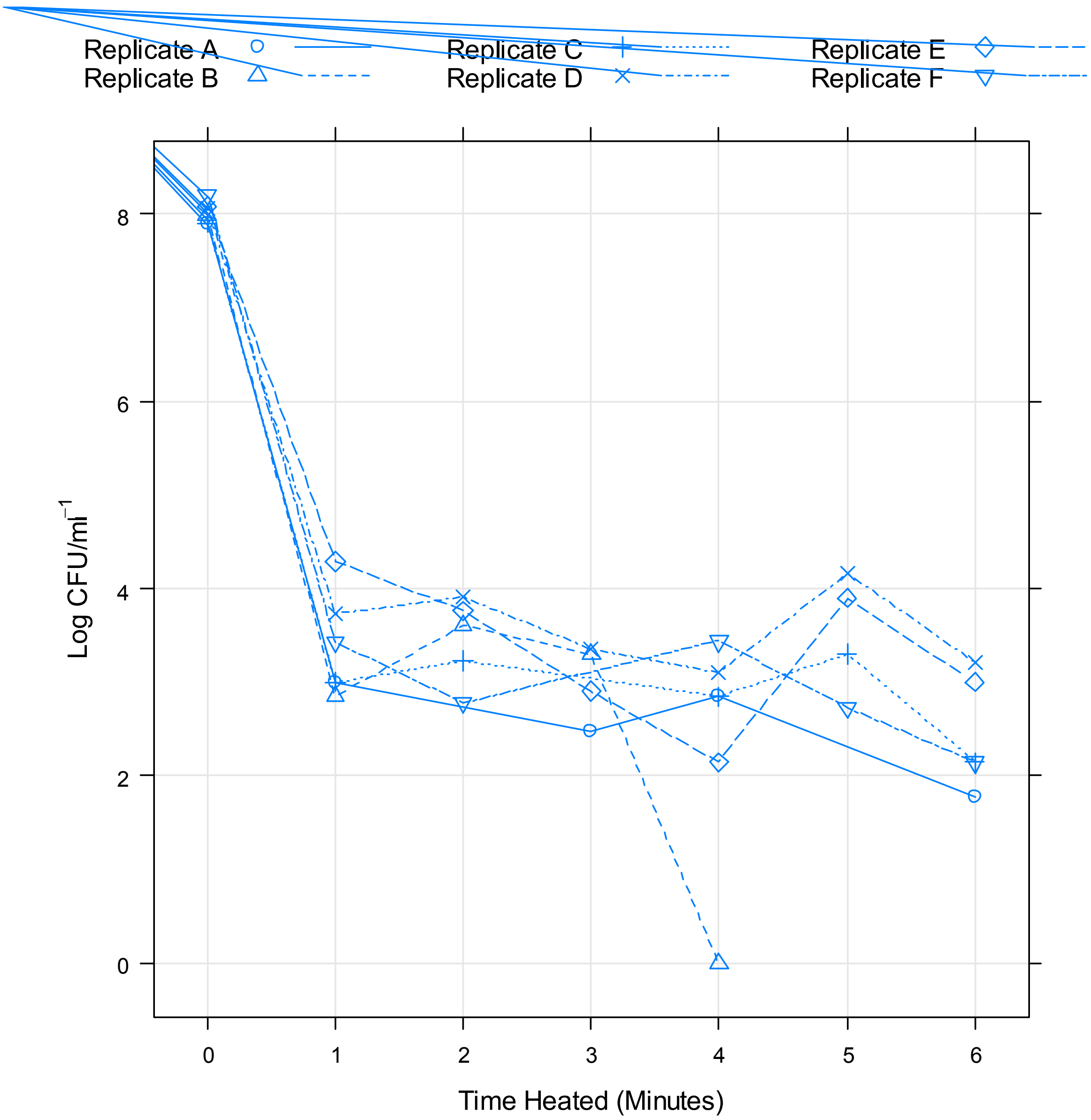

Figure 41. Plot of observed data illustrating survival of strain 13121 (ST-45, CC-45) following heating at 64°C.

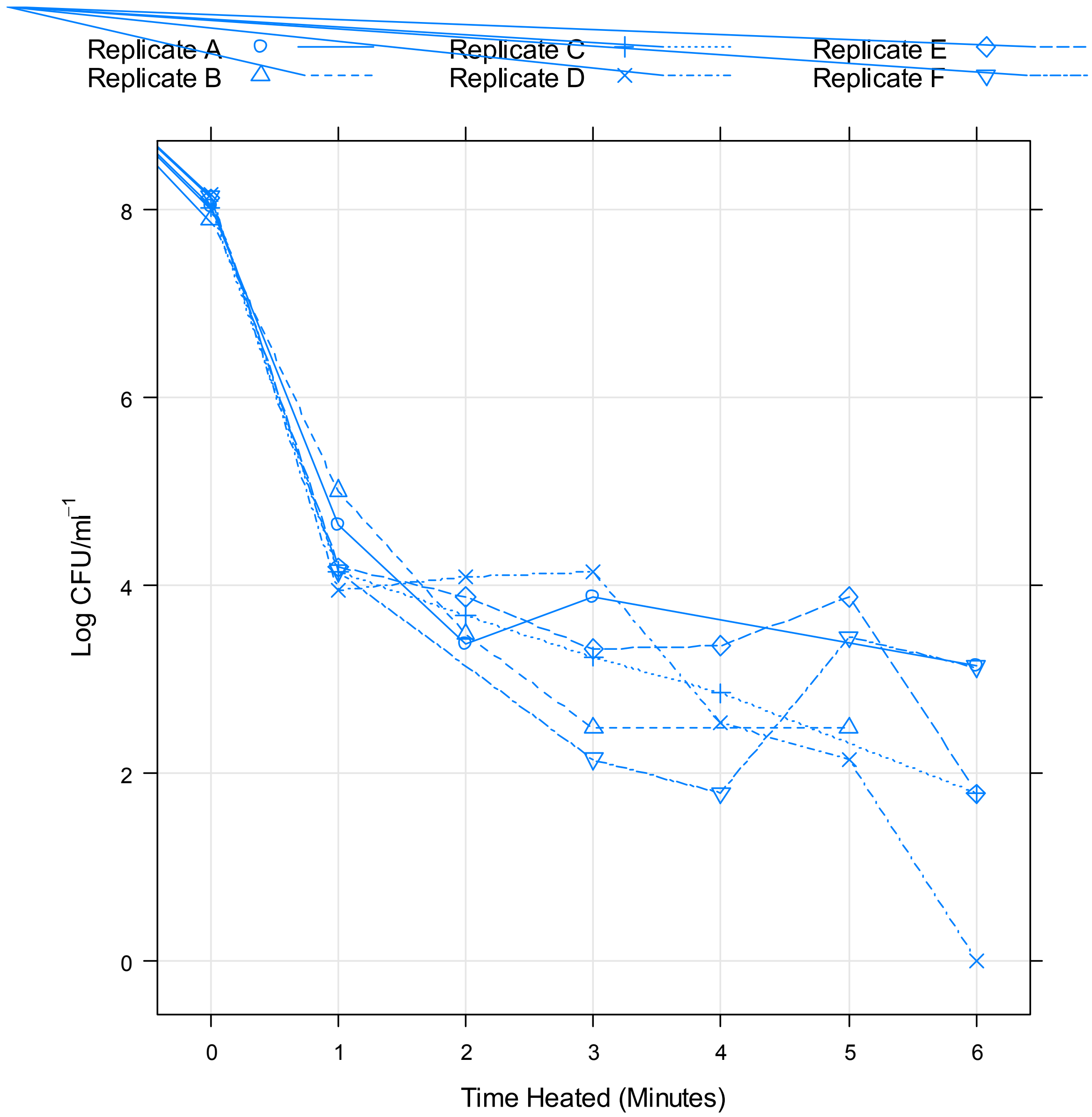

Figure 42. Plot of observed data illustrating survival of strain 13126 (ST-21, CC-21) following heating at 64°C.

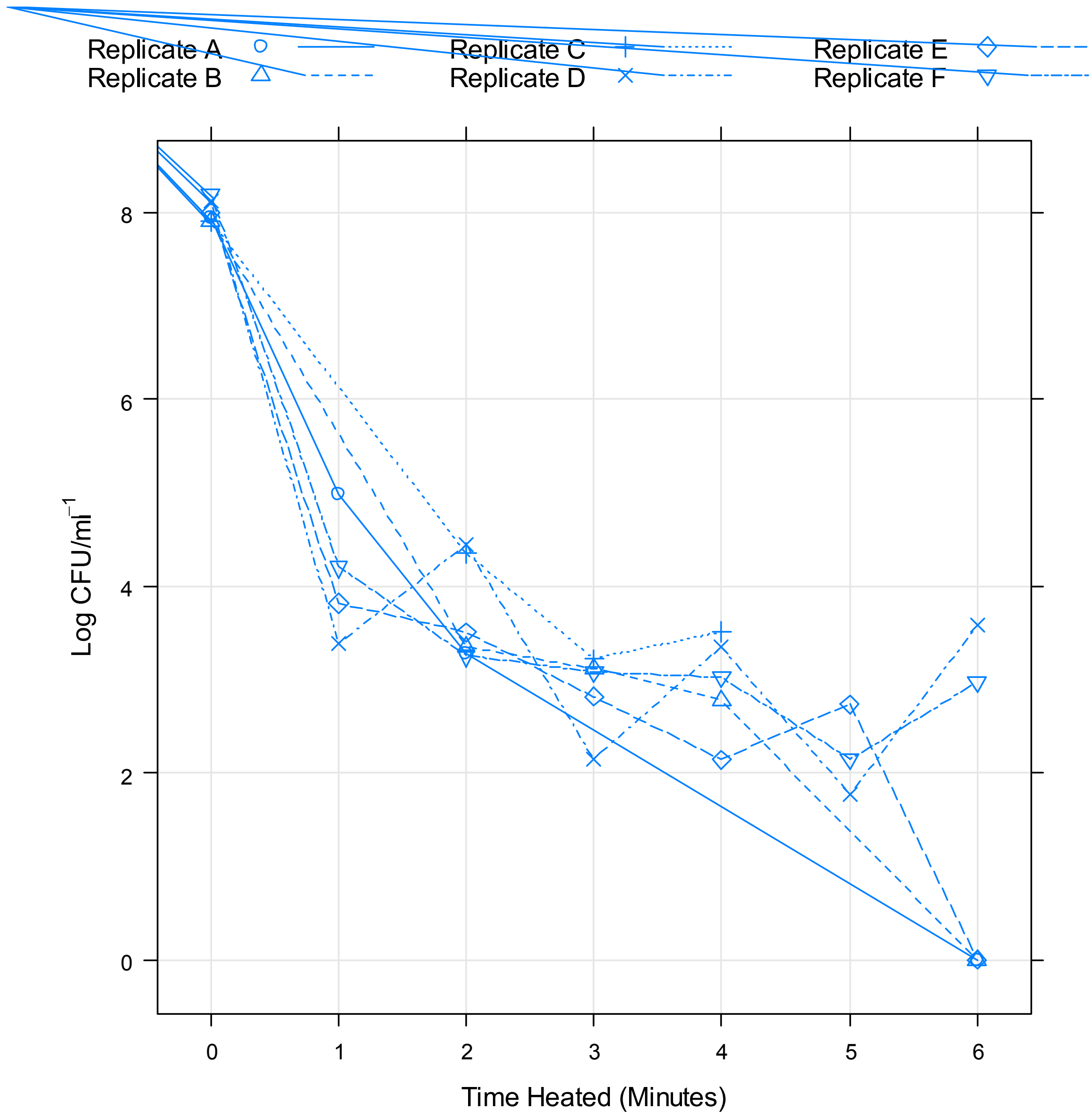

Figure 43. Plot of observed data illustrating survival of strain 13136 (ST-45, CC-45) following heating at 64°C.

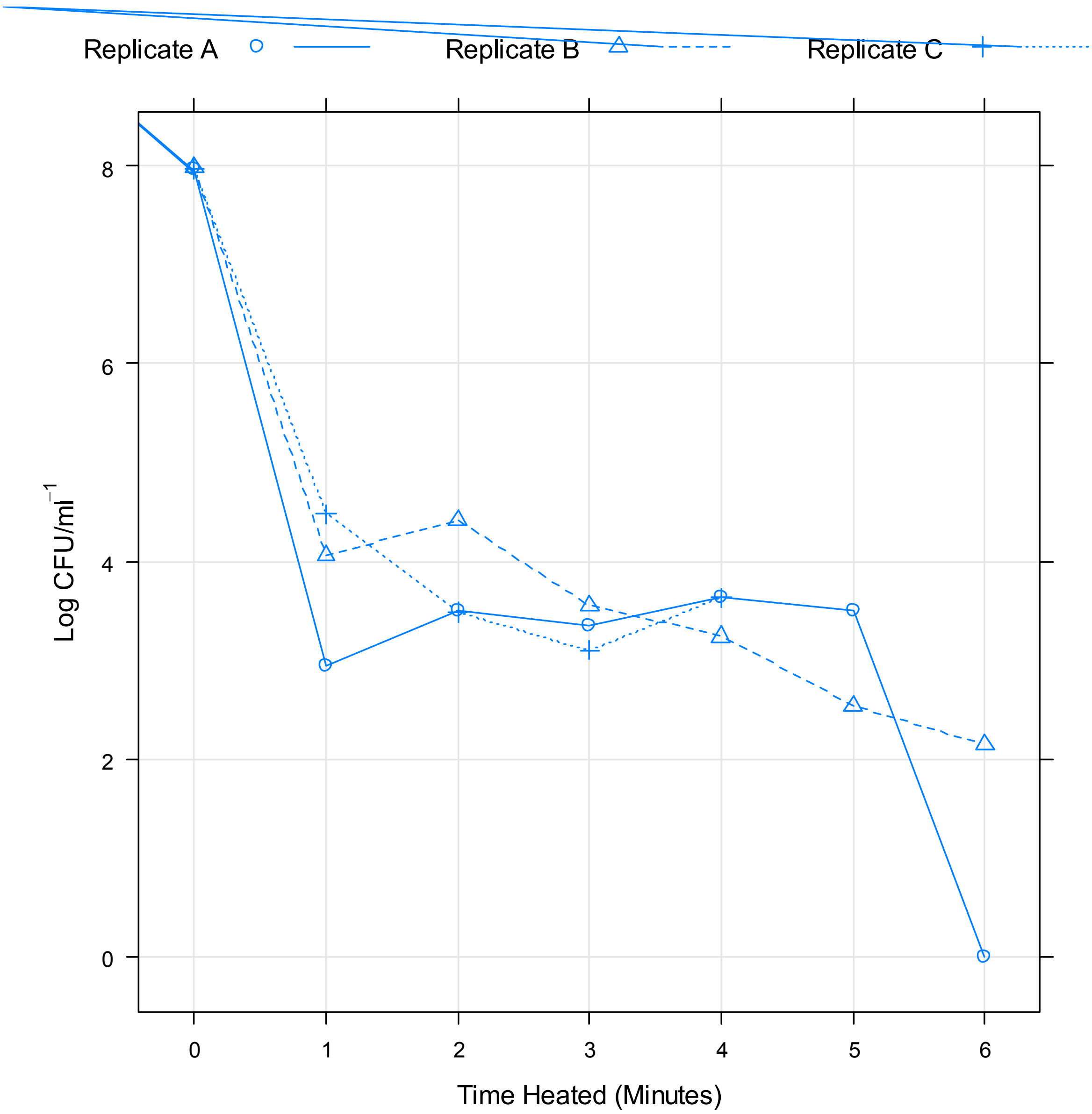

Figure 44. Plot of observed data illustrating survival of strain 13163 (ST-21, CC-21) following heating at 64°C.

1.7 pH and Time-Temperature Simulations:

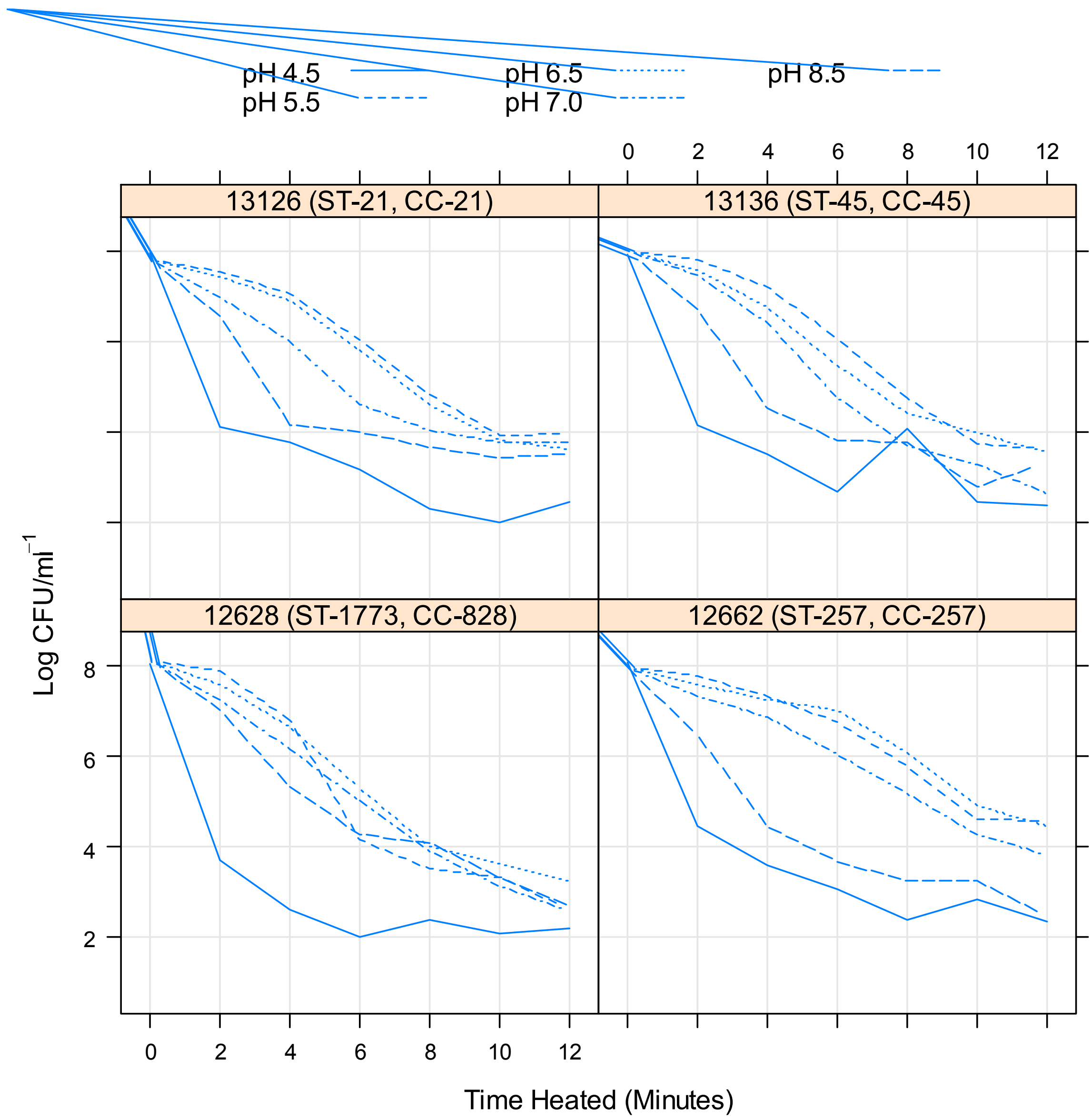

Figure 45. Plot of observed data illustrating survival of four strains following combined pH and time-temperature simulations undertaken at a 56°C.

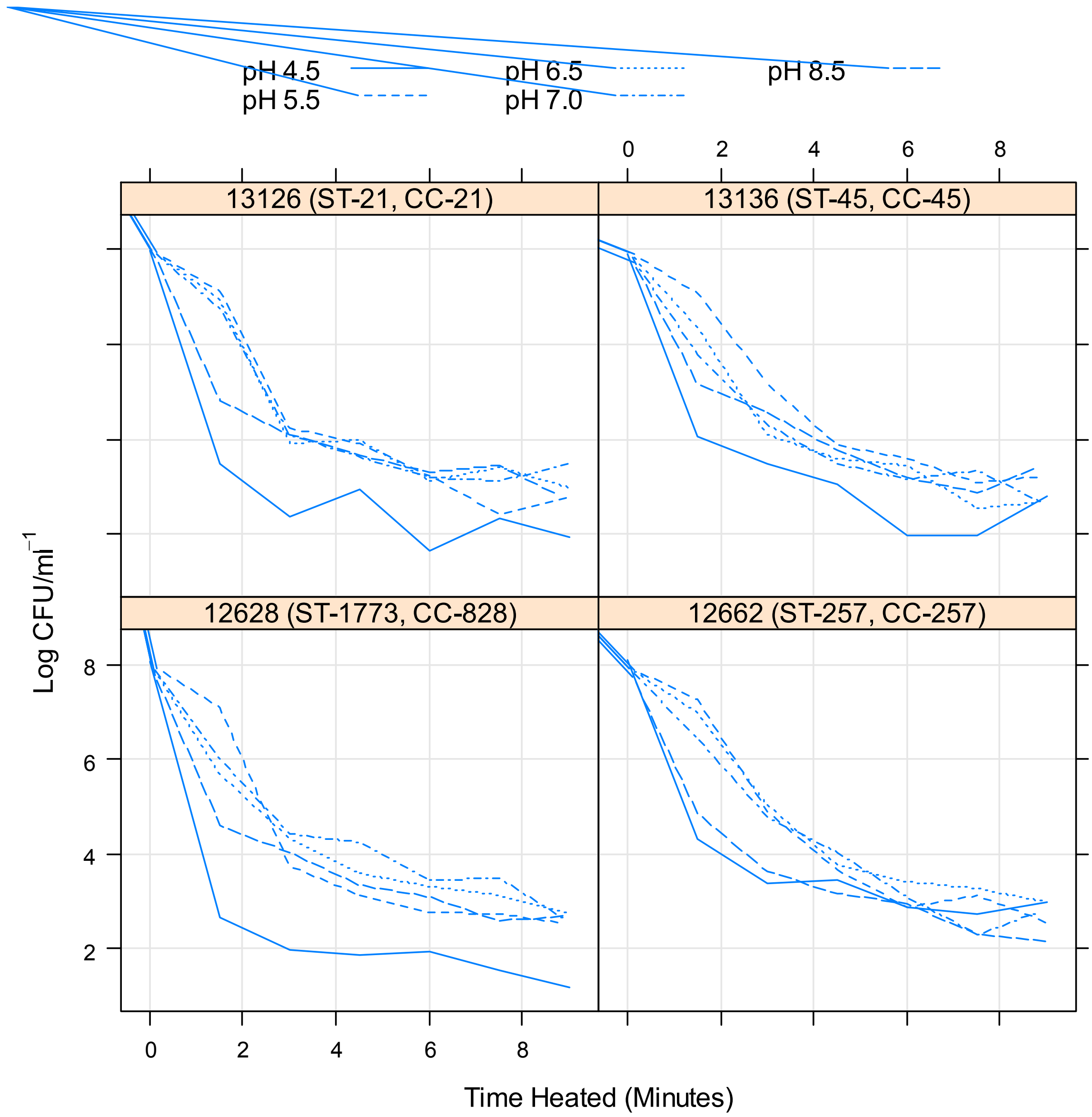

Figure 46. Plot of observed data illustrating survival of four strains following combined pH and time-temperature simulations undertaken at a 60°C.

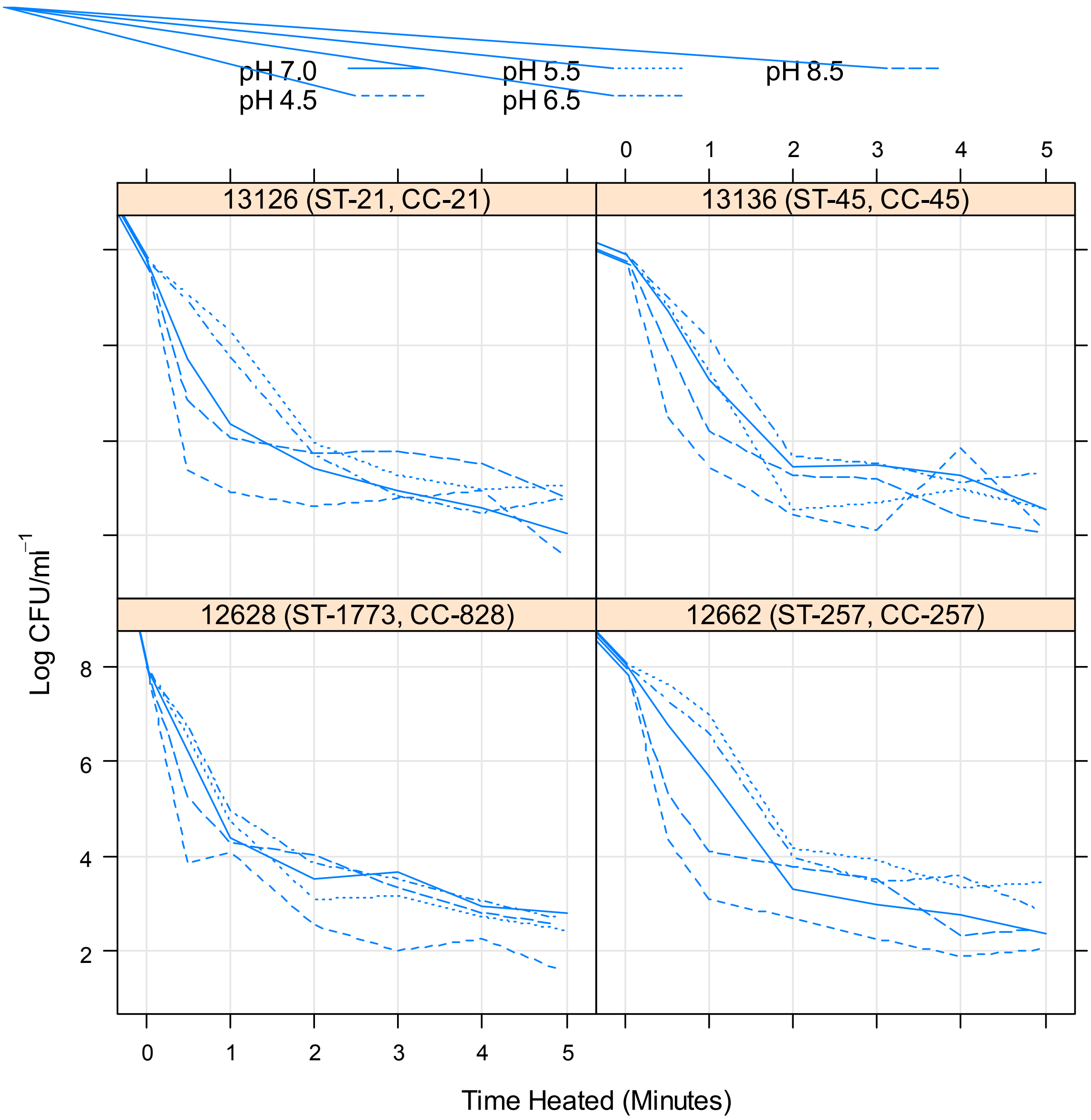

Figure 47. Plot of observed data illustrating survival of four strains following combined pH and time-temperature simulations undertaken at a 64°C.

1.8 Results

1.8.1 Time-temperature Simulations:

1.8.1.1 Non-linear Models

The observed data were compared to the predicted response curves generated for each strain and combination of biophysical and biochemical stress. Predicted response curves for experimental simulations undertaken at 56^{o}C are shown in figures 48 – 61. The predicted response curves for experimental simulations undertaken at 60^{o}C and 64^{o}C are illustrated in figures 72 – 85 and figures 95 – 108 respectively. Predicted response curves relating to the extended experimental simulations are presented in Figures 62 – 63.

The non-linear functions that best described the underlying response of *Campylobacter* were found to be specific to strain, and the type and intensity of biophysical and biochemical stress. Where asymptotic regression, logistic regression, four-parameter logistic regression and four-parameter Weibull models were used to describe the underlying response of *Campylobacter* during simulations undertaken at 56^{o}C (Table 1). In addition, the asymptotic regression and four-parameter logistic regression non-linear functions were used during the extended experimental simulations (Tables 17 and 22). The asymptotic regression and four-parameter logistic regression non-linear functions were used to describe the underlying response of *Campylobacter* during simulations at 60^{o}C (Table 32). By contrast, experimental simulations undertaken at 64^{o}C were described using only the asymptotic regression function (Table 56).

An assessment of relative fit of four-parameter logistic regression and four-parameter Weibull non-linear functions generated for simulations undertaken at 56^{o}C shows that two competing non-linear functions can be used to describe the underlying response of specific *Campylobacter* strains (Table 16). Results of model assessment reveal AIC values to be less than the recommended threshold ($\Delta_i \leq 2$) (Table 16) and as such, either non-linear function can be considered adequate in describing the overall fit to the data.

The absolute goodness-of-fit of models generated for temperature simulations undertaken at 56^{o}C for extended simulations are shown in Tables 1, 17 and 22. The goodness-of-fit of models generated for temperature simulations undertaken at 60^{o}C and 64^{o}C are shown in Tables 32 and 56 respectively.

The concordance correlation coefficient (ρ_c) for simulations undertaken at 56^{o}C, including the extended experimental simulations and 60^{o}C were observed to be high ($\rho_c \geq 0.980$) (Tables 1, 17, 20 and 32). The goodness-of-fit of models for simulations undertaken at 64^{o}C were marginally lower

($\rho_c \geq 0.94$). Comparatively low values of goodness-of-fit were observed for models representing strains 12628 (ST-1773, CC-828) $\rho_c = 0.881$ and 13163 (ST-21, CC-21) $\rho_c = 0.561$ (Table 56). Estimates of individual model parameters for experimental simulations undertaken at 56°C, and also for extended simulations, are described in Tables 2 – 15 and Tables 18 – 19 and 21 – 22 respectively. The estimates of model parameters for simulations undertaken at 60°C and 64°C are described in Tables 33 – 46 and 57 – 70 respectively. In all instances, estimates for the individual model parameters were found to be statistically significant at $P \leq 0.05$.

1.8.1.2 Extended Simulations

Analyses compared the numbers of sub-lethally damaged cells recovered from different inocula for strains 13136 (ST-45, CC-45) and 13121 (ST-45, CC-45). The absolute goodness-of-fit of models describing the response for strains 13121 (ST-45, CC-45) and 13121 (ST-45, CC-45) was $\rho_c = 0.954$ and $\rho_c = 0.991$ respectively (Table 17). Expected and significant differences between initial inocula (6 Log CFU/ml^{-1} and 8 Log CFU /ml^{-1}) were found for the asymptote A parameter for 13121 (ST-45, CC-45) (7.113 +2.947 = 10.060 Log CFU/ml^{-1}, $P = 0.014$) and 13136 (ST-45, CC-45) (6.534 +1.972 = 8.506 Log CFU/ml^{-1}, P-value = 0.014) (Table 20). A significant difference in the numbers of cells recovered for the asymptote B parameter ($P \leq 0.000$) was found when using an inoculum of 8 Log CFU/ml^{-1} (Table 19). The absolute goodness-of-fit of models describing the response for strains 11168 (ST-45, CC-21) and 13121 (ST-45, CC-45) was $\rho_c = 0.965$ and $\rho_c = 0.988$ respectively (Table 20). Analyses comparing experimental simulations of different enumeration media suggest that media type influenced the numbers of cells recovered for strain 11168 (ST-45, CC-21). Fewer numbers of sub-lethally damaged cells were recovered from media type mCCDA in comparison to CAB-FBP (Table 21). Differences in the numbers of sub-lethally damages cells recovered were found for model parameters representing the mid-point (4.782 – 1.470 = 3.042 Log CFU/ml^{-1}, P-value = 0.000) and the scale parameter (4.206-1.384 = 2.822 Log CFU/ml^{-1}, P-value = 0.006) (Table 21). No significant differences were found for the parameters, Asymptotes A and B (Table 21). There were no significant differences in the numbers of sub-lethally damaged cells recovered between media types for strain 13121 (ST-45, CC-45) (Table 22).

1.8.1.3 Mixed Weibull Distribution Model

Predicted response curves for experimental simulations undertaken at 56°C are shown in Figures 64 – 71. The predicted response curves for simulations undertaken at temperatures 60°C and 64°C are illustrated in Figures 86 – 94 and Figures 109 – 114 respectively. The concordance correlation coefficient (ρ_c) was used to assess the absolute goodness-of-fit of mixed Weibull distribution models to the data. The goodness-of-fit of models generated for temperature simulations undertaken at 56°C is shown in Table 23. The absolute goodness-of-fit of models generated for temperature simulations undertaken at 60°C and 64°C are shown in Tables 47 and 71 respectively. The absolute measure of goodness-of-fit of models generated for simulations undertaken at 56°C, 60°C and 64°C was observed to be high ($\rho_c \geq 0.940$).

Estimates of individual model parameters for experimental simulations undertaken at 56°C are described in Tables 24 – 31. The estimates of model parameters for simulations undertaken at 60°C and 64°C are described in Tables 48 – 55 and 72 – 77 respectively. For simulations undertaken at 56°C and 60°C, estimates of model parameters were found to be statistically significant at $P \leq 0.05$ in the majority of cases. However, variability in the precision of estimates for δ2 and/or α parameters was observed for models of some strains. The estimates of parameters δ2 (16.952, P = 0.198) and α (4.651, P = 0.694) for strain 12720 (ST-51, CC-443) undertaken at 56°C are not significant (Table 28). This is also the case for simulations undertaken at 60°C, δ2 (9.999, P = 0.120) (Table 51). The estimates of individual model parameters for simulations undertaken at higher temperature of 64°C showed greater variability (Tables 72 – 77). The estimates of individual parameters (δ1, δ2, *P* and α) for models of strains 12662 (ST-257, CC-257) (Table 74) and 13126 (ST-21, CC-21) (Table 76) were not significant. It was not possible to generate models for all combined simulations due to difficulties encountered during the computational phase.

1.8.2 pH and Time-temperature Simulations:

1.8.2.1 Non-linear Models

The observed data were compared to the predicted response curves for each strain and their respective pH and temperature combinations. Predicted response curves for experimental simulations undertaken at 56°C are shown in Figures 115 – 134. The predicted response curves for experimental simulations undertaken at temperatures 60°C are shown in Figures 152 – 170. The predictive response curves for simulations undertaken at 64°C are shown in Figures 188 – 207.

The non-linear functions used to describe the underlying response of *Campylobacter* was found to be specific to strain and type and intensity of biophysical and biochemical stress. Three non-linear functions were used to describe the underlying response of *Campylobacter* during combined pH (4.5, 5.5, 6.5, 7.5 and 8.5) and temperature (56°C and 60°C and 64°C) simulations; namely asymptotic regression, four-parameter logistic regression and biexponential models (Tables 78, 117 and 155).

An assessment of the goodness-of-fit of models to data is provided by the concordance correlation coefficient (ρ_c) for combined pH and temperature simulations is shown in Tables 78, 117 and 155. The goodness-of-fit of models for simulations undertaken at 56°C was observed to be high. A minimum value of the concordance correlation coefficient ρ_c = 0.793 was recorded for strain 13136 (ST-45, CC-45) for simulation undertaken at pH 8.5 (Table 78). The maximum value of ρ_c = 0.989 was also observed for strain 13136 (ST-45, CC-45) for simulation undertaken at pH 5.5. The absolute measure of goodness-of-fit of models generated for simulations undertaken at 60°C was also observed to be high illustrating an overall good fit to the data. The minimum value of the concordance correlation coefficient ρ_c = 0.922 was recorded for strain 12628 (ST-45, CC-45) for the simulation undertaken at pH 8.5 (Table 117). The maximum value of ρ_c = 0.971 was recorded for strain 12662 (ST-257, CC-257) for simulation undertaken at pH 5.5. The goodness-of-fit of models for simulations undertaken at 64°C was also observed to be high (Table 117). A minimum value of ρ_c = 0.918 was recorded for strain 12628 (ST-45, CC-45) for the simulation undertaken at pH 4.5 (Table 155) and a maximum value of ρ_c = 0.971 was recorded for strain 13136 (ST-45, CC-45) for the simulation undertaken at pH 6.5.

Estimates of individual model parameters for combined pH and temperature simulations undertaken at 56°C are shown in Tables 79 – 98, for simulations undertaken at 60°C simulations individual parameter estimates are shown in Tables 118 – 136. The estimates of model parameters for combined simulations undertaken 64°C are shown in Tables 156 – 175. For simulations undertaken at 56°C estimates of model parameters were found to be statistically significant at P ≤ 0.05 in all but two cases. The estimate for the asymptote for strain 12628 (ST-1773, CC-828) at pH 8.5 was not significant (1.124, P-value = 0.354) (Table 83). The estimate of the LRC parameter for 12662 (ST-257, CC-257) for pH 4.5 was also not significant (-0.421, P-value = 0.393) (Table 84). Similarly, estimates of model parameters for simulations undertaken at 60°C were also found to significant at P ≤ 0.05 in all but two cases. The estimate for the LRC parameter for strain 12662 (ST-257, CC-257) at pH 4.5 was not significant (-0.161, P-value = 0.329) (Table 122). Correspondingly, the estimate of the LRC1 parameter for 12662 (ST-257, CC-257) for pH 8.5 was also not significant (-0.051, P-value = 0.913) (Table 126).

1.8.2.2 Mixed Weibull Distribution Model

Predicted response curves for combined pH simulations undertaken at 56°C are shown in Figures 135 – 151. The predicted response curves for combined pH simulations undertaken at temperatures 60°C and 64°C are illustrated in Figures 171 – 187 and Figures 208 – 227 respectively. The goodness-of-fit of individual models for combined pH and temperature simulations undertaken at 56°C is shown in Table 99. The minimum value of concordance correlation coefficient ρ_c = 0.883 was recorded for strain 13126 (ST-21, CC-21) for simulation undertaken at pH 8.5. In contrast, the maximum value ρ_c = 0.992 was recorded for strain 13126 (ST-21, CC-21) for simulation at pH 8.5. Models were not generated for strain 12662 (ST-257, CC-257) at pH 5.5, 6.5 and 7.5 due to difficulties during computational phase (Table 100). The concordance correlation coefficient for combined pH and temperature simulations undertaken at 60°C is shown in Table 137. The measure of goodness-of-fit of models generated for combined pH and temperature simulations at 60°C was observed to be high. The minimum value $\rho_c = 0.950$ was recorded for strain 12628 (ST-1773, CC-828) at pH 8.5 and a maximum value $\rho_c = 0.986$ was recorded for strain 12662 (ST-257, CC-257) at pH 6.5. Models were not generated for strain 12662 (ST-257, CC-257) at pH 4.5 and for strain 13136 (ST-45, CC-45) at pH 4.5 and 8.5 due to failure during the computational process (Table 137). The goodness-of-fit for models for the combined pH and temperature simulations undertaken at 64°C is shown in Table 176. The overall goodness-of-fit of these models to the data was also observed to be high. The minimum and maximum values of the concordance correlation coefficient were recorded for 12628 (ST-1773, CC-828) at pH 4.5 ($\rho_c = 0.944$) and 8.5 ($\rho_c = 0.990$) respectively (Table 176). Estimates of individual model parameters for combined pH and temperature experimental simulations undertaken at 56°C are described in Tables 100 – 116. The estimates of model parameters for simulations undertaken at 60°C and 64°C are described in Tables 138 – 154 and 177 – 196 respectively.

For simulations undertaken at 56°C estimates of individual model parameters were found to be statistically significant at $P \leq 0.05$ in many cases (Tables 100 - 116). However, variability in the precision of estimates was found for $\delta1$, $\delta2$, *p* and/or α parameters for models of some strains. For example, the estimates of parameters $\delta1$ (1.218, *P* = 0.377), δ2 (14.249, P-value = 0.112) and *p* (2.894, P-value = 0.657) for strain 12628 (ST-1773, CC-828) at pH 4.5 are not significant (Table 100). Estimates of all parameters for the individual model for strain 12662 (ST-1773, CC-828) also undertaken at pH 4.5 were found not to be significant (Table 105). Estimates of parameters $\delta1$, $\delta2$, *p* and α for some individual models examining the combined effects of pH and temperature at 60°C, were also found not to be significant at $P \leq 0.05$ (Tables 138 – 154). For example, $\delta1$ (0.120, P-value = 0.831), δ2 (5.452, *P* = 0.707) and α (0.538, *P* = 0.591) for strain 12662 (ST-1773, CC-828) at pH 4.5 (Table 142). Furthermore, the estimate for the parameter δ2 (20.651, *P* = 0.571) for strain 13126 (ST-21, CC-21) at pH 7.5 is associated with a correspondingly large standard-error ($SE_{\overline{x}}$ = 35.732) (Table 150). In addition, parameter estimates of individual models for combined simulations undertaken at 64°C were found to vary according to strain and type and intensity of stress (Tables 177 – 196). Estimates of parameters $\delta1$, $\delta2$, *p* and α for individual models corresponding to strain 12628 (ST-1773, CC-828) at pH 4.5 (Table 177) and pH 8.5 (Table 181) were not significant at $P \leq 0.05$.

Furthermore, the estimate for the parameter δ2 (85.295, P-value = 0.961) for strain 13126 (ST-21, CC-21) at pH 6.5 is associated with a large standard-error ($SE_{\overline{x}}$ = 1723.532) (Table 189).

1.8.3 Predictive Models: Time-temperature Simulations: 56^{o}C

Table 1. An assessment of the goodness of fit of models analysing the survival of each strain following heating at 56^{o}C.

Strain	Non-linear Function	AIC	logLik	ρ_c
11253 (ST-825, CC-828)	Four-parameter logistic	18.413	-4.207	0.988
11368 (ST-574, CC-574)	Four-parameter logistic	17.209	-3.604	0.986
11762 (ST-829, CC-828)	Four-parameter logistic	7.177	1.411	0.993
12610 (ST-825, CC-828)	Four-parameter logistic	34.164	-12.082	0.982
12628 (ST-1773, CC-828)	Four-parameter Weibull	9.621	0.189	0.993
12645 (ST-51, CC-443)	Four-parameter logistic	12.366	-1.183	0.990
12662 (ST-257, CC-257)	Four-parameter logistic	8.374	0.813	0.987
12720 (ST-51, CC-443)	Four-parameter logistic	5.185	2.408	0.993
12745 (ST-257, CC-257)	Logistic Regression	38.241	-15.121	0.940
12783 (ST-574, CC-574)	Four-parameter logistic	17.988	-3.994	0.985
13121 (ST-45, CC-45)	Asymptotic Regression	36.992	-14.496	0.978
13126 (ST-21, CC-21)	Four-parameter logistic	15.811	-2.906	0.989
13136 (ST-45, CC-45)	Four-parameter logistic	14.972	-2.486	0.990
13163 (ST-21, CC-21)	Four-parameter logistic	3.719	3.141	0.993

Table 2. Four-parameter logistic regression model analysing survival of strain 11253 (ST-825, CC-828) following heating at 56^{o}C.

Parameter	Estimate	Standard Error	*t*-value	*P*-value
Asymptote A	8.357	0.271	30.791	0.000
Asymptote B	3.119	0.197	15.812	0.000
Mid-point	4.280	0.237	18.019	0.000
Scale Parameter	1.226	0.234	5.245	0.000

Table 3. Four-parameter logistic regression model analysing survival of strain 11368 (ST-574, CC-574) following heating at 56^{o}C.

Parameter	Estimate	Standard Error	*t*-value	*P*-value
Asymptote A	8.009	0.218	36.712	0.000
Asymptote B	3.548	0.120	17.760	0.000
Mid-point	4.777	0.253	18.900	0.000
Scale Parameter	1.180	0.239	4.938	0.000

Table 4. Four-parameter logistic regression model analysing survival of strain 11762 (ST-829, CC-828) following heating at 56°C.

Parameter	**Estimate**	**Standard Error**	***t*-value**	***P*-value**
Asymptote A	8.356	0.242	34.505	0.000
Asymptote B	3.405	0.179	19.063	0.000
Mid-point	4.397	0.228	19.273	0.000
Scale Parameter	1.456	0.237	6.134	0.000

Table 5. Four-parameter logistic regression model analysing survival of strain 12610 (ST-825, CC-828) following heating at 56°C.

Parameter	**Estimate**	**Standard Error**	***t*-value**	***P*-value**
Asymptote A	8.356	0.242	34.505	0.000
Asymptote B	3.405	0.179	19.063	0.000
Mid-point	4.397	0.228	19.273	0.000
Scale Parameter	1.456	0.237	6.134	0.000

Table 6. Four-parameter logistic regression model analysing survival of strain 12628 (ST-1773, CC-828) following heating at 56°C.

Parameter	**Estimate**	**Standard Error**	***t*-value**	***P*-value**
Asymptote A	8.366	0.148	56.527	0.000
Asymptote B	3.083	0.102	30.137	0.000
Mid-point	4.186	0.125	33.400	0.000
Scale Parameter	1.238	0.124	9.988	0.000

Table 7. Four-parameter logistic regression model analysing survival of strain 12645 (ST-51, CC-443) following heating at 56°C.

Parameter	**Estimate**	**Standard Error**	***t*-value**	***P*-value**
Asymptote A	8.248	0.312	26.436	0.000
Asymptote B	2.035	0.790	2.576	0.000
Mid-point	6.614	0.574	12.084	0.000
Scale Parameter	2.101	0.522	4.027	0.000

Table 8. Four-parameter logistic regression model analysing survival of strain 12662 (ST-257, CC-257) following heating at 56°C.

Parameter	**Estimate**	**Standard Error**	***t*-value**	***P*-value**
Asymptote A	8.325	0.517	16.108	0.000
Asymptote B	3.003	7.120	4.219	0.000
Mid-point	5.581	0.573	9.739	0.000
Scale Parameter	2.503	0.811	3.085	0.008

Table 9. Four-parameter logistic regression model analysing survival of strain 12720 (ST-51, CC-443) following heating at 56°C.

Parameter	**Estimate**	**Standard Error**	***t*-value**	***P*-value**
Asymptote A	8.440	0.319	26.438	0.000
Asymptote B	2.303	0.607	3.795	0.002
Mid-point	6.133	0.426	14.402	0.000
Scale Parameter	2.230	0.483	4.620	0.000

Table 10. Logistic regression model analysing survival of strain 12745 (ST-257, CC-257) following heating at 56°C.

Parameter	**Estimate**	**Standard Error**	***t*-value**	***P*-value**
Asymptote (Intercept)	8.698	0.953	9.130	0.000
Mid-point	8.391	0.906	9.264	0.000
Scale Parameter	-3.697	1.066	-0.347	0.003

Table 11. Four-parameter logistic regression model analysing survival of strain 12783 (ST-574, CC-574) following heating at 56°C.

Parameter	**Estimate**	**Standard Error**	***t*-value**	***P*-value**
Asymptote A	7.976	0.319	24.957	0.000
Asymptote B	3.131	0.295	10.615	0.000
Mid-point	4.847	0.337	14.386	0.000
Scale Parameter	1.563	0.368	4.242	0.000

Table 12. Asymptotic regression model analysing survival of strain 13121 (ST-45, CC-45) following heating at 56^{o}C.

Parameter	**Estimate**	**Standard Error**	***t*-value**	***P*-value**
R0 (Intercept)	8.017	0.150	53.548	0.000
Asymptote	2.456	0.293	8.374	0.000
LRC	-1.476	0.132	-11.211	0.000

Table 13. Four-parameter logistic regression model analysing survival of strain 13126 (ST-21, CC-21) following heating at 56^{o}C.

Parameter	**Estimate**	**Standard Error**	***t*-value**	***P*-value**
Asymptote A	8.346	0.337	24.746	0.000
Asymptote B	3.140	0.204	15.394	0.000
Mid-point	4.011	0.281	14.280	0.000
Scale Parameter	1.419	0.282	5.038	0.000

Table 14. Four-parameter logistic regression model analysing survival of strain 13136 (ST-45, CC-45) following heating at 56^{o}C.

Parameter	**Estimate**	**Standard Error**	***t*-value**	***P*-value**
Asymptote A	9.611	1.282	8.540	0.000
Asymptote B	1.741	0.278	6.687	0.000
Mid-point	4.782	0.794	6.027	0.000
Scale Parameter	4.206	0.724	5.813	0.000

Table 15. Four-parameter logistic regression model analysing survival of strain 13163 (ST-21, CC-21) following heating at 56^{o}C.

Parameter	**Estimate**	**Standard Error**	***t*-value**	***P*-value**
Asymptote A	8.284	0.270	30.704	0.000
Asymptote B	3.015	0.298	10.124	0.000
Mid-point	5.177	0.276	18.777	0.000
Scale Parameter	1.874	0.337	5.563	0.000

Table 16. An Information Theoretic assessment of the relative performance of non-linear functions used to describe underlying response of Campylobacter following heating at 56°C.

Strain	Non-linear Function	AIC	logLik	ρ_c	Δ_i
11253 (ST-825, CC-828)	Four-parameter Logistic	18.413	-4.207	0.988	0.179
	Four-parameter Weibull	18.592	-4.296	0.988	
11368 (ST-574, CC-574)	Four-parameter Logistic	17.209	-3.605	0.986	0.976
	Weibull Four-parameter	18.185	-4.092	0.985	
11762 (ST-829, CC-828)	Four-parameter Logistic	7.177	1.411	0.993	0.200
	Weibull Four-parameter	7.377	1.312	0.993	
12610 (ST-825, CC-828)	Four-parameter Logistic	34.164	-12.082	0.982	0.713
	Weibull Four-parameter	34.877	-12.438	0.982	
12628 (ST-1773, CC-828)	Weibull Four-parameter	9.621	0.189	0.993	0.188
	Four-parameter Logistic	9.809	0.095	0.993	
12645 (ST-51, CC-443)	Four-parameter Logistic	12.366	-1.183	0.990	1.772
	Weibull Four-parameter	14.138	-2.069	0.989	
12662 (ST-257, CC-257)	Four-parameter Logistic	8.374	0.813	0.987	1.235
	Weibull Four-parameter	9.609	0.195	0.987	
12720 (ST-51, CC443)	Four-parameter Logistic	5.185	2.408	0.993	1.501
	Weibull Four-parameter	6.686	1.657	0.992	
12783 (ST-574, CC-574)	Four-parameter Logistic	17.988	-3.994	0.985	0.581
	Weibull Four-parameter	18.569	-4.285	0.984	
13126 (ST-21, CC-21)	Four-parameter Logistic	15.811	-2.906	0.989	1.190
	Weibull Four-parameter	17.001	-3.505	0.988	
13136 (ST-45, CC-45)	Four-parameter Logistic	14.972	-2.486	0.990	1.534
	Weibull Four-parameter	16.506	-3.253	0.989	
13163 (ST-21, CC-21)	Four-parameter Logistic	3.719	3.14	0.993	1.620
	Weibull Four-parameter	5.339	2.33	0.992	

1.8.4 Extended Time-temperature Simulations: 56°C

Table 17. An assessment of the goodness of fit of four-parameter logistic regression models comparing the survival of two strains of *Campylobacter* using different initial inocula following heating at 56°C.

Strain	Non-linear Function	ρ_c
13121 (ST-45, CC-45)	Four-parameter Logistic	0.954
13136 (ST-45, CC-45)	Four-parameter Logistic	0.991

Table 18. Four-parameter logistic regression model comparing the survival of strain 13121 (ST-45, CC-45) using different inocula following heating at 56^{o}C.

Parameter	**Estimate**	**Standard Error**	***t*-value**	***P*-value**
Asymptote A (Intercept: 6 Log CFU/ml^{-1})	7.113	0.521	13.656	0.000
Asymptote A (8 Log CFU/ml^{-1})	2.947	1.156	2.549	0.014
Asymptote B (Intercept: 6 Log CFU/ml^{-1})	0.683	0.913	0.748	0.458
Asymptote B (8 Log CFU/ml^{-1})	1.580	1.162	1.359	0.180
Midpoint (Intercept: 6 Log CFU/ml^{-1})	4.848	0.722	6.718	0.000
Midpoint (8 Log CFU/ml^{-1})	-1.116	1.058	-1.055	0.296
Scaling Parameter (Intercept: 6 Log CFU/ml^{-1})	2.671	0.722	3.699	0.001
Scaling Parameter (8 Log CFU/ml^{-1})	0.608	1.157	0.525	0.601

Table 19. Four-parameter logistic regression model comparing the survival of strain 13136 (ST-45, CC-45) using different inocula following heating at 56^{o}C.

Parameter	**Estimate**	**Standard Error**	***t*-value**	***P*-value**
Asymptote A (Intercept: 6 Log CFU/ml^{-1})	6.534	0.219	29.804	0.000
Asymptote A (8 Log CFU/ml^{-1})	1.972	0.202	9.754	0.000
Asymptote B (Intercept: 6 Log CFU/ml^{-1})	0.634	0.172	3.699	0.001
Asymptote B (8 Log CFU/ml^{-1})	1.753	0.176	9.956	0.000
Midpoint (Intercept)	6.140	0.240	25.578	0.000
Scaling Parameter (Intercept)	2.268	0.226	10.047	0.000

Table 20. Properties of each strain heated at 56^{o}C, the underlying non-linear functional form of each model and assessment of model fit used to compare media.

Strain	**Non-linear Function**	ρ_c
11168C (ST-45, CC-21)	Four-parameter Logistic	0.965
13121 (ST-45, CC-45)	Asymptotic Regression	0.988

Table 21. Four-parameter logistic regression model comparing survival by means of different media of strain 11168C (ST-45, CC-21) following heating at 56^{o}C.

Parameter	**Estimate**	**Standard Error**	***t*-value**	***P*-value**
Asymptote A (Intercept: CAB-FBP)	9.611	1.282	8.540	0.000
Asymptote B (Intercept: CAB-FBP)	1.741	0.278	6.687	0.000
Asymptote B (mCCDA)	0.425	0.333	1.277	0.206
Mid-point (Intercept: CAB-FBP)	4.782	0.794	6.027	0.000
Mid-point (mCCDA)	-1.740	0.423	-4.113	0.000
Scale Parameter (Intercept: CAB-FBP)	4.206	0.724	5.813	0.000
Scale Parameter (mCCDA)	-1.384	0.486	-2.851	0.006

Table 22. Asymptotic regression model comparing survival by means of different media of strain 13121 (ST-45, CC-45) following heating at 56^{o}C.

Parameter	**Estimate**	**Standard Error**	***t*-value**	***P*-value**
Asymptote (Intercept: CAB-FBP)	1.590	0.403	3.945	0.000
Asymptote (mCCDA)	0.407	0.491	0.830	0.410
R0 (Intercept: CAB-FBP)	8.134	0.317	25.648	0.000
R0 (mCCDA)	0.457	0.606	0.755	0.453
LRC (Intercept: CAB-FBP)	-1.8427	0.1739	-10.595	0.000
LRC (mCCDA)	0.3736	0.2439	1.5315	0.131

1.8.5 Time-Temperature Simulations: 56°C

Mixed Weibull Distribution Model:

Table 23. An assessment of the goodness of fit for Mixed Weibull distribution models analysing the survival of each strain following heating at 56°C.

Strain	Non-linear Function	ρ_c
11253 (ST-825, CC-828)	Mixed Weibull Distribution	0.988
11368 (ST-574, CC-574)	Mixed Weibull Distribution	
11762 (ST-829, CC-828)	Mixed Weibull Distribution	0.992
12610 (ST-825, CC-828)	Mixed Weibull Distribution	0.983
12628 (ST-1773, CC-828)	Mixed Weibull Distribution	0.991
12645 (ST-51, CC-443)	Mixed Weibull Distribution	
12662 (ST-257, CC-257)	Mixed Weibull Distribution	
12720 (ST-51, CC-443)	Mixed Weibull Distribution	0.993
12745 (ST-257, CC-257)	Mixed Weibull Distribution	
12783 (ST-574, CC-574)	Mixed Weibull Distribution	
13121 (ST-45, CC-45)	Mixed Weibull Distribution	
13126 (ST-21, CC-21)	Mixed Weibull Distribution	0.991
13136 (ST-45, CC-45)	Mixed Weibull Distribution	0.990
13163 (ST-574,CC-574)	Mixed Weibull Distribution	0.993

Table 24. Mixed Weibull distribution model analysing the survival of strain 11253 (ST-825, CC-828) following heating at 56°C.

Parameter	Estimate	Standard Error	*t*-value	*P*-value
α	4.078	0.739	5.521	0.000
δ1	2.598	0.375	6.938	0.000
P	1.758	0.320	5.494	0.000
N0	8.225	0.199	41.436	0.000
δ2	9.796	4.573	2.142	0.052

Table 25. Mixed Weibull distribution model analysing the survival of strain 11762 (ST-829, CC-828) following heating at 56°C.

Parameter	Estimate	Standard Error	*t*-value	*P*-value
α	3.833	0.284	13.519	0.000
δ1	2.940	0.329	8.939	0.000
P	2.279	0.634	3.594	0.003
δ2	11.327	2.349	4.823	0.000
N0	8.190	0.154	53.327	0.000

Table 26. Mixed Weibull distribution model analysing the survival of strain 12610 (ST-825, CC-828) following heating at 56°C.

Parameter	Estimate	Standard Error	*t*-value	*P*-value
α	3.972	0.674	5.893	0.000
δ1	2.653	0.314	8.453	0.000
P	1.569	0.217	7.228	0.000
N0	8.151	0.143	57.002	0.000
δ2	13.274	9.987	1.329	0.194

Table 27. Mixed Weibull distribution model analysing the survival of strain 12628 (ST-1773, CC-828) following heating at 56°C.

Parameter	Estimate	Standard Error	*t*-value	*P*-value
α	4.651	0.460	10.122	0.000
δ1	2.430	0.196	12.396	0.000
P	1.606	0.138	11.610	0.000
N0	8.230	0.105	78.191	0.000
δ2	16.952	12.872	1.317	0.198

Table 28. Mixed Weibull distribution model analysing the survival of strain 12720 (ST-51, CC-443) following heating at 56°C.

Parameter	Estimate	Standard Error	*t*-value	*P*-value
α	4.592	11.409	0.403	0.694
δ1	3.240	0.410	7.911	0.000
N0	8.084	0.141	57.473	0.000
P	1.540	0.293	5.267	0.000
δ2	20.859	473.314	0.044	0.966

Table 29. Mixed Weibull distribution model analysing the survival of strain 13126 (ST-21, CC-21) following heating at 56°C.

Parameter	Estimate	Standard Error	*t*-value	*P*-value
α	3.624	0.514	7.048	0.000
δ1	2.462	0.335	7.341	0.000
P	1.681	0.335	5.019	0.000
N0	8.047	0.170	47.391	0.000
δ2	8.684	2.402	3.615	0.003

Table 30. Mixed Weibull distribution model analysing the survival of strain 13136 (ST-45, CC-45) following heating at 56°C.

Parameter	**Estimate**	**Standard Error**	***t*-value**	***P*-value**
α	3.923	1.262	3.108	0.008
δ1	3.027	0.440	6.875	0.000
P	1.684	0.331	5.083	0.000
N0	8.138	0.179	45.482	0.000
δ2	9.017	5.765	1.564	0.142

Table 31. Mixed Weibull distribution model analysing the survival of strain 13163 (ST-21, CC-21) following heating at 56°C.

Parameter	**Estimate**	**Standard Error**	***t*-value**	***P*-value**
α	3.704	1.546	2.396	0.032
δ1	2.981	0.352	8.460	0.000
P	1.514	0.243	6.240	0.000
N0	7.992	0.132	60.667	0.000
δ2	10.933	12.817	0.853	0.409

1.8.6 Predicted Response Curves Non-linear Model: Time-Temperature Profile 56°C

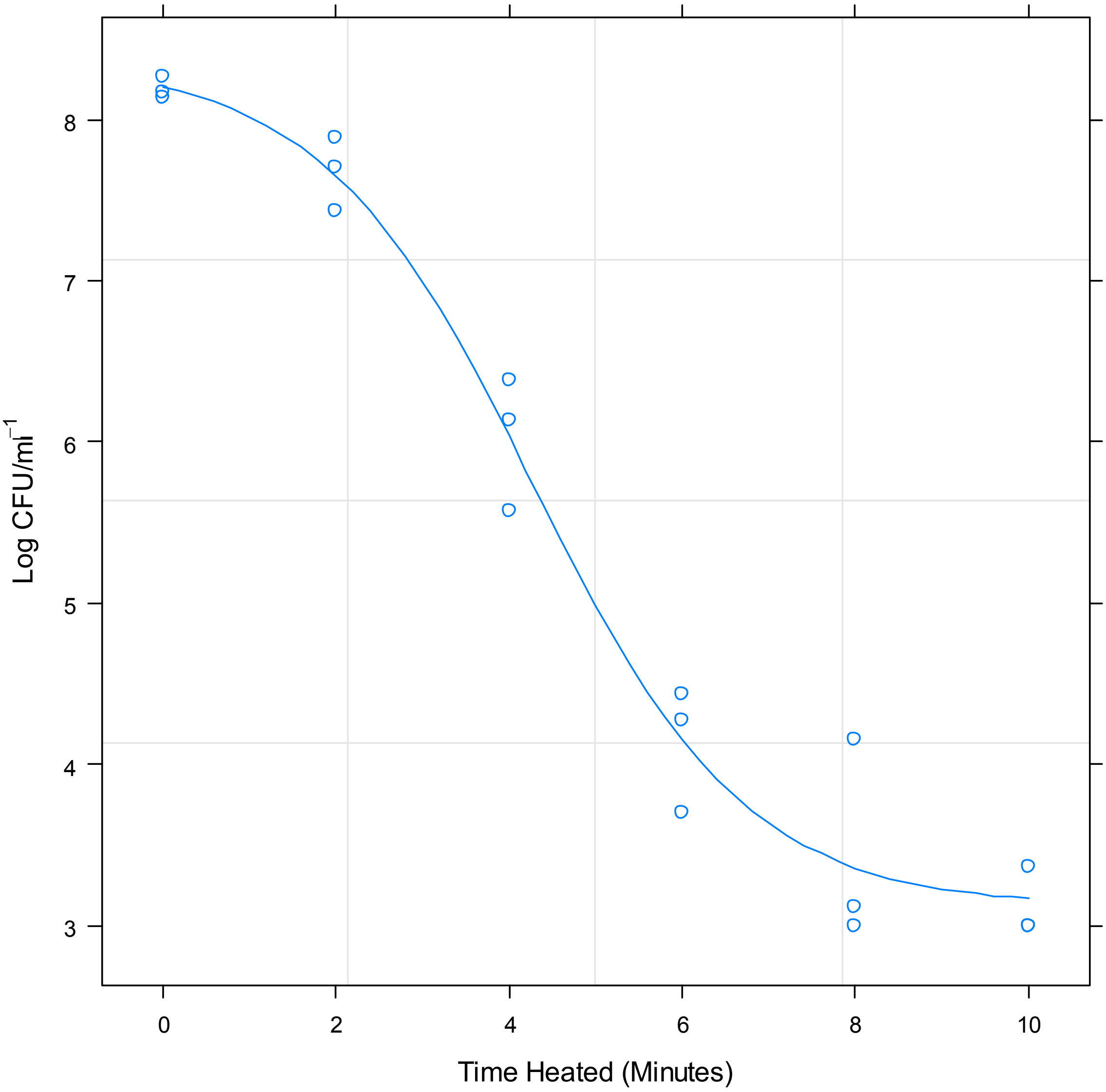

Figure 48. Plot illustrating predicted response using a four-parameter logistic regression model curve for strain 11253 (ST-825, CC-828) following heating at 56°C.

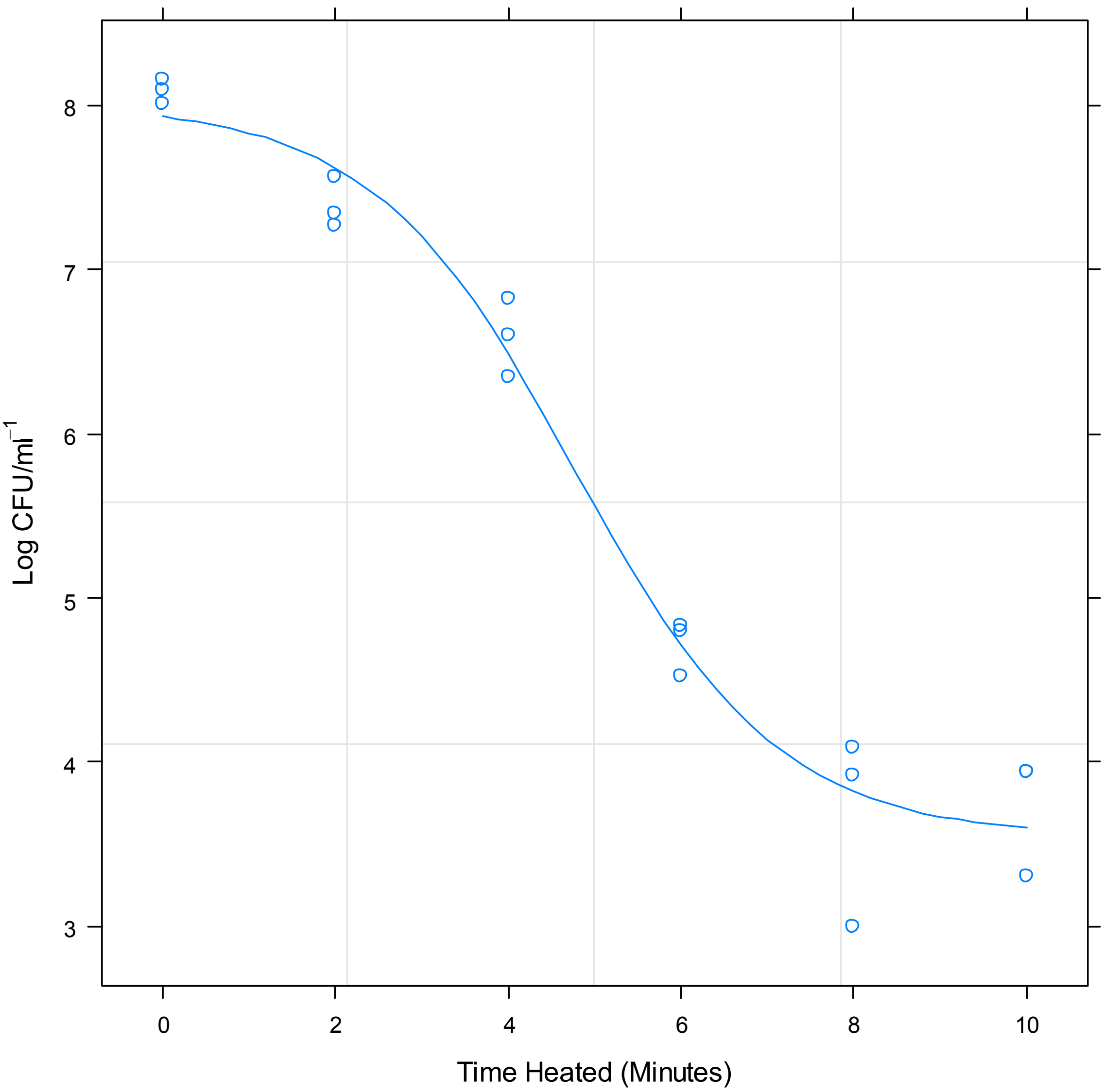

Figure 49. Plot illustrating predicted response curve using a four-parameter logistic regression model for strain 11368 (ST-574, CC-574) following heating at 56°C.

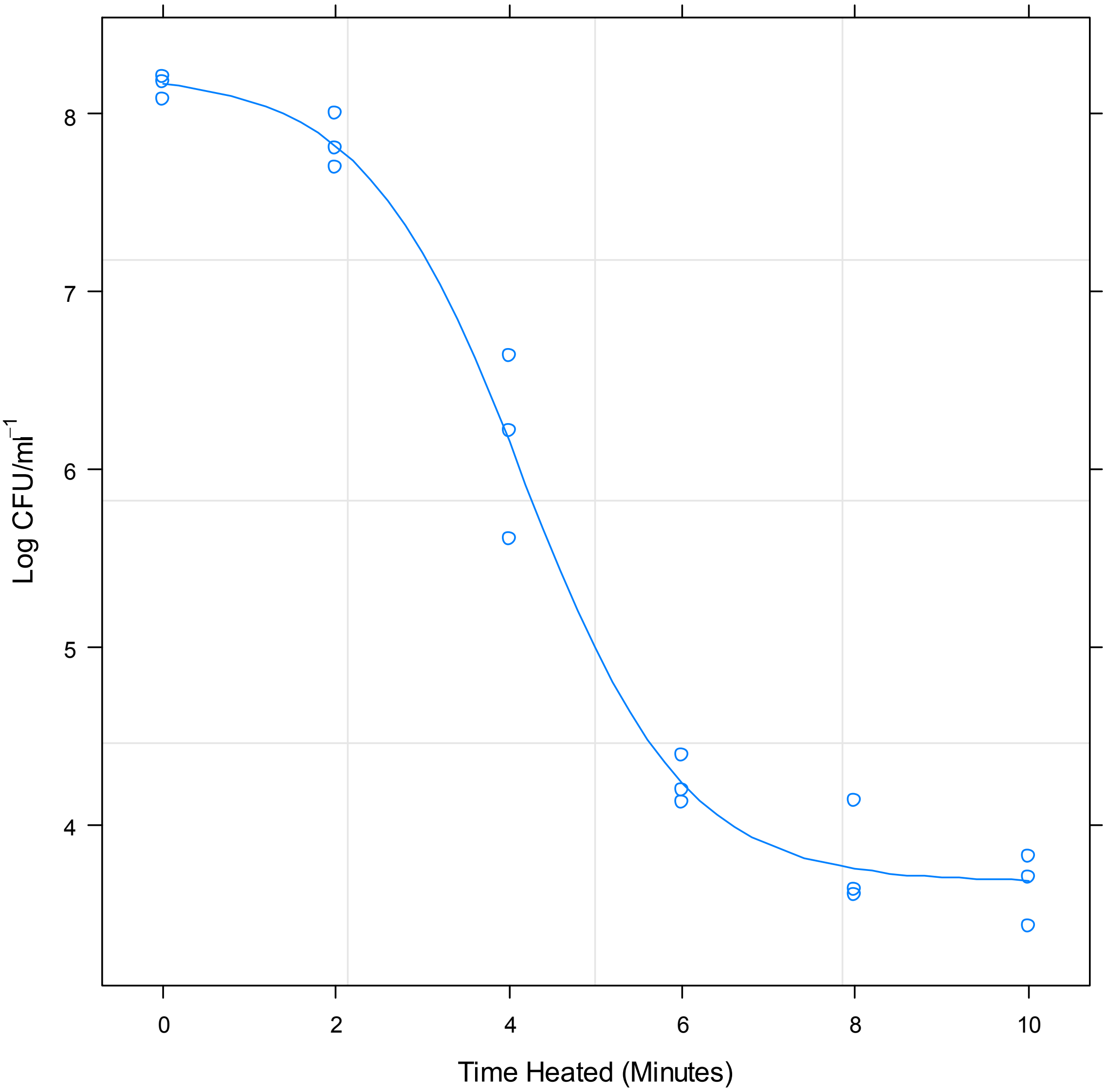

Figure 50. Plot illustrating predicted response curve using a four-parameter logistic regression model for strain 11762 (ST-829, CC-828) following heating at 56°C.

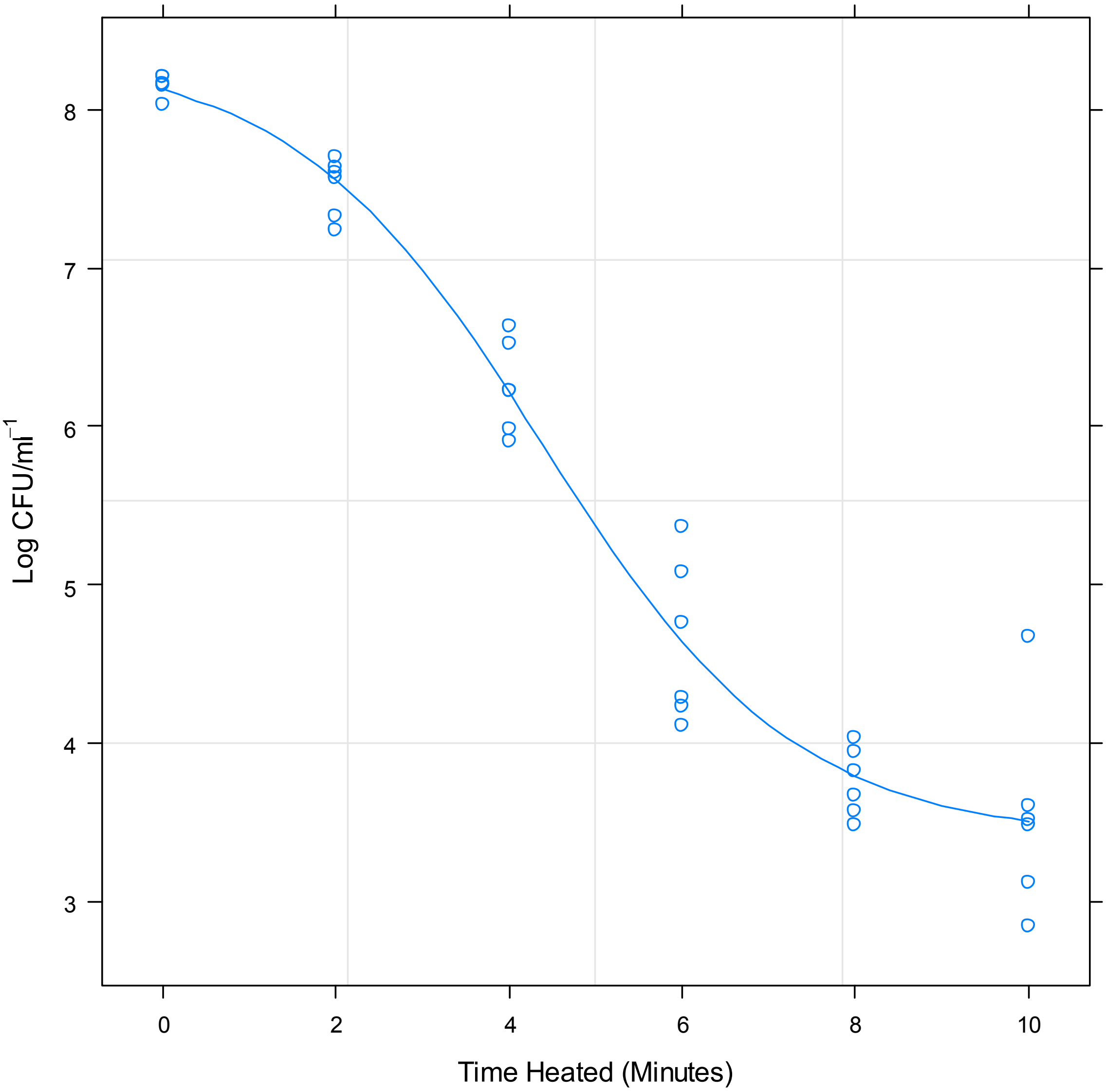

Figure 51. Plot illustrating predicted response curve using a four-parameter logistic regression model for strain 12610 (ST-825, CC-828) following heating at 56°.

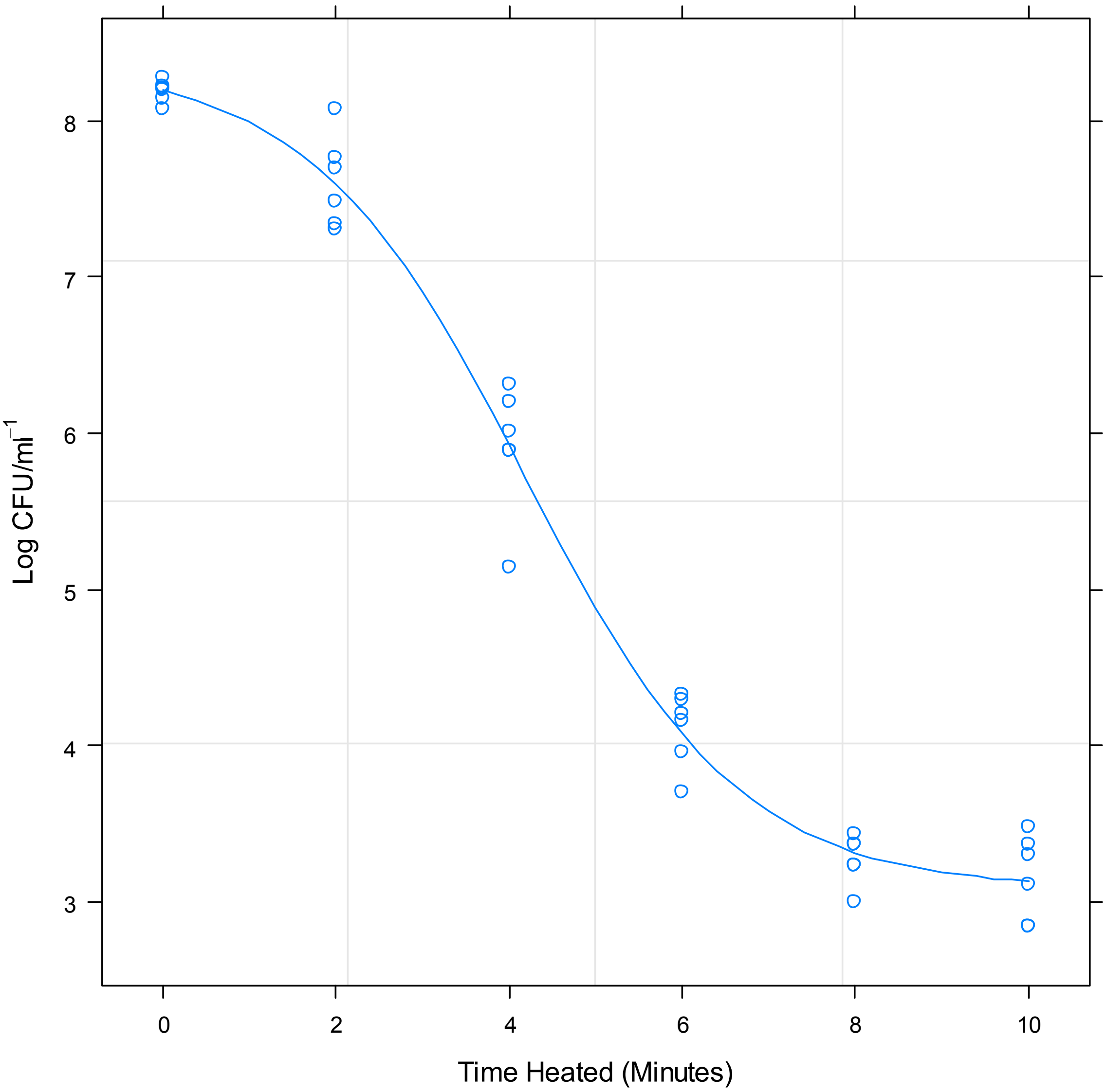

Figure 52. Plot illustrating predicted response curve using a four-parameter logistic regression model for strain 12628 (ST-1773, CC-828) following heating at 56°C.

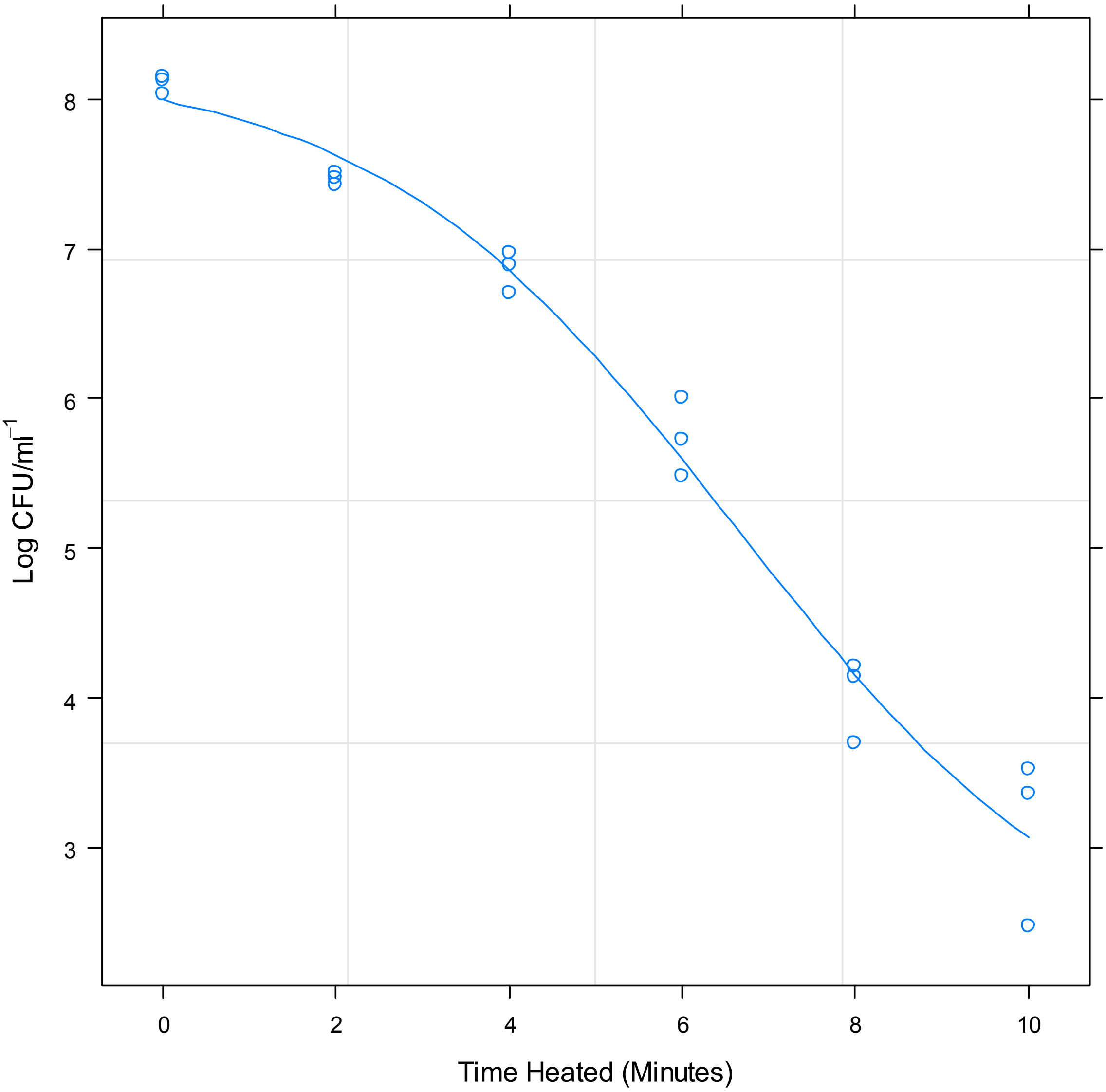

Figure 53. Plot illustrating predicted response curve using a four-parameter logistic regression model for strain 12645 (ST-51, CC-443) following heating at 56°C.

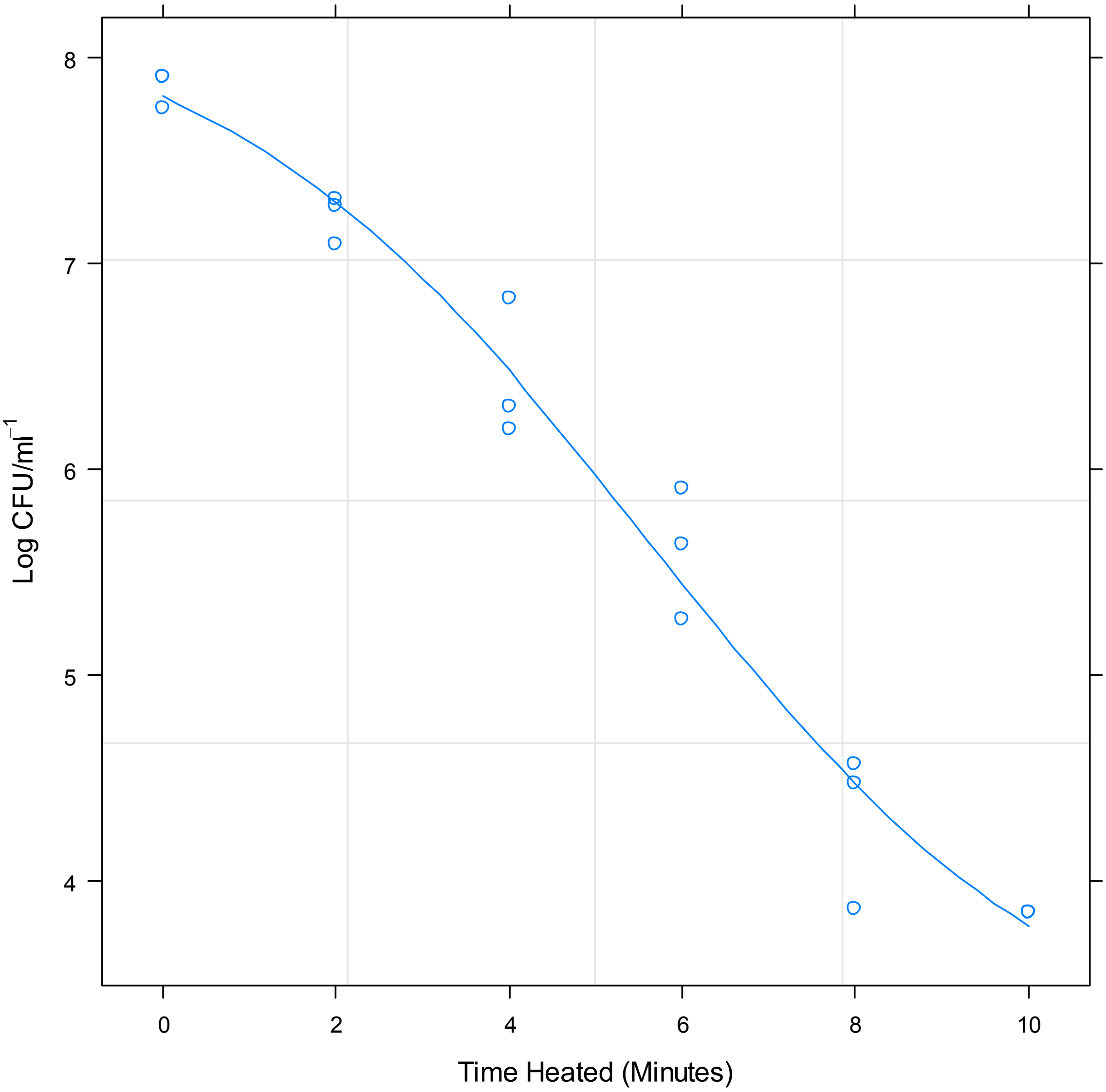

Figure 54. Plot illustrating predicted response curve using a four-parameter logistic regression model for strain 12662 (ST-257, CC-257) following heating at 56°.

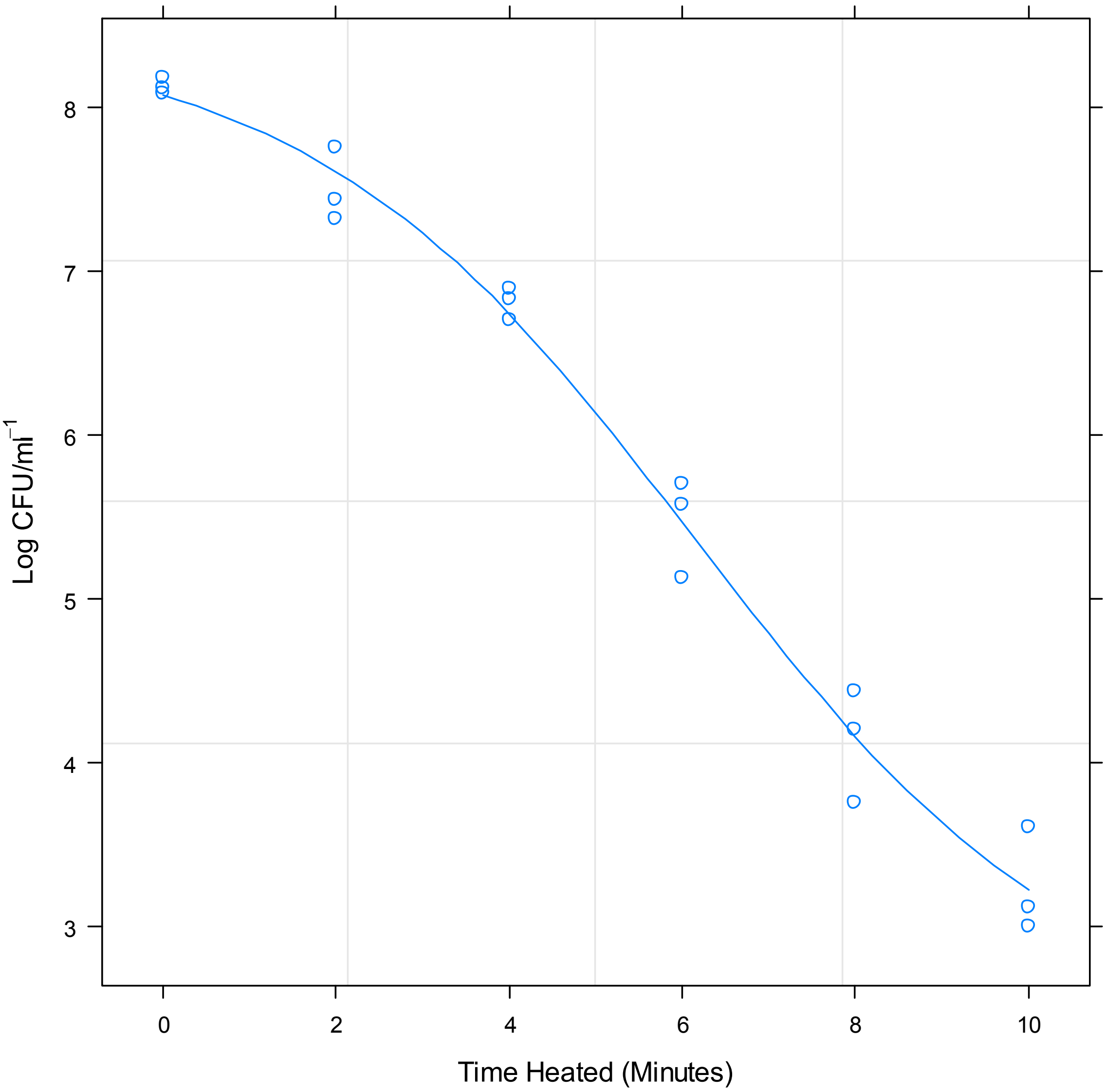

Figure 55. Plot illustrating the predicted response curve using a four-parameter logistic regression model for strain 12720 (ST-51, CC-443) following heating at 56°C.

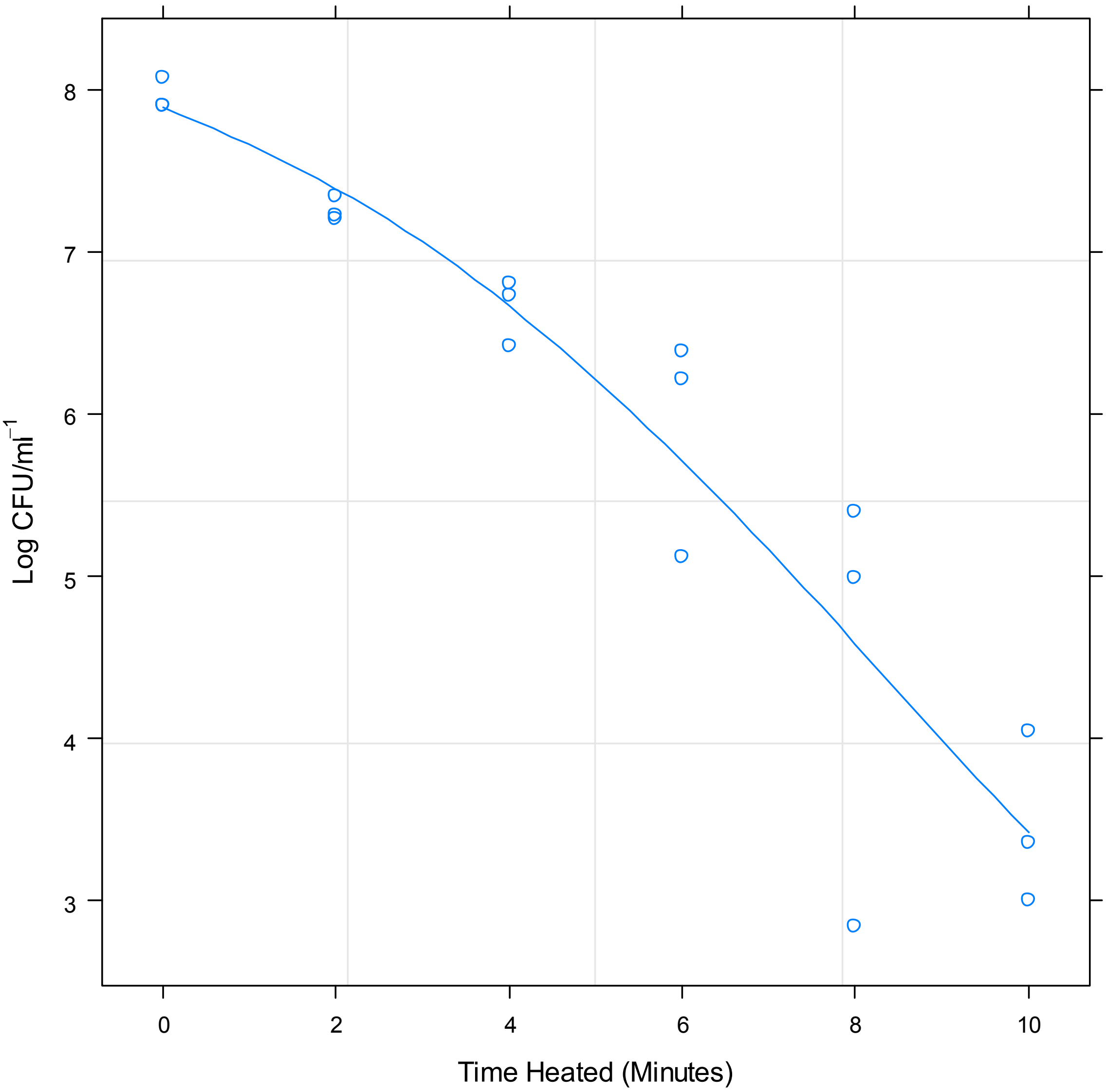

Figure 56. Plot illustrating predicted response curve using a logistic regression model for strain 12745 (ST-257, CC-257) following heating at 56°C.

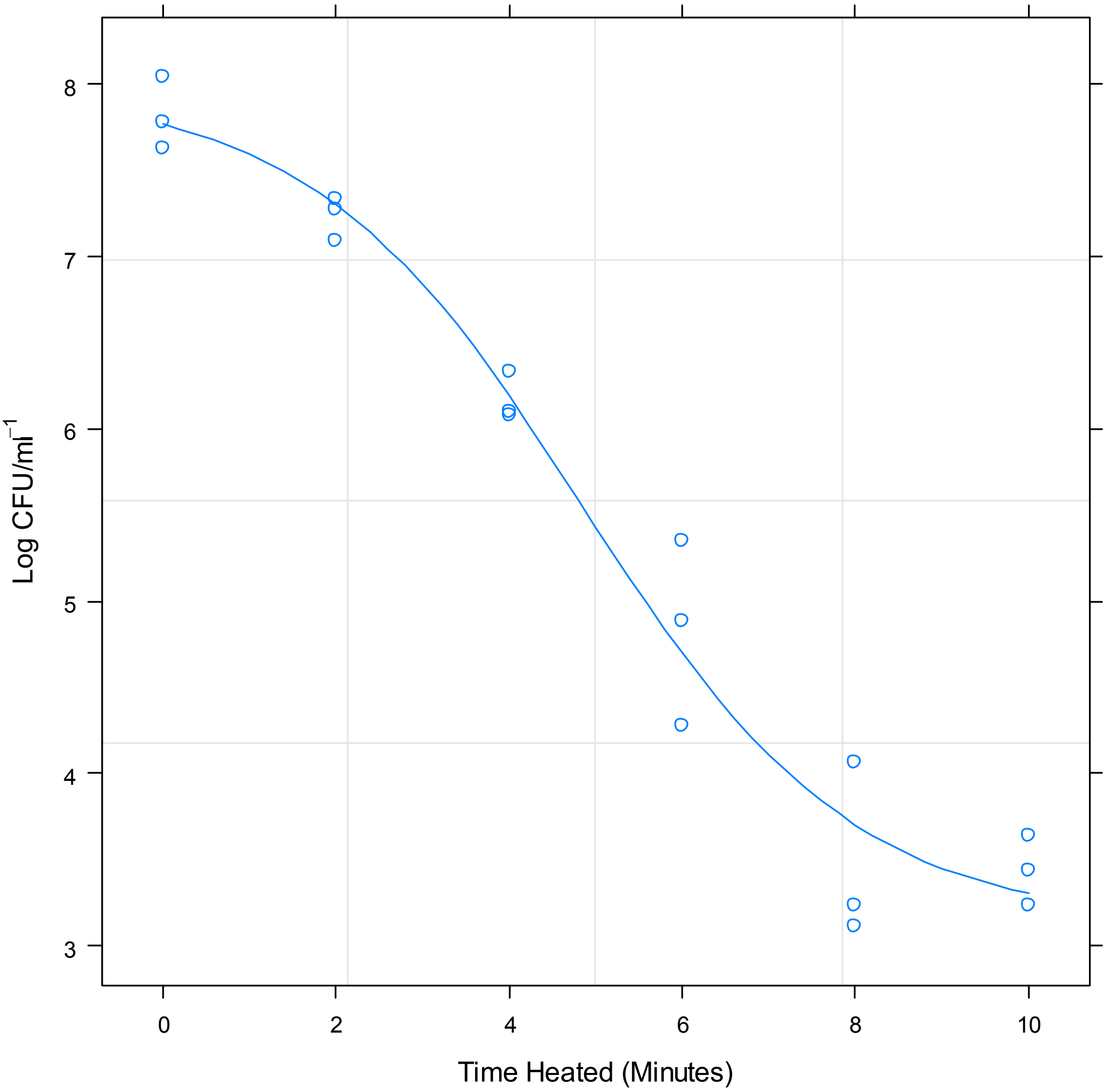

Figure 57. Plot illustrating predicted response curve using a four-parameter logistic regression model for strain 12783 (ST-574, CC-574) following heating at 56°C.

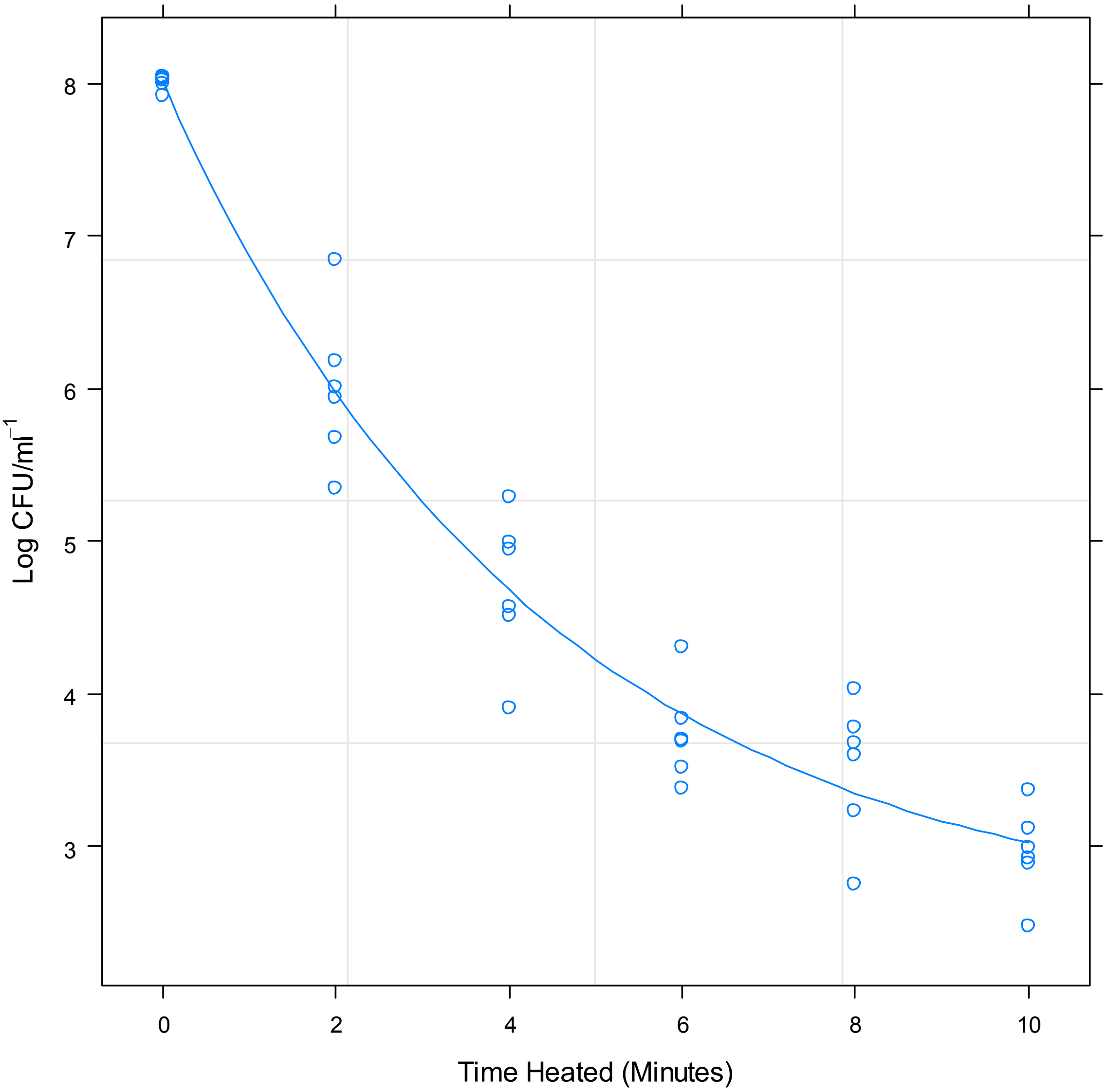

Figure 58. Plot illustrating predicted response curve using an asymptotic regression model for strain 13121 (ST-45, CC-45) following heating at 56°C.

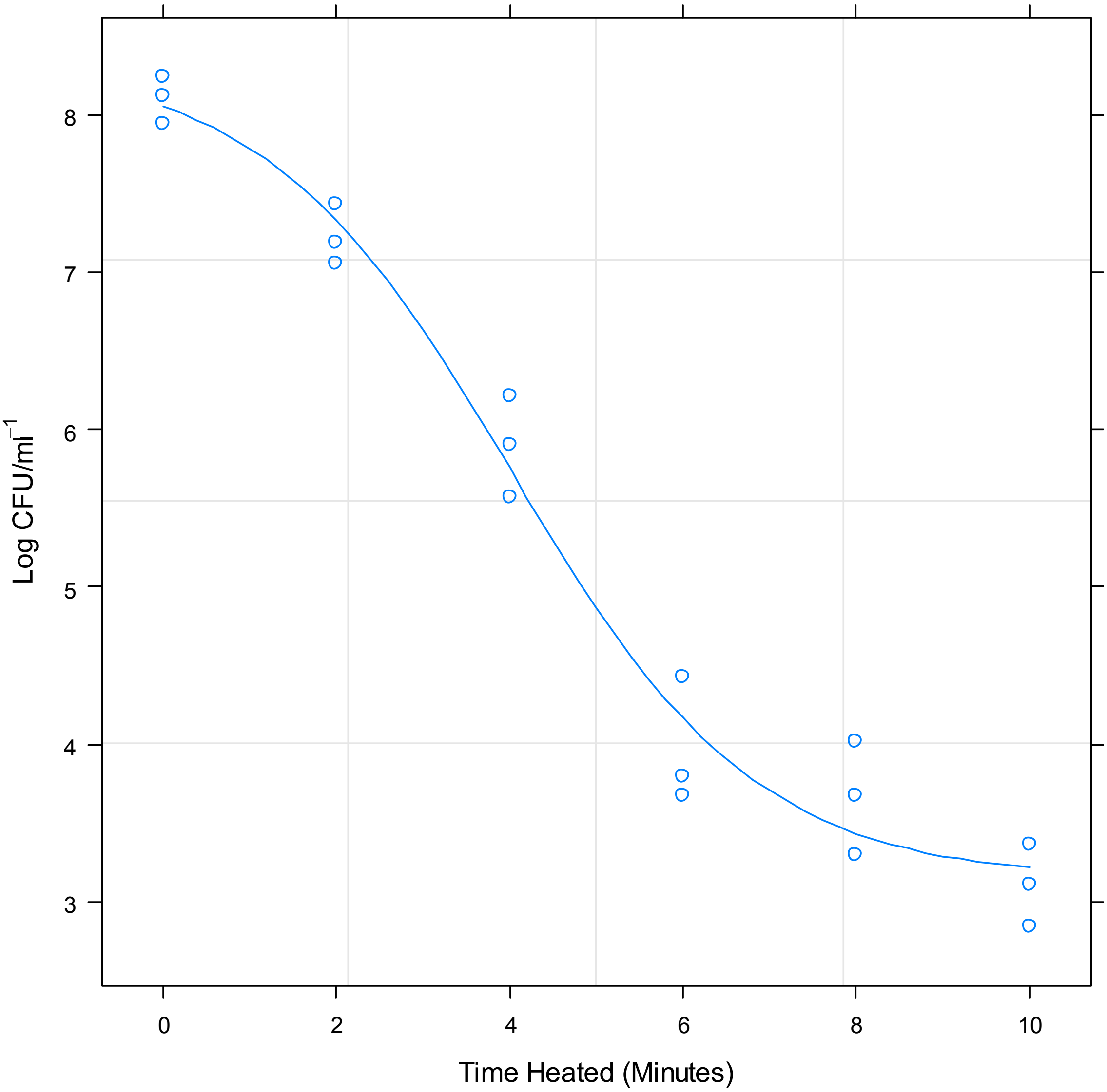

Figure 59. Plot illustrating predicted response curve using a four-parameter logistic regression model for strain 13126 (ST-21, CC-21) following heating at 56°C.

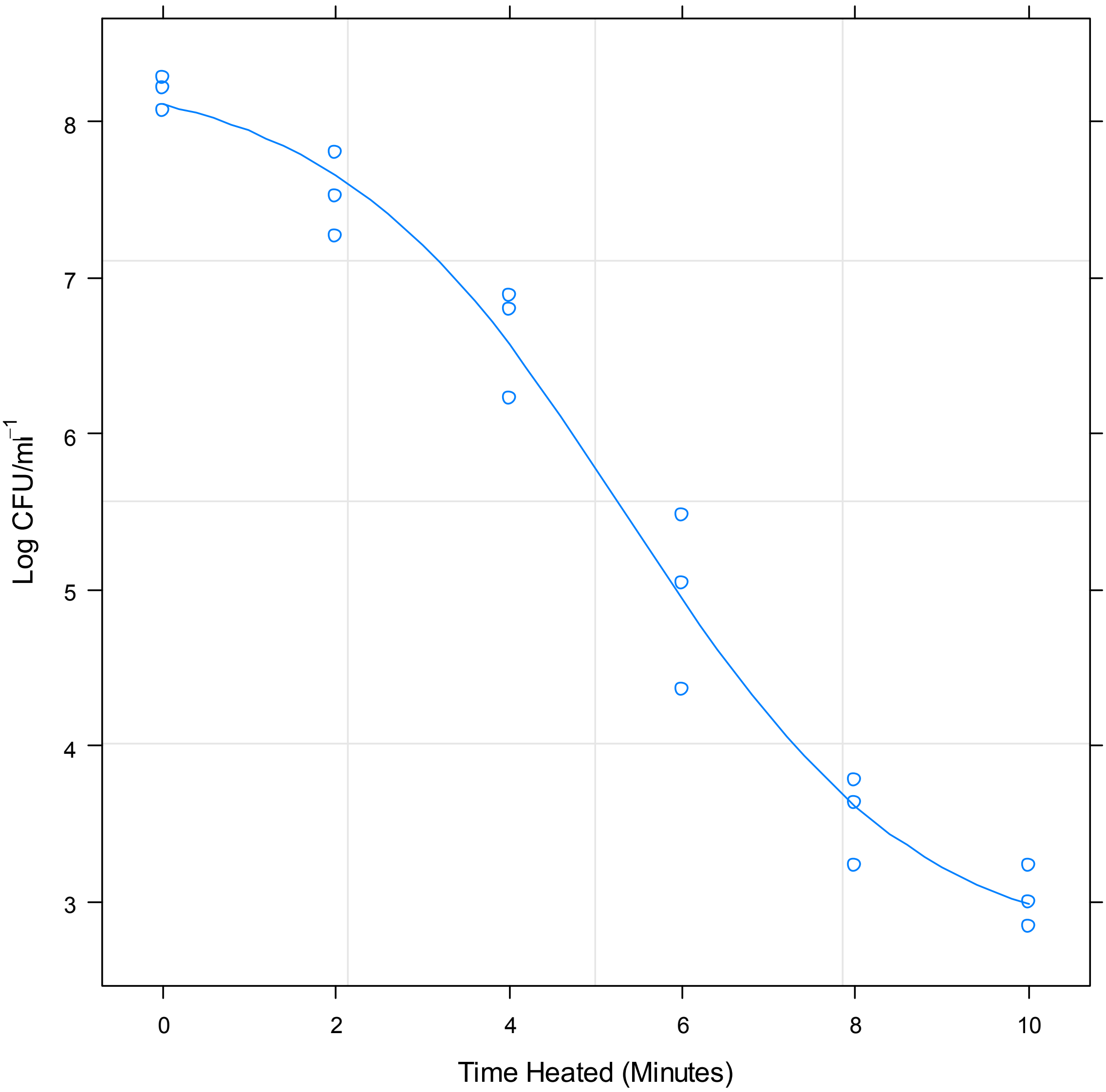

Figure 60. Plot illustrating predicted response curve using a four-parameter logistic regression model for strain 13136 (ST-45, CC-45) following heating at 56°C using a four-parameter logistic regression model.

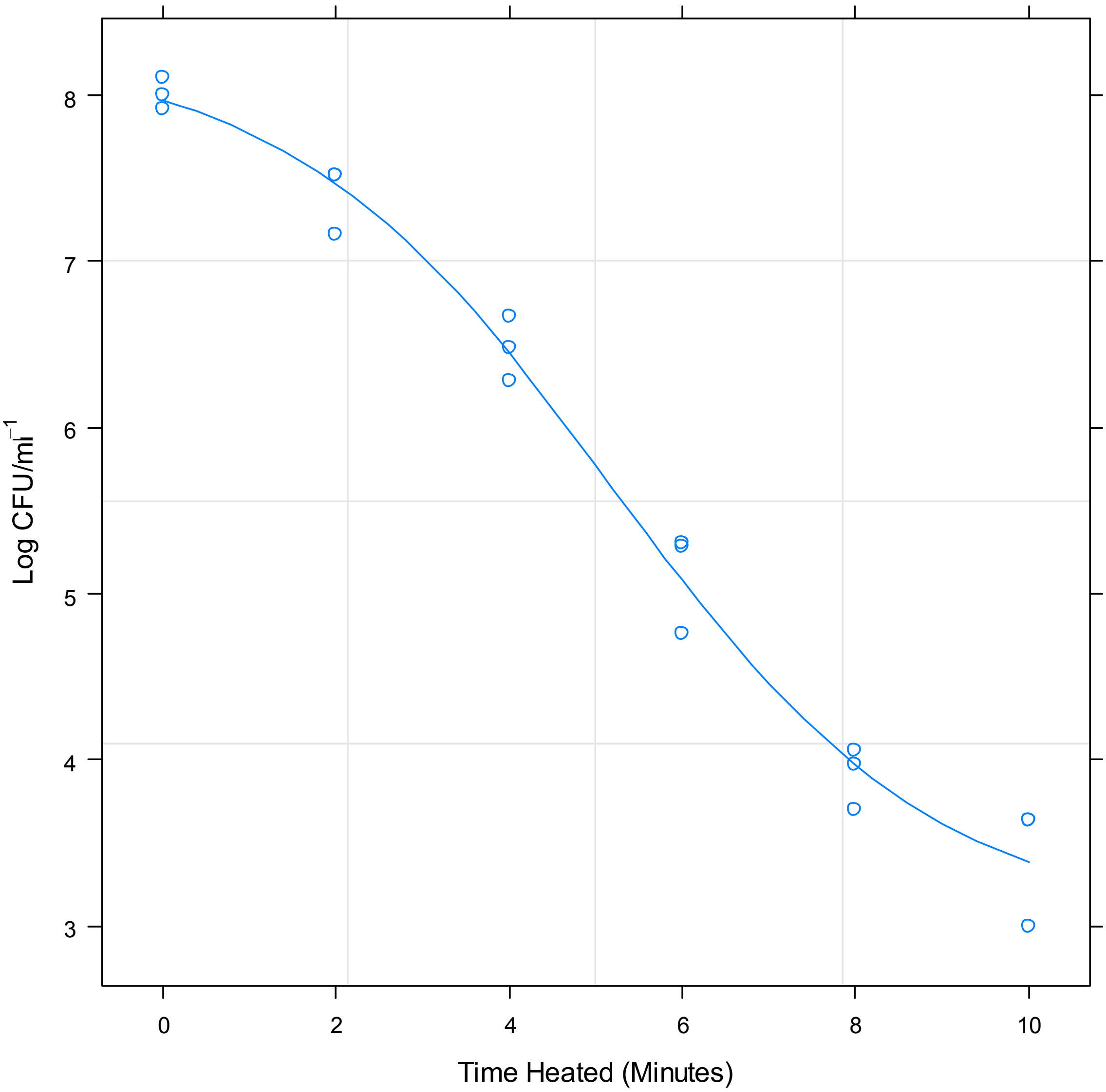

Figure 61. Plot illustrating predicted response curve using a four-parameter logistic regression model for strain 13163 (ST-21, CC-21) following heating at 56°C.

1.8.7 Extended Analysis Predicted Response Curves: Time-Temperature Profile 56°C

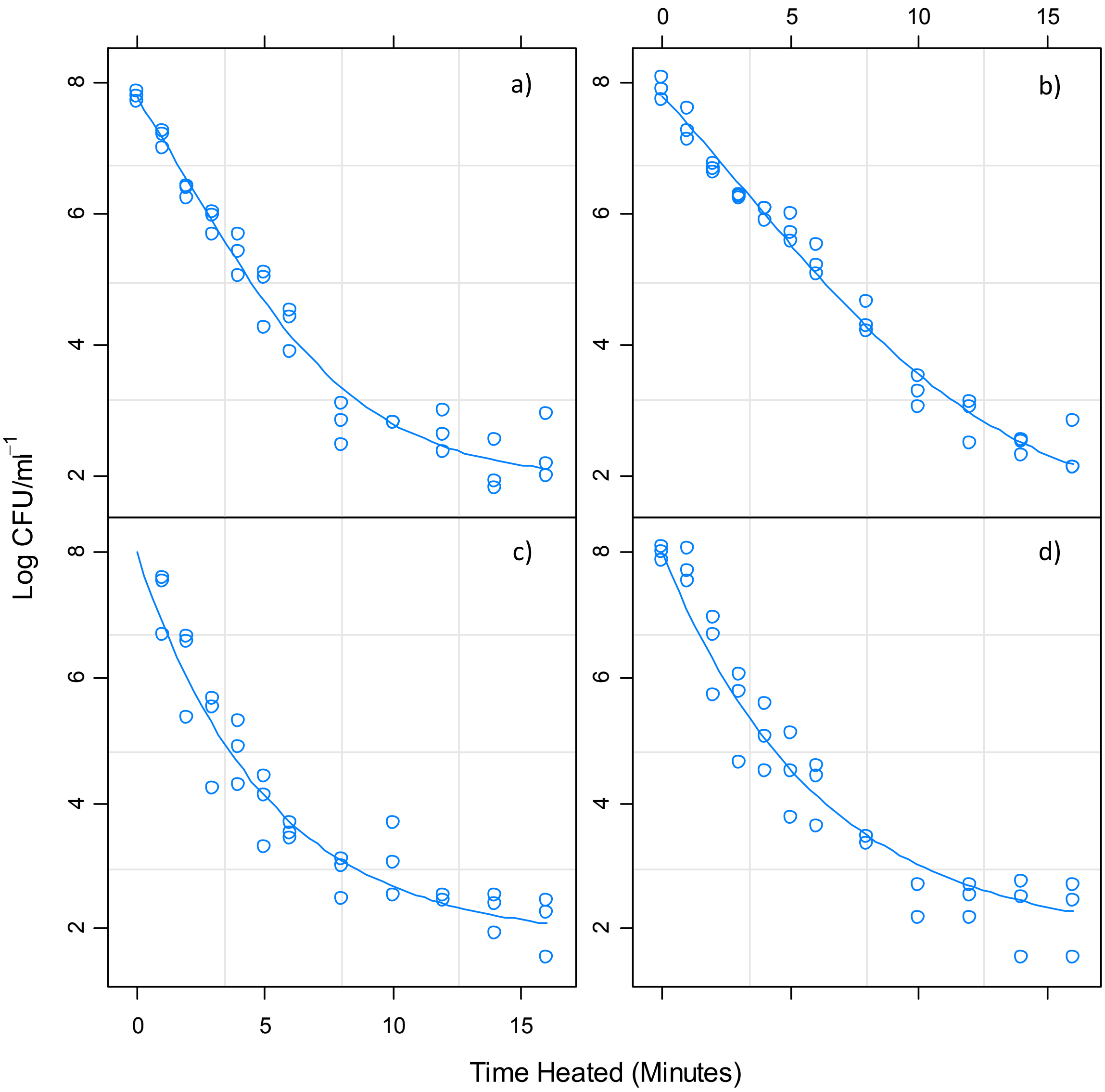

Figure 62. Plot illustrating predicted response curves using asymptotic regression models for two strains following heating at 56°C. Simulations were repeated using two media, Columbia agar base (5% defibrinated blood) (CAB) plus ferrous sulphate, sodium meta-bisulphite, sodium pyruvate (FBP) and modified charcoal cefoperazone deoxycholate agar (mCCDA); strain 11168C (ST-43, CC-21) a) mCCDA, b) CAB-FBP and strain 13121 (ST-45, CC-45) c) mCCDA, d) CAB-FBP.

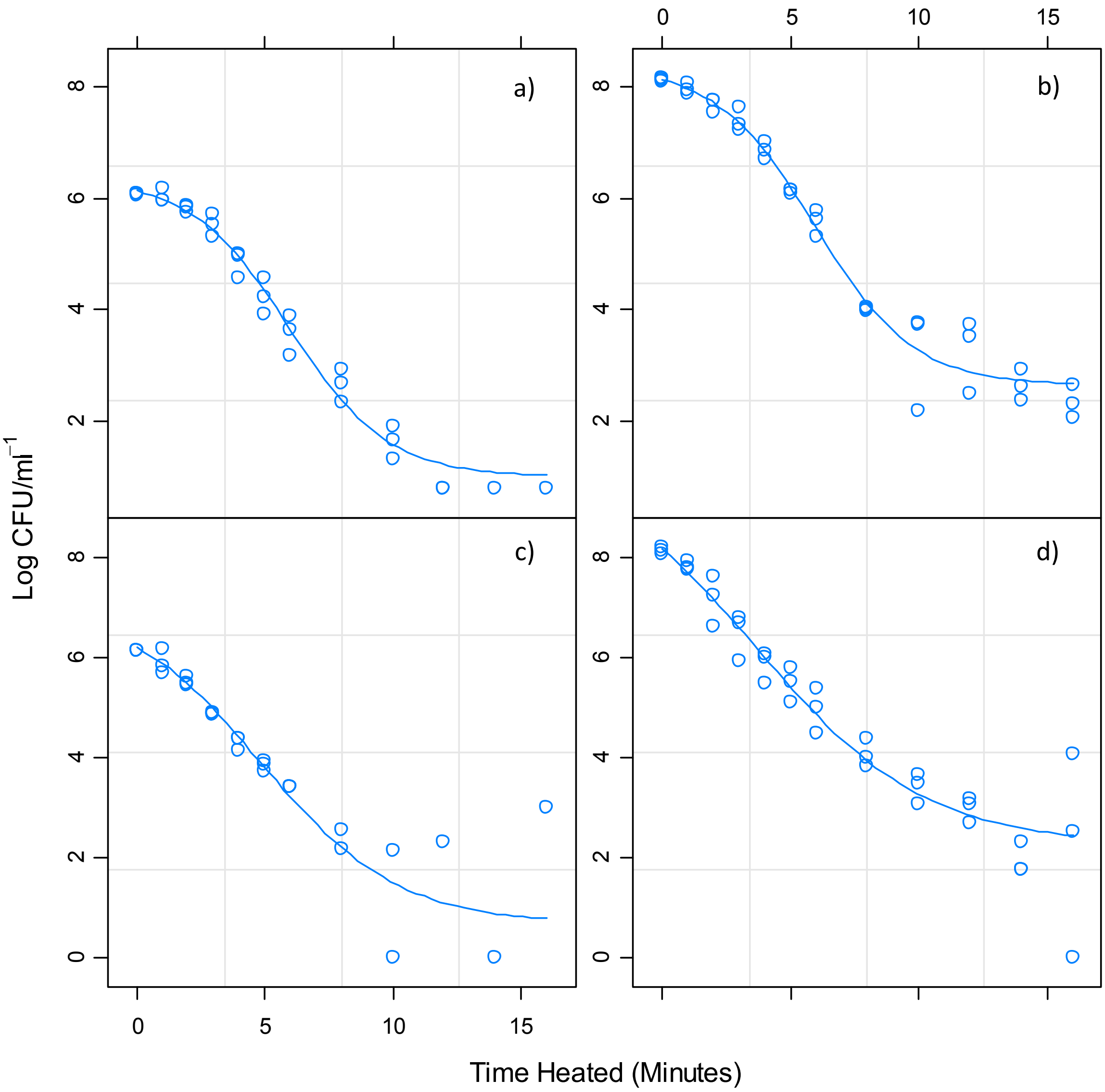

Figure 63. Plot illustrating predicted response curves using a four-parameter logistic regression model for two strains following heating at 56°C. Simulations were repeated using inoculum at 6 Log CFU/ml^{-1} and 8 Log CFU/ml^{-1}; strain 13136 (ST-45, CC-45) a) 6 Log CFU/ml^{-1}, b) 8 Log CFU/ml^{-1} and strain 13121 (ST-45, CC-45) c) 6 Log CFU/ml^{-1}, d) 8 Log CFU/ml^{-1}.

1.8.8 Time-Temperature Simulations: 56°C

Mixed Weibull Distribution Model Predicted Response Curves:

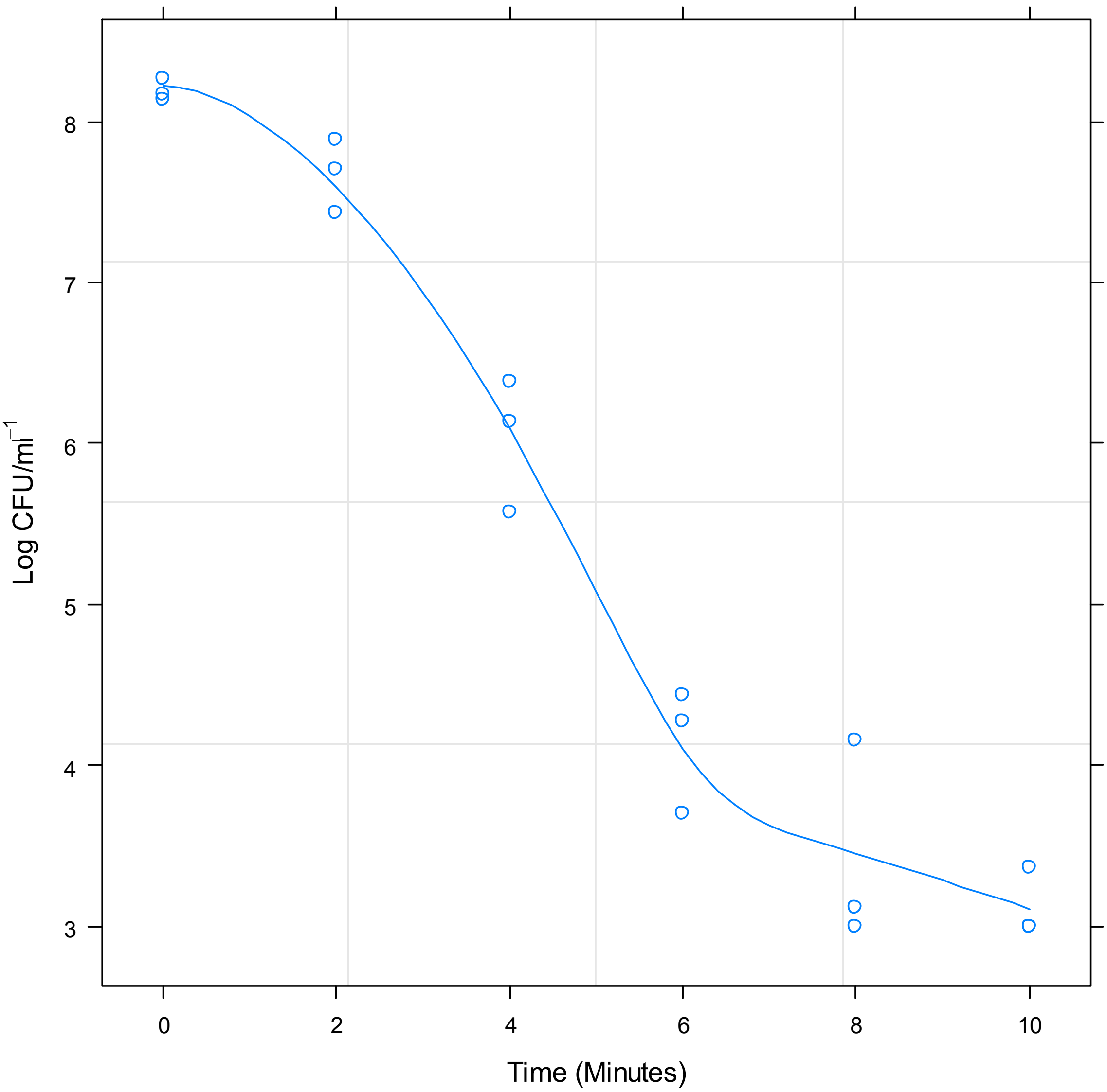

Figure 64. Plot illustrating predicted response curve using a mixed Weibull distribution model for strain 11253 (ST-825, CC-828) following heating at 56°C.

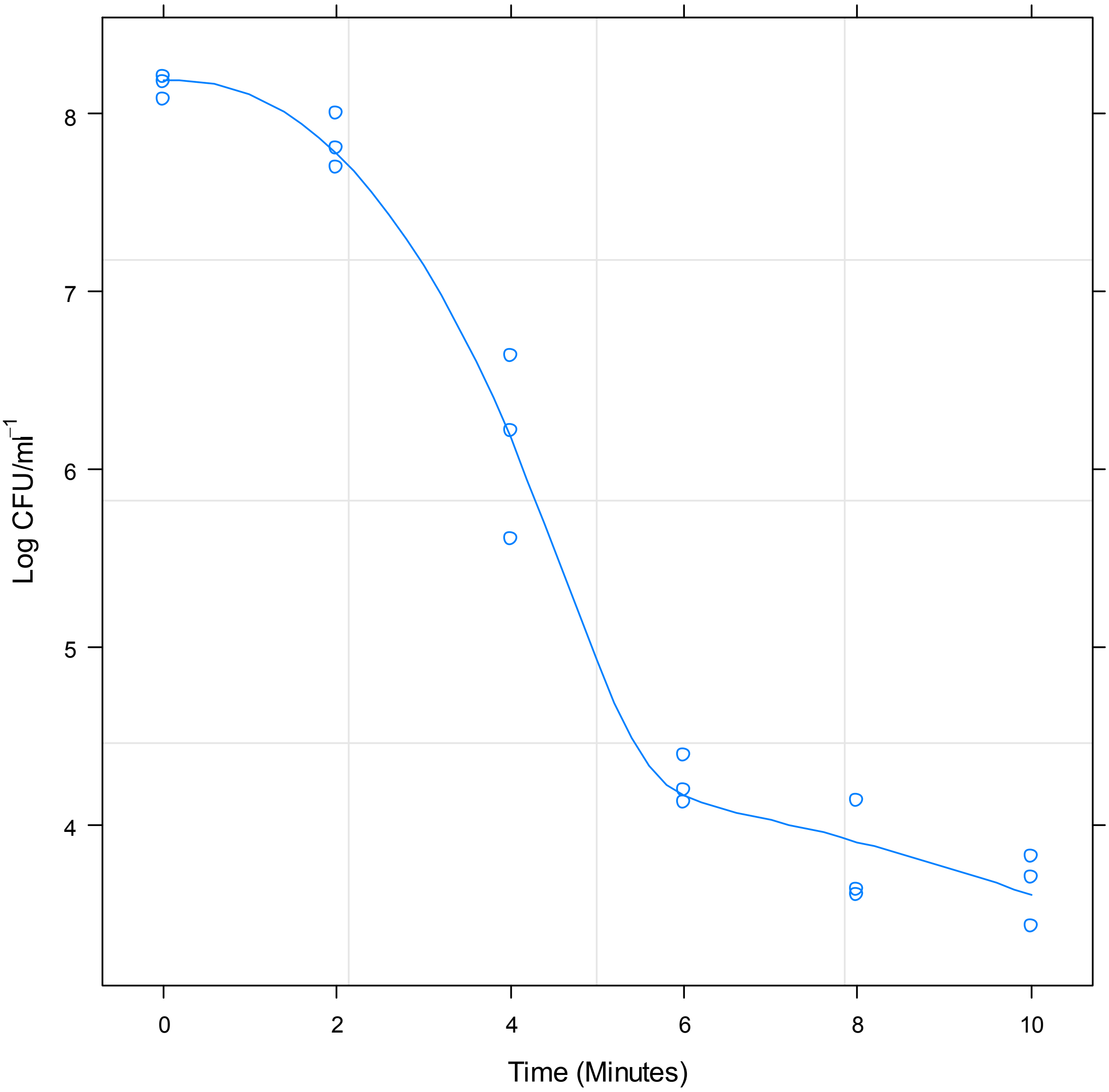

Figure 65. Plot illustrating predicted response curve using a mixed Weibull distribution model for strain 11762 (ST-829, CC-828) following heating at 56°C.

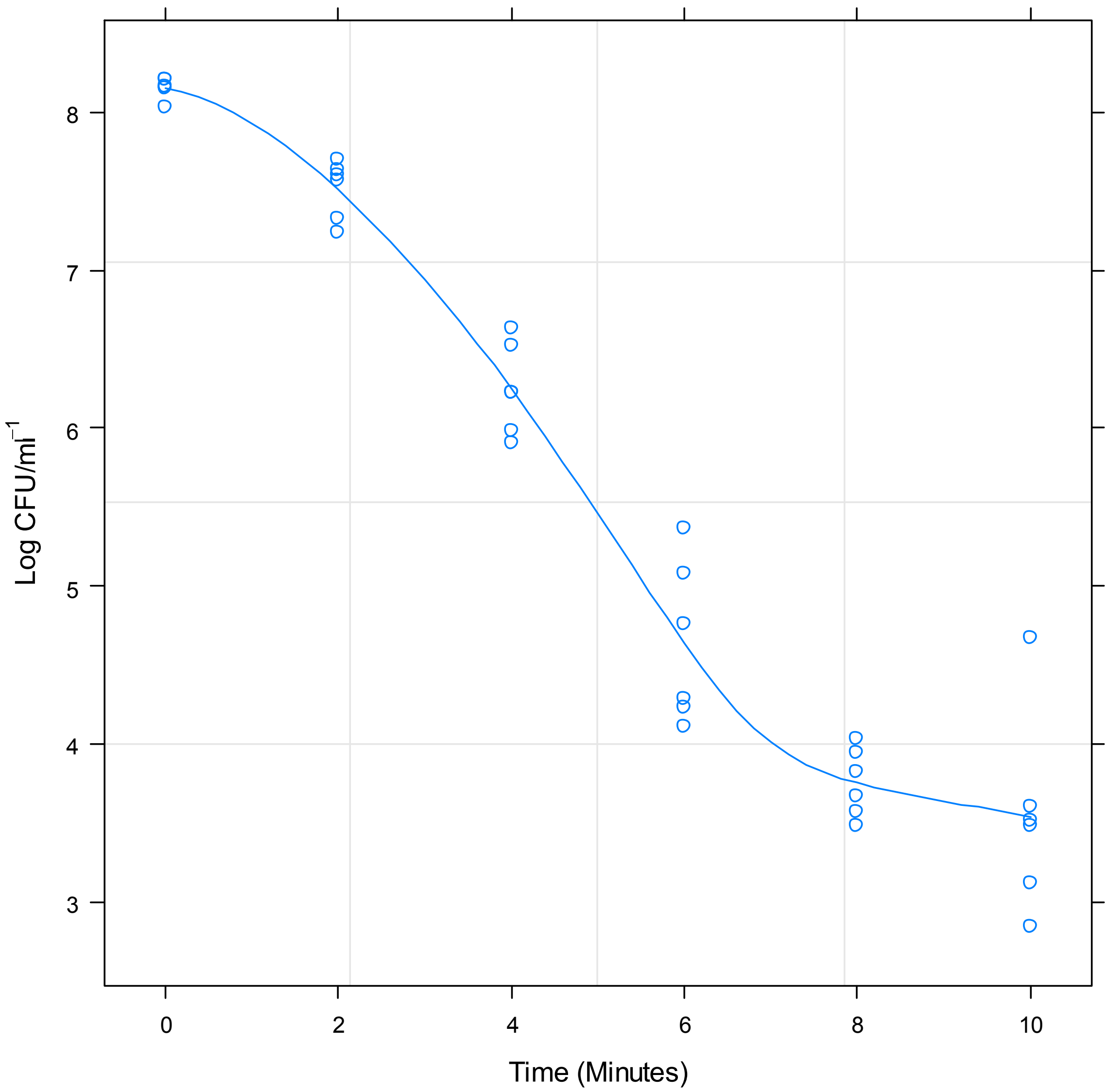

Figure 66. Plot illustrating predicted response curve using a mixed Weibull distribution model for strain 12610 (ST-825, CC-828) following heating at 56°C.

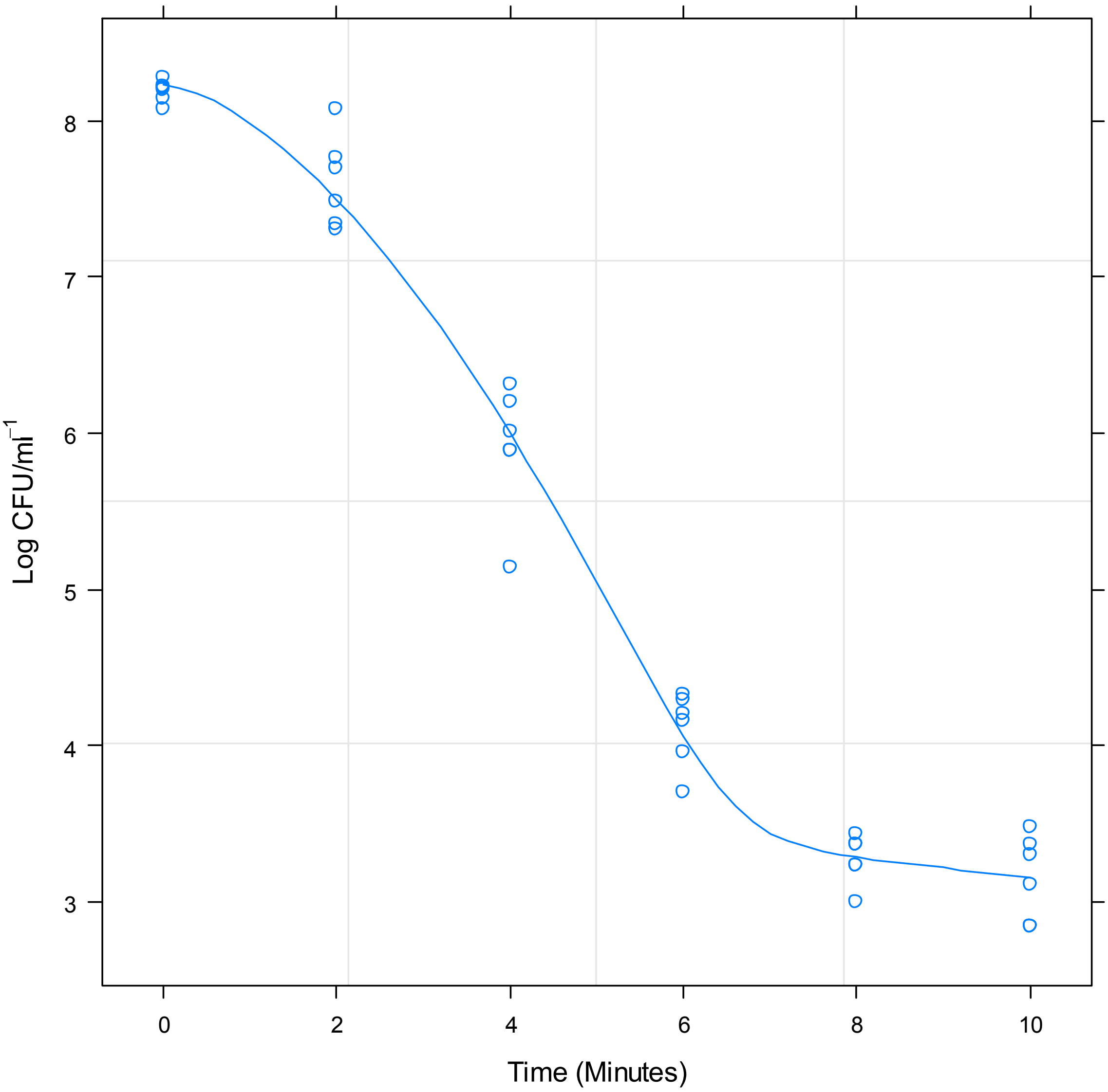

Figure 67. Plot illustrating predicted response curve using a mixed Weibull distribution model for strain 12628 (ST-1773, CC-828) following heating at 56°C.

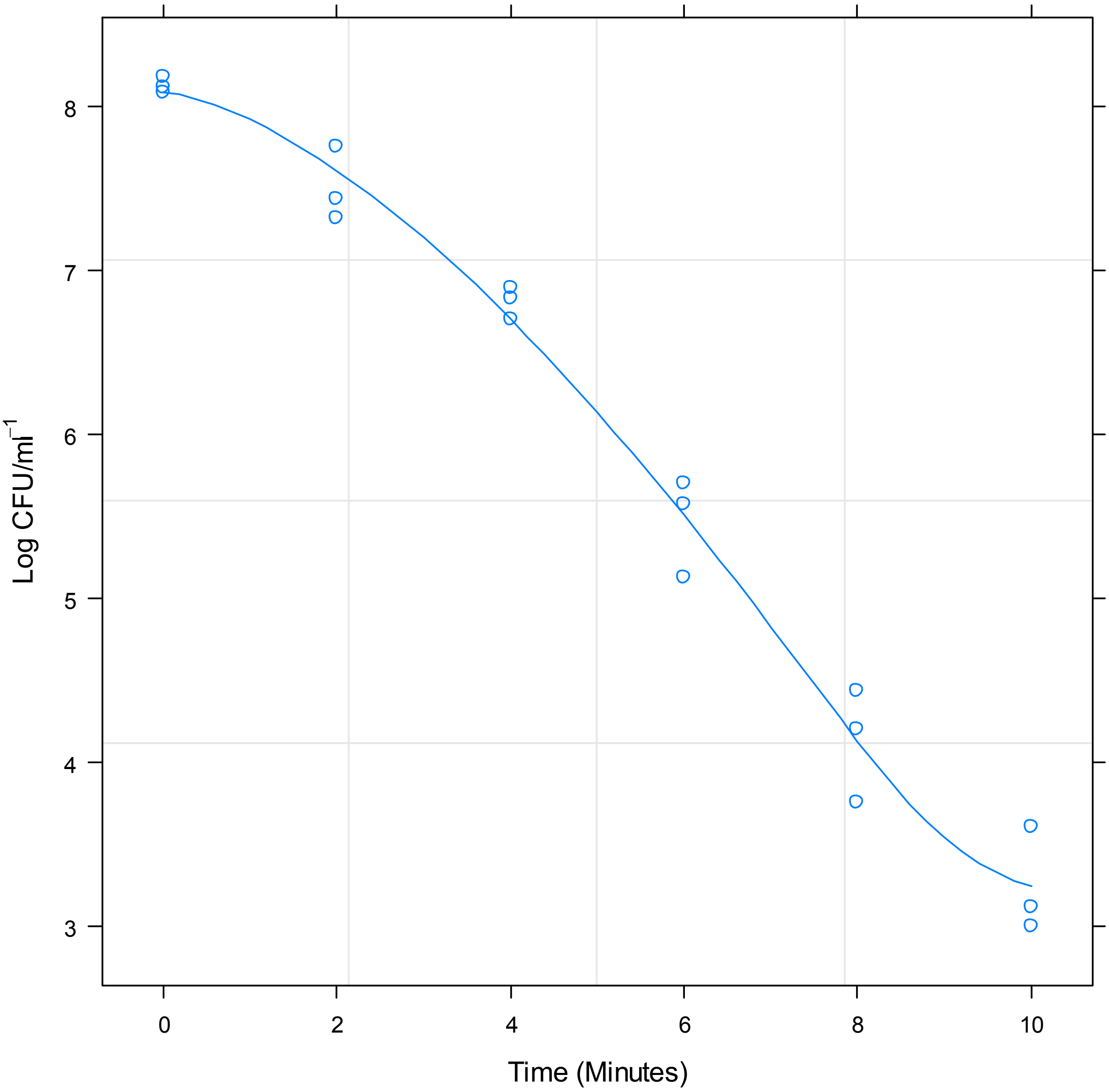

Figure 68. Plot illustrating predicted response curve using a mixed Weibull distribution model for strain 12720 (ST-51, CC-443) following heating at 56°C.

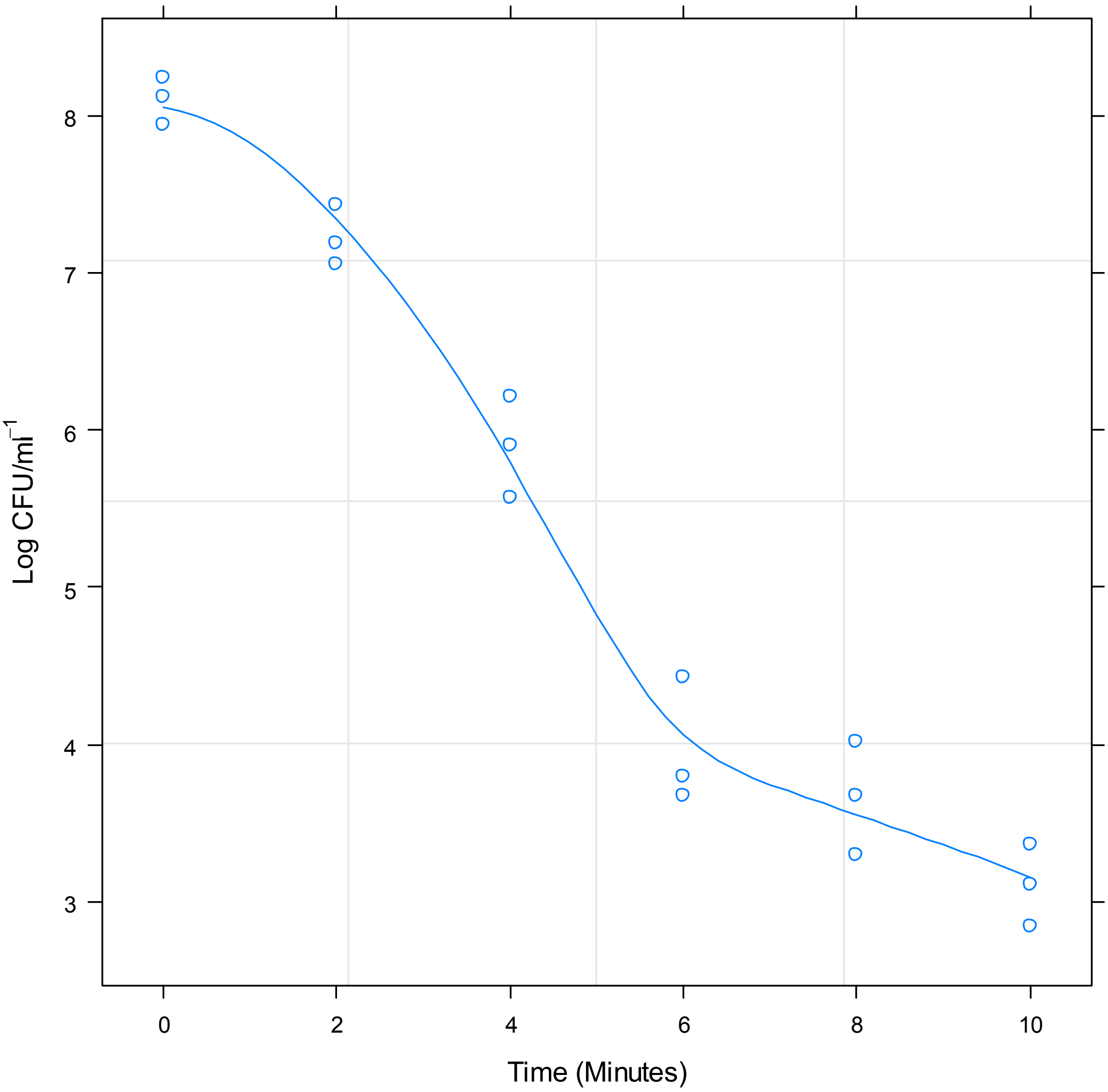

Figure 69. Plot illustrating predicted response curve using a mixed Weibull distribution model for strain 13126 (ST-21, CC-21) following heating at 56°C.

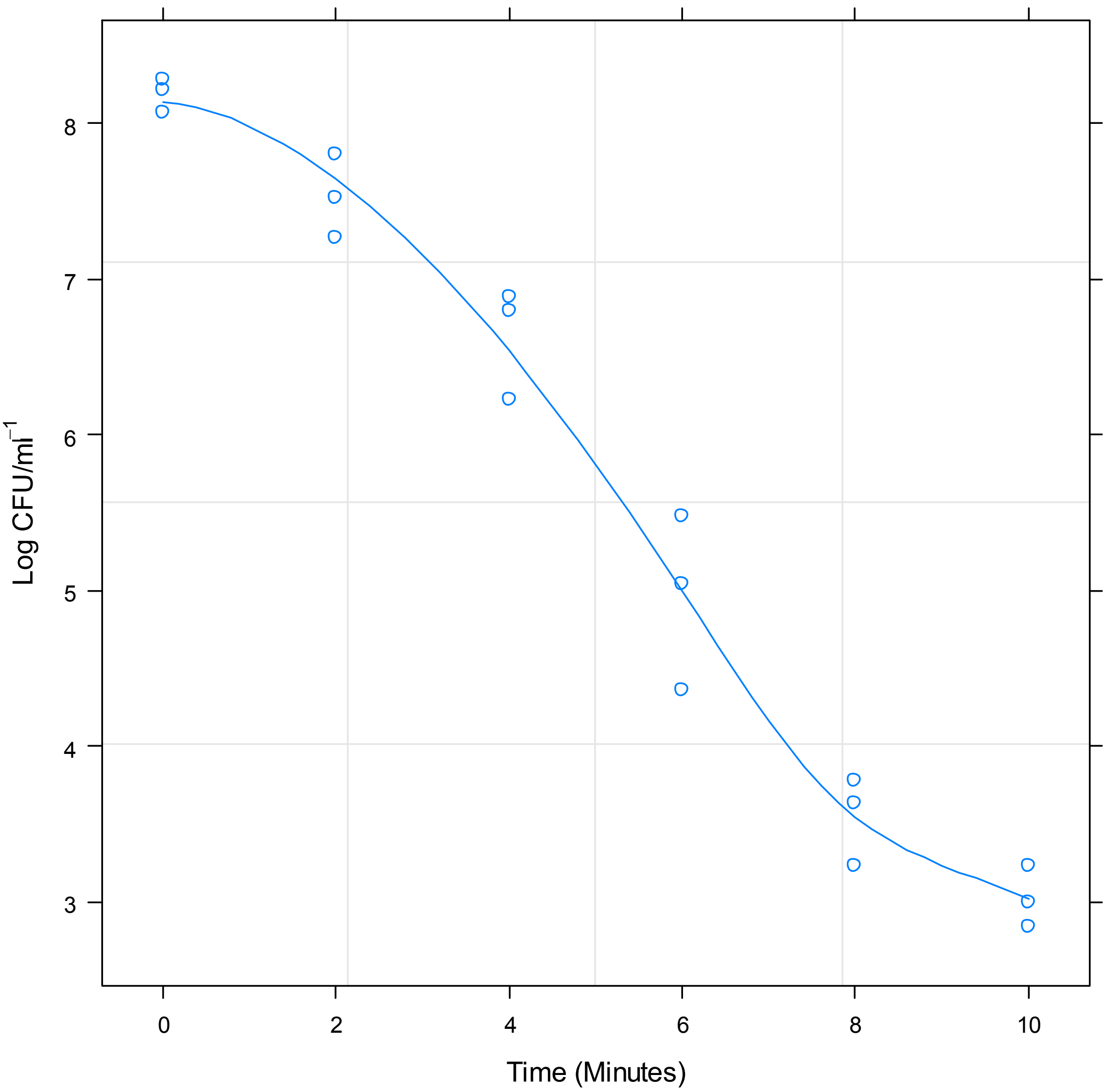

Figure 70. Plot illustrating predicted response curve using a mixed Weibull distribution model for strain 13136 (ST-45, CC-45) following heating at 56°C.

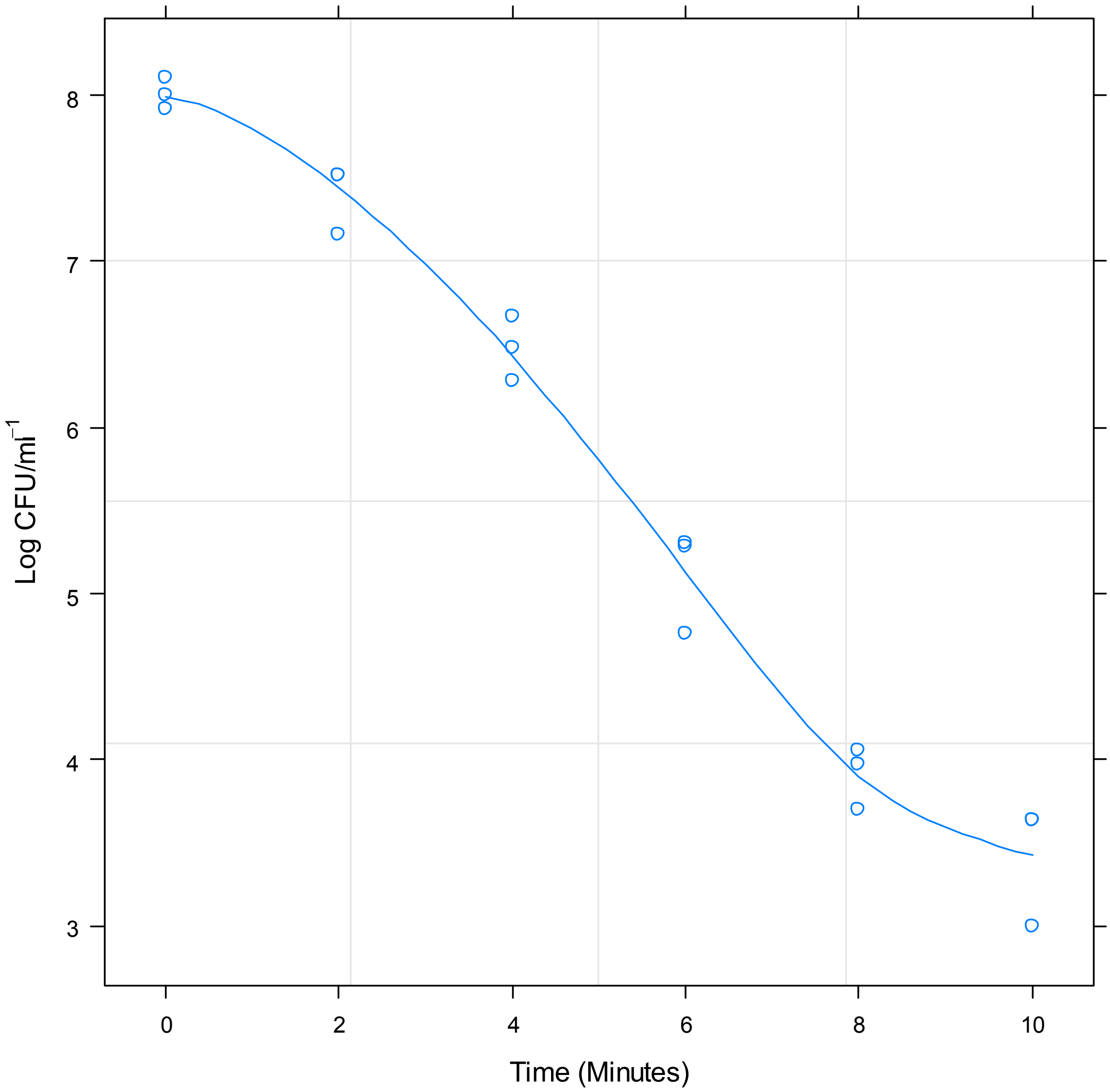

Figure 71. Plot illustrating predicted response curve using a mixed Weibull distribution model for strain 13163 (ST-21, CC-21) following heating at 56°C.

1.8.9 Time-Temperature Simulations: 60°C

Table 32. An assessment of the goodness of fit of models analysing the survival of each strain following heating at 60°C.

Strain	**Non-linear Function**	$\boldsymbol{\rho_c}$
11253 (ST-825, CC-828)	Four-parameter logistic	0.946
11368 (ST-574, CC-574)	Four-parameter logistic	0.959
11762 (ST-829, CC-828)	Asymptotic Regression	0.989
12610 (ST-825, CC-828)	Four-parameter logistic	0.958
12628 (ST-1773, CC-828)	Asymptotic Regression	0.983
12645 (ST-51, CC-443)	Four-parameter logistic	0.978
12662 (ST-257, CC-257)	Four-parameter logistic	0.986
12720 (ST-51, CC-443)	Four-parameter logistic	0.990
12745 (ST-257, CC-257)	Four-parameter logistic	0.971
12783 (ST-574, CC-574)	Four-parameter logistic	0.982
13121 (ST-45, CC-45)	Asymptotic Regression	0.978
13126 (ST-21, CC-21)	Four-parameter logistic	0.981
13136 (ST-45, CC-45)	Four-parameter logistic	0.973
13163 (ST-21, CC-21)	Four-parameter logistic	0.961

Table 33. Four-parameter logistic regression model analysing survival of strain 11253 (ST-825, CC-828) following heating at 60°C.

Parameter	**Estimate**	**Standard Error**	***t*-value**	***P*-value**
Asymptote A	8.212	0.162	50.576	0.000
Asymptote B	2.615	0.184	14.234	0.000
Mid-point	2.178	0.106	20.589	0.000
Scale Parameter	0.657	0.098	6.705	0.000

Table 34. Four-parameter logistic regression model analysing survival of strain 11368 (ST-574, CC-574) following heating at 60°C.

Parameter	**Estimate**	**Standard Error**	***t*-value**	***P*-value**
Asymptote A	8.127	0.102	79.279	0.000
Asymptote B	3.127	0.203	15.443	0.000
Mid-point	2.260	0.010	22.698	0.000
Scale Parameter	0.657	0.082	8.031	0.000

Table 35. Asymptotic regression model analysing survival of strain 11762 (ST-829, CC-828) following heating at 60°C.

Parameter	Estimate	Standard Error	*t*-value	*P*-value
Asymptote	2.631	0.320	8.216	0.000
R0	7.883	0.585	13.469	0.000
LRC	-0.875	0.241	-3.633	0.003

Table 36. Four-parameter logistic regression model analysing survival of strain 12610 (ST-825, CC-828) following heating at 60°C.

Parameter	Estimate	Standard Error	*t*-value	*P*-value
Asymptote A	8.533	0.234	36.489	0.000
Asymptote B	2.745	0.294	9.332	0.000
Mid-point	1.801	0.087	20.745	0.000
Scale Parameter	0.627	0.156	4.026	0.002

Table 37. Asymptotic regression model analysing survival of strain 12628 (ST-45, CC-45) following heating at 60°C.

Parameter	Estimate	Standard Error	*t*-value	*P*-value
Asymptote	0.649	1.907	0.341	0.000
R0	8.146	0.187	43.605	0.000
LRC	-1.506	0.405	-3.722	0.003

Table 38. Four-parameter logistic regression model analysing survival of strain 12645 (ST-51, CC-443) following heating at 60°C.

Parameter	Estimate	Standard Error	*t*-value	*P*-value
Asymptote A	8.151	0.124	65.579	0.000
Asymptote B	3.196	0.188	17.037	0.000
Mid-point	2.095	0.101	20.818	0.000
Scale Parameter	0.612	0.096	6.403	0.000

Table 39. Four-parameter logistic regression model analysing survival of strain 12662 (ST-257, CC-257) following heating at 60^{o}C.

Parameter	Estimate	Standard Error	*t*-value	*P*-value
Asymptote A	8.746	0.253	34.906	0.000
Asymptote B	3.062	0.219	13.961	0.000
Mid-point	1.913	0.096	19.938	0.000
Scale Parameter	0.938	0.143	6.540	0.000

Table 40. Four-parameter logistic regression model analysing survival of strain 12720 (ST-51, CC-443) following heating at 60^{o}C.

Parameter	Estimate	Standard Error	*t*-value	*P*-value
Asymptote A	8.162	0.135	60.451	0.000
Asymptote B	3.266	0.184	17.728	0.000
Mid-point	1.952	0.086	22.566	0.000
Scale Parameter	0.631	0.112	5.640	0.000

Table 41. Four-parameter logistic regression model analysing survival of strain 12745 (ST-257, CC-257) following heating at 60^{o}C.

Parameter	Estimate	Standard Error	*t*-value	*P*-value
Asymptote A	8.459	0.614	13.784	0.000
Asymptote B	3.222	0.243	13.244	0.000
Mid-point	2.053	0.303	6.775	0.000
Scale Parameter	0.727	0.238	3.049	0.009

Table 42. Four-parameter logistic regression model analysing survival of strain 12783 (ST-574, CC-574) following heating at 60^{o}C.

Parameter	Estimate	Standard Error	*t*-value	*P*-value
Asymptote A	8.553	0.476	17.983	0.000
Asymptote B	3.015	0.209	14.450	0.000
Mid-point	1.698	0.182	9.335	0.000
Scale Parameter	0.811	0.204	3.972	0.000

Table 43. Asymptotic regression model analysing survival of strain 13121 (ST-45, CC-45) following heating at 60°C.

Parameter	Estimate	Standard Error	*t*-value	*P*-value
Asymptote	3.397	0.198	17.175	0.000
R0	7.930	0.039	202.835	0.000
LRC	-0.275	0.120	-2.283	0.041

Table 44. Four-parameter logistic regression model analysing survival of strain 13126 (ST-21, CC-21) following heating at 60°C.

Parameter	Estimate	Standard Error	*t*-value	*P*-value
Asymptote A	8.411	0.176	47.871	0.000
Asymptote B	3.327	0.169	19.172	0.000
Mid-point	1.905	0.083	23.052	0.000
Scale Parameter	0.735	0.117	6.296	0.000

Table 45. Four-parameter logistic regression model analysing survival of strain 13136 (ST-45, CC-45) following heating at 60°C.

Parameter	Estimate	Standard Error	*t*-value	*P*-value
Asymptote A	8.617	0.377	22.873	0.000
Asymptote B	3.147	0.175	17.999	0.000
Mid-point	1.730	0.156	11.078	0.000
Scale Parameter	0.828	0.164	5.058	0.000

Table 46. Four-parameter logistic regression model analysing survival of strain 13163 (ST-21, CC-21) following heating at 60°C.

Parameter	Estimate	Standard Error	*t*-value	*P*-value
Asymptote A	8.084	0.326	24.784	0.000
Asymptote B	3.535	0.182	19.377	0.000
Mid-point	2.035	0.188	10.799	0.000
Scale Parameter	0.550	0.135	4.081	0.002

1.8.10 Time-temperature Simulations: 60°C

Mixed Weibull Distribution Model:

Table 47. An assessment of the goodness of fit for Mixed Weibull distribution models analysing the survival of each strain following heating at 60°C.

Strain	Non-linear Function	ρ_c
11253 (ST-825, CC-828)	Mixed Weibull Distribution	
11368 (ST-574, CC-574)	Mixed Weibull Distribution	0.990
11762 (ST-828, CC-829)	Mixed Weibull Distribution	
12610 (ST-825, CC-828)	Mixed Weibull Distribution	
12628 (ST-1773, CC-828)	Mixed Weibull Distribution	
12645 (ST-51, CC-443)	Mixed Weibull Distribution	0.983
12662 (ST-257, CC-257)	Mixed Weibull Distribution	0.977
12720 (ST-51, CC-443)	Mixed Weibull Distribution	0.983
12745 (ST-257, CC-257)	Mixed Weibull Distribution	0.973
12783 (ST-574, CC-574)	Mixed Weibull Distribution	0.960
13121 (ST-45, CC-45)	Mixed Weibull Distribution	0.988
13126 (ST-21, CC-21)	Mixed Weibull Distribution	0.977
13136 (ST-45, CC-45)	Mixed Weibull Distribution	0.982
13163 (ST-574,CC-574)	Mixed Weibull Distribution	

Table 48. Mixed Weibull distribution model analysing the survival of strain 11368 (ST-574, CC-574) following heating at 60°C.

Parameter	Estimate	Standard Error	*t*-value	*P*-value
α	4.728	0.395	11.957	0.000
δ1	1.466	0.218	6.720	0.000
p	1.799	0.337	5.347	0.000
N0	7.971	0.192	41.556	0.000
δ2	29.098	93.782	0.310	0.762

Table 49. Mixed Weibull distribution model analysing the survival of strain 12645 (ST-51, CC-443) following heating at 60°C.

Parameter	Estimate	Standard Error	*t*-value	*P*-value
α	4.404	0.472	9.337	0.000
δ1	1.340	0.247	5.419	0.000
p	1.736	0.369	4.708	0.000
N0	8.001	0.242	33.080	0.000
δ2	11.084	7.316	1.515	0.154

Table 50. Mixed Weibull distribution model analysing the survival of strain 12662 (ST-257, CC-257) following heating at 60°C.

Parameter	Estimate	Standard Error	*t*-value	*P*-value
α	3.567	0.428	8.334	0.000
δ1	1.076	0.188	5.728	0.000
p	1.343	0.233	5.769	0.000
N0	8.090	0.185	43.722	0.000
δ2	4.847	1.229	3.943	0.001

Table 51. Mixed Weibull distribution model analysing the survival of strain 12720 (ST-51, CC-443) following heating at 60°C.

Parameter	Estimate	Standard Error	*t*-value	*P*-value
α	4.187	0.482	8.682	0.000
δ1	1.207	0.231	5.217	0.000
p	1.565	0.323	4.843	0.000
N0	7.954	0.235	33.795	0.000
δ2	9.999	6.013	1.663	0.120

Table 52. Mixed Weibull distribution model analysing the survival of strain 12745 (ST-257, CC-257) following heating at 60°C.

Parameter	Estimate	Standard Error	*t*-value	*P*-value
α	3.982	0.532	7.484	0.000
δ1	1.403	0.162	8.665	0.000
p	3.536	3.106	1.138	0.276
N0	8.134	0.314	25.911	0.000
δ2	6.718	1.120	5.999	0.000

Table 53. Mixed Weibull distribution model analysing the survival of strain 12783 (ST-574, CC-574) following heating at 60°C.

Parameter	Estimate	Standard Error	*t*-value	*P*-value
α	4.221	0.610	6.921	0.000
δ1	0.915	0.225	4.075	0.000
p	1.208	0.254	4.756	0.000
N0	7.943	0.238	33.452	0.000
δ2	8.689	6.500	1.337	0.191

Table 54. Mixed Weibull distribution model analysing the survival of strain 13126 (ST-21, CC-21) following heating at 60°C.

Parameter	Estimate	Standard Error	*t*-value	*P*-value
α	3.631	0.456	7.957	0.000
$\delta 1$	1.224	0.193	6.330	0.000
p	1.990	1.306	1.524	0.138
N0	8.056	0.169	47.672	0.000
$\delta 2$	6.139	1.574	3.900	0.001

Table 55. Mixed Weibull distribution model analysing the survival of strain 13136 (ST-45, CC-45) following heating at 60°C.

Parameter	Estimate	Standard Error	*t*-value	*P*-value
α	3.671	0.294	12.506	0.000
$\delta 1$	1.017	0.165	6.145	0.000
p	1.423	0.354	4.021	0.000
N0	8.012	0.163	49.107	0.000
$\delta 2$	5.621	1.058	5.313	0.000

1.8.11 Time-Temperature Profile 60°C:

Predicted Response Curves:

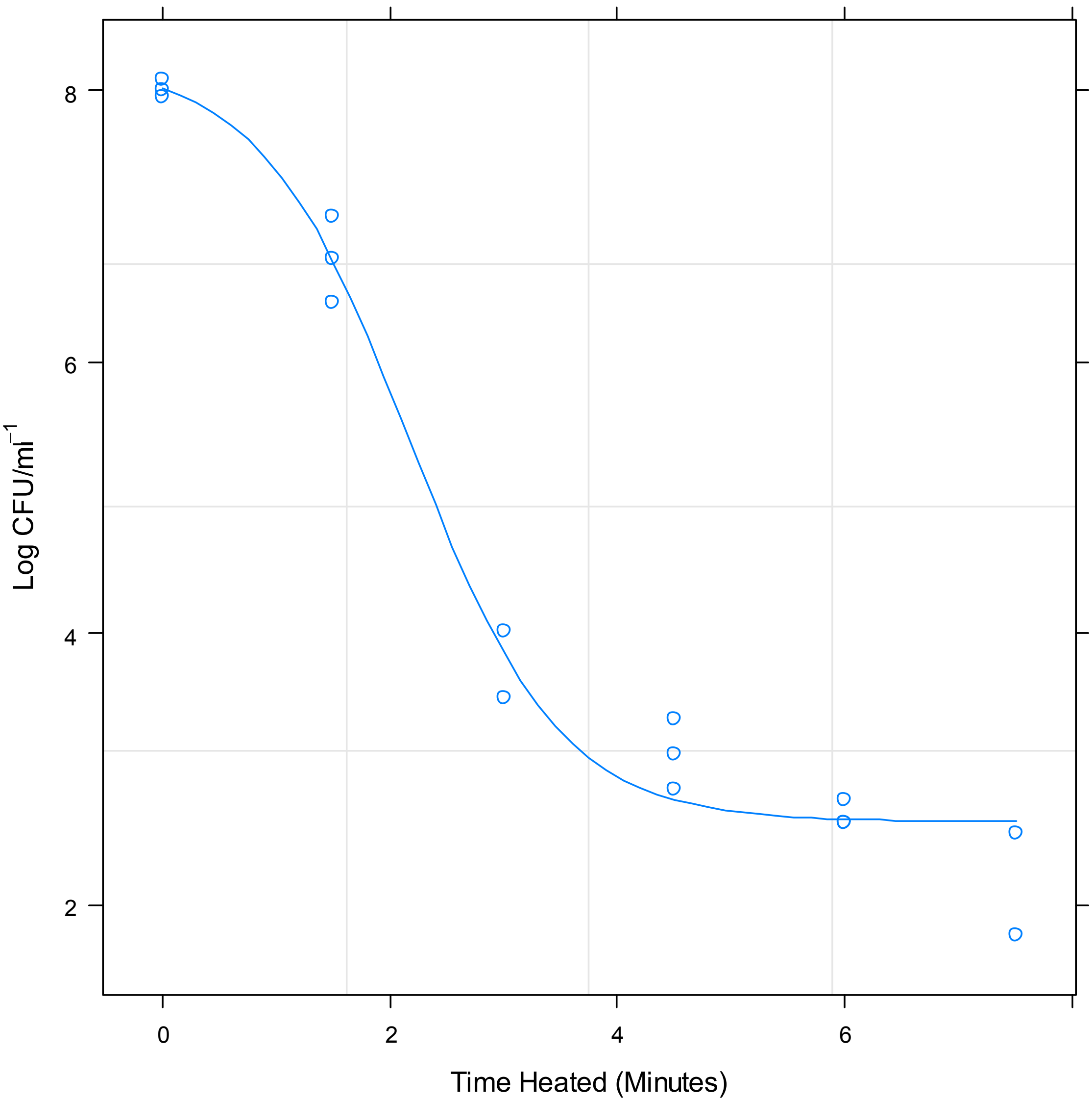

Figure 72. Plot illustrating predicted response curve using a four-parameter logistic regression model for strain 11253 (ST-825, CC-828) following heating at 60°C.

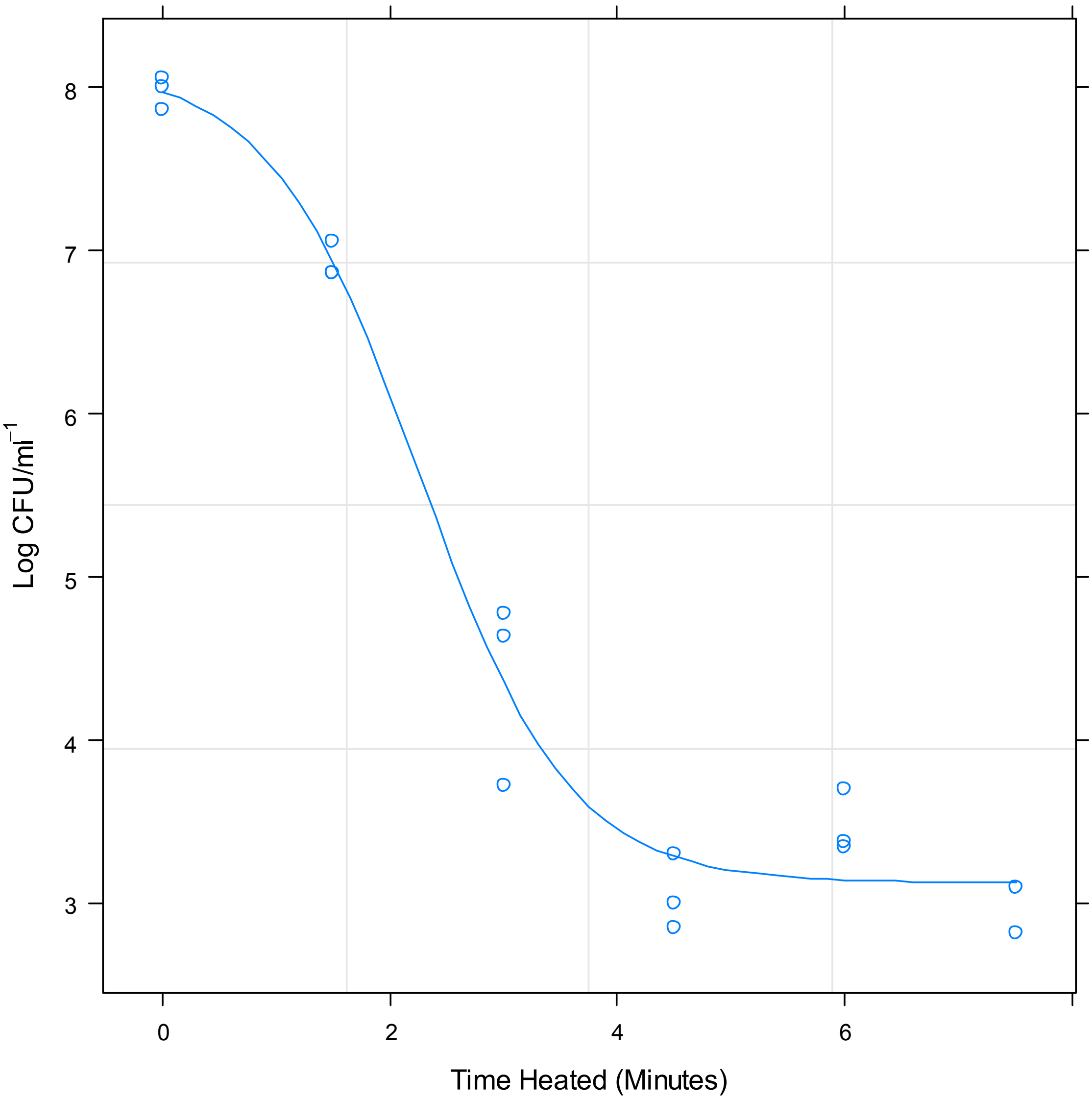

Figure 73. Plot illustrating predicted response curve using a four-parameter logistic regression model for strain 11368 (ST-574, CC-574) following heating at 60°C.

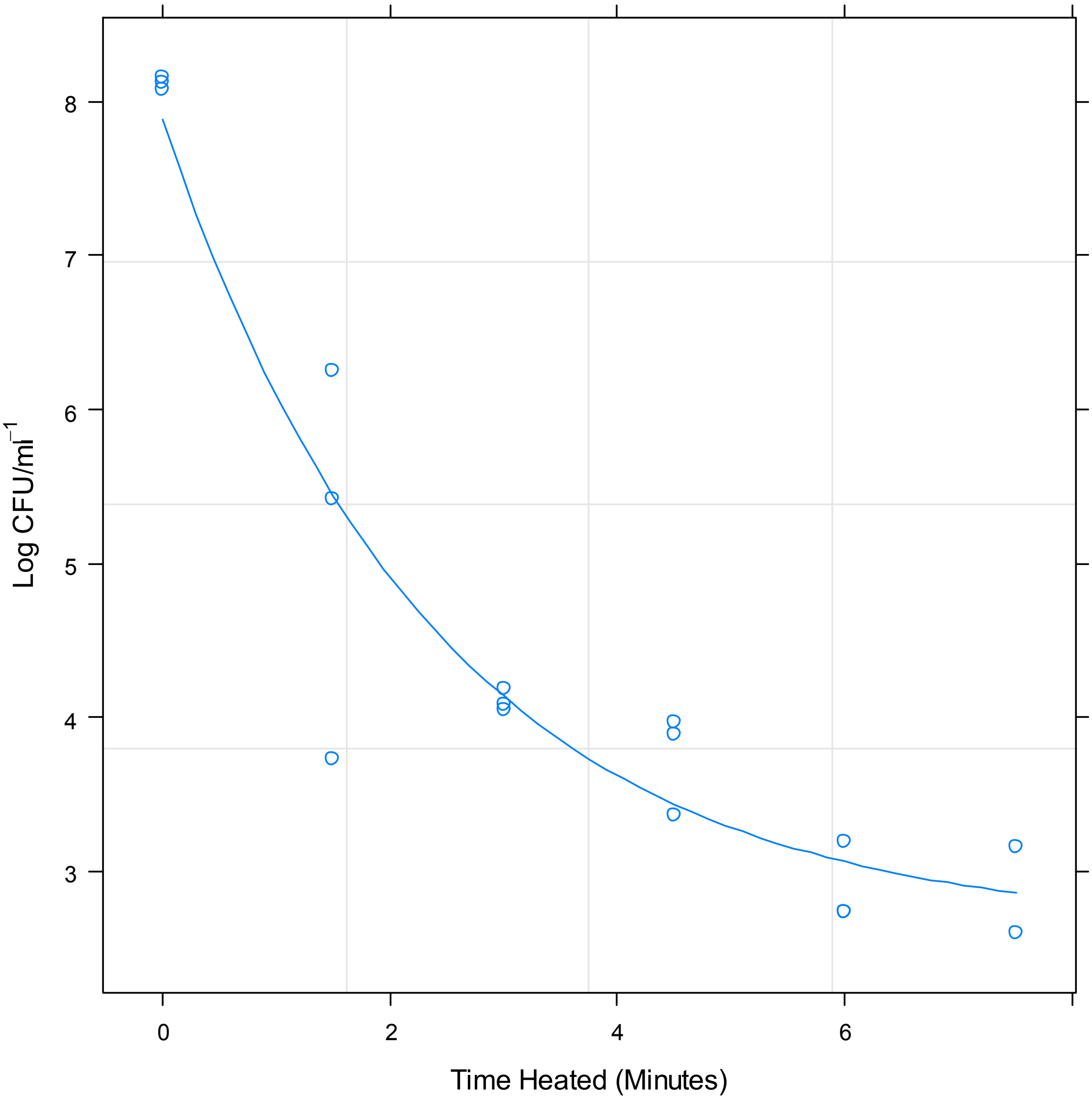

Figure 74. Plot illustrating predicted response curve using an asymptotic regression model for strain 11762 (ST-829, CC-828) following heating at 60°C.

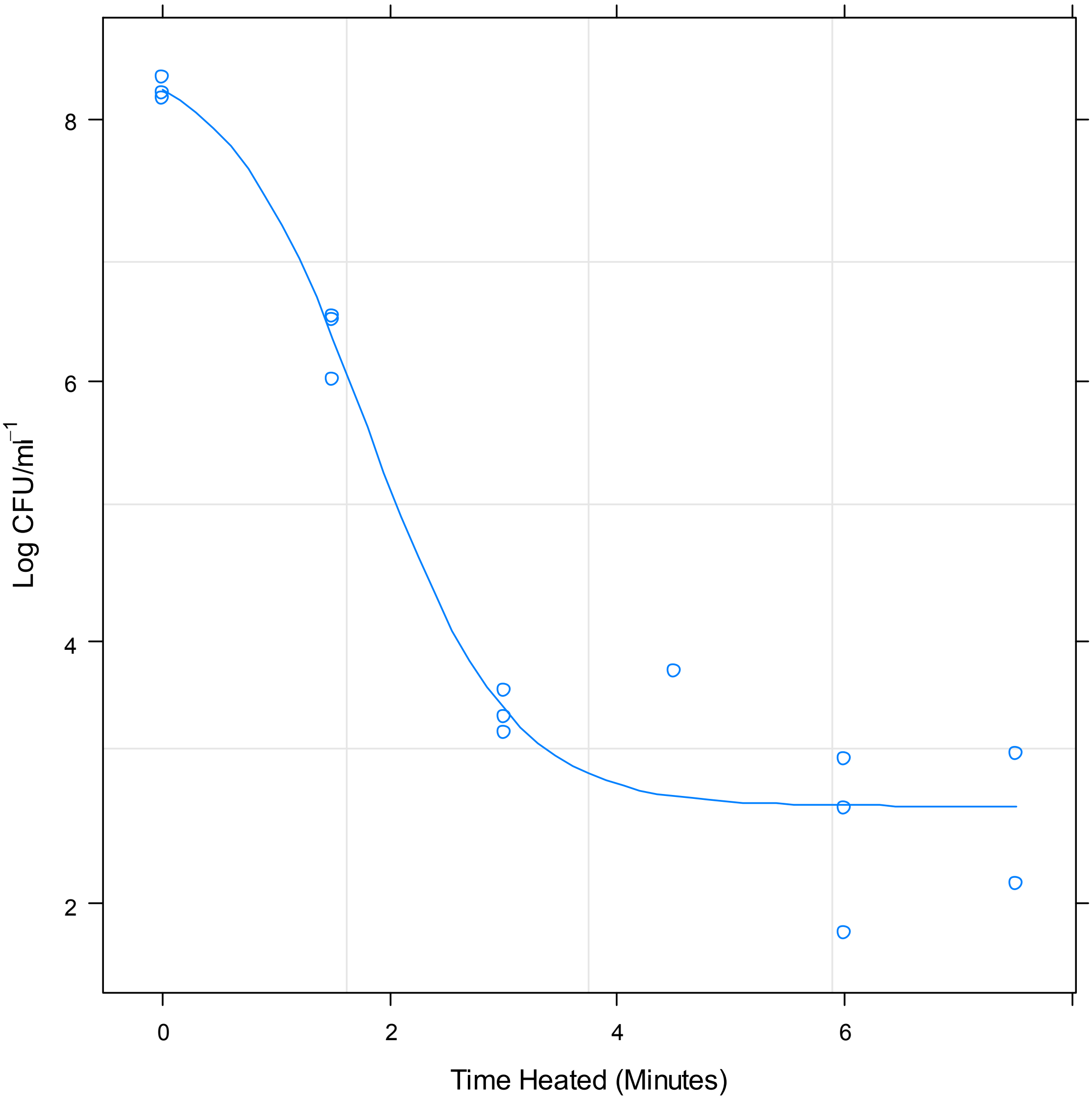

Figure 75. Plot illustrating predicted response curve using a four-parameter logistic regression model for strain 12610 (ST-825, CC-828) following heating at 60°C.

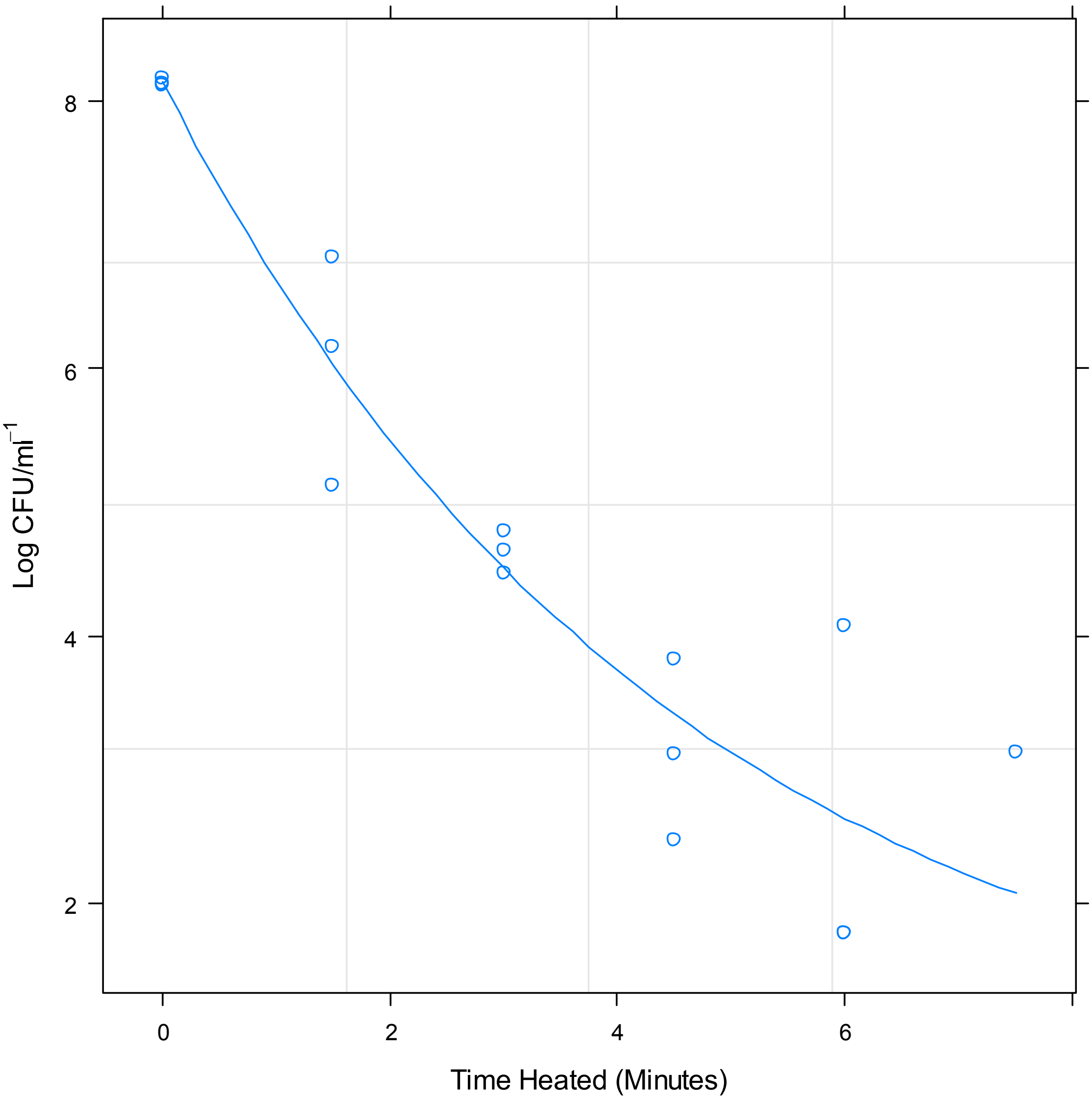

Figure 76. Plot illustrating predicted response curve using an asymptotic regression model for strain 12628 (ST-1773, CC-828) following heating at 60^{o}C.

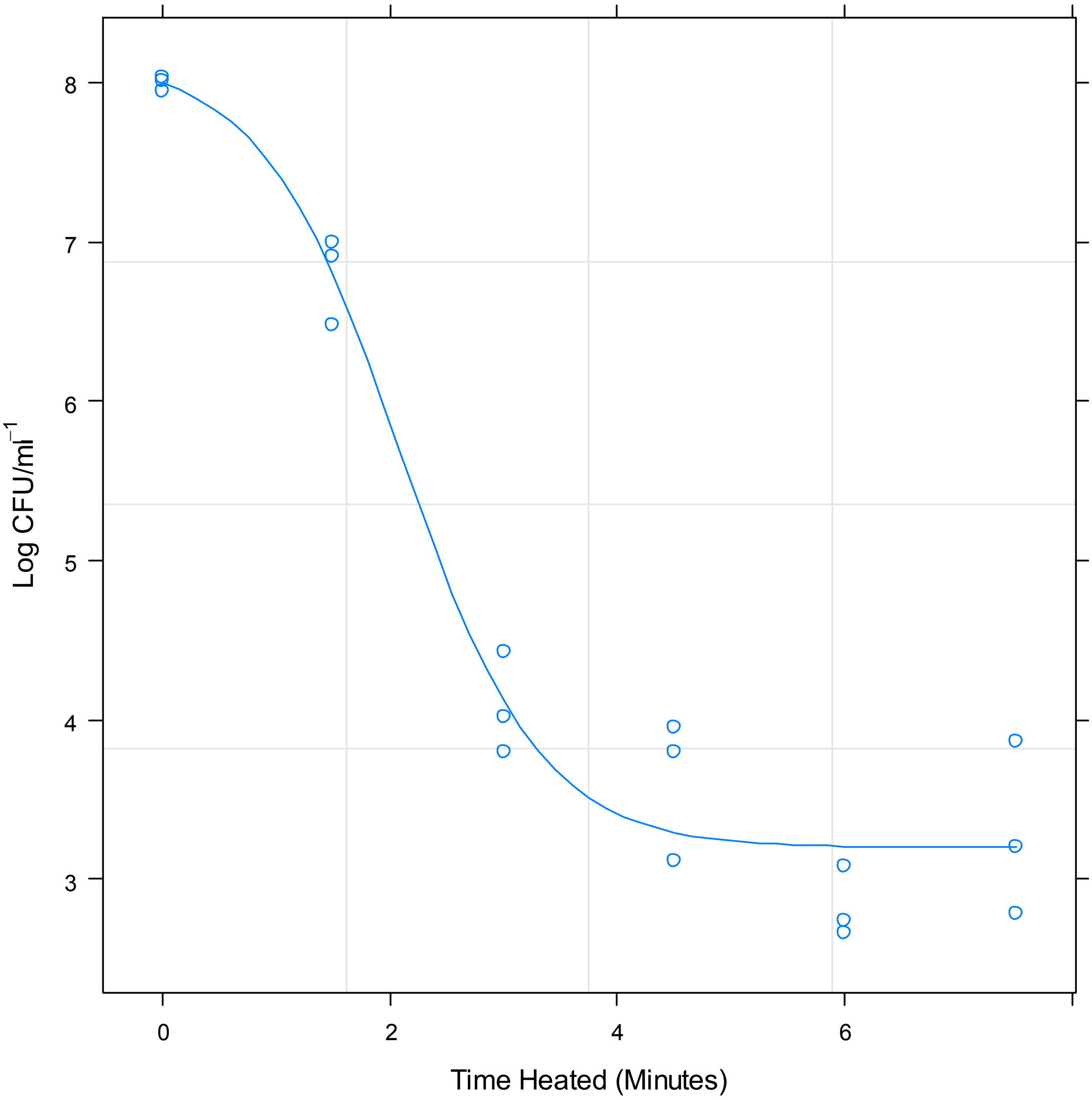

Figure 77. Plot illustrating predicted response curve using a four-parameter logistic regression model for strain 12645 (ST-51, CC-443) following heating at 60°C.

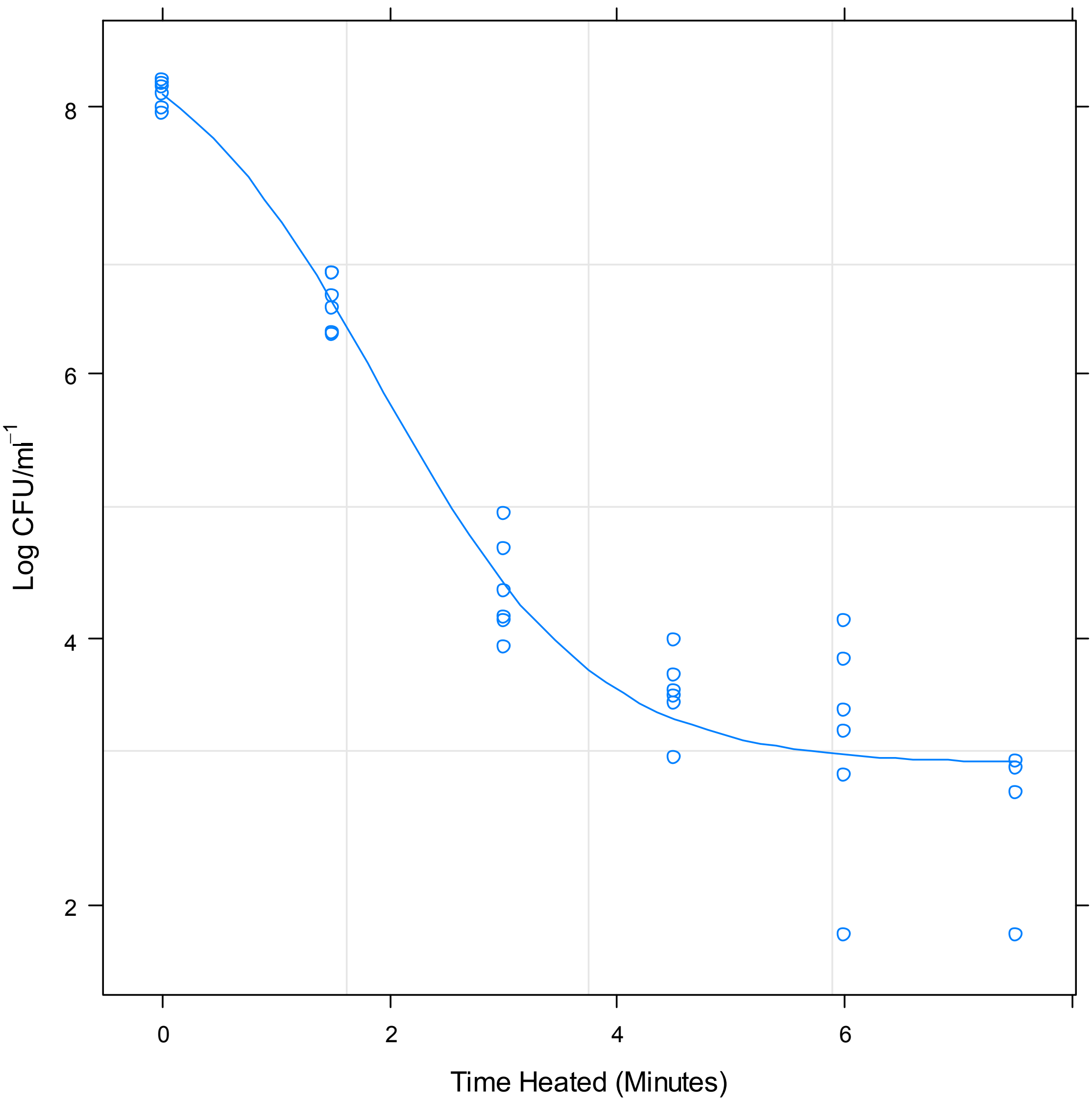

Figure 78. Plot illustrating predicted response curve using a four-parameter logistic regression model for strain 12662 (ST-257, CC-257) following heating at 60°C.

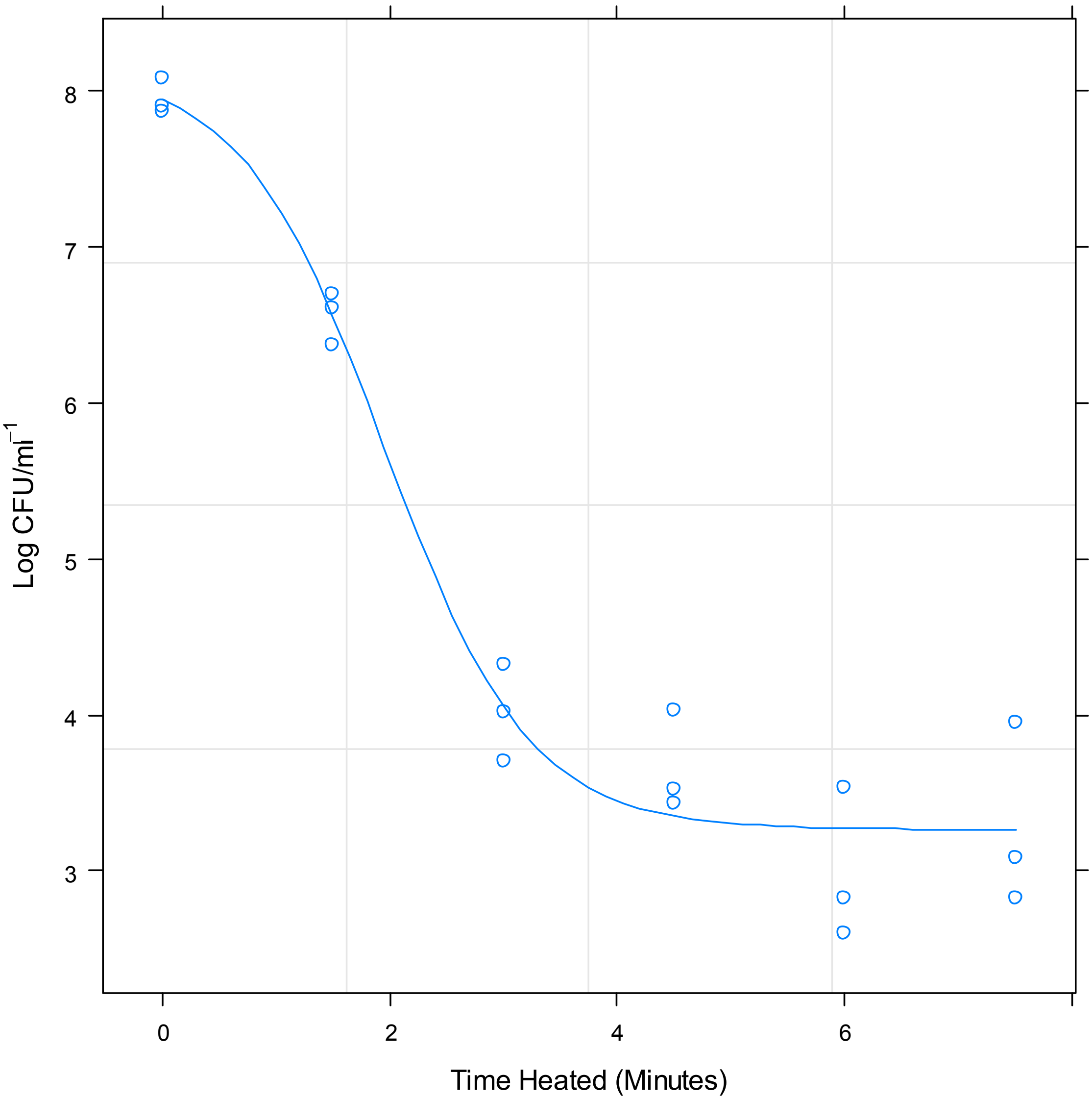

Figure 79. Plot illustrating the predicted response curve using a four-parameter logistic regression model for strain 12720 (ST-51, CC-443) following heating at 60°C.

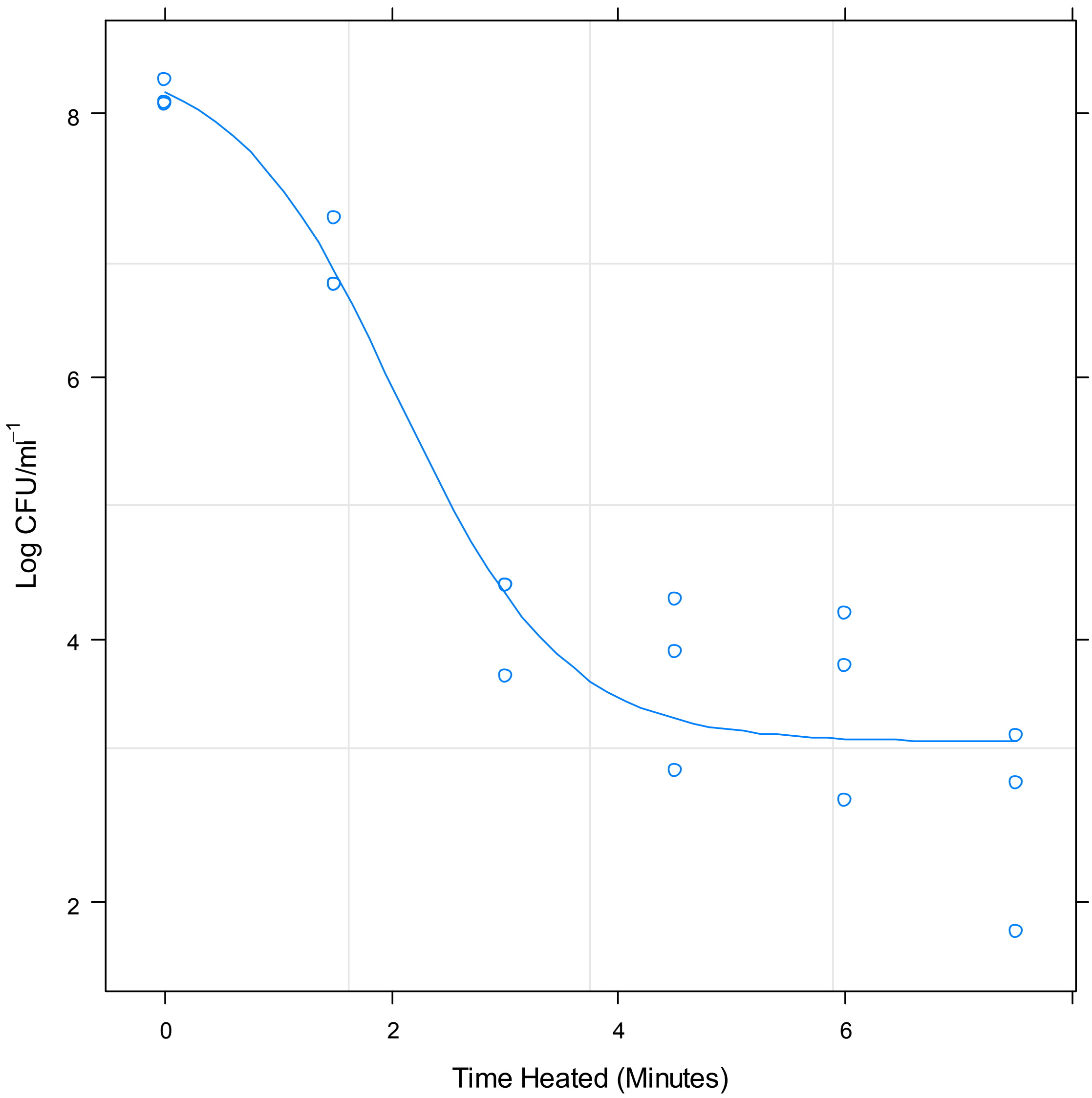

Figure 80. Plot illustrating predicted response curve using a four-parameter logistic regression model for strain 12745 (ST-257, CC-257) following heating at 60°C.

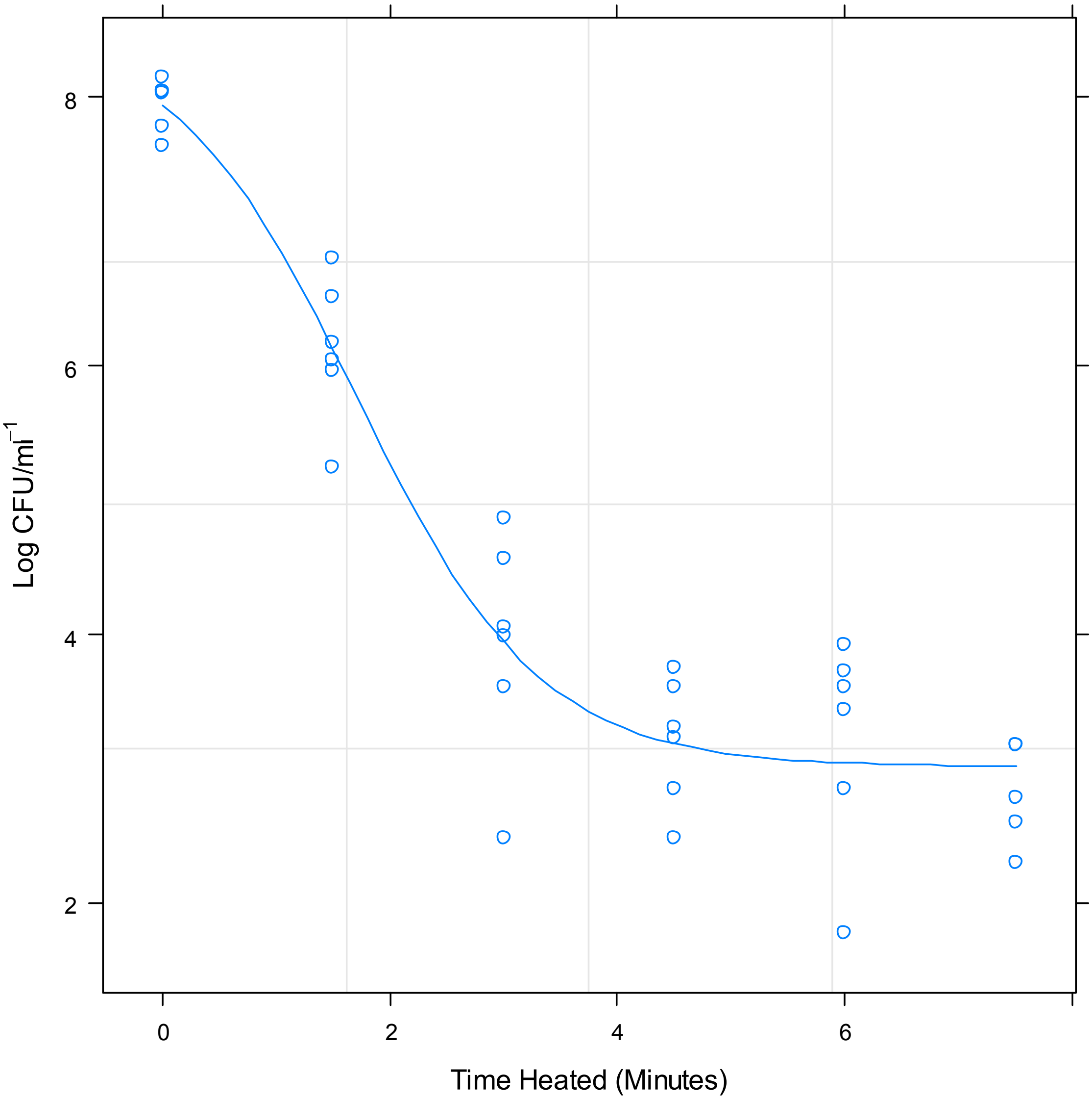

Figure 81. Plot illustrating predicted response curve using a four-parameter logistic regression model for strain 12783 (ST-574, CC-574) following heating at 60°C.

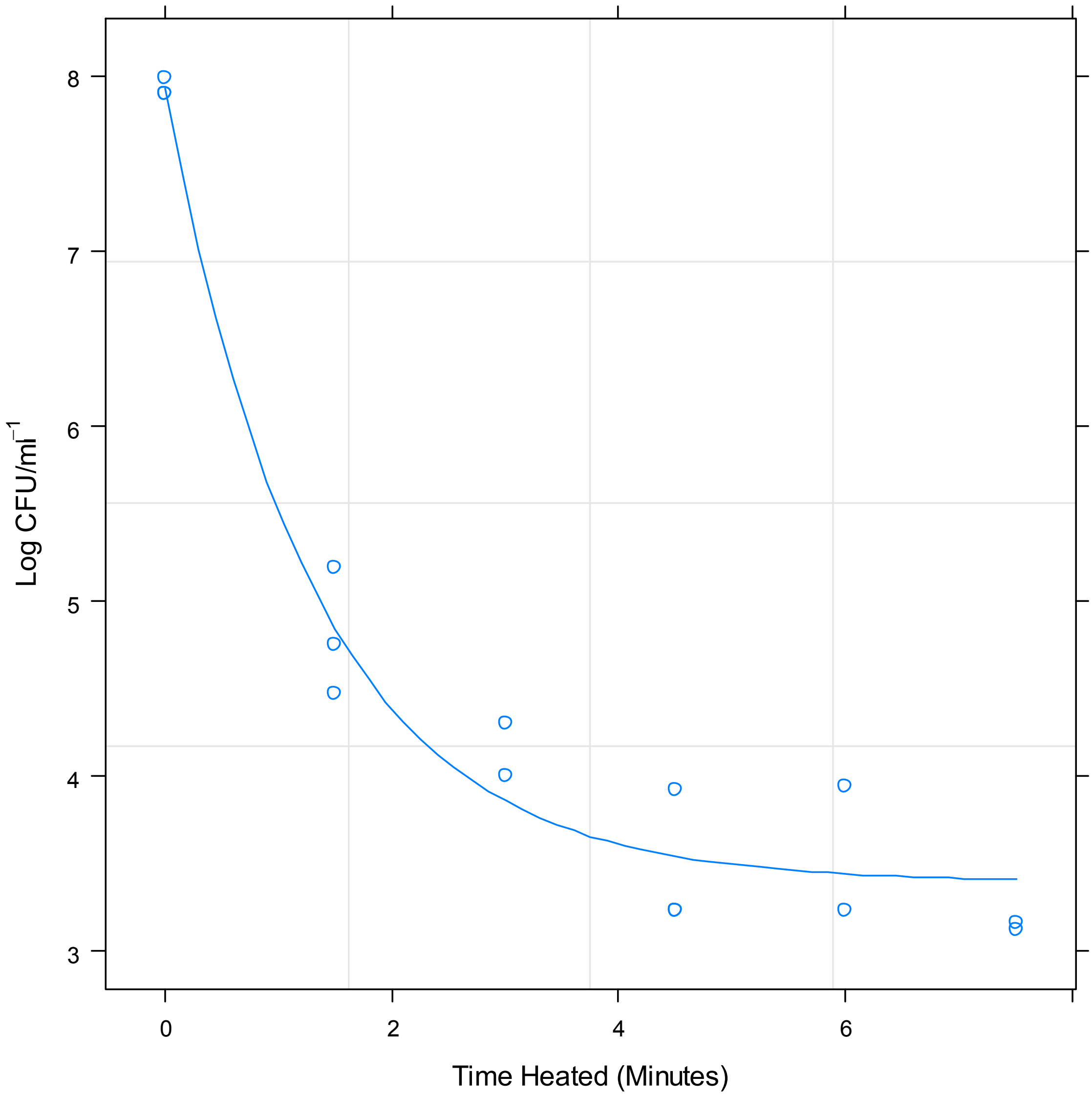

Figure 82. Plot illustrating predicted response curve using an asymptotic regression model for strain 13121 (ST-45, CC-45) following heating at 60°C.

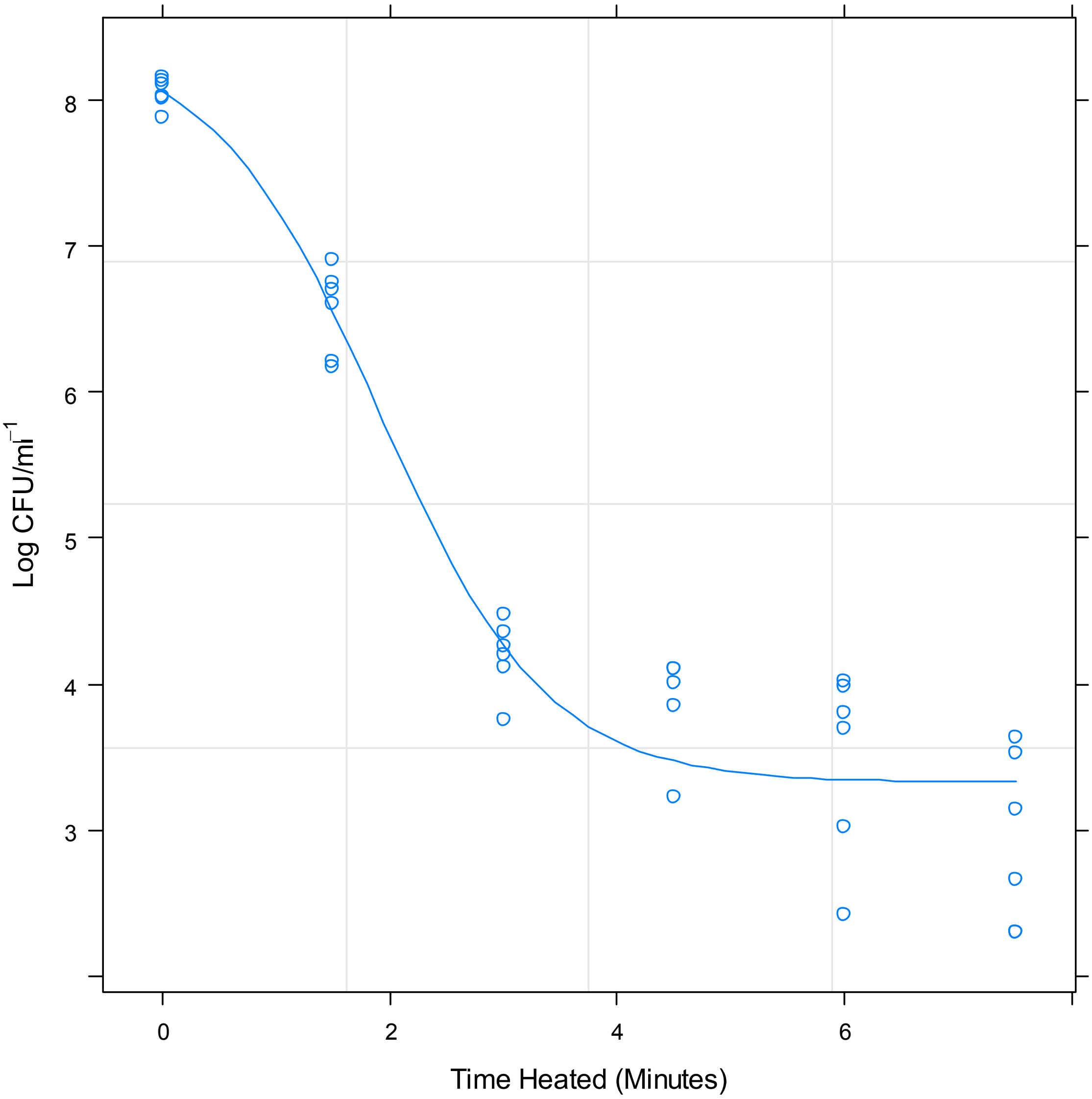

Figure 83. Plot illustrating predicted response curve using a four-parameter logistic regression model for strain 13126 (ST-21, CC-21) following heating at 60°C.

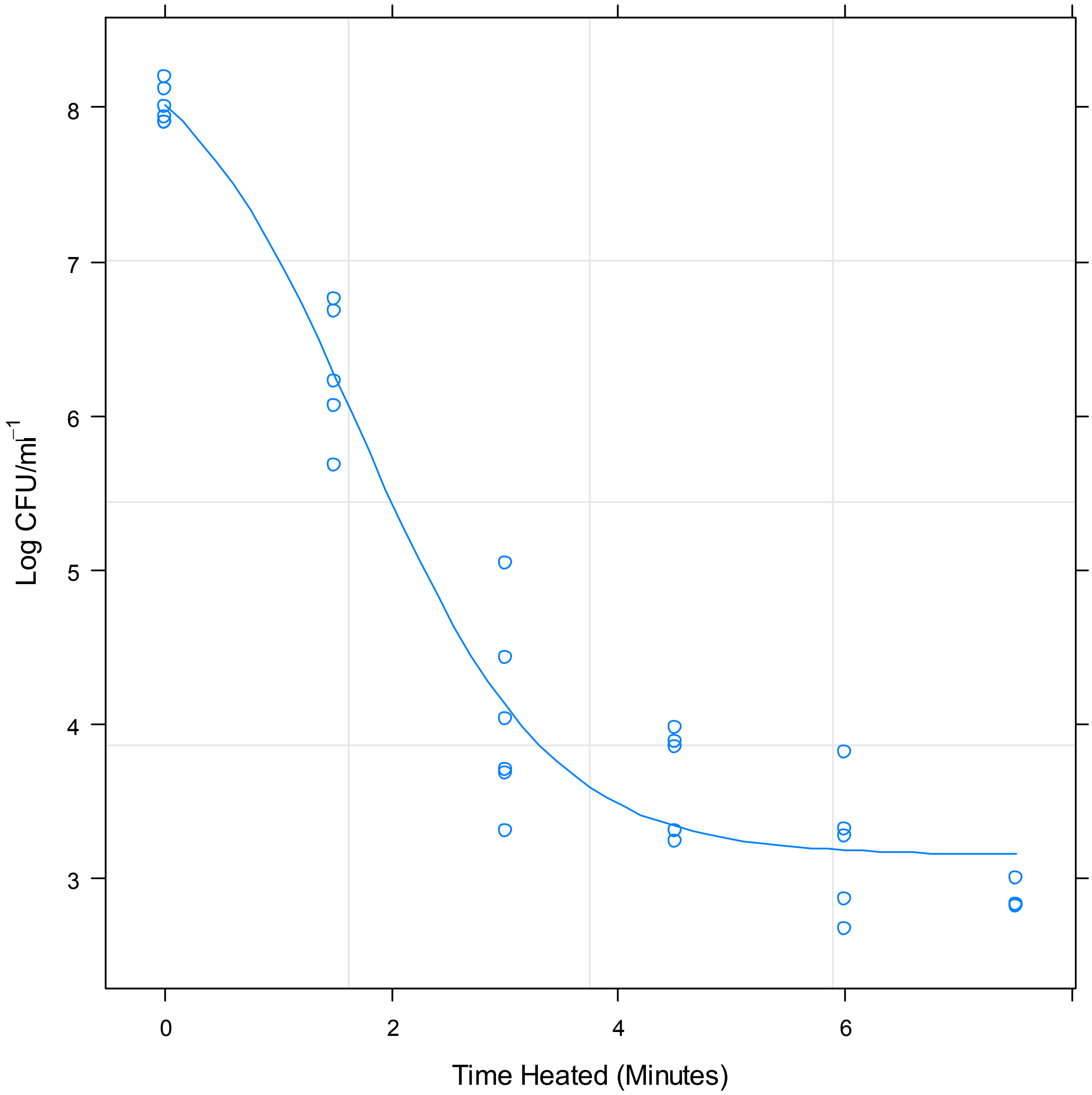

Figure 84. Plot illustrating predicted response curve using a four-parameter logistic regression model for strain 13136 (ST-45, CC-45) following heating at 60°C.

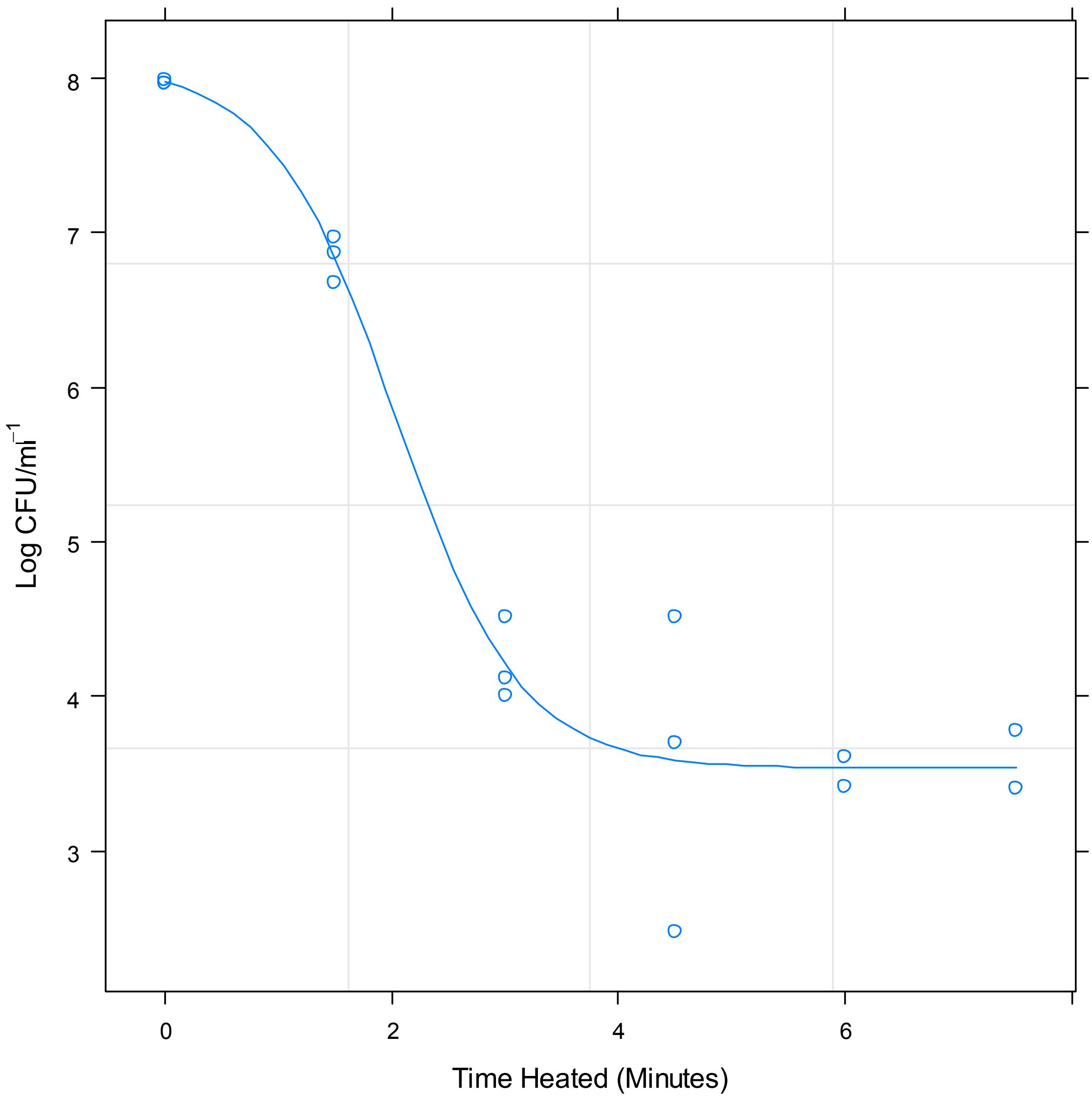

Figure 85. Plot illustrating predicted response curve using a four-parameter logistic regression model for strain 13163 (ST-21, CC-21) following heating at 60°C.

1.8.12 Time-Temperature Simulations: 60°C

Mixed Weibull Distribution Model Predicted Response Curves:

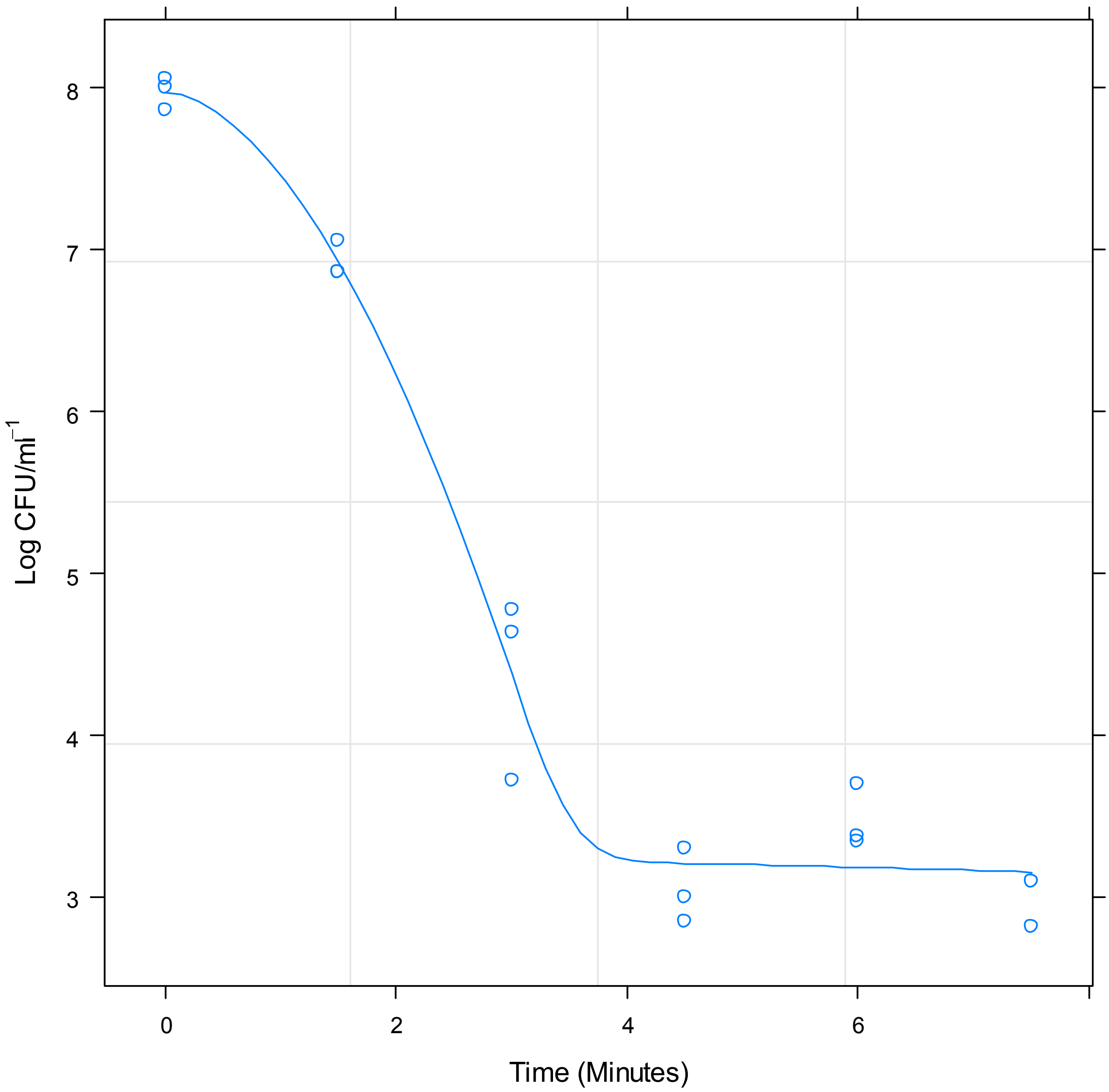

Figure 86. Plot illustrating predicted response curve using a mixed Weibull distribution model for strain 11368 (ST-574, CC-574) following heating at 60°C.

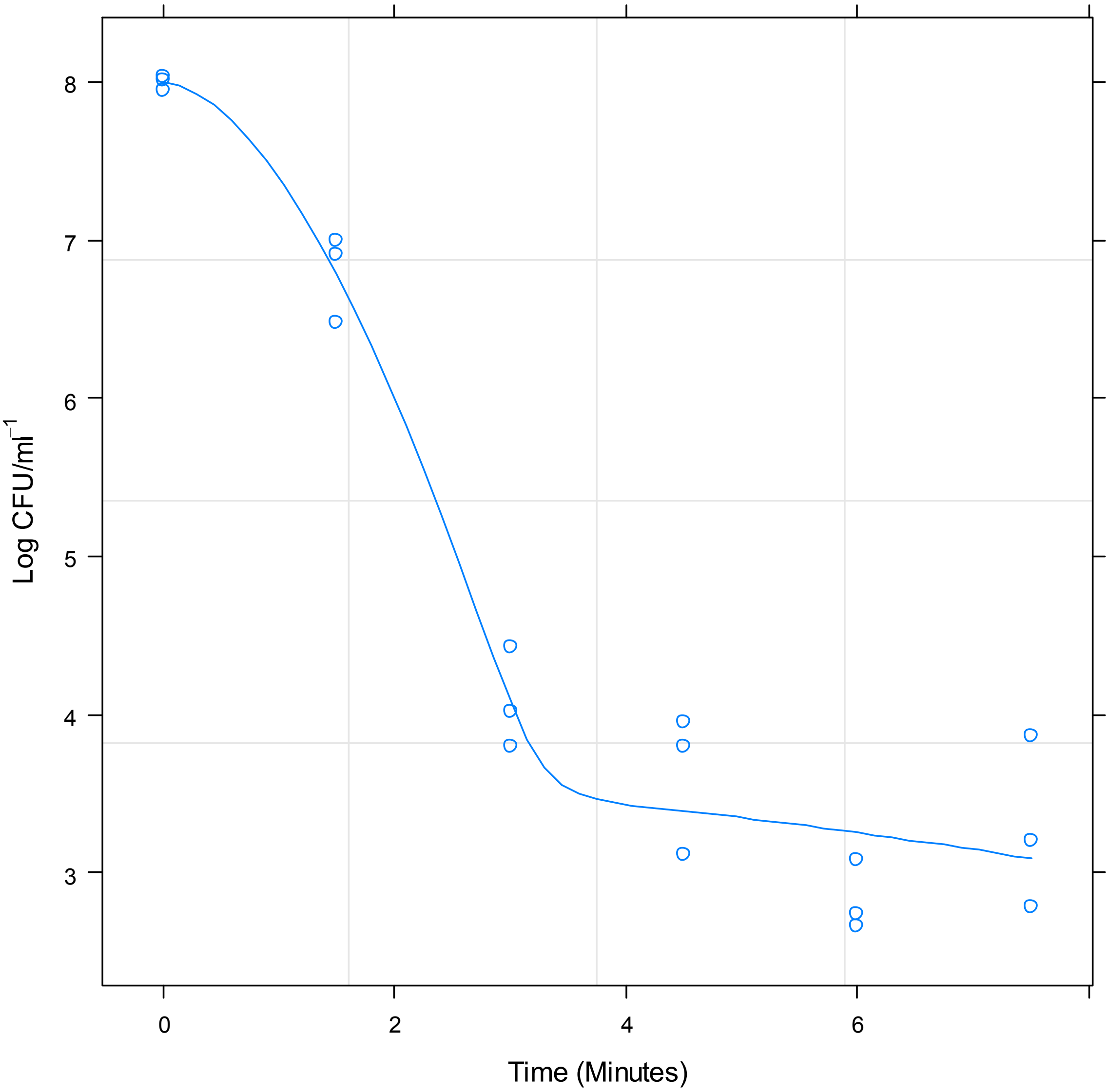

Figure 87. Plot illustrating predicted response curve using a mixed Weibull distribution model for strain 12645 (ST-51, CC-443) following heating at 60°C.

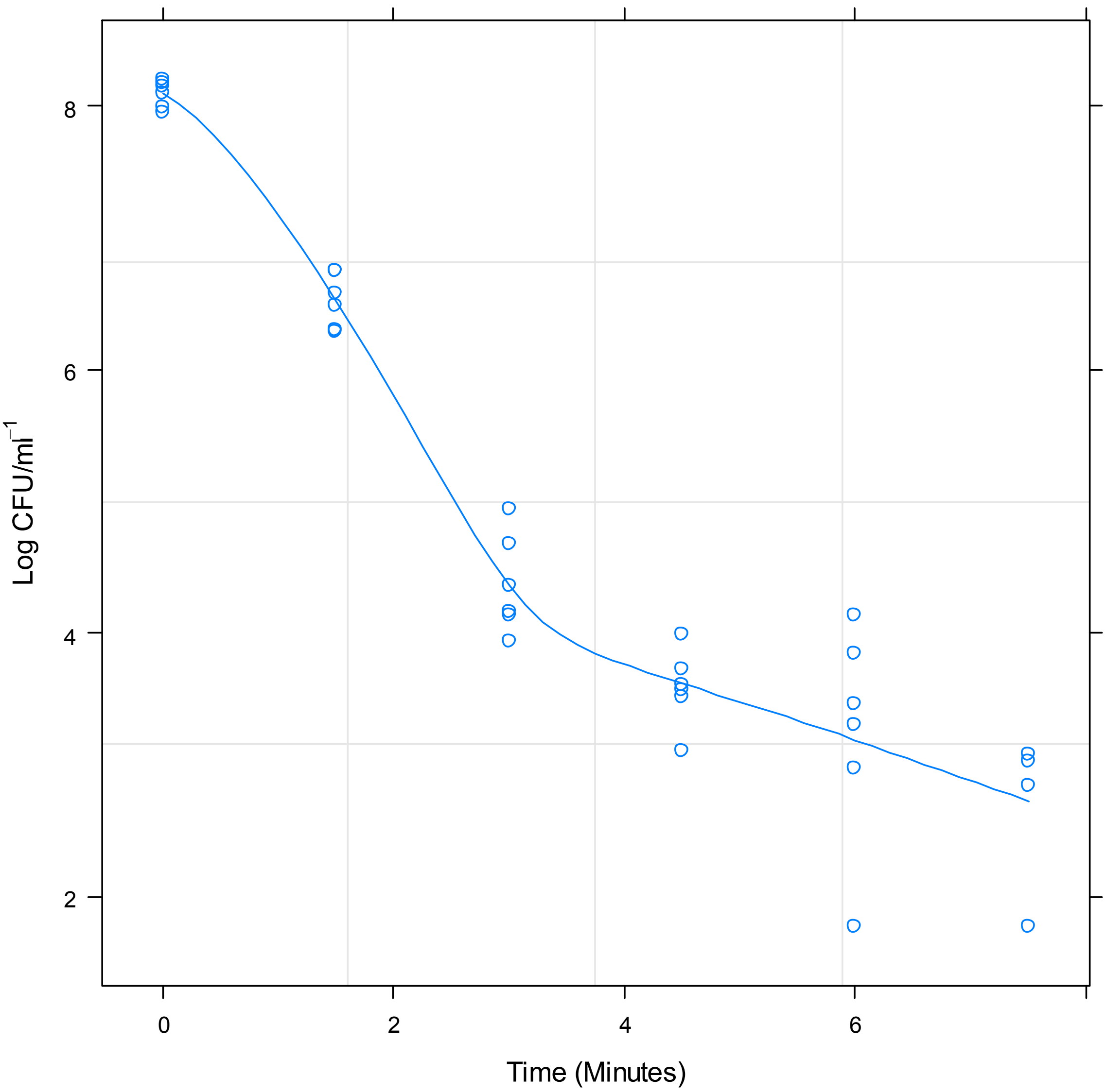

Figure 88. Plot illustrating predicted response curve using a mixed Weibull distribution model for strain 12662 (ST-257, CC-257) following heating at 60°C.

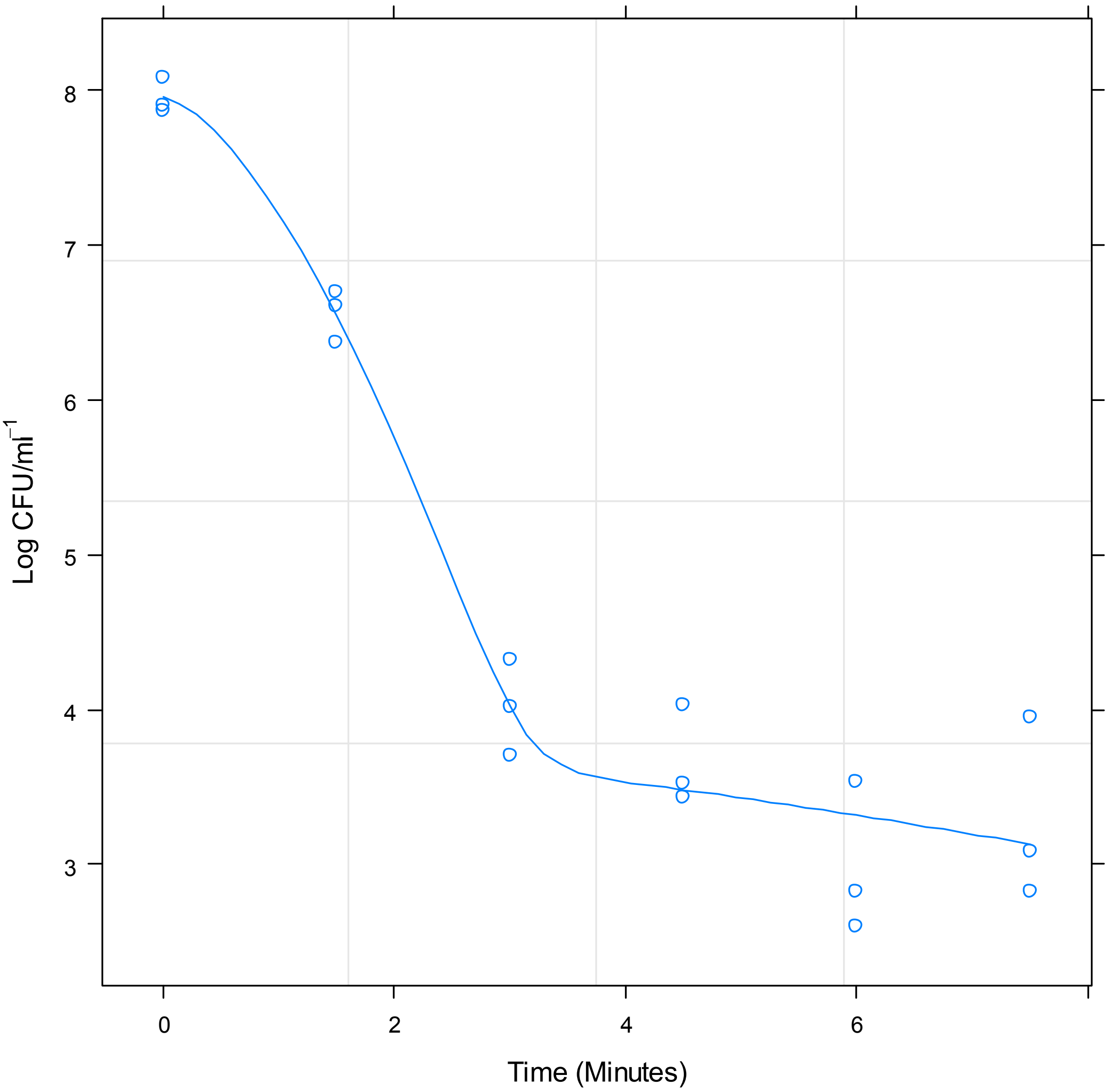

Figure 89. Plot illustrating the predicted response curve using a mixed Weibull distribution model for strain 12720 (ST-51, CC-443) following heating at 60°C.

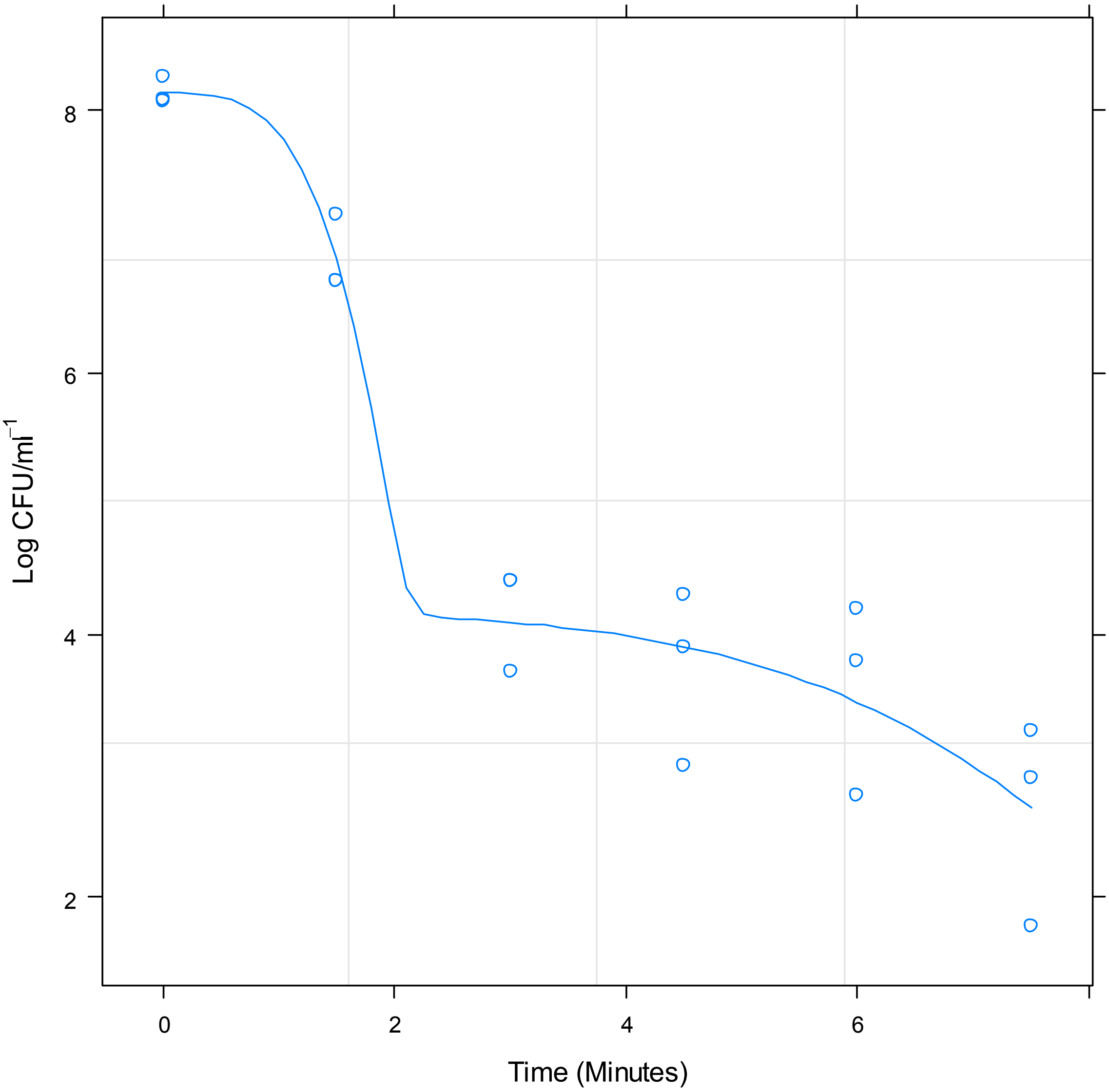

Figure 90. Plot illustrating predicted response curve using a mixed Weibull distribution model for strain 12745 (ST-257, CC-257) following heating at 60°C.

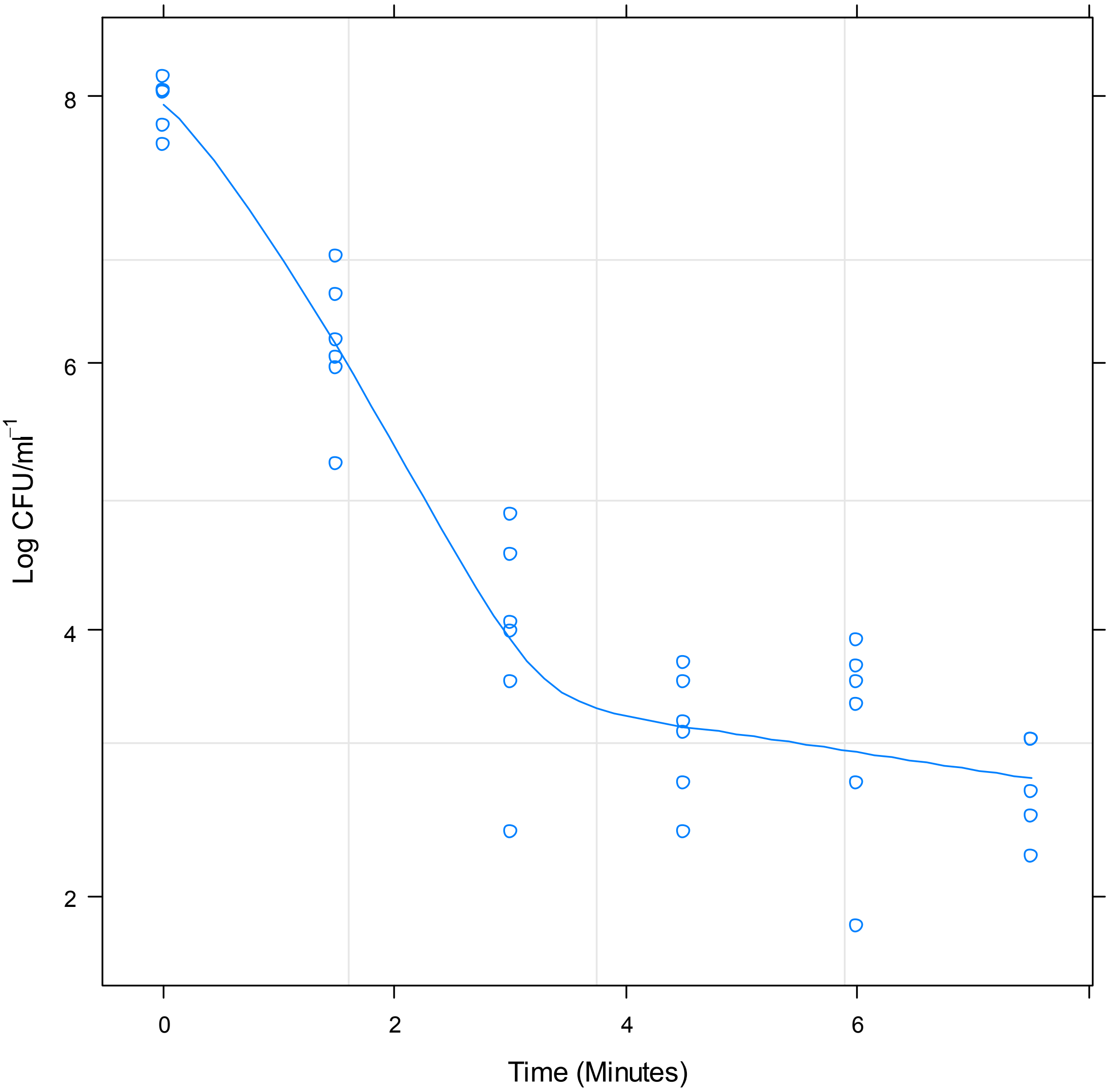

Figure 91. Plot illustrating predicted response curve using a mixed Weibull distribution model for strain 12783 (ST-574, CC-574) following heating at 60°C.

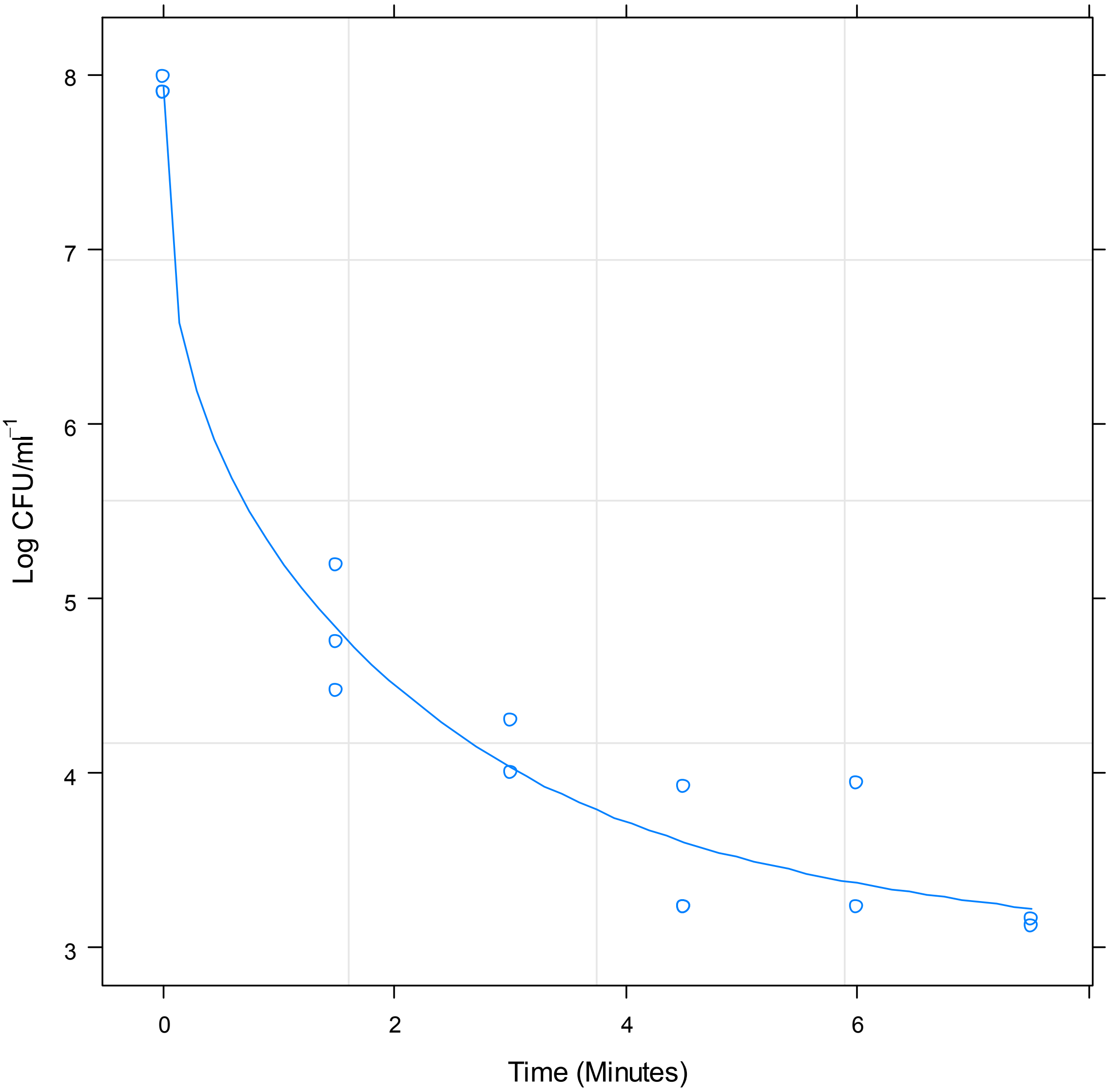

Figure 92. Plot illustrating predicted response curve using a mixed Weibull distribution model for strain 13126 (ST-21, CC-21) following heating at 60°C.

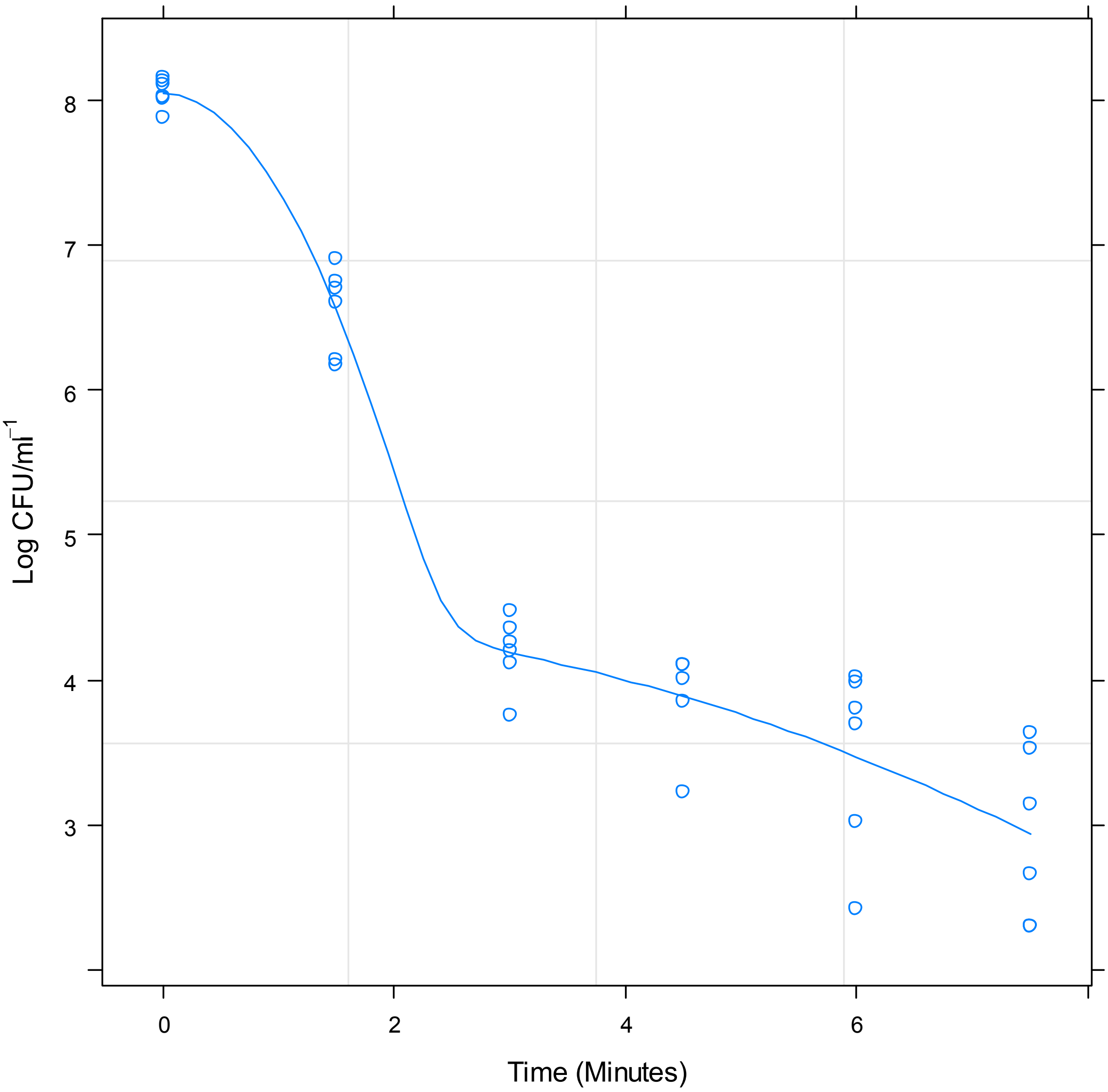

Figure 93. Plot illustrating predicted response curve using a mixed Weibull distribution model for strain 13126 (ST-21, CC-21) following heating at 60°C.

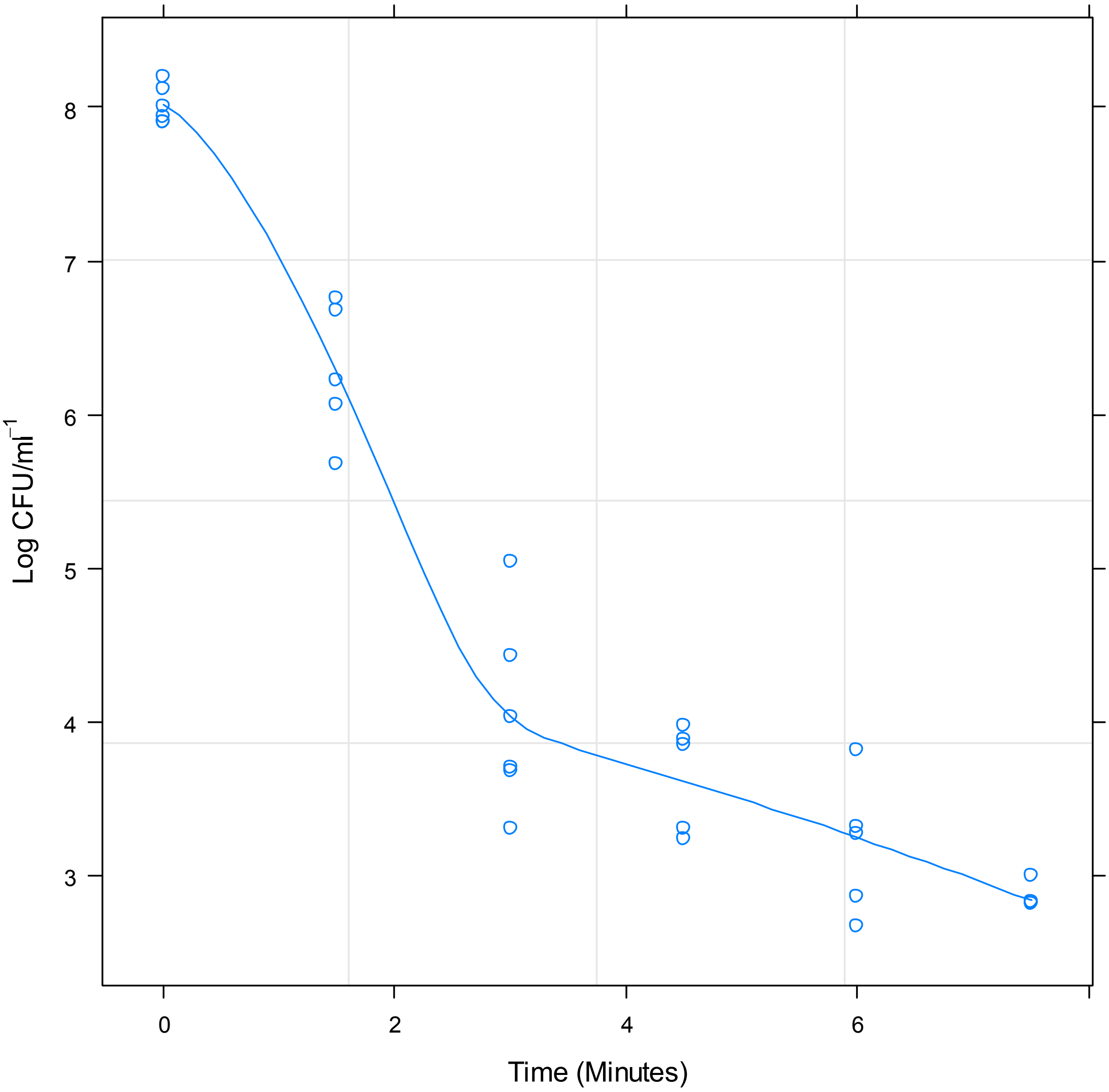

Figure 94. Plot illustrating predicted response curve using a mixed Weibull distribution model for strain 13136 (ST-45, CC-45) following heating at 60°C.

1.8.13 Time-Temperature Simulations: 64⁰C

Table 56. An assessment of the goodness of fit of models analysing the survival of each strain following heating at 64°C.

Strain	**Non-linear Function**	ρ_c
11253 (ST-825, CC-828)	Asymptotic Regression	0.936
11368 (ST-21, CC-21)	Asymptotic Regression	0.968
11762 (ST-829, CC-828)	Asymptotic Regression	0.955
12610 (ST-825, CC-828)	Asymptotic Regression	0.909
12628 (ST-1773, CC-828)	Asymptotic Regression	0.881
12662 (ST-257, CC-257)	Asymptotic Regression	0.926
12645 (ST-51, CC-443)	Asymptotic Regression	0.977
12720 (ST-51, CC-443)	Asymptotic Regression	0.903
12745 (ST-257, CC-257)	Asymptotic Regression	0.934
12783 (ST-574, CC-574)	Asymptotic Regression	0.906
13121 (ST-45, CC-45)	Asymptotic Regression	0.931
13126 (ST-21, CC-21)	Asymptotic Regression	0.932
13136 (ST-45, CC-45)	Asymptotic Regression	0.905
13163 (ST-574, CC-574)	Asymptotic Regression	0.561

Table 57. Asymptotic regression model analysing survival of strain 11253 (ST-825, CC-828) following heating at 64°C.

Parameter	**Estimate**	**Standard Error**	***t*-value**	***P*-value**
R0	8.011	0.038	208.090	0.000
Asymptote	1.966	0.371	5.292	0.000
LRC	0.075	0.142	0.528	0.605

Table 58. Asymptotic regression model analysing survival of strain 11368 (ST-574, CC-574) following heating at 64°C.

Parameter	**Estimate**	**Standard Error**	***t*-value**	***P*-value**
R0	7.972	0..052	152.437	0.000
Asymptote	2.909	0.235	12.374	0.000
LRC	0.425	0.194	2.192	0.047

Table 59. Asymptotic regression model analysing survival of strain 11762 (ST-829, CC-828) following heating at 64°C.

Parameter	Estimate	Standard Error	*t*-value	*P*-value
R0	8.119	0.037	220.688	0.000
Asymptote	2.054	0.321	6.393	0.000
LRC	0.055	0.172	0.375	0.712

Table 60. Asymptotic regression model analysing survival of strain 12610 (ST-825, CC-828) following heating at 64°C.

Parameter	Estimate	Standard Error	*t*-value	*P*-value
R0	8.222	0.060	137.731	0.000
Asymptote	1.854	0.464	3.995	0.001
LRC	0.059	0.208	0.286	0.778

Table 61. Asymptotic regression model analysing survival of strain 12628 (ST-1773, CC-828) following heating at 64°C.

Parameter	Estimate	Standard Error	*t*-value	*P*-value
R0	8.139	0.061	132.493	0.000
Asymptote	2.477	0.565	4.350	0.001
LRC	0.027	0.227	0.120	0.906

Table 62. Asymptotic regression model analysing survival of strain 12645 (ST-51, CC-443) following heating at 64°C.

Parameter	Estimate	Standard Error	*t*-value	*P*-value
R0	7.994	0.023	350.455	0.000
Asymptote	3.012	0.178	16.913	0.000
LRC	0.130	0.094	1.387	0.185

Table 63. Asymptotic regression model analysing survival of strain 12662 (ST-257, CC-257) following heating at 64°C.

Parameter	Estimate	Standard Error	*t*-value	*P*-value
R0	8.173	0.017	490.356	0.000
Asymptote	2.528	0.399	6.344	0.000
LRC	0.004	0.160	0.027	0.979

Table 64. Asymptotic regression model analysing survival of strain 12720 (ST-51, CC-443) following heating at 64°C.

Parameter	Estimate	Standard Error	*t*-value	*P*-value
R0	7.946	0.061	129.649	0.000
Asymptote	2.826	0.380	7.418	0.000
LRC	-0.171	0.188	-0.911	0.375

Table 65. Asymptotic regression model analysing survival of strain 12745 (ST-257, CC-257) following heating at 64°C.

Parameter	Estimate	Standard Error	*t*-value	*P*-value
R0	8.134	0.052	155.005	0.000
Asymptote	3.383	0.210	16.137	0.000
LRC	0.880	0.405	2.173	0.044

Table 66. Asymptotic regression model analysing survival of strain 12783 (ST-574, CC-574) following heating at 64°C.

Parameter	Estimate	Standard Error	*t*-value	*P*-value
R0	8.071	0.055	146.798	0.000
Asymptote	1.837	0.588	3.126	0.007
LRC	-0.036	0.195	-0.187	0.854

Table 67. Asymptotic regression model analysing survival of strain 13121 (ST-45, CC-45) following heating at 64°C.

Parameter	Estimate	Standard Error	*t*-value	*P*-value
R0	8.021	0.044	182.397	0.000
Asymptote	2.892	0.184	15.684	0.000
LRC	0.813	0.253	3.218	0.003

Table 68. Asymptotic regression model analysing survival of strain 13126 (ST-21, CC-21) following heating at 64°C.

Parameter	Estimate	Standard Error	*t*-value	*P*-value
R0	8.055	0.039	204.506	0.000
Asymptote	2.751	0.230	11.973	0.000
LRC	0.149	0.119	1.253	0.219

Table 69. Asymptotic regression model analysing survival of strain 13136 (ST-45, CC-45) following heating at 64^{o}C.

Parameter	**Estimate**	**Standard Error**	***t*-value**	***P*-value**
R0	8.009	0.055	145.333	0.000
Asymptote	2.496	0.310	8.043	0.000
LRC	0.118	0.166	0.712	0.482

Table 70. Asymptotic regression model analysing survival of strain 13163 (ST-21, CC-21) following heating at 64^{o}C.

Parameter	**Estimate**	**Standard Error**	***t*-value**	***P*-value**
R0	7.975	0.006	1378.543	0.000
Asymptote	3.027	0.364	8.328	0.000
LRC	0.562	0.298	1.887	0.078

1.8.14 Time-Temperature Profile 64^{0}C

Mixed Weibull Distribution Model:

Table 71. An assessment of the goodness of fit of mixed Weibull distribution models analysing the survival of each strain following heating at 64^{o}C.

Strain	**Non-linear Function**	ρ_c
11253 (ST-825, CC-828)	Mixed Weibull Distribution	0.947
11368 (ST-21, CC-21)	Mixed Weibull Distribution	
11762 (ST-828, CC-829)	Mixed Weibull Distribution	0.964
12610 (ST-825, CC-828)	Mixed Weibull Distribution	
12628 (ST-1773, CC-828)	Mixed Weibull Distribution	
12645 (ST-51, CC-443)	Mixed Weibull Distribution	
12662 (ST-257, CC-257)	Mixed Weibull Distribution	0.951
12720 (ST-51, CC-443)	Mixed Weibull Distribution	
12745 (ST-257, CC-257)	Mixed Weibull Distribution	
12783 (ST-574, CC-574)	Mixed Weibull Distribution	0.953
13121 (ST-45, CC-45)	Mixed Weibull Distribution	
13126 (ST-21, CC-21)	Mixed Weibull Distribution	0.950
13136 (ST-45, CC-45)	Mixed Weibull Distribution	0.940
13163 (ST-574,CC-574)	Mixed Weibull Distribution	

Table 72. Mixed Weibull distribution model analysing the survival of strain 11253 (ST-825, CC-828) following heating at 64^{o}C.

Parameter	**Estimate**	**Standard Error**	***t*-value**	***P*-value**
N0	8.011	0.486	16.491	0.000
δ1	0.535	0.465	1.152	0.269
δ2	4.657	2.454	1.898	0.079
p	2.238	3.074	0.728	0.479
α	5.101	1.049	4.863	0.000

Table 73. Mixed Weibull distribution model analysing the survival of strain 11762 (ST-829, CC-828) following heating at 64^{o}C.

Parameter	**Estimate**	**Standard Error**	***t*-value**	***P*-value**
N0	8.120	0.382	21.280	0.000
δ1	0.698	0.277	2.520	0.024
δ2	5.708	0.755	7.558	0.000
p	3.852	4.234	0.910	0.377
α	5.381	0.536	10.034	0.000

Table 74. Mixed Weibull distribution model analysing the survival of strain 12662 (ST-257, CC-257) following heating at 64°C.

Parameter	**Estimate**	**Standard Error**	***t*-value**	***P*-value**
N0	8.173	0.441	18.521	0.000
δ1	0.288	0.670	0.429	0.674
δ2	2.297	5.512	0.417	0.683
p	1.102	1.835	0.601	0.558
α	3.550	2.806	1.265	0.227

Table 75. Mixed Weibull distribution model analysing the survival of strain 12783 (ST-574, CC-574) following heating at 64°C.

Parameter	**Estimate**	**Standard Error**	***t*-value**	***P*-value**
N0	8.072	0.513	15.737	0.000
δ1	0.589	0.240	2.4504	0.029
δ2	3.946	1.501	2.630	0.021
p	2.615	1.924	1.359	0.197
α	4.654	0.948	4.907	0.000

Table 76. Mixed Weibull distribution model analysing the survival of strain 13126 (ST-21, CC-21) following heating at 64°C.

Parameter	**Estimate**	**Standard Error**	***t*-value**	***P*-value**
N0	8.056	0.288	27.978	0.000
δ1	0.251	0.648	0.388	0.701
δ2	2.672	6.394	0.418	0.679
p	1.001	1.738	0.576	0.569
α	3.677	2.394	1.536	0.135

Table 77. Mixed Weibull distribution model analysing the survival of strain 13136 (ST-45, CC-45) following heating at 64°C.

Parameter	**Estimate**	**Standard Error**	***t*-value**	***P*-value**
N0	8.011	0.334	23.982	0.000
δ1	0.506	0.282	1.795	0.083
δ2	3.915	1.670	2.344	0.026
p	2.095	1.549	1.353	0.187
α	4.203	0.793	5.298	0.000

1.8.15 Time-Temperature Simulations: 64°C

Predicted Response Curves Models:

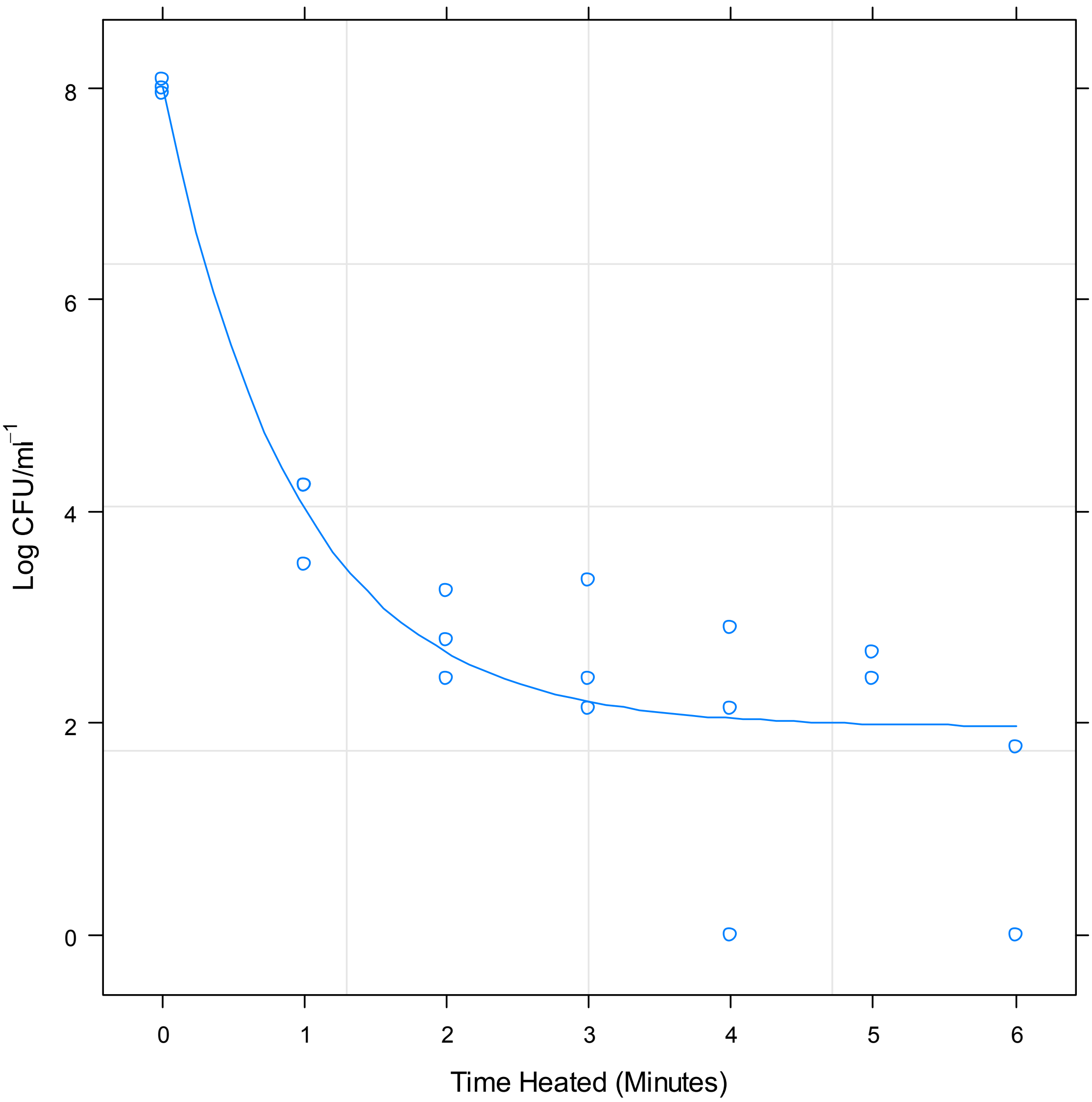

Figure 95. Plot illustrating predicted response curve using an asymptotic regression model for strain 11253 (ST-825, CC-828) following heating at 64°C.

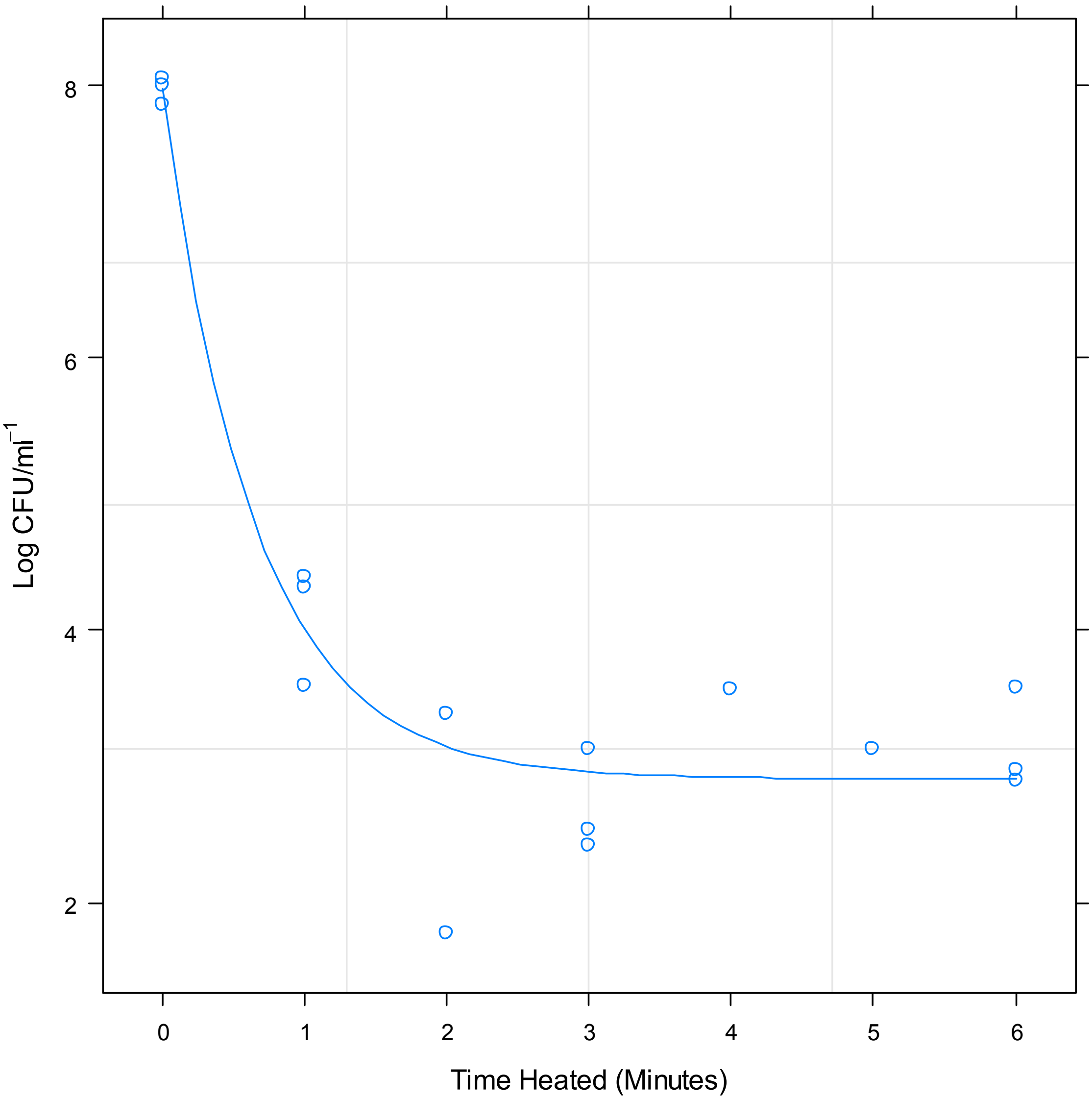

Figure 96. Plot illustrating predicted response curve using an asymptotic regression model for strain 11368 (ST-574, CC5-74) following heating at 64°C.

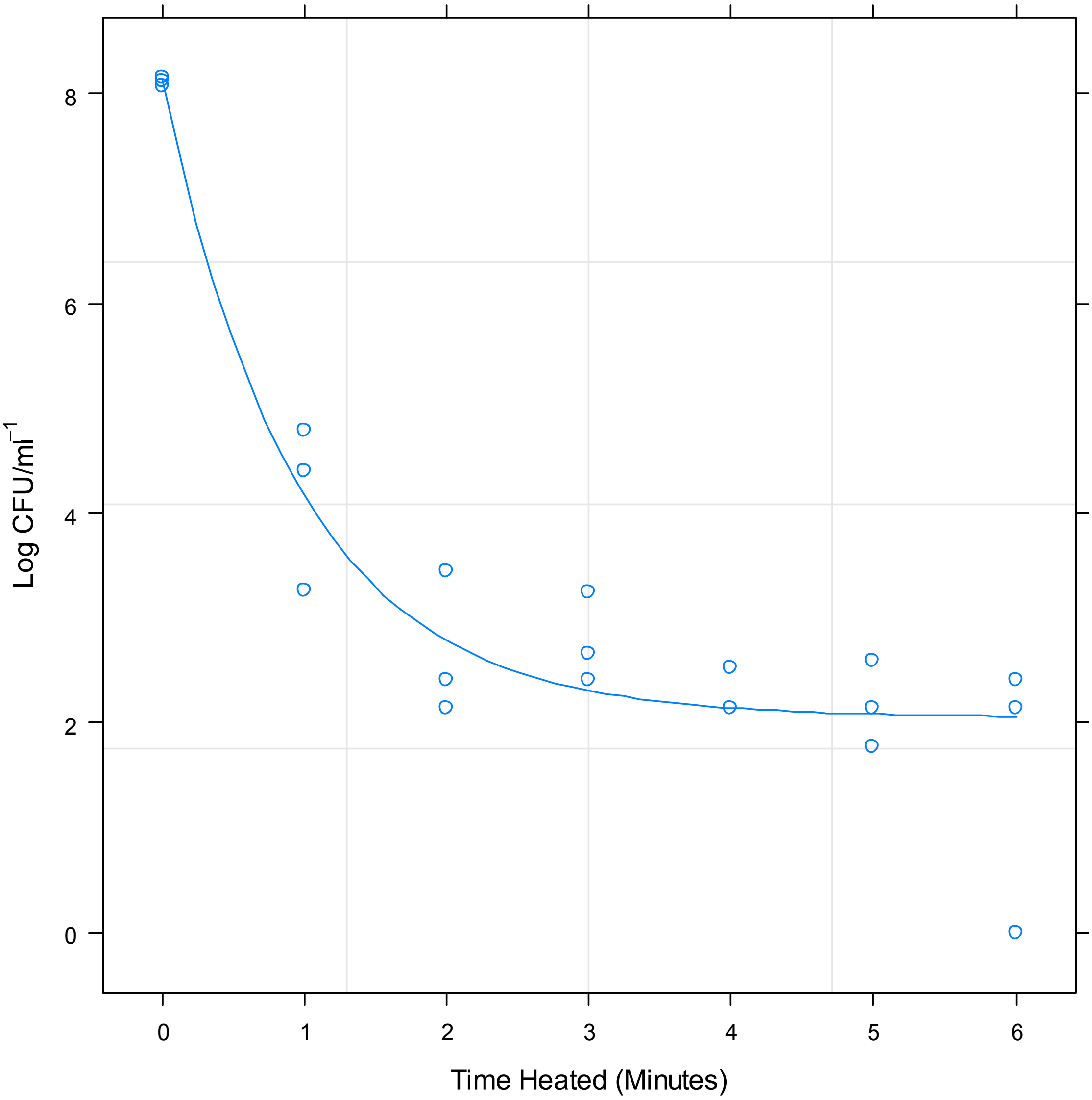

Figure 97. Plot illustrating predicted response curve using an asymptotic regression model for strain 11762 (ST-829, CC-828) following heating at 64°C.

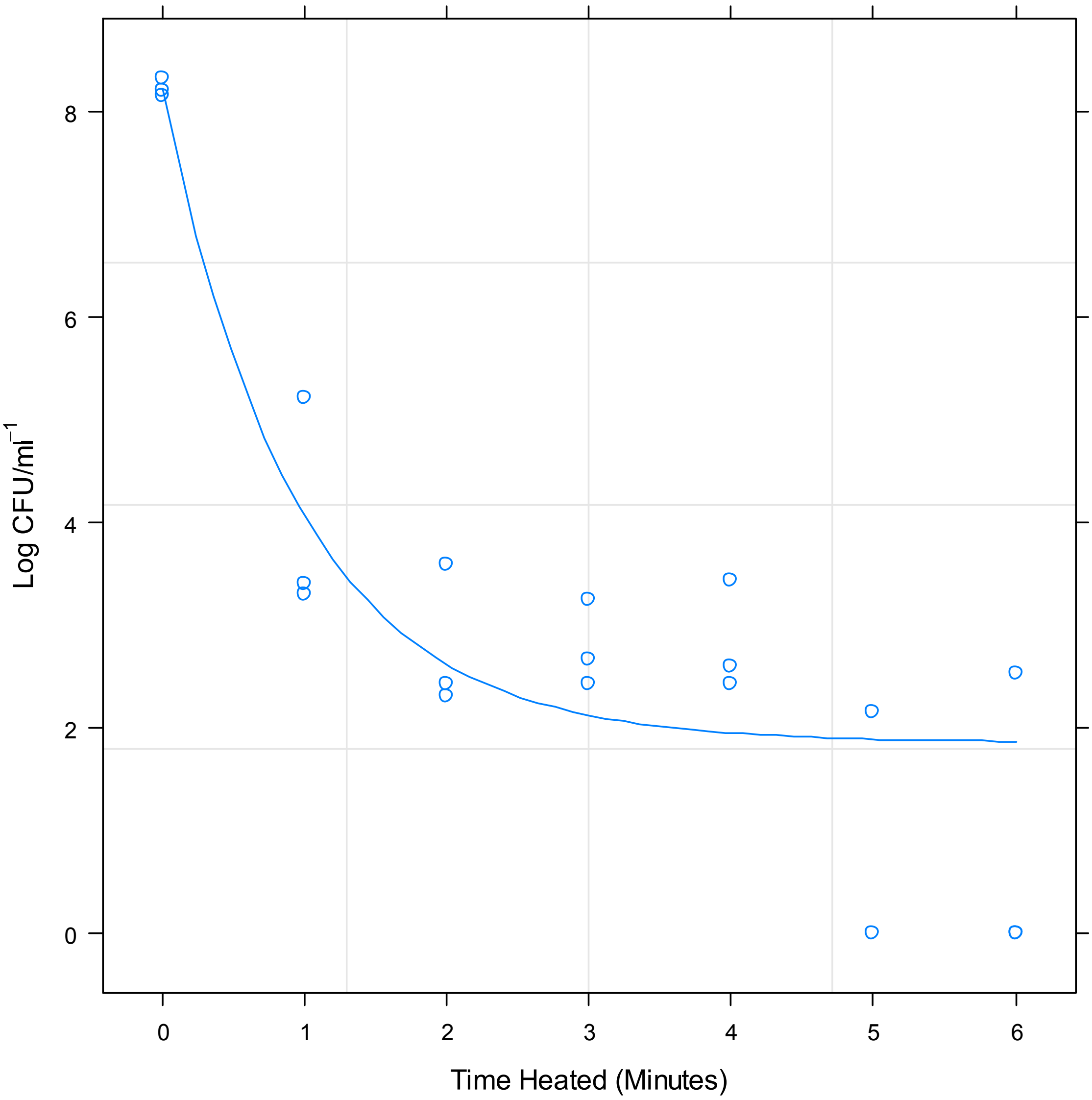

Figure 98. Plot illustrating predicted response curve using an asymptotic regression model for strain 12610 (ST-825, CC-828) following heating at 64°C.

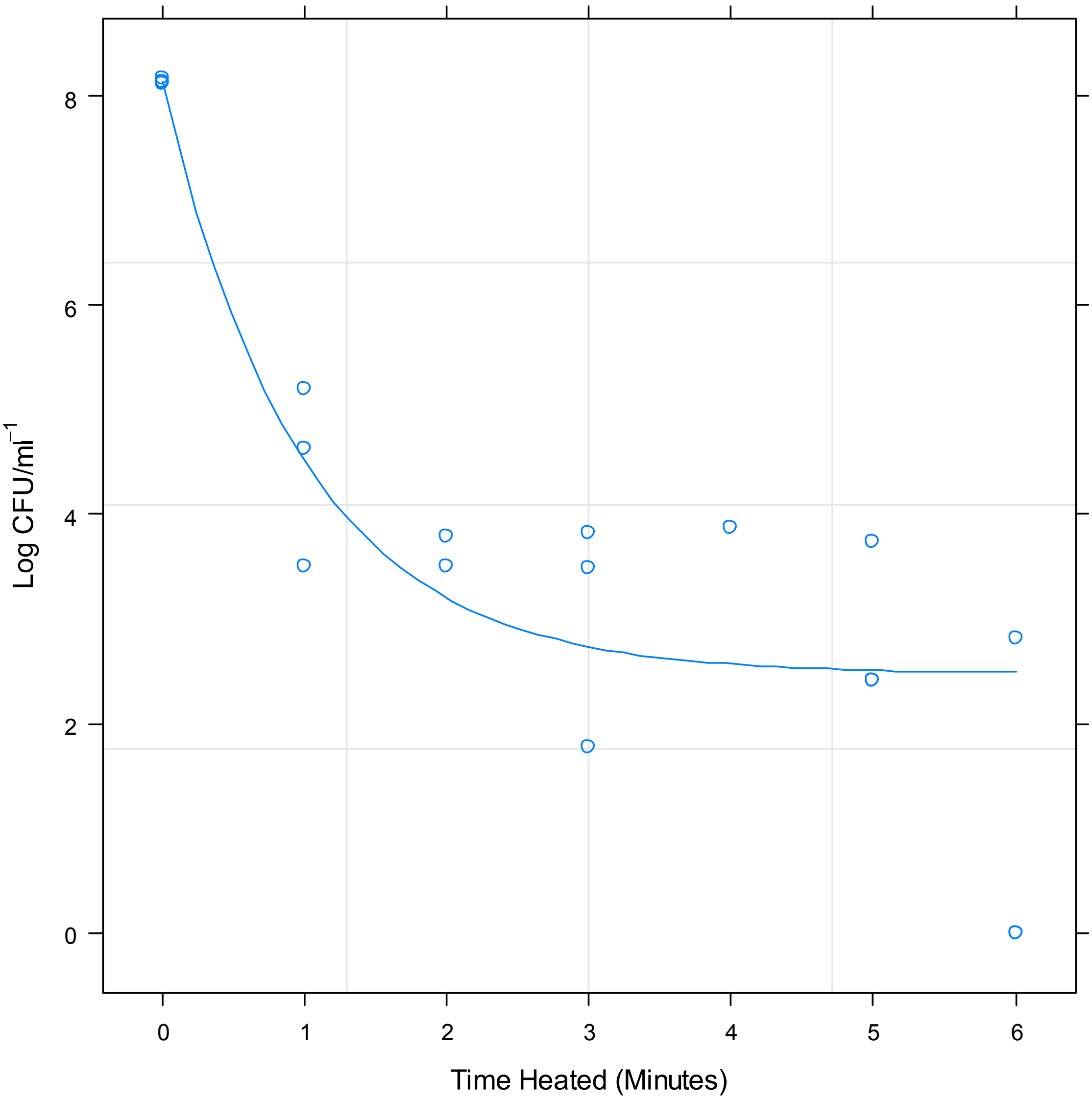

Figure 99. Plot illustrating predicted response curve using an asymptotic regression model for strain 12628 (ST-1773, CC-828) following heating at 64°C.

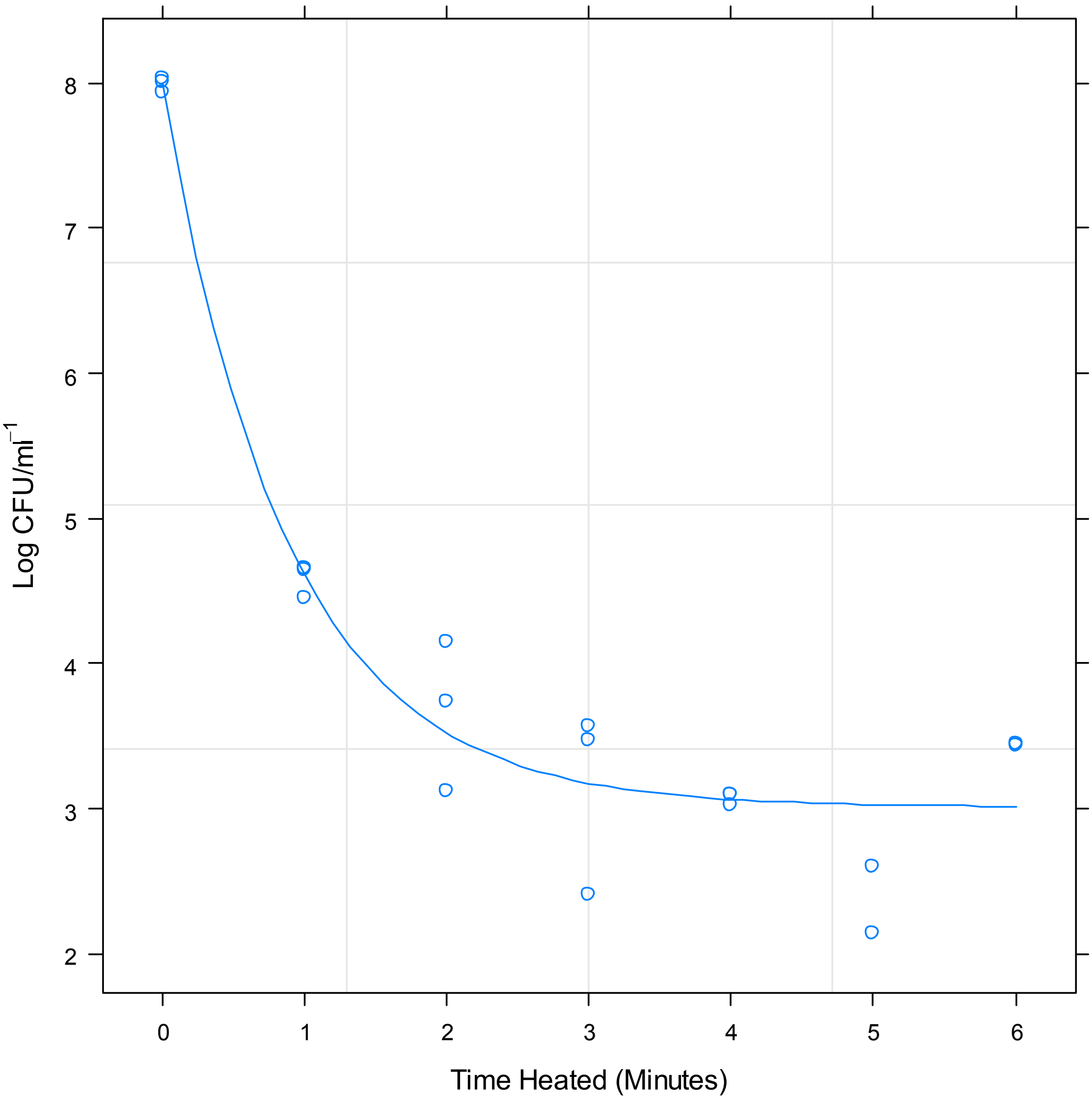

Figure 100. Plot illustrating predicted response curve using an asymptotic regression model for strain 12645 (ST-51, CC-443) following heating at 64°C.

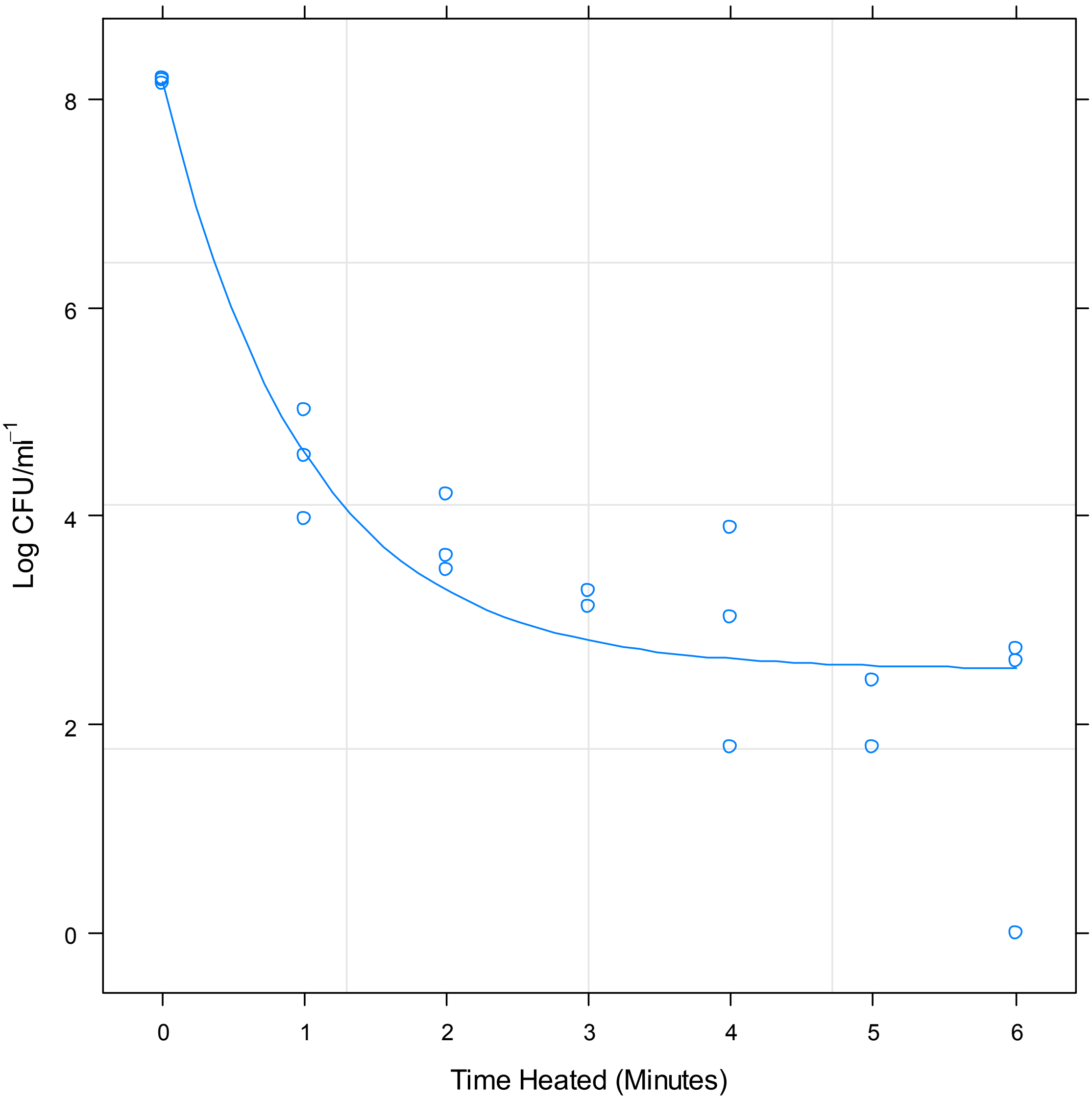

Figure 101. Plot illustrating predicted response curve using an asymptotic regression model for strain 12662 (ST-257, CC-257) following heating at 64°C.

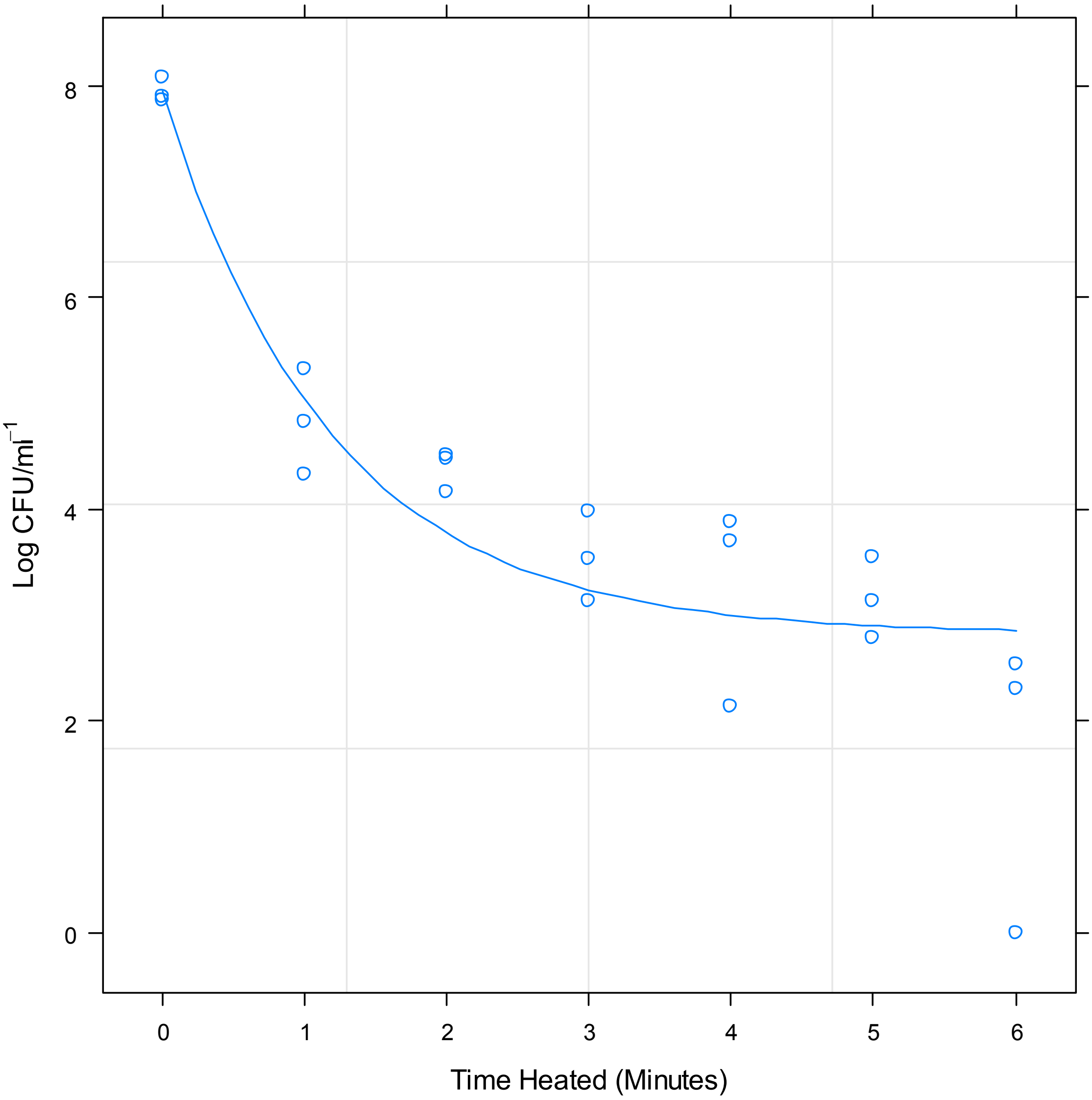

Figure 102. Plot illustrating the predicted response curve using an asymptotic regression model for strain 12720 (ST-51, CC-443) following heating at 64°C.

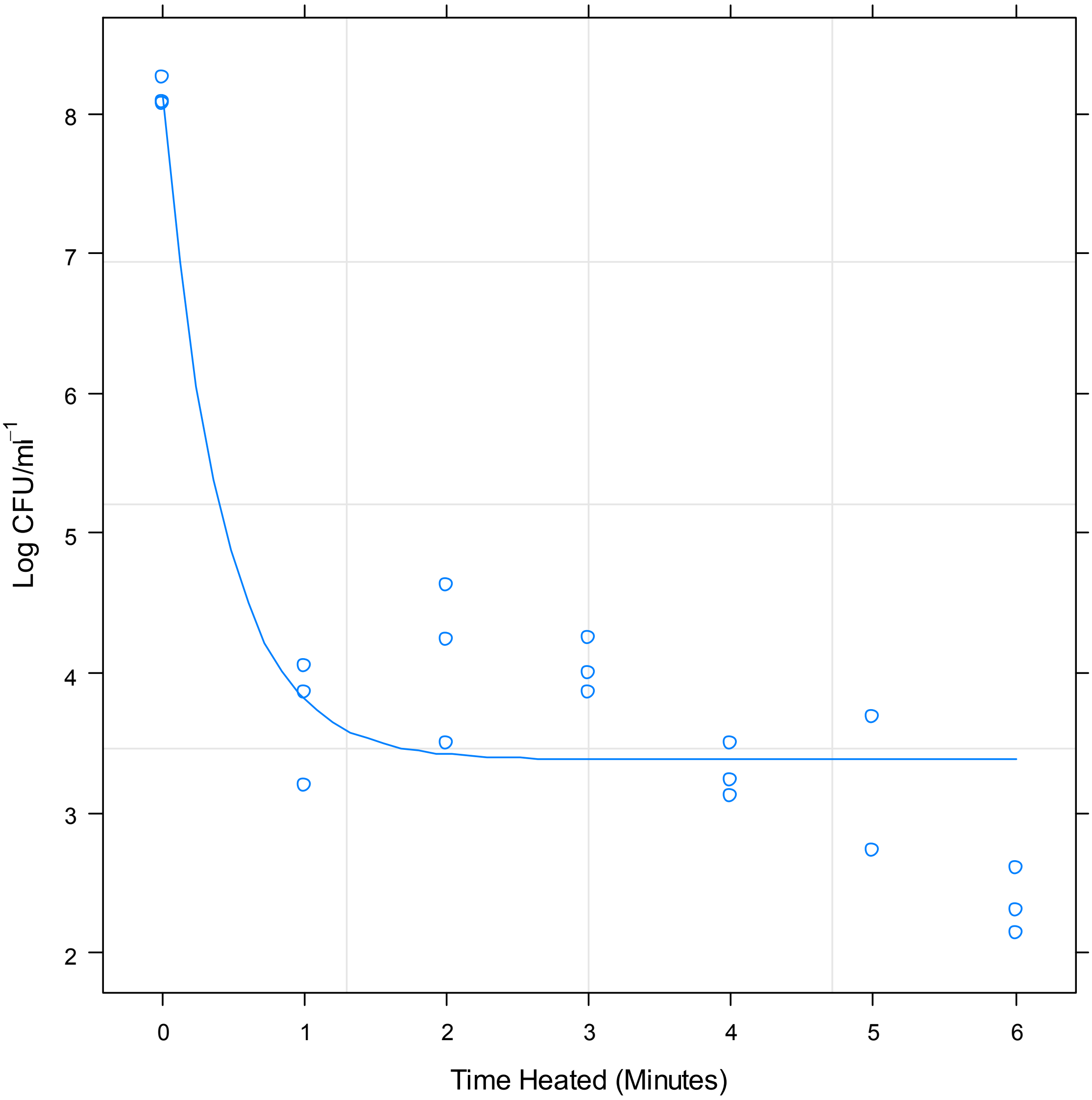

Figure 103. Plot illustrating predicted response curve using an asymptotic regression model for strain 12745 (ST-257, CC-257) following heating at 64°C.

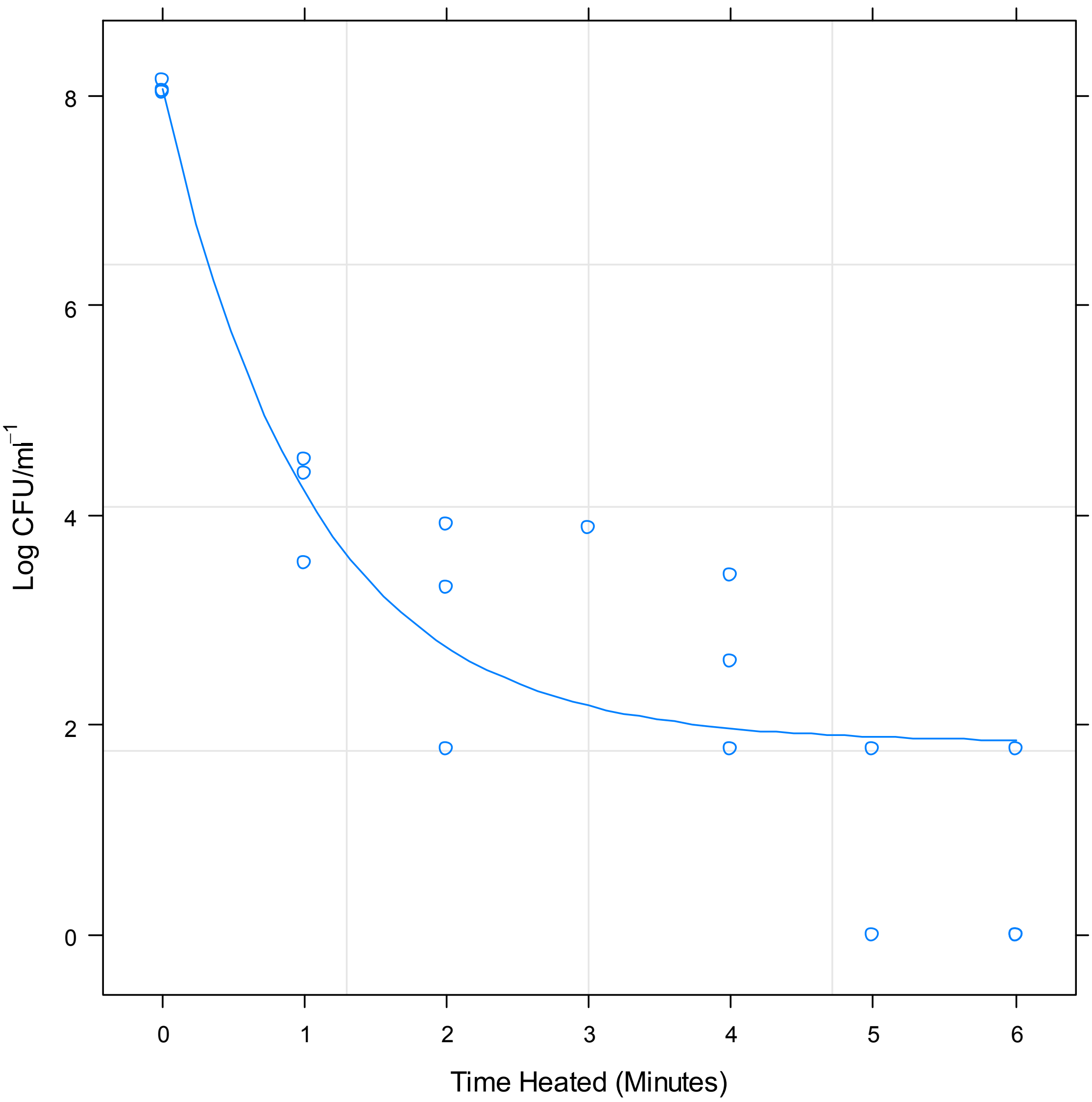

Figure 104. Plot illustrating predicted response curve using an asymptotic regression model for strain 12783 (ST-574, CC-574) following heating at 64°C.

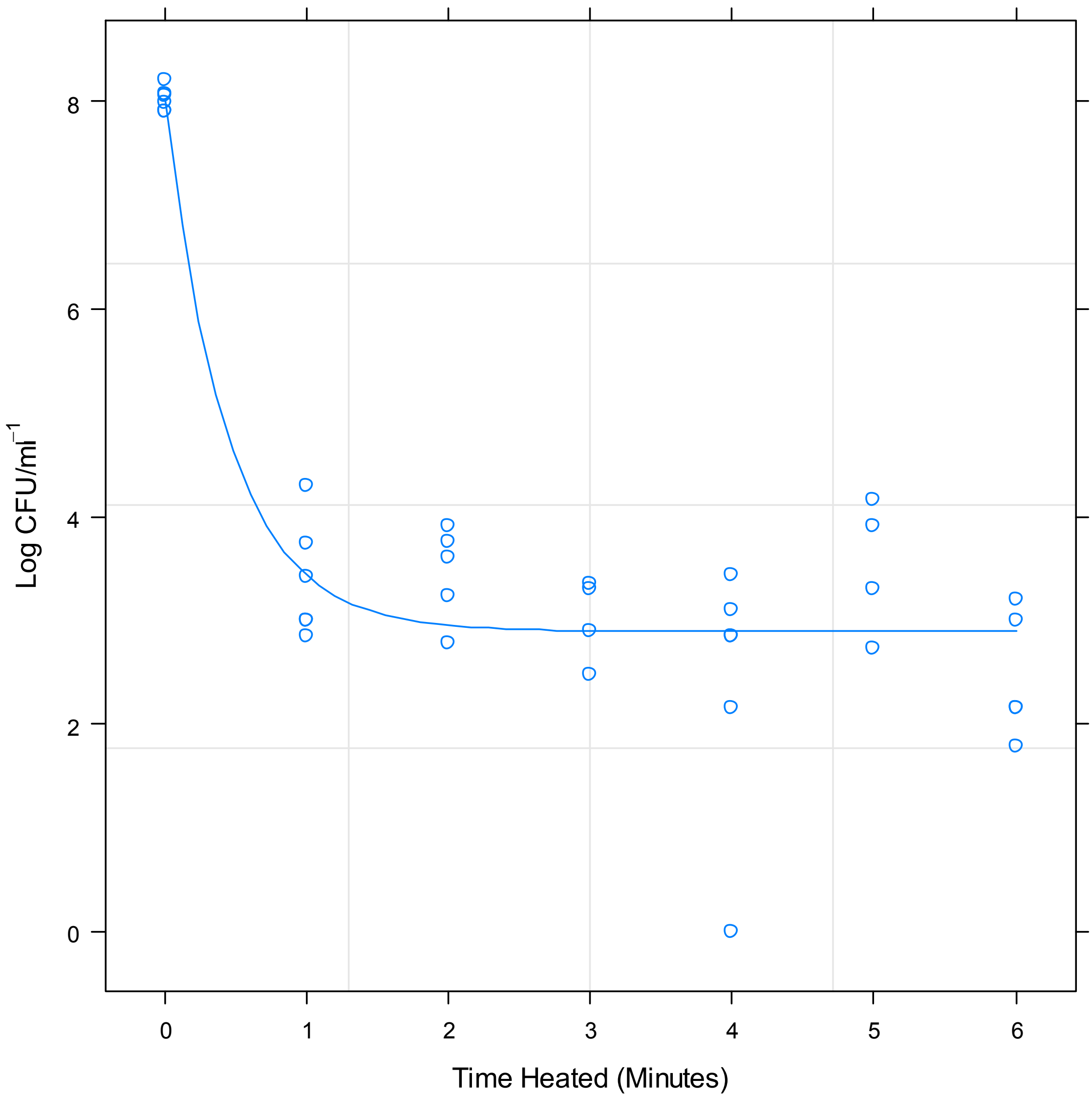

Figure 105. Plot illustrating predicted response curve using an asymptotic regression model for strain 13121 (ST-45, CC-45) following heating at 64°C.

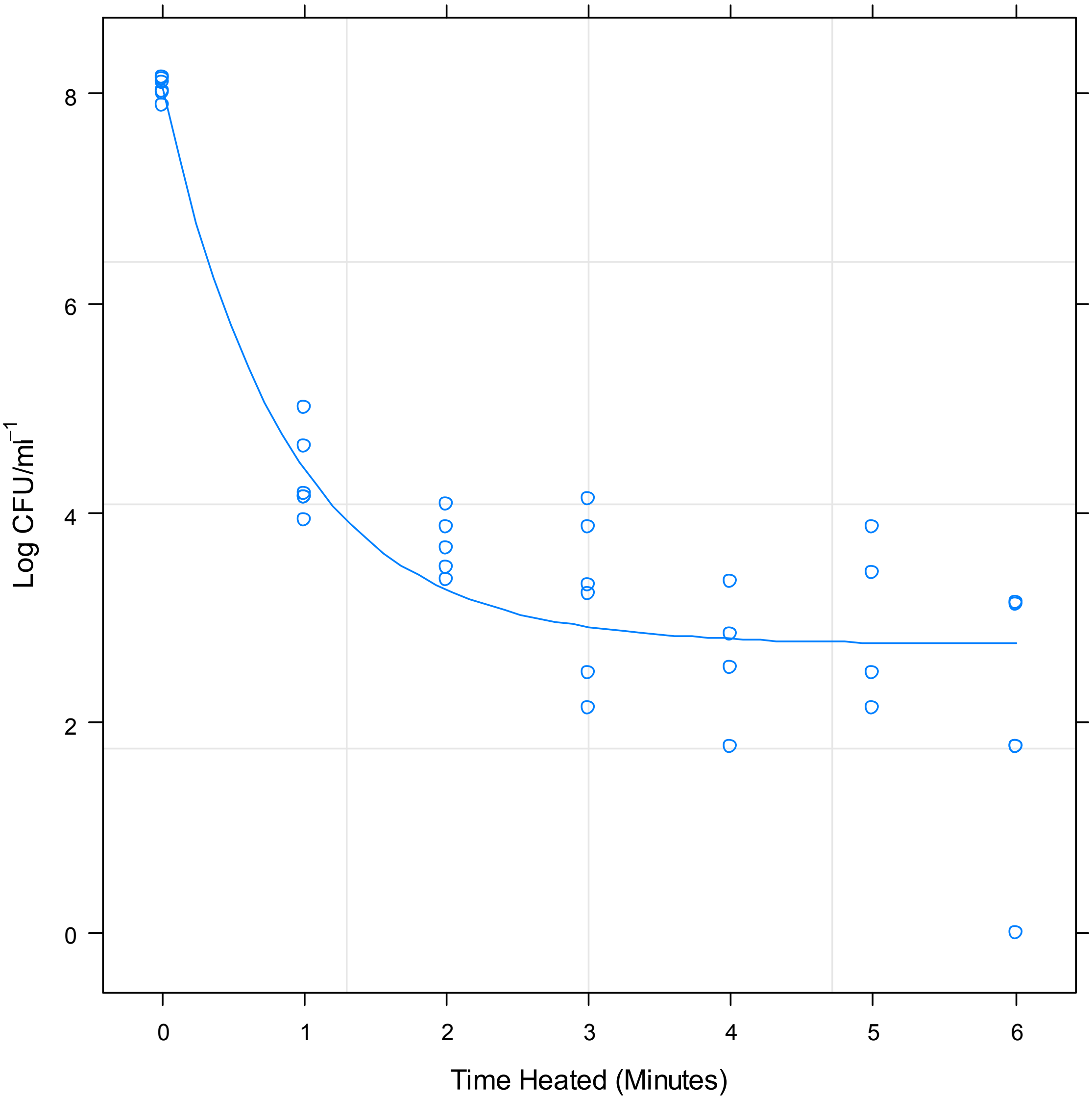

Figure 106. Plot illustrating predicted response curve using an asymptotic regression model for strain 13126 (ST-21, CC-21) following heating at 64°C.

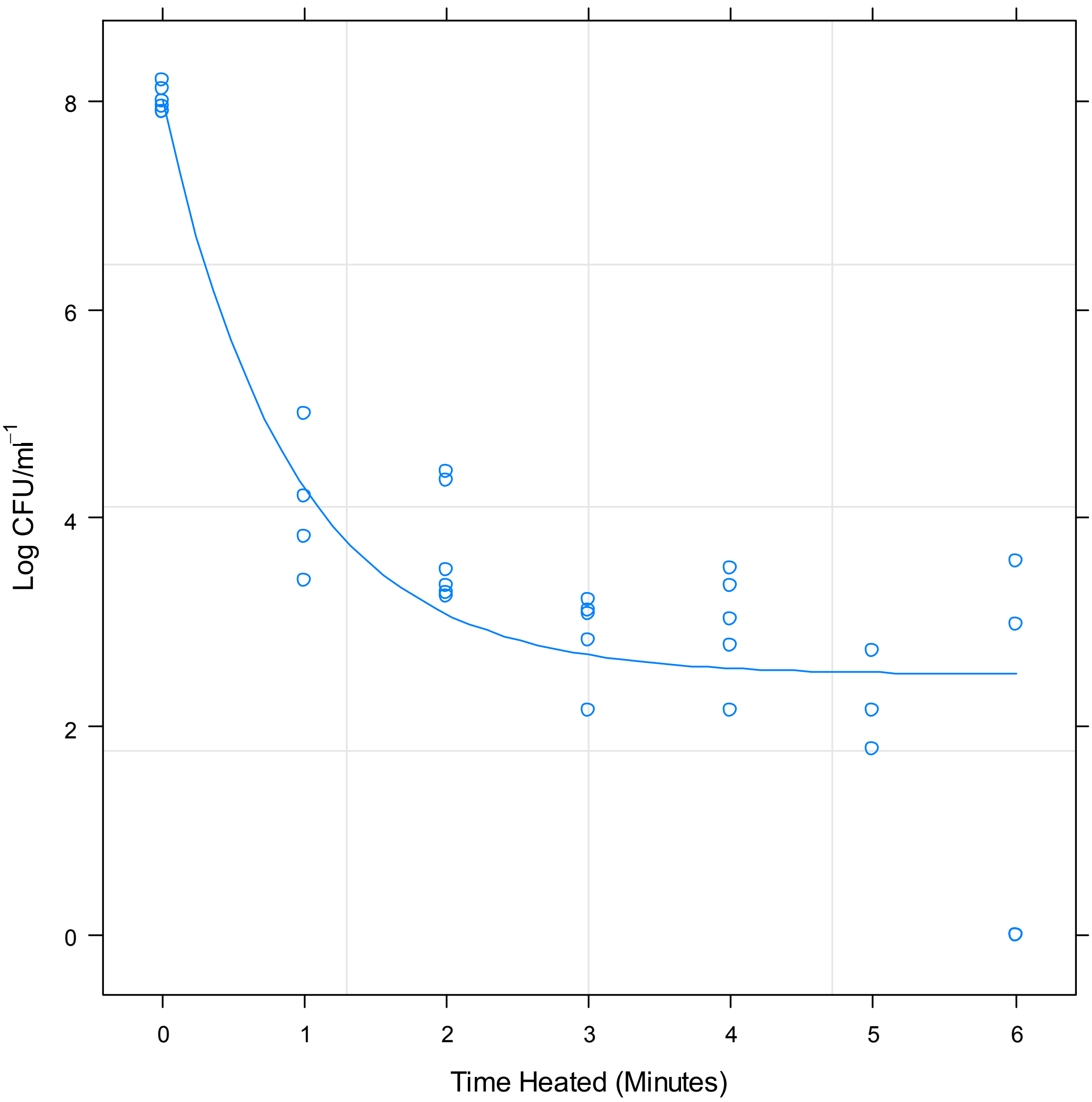

Figure 107. Plot illustrating predicted response curve using an asymptotic regression model for strain 13136 (ST-45, CC-45) following heating at 64°C.

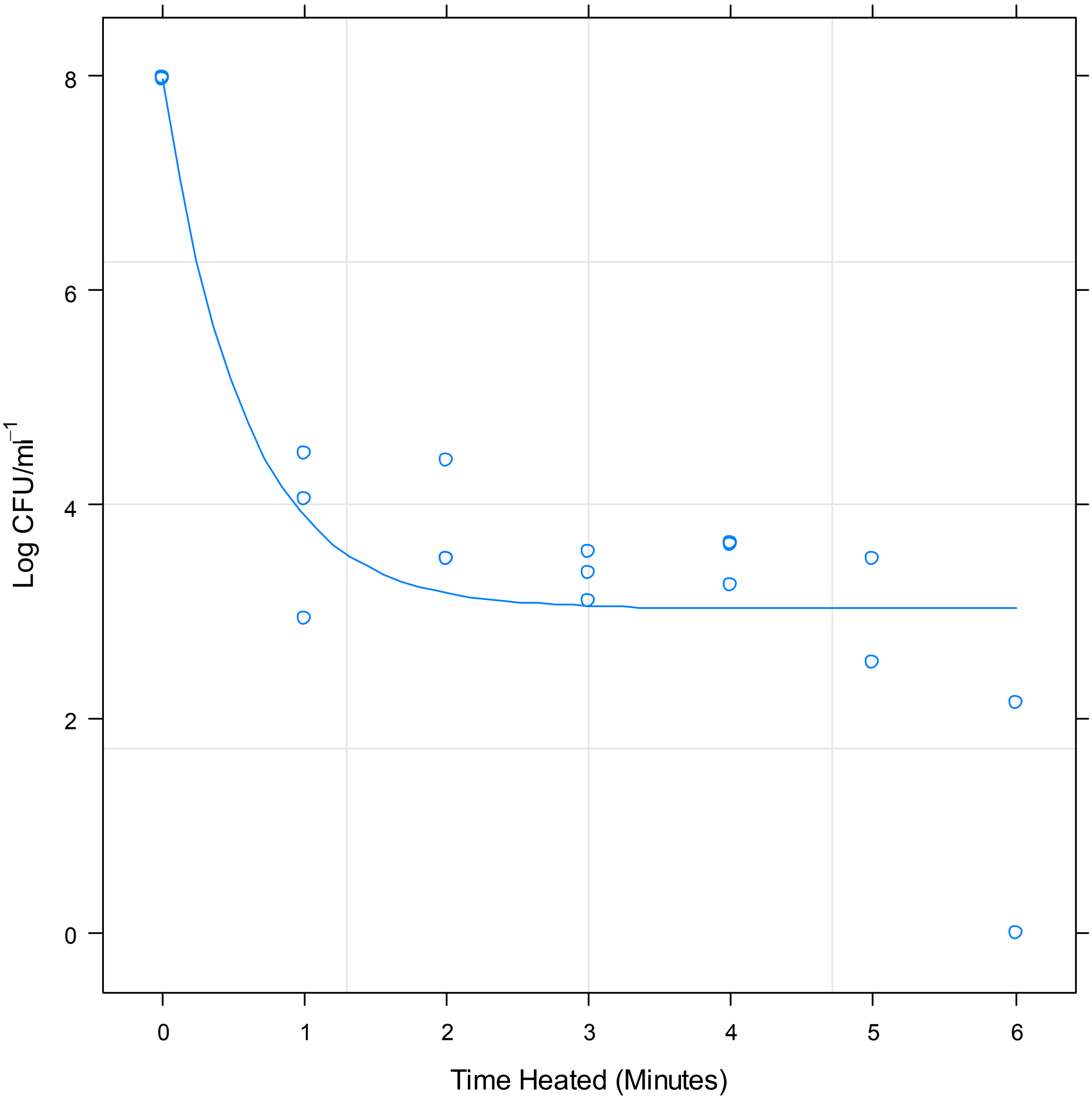

Figure 108. Plot illustrating predicted response curve using an asymptotic regression model for strain 13163 (ST-21, CC-21) following heating at 64°C.

1.8.16 Time-Temperature Simulations: 64°C

Mixed Weibull Distribution Model Predicted Response Curves:

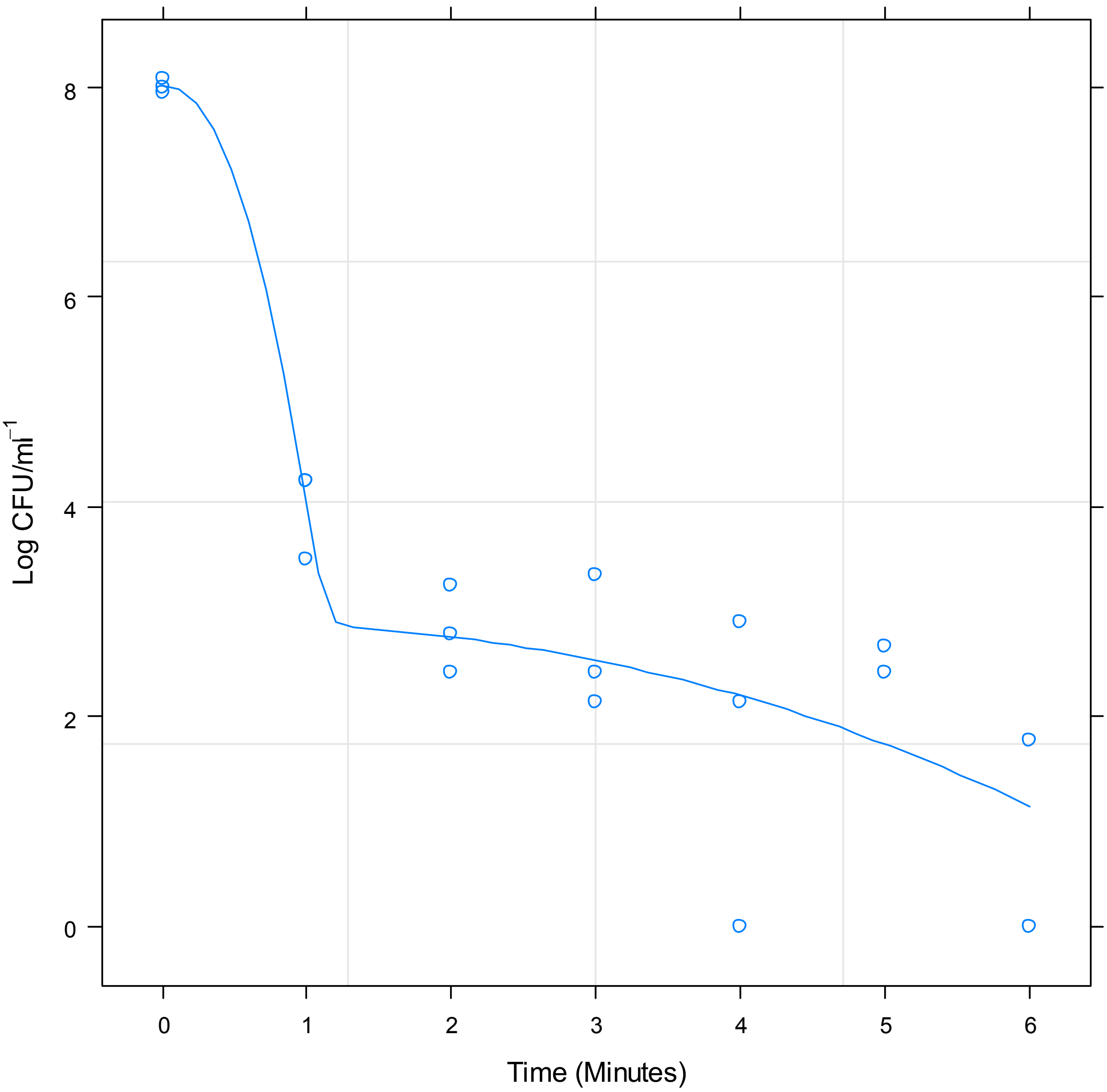

Figure 109. Plot illustrating the predicted response curve using a mixed Weibull distribution model for strain 11253 (ST-825, CC-828) following heating at 64°C.

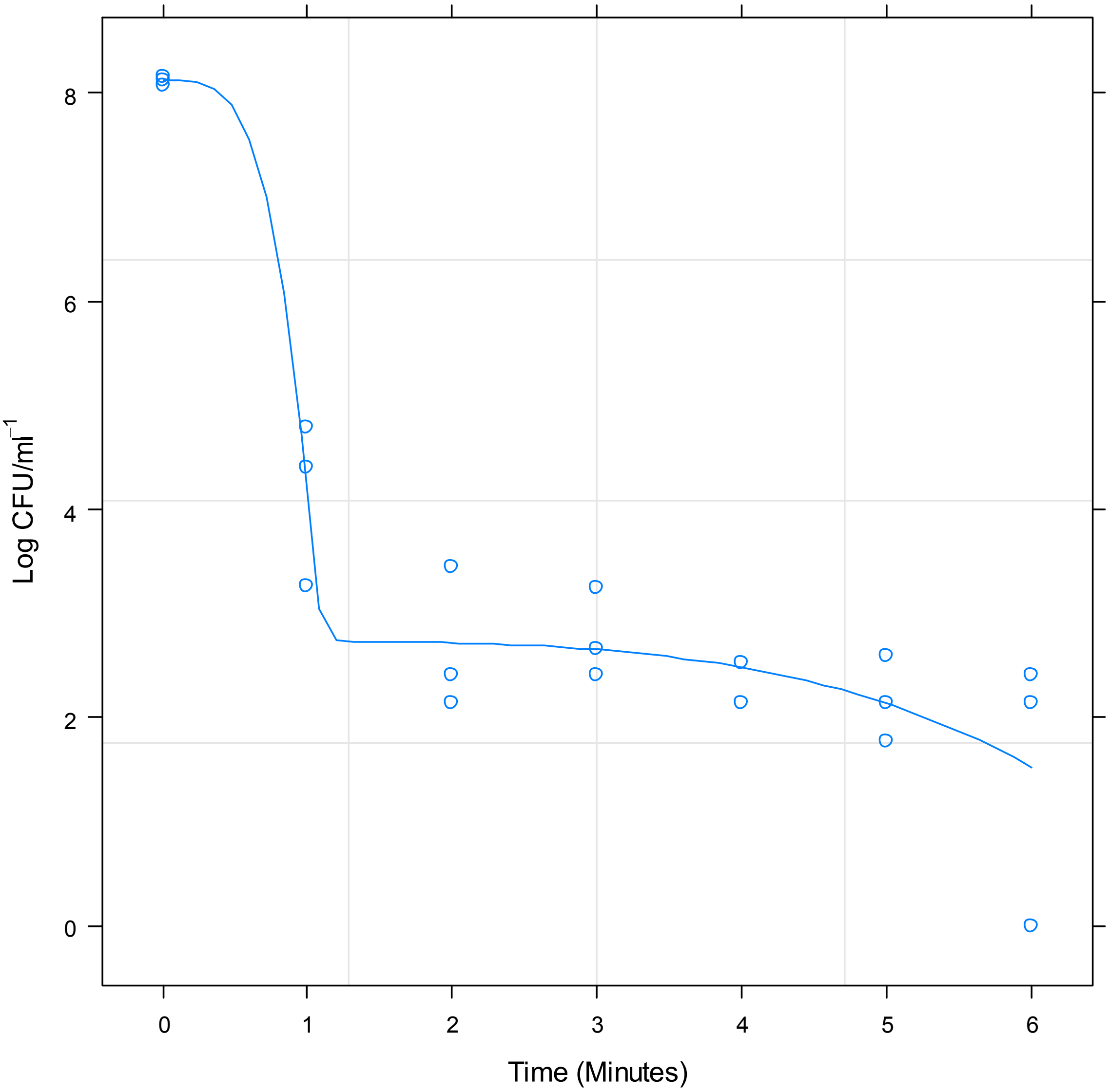

Figure 110. Plot illustrating predicted response curve using a mixed Weibull distribution model for strain 11762 (ST-829, CC-828) following heating at 64°C.

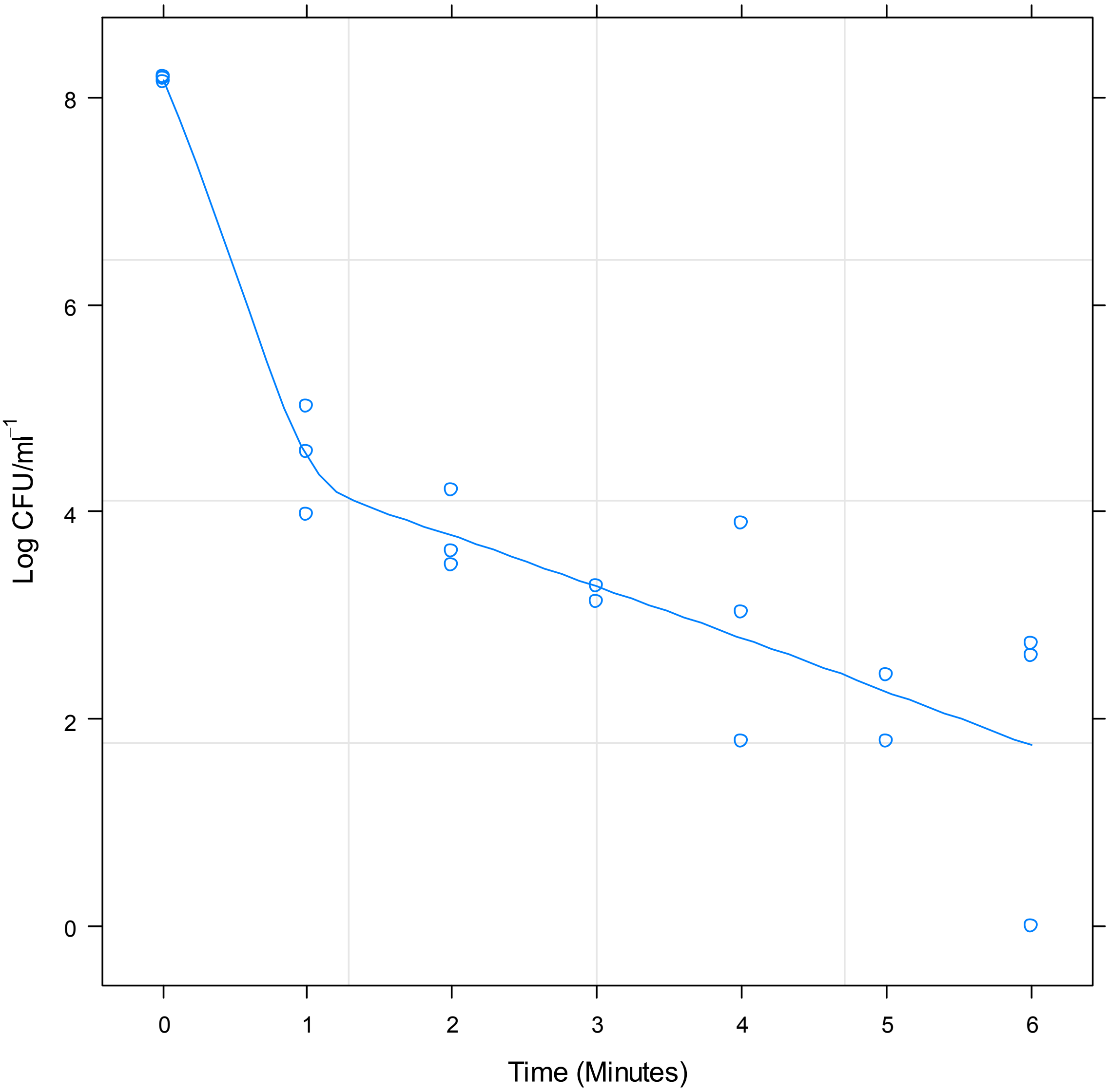

Figure 111. Plot illustrating predicted response curve using a mixed Weibull distribution model for strain 12662 (ST-257, CC-257) following heating at 64°C.

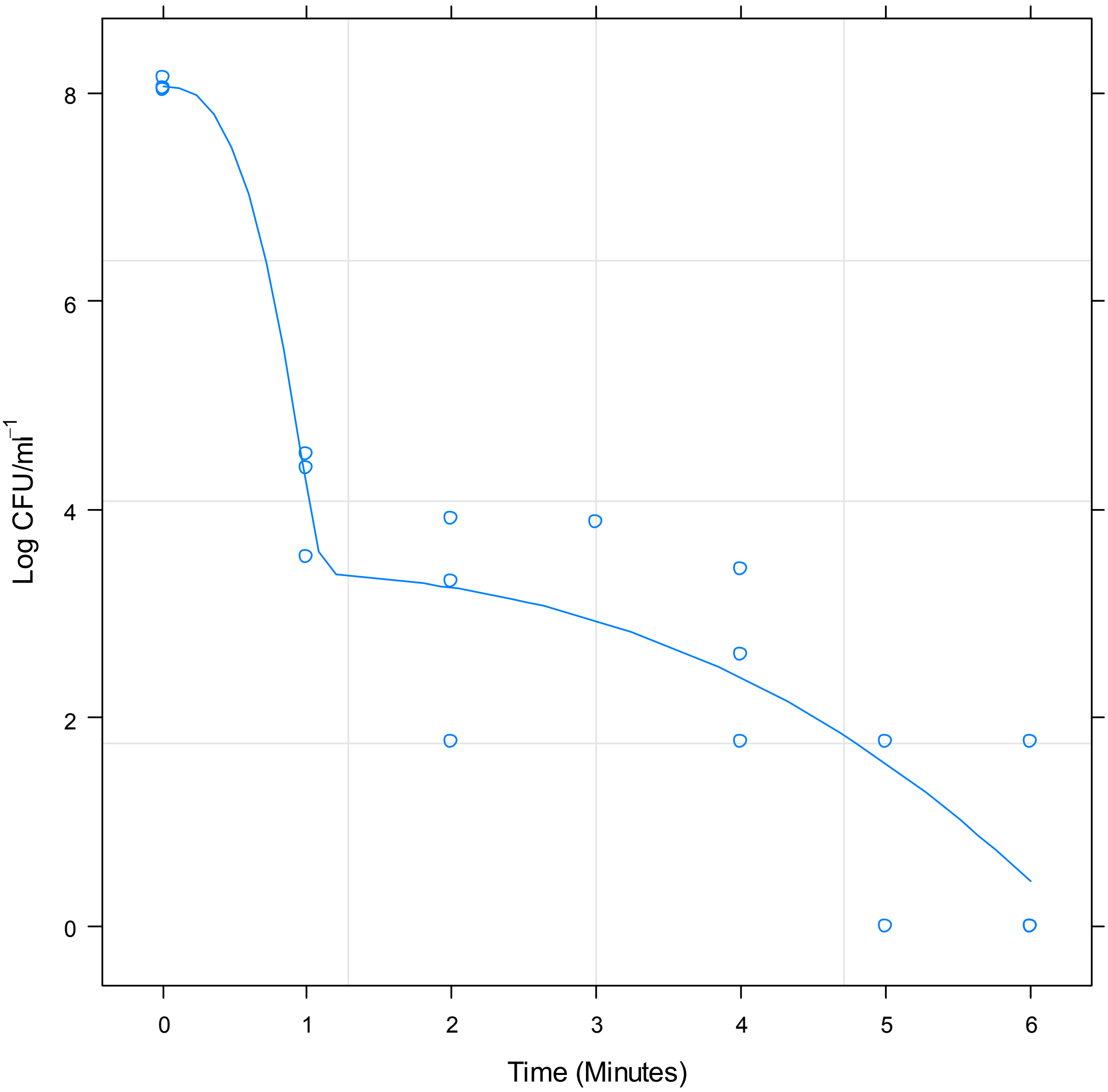

Figure 112. Plot illustrating predicted response curve using a mixed Weibull distribution model for strain 12783 (ST-574, CC-574) following heating at 64°C.

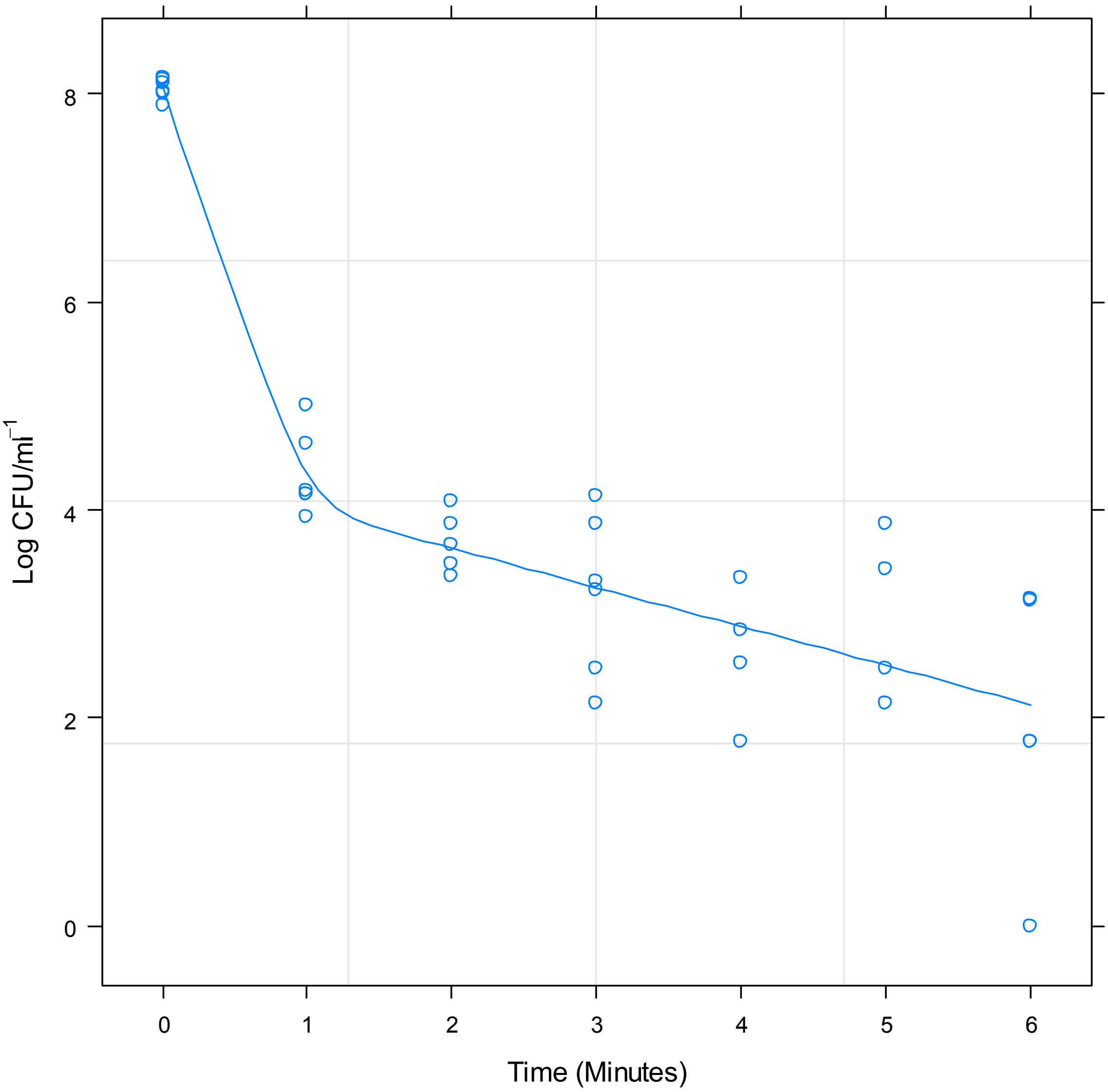

Figure 113. Plot illustrating predicted response curve using a mixed Weibull distribution model for strain 13126 (ST-21, CC-21) following heating at 64°C.

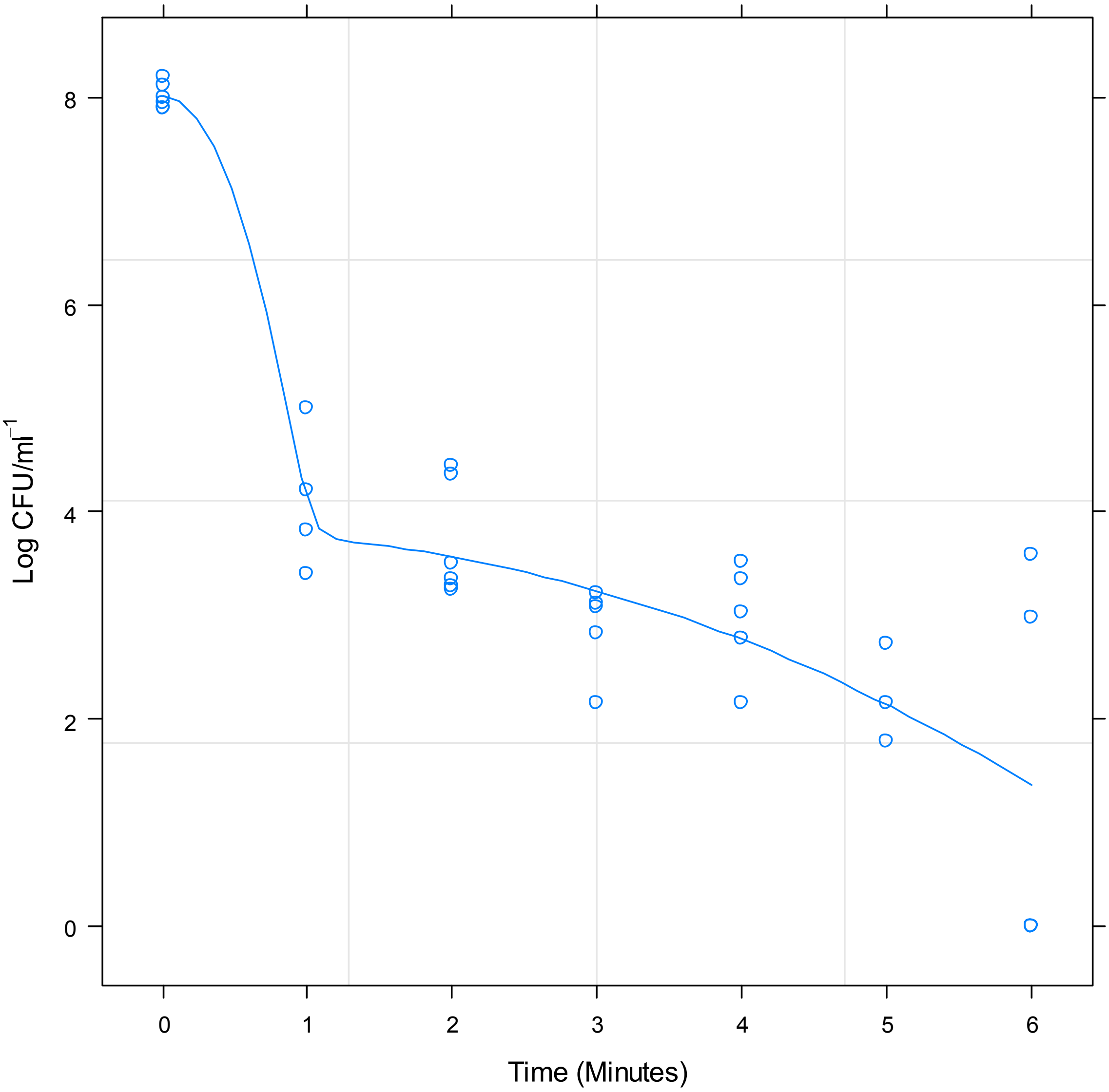

Figure 114. Plot illustrating predicted response curve using a mixed Weibull distribution model for strain 13136 (ST-45, CC-45) following heating at 64°C.

1.8.17 *pH and Time-Temperature Simulations: 56°C*

Table 78. An assessment of the goodness of fit for models analysing the survival of each strain for individual levels of pH at 56°C.

Strain	pH	Non-linear Function	ρ_c
12628 (ST-1773, CC-828)	4.5	Asymptotic Regression	0.974
12628 (ST-1773, CC-828)	5.5	Four-parameter Logistic	0.912
12628 (ST-1773, CC-828)	6.5	Four-parameter Logistic	0.983
12628 (ST-1773, CC-828)	7.5	Four-parameter Logistic	0.980
12628 (ST-1773, CC-828)	8.5	Asymptotic Regression	0.967
12662 (ST-257, CC-257)	4.5	Biexponential	0.921
12662 (ST-257, CC-257)	5.5	Four-parameter Logistic	0.964
12662 (ST-257, CC-257)	6.5	Four-parameter Logistic	0.982
12662 (ST-257, CC-257)	7.5	Four-parameter Logistic	0.973
12662 (ST-257, CC-257)	8.5	Asymptotic Regression	0.945
13126 (ST-21, CC-21)	4.5	Asymptotic Regression	0.917
13126 (ST-21, CC-21)	5.5	Four-parameter Logistic	0.965
13126 (ST-21, CC-21)	6.5	Four-parameter Logistic	0.983
13126 (ST-21, CC-21)	7.5	Four-parameter Logistic	0.960
13126 (ST-21, CC-21)	8.5	Four-parameter Logistic	0.970
13136 (ST-45, CC-45)	4.5	Asymptotic Regression	0.883
13136 (ST-45, CC-45)	5.5	Four-parameter Logistic	0.989
13136 (ST-45, CC-45)	6.5	Four-parameter Logistic	0.978
13136 (ST-45, CC-45)	7.5	Four-parameter Logistic	0.979
13136 (ST-45, CC-45)	8.5	Four-parameter Logistic	0.793

Table 79. Asymptotic regression model analysing survival of strain 12628 (ST-1773, CC-828) at pH 4.5 following heating at 56°C.

Parameter	Estimate	Standard Error	*t*-value	*P*-value
R0	8.064	0.219	36.889	0.000
Asymptote	2.087	0.136	15.375	0.000
LRC	-0.425	0.118	-3.586	0.003

Table 80. Four-parameter logistic regression model analysing survival rate for strain 12628 (ST-1773, CC-828) at pH 5.5 following heating at 56°C.

Parameter	Estimate	Standard Error	*t*-value	*P*-value
Asymptote A	8.151	0.389	20.947	0.000
Asymptote B	3.044	0.288	10.556	0.000
Mid-point	4.909	0.389	12.634	0.000
Scale Parameter	0.958	0.316	3.030	0.008

Table 81. Four-parameter logistic regression model analysing survival rate for strain 12628 (ST-1773, CC-828) at pH 6.5 following heating at 56°C.

Parameter	Estimate	Standard Error	*t*-value	*P*-value
Asymptote A	8.358	0.259	32.303	0.000
Asymptote B	3.169	0.187	16.927	0.000
Mid-point	5.273	0.271	19.493	0.000
Scale Parameter	1.790	0.285	6.279	0.000

Table 82. Four-parameter logistic regression model analysing survival rate for strain 12628 (ST-1773, CC-828) at pH 7.5 following heating at 56°C.

Parameter	Estimate	Standard Error	*t*-value	*P*-value
Asymptote A	9.529	1.107	8.608	0.000
Asymptote B	1.782	0.667	2.670	0.016
Mid-point	4.876	0.729	6.692	0.000
Scale Parameter	3.252	0.974	3.339	0.004

Table 83. Asymptotic regression model analysing survival of strain 12628 (ST-1773, CC-828) at pH 8.5 following heating at 56°C.

Parameter	Estimate	Standard Error	*t*-value	*P*-value
R0	8.222	0.273	30.134	0.000
Asymptote	1.124	1.182	0.951	0.354
LRC	-2.114	0.315	-6.719	0.000

Table 84. Biexponential model analysing survival of strain 12662 (ST-257, CC-257) at pH 4.5 following heating at 56°C.

Parameter	Estimate	Standard Error	*t*-value	*P*-value
Asymptote 1	4.529	1.207	3.751	0.002
LRC 1	-0.421	0.480	-0.877	0.393
Asymptote 2	3.552	1.174	3.026	0.008
LRC 2	-3.405	1.049	-3.245	0.005

Table 85. Four-parameter logistic regression model analysing survival rate for strain 12662 (ST-257, CC-257) at pH 5.5 following heating at 56°C.

Parameter	**Estimate**	**Standard Error**	***t*-value**	***P*-value**
Asymptote A	7.938	0.166	47.886	0.000
Asymptote B	4.259	0.276	15.421	0.000
Mid-point	7.188	0.382	18.815	0.000
Scale Parameter	1.646	0.376	4.378	0.000

Table 86. Four-parameter logistic regression model analysing survival rate for strain 12628 (ST-257, CC-257) at pH 6.5 following heating at 56°C.

Parameter	**Estimate**	**Standard Error**	***t*-value**	***P*-value**
Asymptote A	7.868	0.122	64.583	0.000
Asymptote B	3.827	0.378	10.129	0.000
Mid-point	8.337	0.442	18.854	0.000
Scale Parameter	2.005	0.368	5.445	0.000

Table 87. Four-parameter logistic regression model analysing survival rate for strain 12662 (ST-257, CC-257) at pH 7.5 following heating at 56°C.

Parameter	**Estimate**	**Standard Error**	***t*-value**	***P*-value**
Asymptote A	8.564	0.655	13.075	0.000
Asymptote B	2.770	0.927	2.987	0.008
Mid-point	6.780	0.801	8.463	0.000
Scale Parameter	3.312	1.193	2.776	0.013

Table 88. Asymptotic regression model analysing survival of strain 12662 (ST-257, CC-257) at pH 8.5 following heating at 56°C.

Parameter	**Estimate**	**Standard Error**	***t*-value**	***P*-value**
R0	8.098	0.269	30.053	0.000
Asymptote	2.156	0.436	4.940	0.000
LRC	-1.563	0.196	-7.969	0.000

Table 89. Asymptotic regression model analysing survival of strain 13126 (ST-21, CC-21) at pH 4.5 following heating at 56°C.

Parameter	**Estimate**	**Standard Error**	***t*-value**	***P*-value**
R0	7.872	0.352	22.367	0.000
Asymptote	2.394	0.238	10.079	0.000
LRC	-0.777	0.191	-4.071	0.001

Table 90. Four-parameter logistic regression model analysing survival rate for strain 13126 (ST-21, CC-21) at pH 5.5 following heating at 56°C.

Parameter	**Estimate**	**Standard Error**	***t*-value**	***P*-value**
Asymptote A	7.832	0.207	37.824	0.000
Asymptote B	3.732	0.239	15.593	0.000
Mid-point	6.351	0.341	18.604	0.000
Scale Parameter	1.560	0.346	4.509	0.000

Table 91. Four-parameter logistic regression model analysing survival rate for strain 13126 (ST-21, CC-21) at pH 6.5 following heating at 56°C.

Parameter	**Estimate**	**Standard Error**	***t*-value**	***P*-value**
Asymptote A	7.899	0.181	43.645	0.000
Asymptote B	3.405	0.199	17.085	0.000
Mid-point	6.219	0.264	23.559	0.000
Scale Parameter	1.757	0.283	6.218	0.000

Table 92. Four-parameter logistic regression model analysing survival rate for strain 13126 (ST-21, CC-21) at pH 7.5 following heating at 56°C.

Parameter	**Estimate**	**Standard Error**	***t*-value**	***P*-value**
Asymptote A	8.160	0.465	17.554	0.000
Asymptote B	3.678	0.183	20.101	0.000
Mid-point	3.920	0.474	8.274	0.000
Scale Parameter	1.659	0.418	3.972	0.001

Table 93. Four-parameter logistic regression model analysing survival rate for strain 13126 (ST-21, CC-21) at pH 8.5 following heating at 56°C.

Parameter	Estimate	Standard Error	*t*-value	*P*-value
Asymptote A	8.007	0.281	28.445	0.000
Asymptote B	3.610	0.105	34.499	0.000
Mid-point	2.541	0.203	12.518	0.000
Scale Parameter	0.796	0.163	4.876	0.000

Table 94. Asymptotic regression model analysing survival of strain 13136 (ST-45, CC-45) at pH 4.5 following heating at 56°C.

Parameter	Estimate	Standard Error	*t*-value	*P*-value
R0	7.875	0.416	18.931	0.000
Asymptote	2.615	0.259	10.079	0.000
LRC	-0.598	0.237	-2.523	0.023

Table 95. Four-parameter logistic regression model analysing survival rate for strain 13136 (ST-45, CC-45) at pH 5.5 following heating at 56°C.

Parameter	Estimate	Standard Error	*t*-value	*P*-value
Asymptote A	8.077	0.133	60.736	0.000
Asymptote B	3.397	0.161	21.067	0.000
Mid-point	6.460	0.197	32.727	0.000
Scale Parameter	1.606	0.202	7.967	0.000

Table 96. Four-parameter logistic regression model analysing survival rate for strain 13136 (ST-45, CC-45) at pH 6.5 following heating at 56°C.

Parameter	Estimate	Standard Error	*t*-value	*P*-value
Asymptote A	8.215	0.244	33.614	0.000
Asymptote B	3.416	0.320	10.690	0.000
Mid-point	5.505	0.336	16.405	0.000
Scale Parameter	1.839	0.337	5.455	0.000

Table 97. Four-parameter logistic regression model analysing survival rate for strain 13136 (ST-45, CC-45) at pH 7.5 following heating at 56°C.

Parameter	**Estimate**	**Standard Error**	***t*-value**	***P*-value**
Asymptote A	8.410	0.371	22.681	0.000
Asymptote B	2.627	0.248	10.592	0.000
Mid-point	5.127	0.338	15.178	0.000
Scale Parameter	1.938	0.364	5.327	0.000

Table 98. Four-parameter logistic regression model analysing survival rate for strain 13136 (ST-45, CC-45) at pH 8.5 following heating at 56°C.

Parameter	**Estimate**	**Standard Error**	***t*-value**	***P*-value**
Asymptote A	8.827	0.860	10.261	0.000
Asymptote B	3.228	0.178	18.150	0.000
Mid-point	2.581	0.584	4.416	0.000
Scale Parameter	1.432	0.405	3.533	0.003

1.8.18 pH and Time-Temperature Simulations: 56^{0}C

Mixed Weibull Distribution Model:

Table 99. An assessment of the goodness of fit for Mixed Weibull Distribution analysing the survival of each strain for individual levels of pH at 56^{o}C.

Strain	pH	Non-linear Function	ρ_c
12628 (ST-1773, CC-828)	4.5	Mixed Weibull Distribution	0.982
12628 (ST-1773, CC-828)	5.5	Mixed Weibull Distribution	0.948
12628 (ST-1773, CC-828)	6.5	Mixed Weibull Distribution	0.992
12628 (ST-1773, CC-828)	7.5	Mixed Weibull Distribution	0.990
12628 (ST-1773, CC-828)	8.5	Mixed Weibull Distribution	0.974
12662 (ST-257, CC-257)	4.5	Mixed Weibull Distribution	0.956
12662 (ST-257, CC-257)	5.5	Mixed Weibull Distribution	
12662 (ST-257, CC-257)	6.5	Mixed Weibull Distribution	
12662 (ST-257, CC-257)	7.5	Mixed Weibull Distribution	
12662 (ST-257, CC-257)	8.5	Mixed Weibull Distribution	0.978
13126 (ST-21, CC-21)	4.5	Mixed Weibull Distribution	0.980
13126 (ST-21, CC-21)	5.5	Mixed Weibull Distribution	0.966
13126 (ST-21, CC-21)	6.5	Mixed Weibull Distribution	0.991
13126 (ST-21, CC-21)	7.5	Mixed Weibull Distribution	0.978
13126 (ST-21, CC-21)	8.5	Mixed Weibull Distribution	0.883
13136 (ST-45, CC-45)	4.5	Mixed Weibull Distribution	0.891
13136 (ST-45, CC-45)	5.5	Mixed Weibull Distribution	0.991
13136 (ST-45, CC-45)	6.5	Mixed Weibull Distribution	0.989
13136 (ST-45, CC-45)	7.5	Mixed Weibull Distribution	0.991
13136 (ST-45, CC-45)	8.5	Mixed Weibull Distribution	0.969

Table 100. Mixed Weibull distribution model analysing the survival of strain 12628 (ST-1773, CC-828) at pH 4.5 following heating at 56^{o}C.

Parameter	Estimate	Standard Error	*t*-value	*P*-value
α	5.390	0.333	16.176	0.000
δ1	1.218	1.331	0.914	0.377
p	2.894	6.368	0.455	0.657
N0	7.990	0.044	180.741	0.000
δ2	14.249	8.351	1.706	0.112

Table 101. Mixed Weibull distribution model analysing the survival of strain 12628 (ST-1773, CC-828) at pH 5.5 following heating at 56^{o}C.

Parameter	Estimate	Standard Error	*t*-value	*P*-value
α	3.796	0.214	17.766	0.000
δ1	3.881	0.051	75.760	0.000
p	3.058	0.125	24.388	0.000
N0	8.104	0.013	625.807	0.000
δ2	10.928	1.2901	8.471	0.000

Table 102. Mixed Weibull distribution model analysing the survival of strain 12628 (ST-1773, CC-828) at pH 6.5 following heating at 56^{o}C.

Parameter	Estimate	Standard Error	*t*-value	*P*-value
α	3.574	0.515	6.940	0.000
δ1	3.192	0.379	8.416	0.000
N0	8.100	0.147	55.151	0.000
p	1.664	0.270	6.166	0.000
δ2	10.385	2.872	3.616	0.002

Table 103. Mixed Weibull distribution model analysing the survival of strain 12628 (ST-1773, CC-828) at pH 7.5 following heating at 56^{o}C.

Parameter	Estimate	Standard Error	*t*-value	*P*-value
α	3.120	1.664	1.875	0.079
δ1	2.270	0.427	5.319	0.000
p	1.179	0.207	5.708	0.000
N0	8.118	0.183	44.305	0.000
δ2	5.619	3.101	1.812	0.089

Table 104. Mixed Weibull distribution model analysing the survival of strain 12628 (ST-1773, CC-828) at pH 8.5 following heating at 56^{o}C.

Parameter	Estimate	Standard Error	*t*-value	*P*-value
α	2.806	0.546	5.141	0.000
δ1	1.946	0.507	3.841	0.001
p	1.509	0.476	3.169	0.006
N0	8.098	0.282	28.749	0.000
δ2	6.449	2.131	3.026	0.008

Table 105. Mixed Weibull distribution model analysing the survival of strain 12662 (ST-1773, CC-828) at pH 4.5 following heating at 56^{o}C.

Parameter	Estimate	Standard Error	*t*-value	*P*-value
α	5.539	3.110	1.781	0.094
δ1	0.082	0.120	0.698	0.495
p	0.405	0.160	2.526	0.023
N0	8.043	0.280	29.204	0.000
δ2	1403.846	7.92E+04	0.018	0.986

Table 106. Mixed Weibull distribution model analysing the survival of strain 12662 (ST-1773, CC-828) at pH 8.5 following heating at 56^{o}C.

Parameter	Estimate	Standard Error	*t*-value	*P*-value
α	3.669	0.367	9.996	0.000
δ1	1.468	0.112	13.120	0.000
p	1.300	0.115	11.304	0.000
N0	7.973	0.061	131.531	0.000
δ2	8.222	2.447	3.361	0.004

Table 107. Mixed Weibull distribution model analysing the survival of strain 13126 (ST-21, CC-21) at pH 4.5 following heating at 56^{o}C.

Parameter	Estimate	Standard Error	*t*-value	*P*-value
α	5.120	1512.370	0.003	0.998
δ1	0.065	1.366	0.048	0.966
p	0.310	1.052	0.295	0.796
N0	7.490	9.118	0.822	0.498
δ2	2.680	7025.005	0.000	1.000

Table 108. Mixed Weibull distribution model analysing the survival of strain 13126 (ST-21, CC-21) at pH 5.5 following heating at 56^{o}C.

Parameter	Estimate	Standard Error	*t*-value	*P*-value
α	2.252	0.314	7.000	0.000
δ1	4.445	0.015	302.000	0.000
p	2.026	0.004	506.000	0.000
N0	7.799	0.000	4.4E+09	0.000
δ2	10.020	1.387	7.000	0.000

Table 109. Mixed Weibull distribution model analysing the survival of strain 13126 (ST-21, CC-21) at pH 6.5 following heating at 56°C.

Parameter	Estimate	Standard Error	*t*-value	*P*-value
α	3.596	0.778	4.619	0.000
δ1	4.136	0.405	10.208	0.000
p	1.807	0.267	6.763	0.000
N0	7.794	0.128	60.680	0.000
δ2	16.001	12.726	1.257	0.227

Table 110. Mixed Weibull distribution model analysing the survival of strain 13126 (ST-21, CC-21) at pH 7.5 following heating at 56°C.

Parameter	Estimate	Standard Error	*t*-value	*P*-value
α	3.579	0.699	5.120	0.000
δ1	2.455	0.491	5.000	0.000
p	1.327	0.290	4.583	0.000
N0	7.804	0.206	37.855	0.000
δ2	20.243	25.111	0.806	0.432

Table 111. Mixed Weibull distribution model analysing the survival of strain 13126 (ST-21, CC-21) at pH 8.5 following heating at 56°C.

Parameter	Estimate	Standard Error	*t*-value	*P*-value
α	3.4384	0.237	14.519	0.005
δ1	1.8350	0.230	7.964	0.015
p	3.2468	4.716	0.688	0.562
N0	7.7993	0.010	794.914	0.000
δ2	9.8981	3.185	3.108	0.089

Table 112. Mixed Weibull distribution model analysing the survival of strain 13136 (ST-45, CC-45) at pH 4.5 following heating at 56°C.

Parameter	Estimate	Standard Error	*t*-value	*P*-value
α	4.887	0.136	35.860	0.000
δ1	1.348	0.229	5.891	0.000
p	3.291	1.412	2.330	0.035
N0	7.831	0.025	308.450	0.000
δ2	9.489	0.931	10.190	0.000

Table 113. Mixed Weibull distribution model analysing the survival of strain 13136 (ST-45, CC-45) at pH 5.5 following heating at 56°C.

Parameter	**Estimate**	**Standard Error**	***t*-value**	***P*-value**
α	2.955	0.052	56.794	0.000
δ1	4.559	0.016	292.621	0.000
p	2.267	0.020	110.977	0.000
N0	7.905	0.004	1787.696	0.000
δ2	9.645	0.164	58.880	0.000

Table 114. Mixed Weibull distribution model analysing the survival of strain 13136 (ST-45, CC-45) at pH 6.5 following heating at 56°C.

Parameter	**Estimate**	**Standard Error**	***t*-value**	***P*-value**
α	3.059	1.021	2.996	0.012
δ1	3.494	0.189	18.454	0.000
p	1.707	0.191	8.915	0.000
N0	7.985	0.055	146.414	0.000
δ2	9.984	6.063	1.647	0.128

Table 115. Mixed Weibull distribution model analysing the survival of strain 13136 (ST-45, CC-45) at pH 7.5 following heating at 56°C.

Parameter	**Estimate**	**Standard Error**	***t*-value**	***P*-value**
α	3.3237	0.4812	6.9071	0.000
δ1	3.0560	0.2440	12.5245	0.000
p	1.7715	0.2151	8.2363	0.000
N0	7.9810	0.0889	89.8257	0.000
δ2	8.1456	1.6049	5.0756	0.000

Table 116. Mixed Weibull distribution model analysing the survival of strain 13136 (ST-45, CC-45) at pH 8.5 following heating at 56°C.

Parameter	**Estimate**	**Standard Error**	***t*-value**	***P*-value**
α	3.762	0.439	8.570	0.000
δ1	1.686	0.197	8.555	0.000
p	1.479	0.221	6.547	0.000
N0	7.993	0.109	73.621	0.000
δ2	10.473	3.721	2.815	0.013

1.8.19 pH and Time-Temperature Simulations: 56°C

Predicted Response Curves:

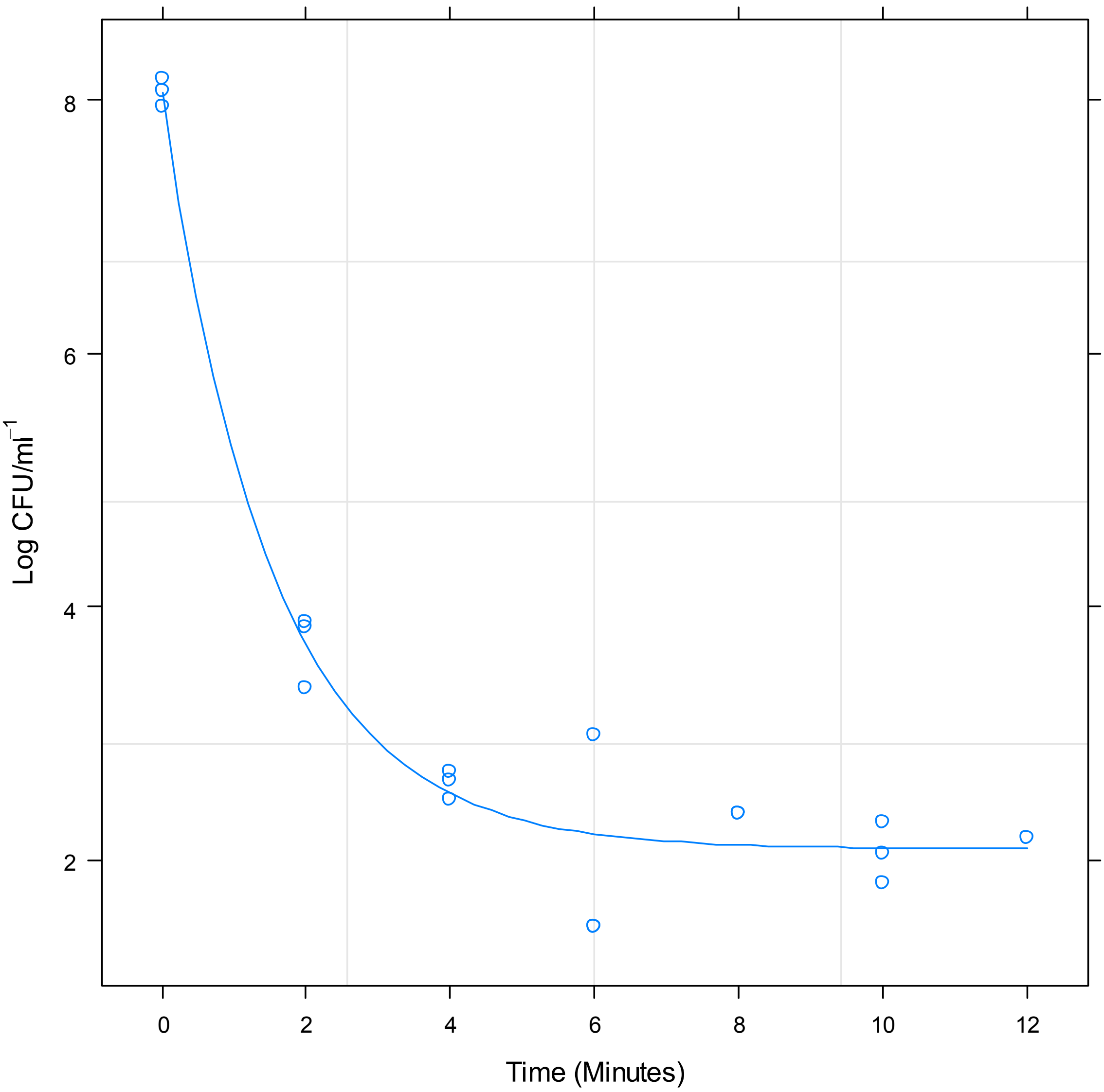

Figure 115. Predicted response curve using an asymptotic regression model for strain 12628 (ST1773-CC828) at pH 4.5 following heating at 56°C.

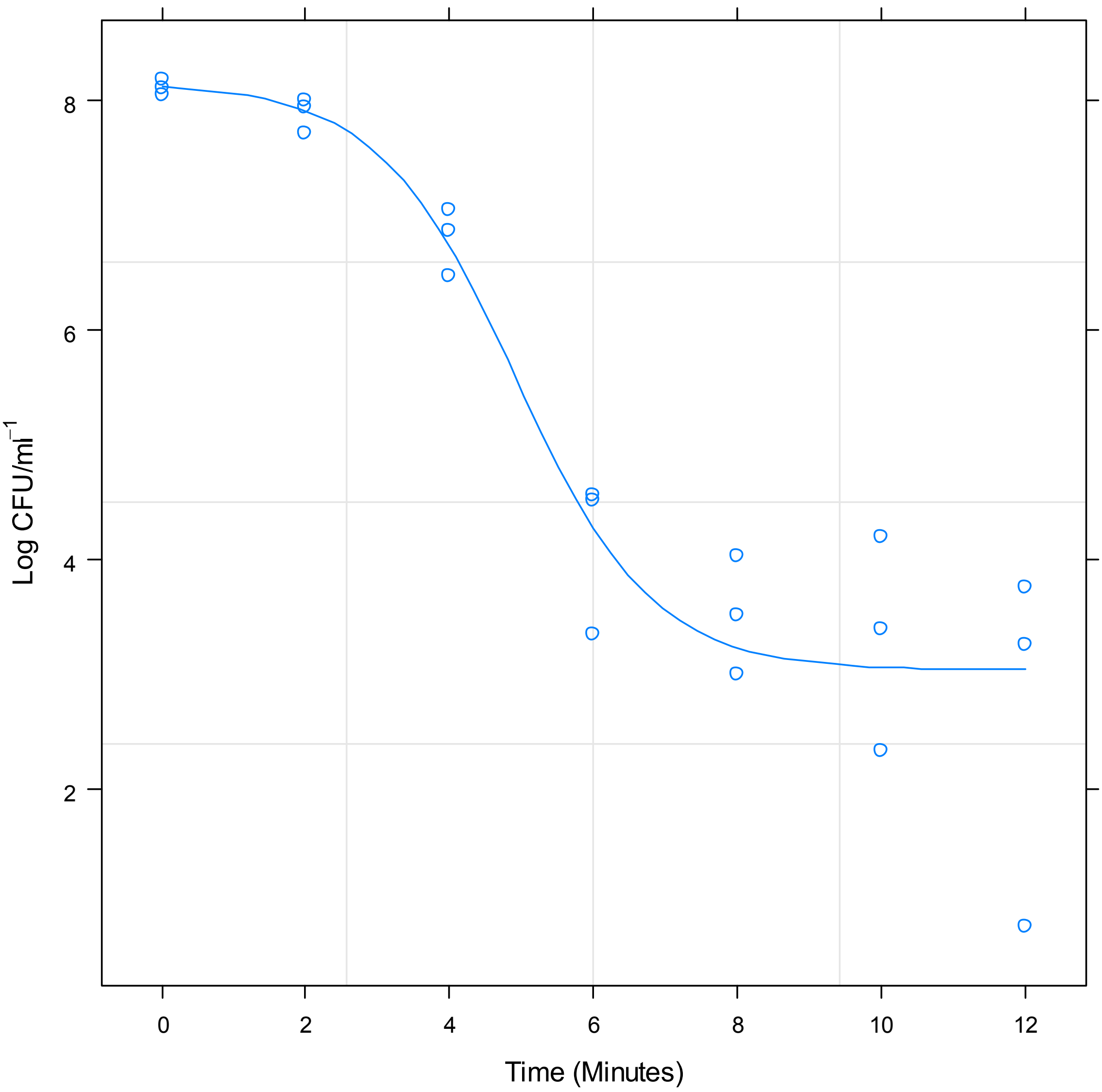

Figure 116. Predicted response curve using a four-parameter logistic regression model for strain 12628 (ST1773-CC828) at pH 5.5 following heating at 56^{o}C.

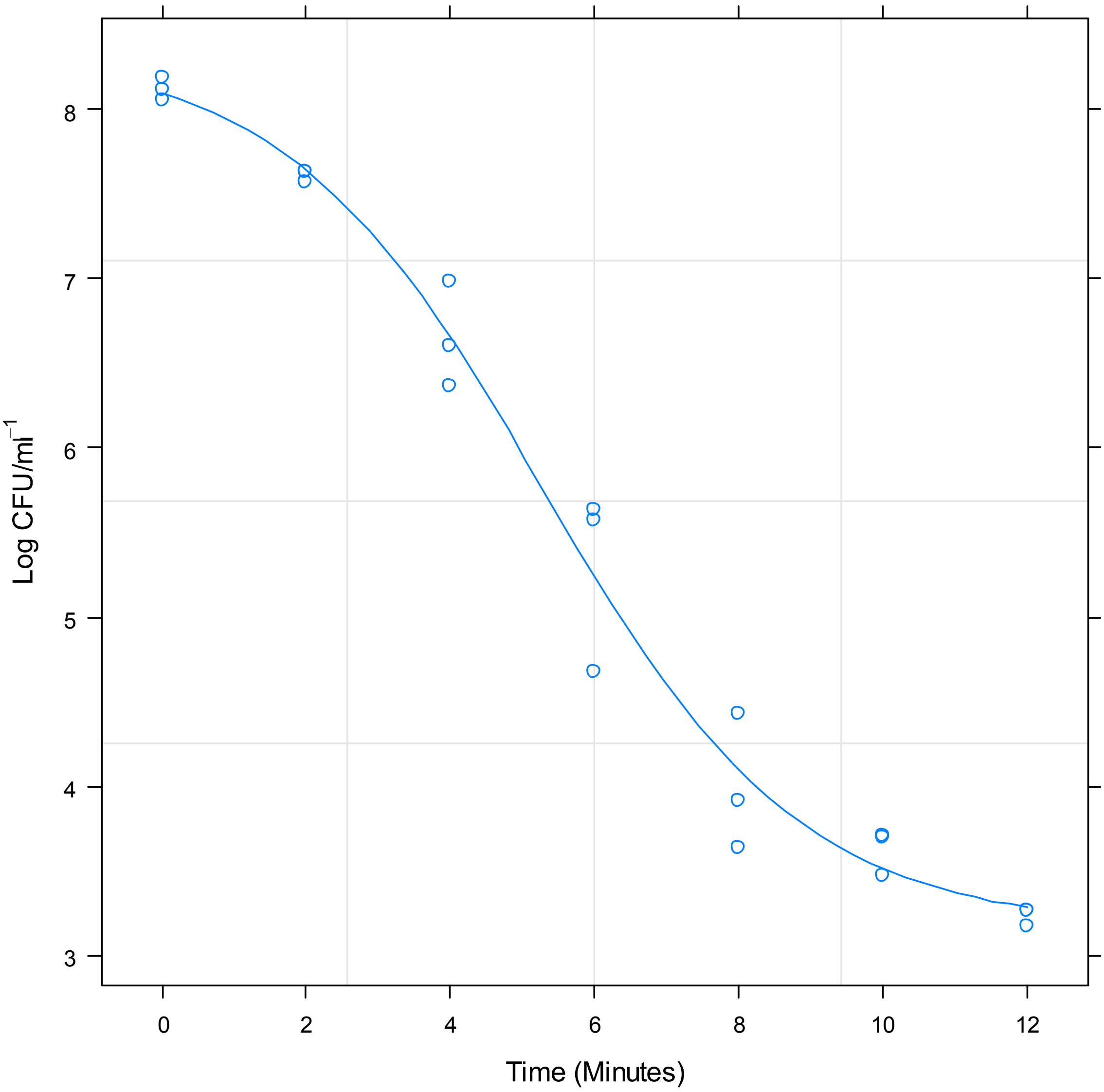

Figure 117. Predicted response curve using a four-parameter logistic regression model for strain 12628 (ST1773-CC828) at pH 6.5 and following heating at 56^{o}C.

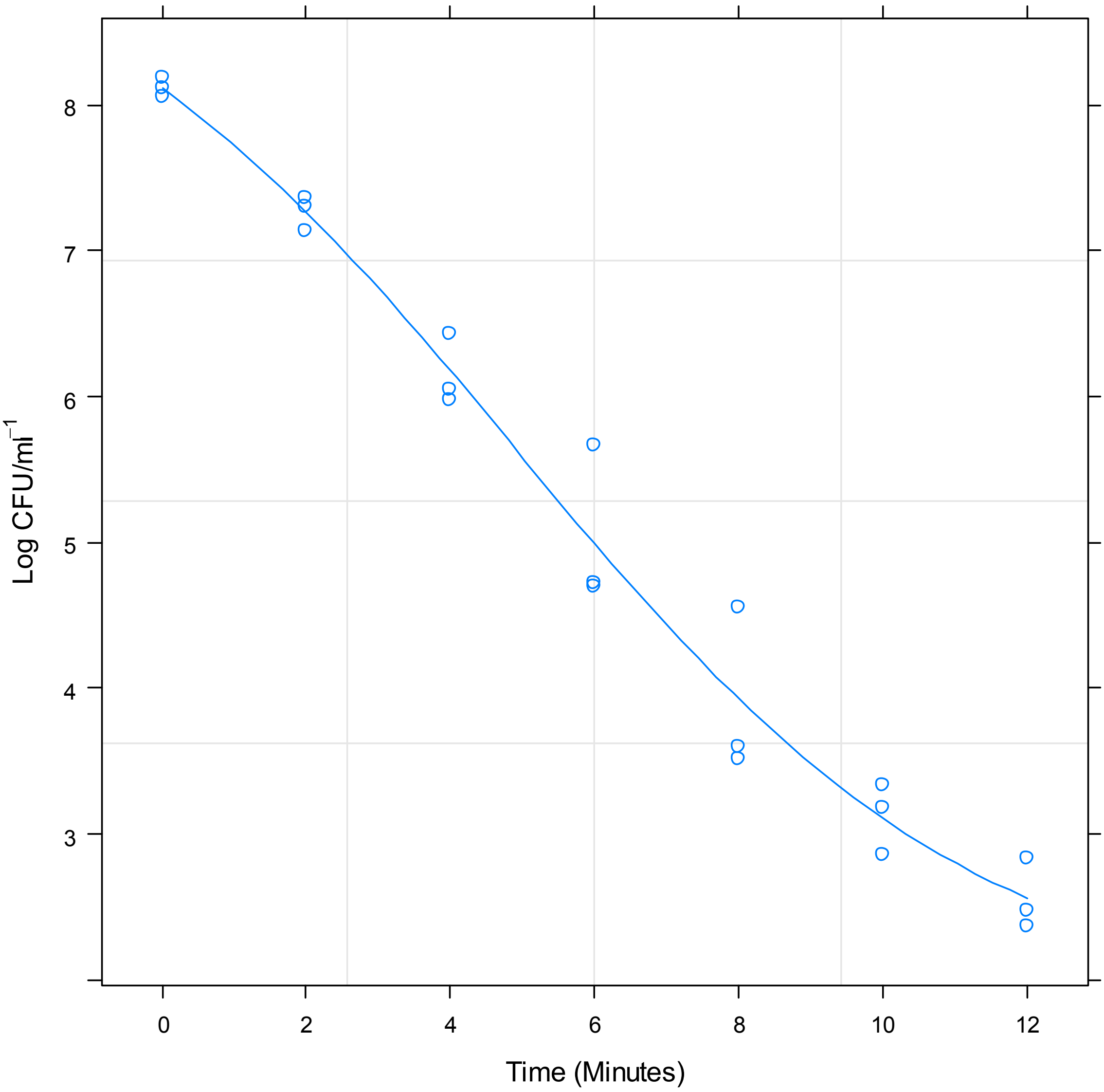

Figure 118. Predicted response curve using a four-parameter logistic regression model for strain 12628 (ST1773-CC828) at pH 7.5 following heating at 56°C.

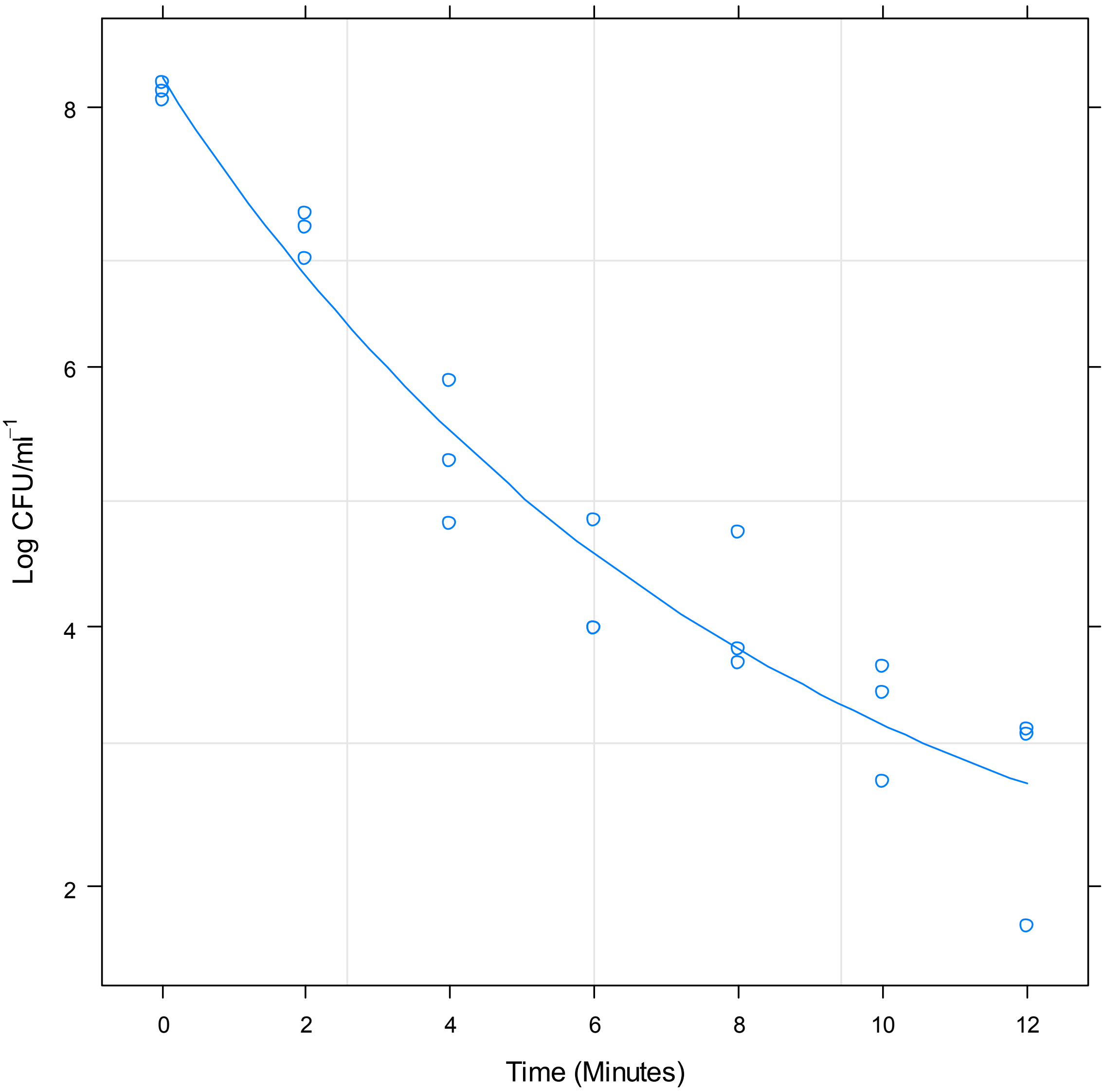

Figure 119. Predicted response curve using an asymptotic regression model for strain 12628 (ST1773-CC828) at pH 8.5 and following heating at 56°C.

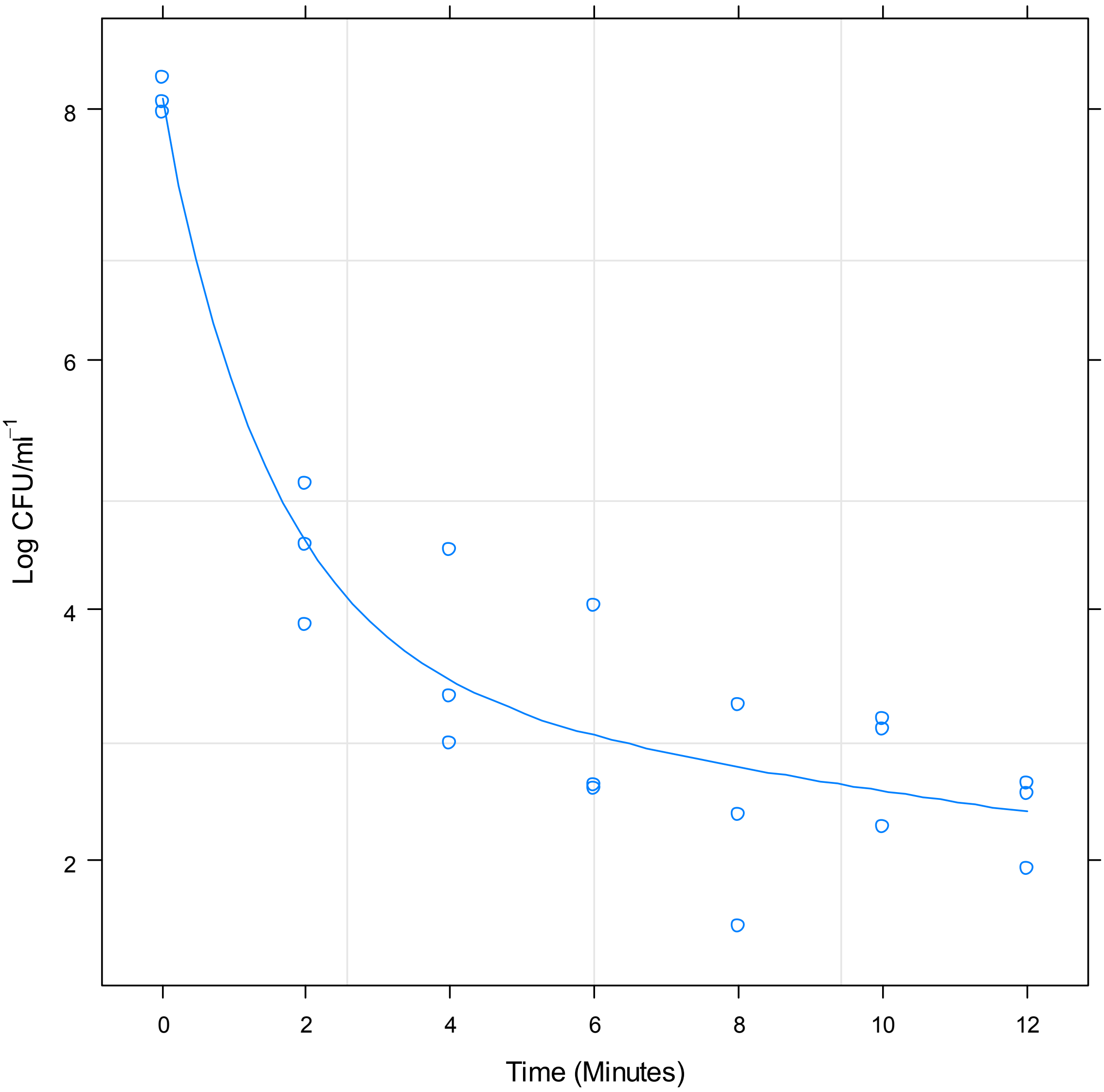

Figure 120. Predicted response curve using a biexponential model for strain 12662 (ST-257, CC-257) at pH 4.5 and following heating at 56°C.

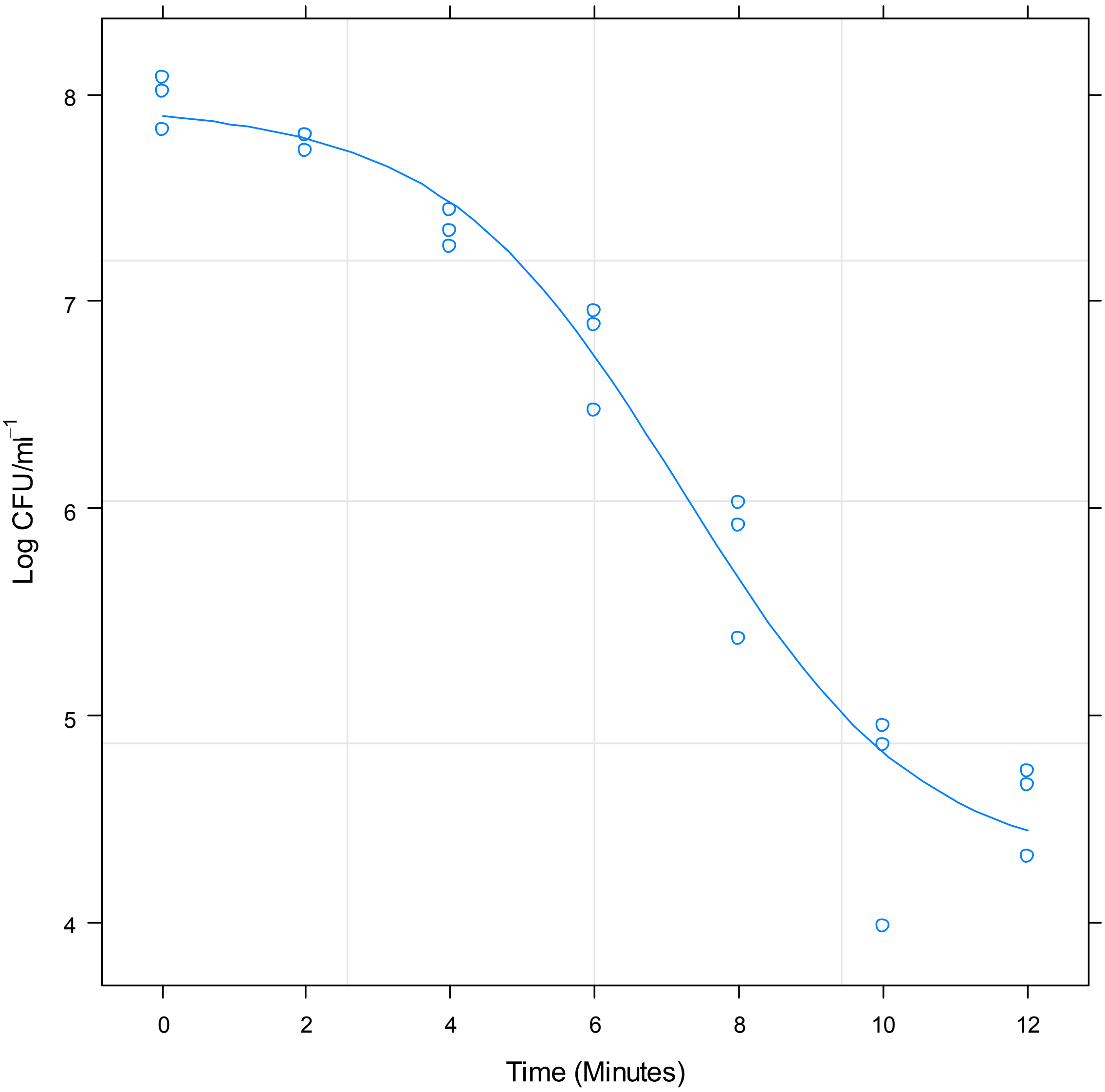

Figure 121. Predicted response curve using a four-parameter logistic regression model for strain 12662 (ST-257, CC-828) at pH 5.5 following heating at 56^{o}C.

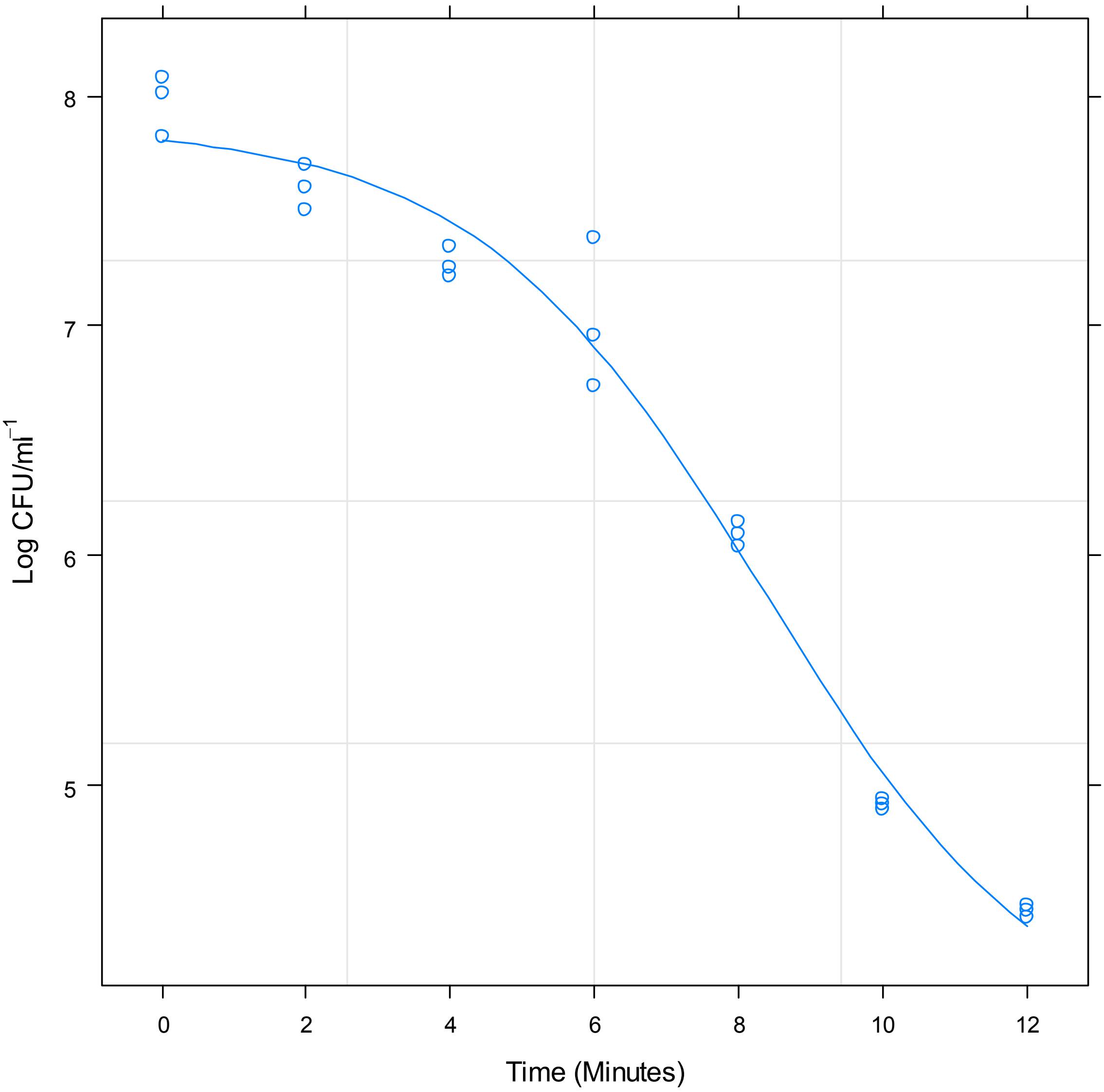

Figure 122. Predicted response curve using a four-parameter logistic regression model for strain 12662 (ST-257, CC-828) at pH 6.5 following heating at 56^{o}C.

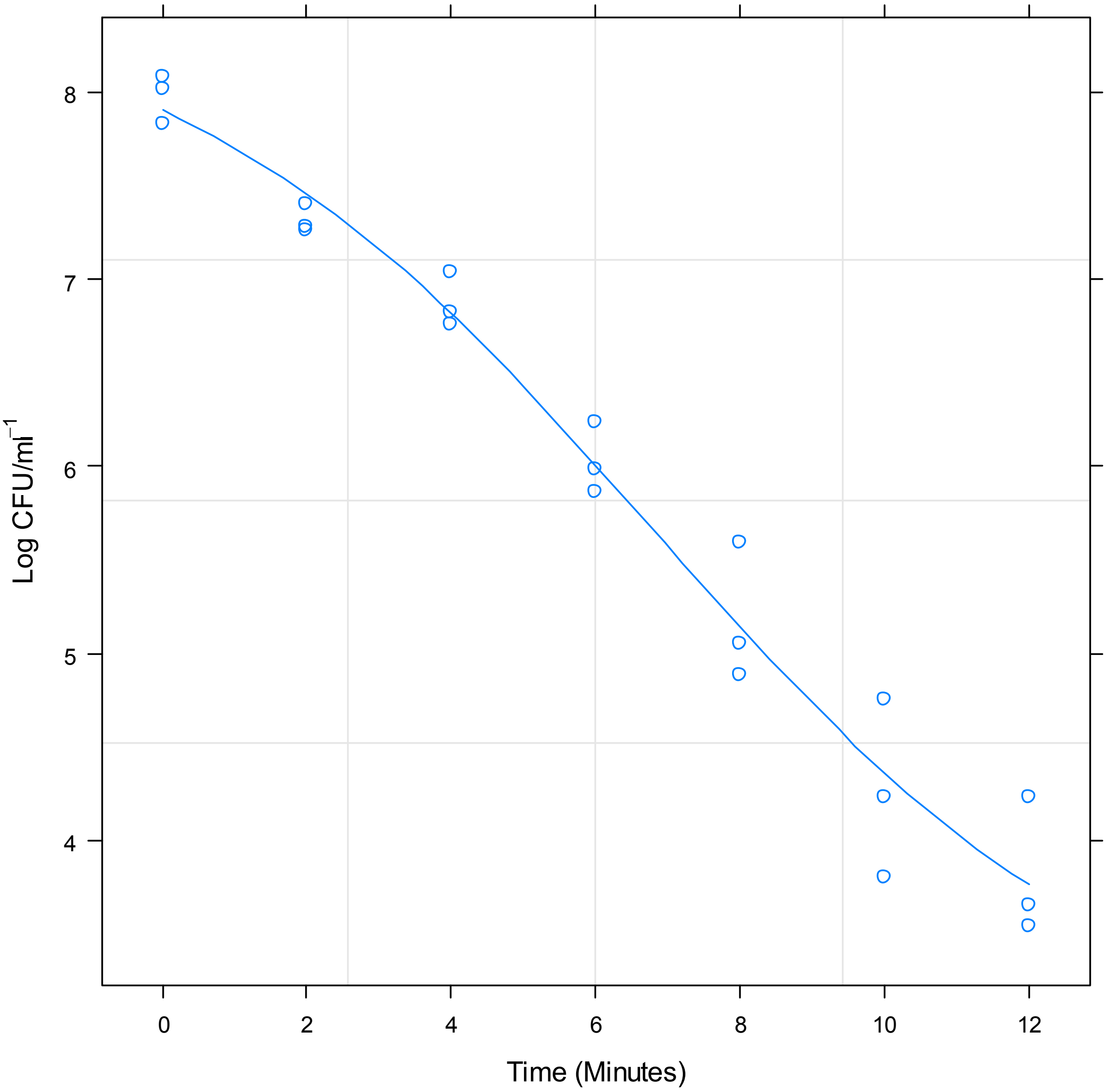

Figure 123. Predicted response curve using a four-parameter logistic regression model for strain 12662 (ST-257, CC-828) at pH 7.5 following heating at 56^{o}C.

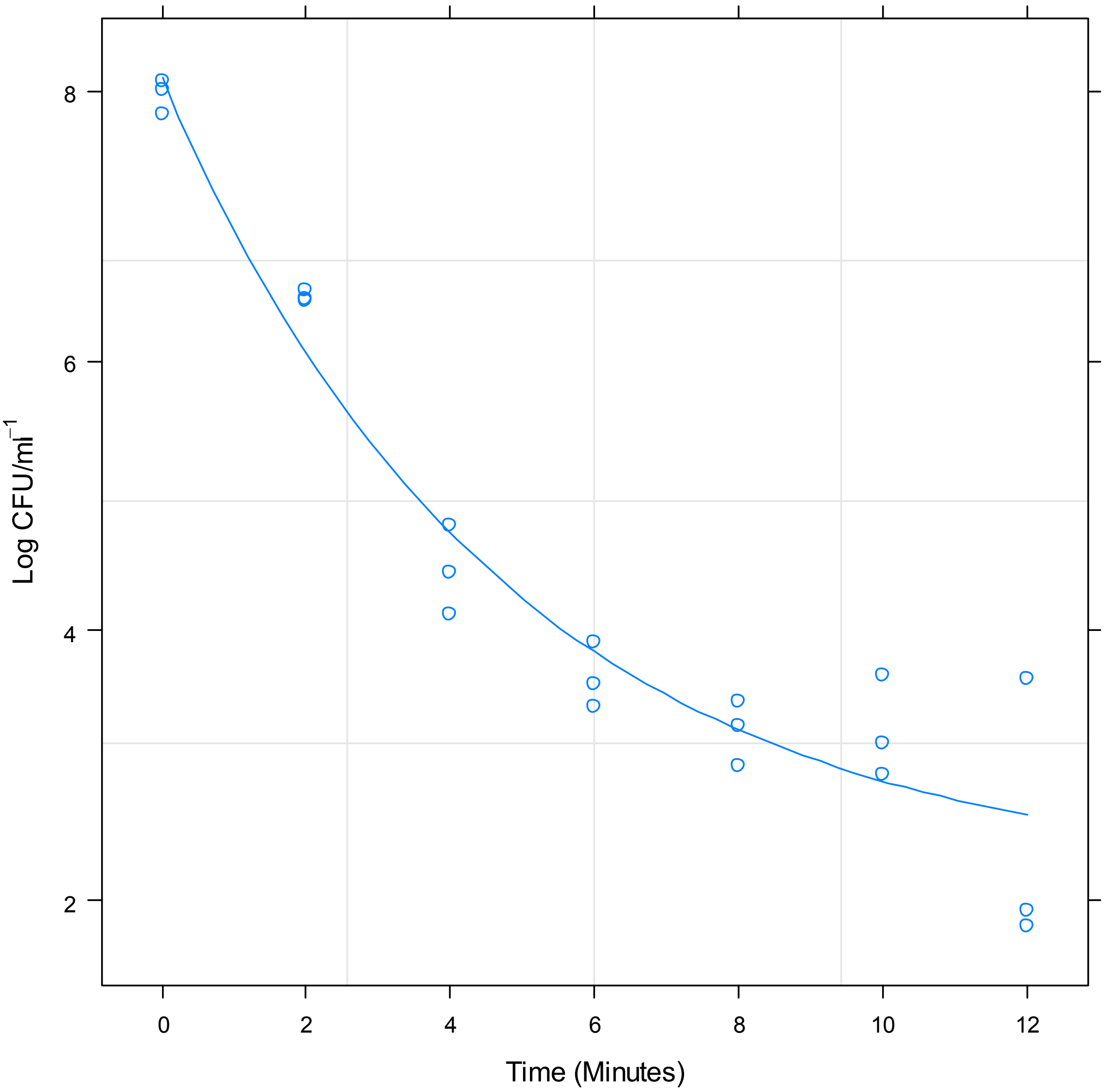

Figure 124. Predicted response curve using an asymptotic regression model for strain 12662 (ST-257, CC-828) at pH 8.5 following heating at 56°C.

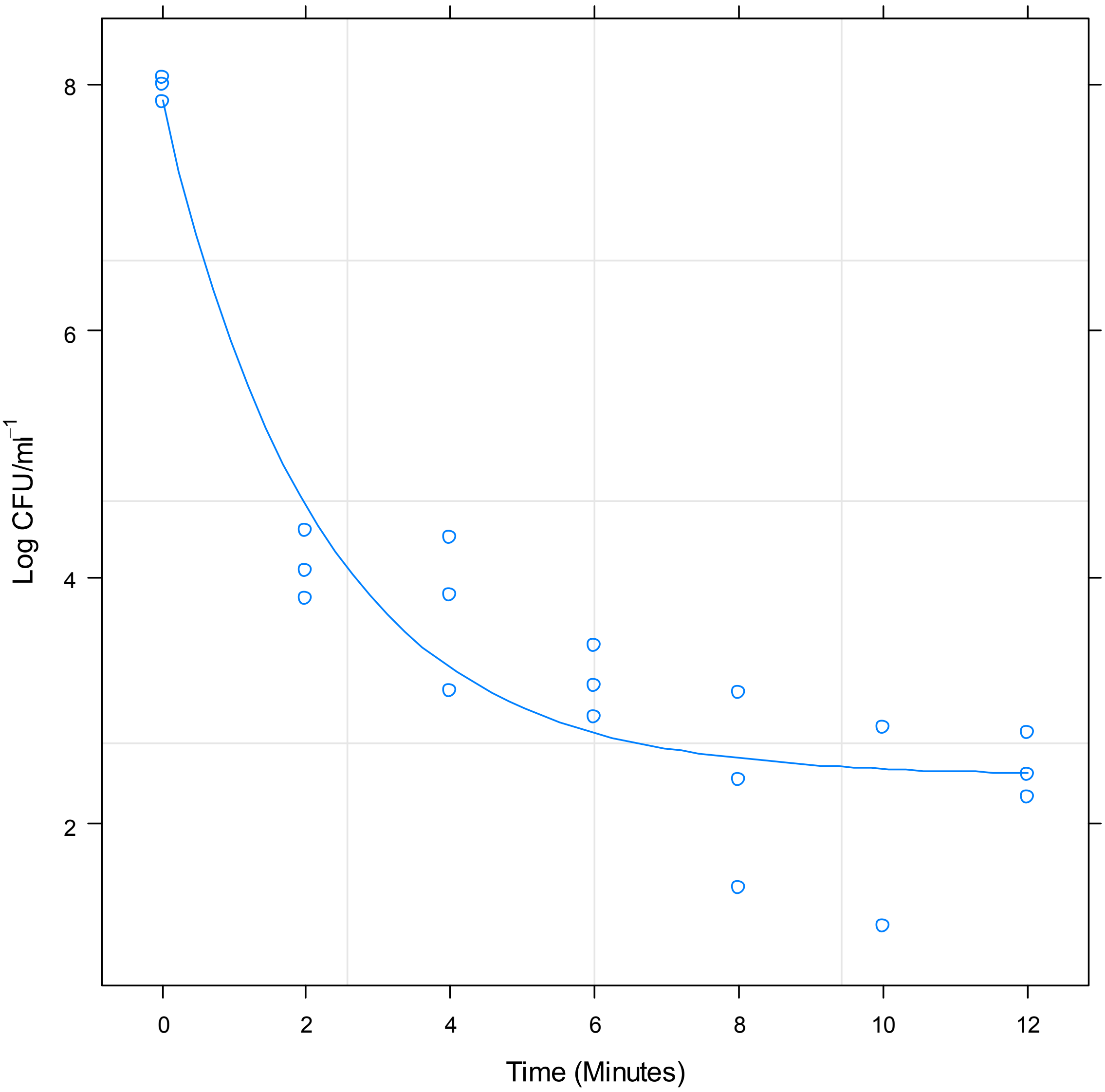

Figure 125. Predicted response curve using an asymptotic regression model for strain 13126 (ST-21, CC-21) at pH 4.5 following heating at 56°C.

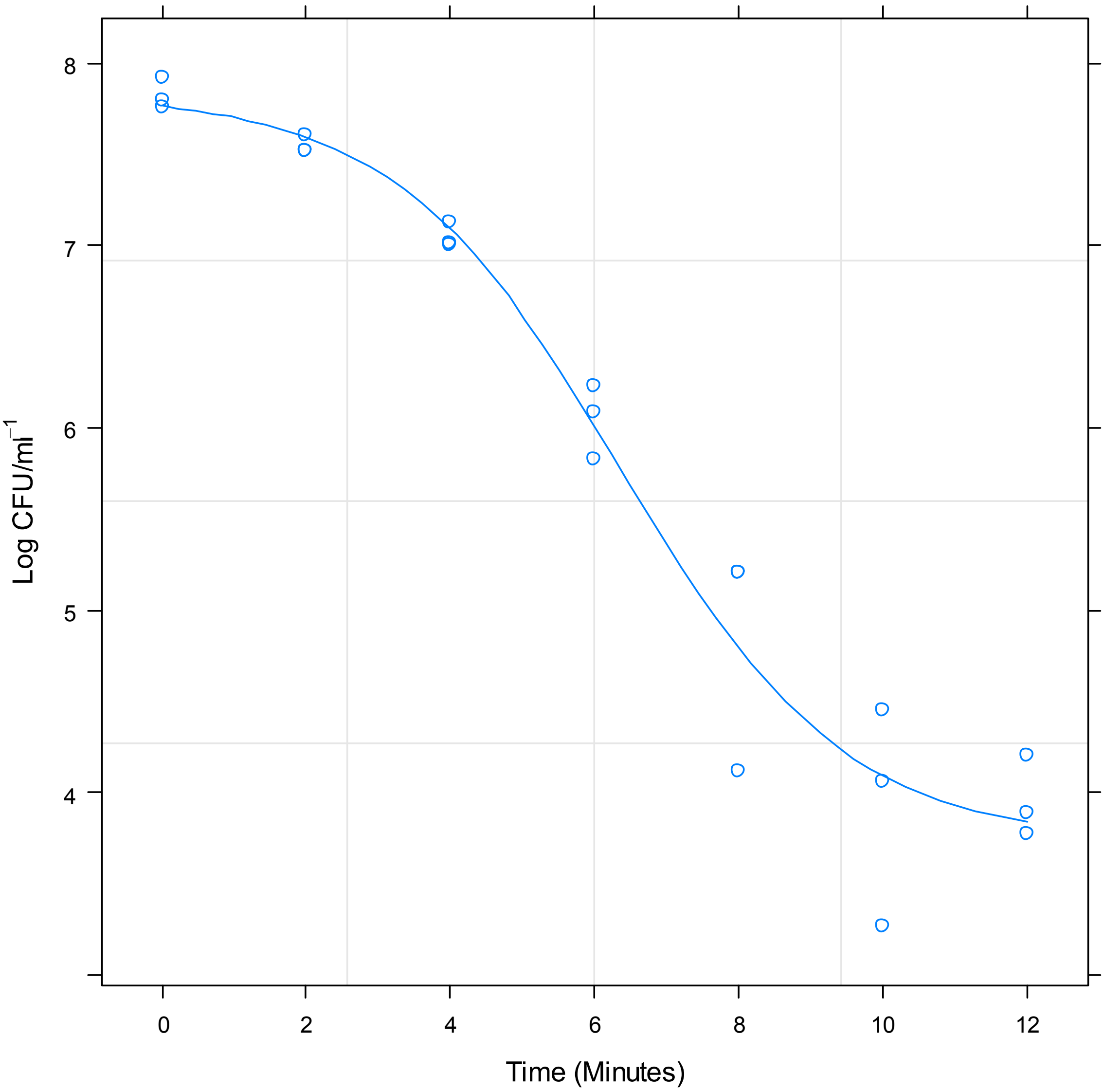

Figure 126. Predicted response curve using a four-parameter logistic regression model for strain 13126 (ST-21, CC-21) at pH 5.5 following heating at 56°C.

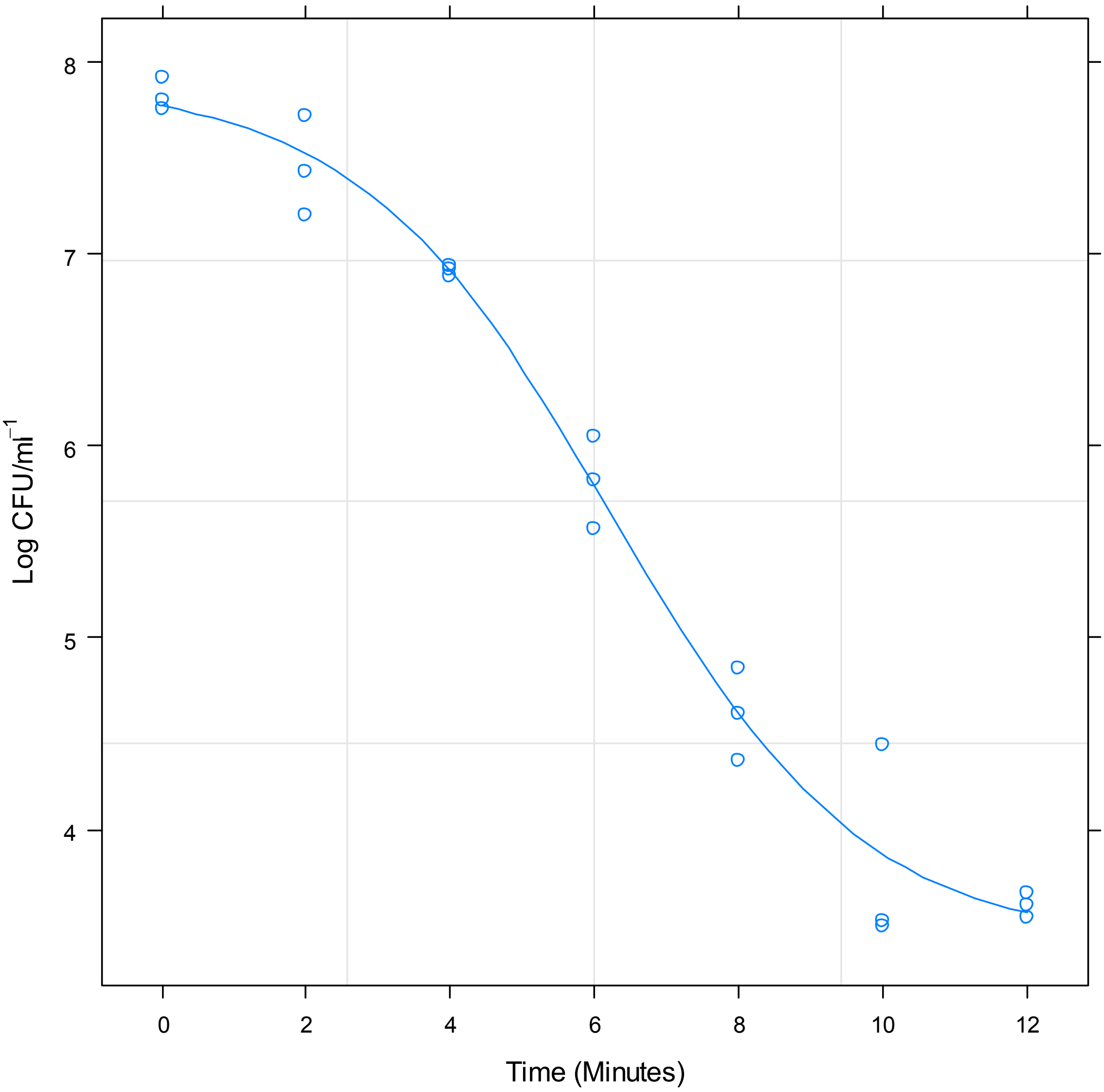

Figure 127. Predicted response curve using a four-parameter logistic regression model for strain 13126 (ST-21, CC-21) at pH 6.5 following heating at 56°C.

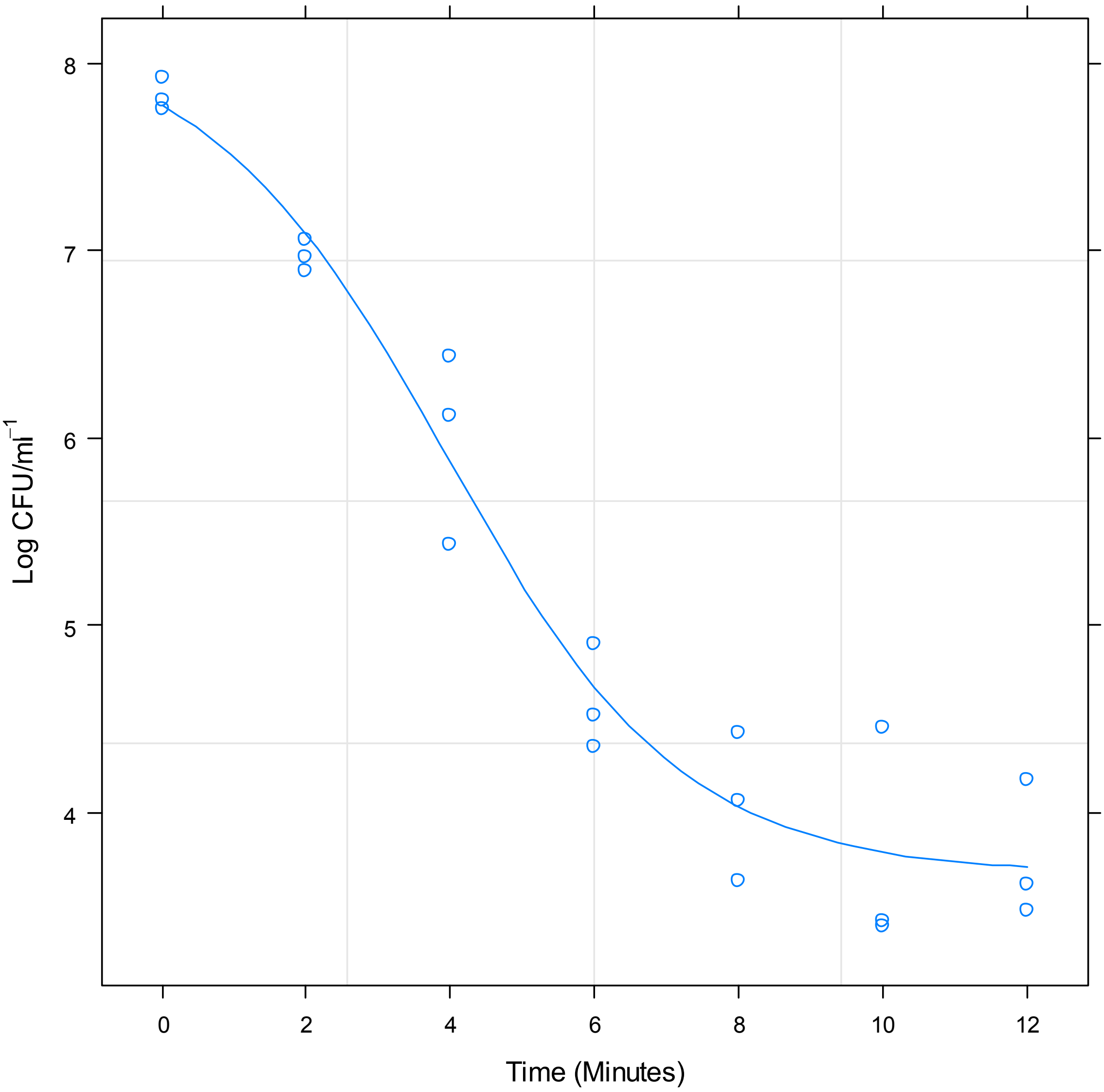

Figure 128. Predicted response curve using a four-parameter logistic regression model for strain 13126 (ST-21, CC-21) at pH 7.5 following heating at 56^{o}C.

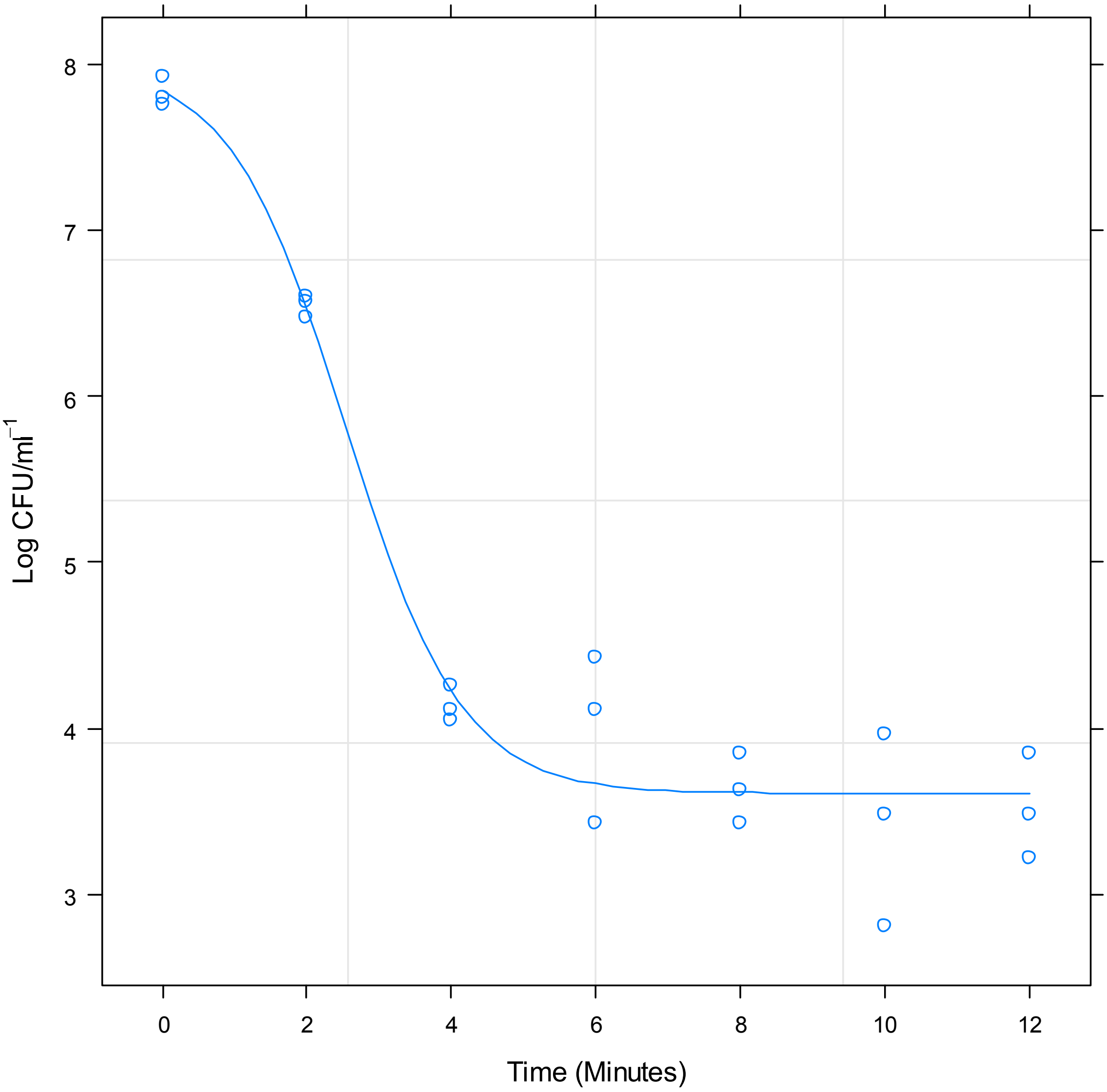

Figure 129. Predicted response curve for strain 13126 (ST-21, CC-21) using a four-parameter logistic regression model following exposure to pH 8.5 and heating at 56°C.

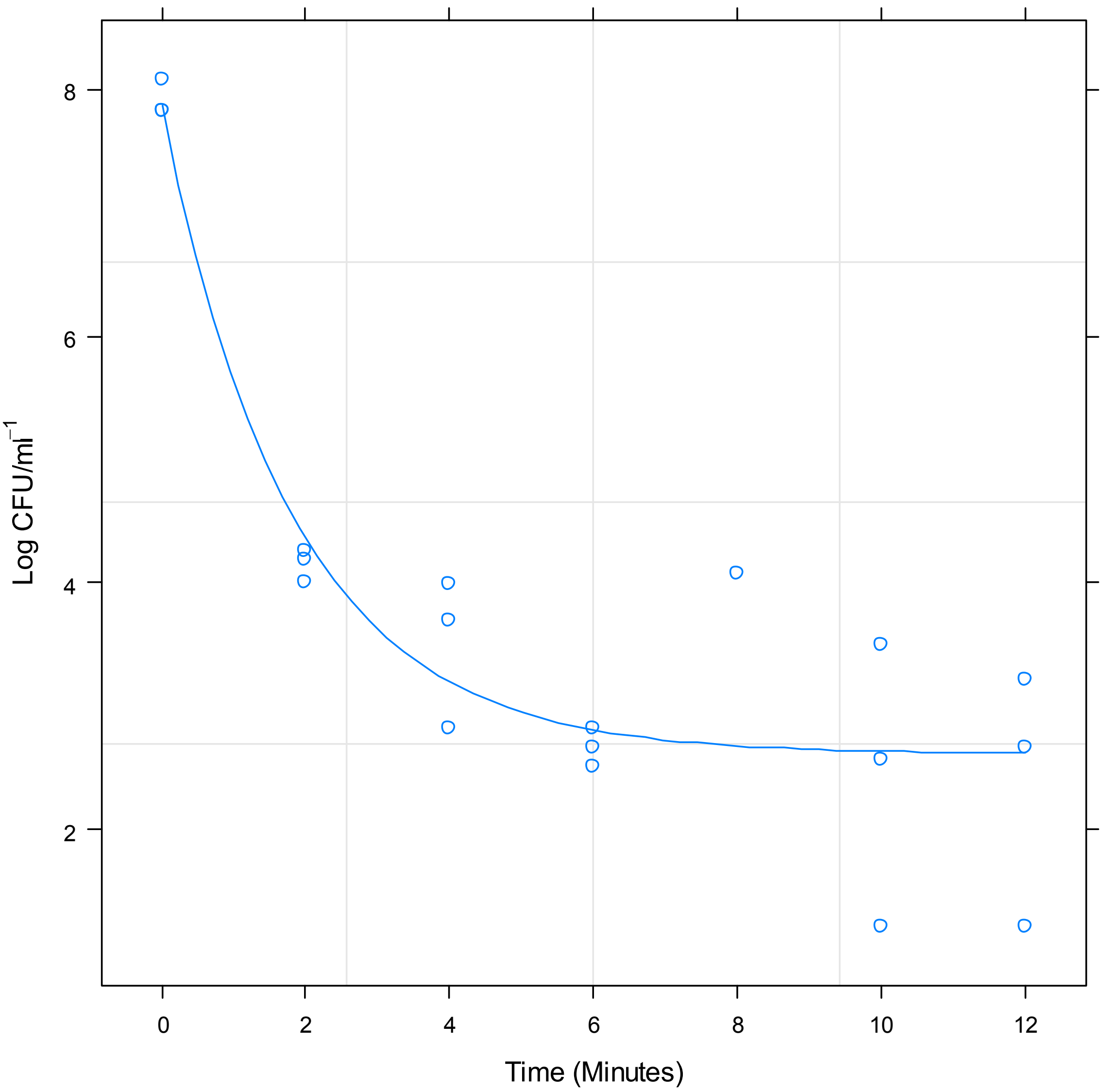

Figure 130. Predicted response curve using an asymptotic regression model for strain 13136 (ST-45, CC-45) at pH 4.5 following heating at 56°C.

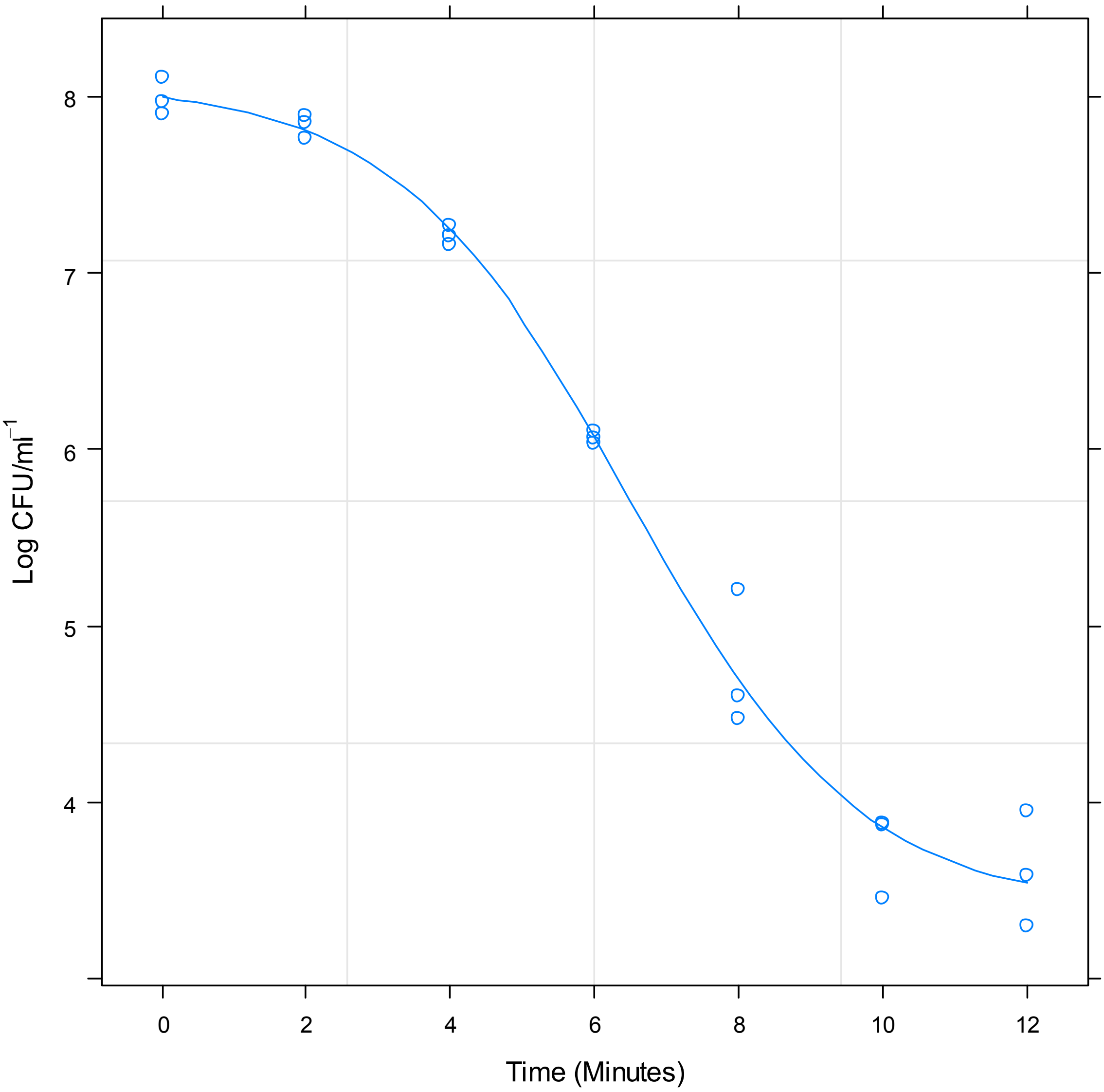

Figure 131. Predicted response curve using a four-parameter logistic regression model for strain 13136 (ST-45, CC-45) at pH 5.5 following heating at 56^{o}C.

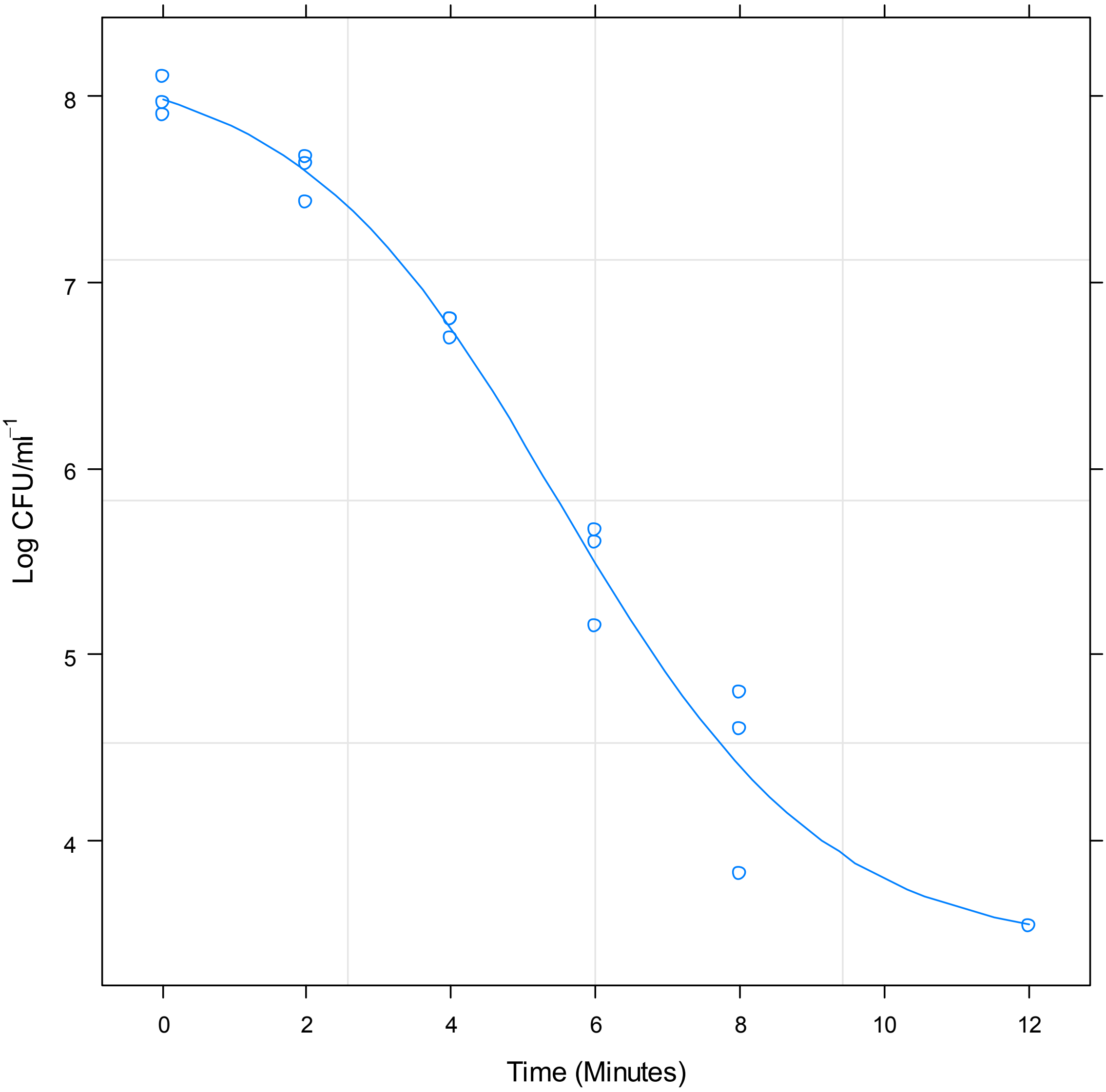

Figure 132. Predicted response curve using a four-parameter logistic regression model for strain 13136 (ST-45, CC-45) at pH 6.5 following heating at 56°C.

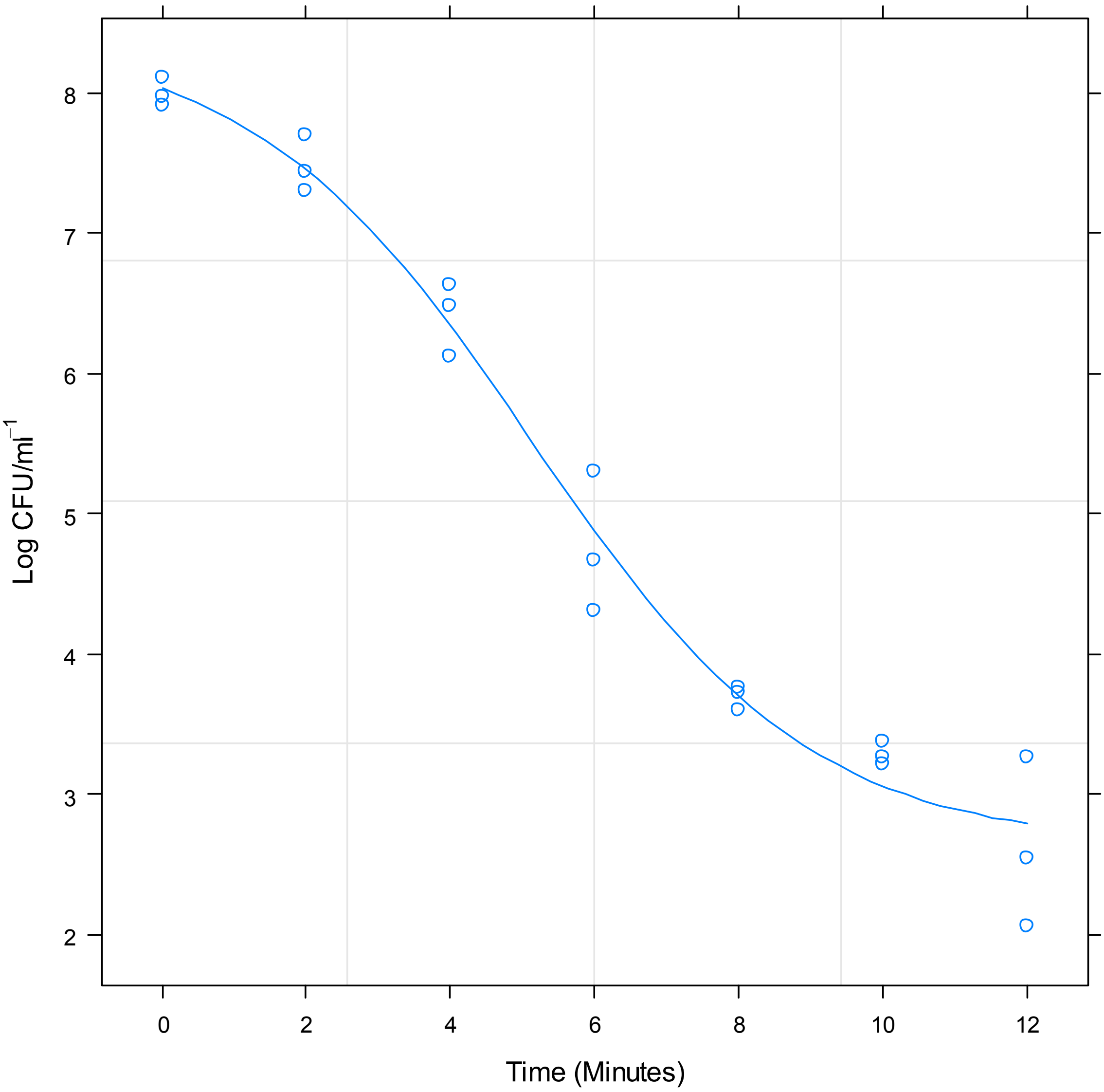

Figure 133. Predicted response using a four-parameter logistic regression model curve for strain 13136 (ST-45, CC-45) at pH 7.5 following heating at 56°C.

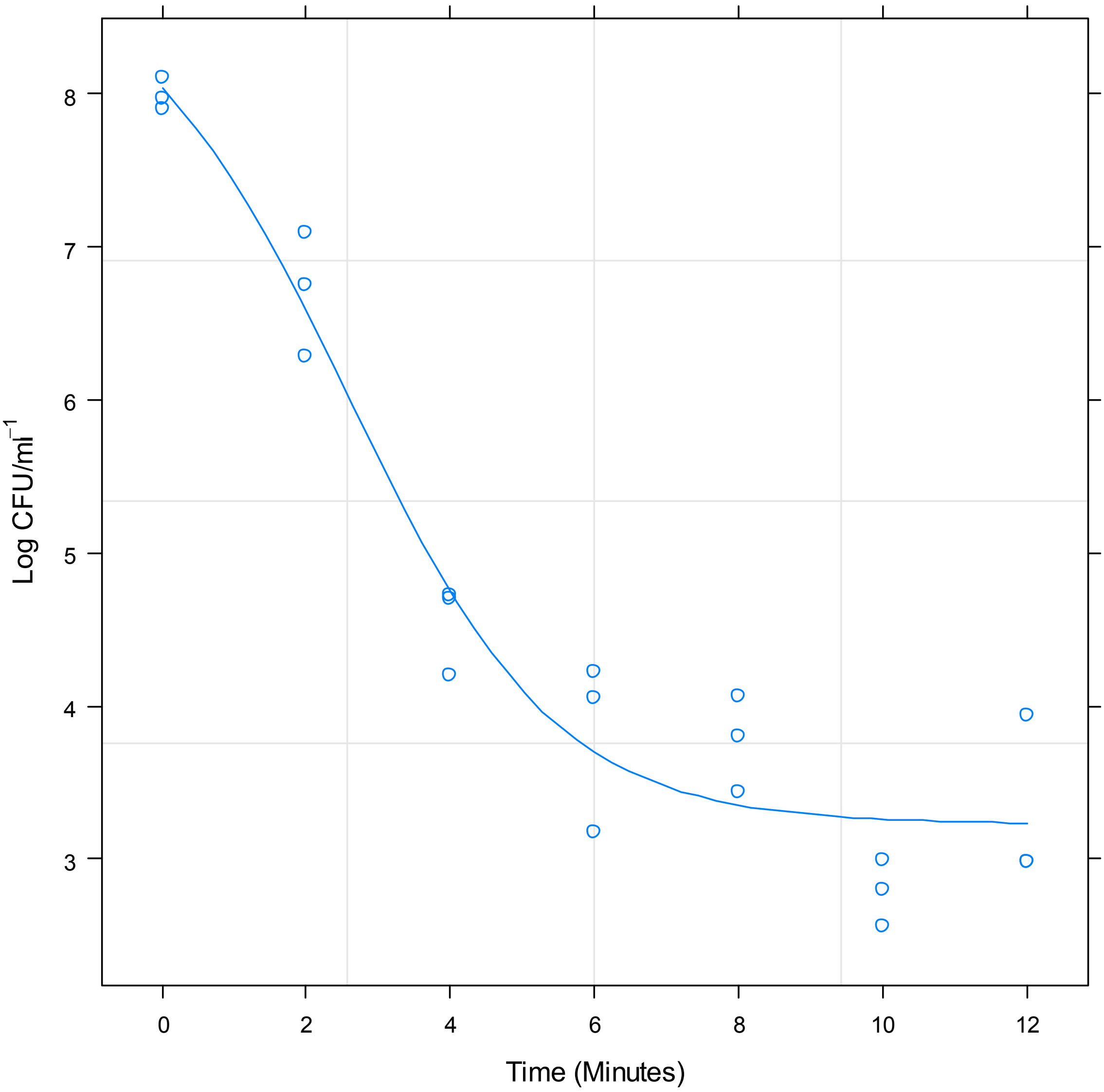

Figure 134. Predicted response curve using a four-parameter logistic regression model for strain 13136 (ST-45, CC-45) at pH 8.5 following heating at 56°C.

1.8.20 pH and Time-Temperature Simulations: 56°C

Mixed Weibull Distribution Model Predicted Response Curves:

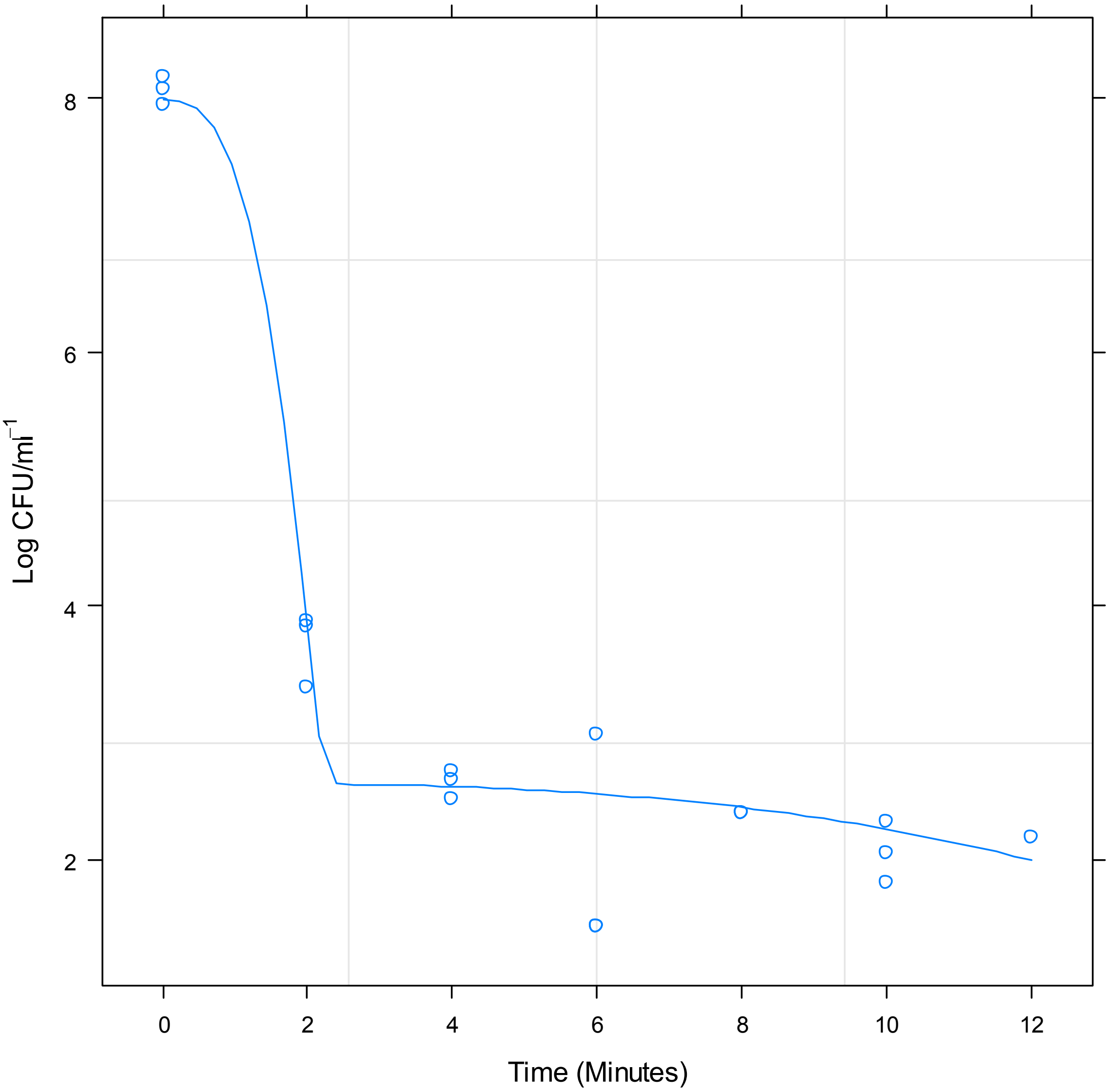

Figure 135. Predicted response curve using a mixed Weibull regression model for strain 12628 (ST1773-CC828) at pH 4.5 following heating at 56°C.

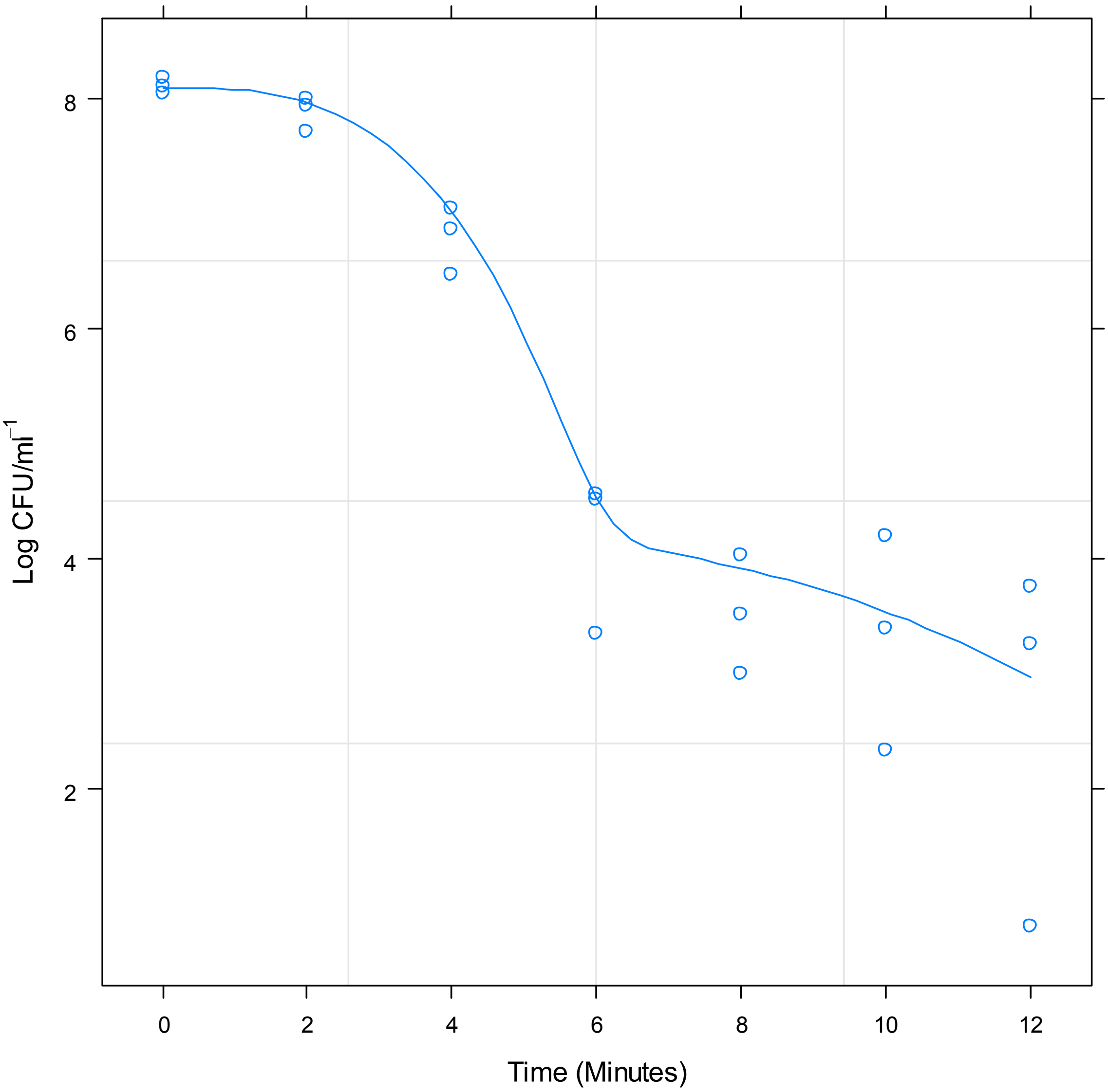

Figure 136. Predicted response curve using a mixed Weibull distribution model of strain 12628 (ST1773-CC828) at pH 5.5 following heating at 56^{o}C.

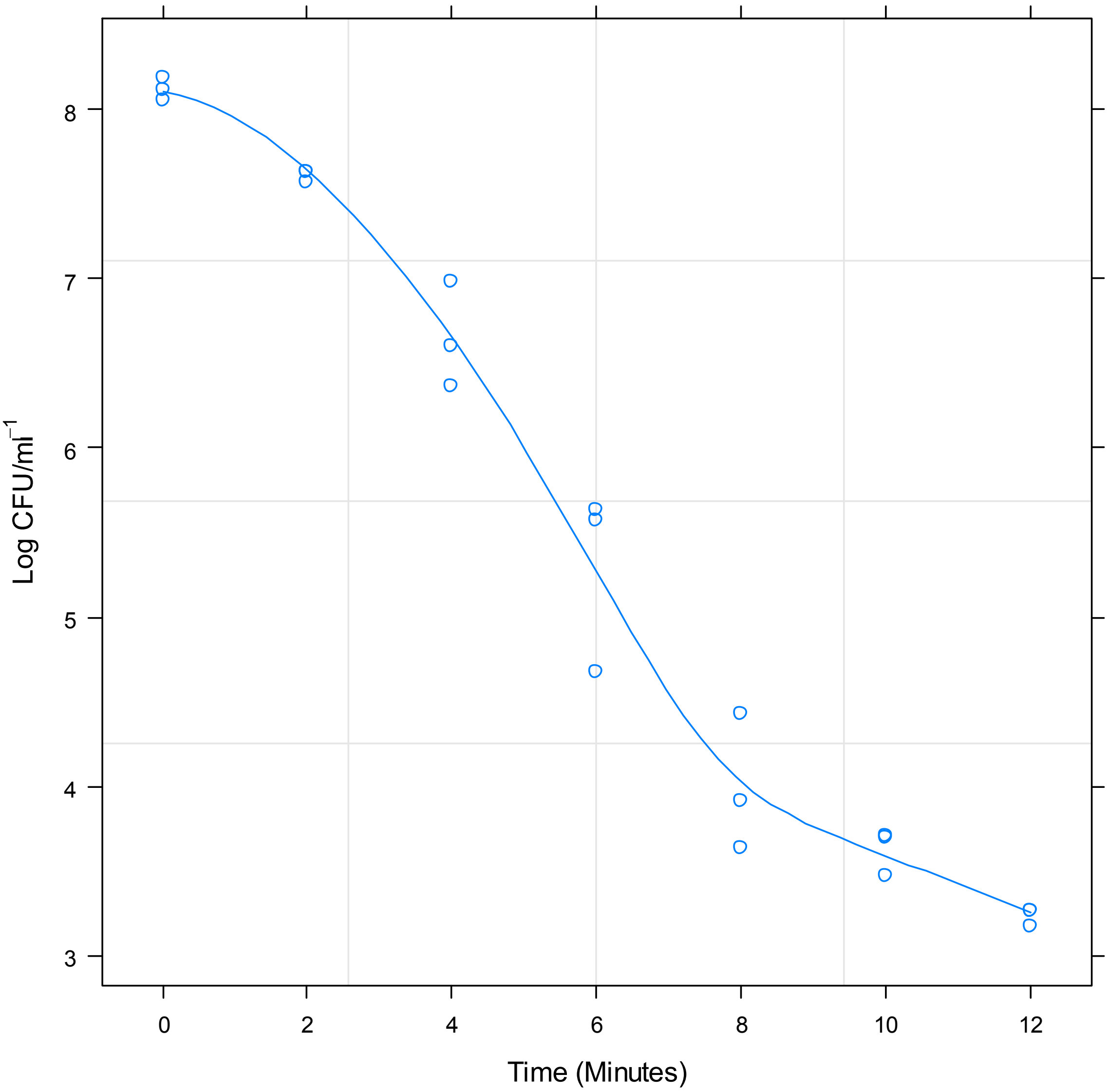

Figure 137. Predicted response curve using a mixed Weibull distribution model of strain 12628 (ST1773-CC828) at pH 6.5 following heating at 56^{o}C.

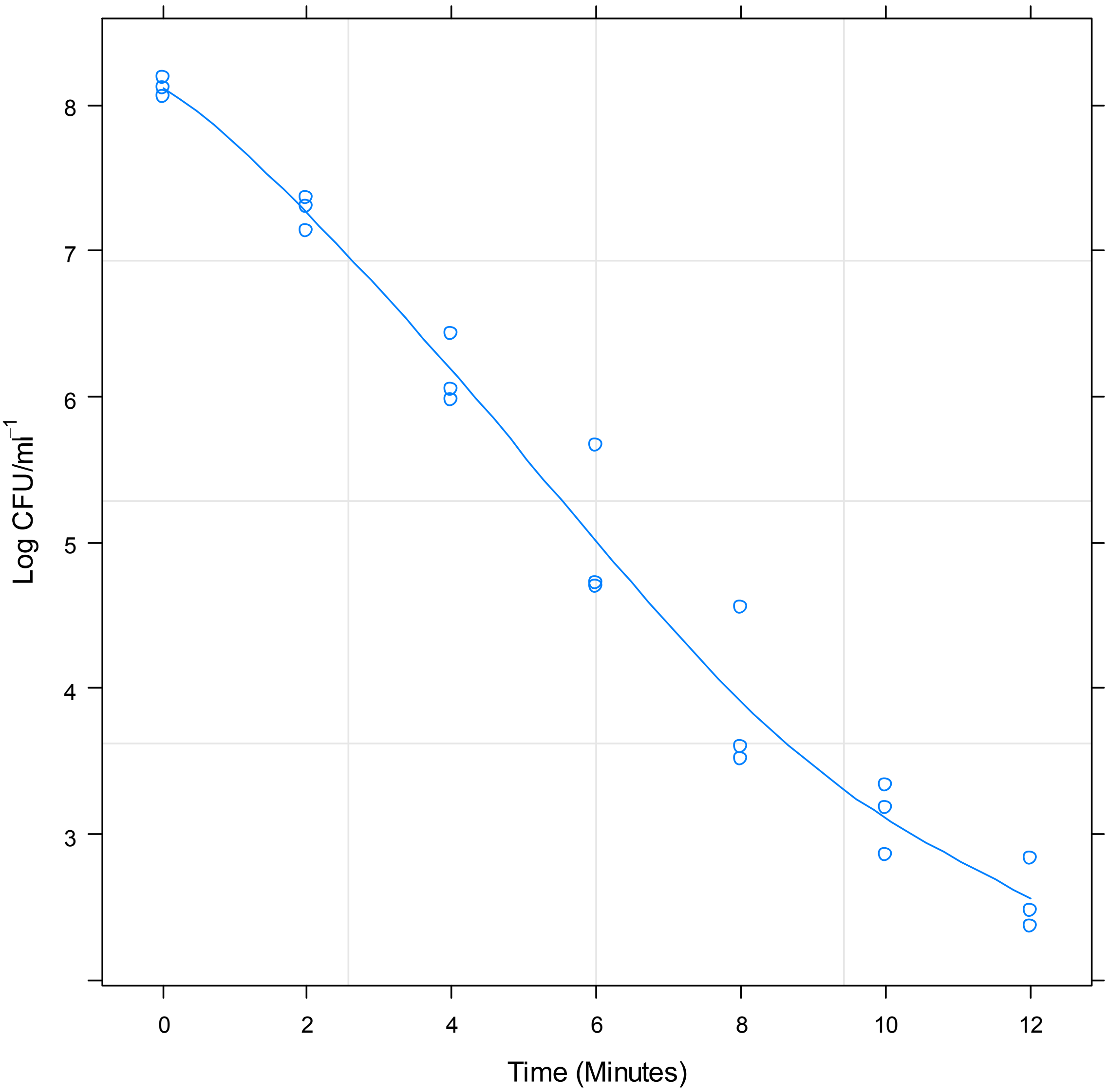

Figure 138. Predicted response curve using a mixed Weibull distribution model of strain 12628 (ST1773-CC828) at pH 7.5 following heating at 56^{o}C.

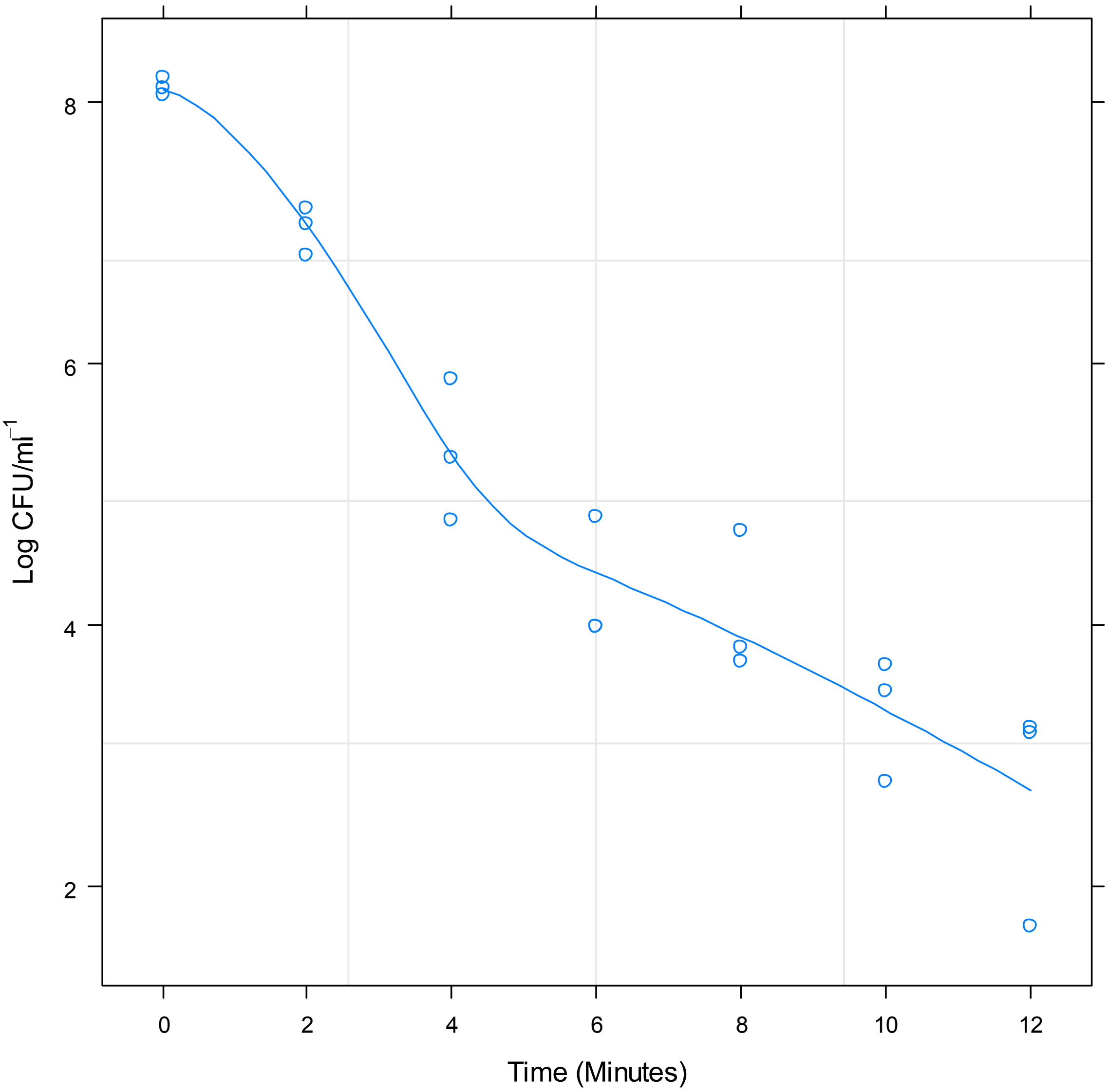

Figure 139. Predicted response curve using a mixed Weibull distribution model of strain 12628 (ST1773-CC828) at pH 8.5 following heating at 56°C.

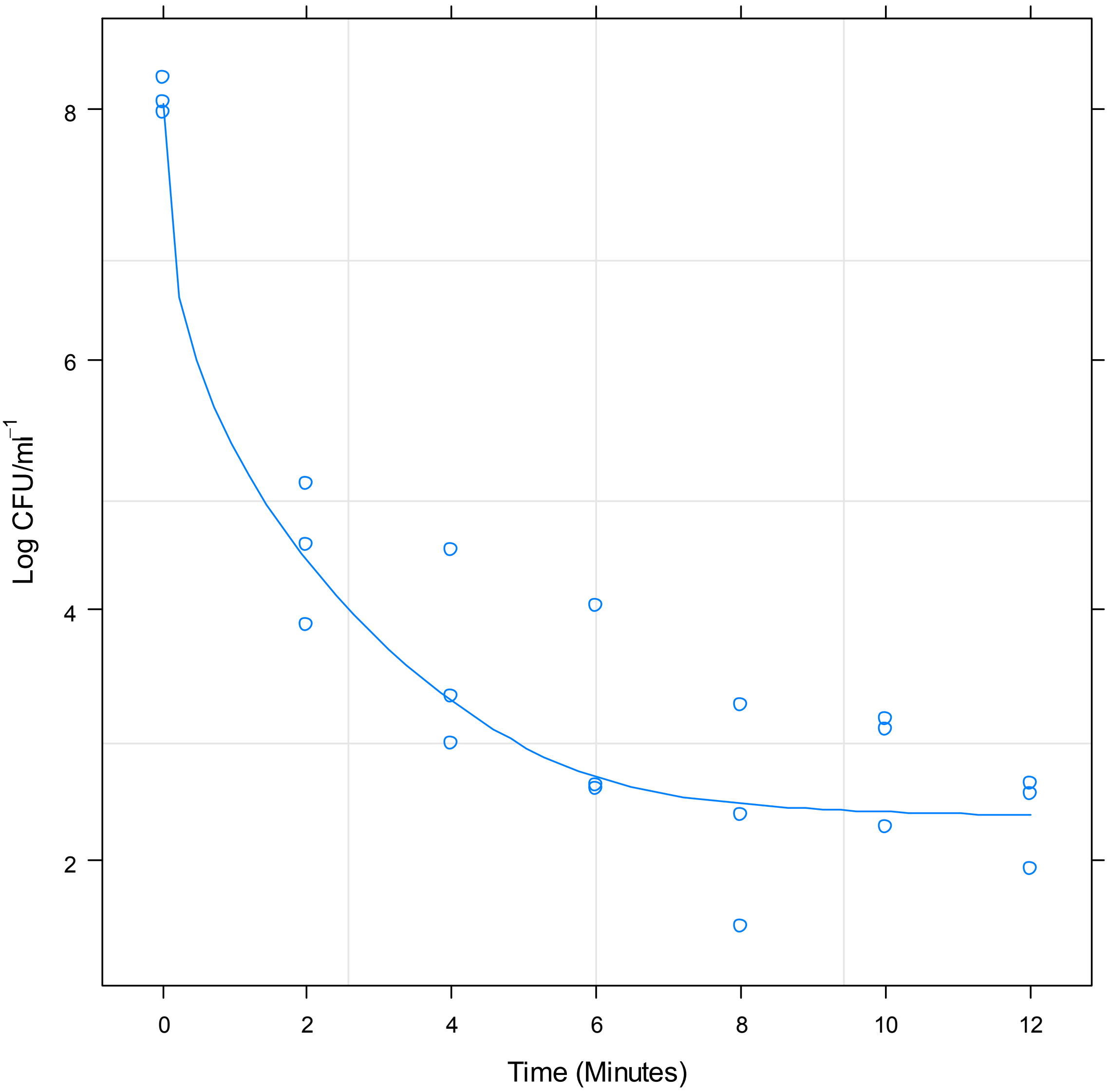

Figure 140. Predicted response curve using a mixed Weibull distribution model of strain 12662 (ST-257, CC-257) at pH 4.5 following heating at 56°C.

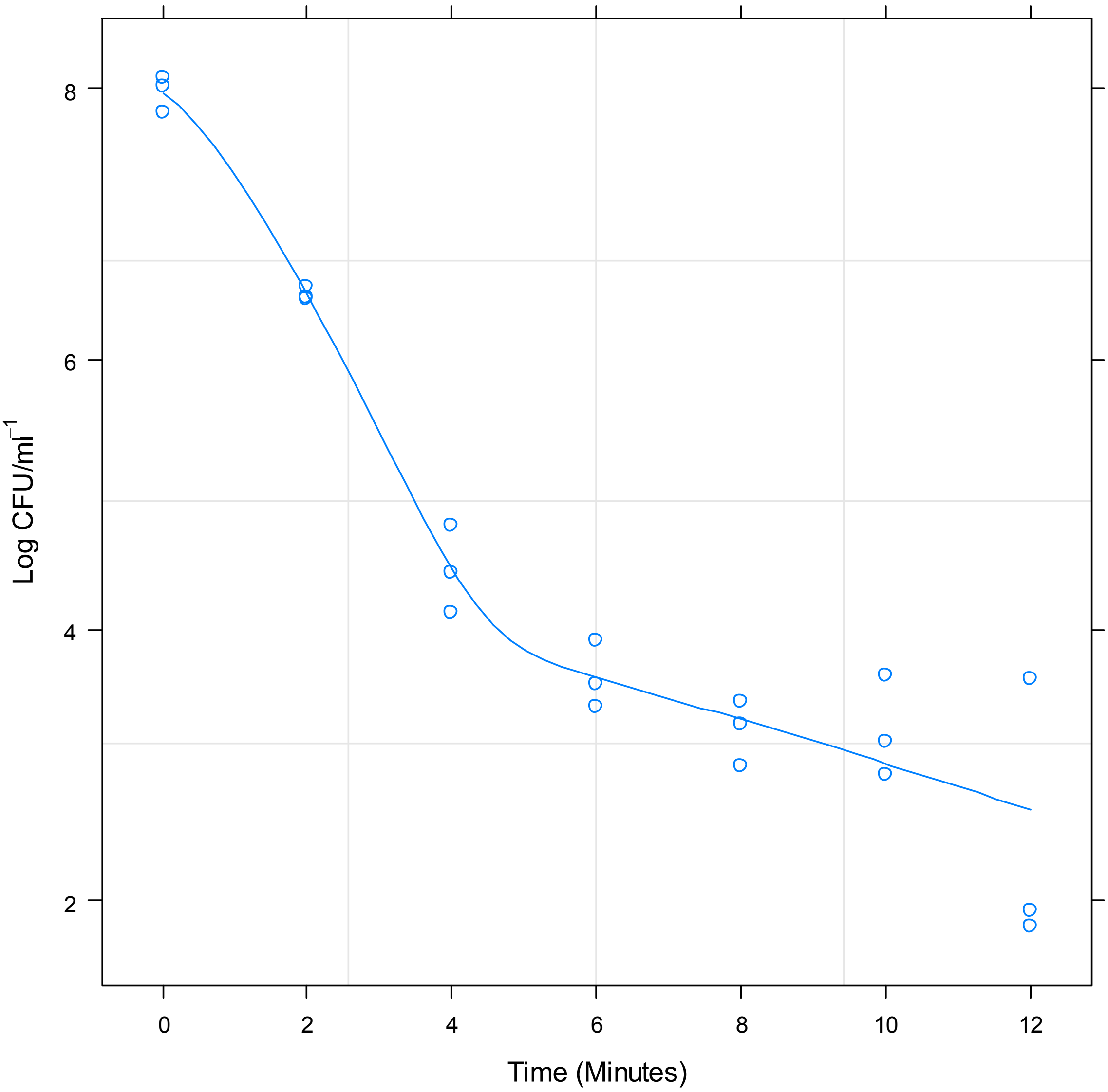

Figure 141. Predicted response curve using a mixed Weibull distribution model of strain 12662 (ST-257, CC-257) at pH 8.5 following heating at 56^{o}C.

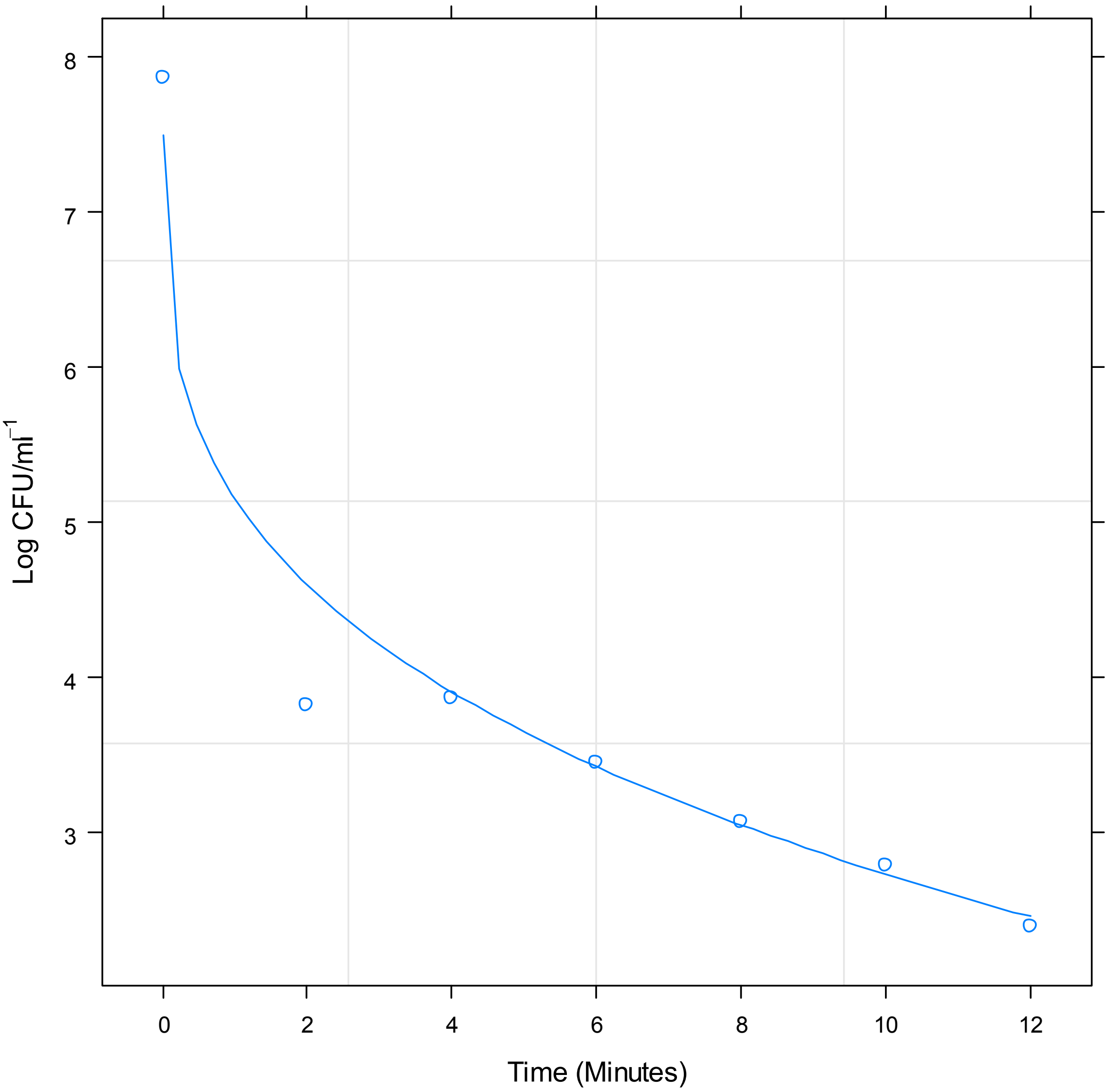

Figure 142. Predicted response curve using a mixed Weibull distribution model of strain 13126 (ST-21, CC-21) at pH 4.5 following heating at 56°C.

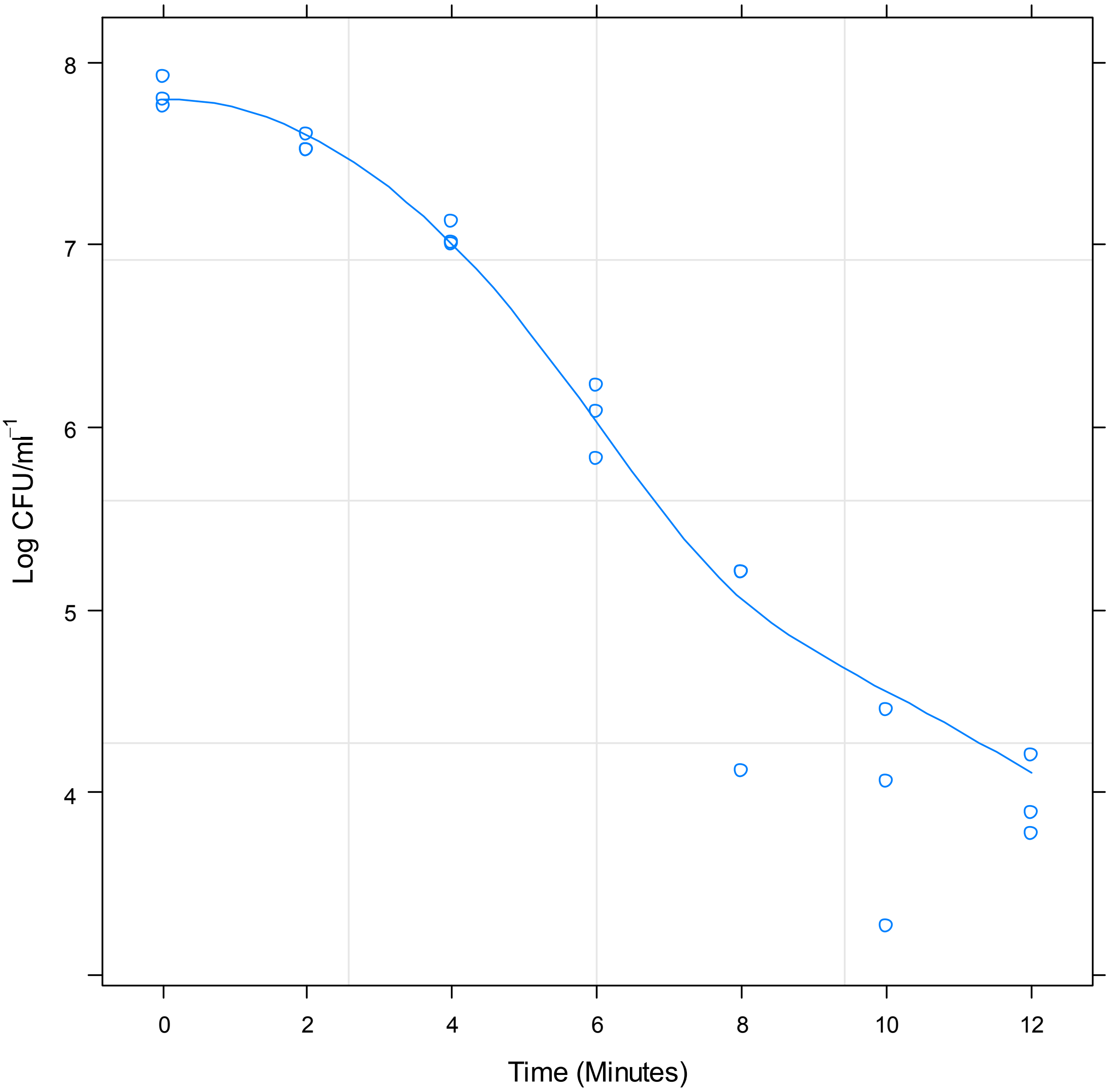

Figure 143. Predicted response curve using a mixed Weibull distribution model of strain 13126 (ST-21, CC-21) at pH 5.5 following heating at 56°C.

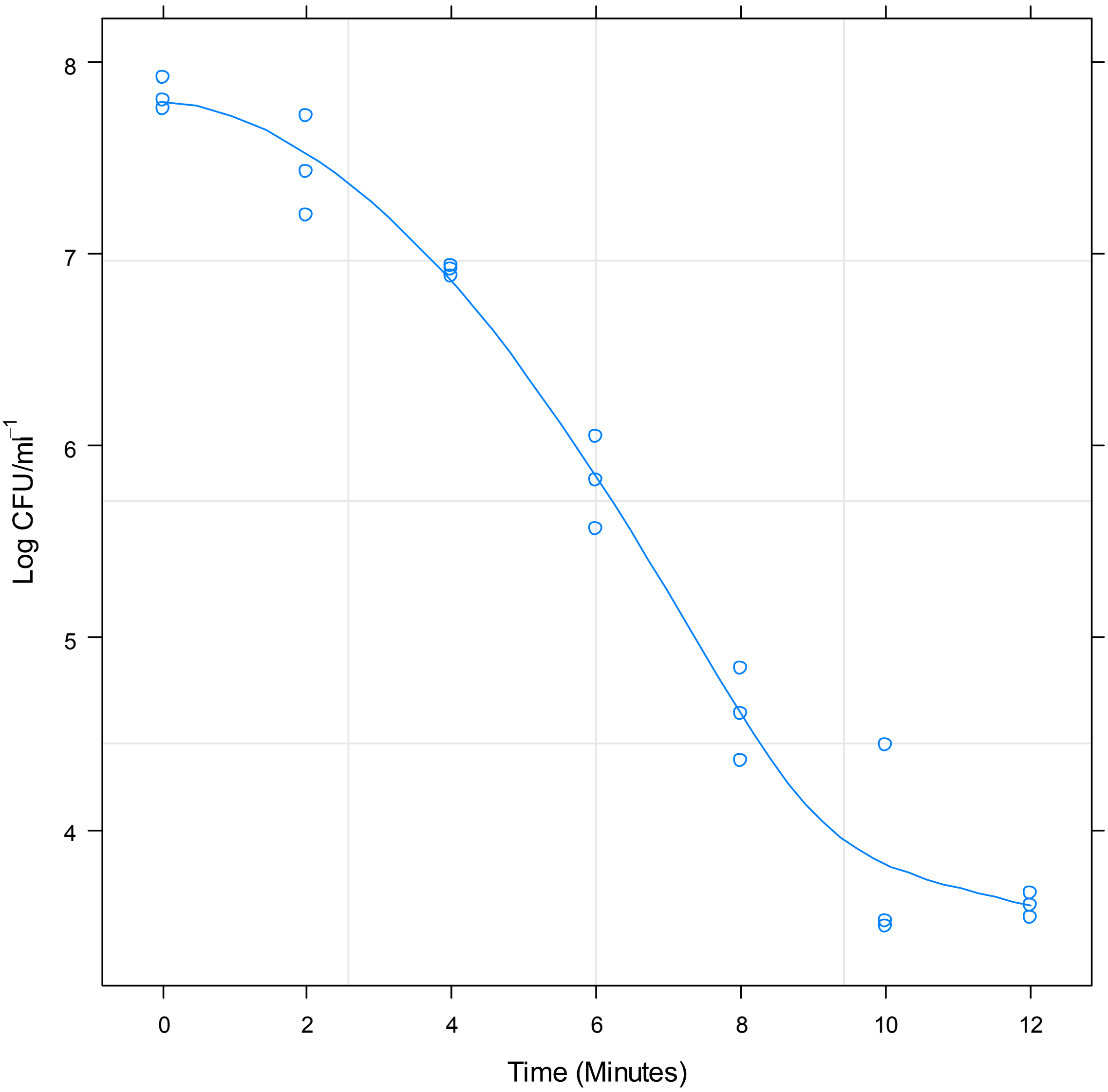

Figure 144. Predicted response curve using a mixed Weibull distribution model of strain 13126 (ST-21, CC-21) at pH 6.5 following heating at 56°C.

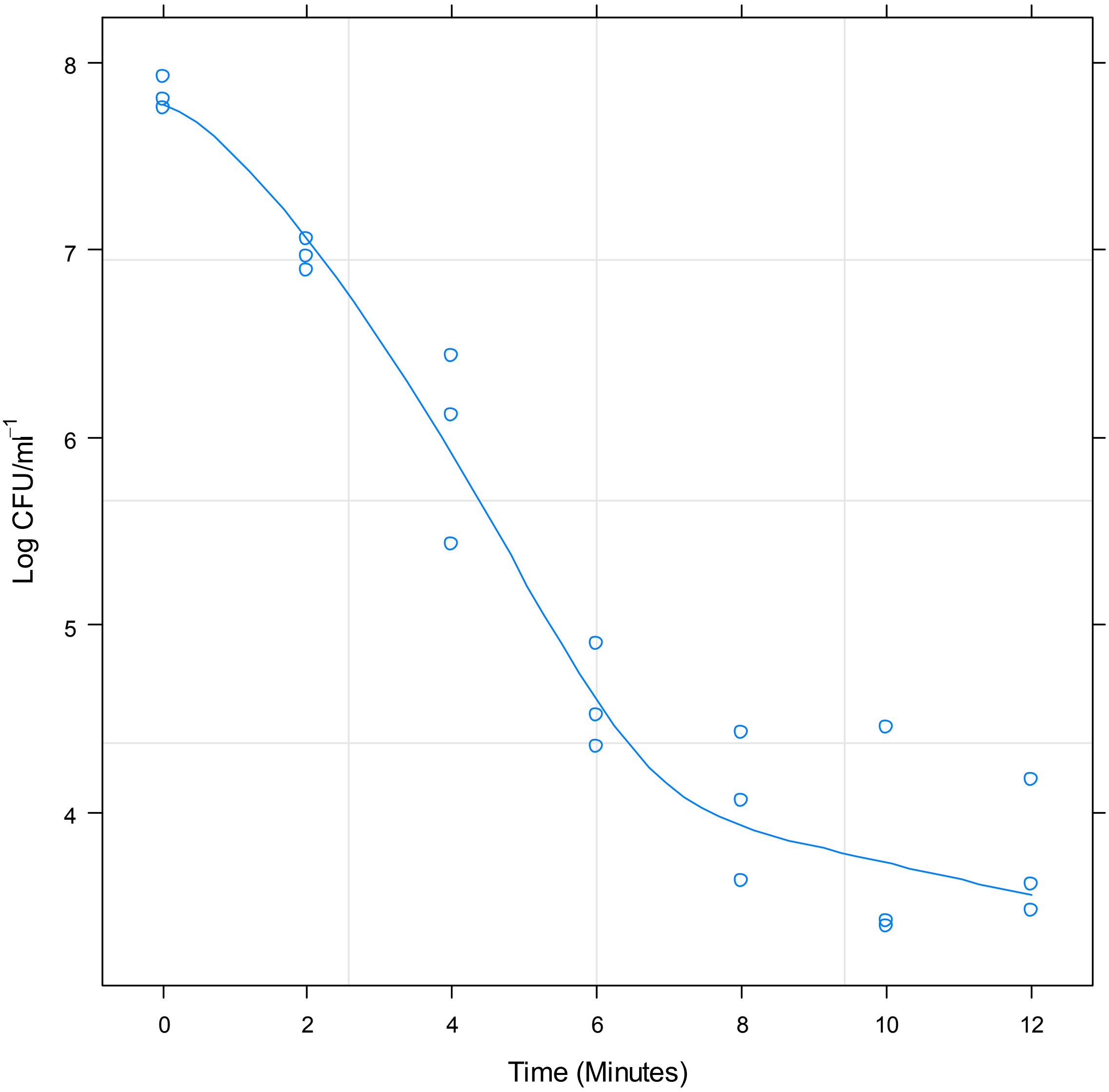

Figure 145. Predicted response curve using a mixed Weibull distribution model of strain 13126 (ST-21, CC-21) at pH 7.5 following heating at 56^{o}C.

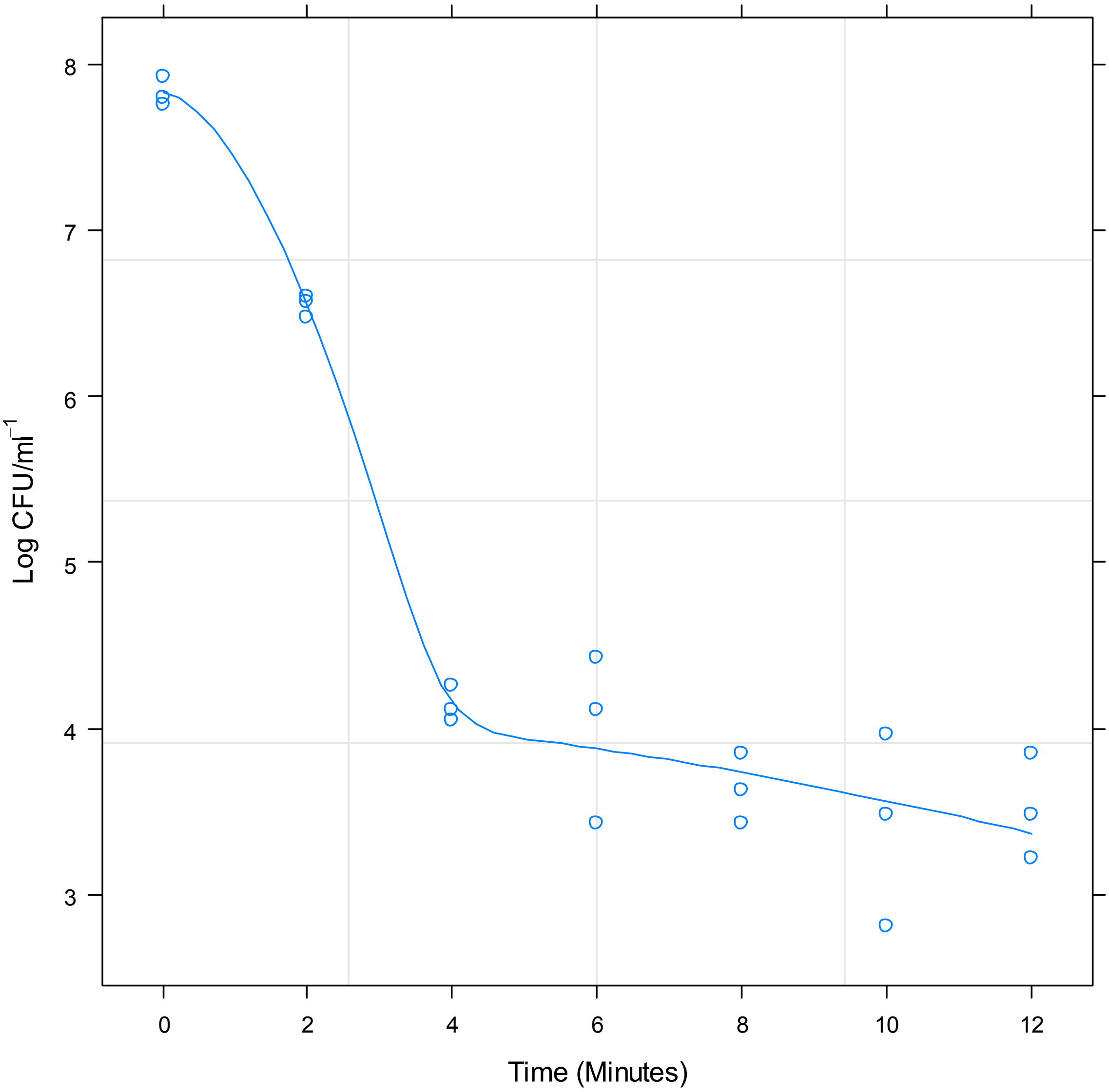

Figure 146. Predicted response curve using a mixed Weibull distribution model of strain 13126 (ST-21, CC-21) at pH 8.5 following heating at 56°C.

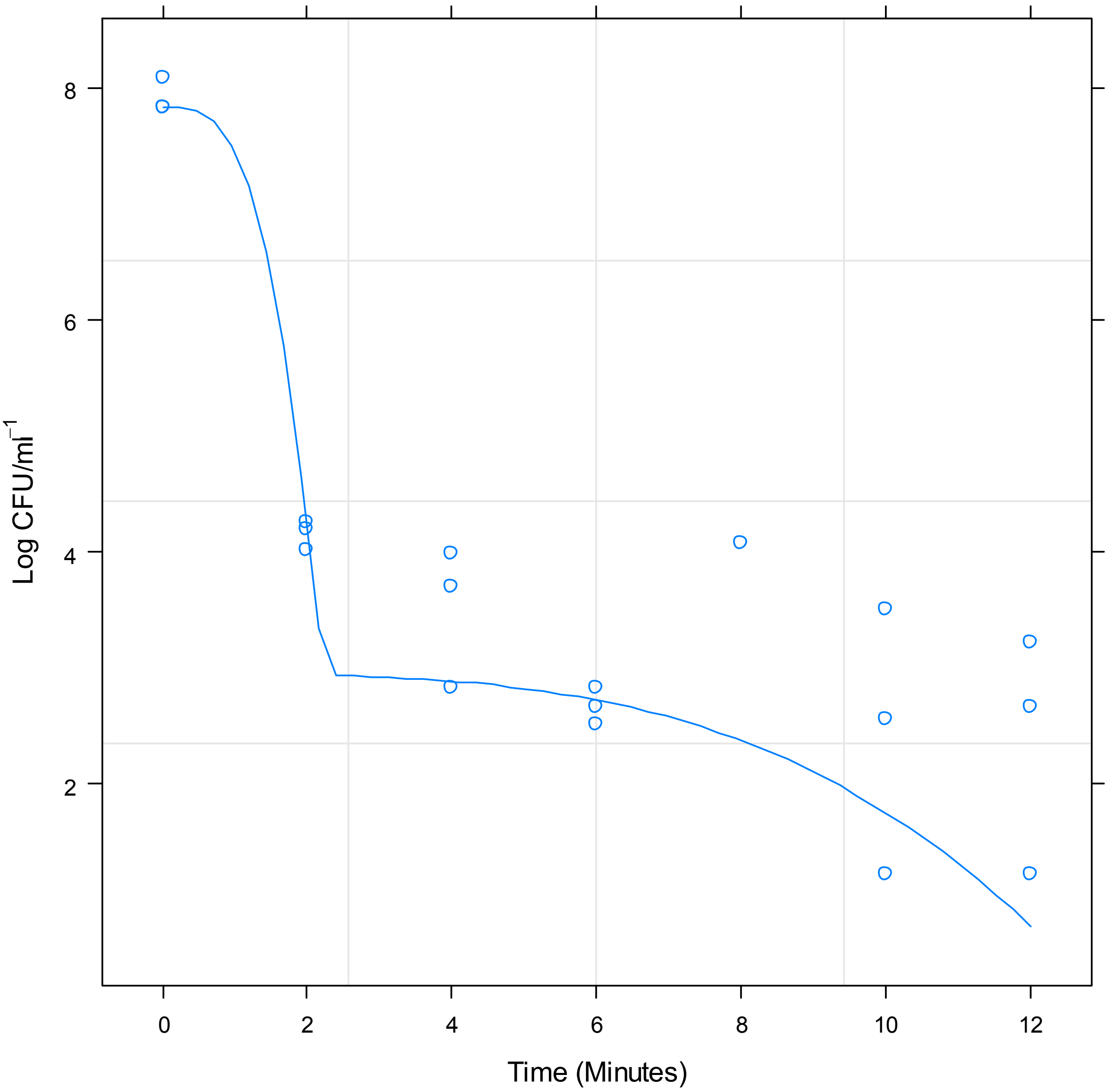

Figure 147. Predicted response curve using a mixed Weibull distribution model of strain 13136 (ST-45, CC-45) at pH 4.5 following heating at 56^{o}C.

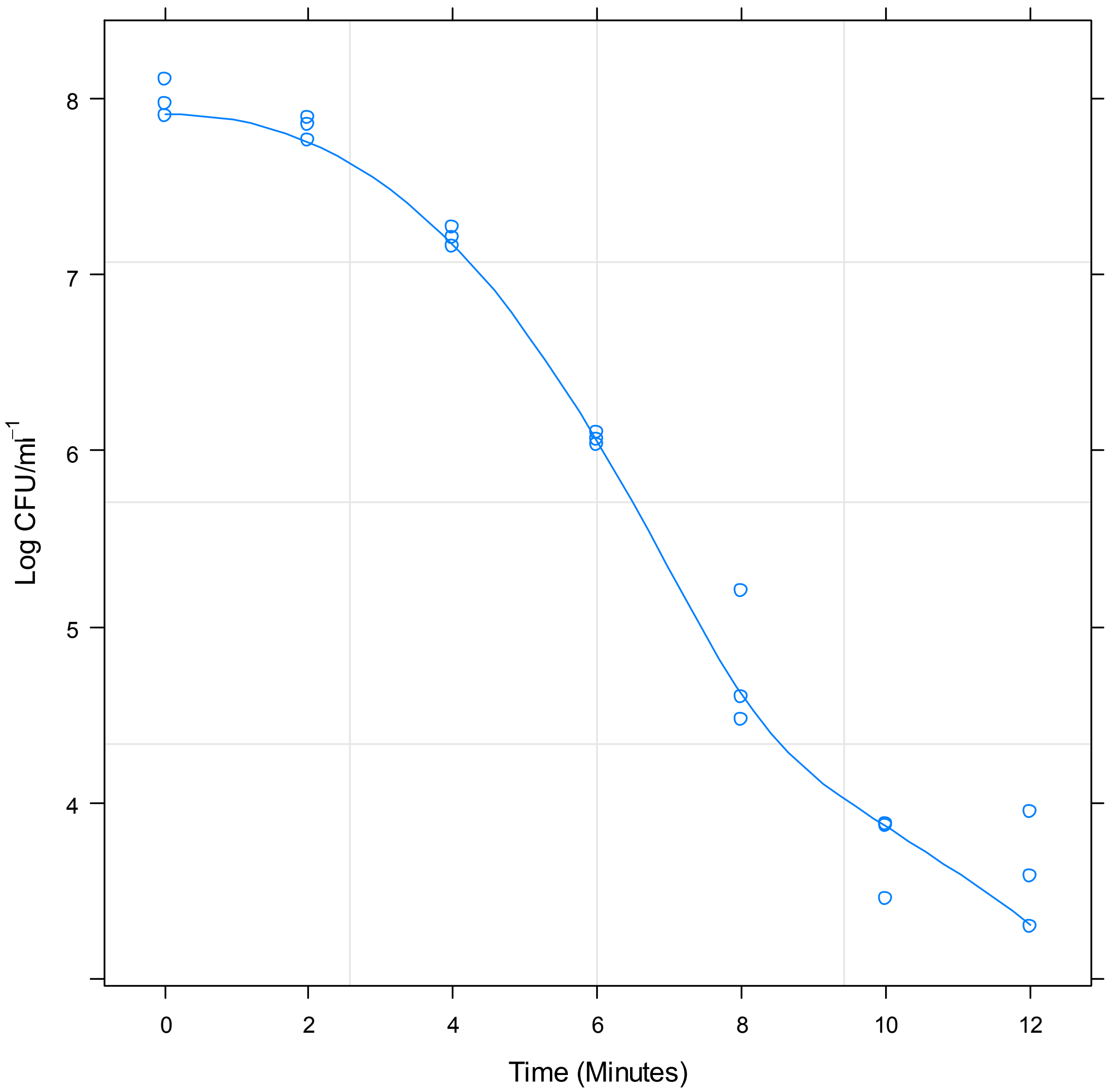

Figure 148. Predicted response curve using a mixed Weibull distribution model of strain 13136 (ST-45, CC-45) at pH 5.5 following heating at 56°C.

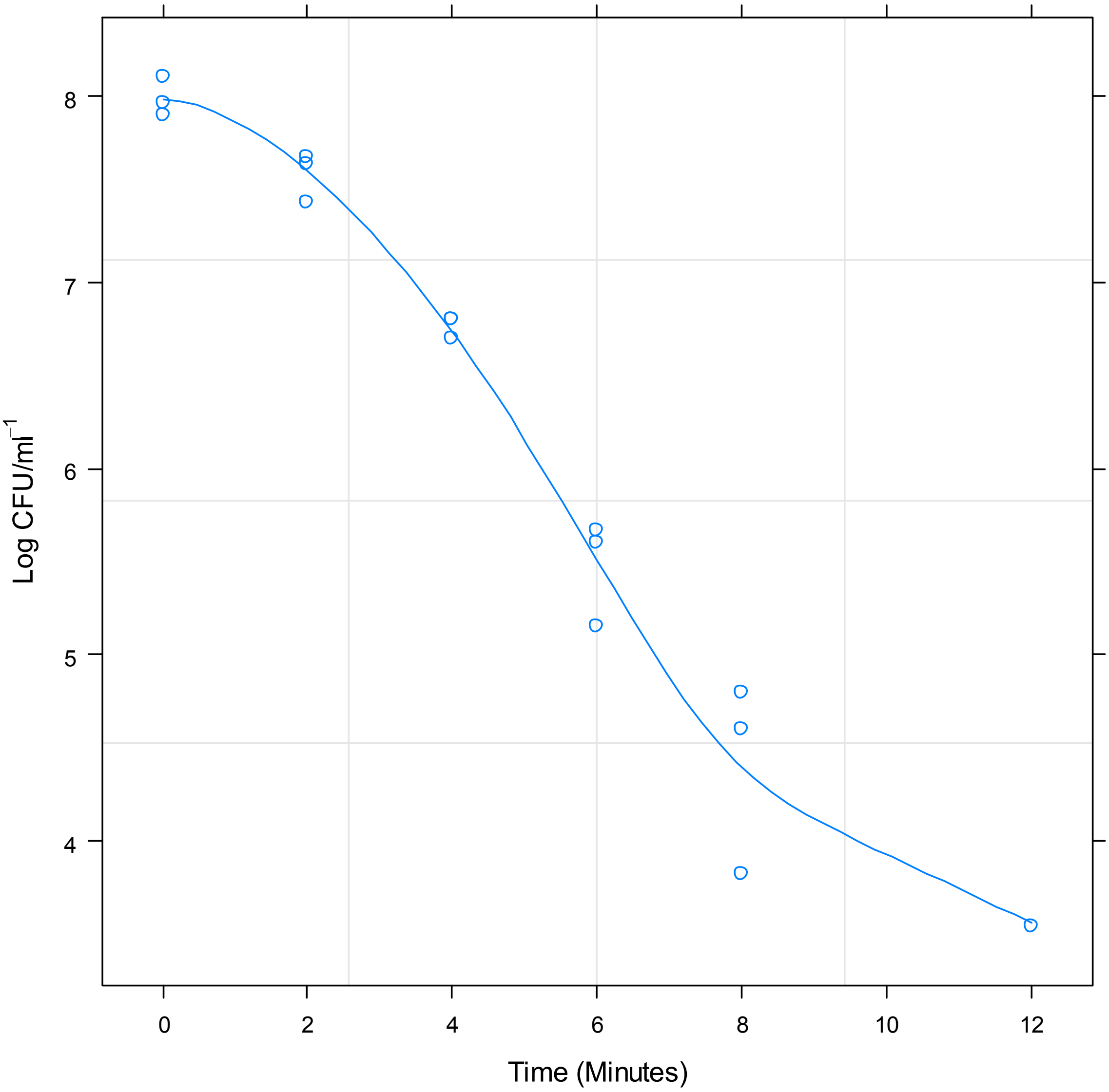

Figure 149. Predicted response curve using a mixed Weibull distribution model of strain 13136 (ST-45, CC-45) at pH 6.5 following heating at 56°C.

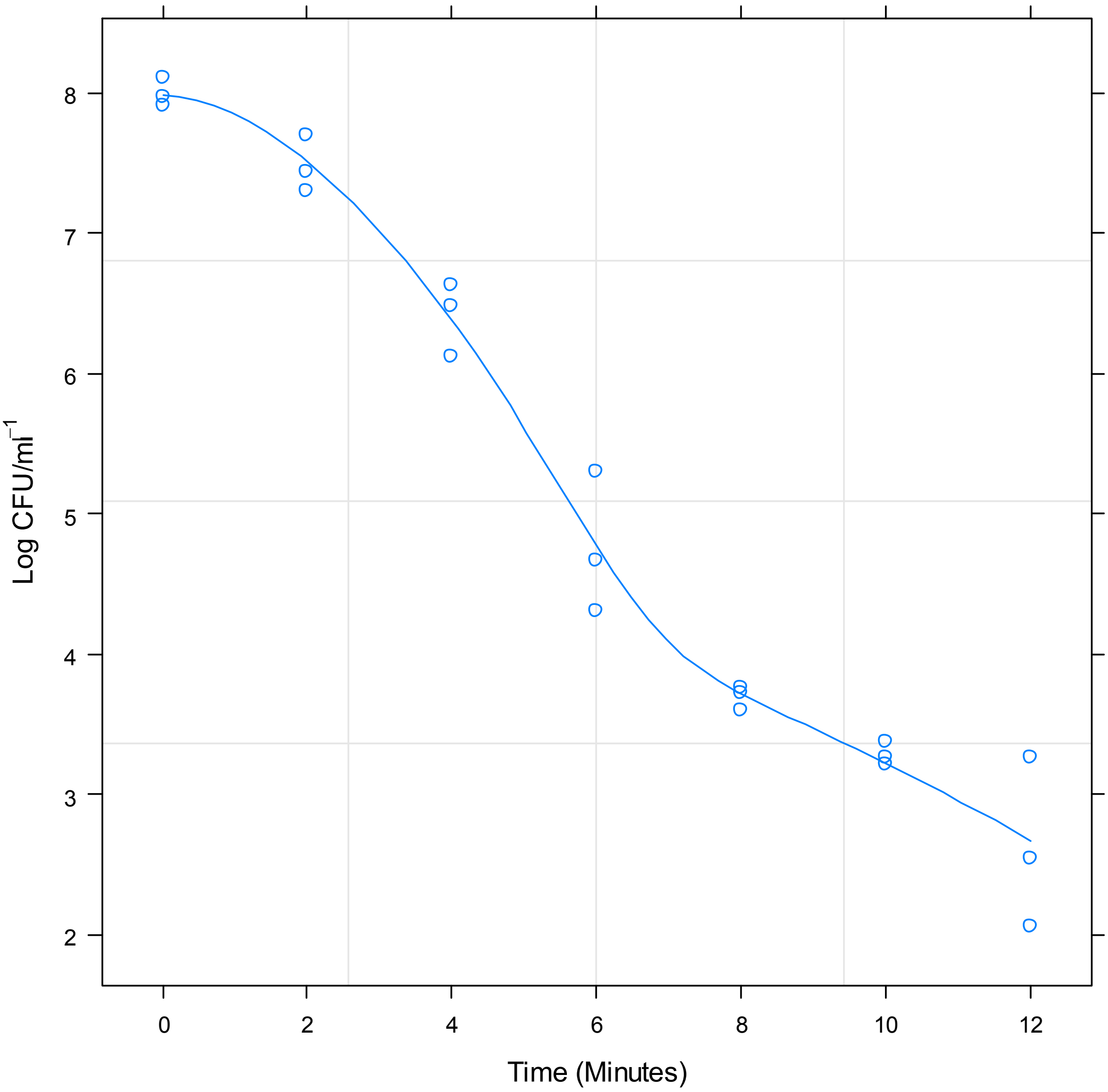

Figure 150. Predicted response curve using a mixed Weibull distribution model of strain 13136 (ST-45, CC-45) at pH 7.5 following heating at 56^{o}C.

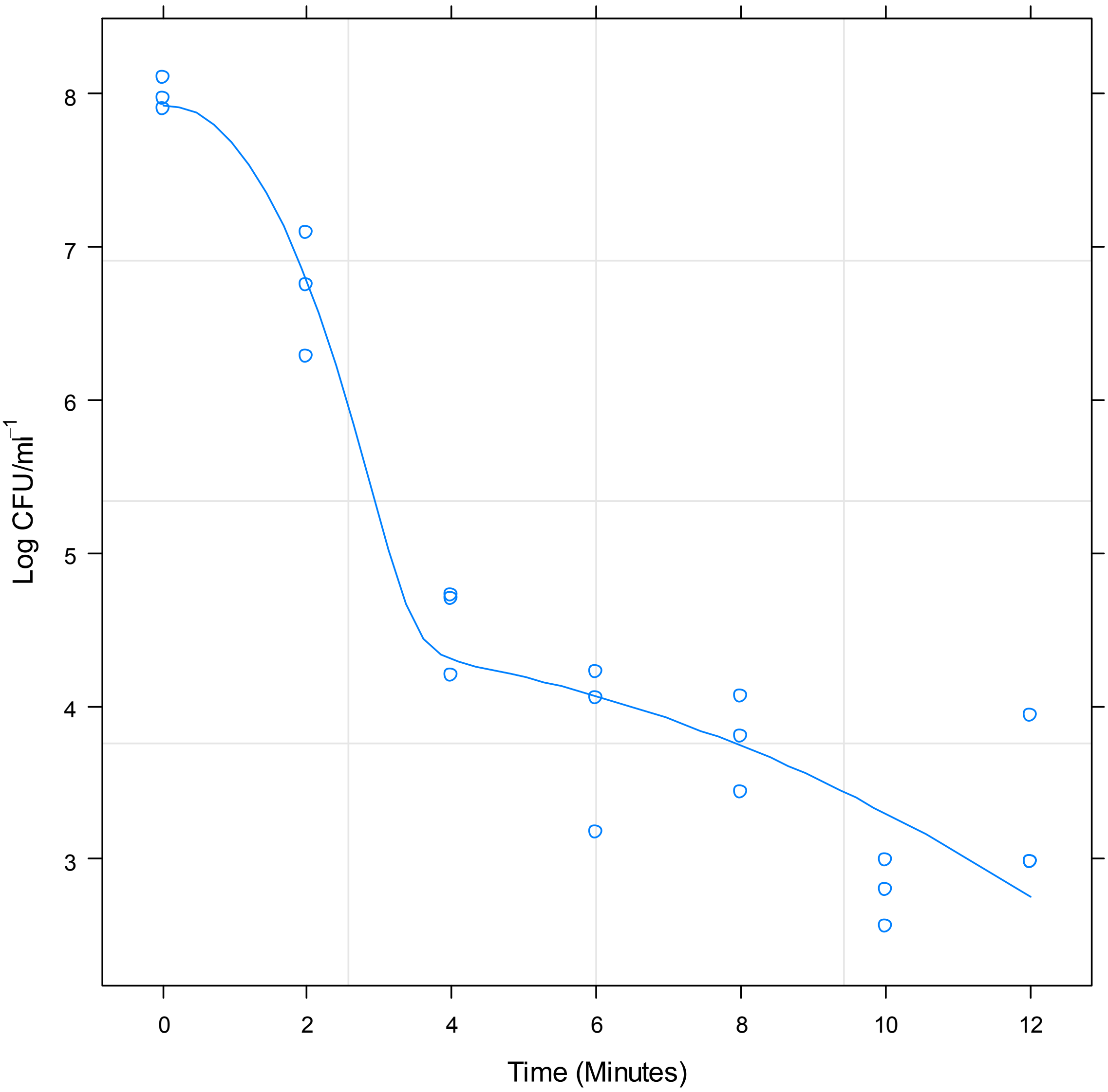

Figure 151. Predicted response curve using a mixed Weibull distribution model of strain 13136 (ST-45, CC-45) at pH 8.5 following heating at 56^{o}C.

1.8.21 pH and Time-Temperature Simulations: 60°C

Table 117. An assessment of the goodness of fit for models analysing the survival of each strain for individual levels of pH at 60°C.

Strain	pH	Non-linear Function	ρ_c
12628 (ST-1773, CC-828)	4.5		
12628 (ST-1773, CC-828)	5.5	Four-parameter Logistic	0.954
12628 (ST-1773, CC-828)	6.5	Asymptotic Regression	0.966
12628 (ST-1773, CC-828)	7.5	Asymptotic Regression	0.955
12628 (ST-1773, CC-828)	8.5	Asymptotic Regression	0.922
12662 (ST-257, CC257)	4.5	Asymptotic Regression	0.944
12662 (ST-257, CC257)	5.5	Four-parameter Logistic	0.943
12662 (ST-257, CC257)	6.5	Four-parameter Logistic	0.971
12662 (ST-257, CC257)	7.5	Asymptotic Regression	0.947
12662 (ST-257, CC257)	8.5	Biexponential	0.954
13126 (ST-21, CC21)	4.5	Asymptotic Regression	0.943
13126 (ST-21, CC21)	5.5	Four-parameter Logistic	0.955
13126 (ST-21, CC21)	6.5	Four-parameter Logistic	0.938
13126 (ST-21, CC21)	7.5	Four-parameter Logistic	0.941
13126 (ST-21, CC21)	8.5	Biexponential	0.955
13136 (ST-45, CC45)	4.5	Asymptotic Regression	0.932
13136 (ST-45, CC45)	5.5	Four-parameter Logistic	0.960
13136 (ST-45, CC45)	6.5	Asymptotic Regression	0.940
13136 (ST-45, CC45)	7.5	Asymptotic Regression	0.956
13136(ST-45, CC45)	8.5	Asymptotic Regression	0.952

Table 118. Four-parameter logistic regression model analysing survival for strain 12628 (ST-1773, CC-828) at pH 5.5 following heating at 60°C.

Parameter	Estimate	Standard Error	*t*-value	*P*-value
Asymptote A	8.133	0.361	22.550	0.000
Asymptote B	2.754	0.158	17.393	0.000
Mid-point	2.246	0.187	12.034	0.000
Scale Parameter	0.536	0.118	4.529	0.000

Table 119. Asymptotic regression model analysing survival rate for strain 12628 (ST-1773, CC-828) at pH 6.5 following heating at 60°C.

Parameter	Estimate	Standard Error	*t*-value	*P*-value
R0	8.030	0.203	39.547	0.000
Asymptote	2.723	0.202	13.480	0.000
LRC	-0.938	0.129	-7.302	0.000

Table 120. Asymptotic regression model analysing survival rate for strain 12628 (ST-1773, CC-828) at pH 7.5 following heating at 60°C.

Parameter	Estimate	Standard Error	*t*-value	*P*-value
R0	7.987	0.226	35.322	0.000
Asymptote	2.565	0.323	7.939	0.000
LRC	-1.196	0.168	-7.110	0.000

Table 121. Asymptotic regression model analysing survival rate for strain 12628 (ST-1773, CC-828) at pH 8.5 following heating at 60°C.

Parameter	Estimate	Standard Error	*t*-value	*P*-value
R0	7.954	0.316	25.181	0.000
Asymptote	2.781	0.213	13.083	0.000
LRC	-0.554	0.179	-3.089	0.006

Table 122. Asymptotic regression model analysing survival rate for strain 12662 (ST-257, CC-257) at pH 4.5 following heating at 60°C.

Parameter	Estimate	Standard Error	*t*-value	*P*-value
R0	8.075	0.267	30.289	0.000
Asymptote	2.972	0.144	20.710	0.000
LRC	-0.161	0.160	-1.004	0.329

Table 123. Four-parameter logistic regression model analysing the survival rate for strain 12662 (ST-257, CC-257) at pH 5.5 following heating at 60°C.

Parameter	Estimate	Standard Error	*t*-value	*P*-value
Asymptote A	8.257	0.488	16.918	0.000
Asymptote B	2.847	0.218	13.081	0.000
Mid-point	2.681	0.291	9.226	0.000
Scale Parameter	0.888	0.260	3.419	0.003

Table 124. Four-parameter logistic regression model analysing survival rate for strain 12662 (ST-257, CC-257) at pH 6.5 following heating at 60°C.

Parameter	Estimate	Standard Error	*t*-value	*P*-value
Asymptote A	8.429	0.454	18.569	0.000
Asymptote B	3.149	0.143	22.093	0.000
Mid-point	2.446	0.261	9.381	0.000
Scale Parameter	1.028	0.210	4.900	0.000

Table 125. Asymptotic regression model analysing survival rate for strain 12662 (ST-257, CC-257) at pH 7.5 following heating at 60^{o}C.

Parameter	**Estimate**	**Standard Error**	***t*-value**	***P*-value**
R0	8.073	0.269	30.054	0.000
Asymptote	1.637	0.596	2.748	0.013
LRC	-1.462	0.218	-6.707	0.000

Table 126. Biexponential regression model analysing survival rate for strain 12662 (ST-257, CC-257) at pH 8.5 following heating at 60^{o}C.

Parameter	**Estimate**	**Standard Error**	***t*-value**	***P*-value**
Asymptote 1	3.513	0.945	3.718	0.002
LRC1	-0.051	0.460	-0.111	0.913
Asymptote 1	4.479	0.914	4.902	0.000
LRC2	-2.516	0.372	-6.768	0.000

Table 127. Asymptotic regression model analysing survival rate for strain 13126 (ST-21, CC-21) at pH 4.5 following heating at 60^{o}C.

Parameter	**Estimate**	**Standard Error**	***t*-value**	***P*-value**
R0	7.967	0.317	25.170	0.000
Asymptote	2.199	0.178	12.362	0.000
LRC	-0.010	0.185	-0.053	0.900

Table 128. Four-parameter logistic regression model analysing survival rate for strain 13126 (ST-21, CC-21) at pH 5.5 following heating at 60^{o}C.

Parameter	**Estimate**	**Standard Error**	***t*-value**	***P*-value**
Asymptote A	8.867	0.990	8.954	0.000
Asymptote B	2.761	0.250	11.040	0.000
Mid-point	2.218	0.488	4.545	0.001
Scale Parameter	1.111	0.364	3.048	0.012

Table 129. Four-parameter logistic regression model analysing survival rate for strain 13126 (ST-21, CC-21) at pH 6.5 following heating at 60^{o}C.

Parameter	**Estimate**	**Standard Error**	***t*-value**	***P*-value**
Asymptote A	8.118	0.368	22.060	0.000
Asymptote B	3.350	0.159	21.012	0.000
Mid-point	2.060	0.202	10.195	0.000
Scale Parameter	0.517	0.134	3.853	0.001

Table 130. Four-parameter logistic regression model analysing survival rate for strain 13126 (ST-21, CC-21) at pH 7.5 following heating at 60^{o}C.

Parameter	**Estimate**	**Standard Error**	***t*-value**	***P*-value**
Asymptote A	8.1968	0.4108	19.9538	0.000
Asymptote B	3.3253	0.1574	21.1230	0.000
Mid-point	2.0153	0.2132	9.4509	0.000
Scale Parameter	0.6095	0.1582	3.8538	0.001

Table 131. Asymptotic regression model analysing survival rate for strain 13126 (ST-21, CC-21) at pH 8.5 following heating at 60^{o}C.

Parameter	**Estimate**	**Standard Error**	***t*-value**	***P*-value**
R0	8.036	0.319	25.172	0.000
Asymptote	3.144	0.203	15.499	0.000
LRC	-0.475	0.191	-2.495	0.030

Table 132. Asymptotic regression model analysing survival rate for strain 13136 (ST-45, CC-45) at pH 4.5 following heating at 60^{o}C.

Parameter	**Estimate**	**Standard Error**	***t*-value**	***P*-value**
R0	7.853	0.315	24.962	0.000
Asymptote	2.382	0.190	12.556	0.000
LRC	-0.393	0.168	-2.338	0.031

Table 133. Four-parameter logistic regression model analysing survival rate for strain 13136 (ST-45, CC-45) at pH 5.5 following heating at 60°C.

Parameter	Estimate	Standard Error	*t*-value	*P*-value
Asymptote A	8.410	0.518	16.241	0.000
Asymptote B	3.202	0.172	18.619	0.000
Mid-point	2.533	0.306	8.274	0.000
Scale Parameter	1.033	0.251	4.111	0.001

Table 134. Asymptotic regression model analysing survival rate for strain 13136 (ST-45, CC-45) at pH 6.5 following heating at 60°C.

Parameter	Estimate	Standard Error	*t*-value	*P*-value
R0	8.091	0.276	29.304	0.000
Asymptote	2.223	0.379	5.863	0.000
LRC	-1.170	0.186	-6.300	0.000

Table 135. Asymptotic regression model analysing survival rate for strain 13136 (ST-45, CC-45) at pH 7.5 following heating at 60°C.

Parameter	Estimate	Standard Error	*t*-value	*P*-value
R0	8.001	0.230	34.870	0.000
Asymptote	2.660	0.236	11.272	0.000
LRC	-0.965	0.147	-6.582	0.000

Table 136. Asymptotic regression model analysing survival rate for strain 13136 (ST-45, CC-45) at pH 8.5 following heating at 60°C.

Parameter	Estimate	Standard Error	*t*-value	*P*-value
R0	7.917	0.226	35.079	0.000
Asymptote	3.115	0.176	17.754	0.000
LRC	-0.719	0.143	-5.019	0.000

1.8.22 pH and Time-temperature Simulations: 60^{0}C

Mixed Weibull Distribution Model:

Table 137. An assessment of the goodness of fit for Mixed Weibull Distribution models analysing the survival of four strains for combined levels of pH at 60^{o}C.

Strain	**pH**	**Non-linear Function**	ρ_c
12628 (ST-1773, CC-828)	4.5	Mixed Weibull Distribution	
12628 (ST-1773, CC-828)	5.5	Mixed Weibull Distribution	0.978
12628 (ST-1773, CC-828)	6.5	Mixed Weibull Distribution	0.983
12628 (ST-1773, CC-828)	7.5	Mixed Weibull Distribution	0.983
12628 (ST-1773, CC-828)	8.5	Mixed Weibull Distribution	0.950
12662 (ST-257, CC-257)	4.5	Mixed Weibull Distribution	0.972
12662 (ST-257, CC-257)	5.5	Mixed Weibull Distribution	0.963
12662 (ST-257, CC-257)	6.5	Mixed Weibull Distribution	0.986
12662 (ST-257, CC-257)	7.5	Mixed Weibull Distribution	0.966
12662 (ST-257, CC-257)	8.5	Mixed Weibull Distribution	0.976
13126 (ST-21, CC-21)	4.5	Mixed Weibull Distribution	0.974
13126 (ST-21, CC-21)	5.5	Mixed Weibull Distribution	0.966
13126 (ST-21, CC-21)	6.5	Mixed Weibull Distribution	0.981
13126 (ST-21, CC-21)	7.5	Mixed Weibull Distribution	0.968
13126 (ST-21, CC-21)	8.5	Mixed Weibull Distribution	0.979
13136 (ST-45, CC-45)	4.5	Mixed Weibull Distribution	
13136 (ST-45, CC-45)	5.5	Mixed Weibull Distribution	0.964
13136 (ST-45, CC-45)	6.5	Mixed Weibull Distribution	0.978
13136 (ST-45, CC-45)	7.5	Mixed Weibull Distribution	0.979
13136 (ST-45, CC-45)	8.5	Mixed Weibull Distribution	

Table 138. Mixed Weibull distribution model analysing the survival of strain 12628 (ST-1773, CC-828) at pH 5.5 following heating at 60^{o}C.

Parameter	**Estimate**	**Standard Error**	***t*-value**	***P*-value**
α	4.826	0.073	66.184	0.000
δ1	1.577	0.003	554.189	0.000
p	2.125	0.007	295.780	0.000
N0	8.013	0.001	6249.173	0.000
δ2	10.236	1.680	6.093	0.000

Table 139. Mixed Weibull distribution model analysing the survival of strain 12628 (ST-1773, CC-828) at pH 6.5 following heating at 60°C.

Parameter	**Estimate**	**Standard Error**	***t*-value**	***P*-value**
α	3.249	0.639	5.085	0.000
δ1	0.478	0.220	2.190	0.046
p	0.750	0.219	3.417	0.004
N0	8.033	0.216	37.185	0.000
δ2	3.583	2.056	1.742	0.101

Table 140. Mixed Weibull distribution model analysing the survival of strain 12628 (ST-1773, CC-828) at pH 7.5 following heating at 60°C.

Parameter	**Estimate**	**Standard Error**	***t*-value**	***P*-value**
α	3.279	0.616	5.321	0.000
δ1	0.993	0.304	3.265	0.005
p	1.741	1.267	1.374	0.186
N0	8.035	0.043	186.740	0.000
δ2	5.874	2.503	2.346	0.032

Table 141. Mixed Weibull distribution model analysing the survival of strain 12628 (ST-1773, CC-828) at pH 8.5 following heating at 60°C.

Parameter	**Estimate**	**Standard Error**	***t*-value**	***P*-value**
α	4.447	0.046	96.856	0.000
δ1	1.127	0.165	6.830	0.000
p	4.533	2.320	1.954	0.068
N0	8.104	0.001	5.77E+03	0.000
δ2	8.160	0.498	16.381	0.000

Table 142. Mixed Weibull distribution model analysing the survival of strain 12662 (ST-257, CC-257) at pH 4.5 following heating at 60°C.

Parameter	**Estimate**	**Standard Error**	***t*-value**	***P*-value**
α	0.538	0.982	0.548	0.591
δ1	0.120	0.554	0.217	0.831
p	3.968	1.318	3.010	0.008
N0	8.091	0.277	29.207	0.000
δ2	5.452	14.248	0.383	0.707

Table 143. Mixed Weibull distribution model analysing the survival of strain 12662 (ST-257, CC-257) at pH 5.5 following heating at 60°C.

Parameter	Estimate	Standard Error	*t*-value	*P*-value
α	2.452	0.0410	59.876	0.000
δ1	1.746	0.0158	110.735	0.000
p	4.398	0.0558	78.869	0.000
N0	7.912	0.0081	971.265	0.000
δ2	9.699	0.6878	14.102	0.000

Table 144. Mixed Weibull distribution model analysing the survival of strain 12662 (ST-257, CC-257) at pH 6.5 following heating at 60°C.

Parameter	Estimate	Standard Error	*t*-value	*P*-value
α	1.548	0.362	4.283	0.001
δ1	1.494	0.277	5.401	0.000
p	3.892	0.345	11.282	0.000
N0	7.966	0.205	38.774	0.000
δ2	8.523	2.245	3.797	0.002

Table 145. Mixed Weibull distribution model analysing the survival of strain 12662 (ST-257, CC-257) at pH 7.5 following heating at 60°C.

Parameter	Estimate	Standard Error	*t*-value	*P*-value
α	1.155	0.158	7.320	0.000
δ1	1.023	0.089	11.519	0.000
p	2.505	0.432	5.800	0.000
N0	7.959	0.049	162.273	0.000
δ2	3.086	0.626	4.929	0.000

Table 146. Mixed Weibull distribution model analysing the survival of strain 12662 (ST-257, CC-257) at pH 8.5 following heating at 60°C.

Parameter	Estimate	Standard Error	*t*-value	*P*-value
α	0.802	0.804	0.997	0.335
δ1	0.350	0.525	0.666	0.516
p	3.334	1.549	2.152	0.048
N0	7.986	0.301	26.512	0.00
δ2	2.824	5.238	0.539	0.598

Table 147. Mixed Weibull distribution model analysing the survival of strain 13126 (ST-21, CC-21) at pH 4.5 following heating at 60°C.

Parameter	**Estimate**	**Standard Error**	***t*-value**	***P*-value**
α	3.968	1.318	3.010	0.008
δ1	0.120	0.554	0.217	0.831
p	0.538	0.981	0.548	0.591
N0	8.091	0.277	29.207	0.000
δ2	5.452	14.248	0.383	0.707

Table 148. Mixed Weibull distribution model analysing the survival of strain 13126 (ST-21, CC-21) at pH 5.5 following heating at 60°C.

Parameter	**Estimate**	**Standard Error**	***t*-value**	***P*-value**
α	2.383	0.115	20.744	0.000
δ1	1.628	0.009	178.353	0.000
p	3.628	0.104	34.854	0.000
N0	7.865	0.002	3.37E+03	0.000
δ2	6.510	0.407	16.001	0.000

Table 149. Mixed Weibull distribution model analysing the survival of strain 13126 (ST-21, CC-21) at pH 6.5 following heating at 60°C.

Parameter	**Estimate**	**Standard Error**	***t*-value**	***P*-value**
α	2.319	1.096	2.116	0.050
δ1	1.451	0.091	15.992	0.000
p	3.996	0.190	21.021	0.000
N0	8.017	0.086	92.958	0.000
δ2	8.375	1.729	4.844	0.000

Table 150. Mixed Weibull distribution model analysing the survival of strain 13126 (ST-21, CC-21) at pH 7.5 following heating at 60°C.

Parameter	**Estimate**	**Standard Error**	***t*-value**	***P*-value**
α	1.683	0.183	9.198	0.000
δ1	1.305	0.084	15.456	0.000
p	4.501	0.483	9.326	0.000
N0	8.016	0.060	134.233	0.000
δ2	20.651	35.732	0.578	0.571

Table 151. Mixed Weibull distribution model analysing the survival of strain 13126 (ST-21, CC-21) at pH 8.5 following heating at 60°C.

Parameter	**Estimate**	**Standard Error**	***t*-value**	***P*-value**
α	1.233	2.102	0.587	0.572
δ1	0.555	0.976	0.569	0.584
p	3.660	1.555	2.354	0.043
N0	8.092	0.306	26.433	0.000
δ2	6.081	8.264	0.736	0.481

Table 152. Mixed Weibull distribution model analysing the survival of strain 13136 (ST-45, CC-45) at pH 5.5 following heating at 60°C.

Parameter	**Estimate**	**Standard Error**	***t*-value**	***P*-value**
α	4.142	0.196	21.103	0.000
δ1	1.605	0.096	16.653	0.000
p	1.676	0.153	10.933	0.000
N0	7.969	0.058	137.009	0.000
δ2	28.006	33.743	0.830	0.419

Table 153. Mixed Weibull distribution model analysing the survival of strain 13136 (ST-45, CC-45) at pH 6.5 following heating at 60°C.

Parameter	**Estimate**	**Standard Error**	***t*-value**	***P*-value**
α	3.658	0.323	11.312	0.000
δ1	1.069	0.111	9.632	0.000
p	1.429	0.248	5.752	0.000
N0	7.970	0.090	88.434	0.000
δ2	5.873	1.303	4.507	0.000

Table 154. Mixed Weibull distribution model analysing the survival of strain 13136 (ST-45, CC-45) at pH 7.5 following heating at 60°C.

Parameter	**Estimate**	**Standard Error**	***t*-value**	***P*-value**
α	3.579	0.671	5.332	0.000
δ1	0.589	0.245	2.410	0.028
p	0.827	0.228	3.629	0.002
N0	7.966	0.241	33.110	0.000
δ2	5.143	3.223	1.596	0.130

1.8.23 pH and Time-Temperature Simulations: 60°C

Predicted Response Curves:

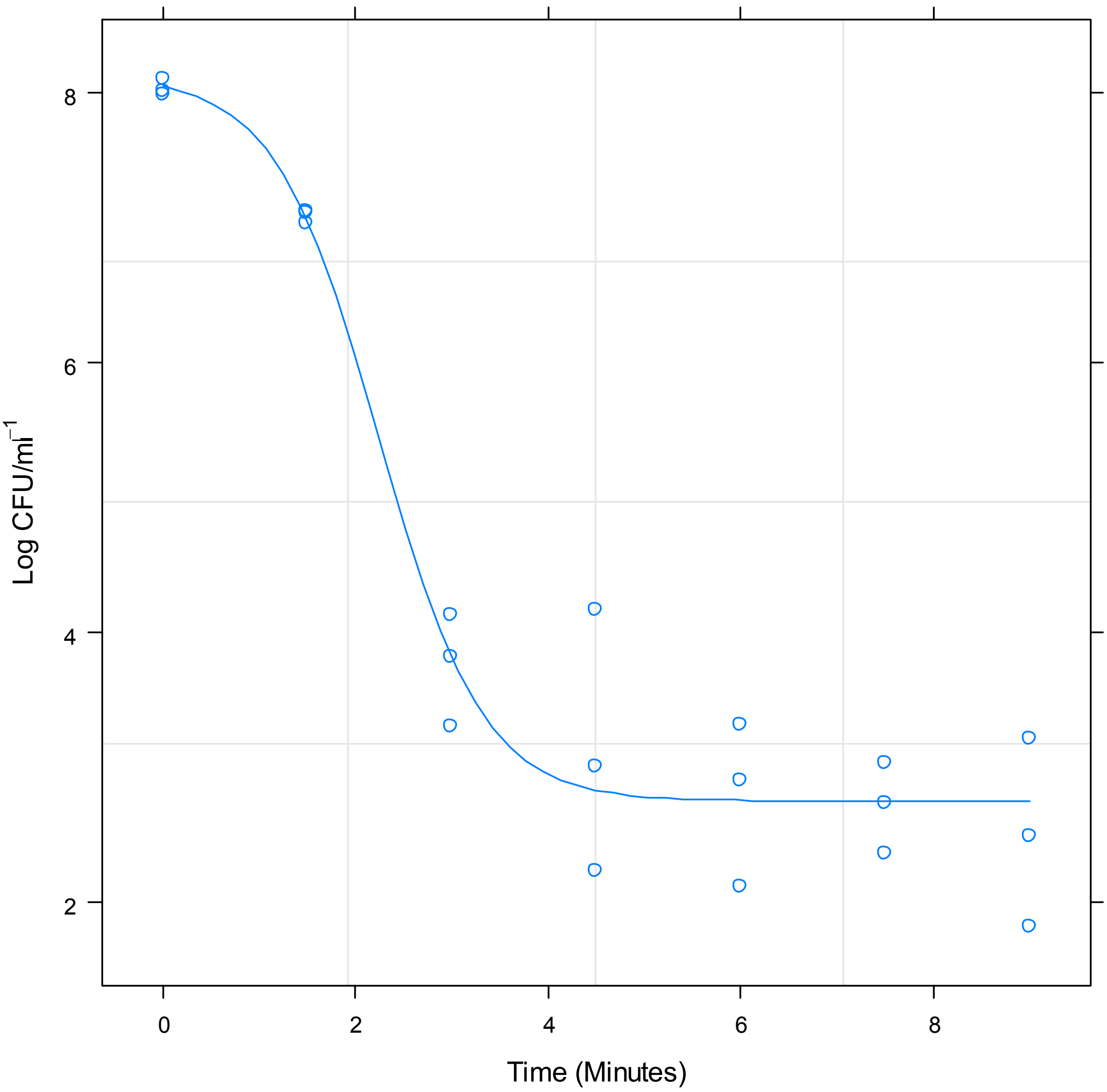

Figure 152. Predicted response curve using a four-parameter logistic regression model for strain 12628 (ST-1773, CC-828) at pH 5.5 following heating at 60°C.

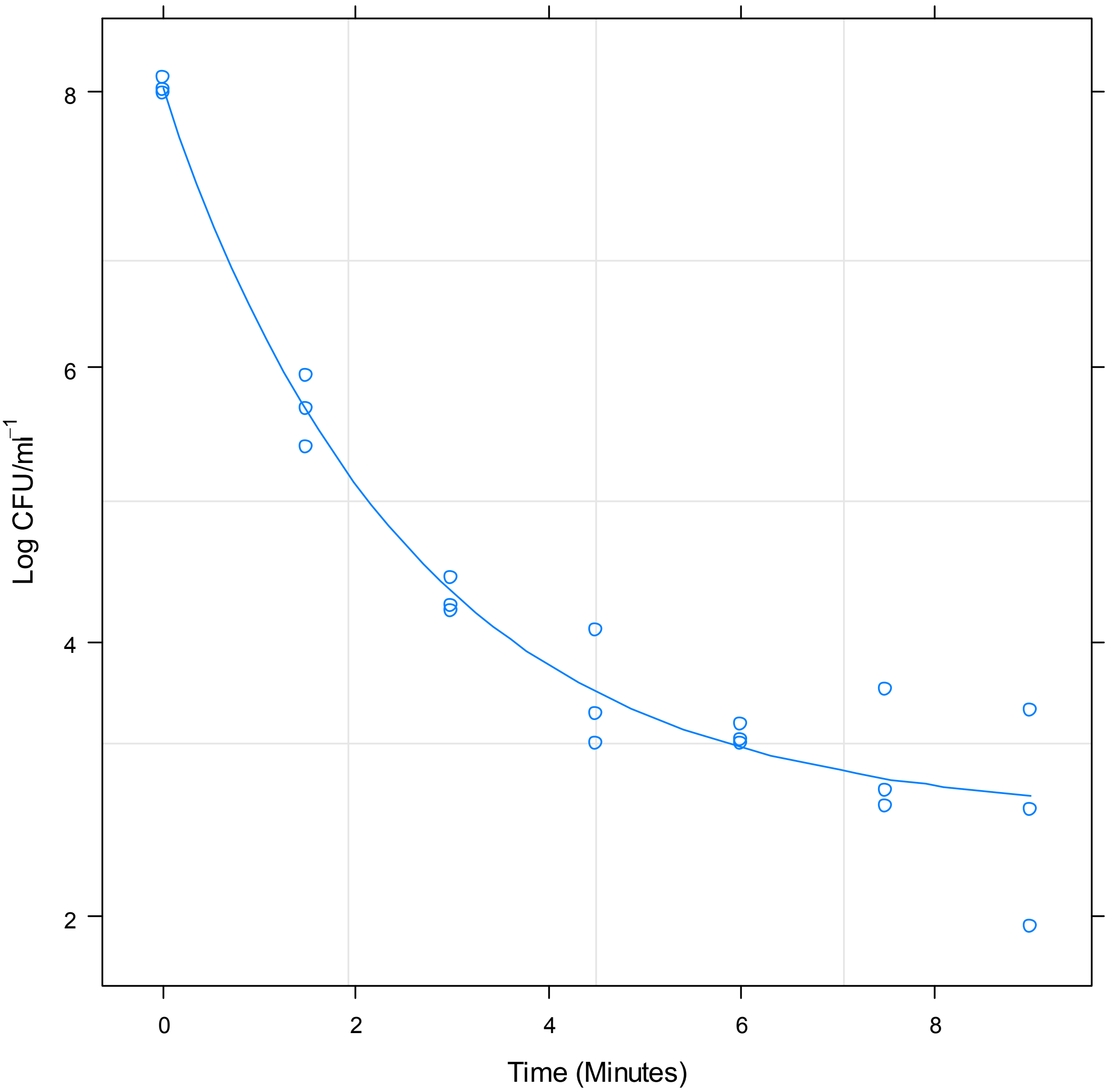

Figure 153. Predicted response curve using an asymptotic regression model for strain 12628 (ST-1773, CC-828) at pH 6.5 following heating at 60°C.

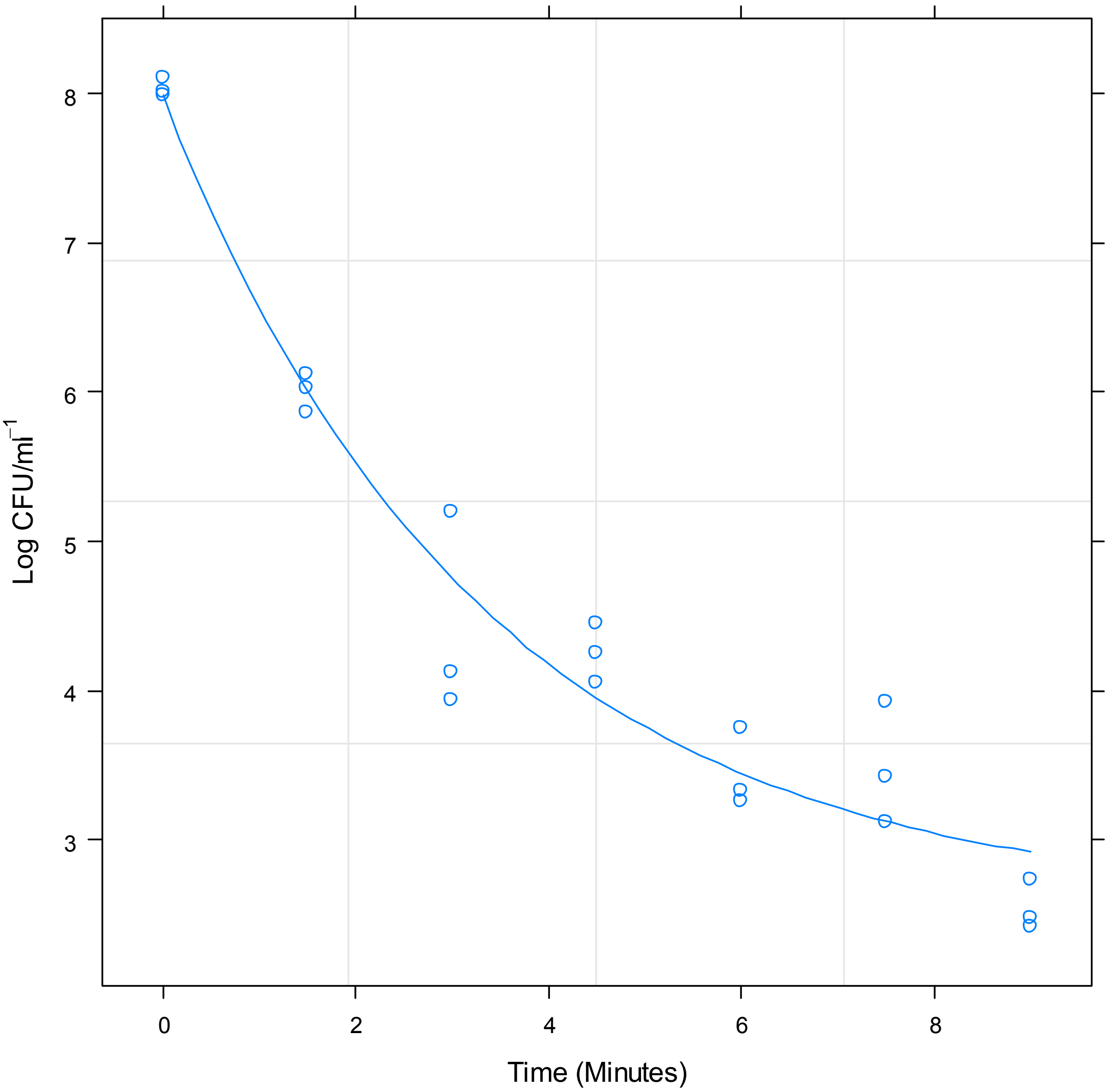

Figure 154. Predicted response curve using an asymptotic regression model for strain 12628 (ST-1773, CC-828) at pH 7.5 following heating at 60^{o}C.

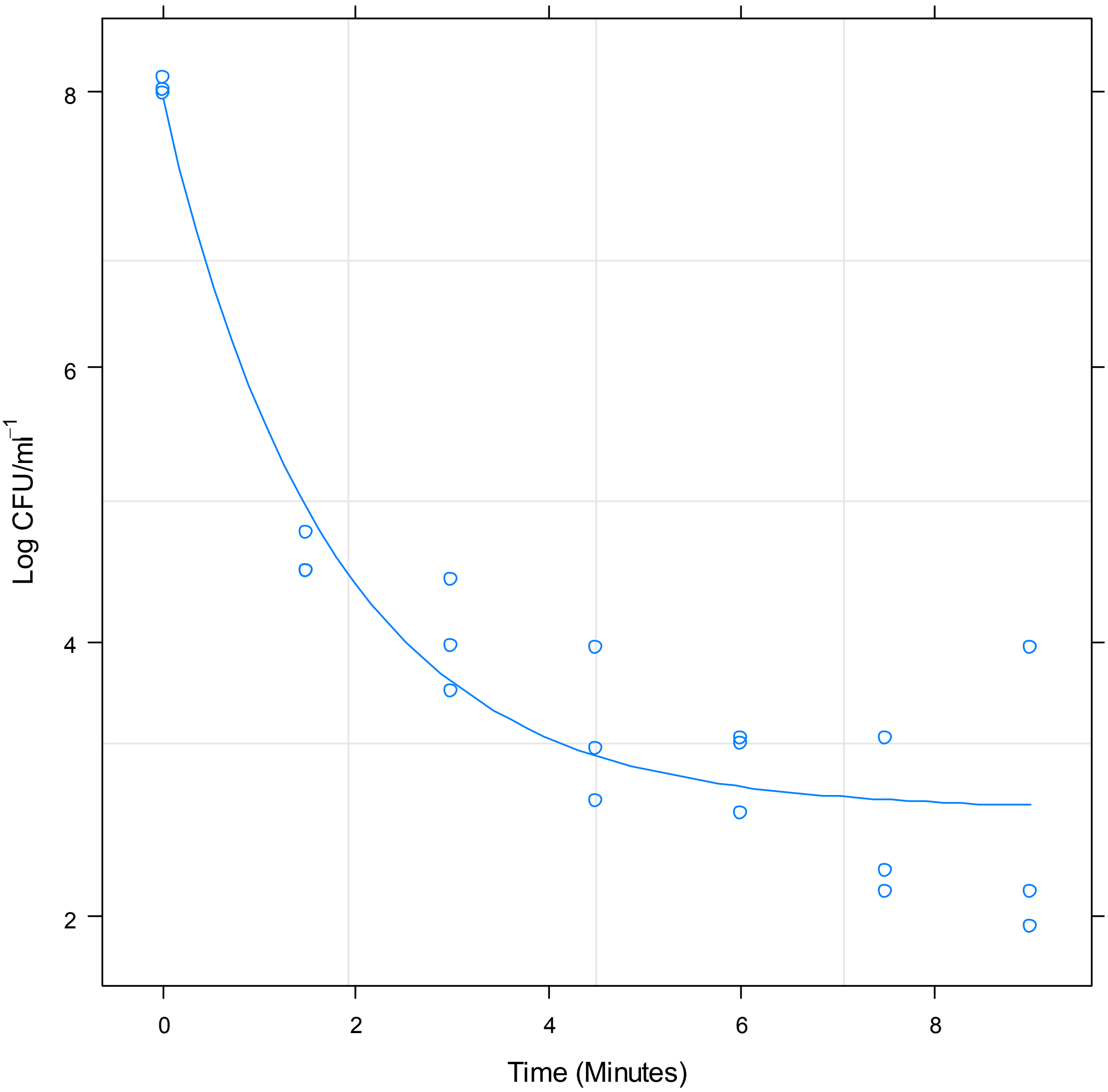

Figure 155. Predicted response curve using an asymptotic regression model for strain 12628 (ST-1773, CC-828) at pH 8.5 following heating at 60^{o}C.

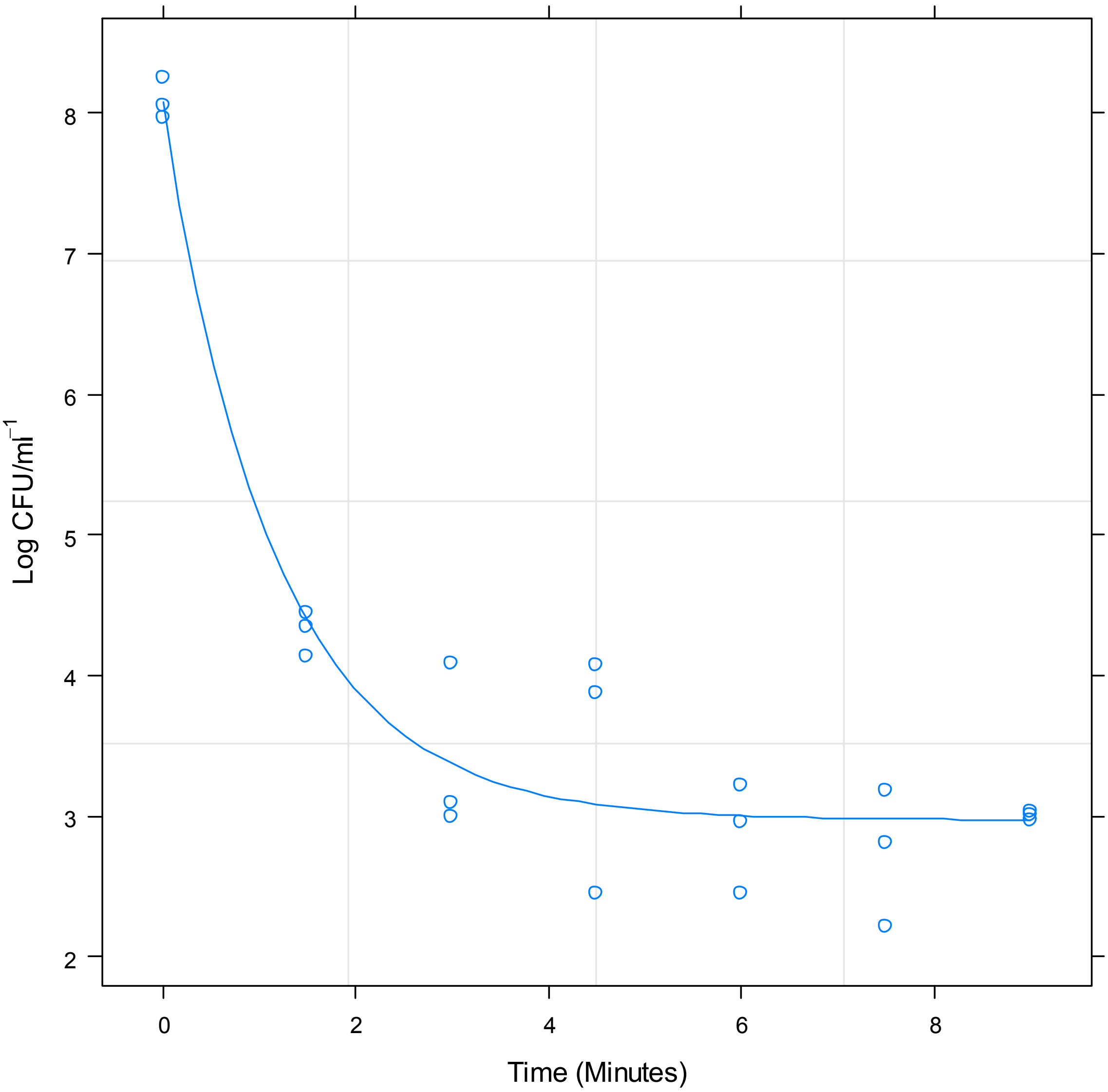

Figure 156. Predicted response curve using an asymptotic regression model for strain 12662 (ST-257, CC-257) at pH 4.5 following heating at 60°C.

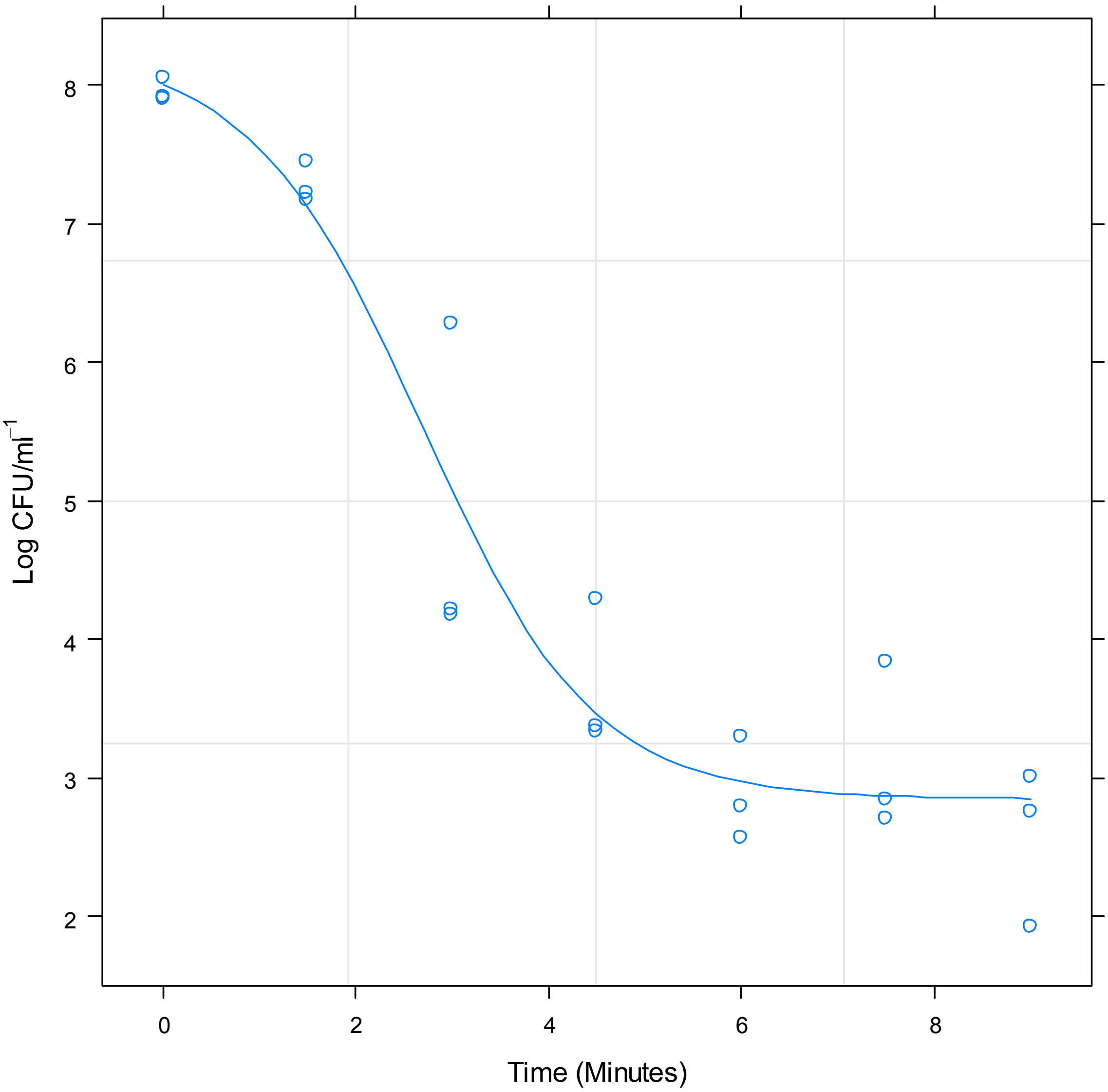

Figure 157. Predicted response curve using a four-parameter logistic regression model for strain 12628 (ST-1773, CC-828) at pH 5.5 following heating at 60°C.

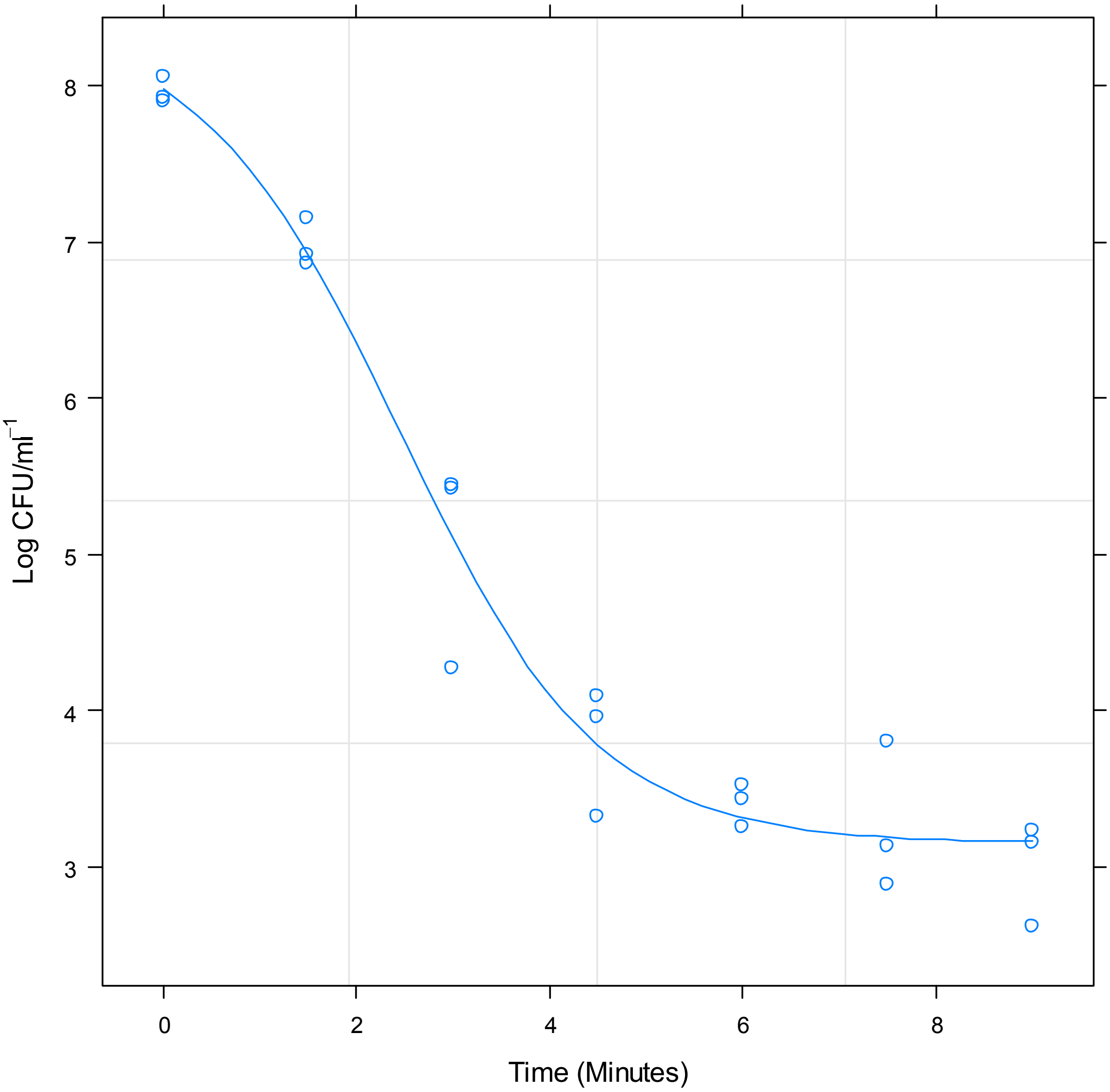

Figure 158. Predicted response curve using a four-parameter logistic regression for strain 12662 (ST-257, CC-257) at pH 6.5 following heating at 60°C.

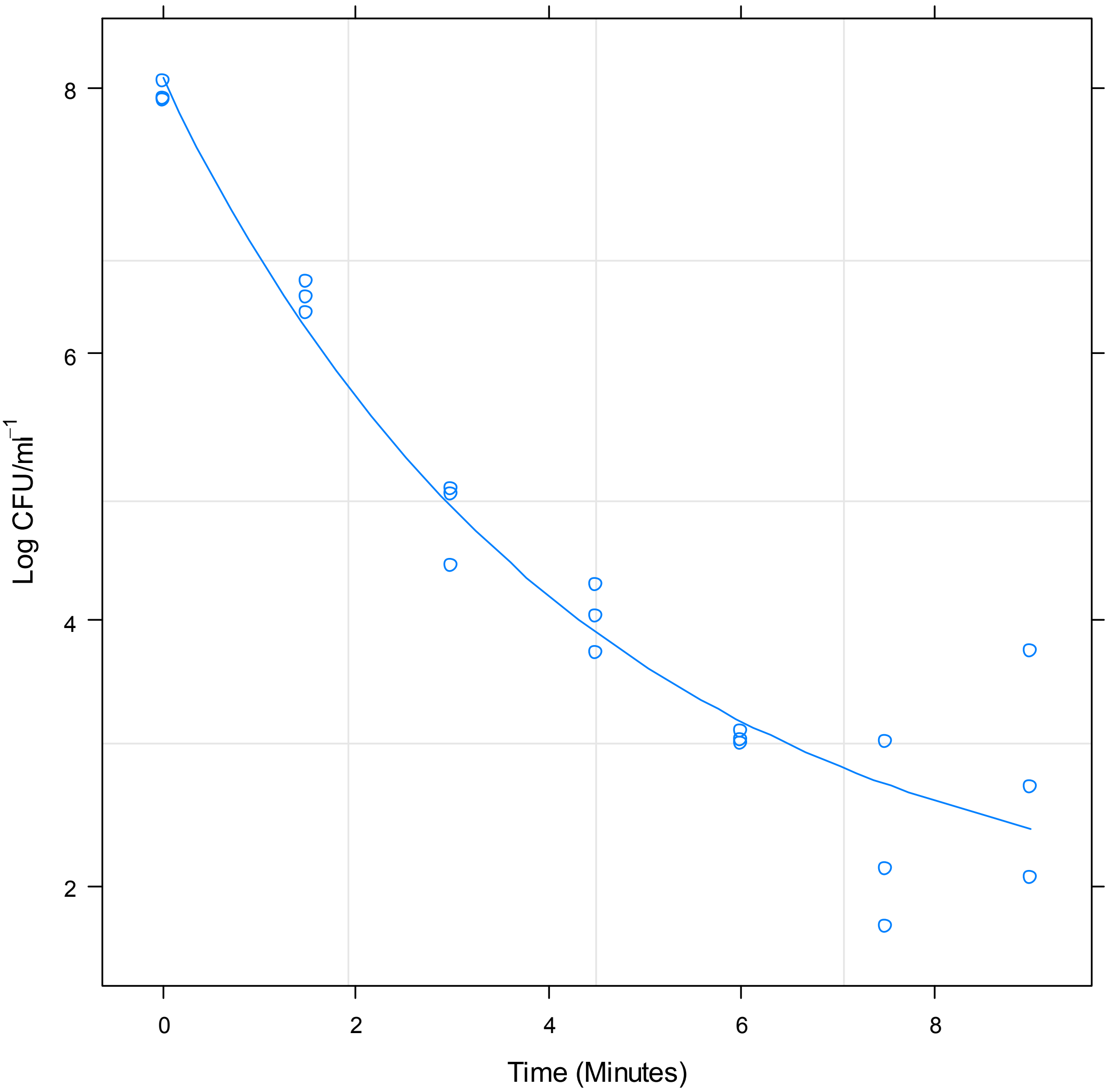

Figure 159. Predicted response curve using an asymptotic regression model for strain 12628 (ST-257, CC-257) at pH 7.5 following heating at 60°C.

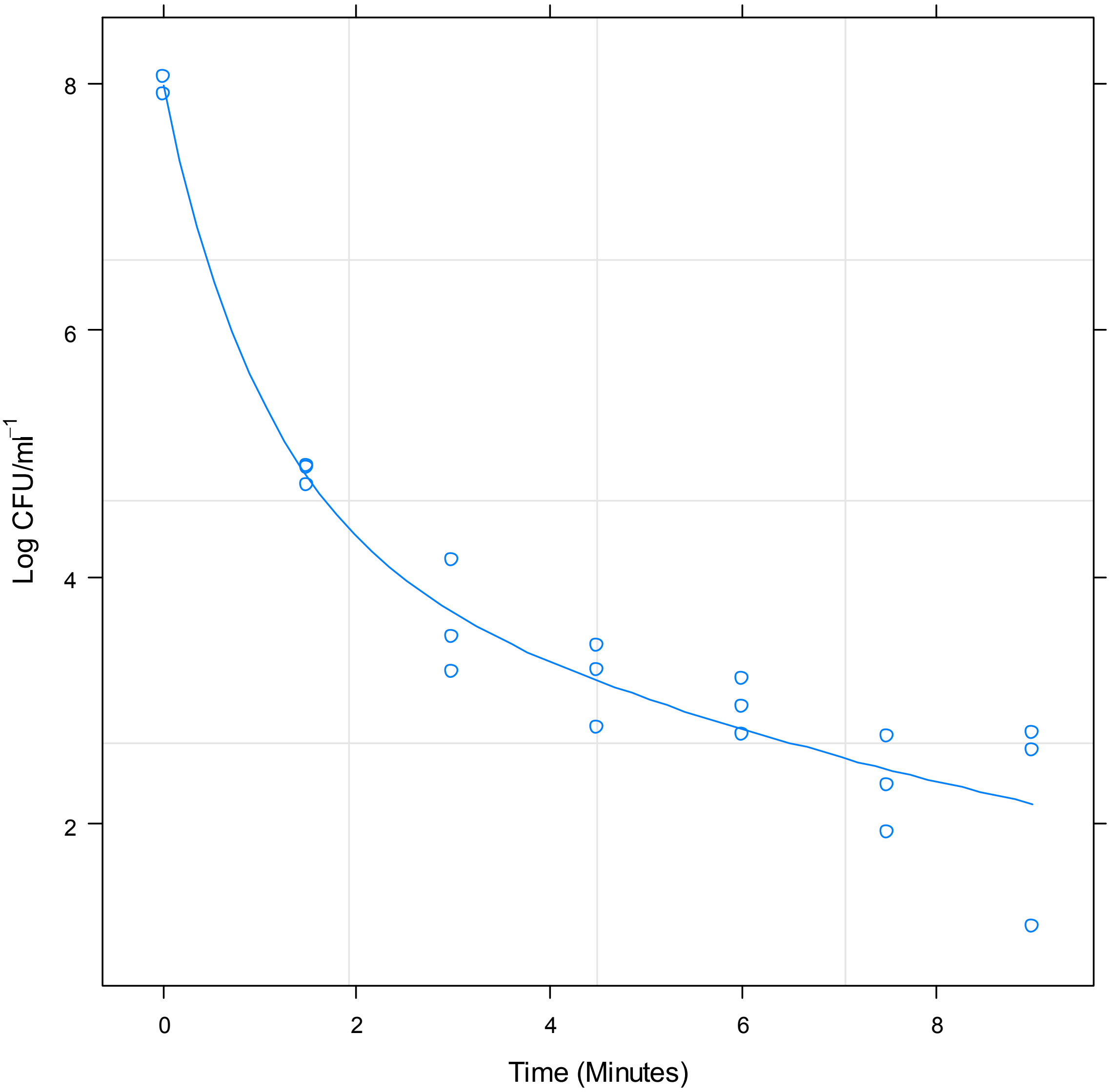

Figure 160. Predicted response curve using a biexponential regression model for strain 12662 (ST-257, CC-257) at pH 8.5 following heating at 60°C.

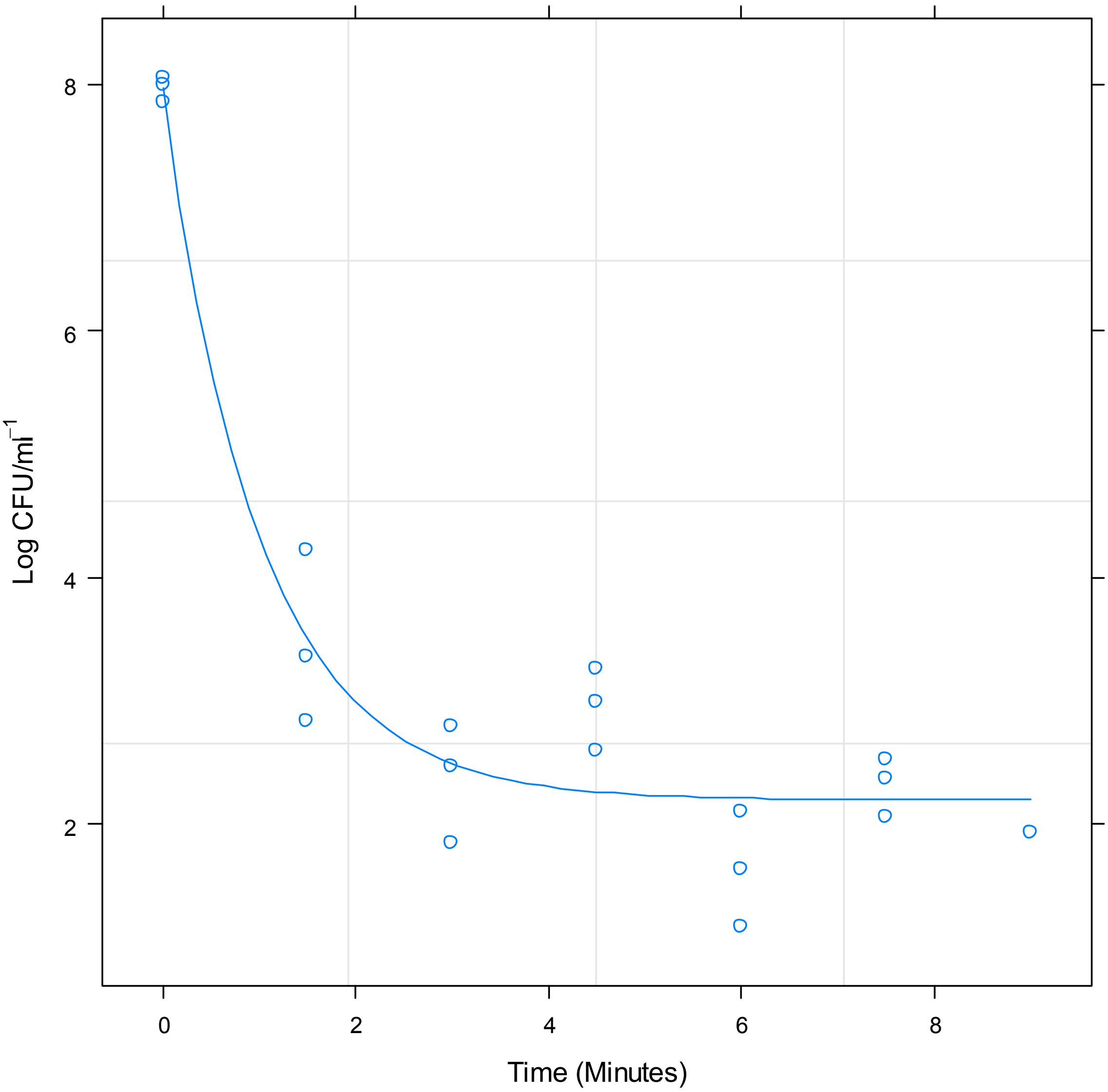

Figure 161. Predicted response curve using an asymptotic regression model for strain 13126 (ST-21, CC-21) at pH 4.5 following heating at 60°C.

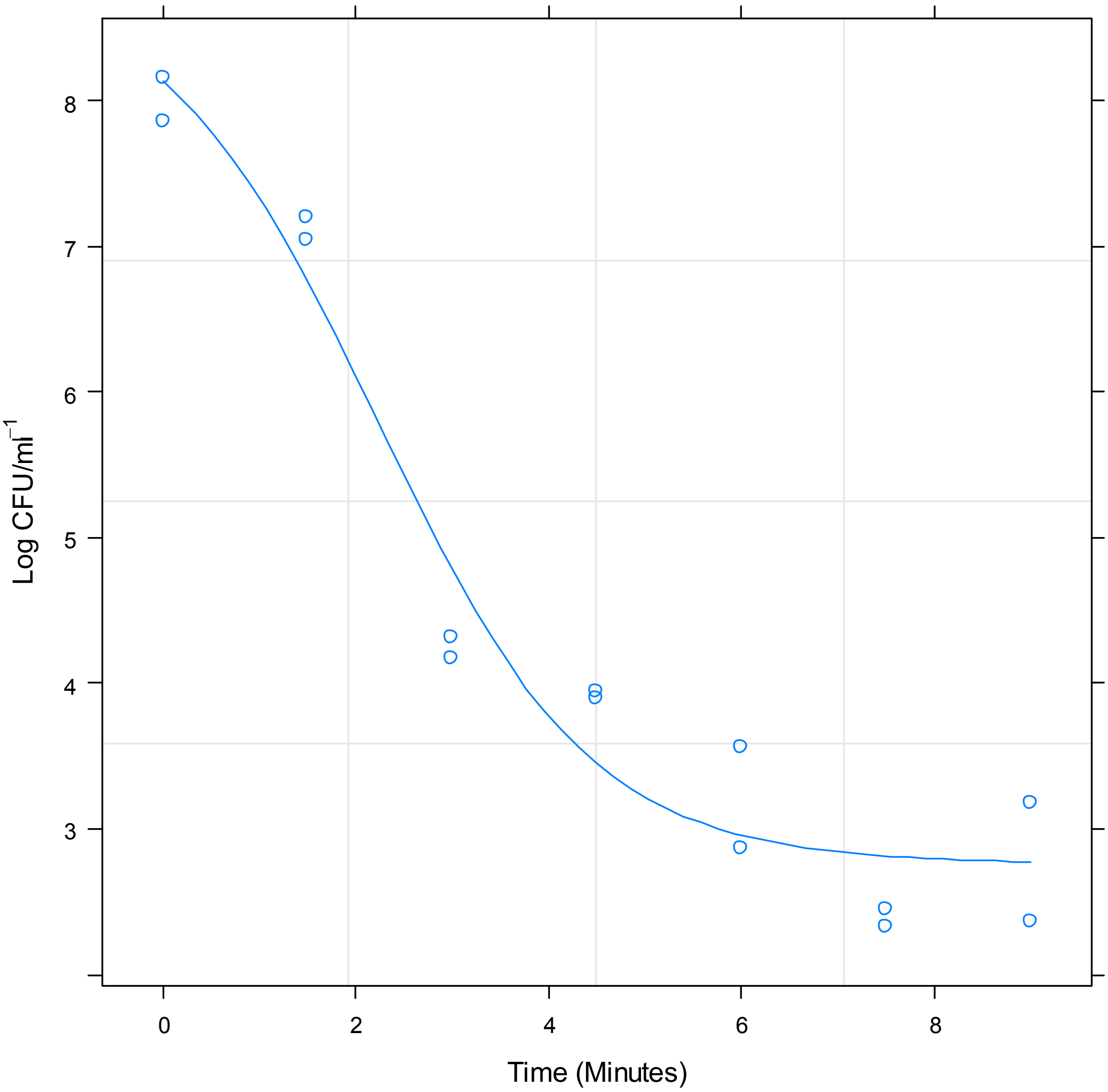

Figure 162. Predicted response curve using a four-parameter logistic regression model for strain 13126 (ST-21, CC-21 at pH 5.5 following heating at 60^{o}C.

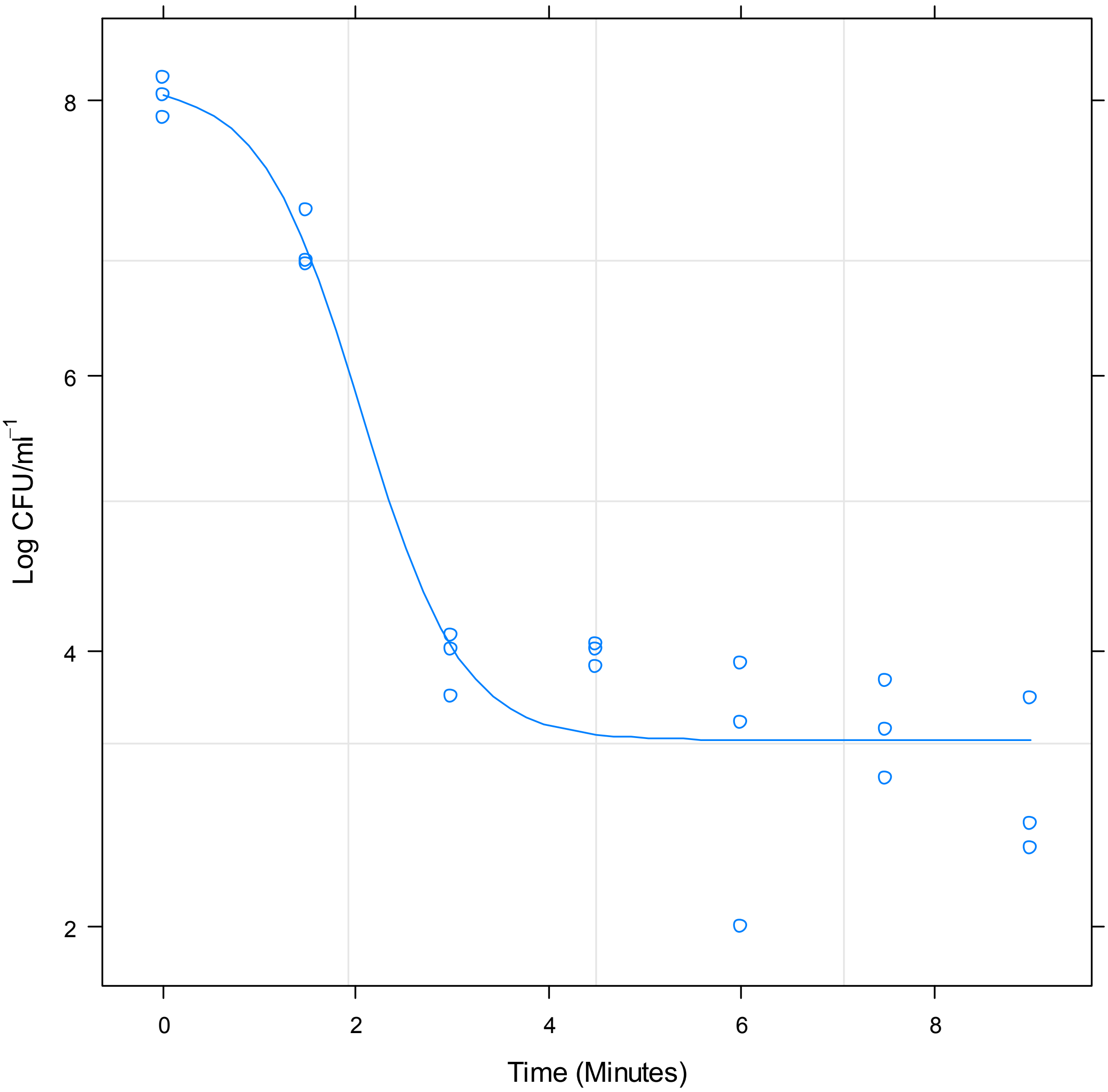

Figure 163. Predicted response curve using a four-parameter logistic regression model for strain 13126 (ST-21, CC-21) at pH 6.5 following heating at 60°C.

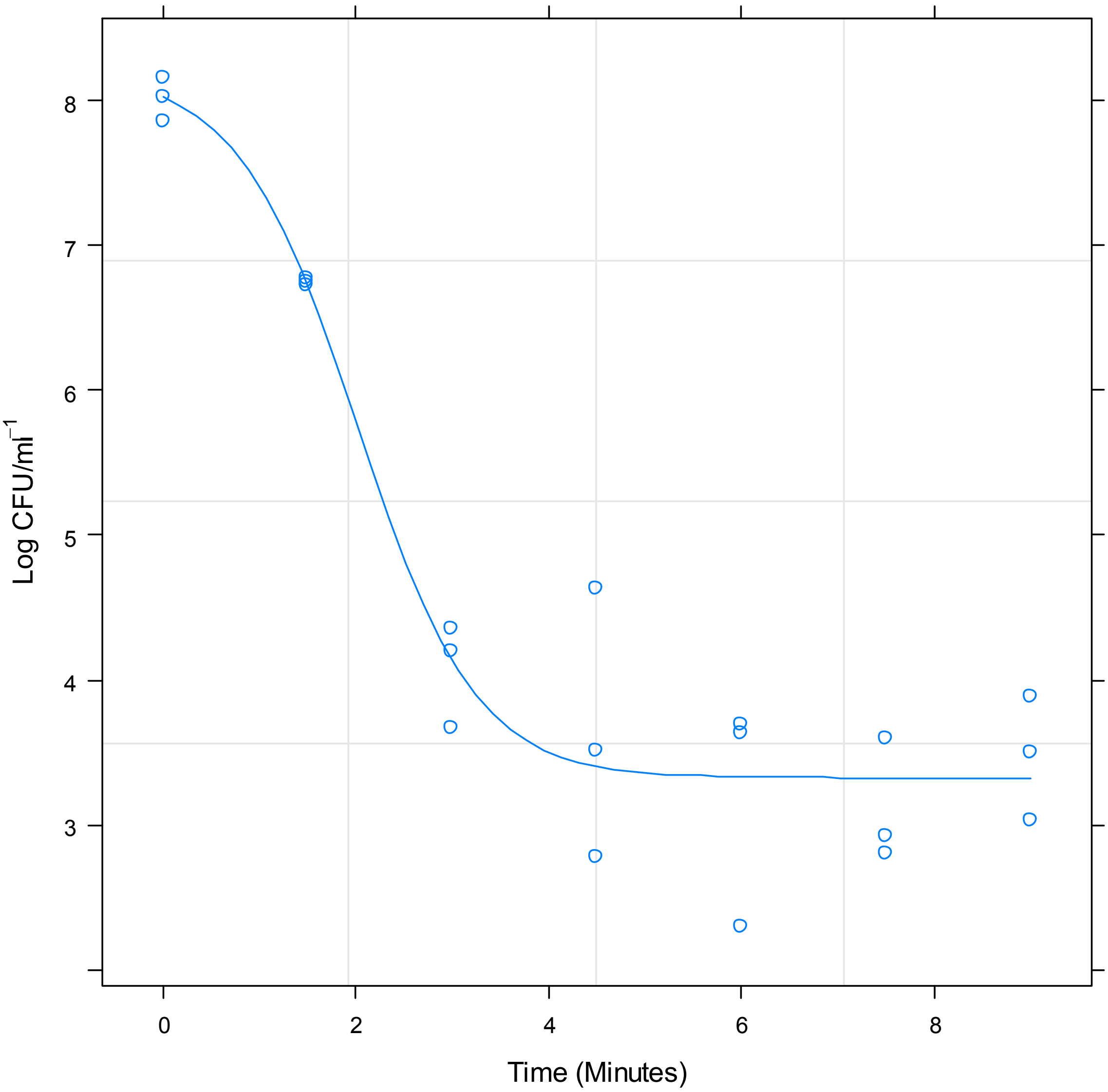

Figure 164. Predicted response curve using a four-parameter logistic regression model for strain 13126 (ST-21, CC-21) at pH 7.5 following heating at 60°C.

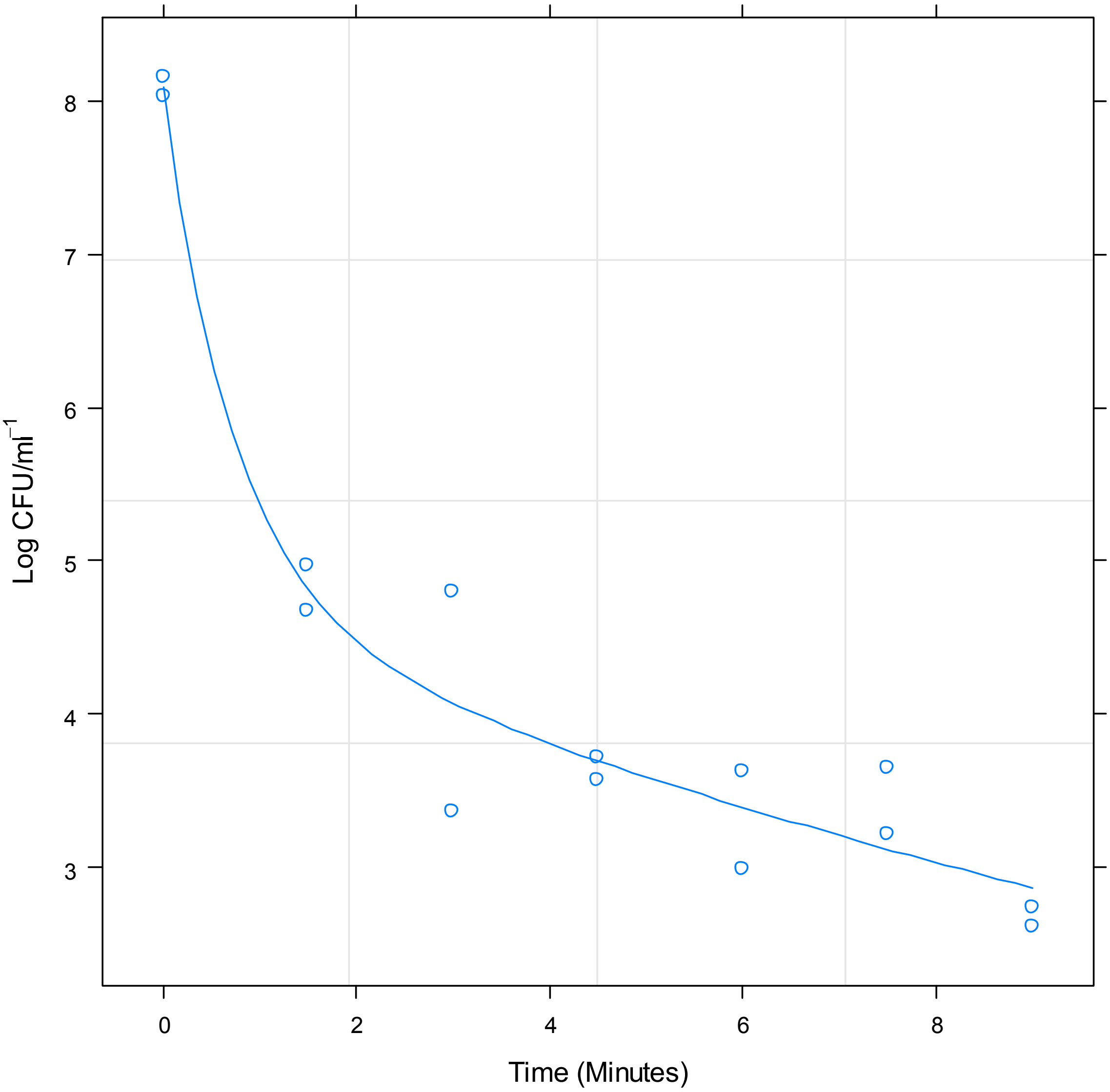

Figure 165. Predicted response curve using a biexponential regression model for strain 13126 (ST-21, CC-21) at pH 8.5 following heating at 60°C.

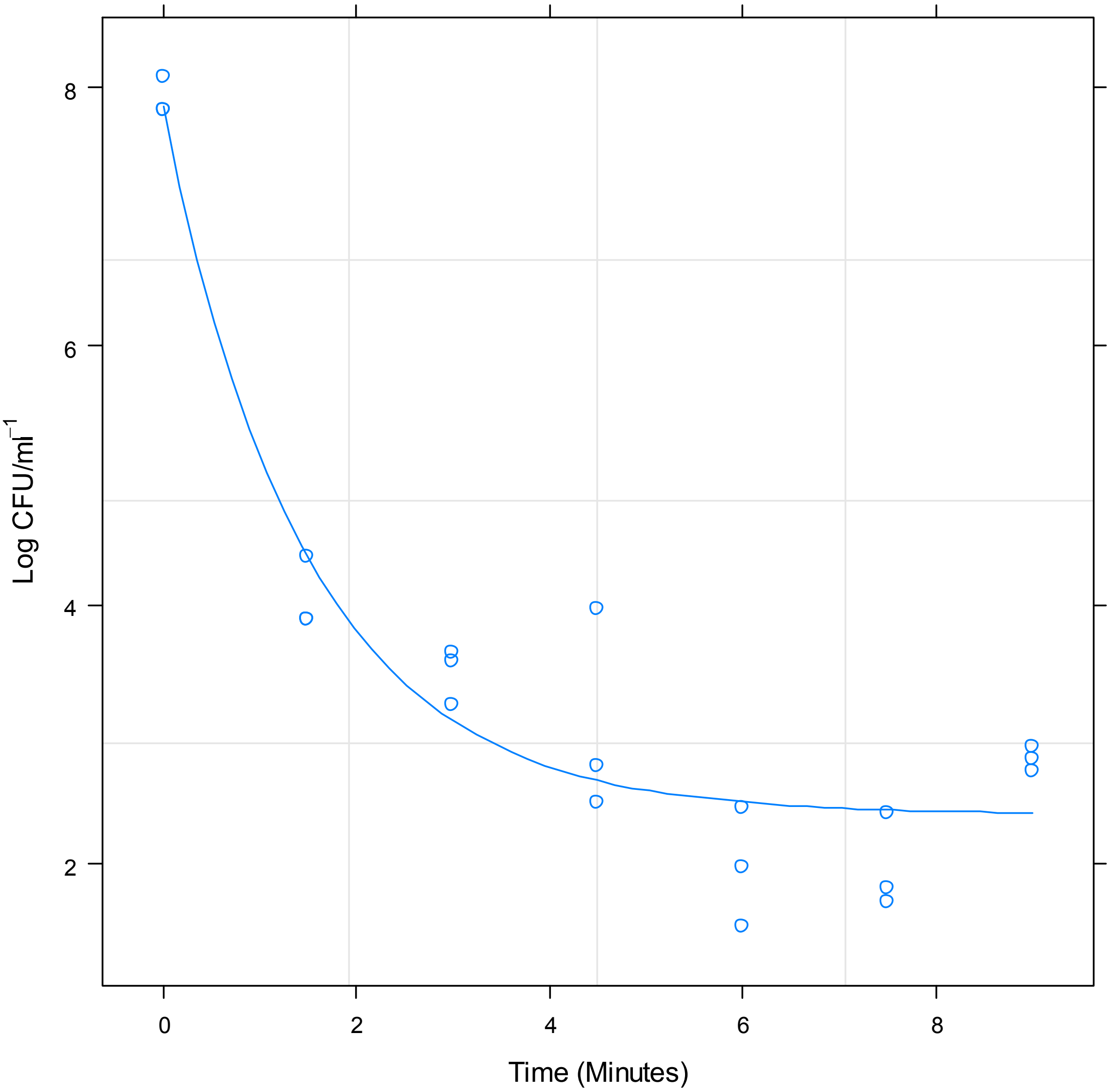

Figure 166. Predicted response curve using an asymptotic regression model for strain 13136 (ST-45, CC-45) at pH 4.5 following heating at 60°C.

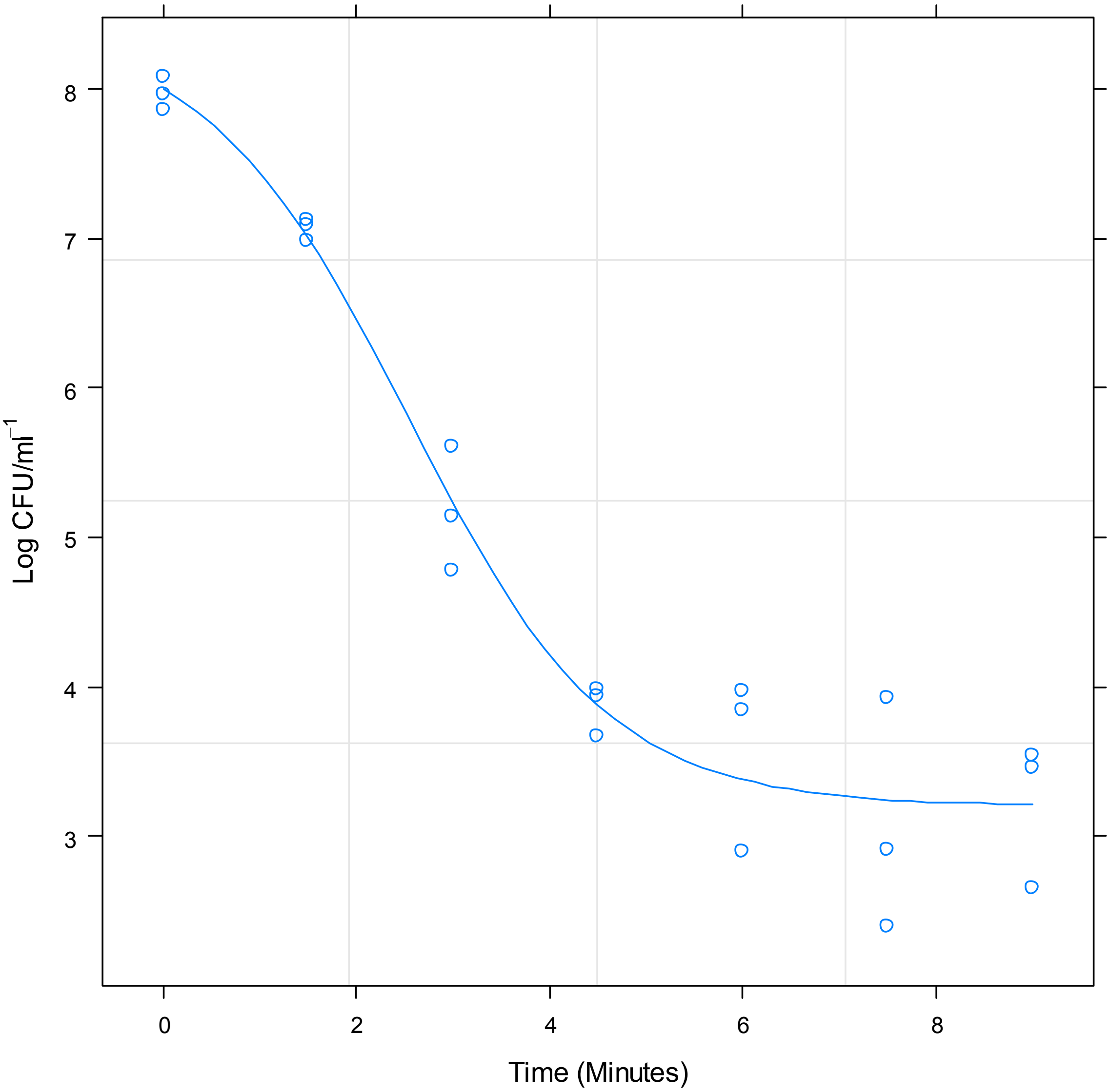

Figure 167. Predicted response curve using a four-parameter logistic regression model for strain 13136 (ST-45, CC-45) at pH 5.5 following heating at 60°C.

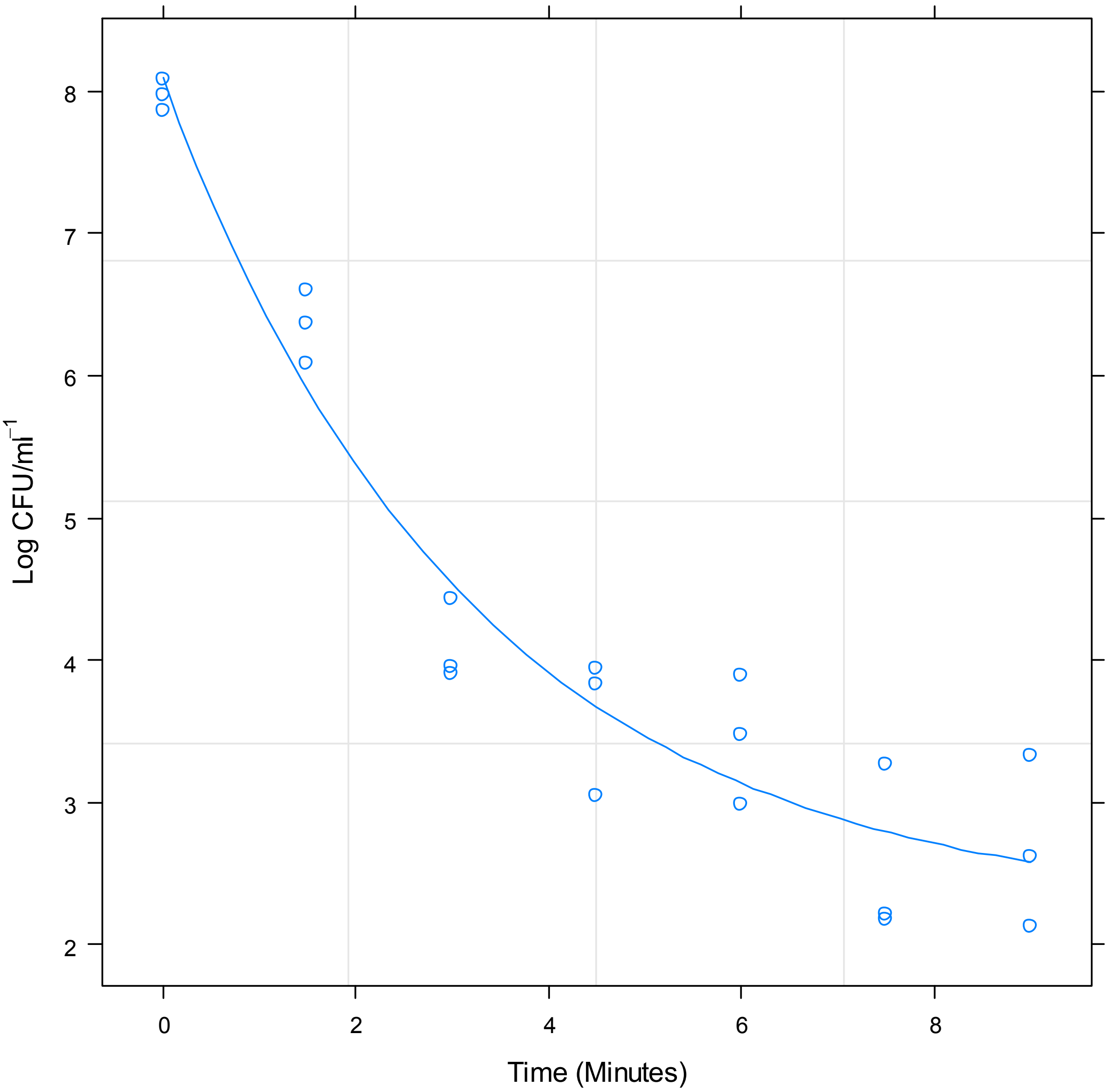

Figure 168. Predicted response curve using an asymptotic regression model for strain 13136 (ST-45, CC-45) at pH 6.5 following heating at 60^{o}C.

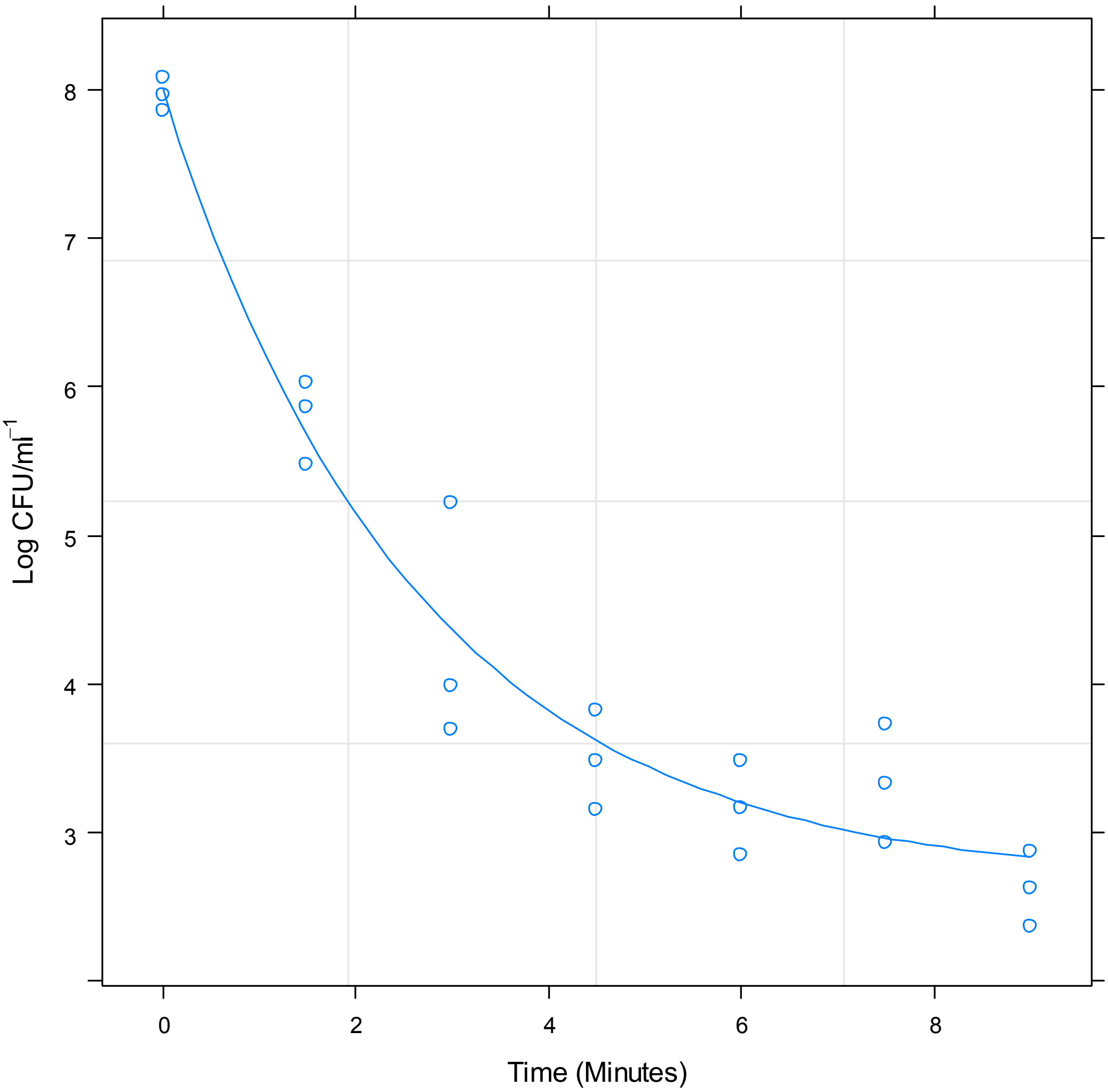

Figure 169. Predicted response curve using an asymptotic regression model for strain 13136 (ST-45, CC-45) at pH 7.5 following heating at 60°C.

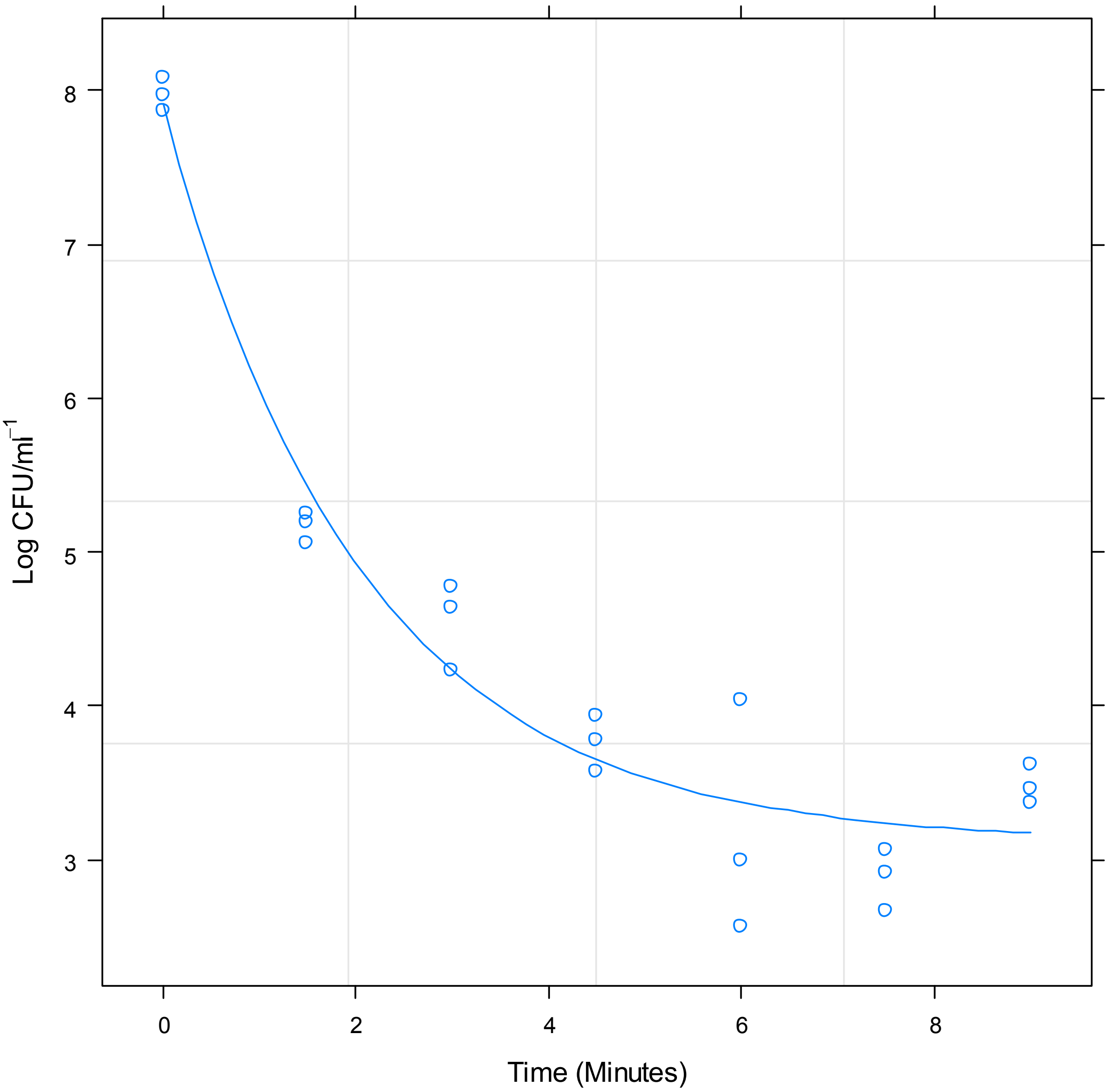

Figure 170. Predicted response curve using an asymptotic regression model for strain 13136 (ST-45, CC-45) at pH 8.5 following heating at 60°C.

1.8.24 pH and Time-Temperature Simulations: 60°C

Mixed Weibull Distribution Model Predicted Response Curves:

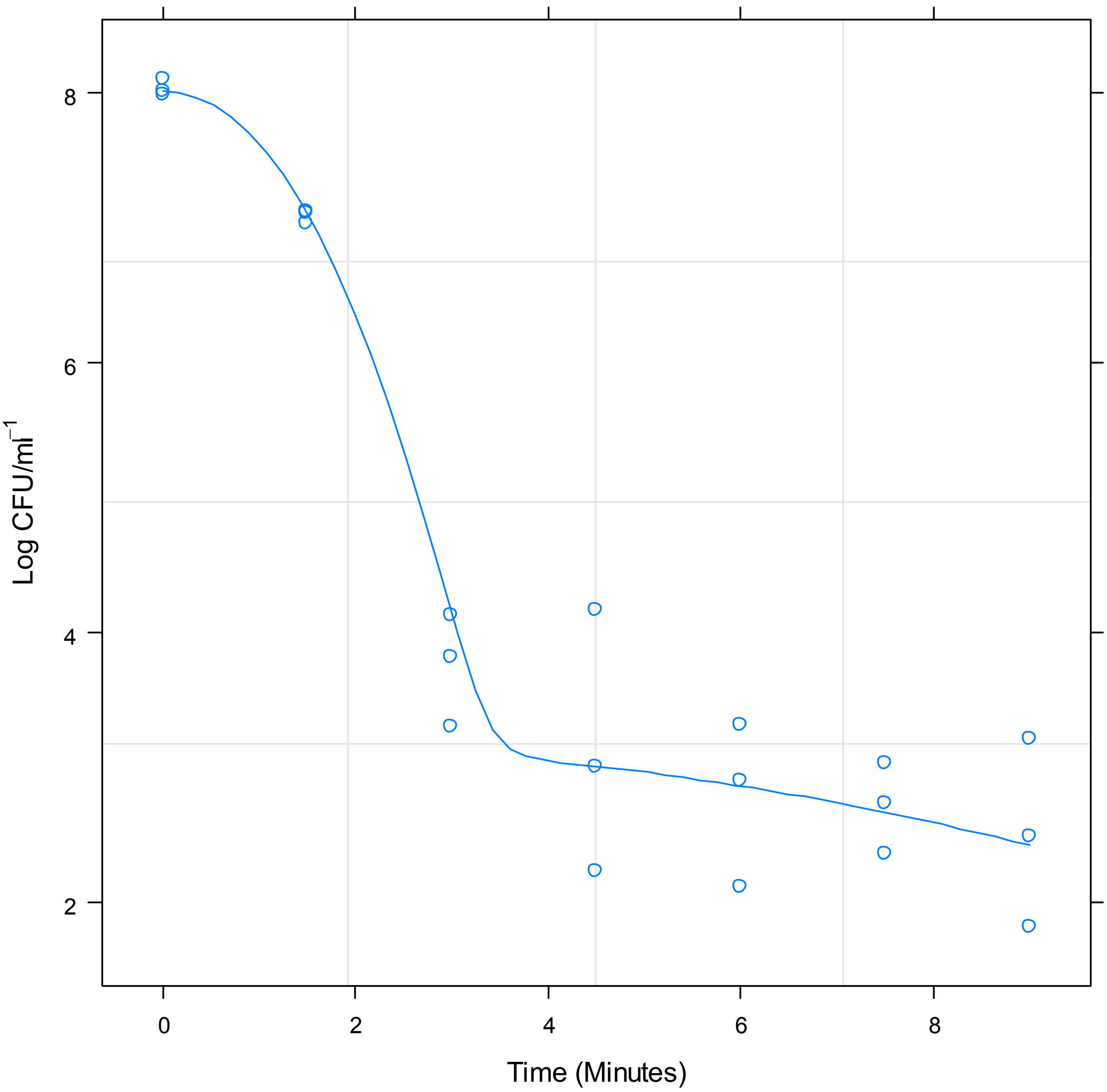

Figure 171. Predicted response curve using a mixed Weibull distribution model of strain 12628 (ST-1773, CC-828) at pH 5.5 following heating at 60°C.

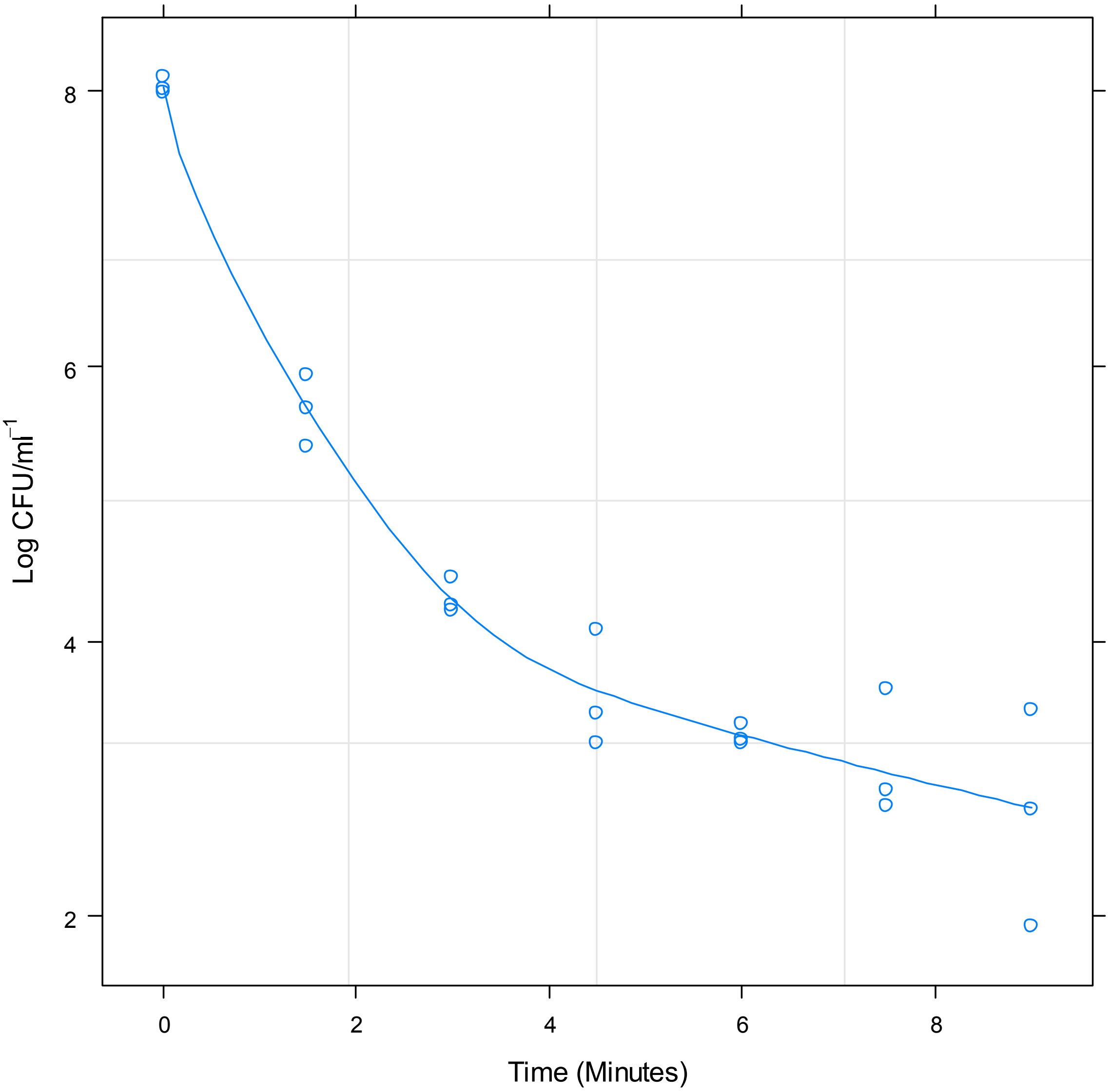

Figure 172. Predicted response curve using a mixed Weibull distribution model of strain 12628 (ST-1773, CC-828) at pH 6.5 following heating at 60^{o}C.

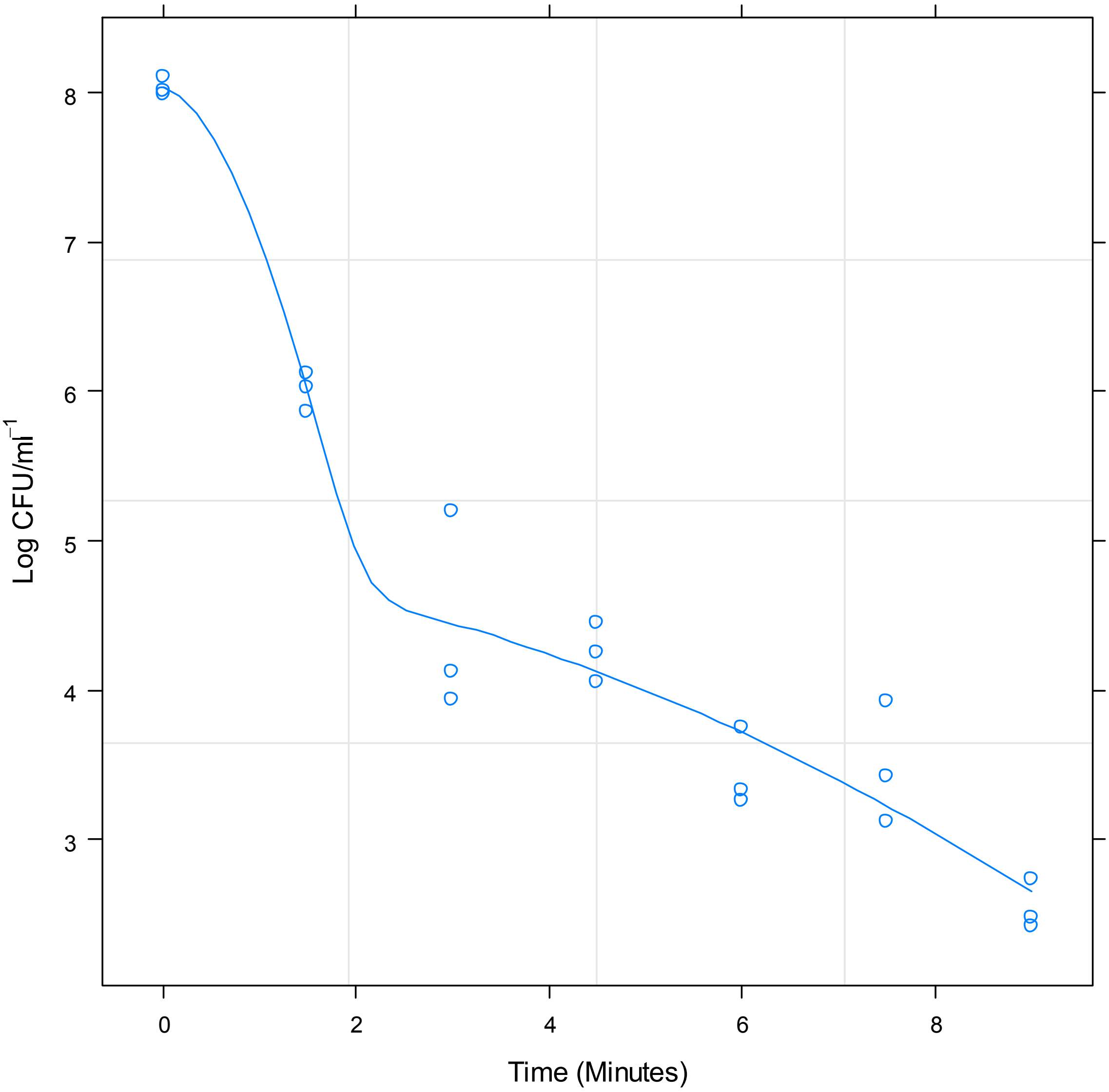

Figure 173. Predicted response curve using a mixed Weibull distribution model of strain 12628 (ST-1773, CC-828) at pH 7.5 following heating at 60°C.

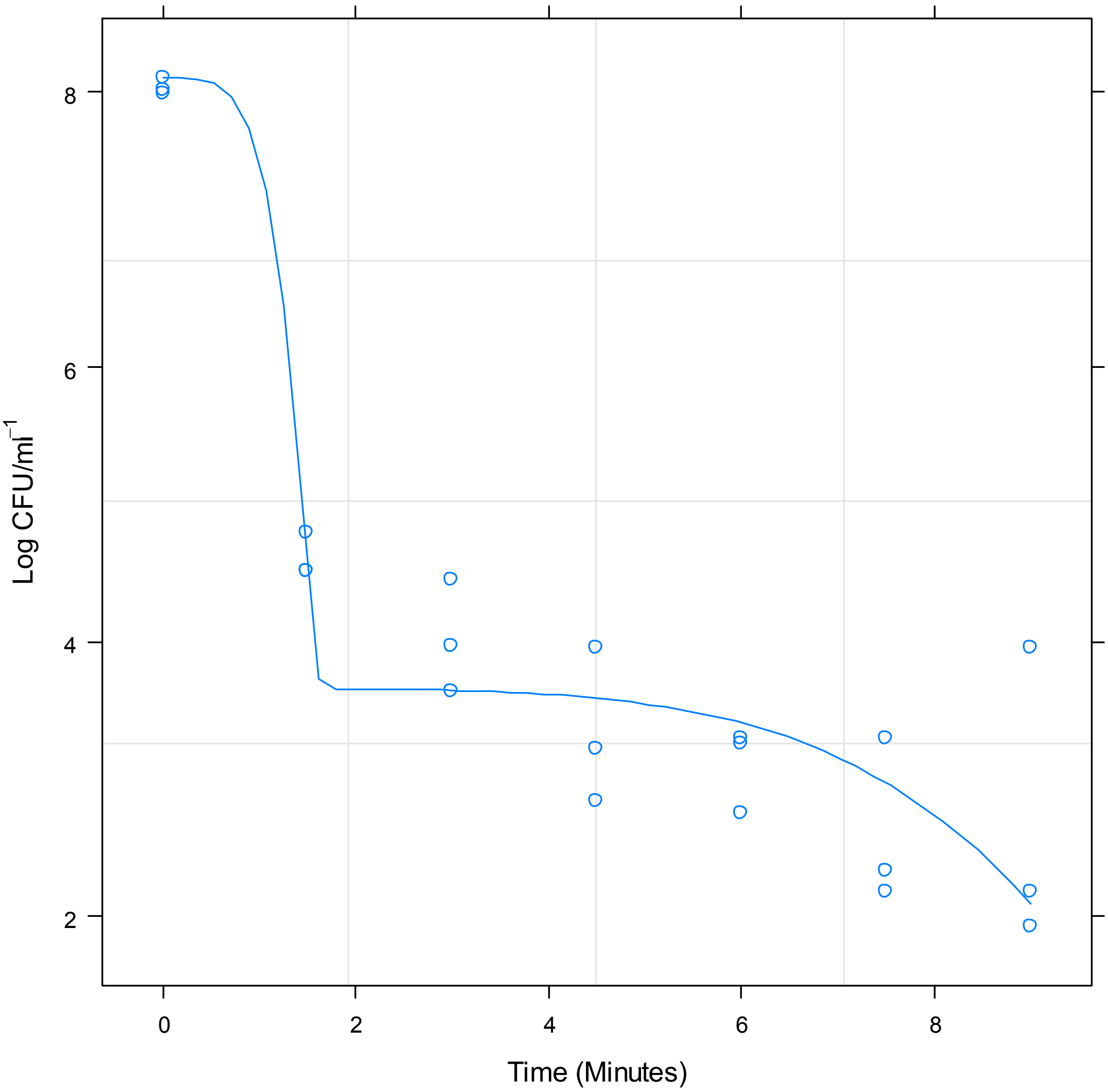

Figure 174. Predicted response curve using a mixed Weibull distribution model of strain 12628 (ST-1773, CC-828) at pH 8.5 following heating at 60^{o}C.

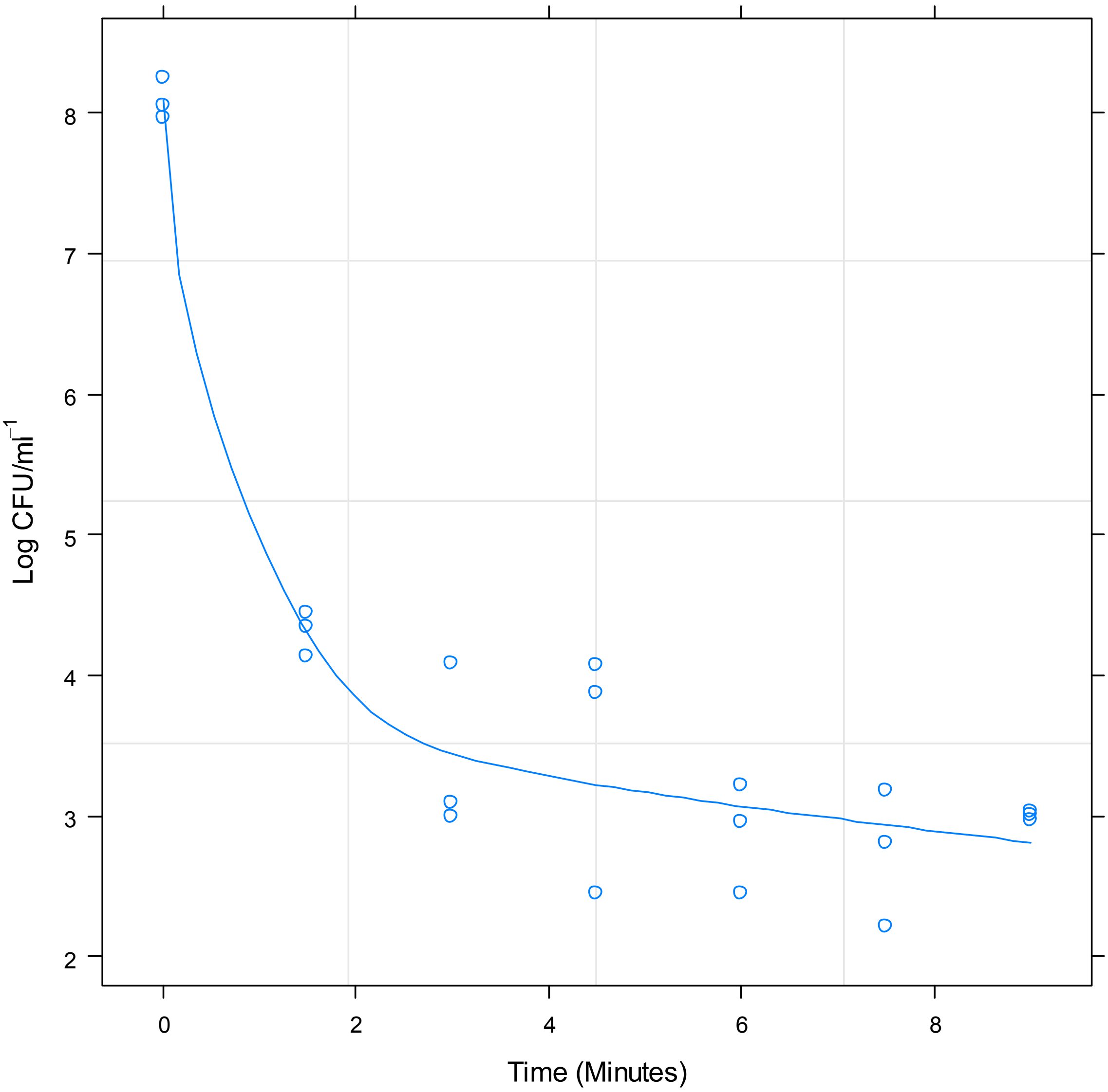

Figure 175. Predicted response curve using a mixed Weibull distribution model of strain 12662 (ST-257, CC-257) at pH 4.5 following heating at 60°C.

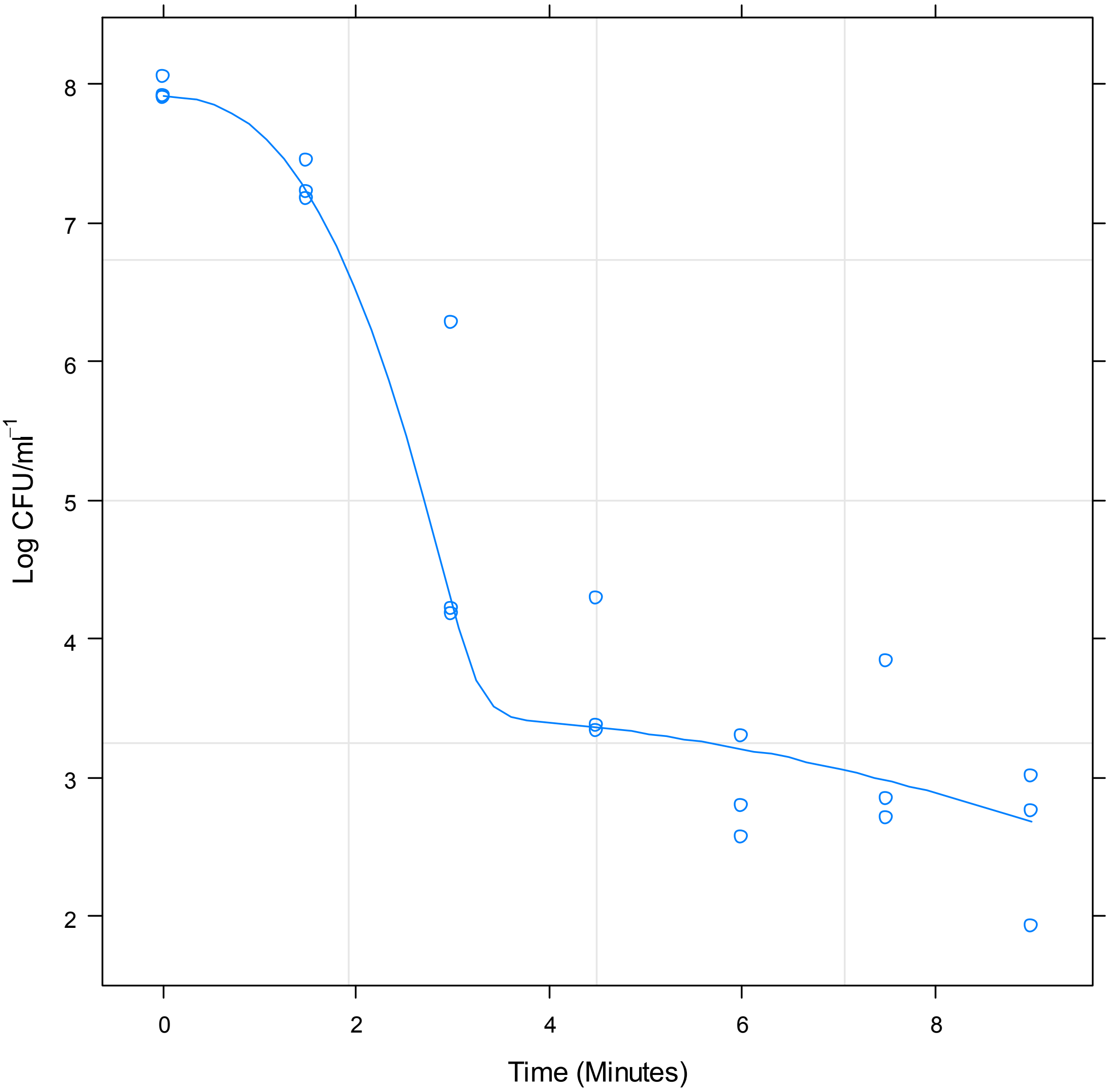

Figure 176. Predicted response curve using a mixed Weibull distribution model of strain 12662 (ST-257, CC-257) at pH 5.5 following heating at 60^{o}C.

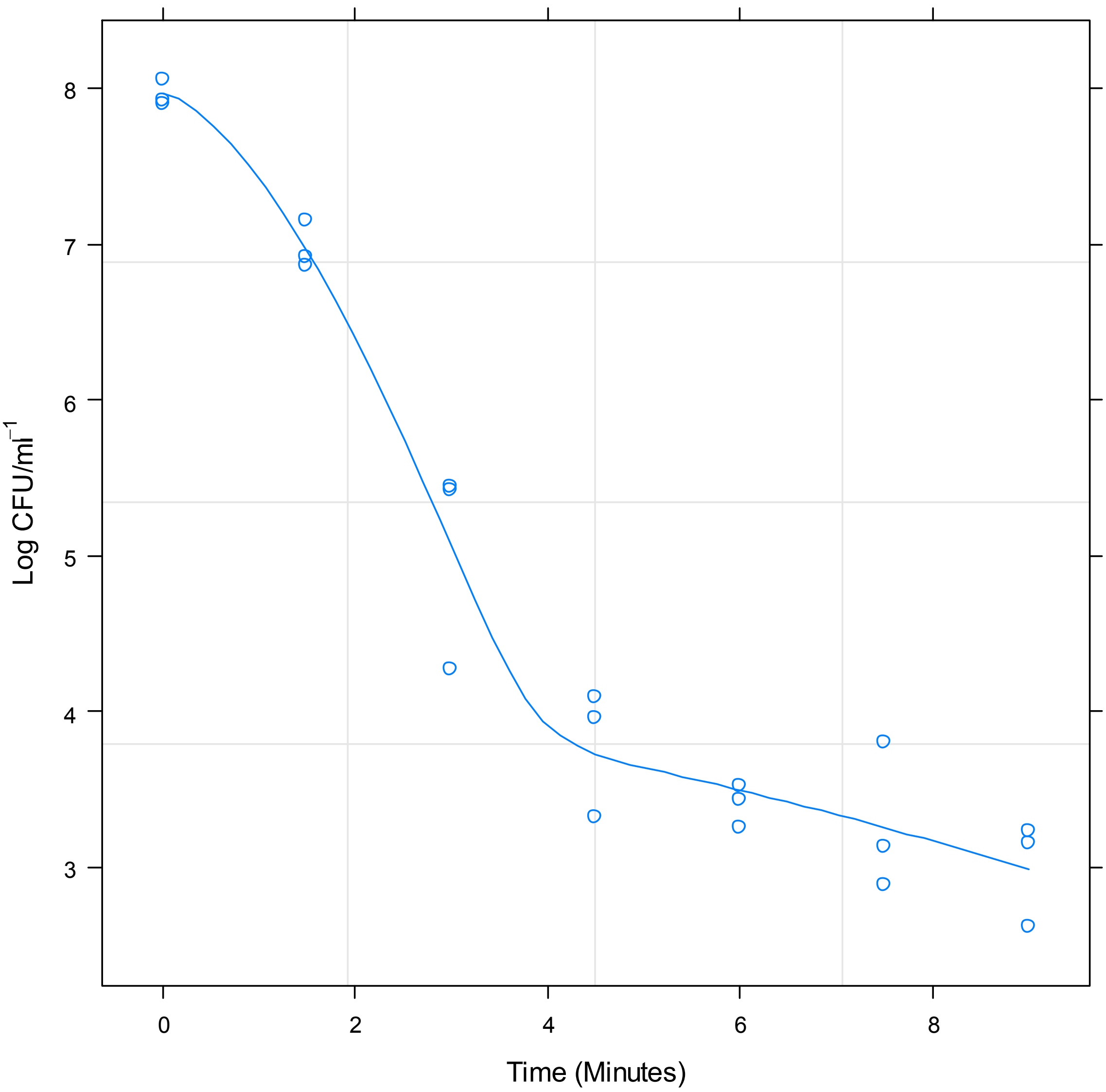

Figure 177. Predicted response curve using a mixed Weibull distribution model of strain 12662 (ST-257, CC-257) at pH 6.5 following heating at 60^{o}C.

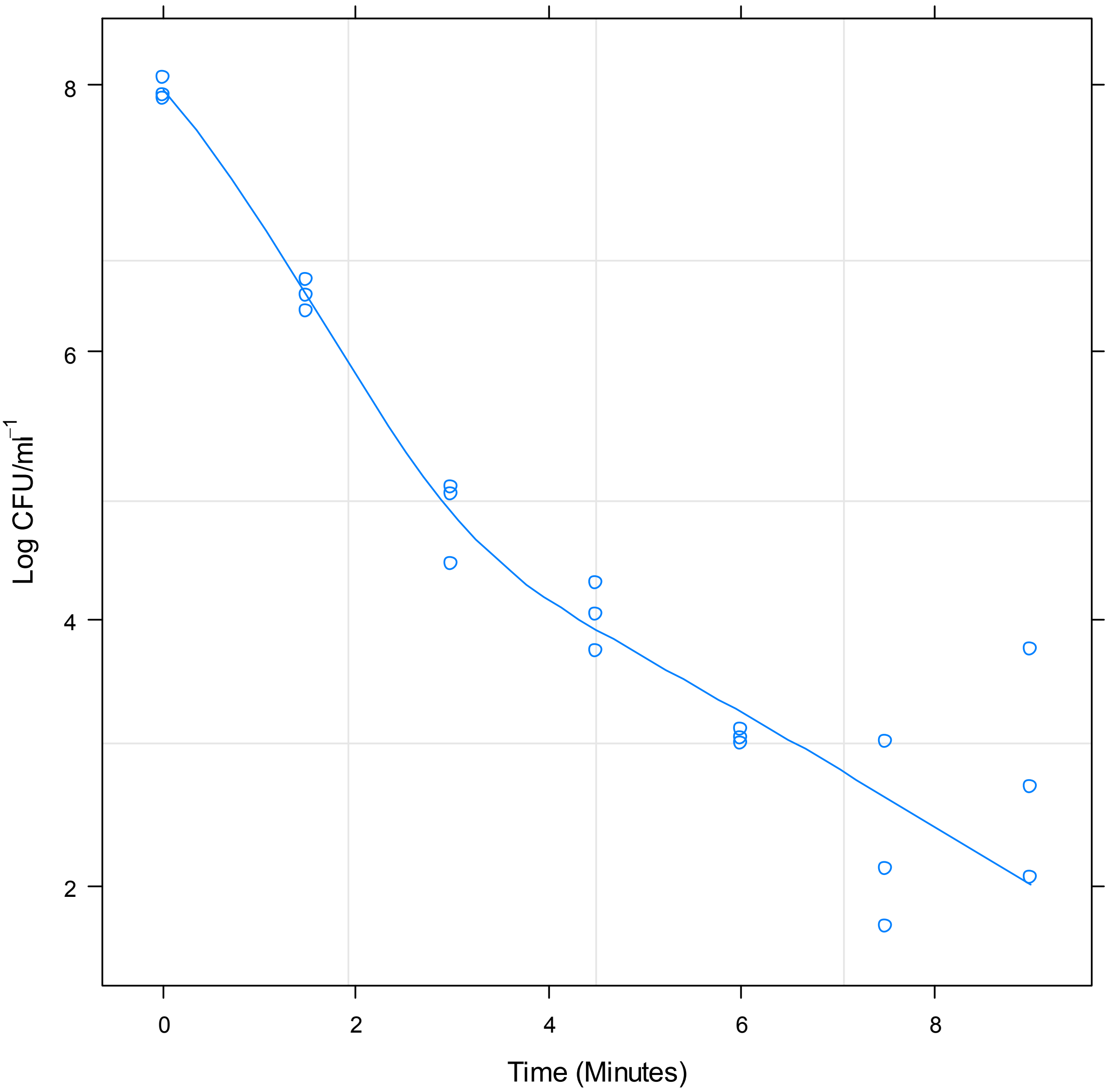

Figure 178. Predicted response curve using a mixed Weibull distribution model of strain 12662 (ST-257, CC-257) at pH 7.5 following heating at 60°C.

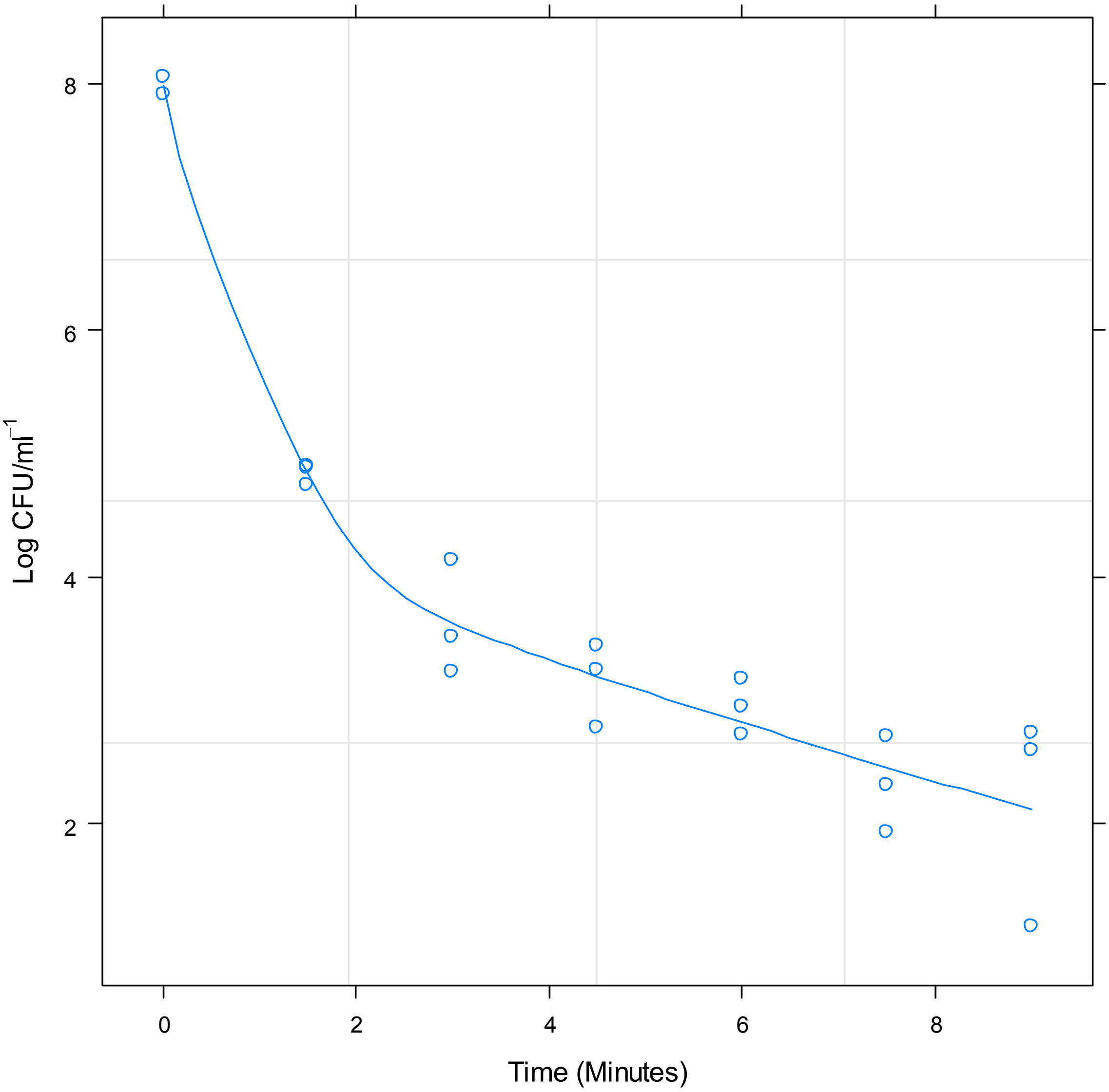

Figure 179. Predicted response curve using a mixed Weibull distribution model of strain 12662 (ST-257, CC-257) at pH 8.5 following heating at 60°C.

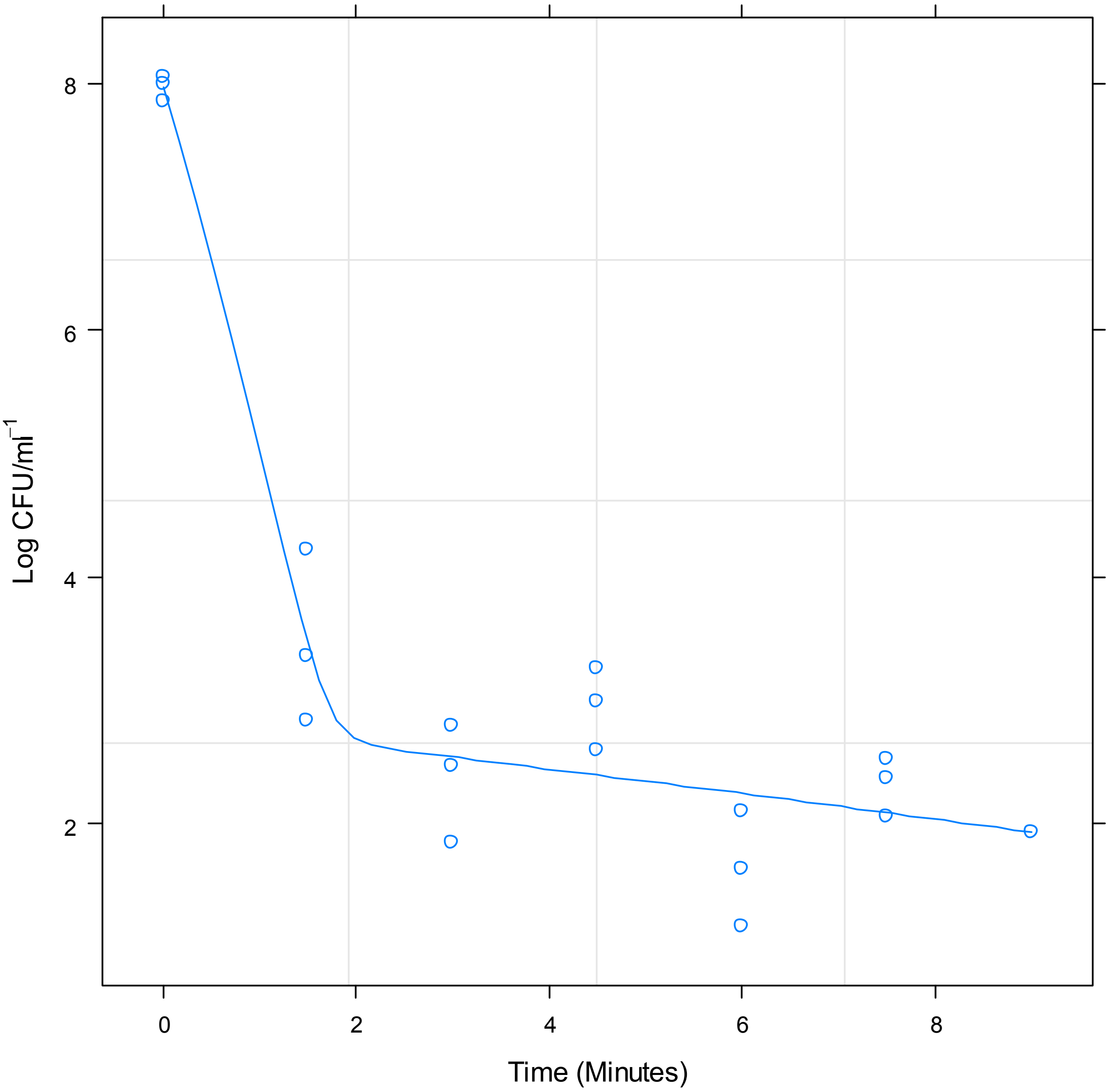

Figure 180. Predicted response curve using a mixed Weibull distribution model of strain 13126 (ST-21, CC-21) at pH 4.5 following heating at 60^{o}C.

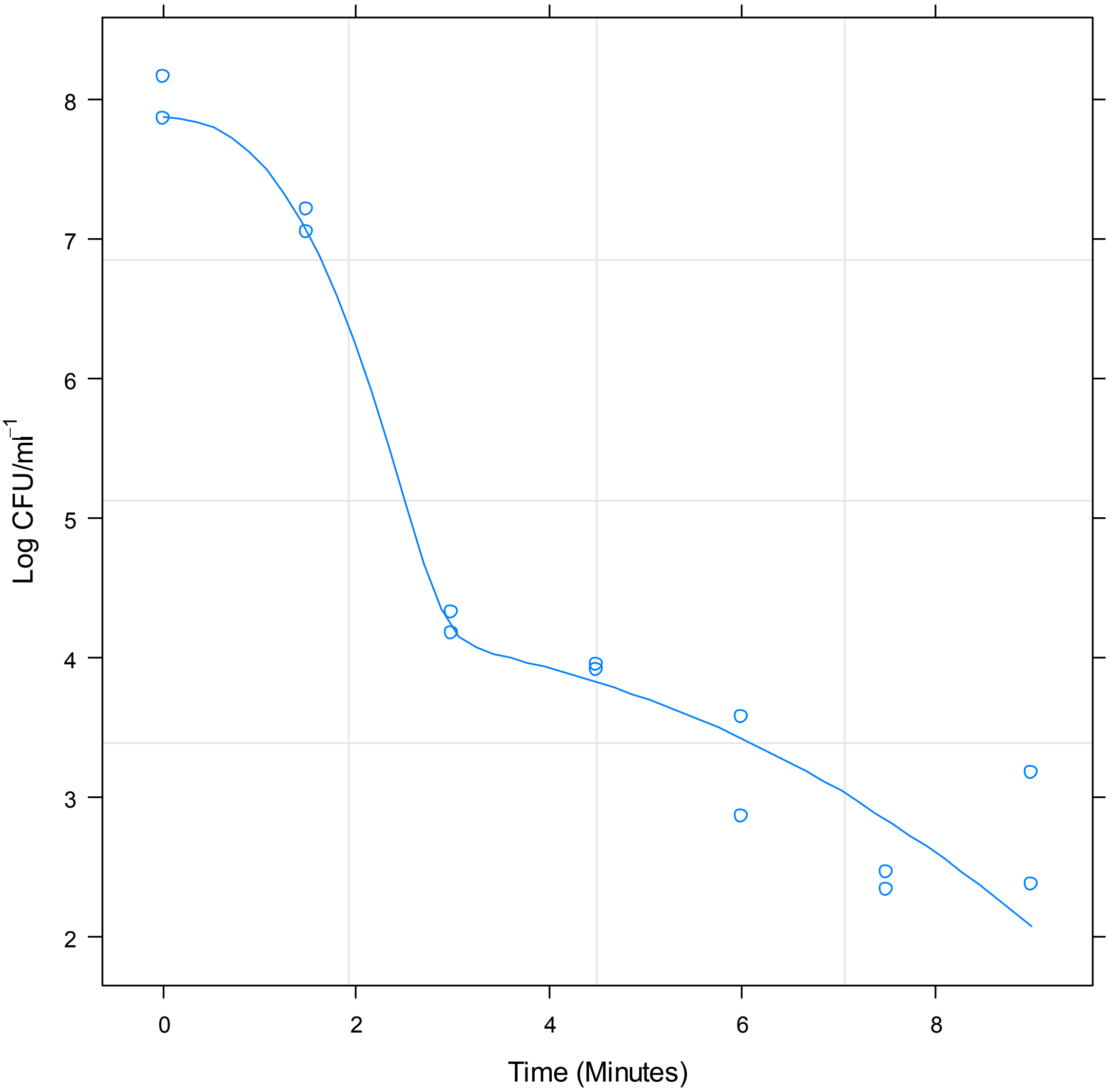

Figure 181. Predicted response curve using a mixed Weibull distribution model of strain 13126 (ST-21, CC-21) at pH 5.5 following heating at 60°C.

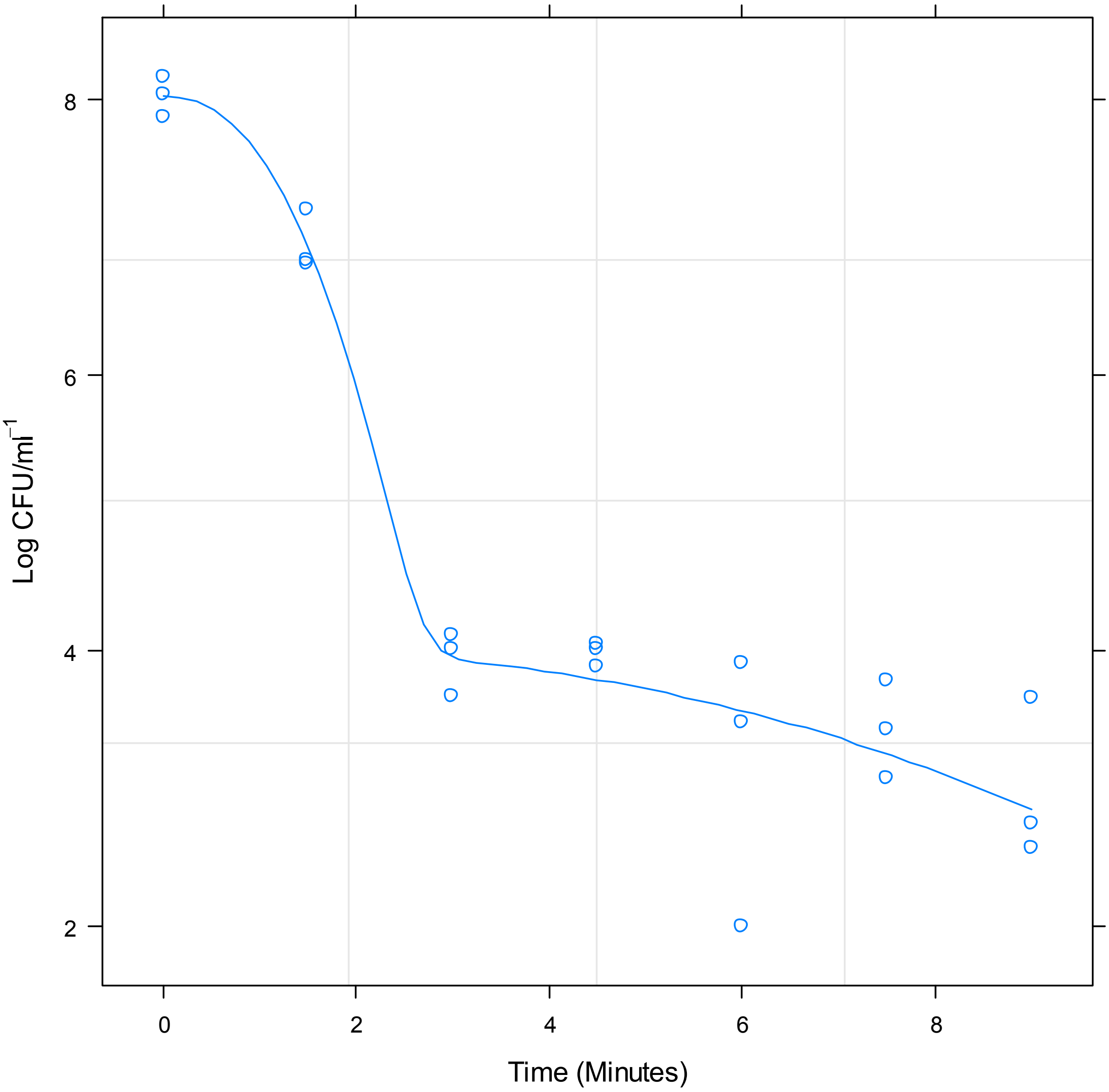

Figure 182. Predicted response curve using a mixed Weibull distribution model of strain 13126 (ST-21, CC-21) at pH 6.5 following heating at 60^{o}C.

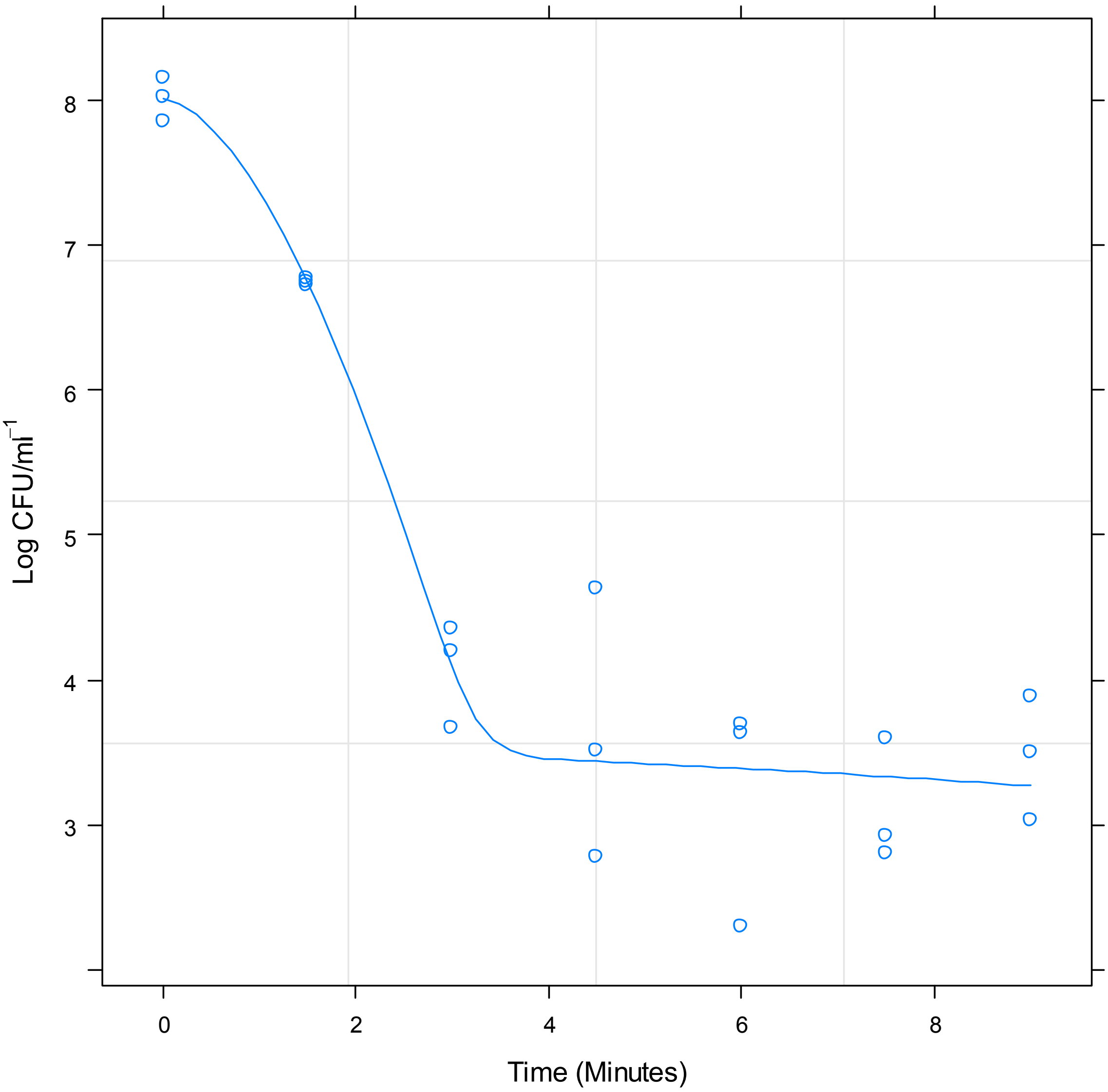

Figure 183. Predicted response curve using a mixed Weibull distribution model of strain 13126 (ST-21, CC-21) at pH 7.5 following heating at 60°C.

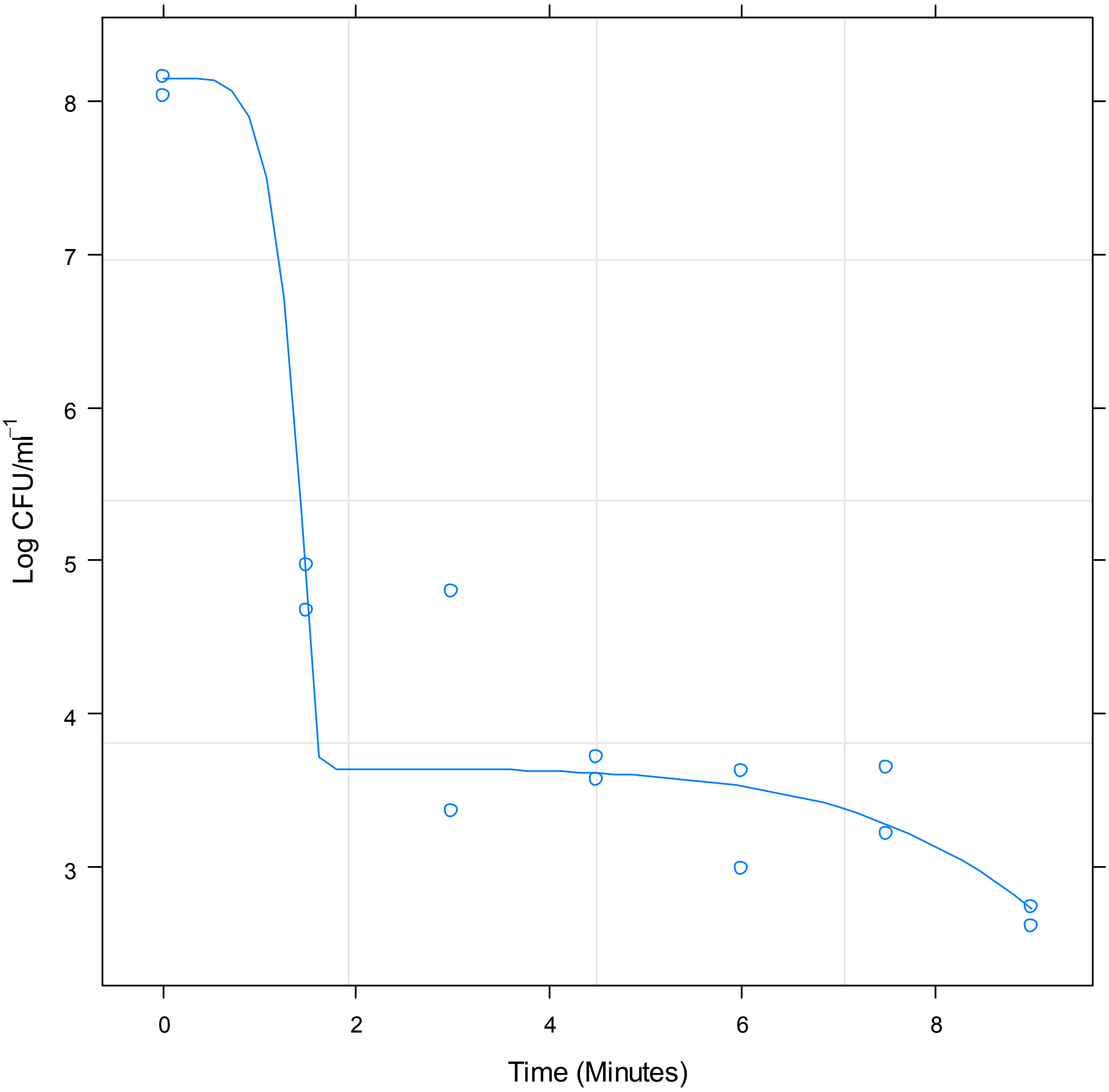

Figure 184. Predicted response curve using a mixed Weibull distribution model of strain 13126 (ST-21, CC-21) at pH 8.5 following heating at 60^{o}C.

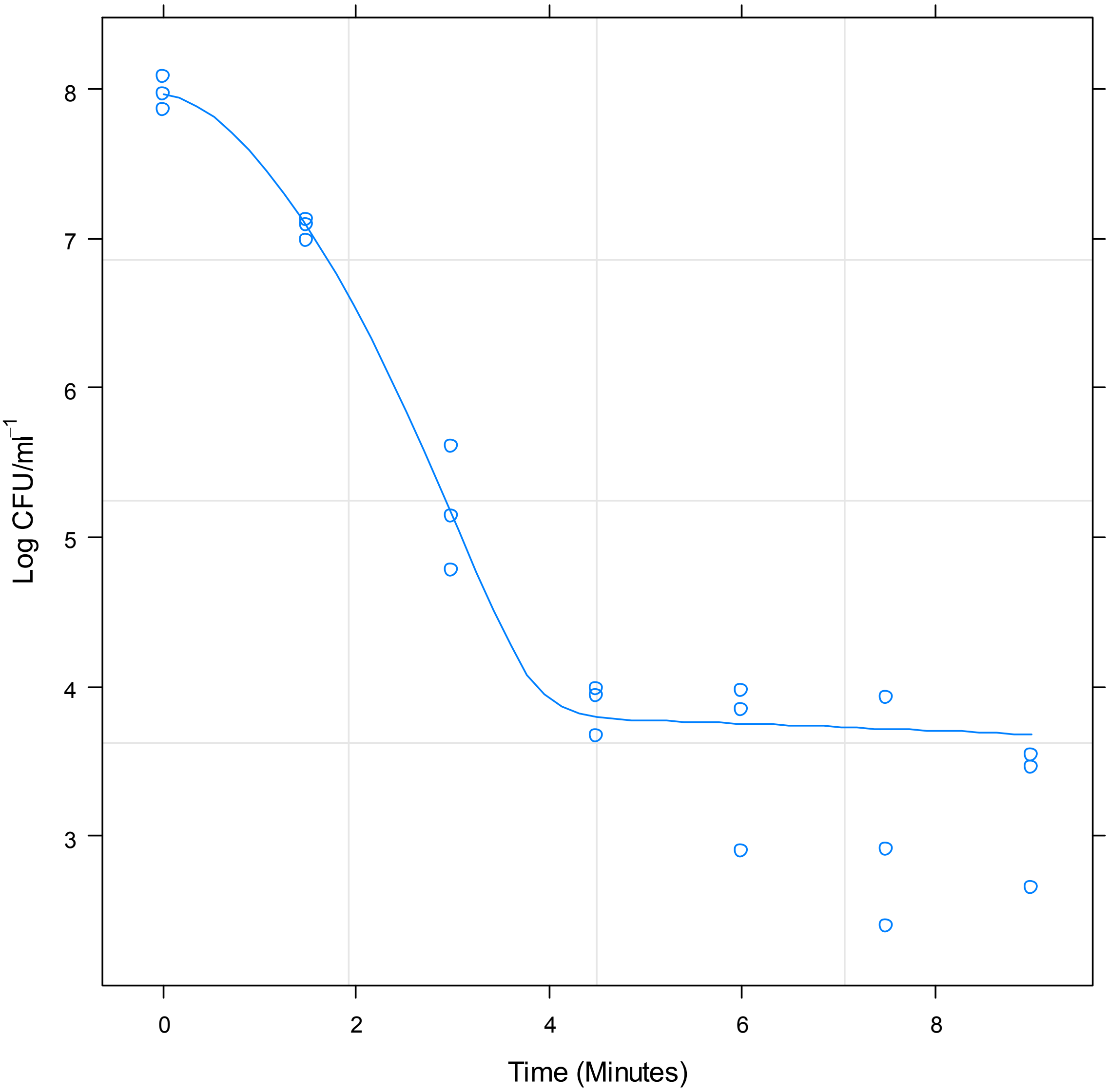

Figure 185. Predicted response curve using a mixed Weibull distribution model of strain 13136 (ST-45, CC-45) at pH 5.5 following heating at 60^{o}C.

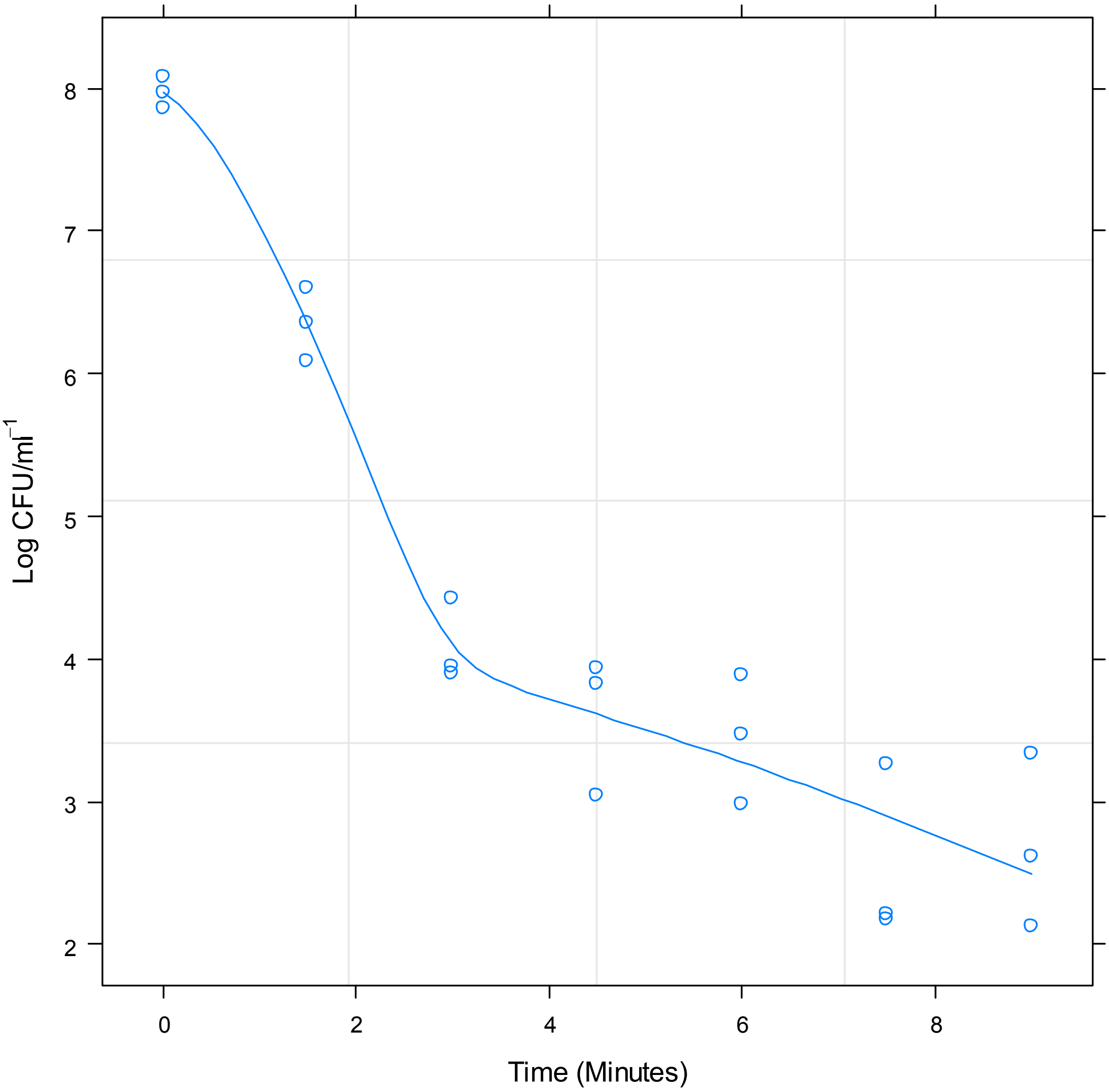

Figure 186. Predicted response curve using a mixed Weibull distribution model of strain 13136 (ST-45, CC-45) at pH 6.5 following heating at 60^{o}C.

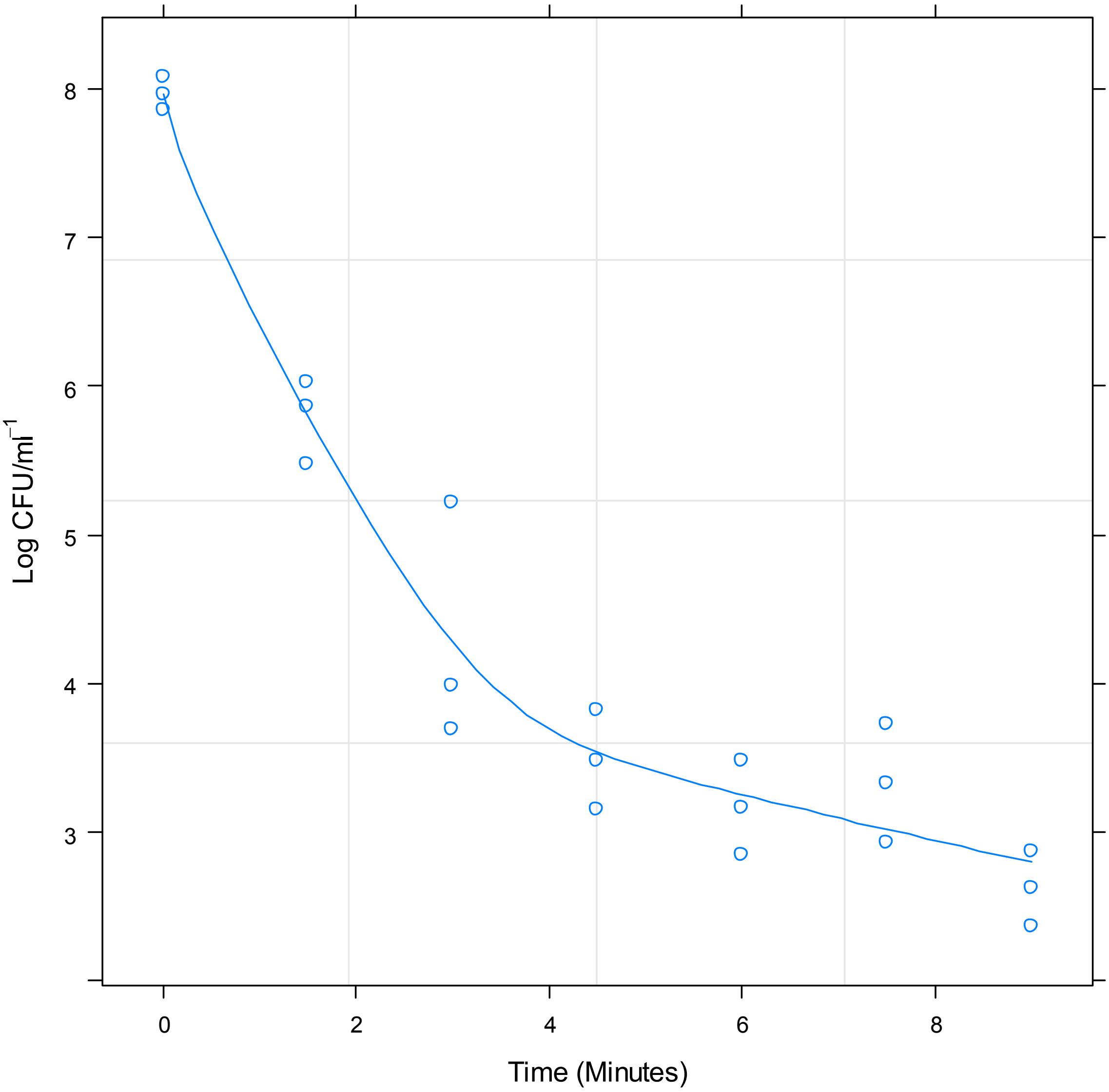

Figure 187. Predicted response curve using a mixed Weibull distribution model of strain 13136 (ST-45, CC-45) at pH 7.5 following heating at 60^{o}C.

1.8.25 pH and Time-Temperature Simulations: 64^{0}C

Table 155. An assessment of the goodness of fit for models analysing the survival of each strain for individual levels of pH at 64^{o}C.

Strain	pH	Non-linear Function	ρ_c
12628 (ST-1773, CC-828)	4.5	Asymptotic Regression	0.915
12628 (ST-1773, CC-828)	5.5	Asymptotic Regression	0.918
12628 (ST-1773, CC-828)	6.5	Asymptotic Regression	0.950
12628 (ST-1773, CC-828)	7.5	Asymptotic Regression	0.953
12628 (ST-1773, CC-828)	8.5	Biexponential	0.941
12662 (ST-257, CC-257)	4.5	Asymptotic Regression	0.944
12662 (ST-257, CC-257)	5.5	Four-parameter Logistic	0.941
12662 (ST-257, CC-257)	6.5	Four-parameter Logistic	0.951
12662 (ST-257, CC-257)	7.5	Asymptotic Regression	0.953
12662 (ST-257, CC-257)	8.5	Biexponential	0.957
13126 (ST-21, CC-21)	4.5	Asymptotic Regression	0.942
13126 (ST-21,CC-21)	5.5	Four-parameter Logistic	0.967
13126 (ST-21, CC-21)	6.5	Four-parameter Logistic	0.953
13126 (ST-21, CC-21)	7.5	Biexponential	0.961
13126 (ST-21, CC-21)	8.5	Biexponential	0.959
13136 (ST-45, CC-45)	4.5	Asymptotic Regression	0.947
13136 (ST-45, CC-45)	5.5	Four-parameter Logistic	0.939
13136 (ST-45, CC-45)	6.5	Four-parameter Logistic	0.969
13136 (ST-45, CC-45)	7.5	Asymptotic Regression	0.953
13136 (ST-45, CC-45)	8.5	Biexponential	0.931

Table 156. Asymptotic regression model analysing survival of strain 12628 (ST-1773, CC-828) at pH 4.5 following heating at 64^{o}C.

Parameter	Estimate	Standard Error	*t*-value	*P*-value
R0	7.858	0.385	20.409	0.000
Asymptote	2.042	0.231	8.856	0.000
LRC	0.442	0.179	2.471	0.024

Table 157. Asymptotic regression model analysing survival of strain 12628 (ST-1773, CC-828) at pH 5.5 following heating at 64^{o}C.

Parameter	Estimate	Standard Error	*t*-value	*P*-value
R0	8.139	0.351	23.166	0.000
Asymptote	2.451	0.303	8.079	0.000
LRC	-0.162	0.198	-0.821	0.422

Table 158. Asymptotic regression model analysing survival of strain 12628 (ST-1773, CC-828) at pH 6.5 following heating at 64°C.

Parameter	Estimate	Standard Error	*t*-value	*P*-value
R0	8.0618	0.2484	32.4499	0.0000
Asymptote	2.7074	0.2530	10.7015	0.0000
LRC	-0.3038	0.1619	-1.8760	0.0770

Table 159. Asymptotic regression model analysing survival of strain 12628 (ST-1773, CC-828) at pH 7.5 following heating at 64°C.

Parameter	Estimate	Standard Error	*t*-value	*P*-value
R0	8.085	0.244	33.175	0.000
Asymptote	2.633	0.254	10.389	0.000
LRC	-0.321	0.158	-2.031	0.057

Table 160. Asymptotic regression model analysing survival of strain 12628 (ST-1773, CC-828) at pH 8.5 following heating at 64°C.

Parameter	Estimate	Standard Error	t-value	P-value
Asymptote 1	3.010	0.593	5.0760	0.000
LRC1	1.240	0.518	2.3945	0.028
Asymptote 2	4.983	0.528	9.4335	0.000
LRC2	-2.013	0.252	-7.9909	0.000

Table 161. Asymptotic regression model analysing survival of strain 12662 (ST-257, CC-257) at pH 4.5 following heating at 64°C.

Parameter	Estimate	Standard Error	*t*-value	*P*-value
R0	8.064	0.313	25.757	0.000
Asymptote	2.226	0.184	12.091	0.000
LRC	0.655	0.149	4.411	0.000

Table 162. Four-parameter logistic regression model analysing survival of strain 12662 (ST-257, CC-257) at pH 5.5 following heating at 64°C.

Parameter	Estimate	Standard Error	*t*-value	*P*-value
Asymptote A	8.116	0.368	22.077	0.000
Asymptote B	3.536	0.193	18.305	0.000
Mid-point	1.377	0.150	9.170	0.000
Scale Parameter	0.367	0.103	3.559	0.002

Table 163. Four-parameter logistic regression model analysing survival of strain 12662 (ST-257, CC-257) at pH 6.5 following heating at 64°C.

Parameter	Estimate	Standard Error	*t*-value	*P*-value
Asymptote A	8.405	0.586	14.340	0.000
Asymptote B	3.145	0.210	14.949	0.000
Mid-point	1.259	0.179	7.046	0.000
Scale Parameter	0.507	0.139	3.659	0.002

Table 164. Asymptotic regression model analysing survival of strain 12662 (ST-257, CC-257) at pH 7.5 following heating at 64°C.

Parameter	Estimate	Standard Error	*t*-value	*P*-value
R0	8.085	0.244	33.175	0.000
Asymptote	2.634	0.253	10.389	0.000
LRC	-0.320	0.158	-2.031	0.057

Table 165. Biexponential regression model analysing survival of strain 12662 (ST-257, CC-257) at pH 8.5 following heating at 64°C.

Parameter	Estimate	Standard Error	*t*-value	*P*-value
Asymptote 1	3.219	0.568	5.664	0.000
LRC1	1.118	0.410	2.725	0.014
Asymptote 2	4.855	0.518	9.366	0.000
LRC2	-1.955	0.236	-8.300	0.000

Table 166. Asymptotic regression model analysing survival of strain 13126 (ST-21, CC-21) at pH 45 following heating at 64°C.

Parameter	Estimate	Standard Error	*t*-value	*P*-value
R0	7.969	0.335	23.769	0.000
Asymptote	2.583	0.239	10.793	0.000
LRC	1.313	0.260	5.048	0.001

Table 167. Four-parameter regression model analysing survival of strain 13126 (ST-21, CC-21) at pH 5.5 following heating at 64°C.

Parameter	Estimate	Standard Error	*t*-value	*P*-value
Asymptote A	8.202	0.501	16.371	0.000
Asymptote B	3.008	0.161	18.724	0.000
Mid-point	1.248	0.154	8.085	0.000
Scale Parameter	0.525	0.118	4.433	0.000

Table 168. Four-parameter regression model analysing survival of strain 13126 (ST-21, CC-21) at pH 6.5 following heating at 64°C.

Parameter	Estimate	Standard Error	*t*-value	*P*-value
Asymptote A	8.857	1.129	7.848	0.000
Asymptote B	2.606	0.218	11.930	0.000
Mid-point	1.007	0.277	3.636	0.002
Scale Parameter	0.628	0.188	3.340	0.004

Table 169. Biexponential regression model analysing survival of strain 13126 (ST-21, CC-21) at pH 7.5 following heating at 64°C.

Parameter	Estimate	Standard Error	*t*-value	*P*-value
Asymptote 1	3.439	0.938	3.665	0.002
LRC1	0.501	0.397	1.262	0.224
Asymptote 2	4.397	0.932	4.716	0.000
LRC2	-1.946	0.395	-4.929	0.000

Table 170. Biexponential regression model analysing survival of strain 13126 (ST-21, CC-21) at pH 8.5 following heating at 64°C.

Parameter	Estimate	Standard Error	*t*-value	*P*-value
Asymptote 1	3.411	0.390	8.749	0.000
LRC1	1.277	0.327	3.901	0.001
Asymptote 2	4.407	0.333	13.216	0.000
LRC2	-2.607	0.316	-8.261	0.000

Table 171. Asymptotic regression model analysing survival of strain 13136 (ST-45, CC-45) at pH 4.5 following heating at 64°C.

Parameter	Estimate	Standard Error	*t*-value	*P*-value
R0	7.871	0.304	25.868	0.000
Asymptote	2.155	0.237	9.091	0.000
LRC	0.496	0.159	3.116	0.008

Table 172. Four-parameter logistic regression model analysing survival of strain 13136 (ST-45, CC-45) at pH 5.5 following heating at 64°C.

Parameter	**Estimate**	**Standard Error**	***t*-value**	***P*-value**
Asymptote A	8.030	0.604	13.295	0.000
Asymptote B	2.652	0.209	12.716	0.000
Mid-point	0.990	0.110	8.979	0.000
Scale Parameter	0.318	0.136	2.344	0.032

Table 173. Four-parameter logistic regression model analysing survival of strain 13136 (ST-45, CC-45) at pH 6.5 following heating at 64°C.

Parameter	**Estimate**	**Standard Error**	***t*-value**	***P*-value**
Asymptote A	8.190	0.420	19.511	0.000
Asymptote B	3.286	0.135	24.385	0.000
Mid-point	1.086	0.110	9.839	0.000
Scale Parameter	0.421	0.100	4.200	0.001

Table 174. Asymptotic regression model analysing survival of strain 13136 (ST-45, CC-45) at pH 7.5 following heating at 64°C.

Parameter	**Estimate**	**Standard Error**	***t*-value**	***P*-value**
R0	8.085	0.244	33.175	0.000
Asymptote	2.634	0.253	10.389	0.000
LRC	-0.320	0.158	-2.031	0.057

Table 175. Biexponential regression model analysing survival of strain 13136 (ST-45, CC-45) at pH 8.5 following heating at 64°C.

Parameter	**Estimate**	**Standard Error**	***t*-value**	***P*-value**
Asymptote 1	3.844	1.435	2.679	0.017
LRC1	0.443	0.521	0.850	0.408
Asymptote 2	4.157	1.434	2.898	0.011
LRC2	-2.036	0.706	-2.881	0.011

1.8.26 pH and Time-temperature Simulations: 64^{0}C

Mixed Weibull Distribution Model:

Table 176. An assessment of the goodness of fit for Mixed Weibull distribution models analysing the survival of each strain following heating at 64^{o}C.

Strain	pH	Non-linear Function	ρ_c
12628 (ST-1773, CC-828)	4.5	Mixed Weibull Distribution	0.990
12628 (ST-1773, CC-828)	5.5	Mixed Weibull Distribution	0.963
12628 (ST-1773, CC-828)	6.5	Mixed Weibull Distribution	0.980
12628 (ST-1773, CC-828)	7.5	Mixed Weibull Distribution	0.965
12628(ST-1773, CC-828)	8.5	Mixed Weibull Distribution	0.944
12662 (ST-257, CC-257)	4.5	Mixed Weibull Distribution	0.970
12662 (ST-257, CC-257)	5.5	Mixed Weibull Distribution	0.968
12662 (ST-257, CC-257)	6.5	Mixed Weibull Distribution	0.978
12662 (ST-257, CC-257)	7.5	Mixed Weibull Distribution	0.970
12662 (ST-257, CC-257)	8.5	Mixed Weibull Distribution	0.972
13126 (ST-21, CC-21)	4.5	Mixed Weibull Distribution	0.964
13126 (ST-21, CC-21)	5.5	Mixed Weibull Distribution	0.982
13126 (ST-21, CC-21)	6.5	Mixed Weibull Distribution	0.957
13126 (ST-21, CC-21)	7.5	Mixed Weibull Distribution	0.976
13126 (ST-21, CC-21)	8.5	Mixed Weibull Distribution	0.982
13136 (ST-45, CC-45)	4.5	Mixed Weibull Distribution	0.976
13136 (ST-45, CC-45)	5.5	Mixed Weibull Distribution	0.967
13136 (ST-45, CC-45)	6.5	Mixed Weibull Distribution	0.985
13136 (ST-45, CC-45)	7.5	Mixed Weibull Distribution	0.984
13136 (ST-45, CC-45)	8.5	Mixed Weibull Distribution	0.967

Table 177. Mixed Weibull distribution model analysing the survival of strain 12628 (ST-1773, CC-828) at 64^{o}C and pH 4.5.

Parameter	Estimate	Standard Error	*t*-value	*P*-value
α	2.990	38.124	0.078	0.945
$\delta 1$	0.010	0.054	0.178	0.875
p	0.309	0.471	0.657	0.579
N0	8.162	0.536	15.226	0.004
$\delta 2$	0.077	1.925	0.040	0.972

Table 178. Mixed Weibull distribution model analysing the survival of strain 12628 (ST-1773, CC-828) at 64°C and pH 5.5.

Parameter	Estimate	Standard Error	*t*-value	*P*-value
α	4.442	0.623	7.129	0.000
δ1	0.369	0.056	6.572	0.000
p	1.180	0.202	5.845	0.000
N0	7.987	0.100	79.749	0.000
δ2	4.877	3.676	1.327	0.203

Table 179. Mixed Weibull distribution model analysing the survival of strain 12628 (ST-1773, CC-828) at 64°C and pH 6.5.

Parameter	Estimate	Standard Error	*t*-value	*P*-value
α	3.582	0.411	8.708	0.000
δ1	0.416	0.107	3.885	0.001
p	1.289	0.343	3.765	0.002
N0	7.986	0.247	32.300	0.000
δ2	3.248	0.972	3.340	0.004

Table 180. Mixed Weibull distribution model analysing the survival of strain 12628 (ST-1773, CC-828) at 64°C and pH 7.5.

Parameter	Estimate	Standard Error	*t*-value	*P*-value
α	3.818	0.517	7.390	0.000
δ1	0.307	0.109	2.822	0.012
P	1.129	0.340	3.326	0.004
N0	7.982	0.313	25.492	0.000
δ2	3.767	1.658	2.272	0.037

Table 181. Mixed Weibull distribution model analysing the survival of strain 12628 (ST-1773, CC-828) at 64°C and pH 8.5.

Parameter	Estimate	Standard Error	*t*-value	*P*-value
α	3.2111	0.998	3.217	0.005
δ1	0.1777	0.164	1.085	0.294
p	1.0040	0.845	1.188	0.252
N0	7.9876	0.285	27.999	0.000
δ2	2.1912	2.299	0.953	0.355

Table 182. Mixed Weibull distribution model analysing the survival of strain 12662 (ST-257, CC-257) at 64^{o}C and pH 4.5.

Parameter	Estimate	Standard Error	*t*-value	*P*-value
α	4.324	0.904	4.782	0.000
δ1	0.058	0.092	0.627	0.541
p	0.651	0.475	1.369	0.193
N0	8.051	0.171	47.127	0.000
δ2	1.539	2.204	0.698	0.496

Table 183. Mixed Weibull distribution model analysing the survival of strain 12662 (ST-257, CC-257) at 64^{o}C and pH 5.5.

Parameter	Estimate	Standard Error	*t*-value	*P*-value
α	3.938	0.596	6.614	0.000
δ1	0.942	0.108	8.693	0.000
p	1.899	0.352	5.395	0.000
N0	8.026	0.129	62.036	0.000
δ2	5.719	3.871	1.477	0.159

Table 184. Mixed Weibull distribution model analysing the survival of strain 12662 (ST-257, CC-257) at 64^{o}C and pH 6.5.

Parameter	Estimate	Standard Error	*t*-value	*P*-value
α	3.868	0.533	7.257	0.000
δ1	0.757	0.172	4.405	0.001
p	1.506	0.375	4.015	0.001
N0	7.986	0.265	30.198	0.000
δ2	4.401	1.643	2.678	0.017

Table 185. Mixed Weibull distribution model analysing the survival of strain 12662 (ST-2573, CC-257) at 64^{o}C and pH 7.5.

Parameter	Estimate	Standard Error	*t*-value	*P*-value
α	4.361	0.750	5.818	0.000
δ1	0.432	0.150	2.879	0.011
p	1.070	0.316	3.392	0.004
N0	8.033	0.321	25.062	0.000
δ2	4.127	2.827	1.460	0.164

Table 186. Mixed Weibull distribution model analysing the survival of strain 12662 (ST-257, CC-257) at 64^{o}C and pH 8.5.

Parameter	**Estimate**	**Standard Error**	***t*-value**	***P*-value**
α	3.812	0.280	13.669	0.000
δ1	0.2790	0.085	3.287	0.005
p	1.750	0.903	1.938	0.071
N0	8.063	0.006	1.37E+03	0.000
δ2	3.189	0.720	4.431	0.000

Table 187. Mixed Weibull distribution model analysing the survival of strain 13126 (ST-21, CC-21) at 64^{o}C and pH 4.5.

Parameter	**Estimate**	**Standard Error**	***t*-value**	***P*-value**
α	3.633	0.896	4.055	0.004
δ1	0.013	0.029	0.430	0.679
p	0.390	0.245	1.591	0.150
N0	7.870	0.148	53.348	0.000
δ2	0.465	1.065	0.437	0.674

Table 188. Mixed Weibull distribution model analysing the survival of strain 13126 (ST-21, CC-21) at 64^{o}C and pH 5.5.

Parameter	**Estimate**	**Standard Error**	***t*-value**	***P*-value**
α	4.424	0.733	6.039	0.000
δ1	0.700	0.089	7.862	0.000
p	1.288	0.165	7.792	0.000
N0	7.795	0.116	67.359	0.000
δ2	10.554	20.159	0.524	0.608

Table 189. Mixed Weibull distribution model analysing the survival of strain 13126 (ST-21, CC-21) at 64^{o}C and pH 6.5.

Parameter	**Estimate**	**Standard Error**	***t*-value**	***P*-value**
α	5.105	0.961	5.312	0.000
δ1	0.504	0.165	3.046	0.008
p	1.038	0.228	4.555	0.003
N0	7.838	0.300	26.131	0.000
δ2	85.295	1.72E+03	0.050	0.961

Table 190. Mixed Weibull distribution model analysing the survival of strain 13126 (ST-21, CC-21) at 64°C and pH 7.5.

Parameter	Estimate	Standard Error	*t*-value	*P*-value
α	3.162	0.523	6.050	0.000
δ1	0.195	0.048	4.040	0.001
p	0.797	0.163	4.879	0.000
N0	7.814	0.066	118.059	0.000
δ2	1.545	0.660	2.340	0.033

Table 191. Mixed Weibull distribution model analysing the survival of strain 13126 (ST-21, CC-21) at 64°C and pH 8.5.

Parameter	Estimate	Standard Error	*t*-value	*P*-value
α	3.956	0.366	10.796	0.000
δ1	0.399	0.037	10.706	0.000
p	4.886	1.890	2.586	0.021
N0	7.814	0.343	22.786	0.000
δ2	4.956	0.148	33.588	0.000

Table 192. Mixed Weibull distribution model analysing the survival of strain 13136 (ST-45, CC-45) at 64°C and pH 4.5.

Parameter	Estimate	Standard Error	*t*-value	*P*-value
α	5.504	3.725	1.478	0.168
δ1	0.021	0.025	0.843	0.417
p	0.388	0.132	2.930	0.014
N0	7.911	0.073	108.084	0.000
δ2	66.256	2.03E+03	0.033	0.975

Table 193. Mixed Weibull distribution model analysing the survival of strain 13136 (ST-45, CC-45) at 64°C and pH 5.5.

Parameter	Estimate	Standard Error	*t*-value	*P*-value
α	5.124	1.084	4.727	0.002
δ1	0.412	0.239	1.726	0.123
p	1.150	0.661	1.741	0.120
N0	8.061	0.507	15.899	0.000
δ2	10.768	32.896	0.327	0.752

Table 194. Mixed Weibull distribution model analysing the survival of strain 13136 (ST-45, CC-45) at 64°C and pH 6.5.

Parameter	Estimate	Standard Error	*t*-value	*P*-value
α	4.384	0.520	8.431	0.000
δ1	0.616	0.120	5.132	0.000
p	1.290	0.238	5.416	0.000
N0	7.901	0.209	37.756	0.000
δ2	14.641	28.794	0.509	0.618

Table 195. Mixed Weibull distribution model analysing the survival of strain 13136 (ST-45, CC-45) at 64°C and pH 7.5.

Parameter	Estimate	Standard Error	*t*-value	*P*-value
α	3.893	0.378	10.301	0.000
δ1	0.452	0.113	4.012	0.001
p	1.247	0.349	3.576	0.003
N0	7.918	0.225	35.202	0.000
δ2	4.039	1.297	3.114	0.007

Table 196. Mixed Weibull distribution model analysing the survival of strain 13136 (ST-45, CC-45) at 64°C and pH 8.5.

Parameter	Estimate	Standard Error	*t*-value	*P*-value
α	3.670	0.569	6.451	0.000
δ1	0.242	0.054	4.447	0.001
p	0.980	0.222	4.421	0.001
N0	7.944	0.091	87.062	0.000
δ2	2.243	0.955	2.349	0.033

1.8.27 pH and Time-Temperature Simulations: 64°C

Predicted Response Curves:

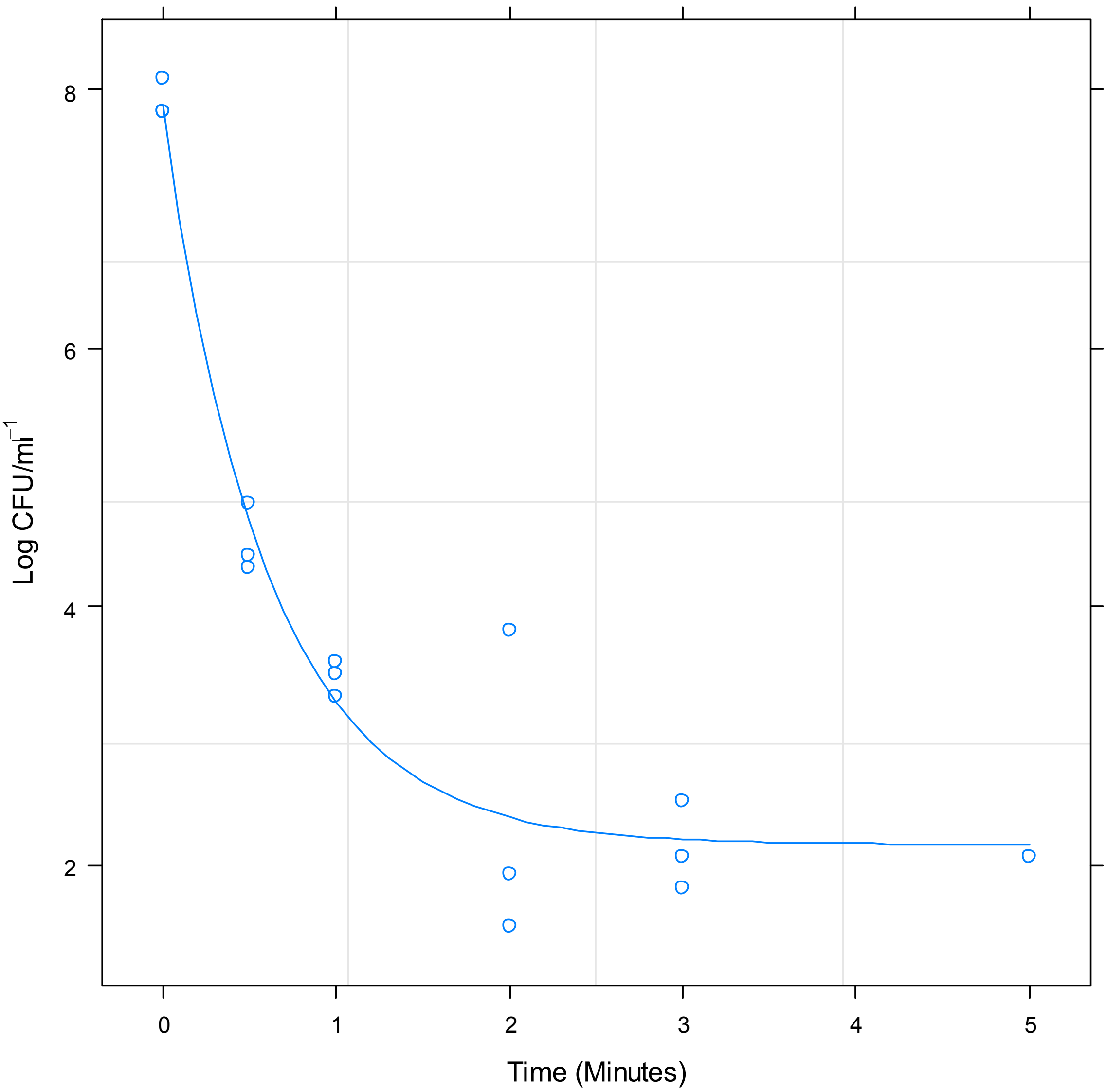

Figure 188. Predicted response curve using an asymptotic regression model for strain 12628 (ST-1773, CC-828) at pH 4.5 following heating at 64°C.

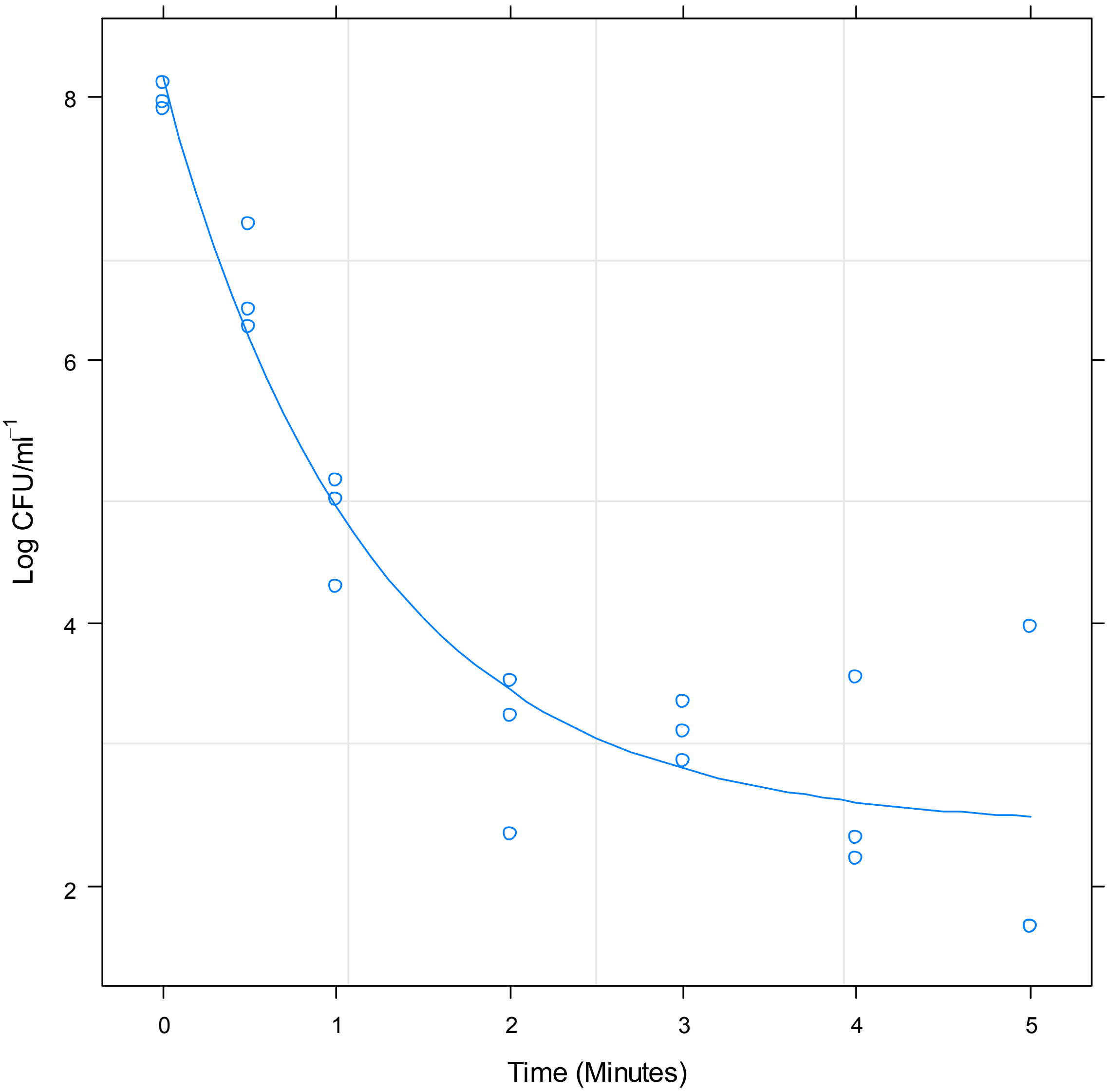

Figure 189. Predicted response curve using an asymptotic regression model for strain 12628 (ST-1773, CC-828) at pH 5.5 following heating at 64°C.

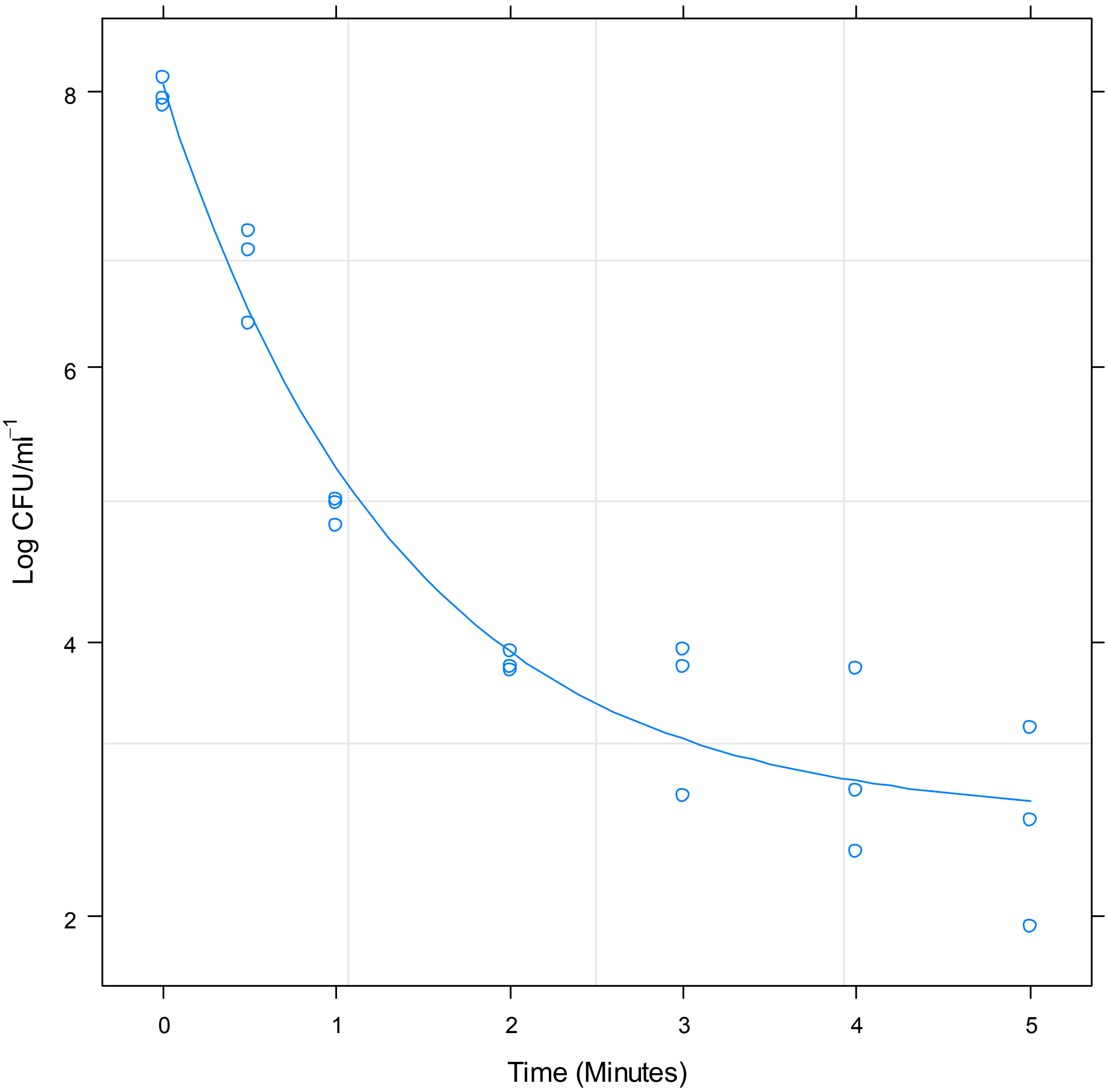

Figure 190. Predicted response curve using an asymptotic regression model for strain 12628 (ST-1773, CC-828) at pH 6.5 following heating at 64°C.

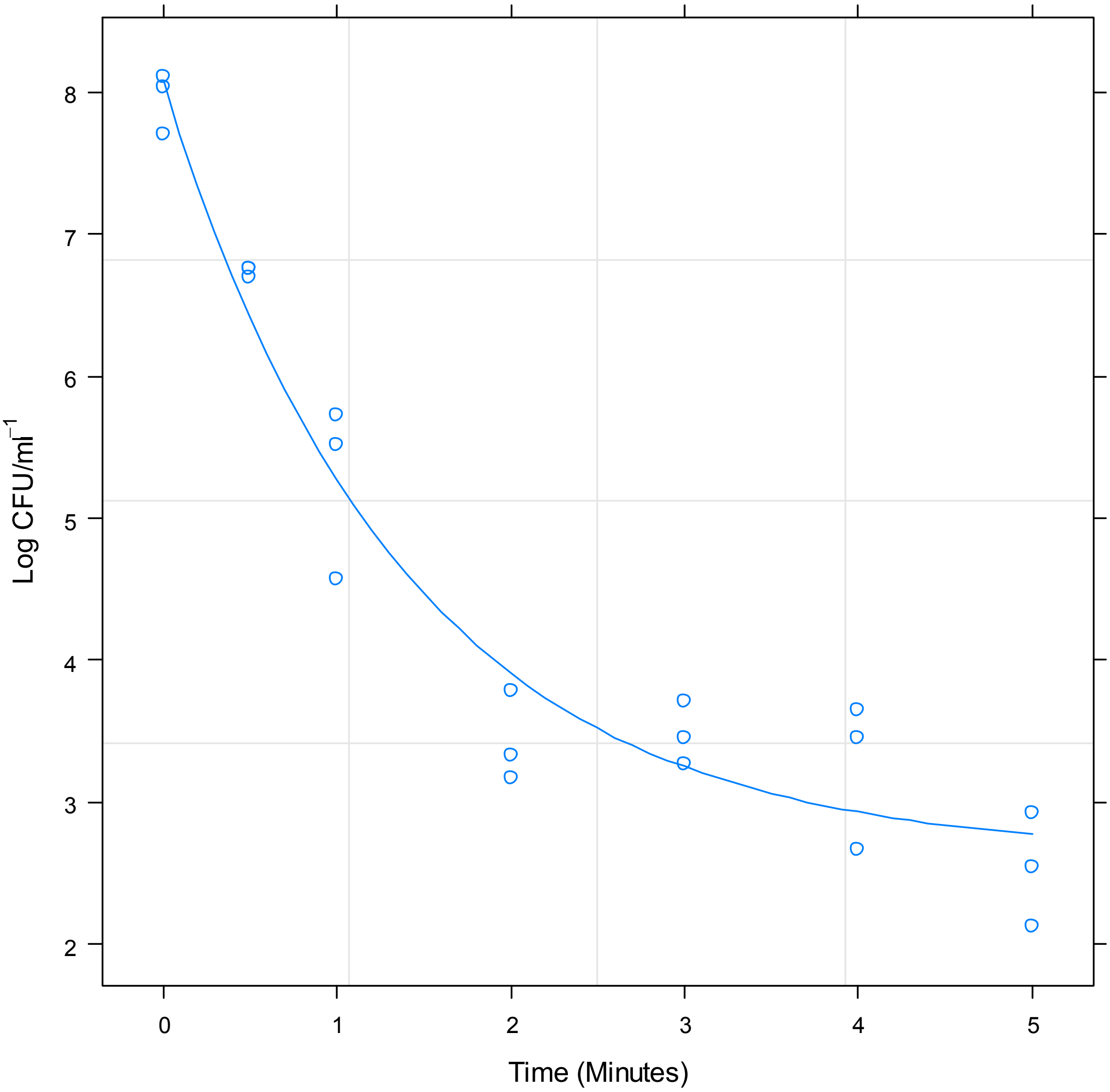

Figure 191. Predicted response curve using an asymptotic regression model for strain 12628 (ST-1773, CC-828) at pH 7.5 following heating at 64°C.

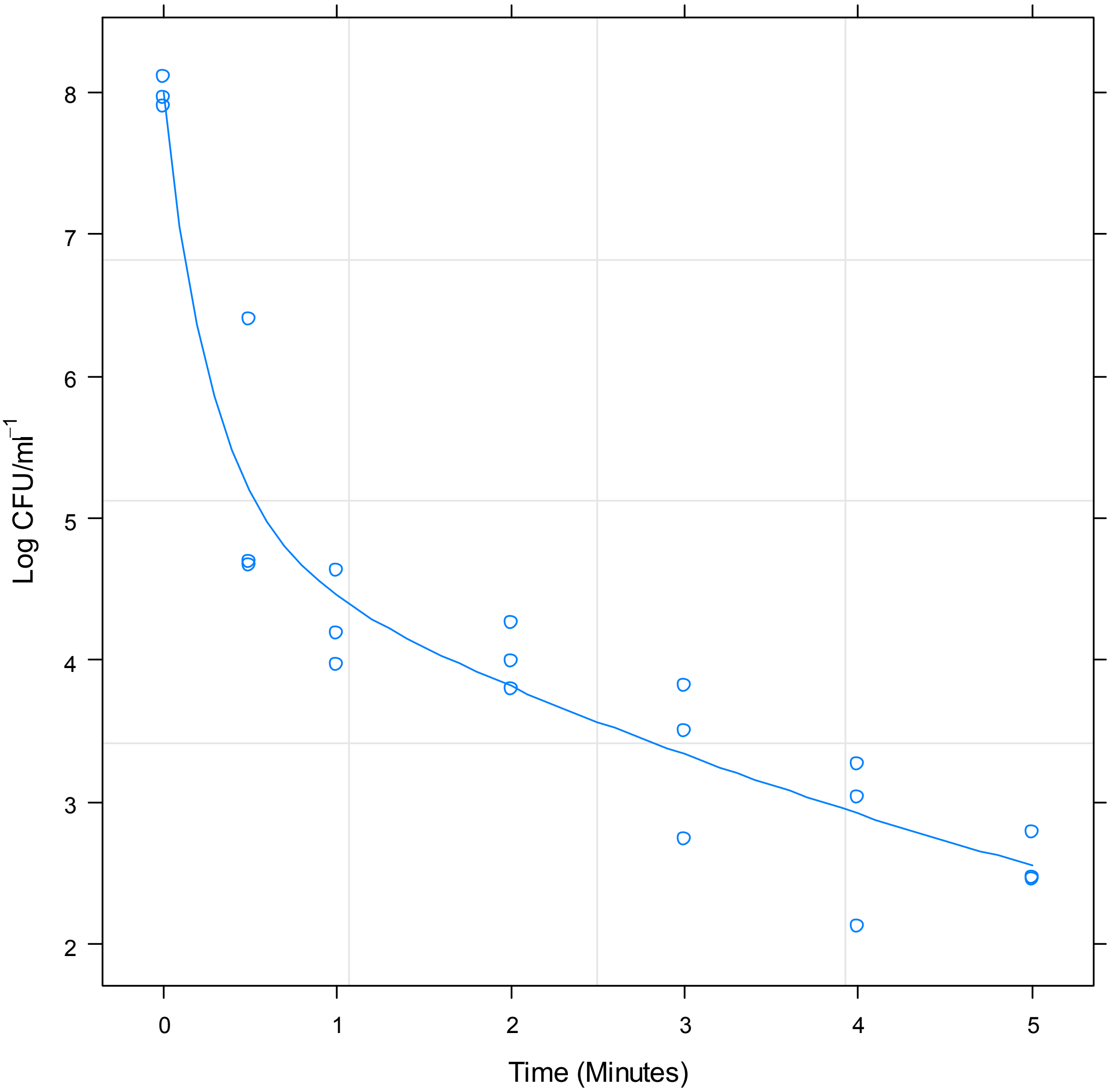

Figure 192. Predicted response curve using a biexponential regression model for strain 12628 (ST-1773, CC-828) at pH 8.5 following heating at 64°C.

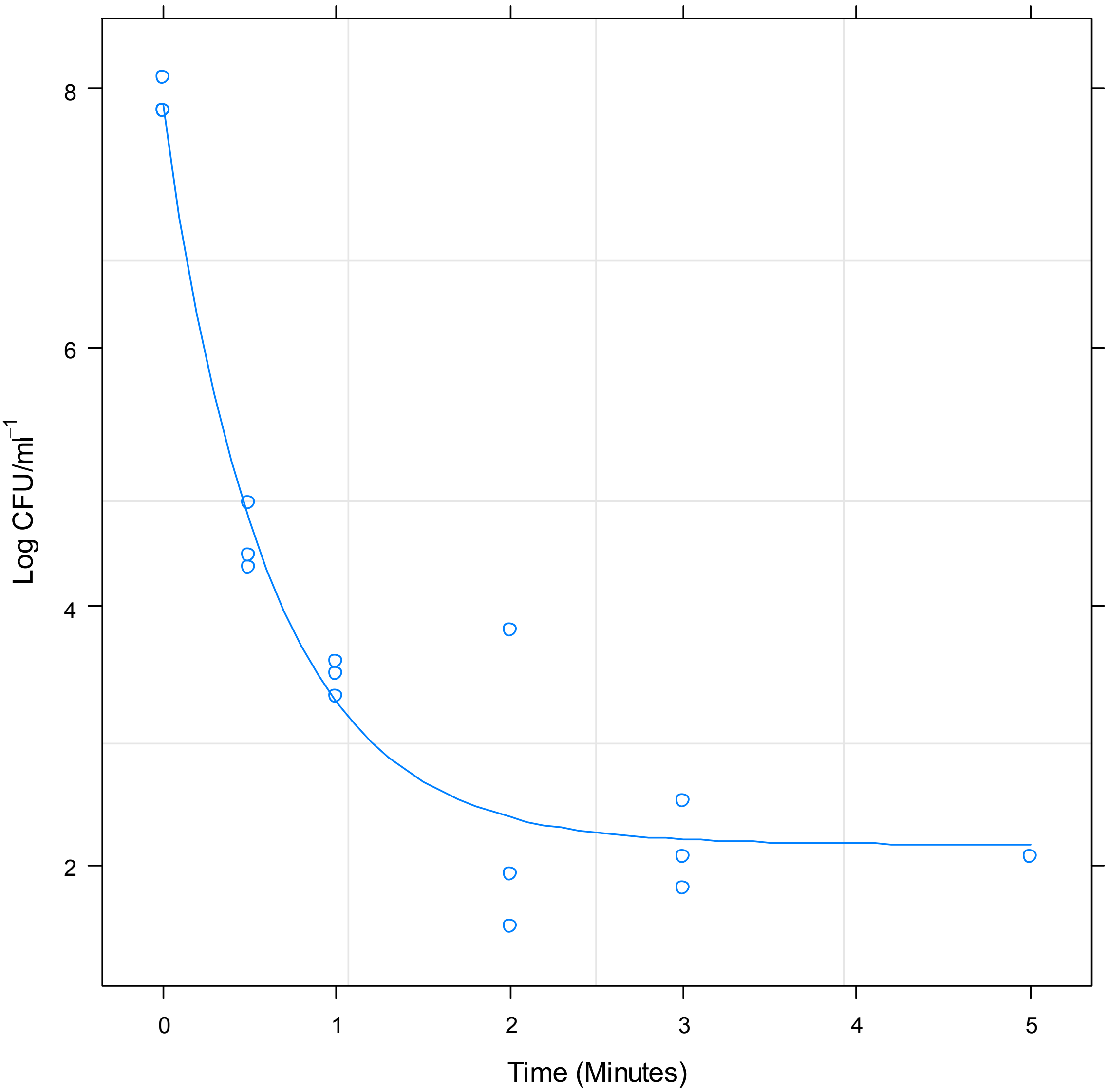

Figure 193. Predicted response curve using an asymptotic regression model for strain 12662 (ST-257, CC-257) at pH 4.5 following heating at 64°C.

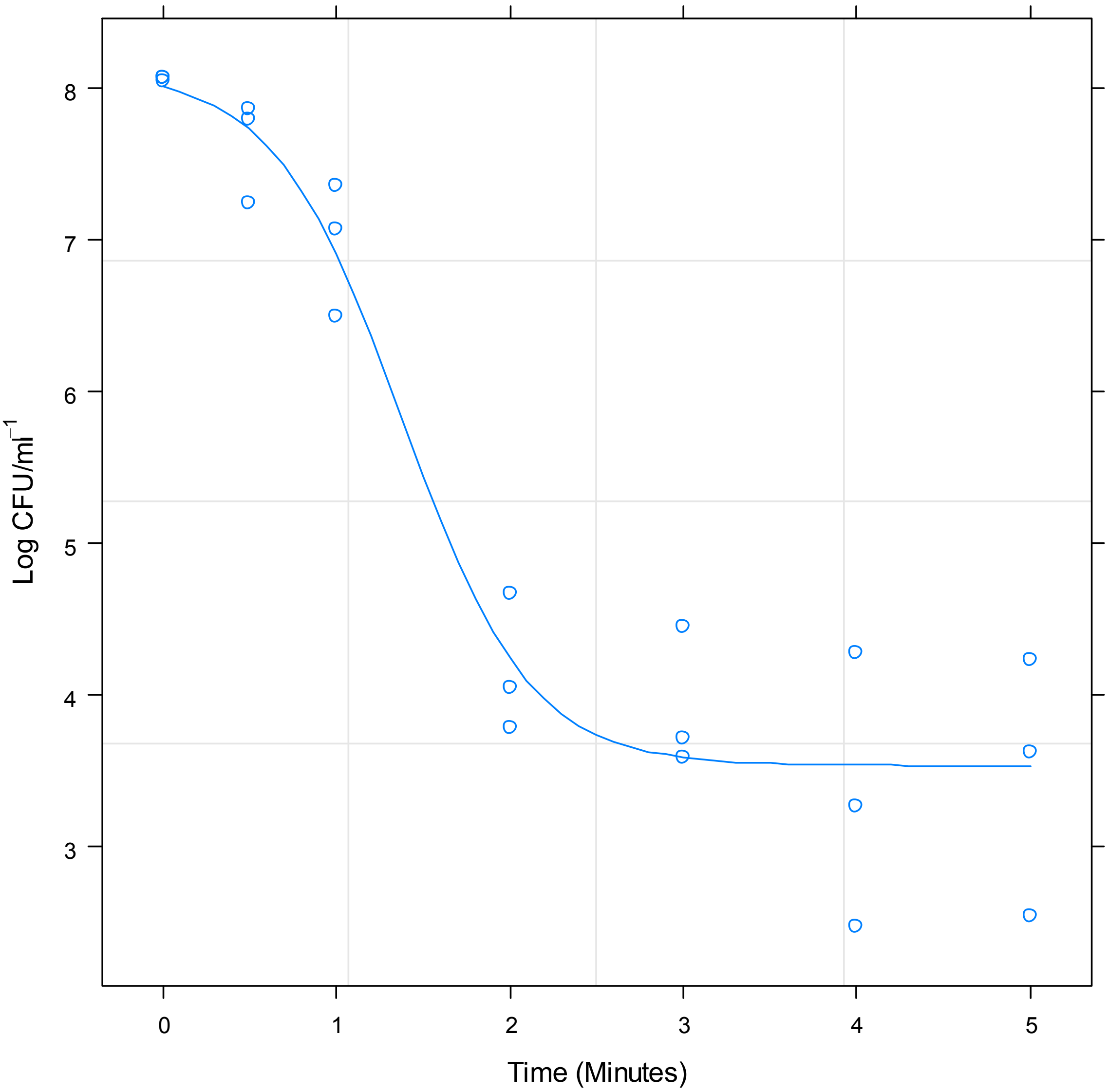

Figure 194. Predicted response curve using a four-parameter logistic regression model for strain 12662 (ST-257, CC-257) at pH 5.5 following heating at 64^{o}C.

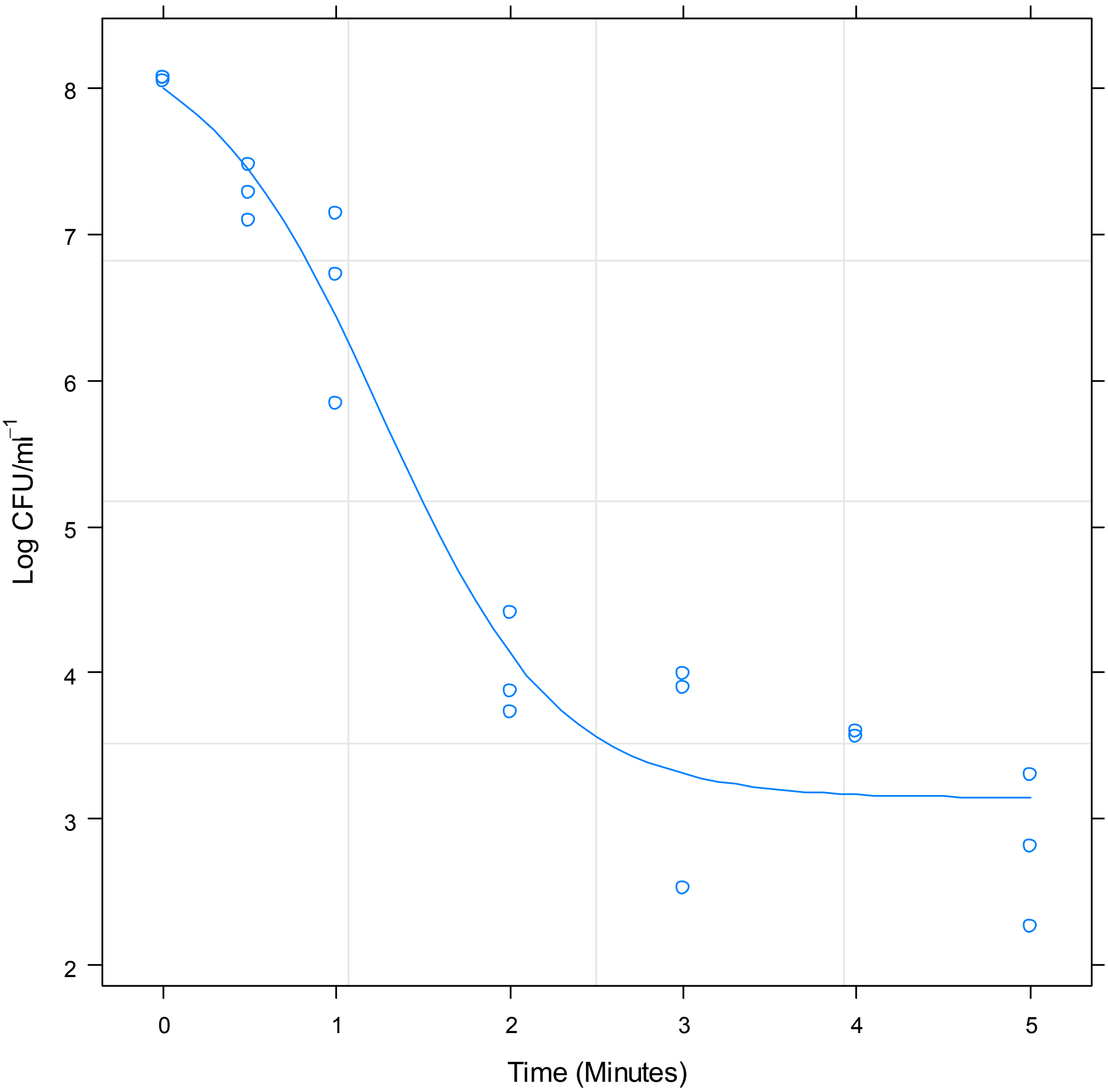

Figure 195. Predicted response curve using a four-parameter logistic regression model for strain 12662 (ST-257, CC-257) at pH 6.5 following heating at 64°C.

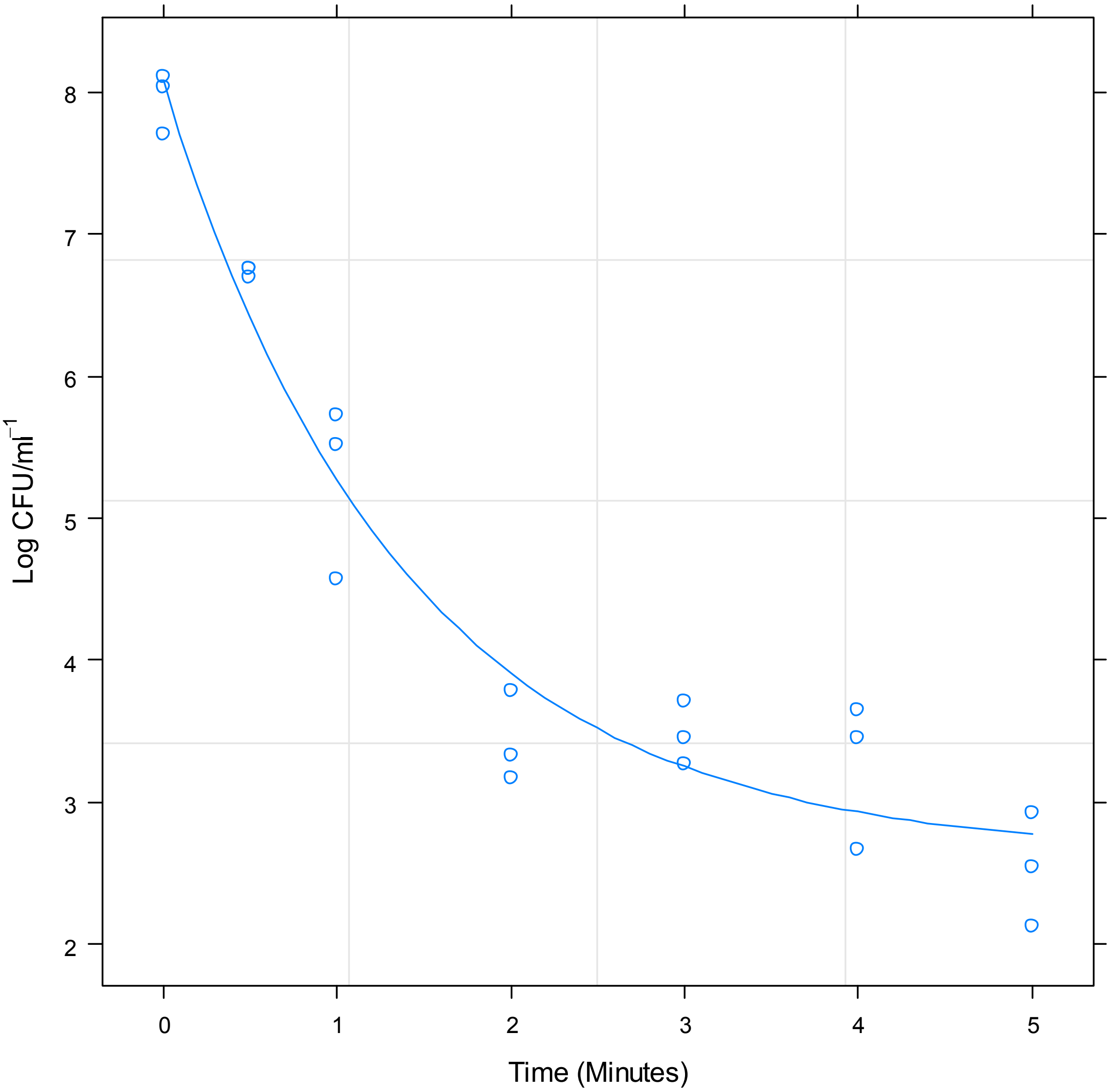

Figure 196. Predicted response curve using an asymptotic regression model for strain 12662 (ST-257, CC-257) at pH 7.5 following heating at 64°C.

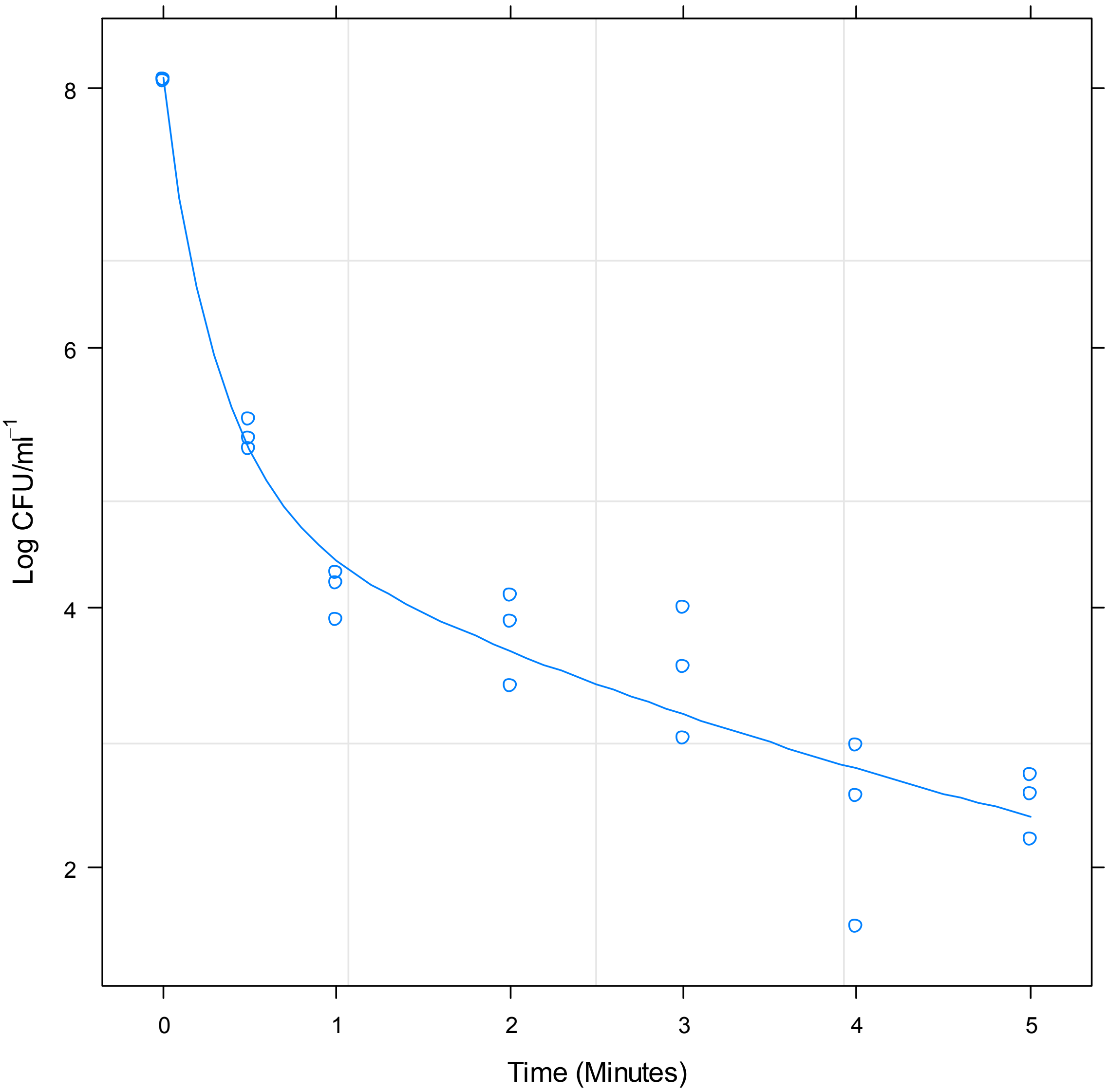

Figure 197. Predicted response curve using a biexponential regression model following for strain 12662 (ST-257, CC-257) at pH 8.5 following heating at 64^{o}C.

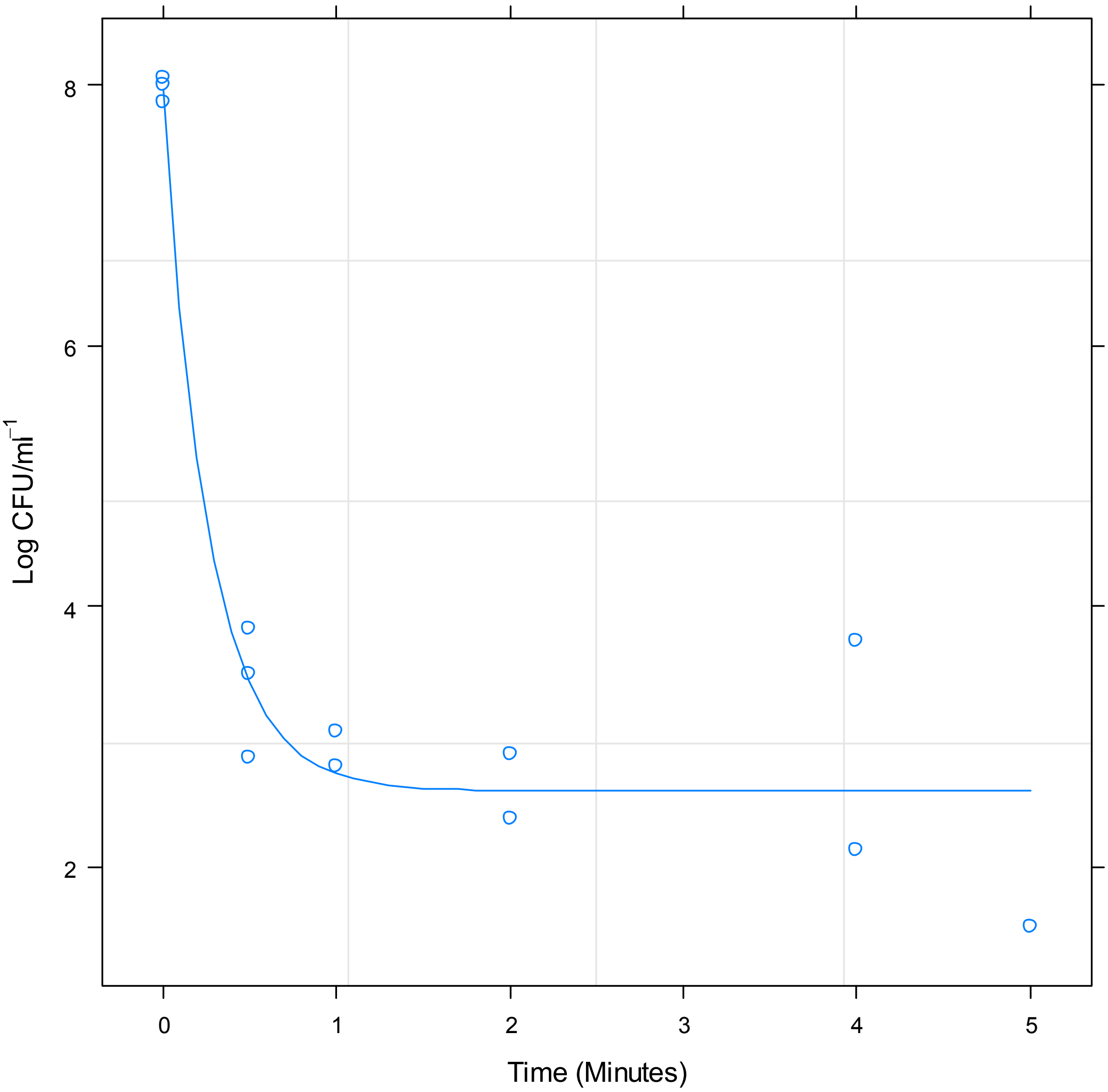

Figure 198. Predicted response curve using an asymptotic regression model for strain 13126 (ST-21, CC-21) at pH 4.5 following heating at 64°C.

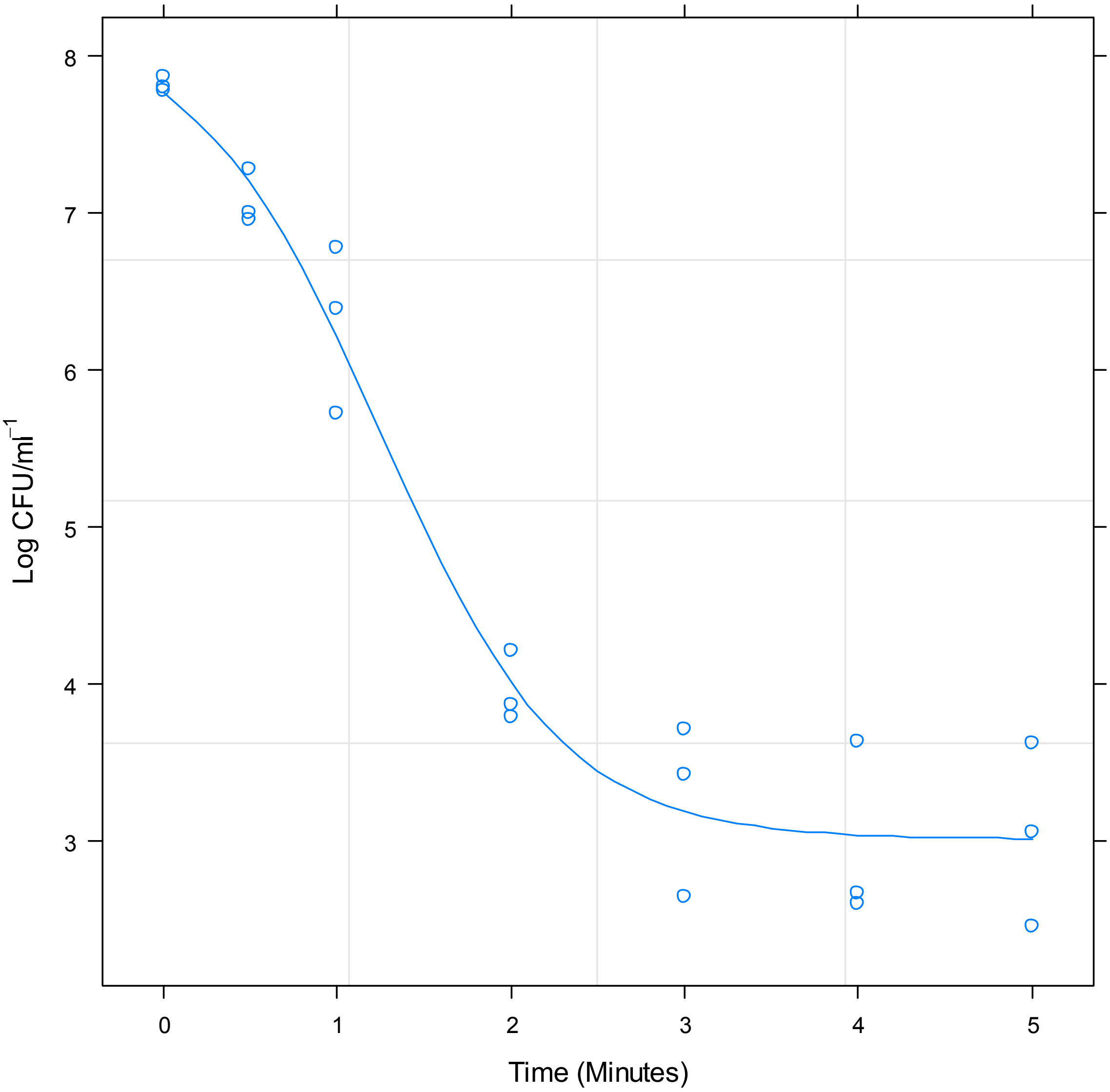

Figure 199. Predicted response curve using a four-parameter logistic regression model for strain 13126 (ST-21, CC-21) at pH 5.5 following heating at 64°C.

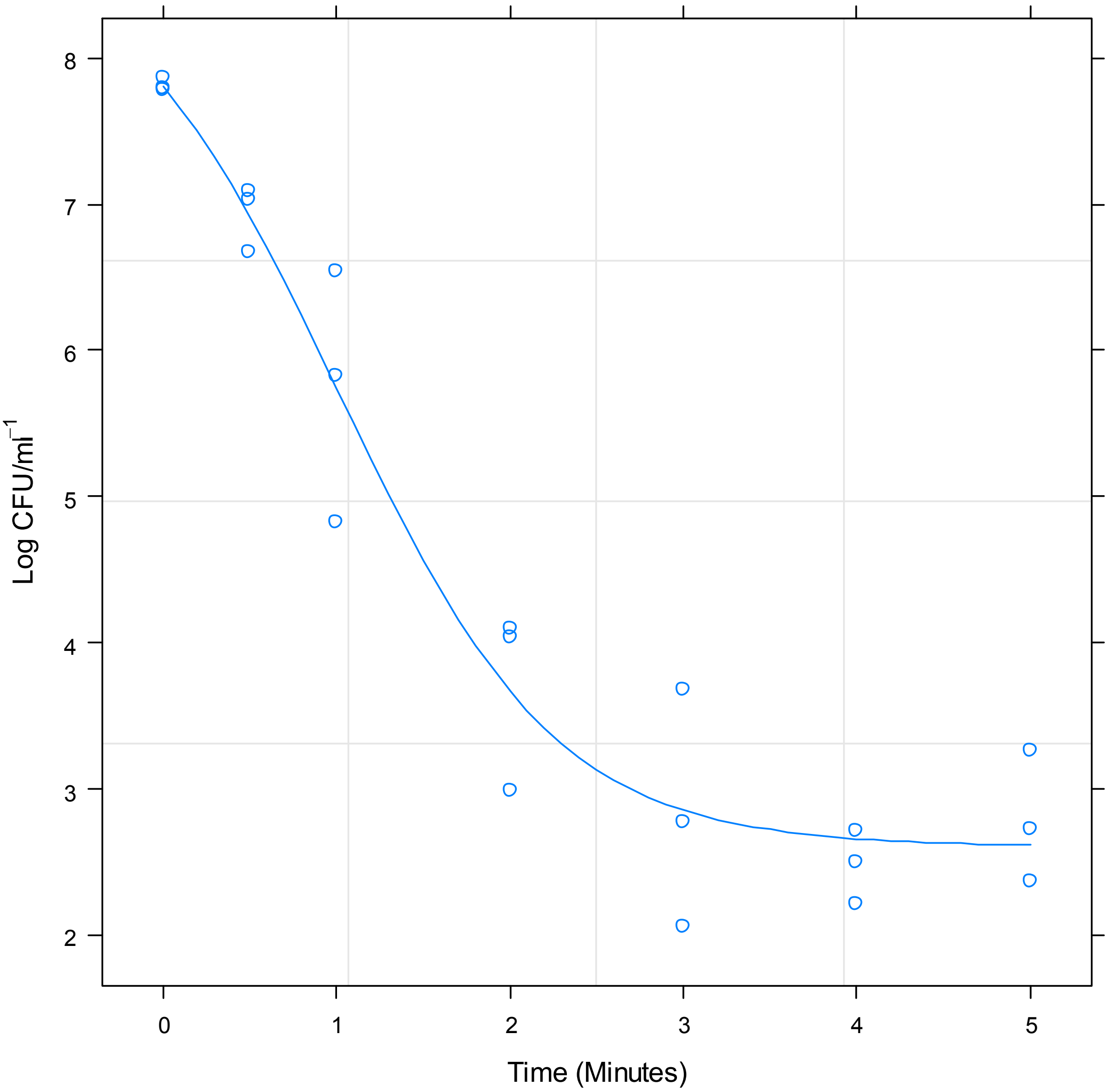

Figure 200. Predicted response curve using a four-parameter logistic regression model for strain 13126 (ST-21, CC-21) at pH 6.5 following heating at 64^{o}C.

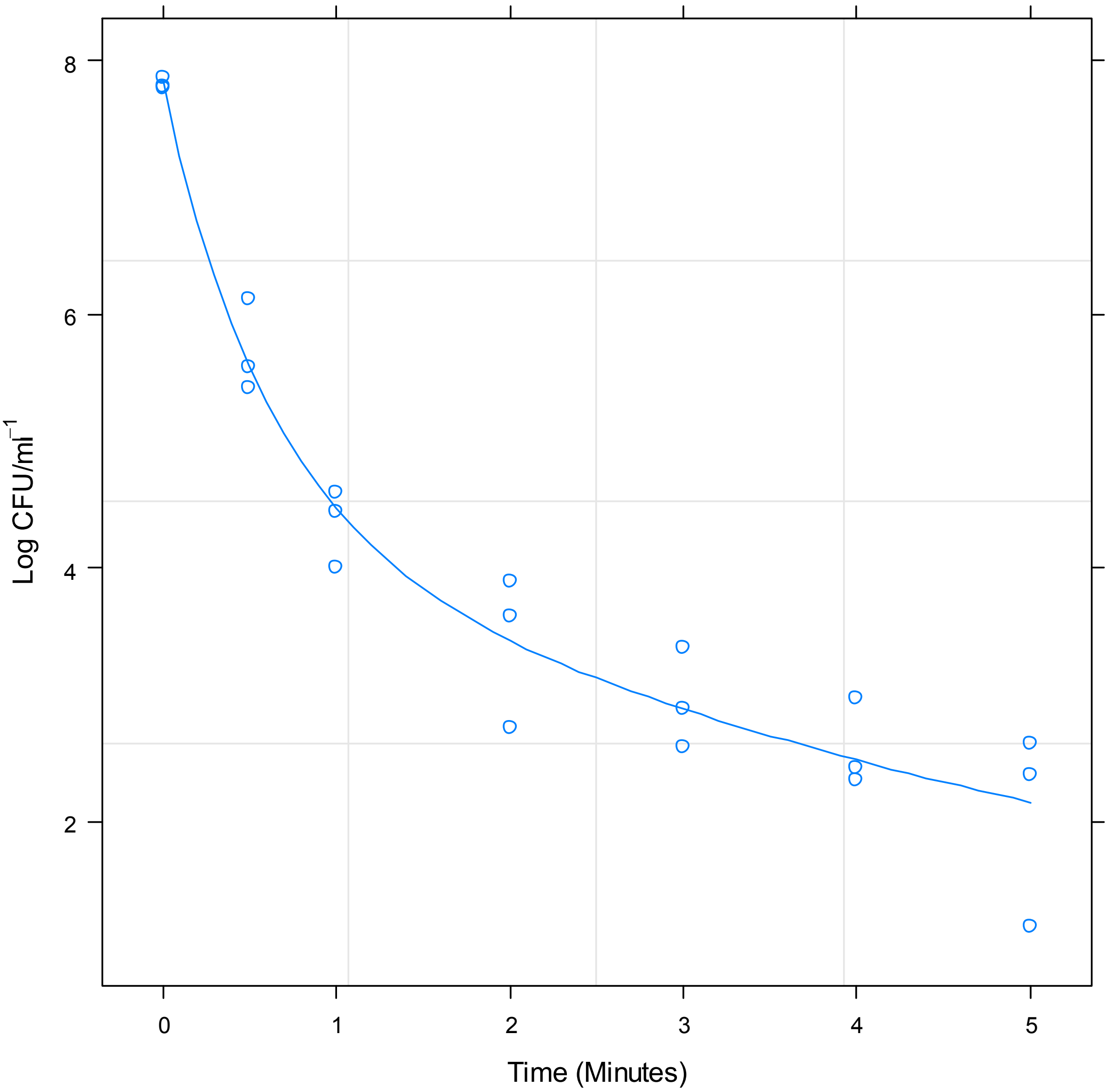

Figure 201. Predicted response curve using a biexponential regression model for strain 13126 (ST-21, CC-21) at pH 7.5 following heating at 64°C.

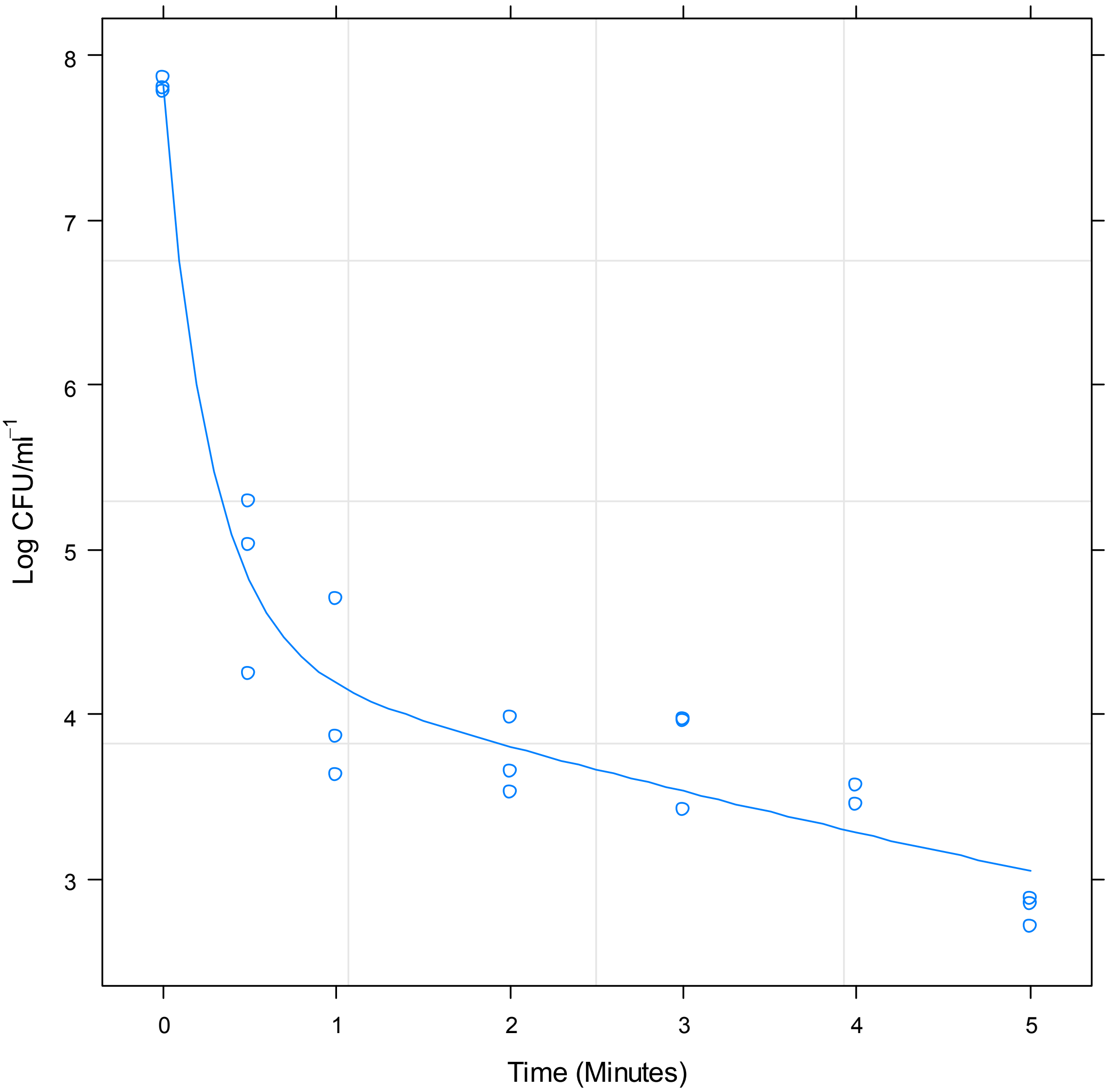

Figure 202. Predicted response curve using a biexponential regression model for strain 13126 (ST-21, CC-21) at pH 8.5 following heating at 64°C.

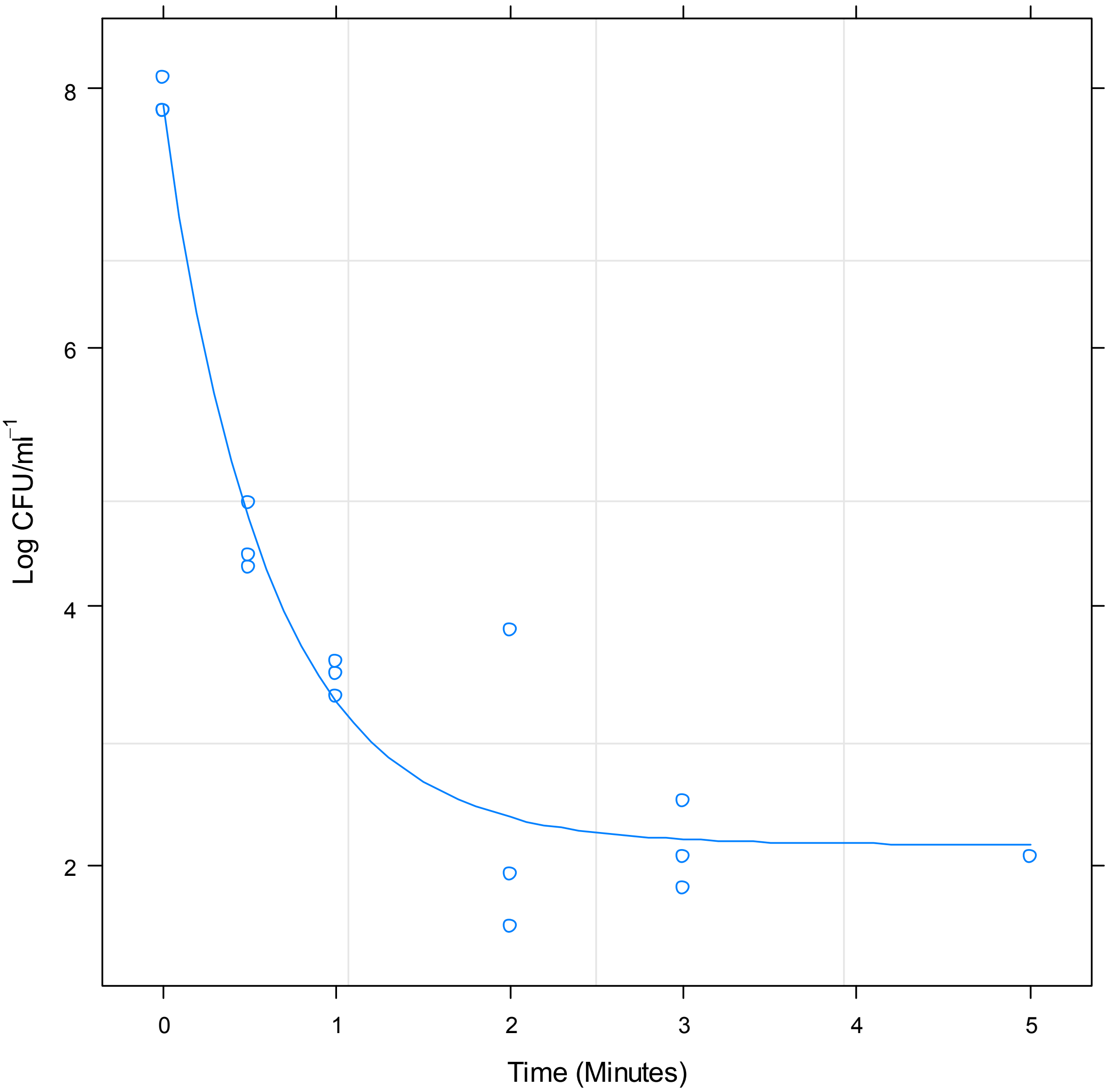

Figure 203. Predicted response curve using an asymptotic regression model for strain 13136 (ST-45, CC-45) at pH 4.5 following heating at 64°C.

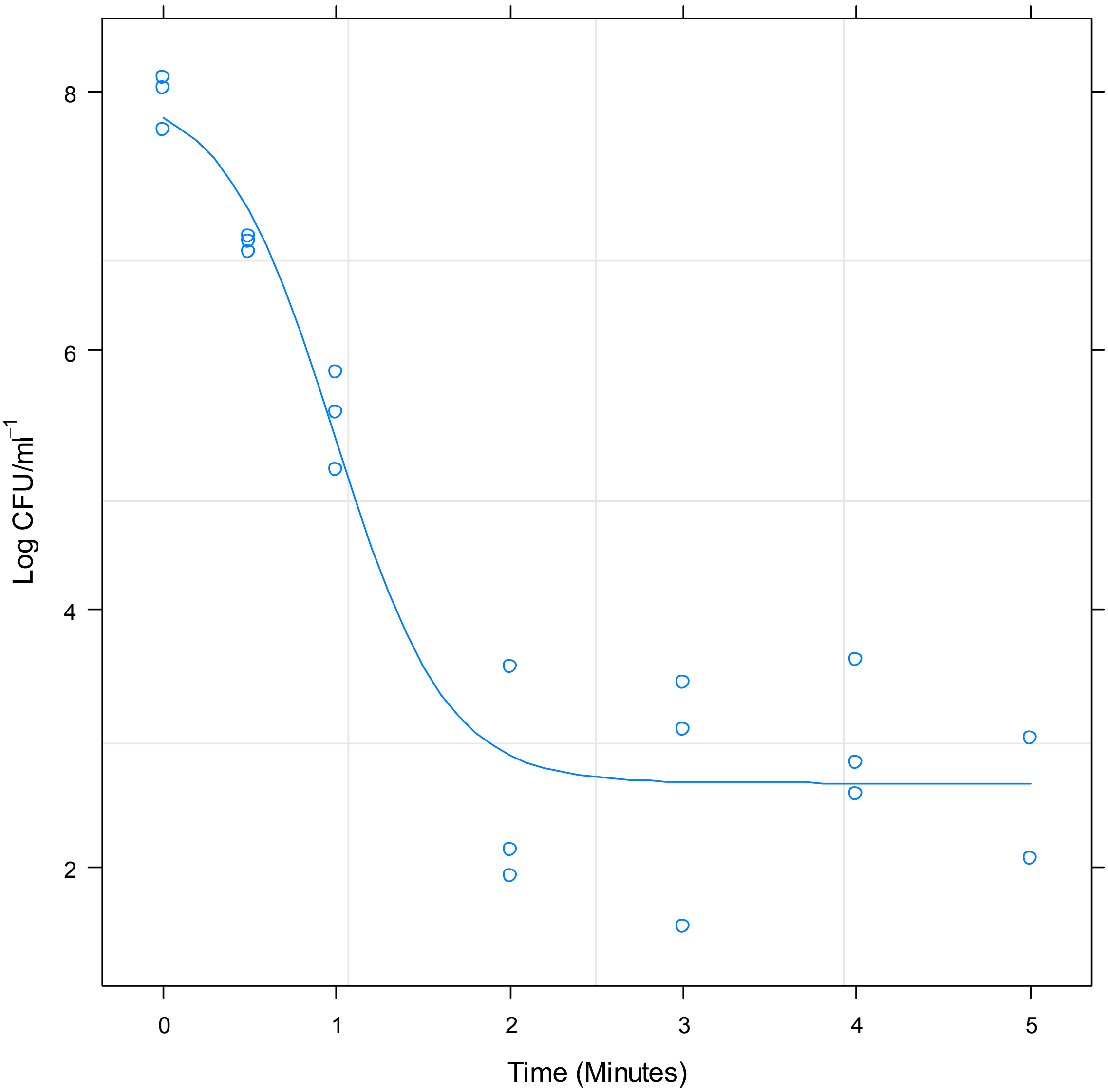

Figure 204. Predicted response curve using a four-parameter logistic regression model for strain 13136 (ST-45, CC-45) at pH 5.5 following heating at 64°C.

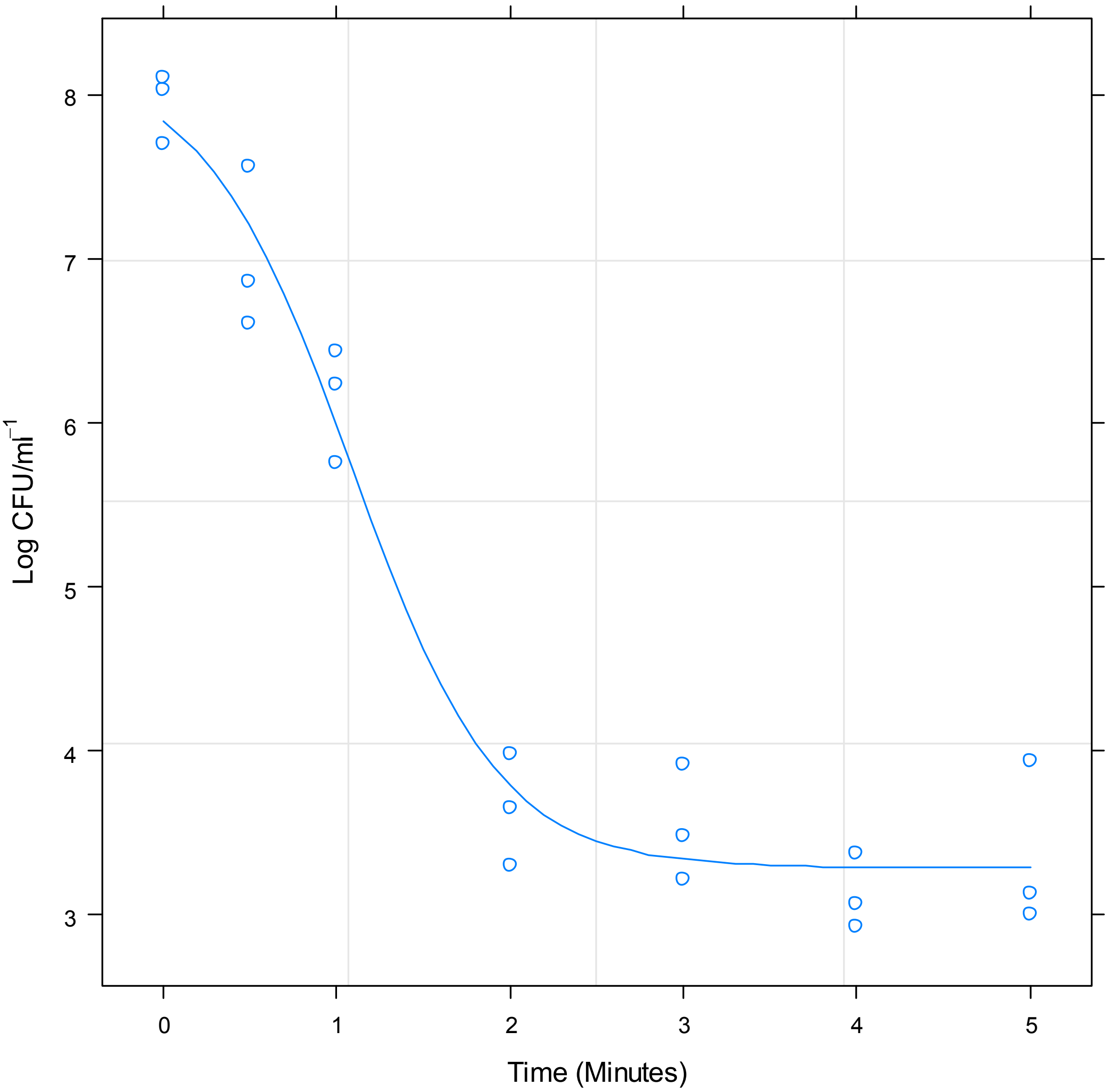

Figure 205. Predicted response curve using a four-parameter logistic regression model for strain 13136 (ST-45, CC-45) at pH 6.5 following heating at 64^{o}C.

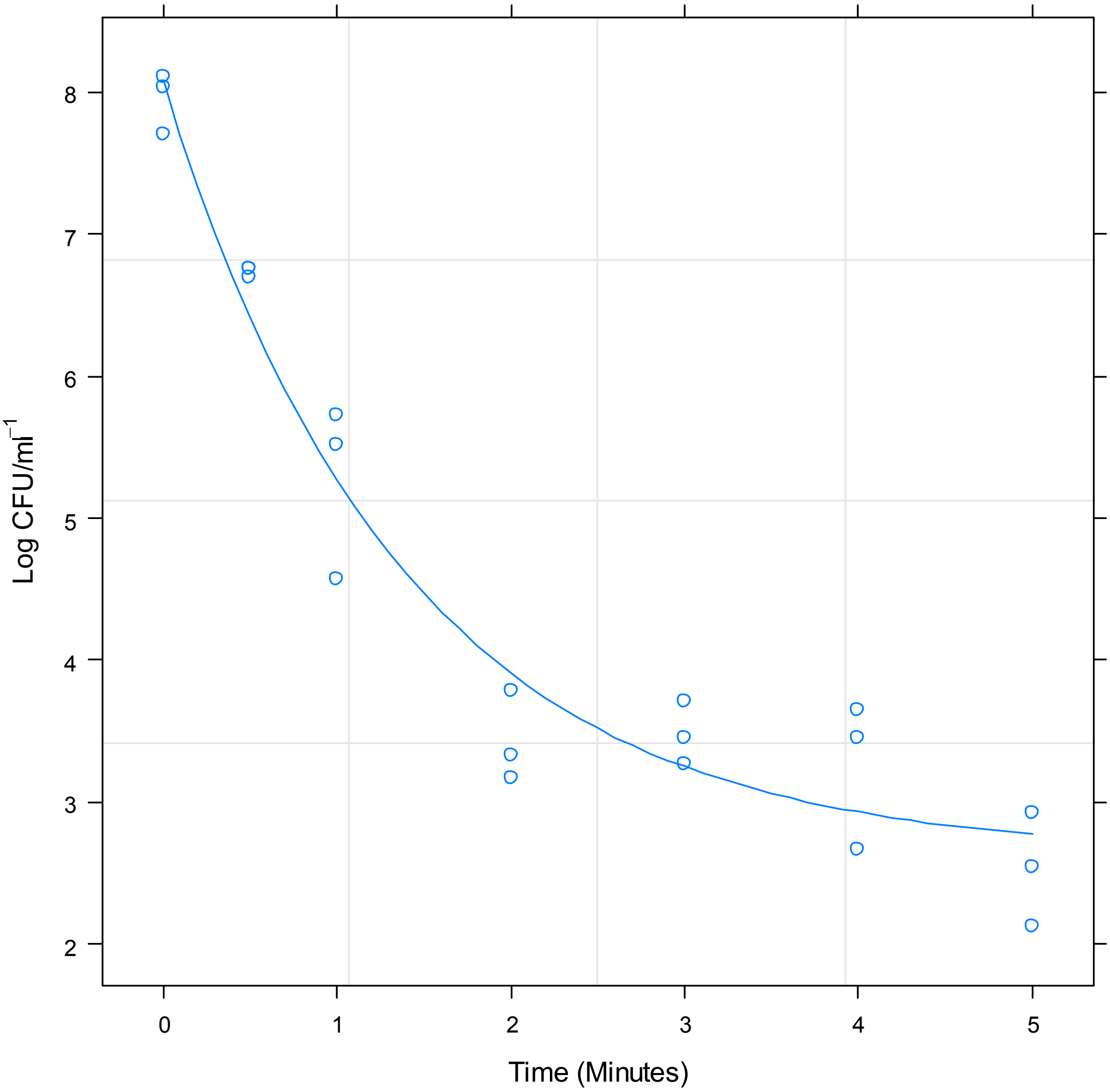

Figure 206. Predicted response curve using an asymptotic regression model for strain 13136 (ST-45, CC-45) at pH 7.5 following heating at 64°C.

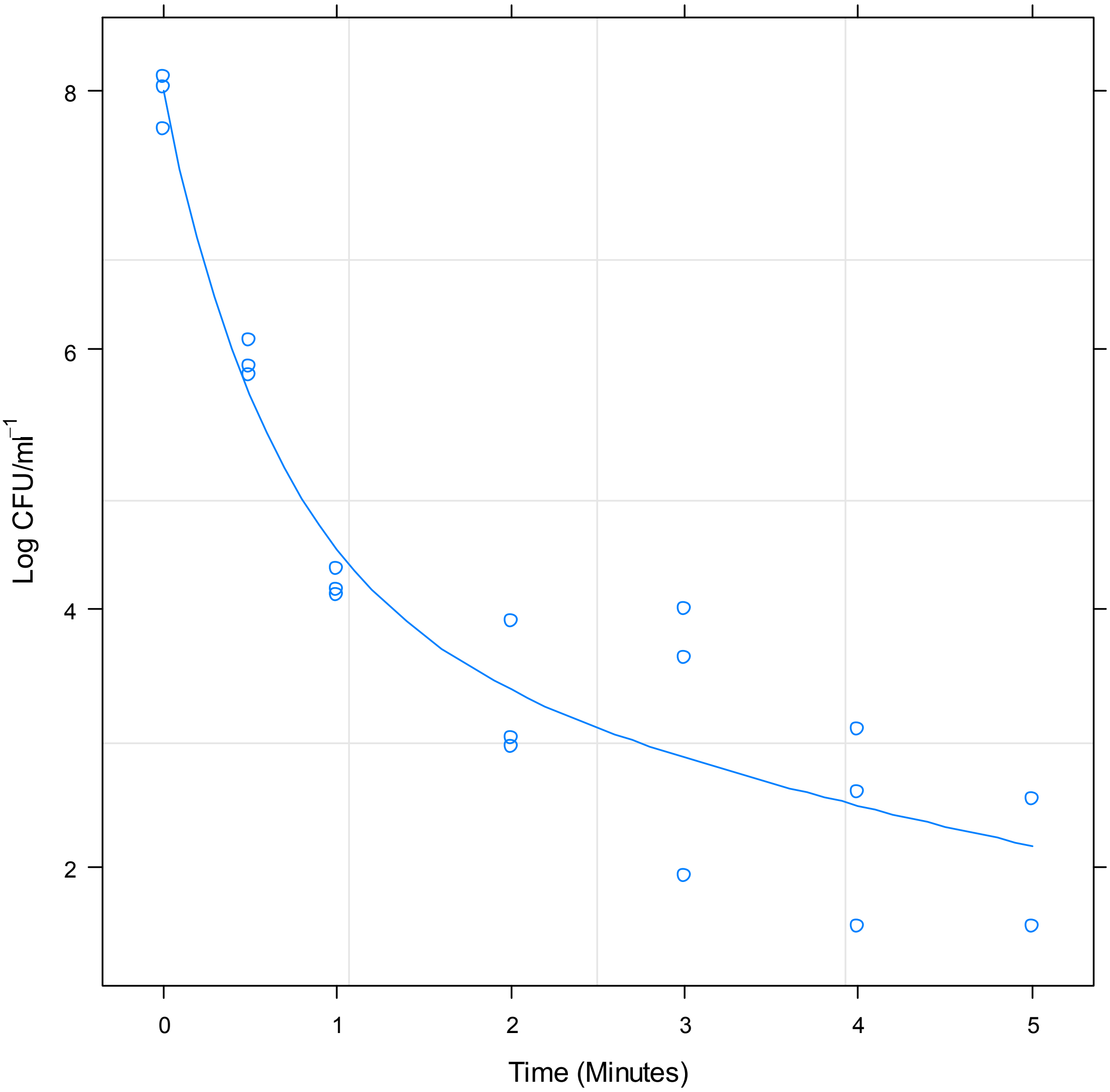

Figure 207. Predicted response curve using a biexponential regression model for strain 13136 (ST-45, CC-45) at pH 8.5 following heating at 64°C.

1.8.28 pH and Time-Temperature Simulations: 64°C

Mixed Weibull Distribution Model Predicted Response Curves:

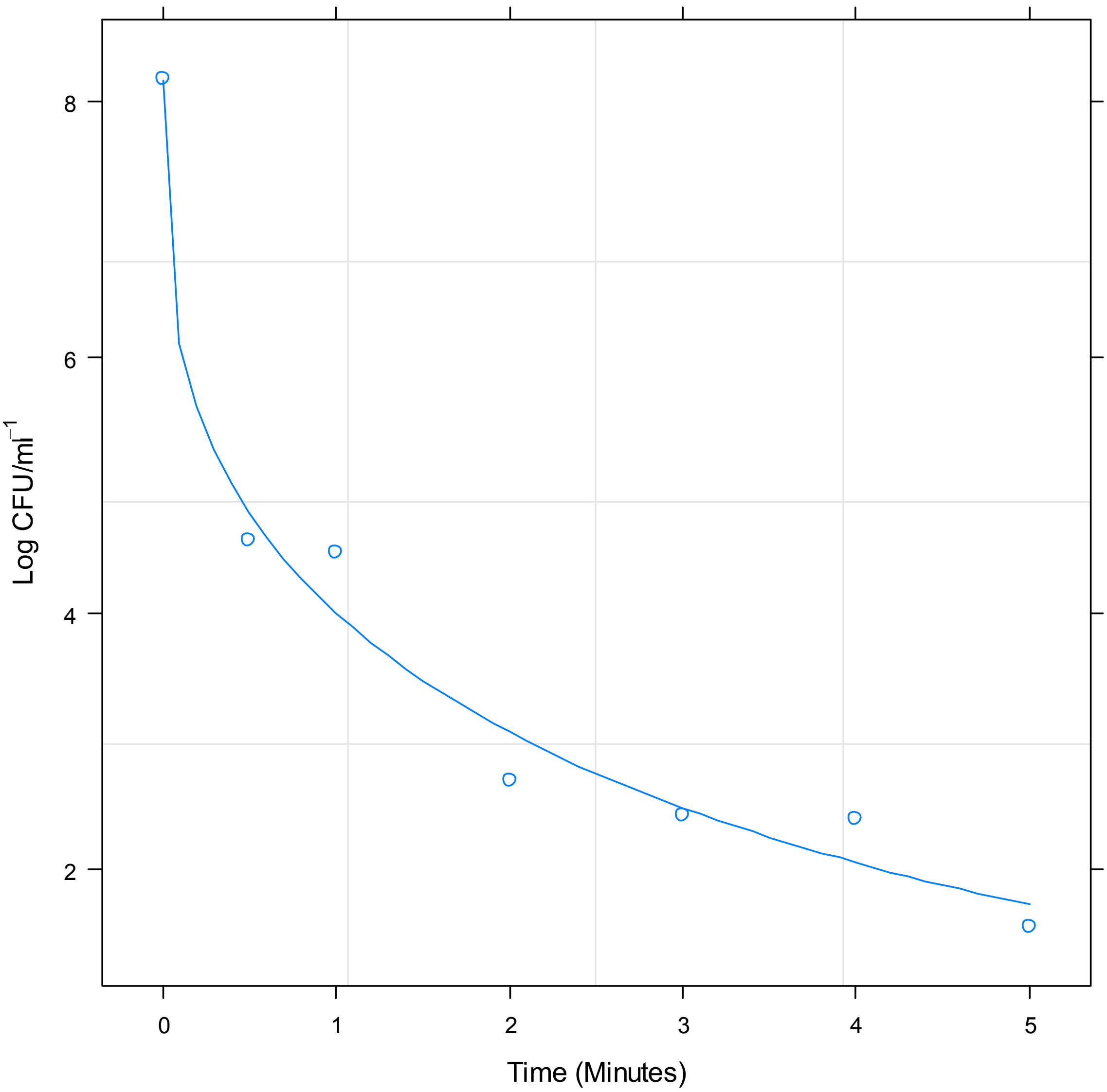

Figure 208. Predicted response curve using a mixed Weibull distribution model of strain 12628 (ST-1773, CC-828) at pH 4.5 following heating at 64°C.

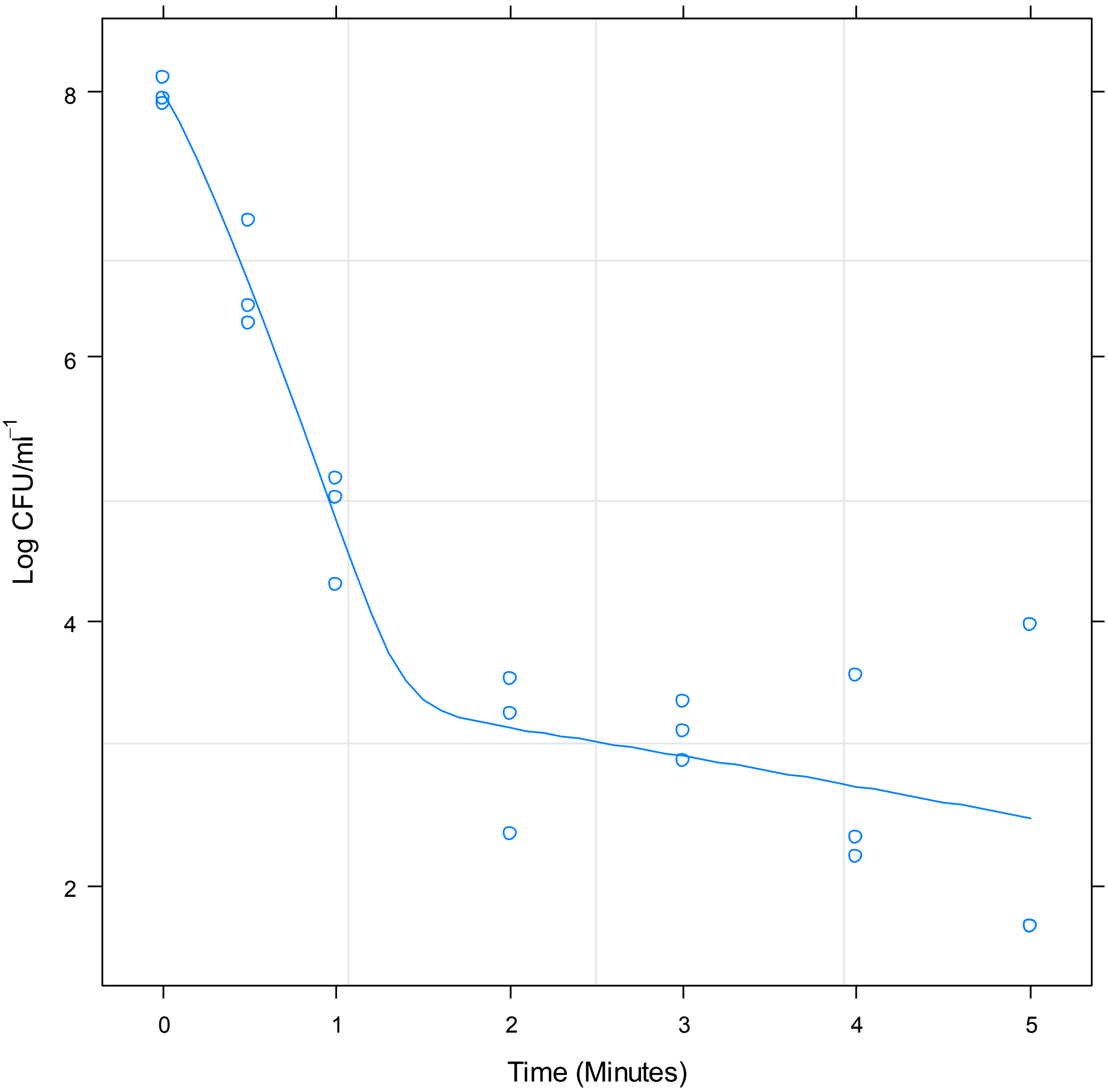

Figure 209. Predicted response curve using a mixed Weibull distribution model of strain 12628 (ST-1773, CC-828) at pH 5.5 following heating at 64°C.

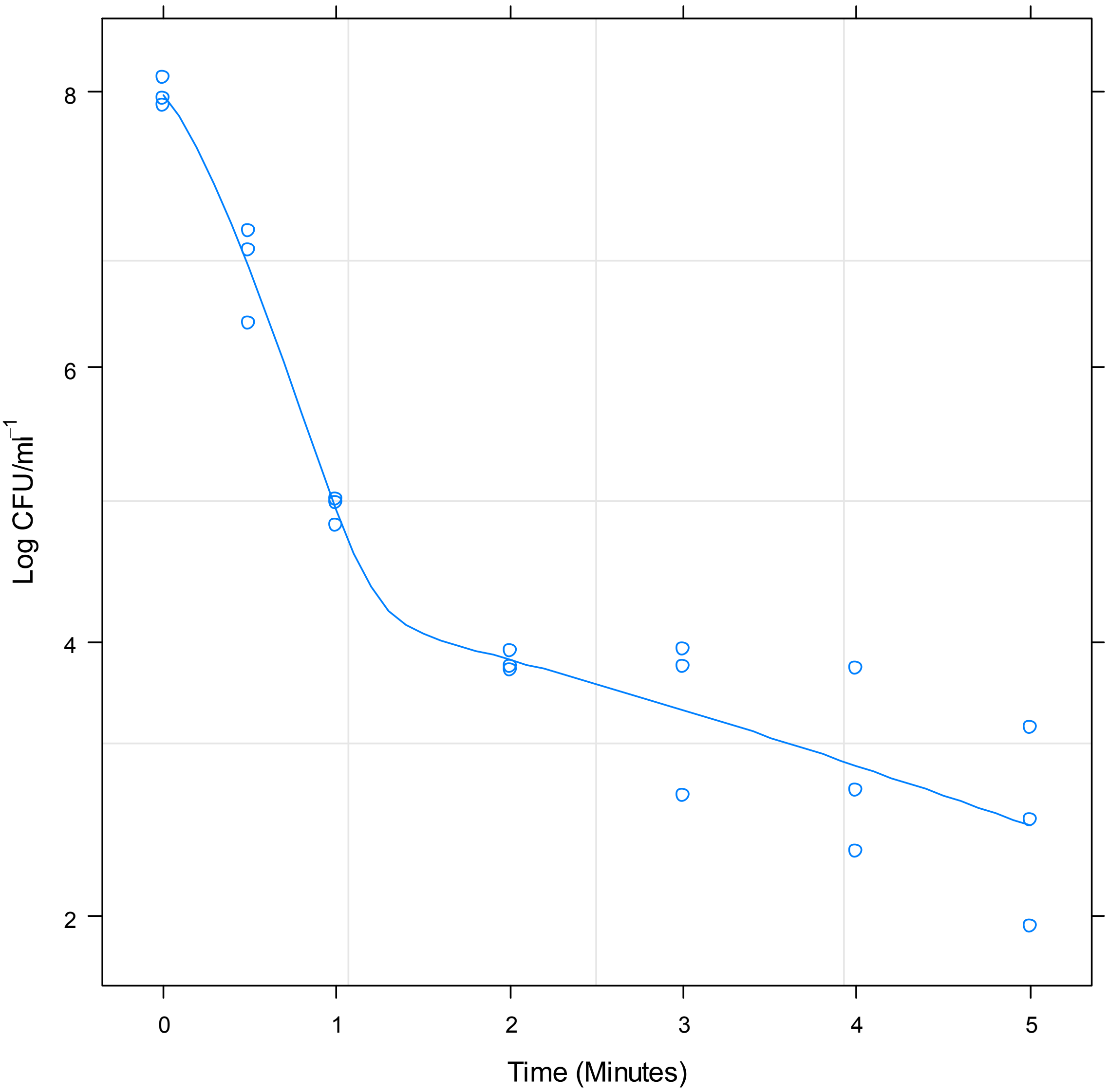

Figure 210. Predicted response curve using a mixed Weibull distribution model of strain 12628 (ST-1773, CC-828) at pH 6.5 following heating at 64^{o}C.

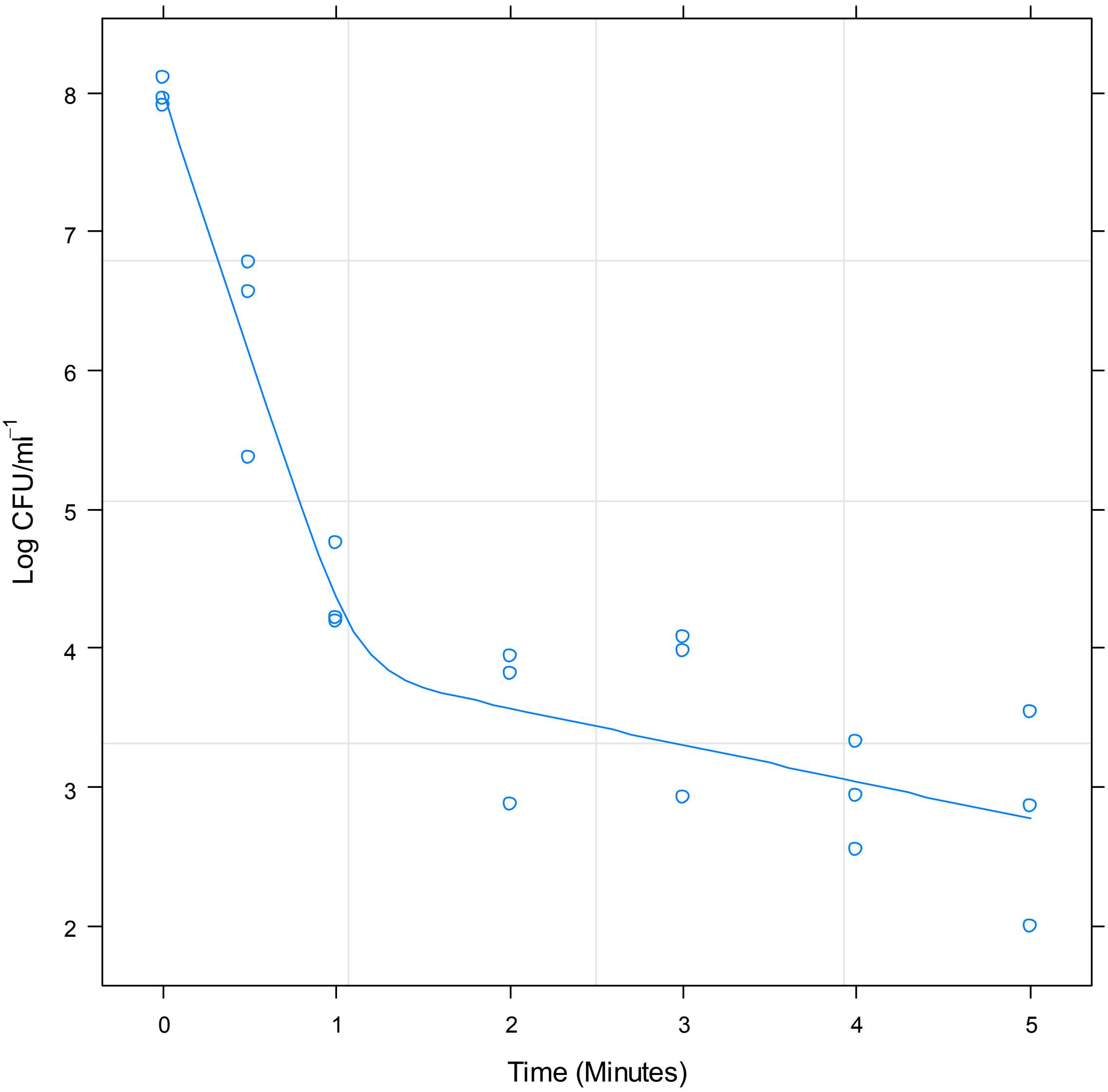

Figure 211. Predicted response curve using a mixed Weibull distribution model of strain 12628 (ST-1773, CC-828) at pH 7.5 following heating at 64°C.

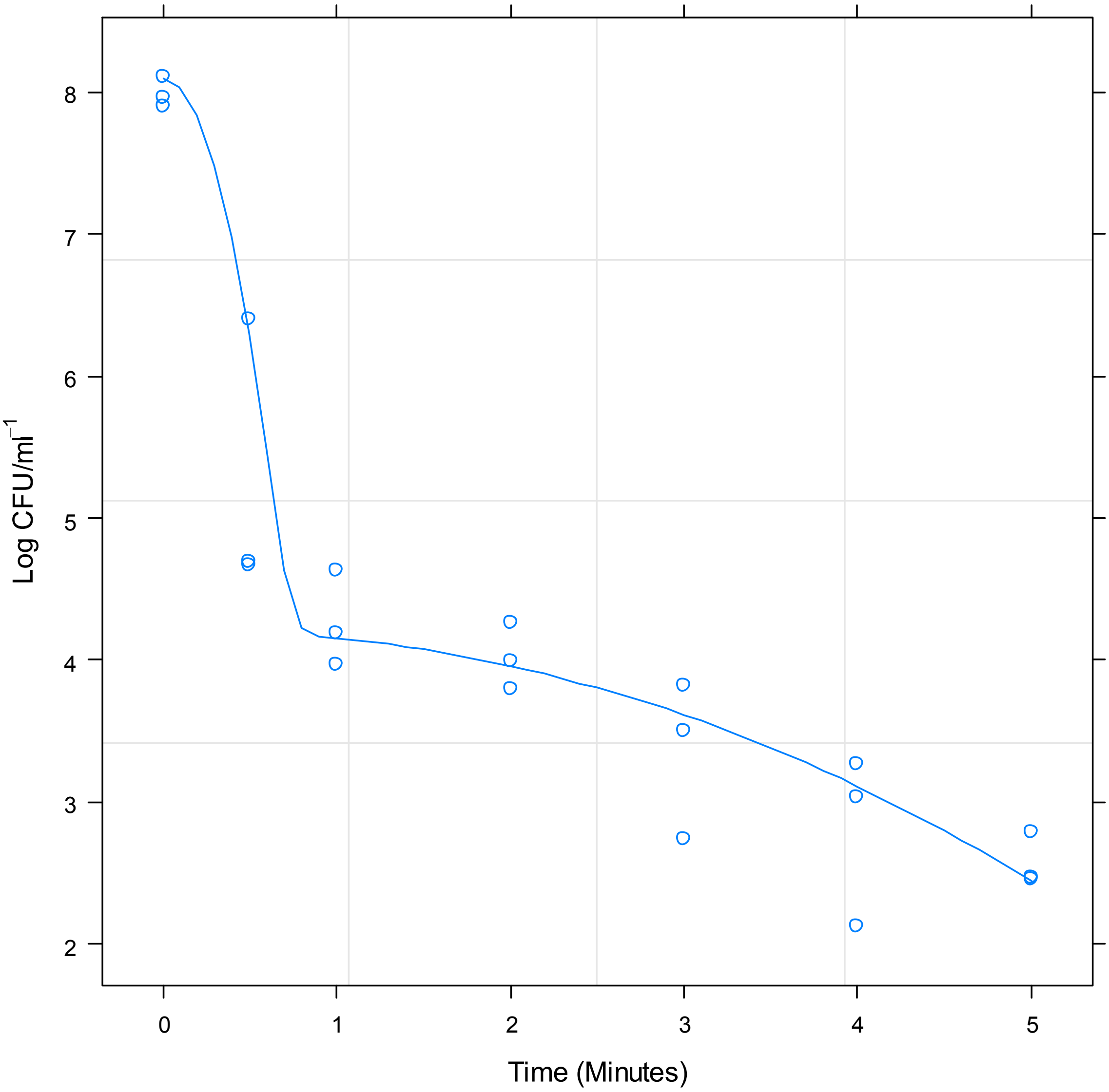

Figure 212. Predicted response curve using a mixed Weibull distribution model of strain 12628 (ST-1773, CC-828) at pH 8.5 following heating at 64°C.

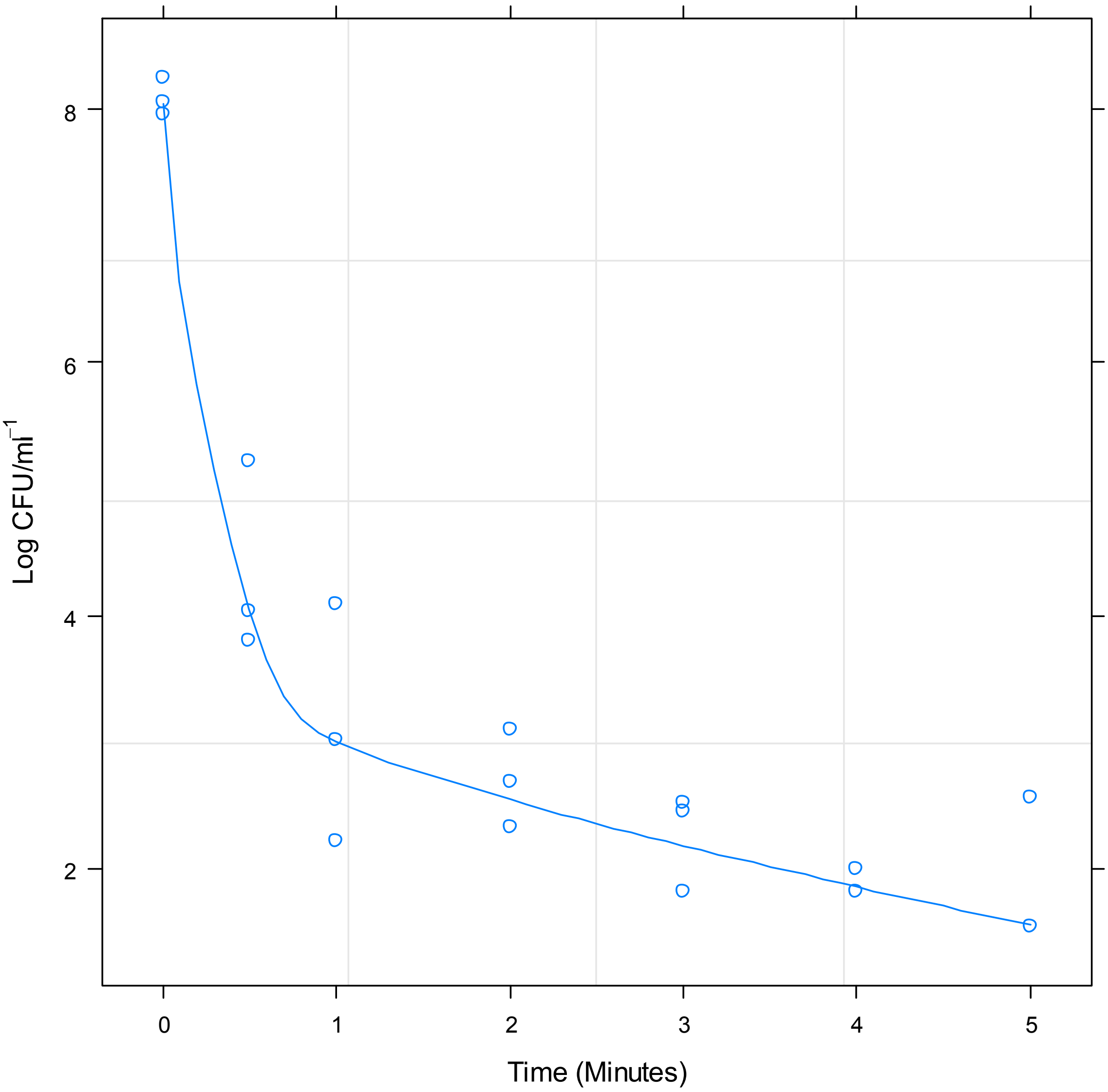

Figure 213. Predicted response curve using a mixed Weibull distribution model of strain 12662 (ST-257, CC-257) at pH 4.5 following heating at 64°C.

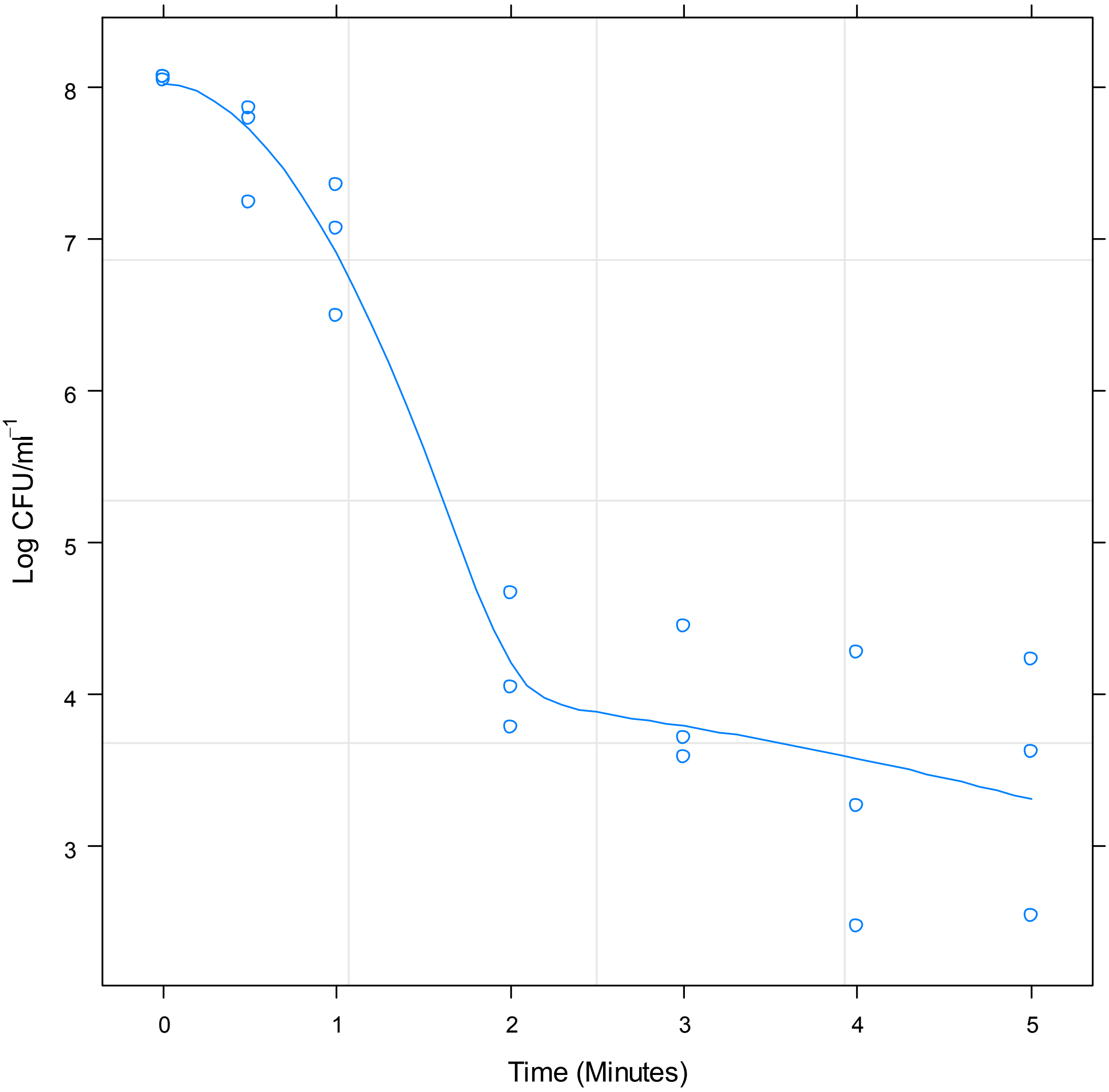

Figure 214. Predicted response curve using a mixed Weibull distribution model of strain 12662 (ST-257, CC-257) at pH 5.5 following heating at 64°C.

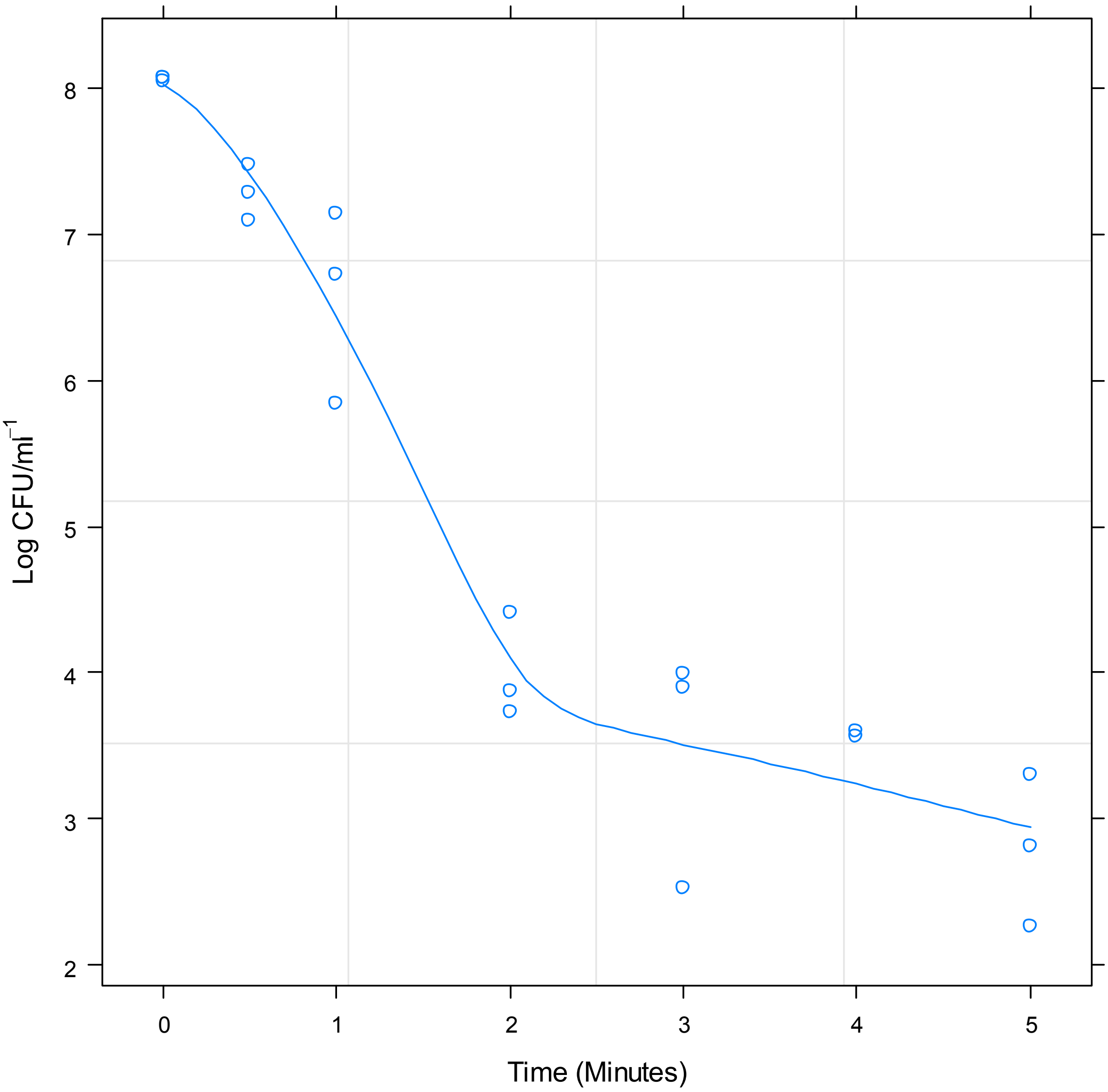

Figure 215. Predicted response curve using a mixed Weibull distribution model of strain 12662 (ST-257, CC-257) at pH 6.5 following heating at 64°C.

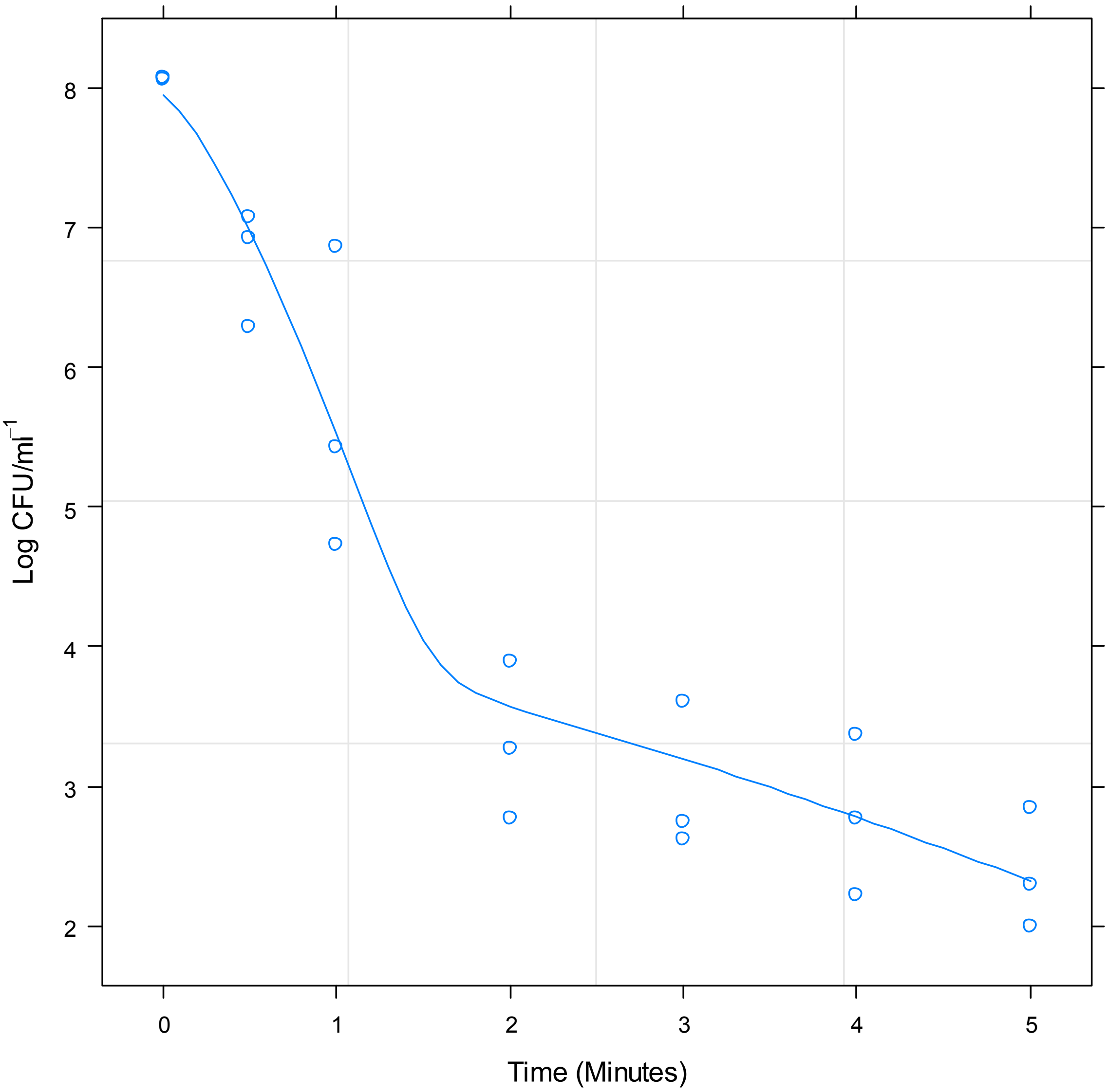

Figure 216. Predicted response curve using a mixed Weibull distribution model of strain 12662 (ST-257, CC-257) at pH 7.5 following heating at 64°C.

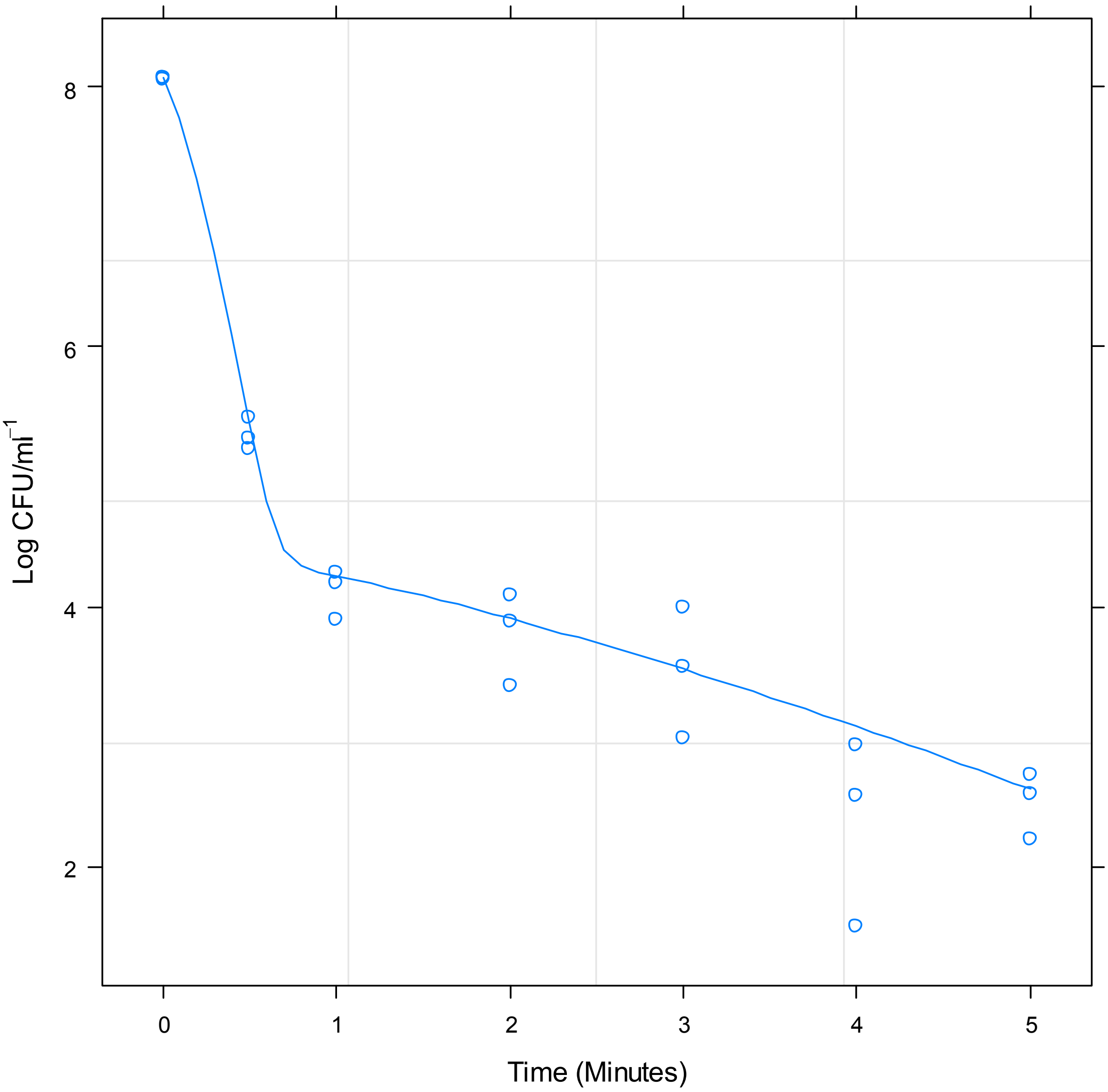

Figure 217. Predicted response curve using a mixed Weibull distribution model of strain 12662 (ST-257, CC-257) at pH 8.5 following heating at 64°C.

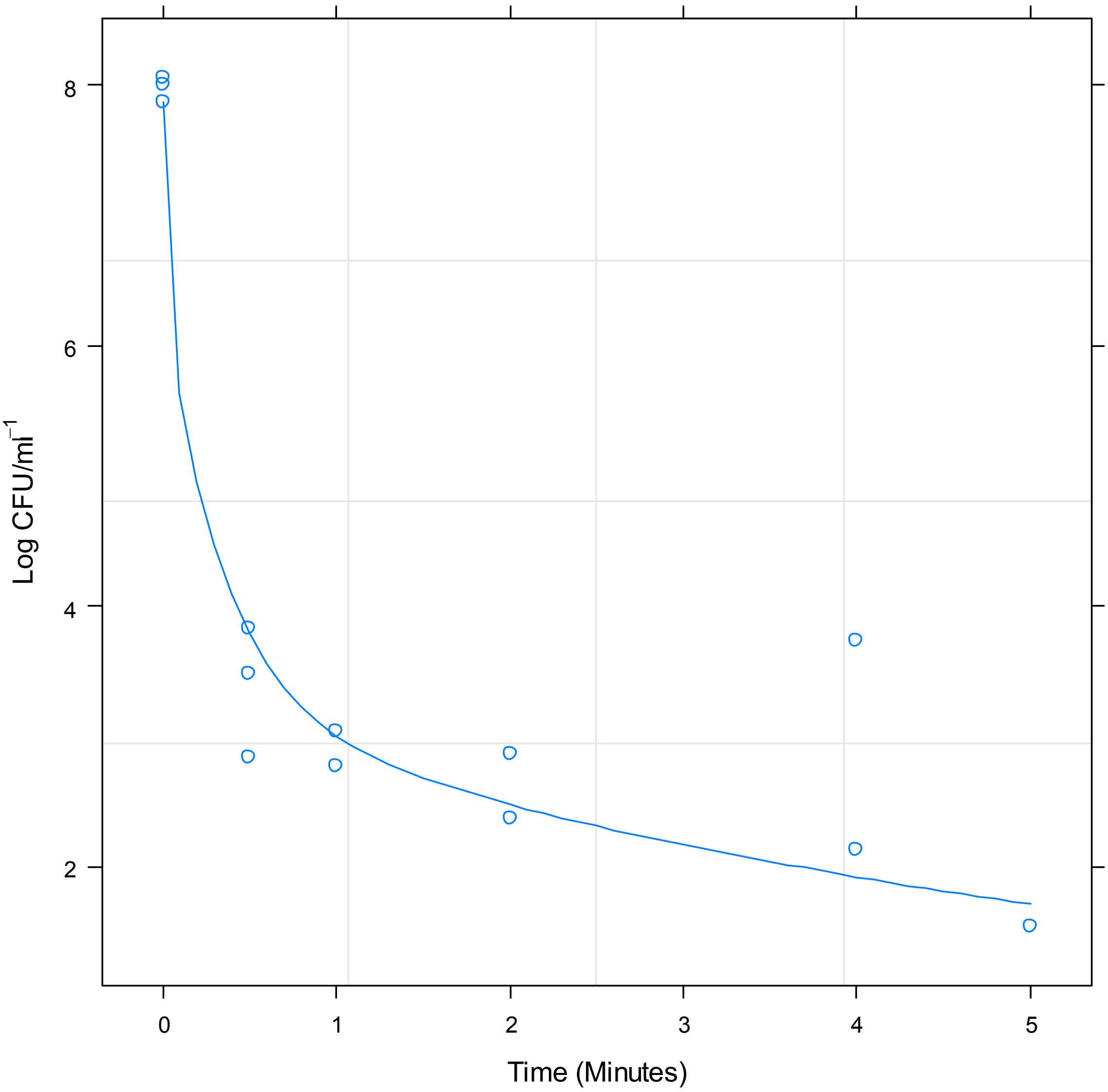

Figure 218. Predicted response curve using a mixed Weibull distribution model of strain 13126 (ST-21, CC-21) at pH 4.5 following heating at 64°C.

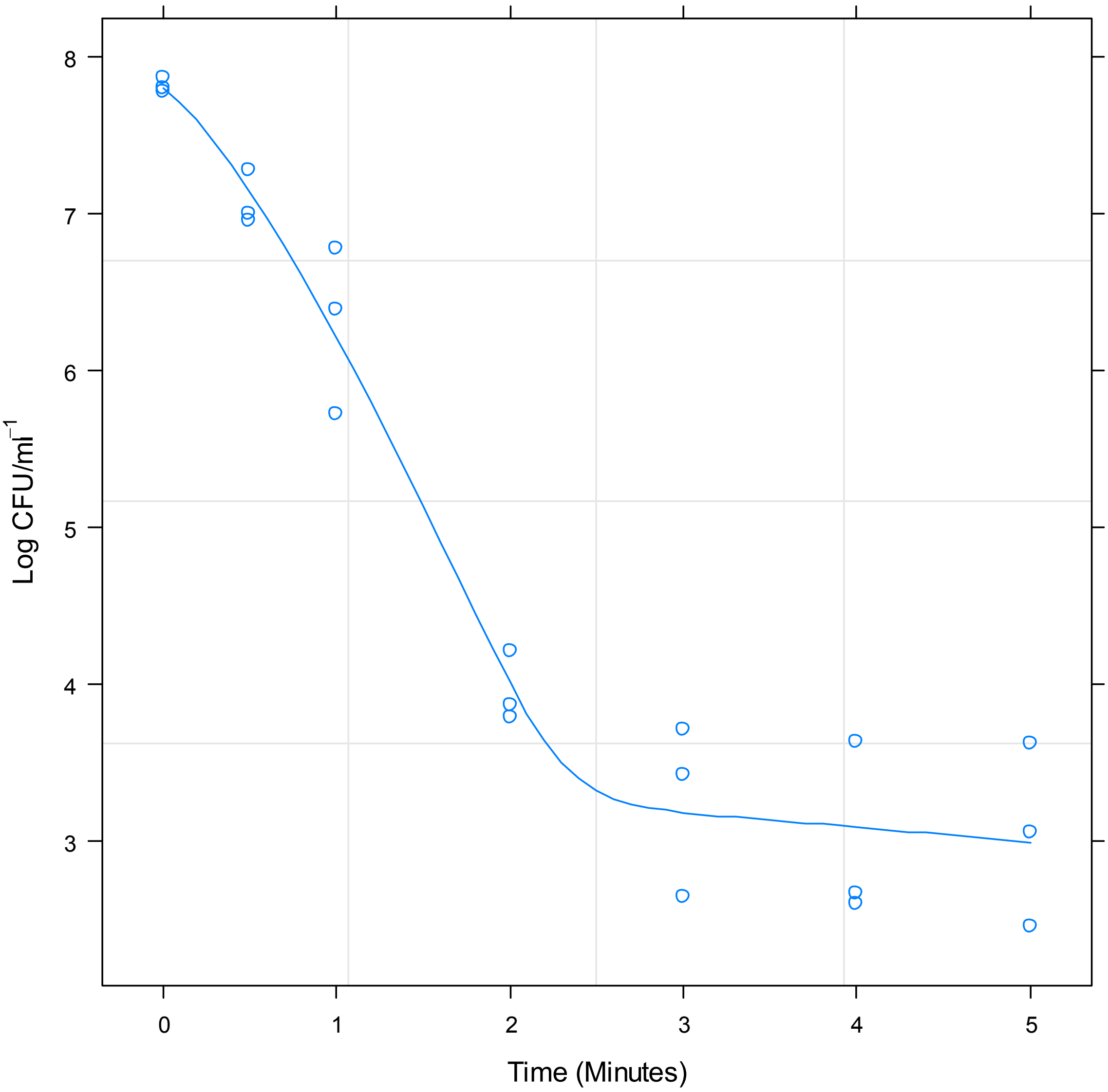

Figure 219. Predicted response curve using a mixed Weibull distribution model of strain 13126 (ST-21, CC-21) at pH 5.5 following heating at 64^{o}C.

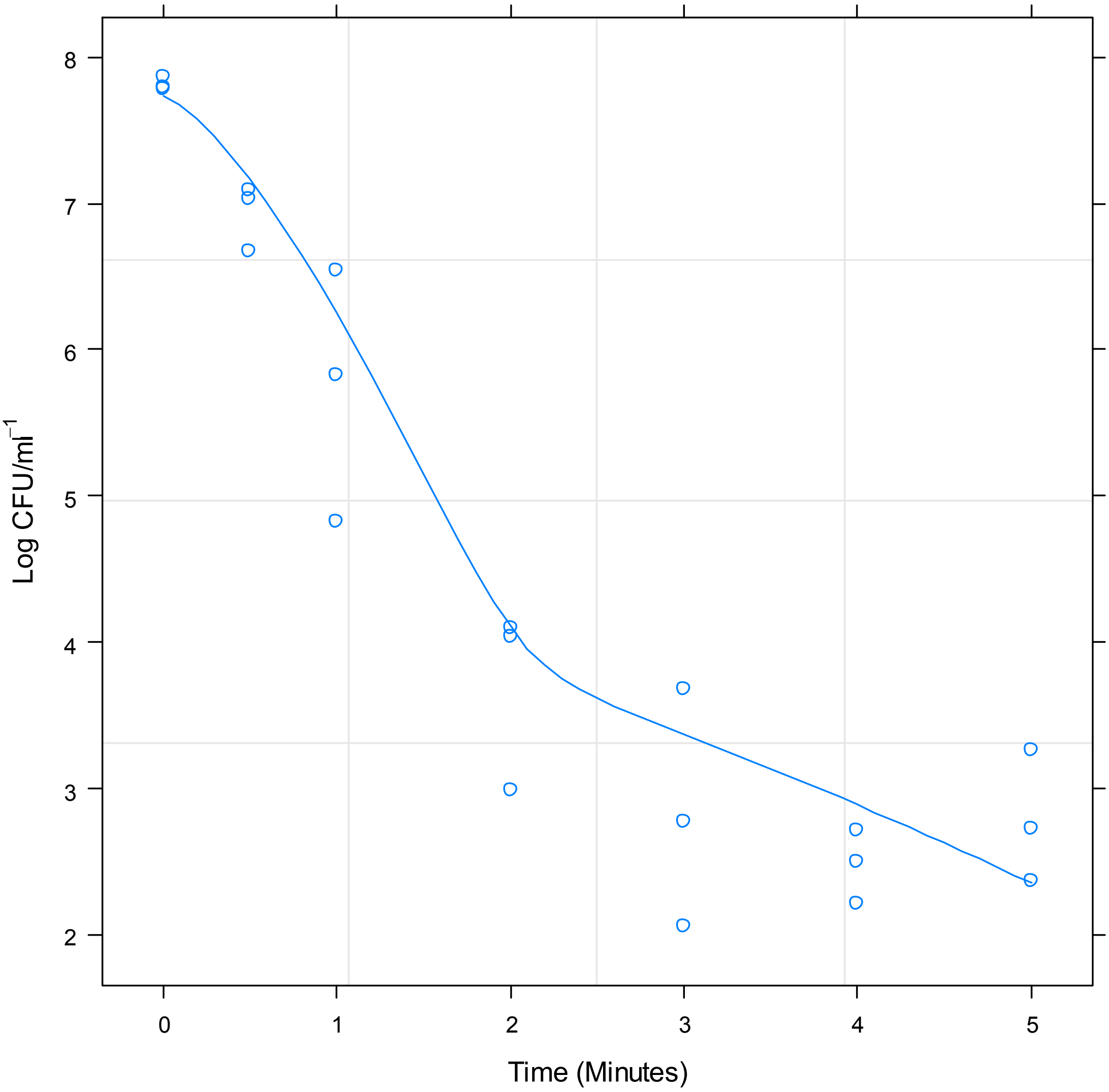

Figure 220. Predicted response curve using a mixed Weibull distribution model of strain 13126 (ST-21, CC-21) at pH 6.5 following heating at 64^{o}C.

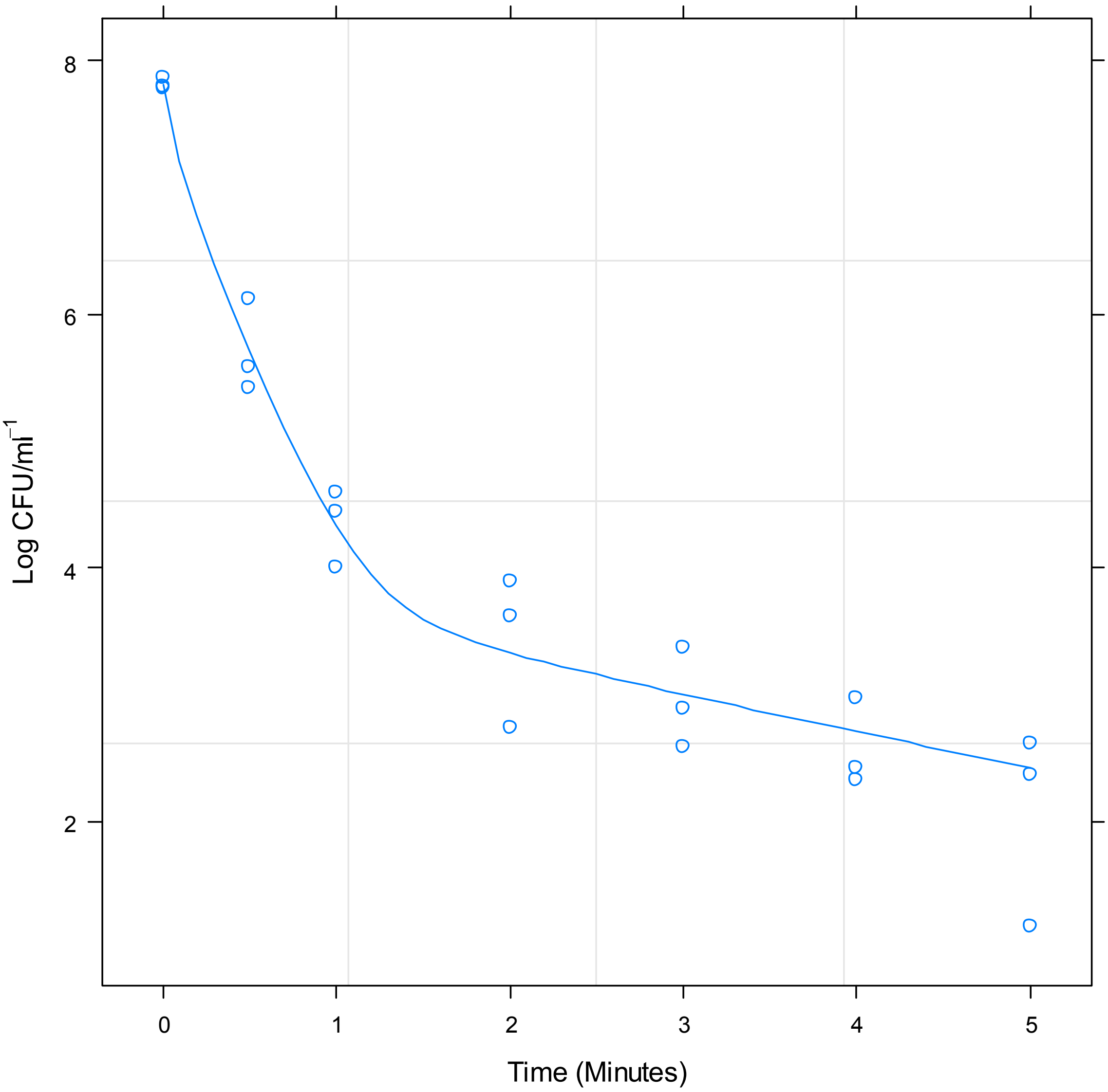

Figure 221. Predicted response curve using a mixed Weibull distribution model of strain 13126 (ST-21, CC-21) at pH 7.5 following heating at 64°C.

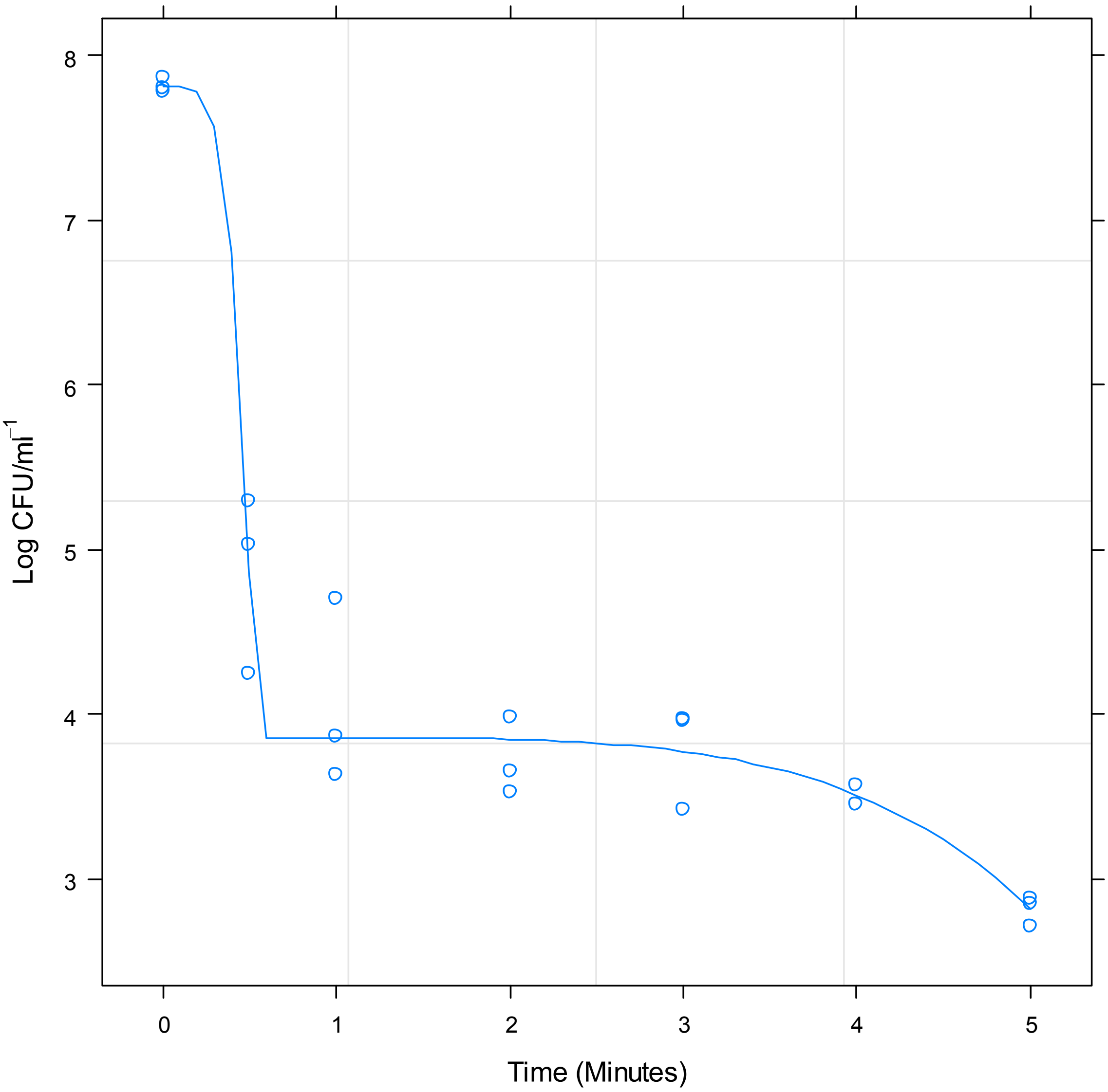

Figure 222. Predicted response curve using a mixed Weibull distribution model of strain 13126 (ST-21, CC-21) at pH 8.5 following heating at 64^{o}C.

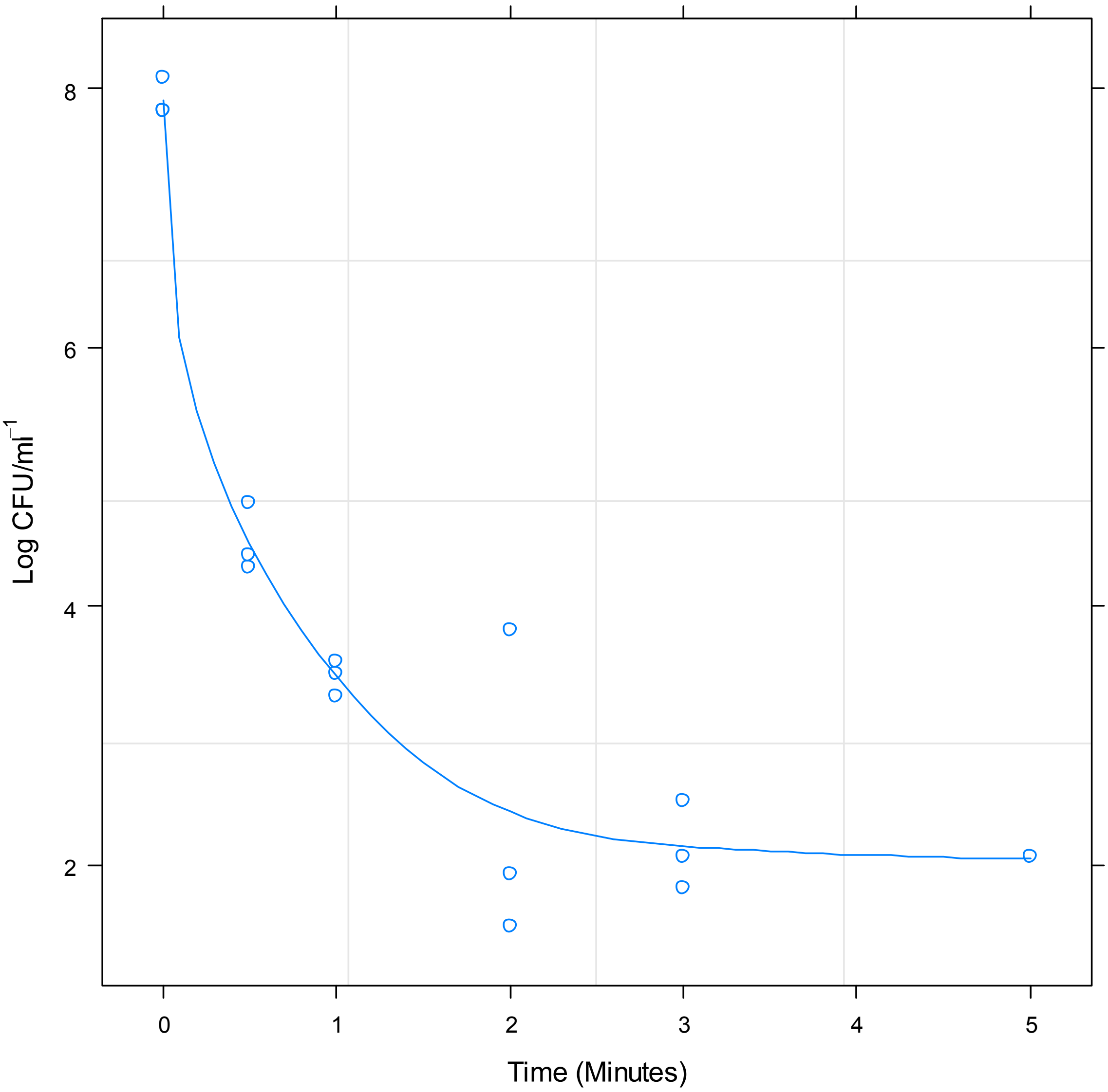

Figure 223. Predicted response curve using a mixed Weibull distribution model of strain 13136 (ST-45, CC-45) at pH 4.5 following heating at 64°C.

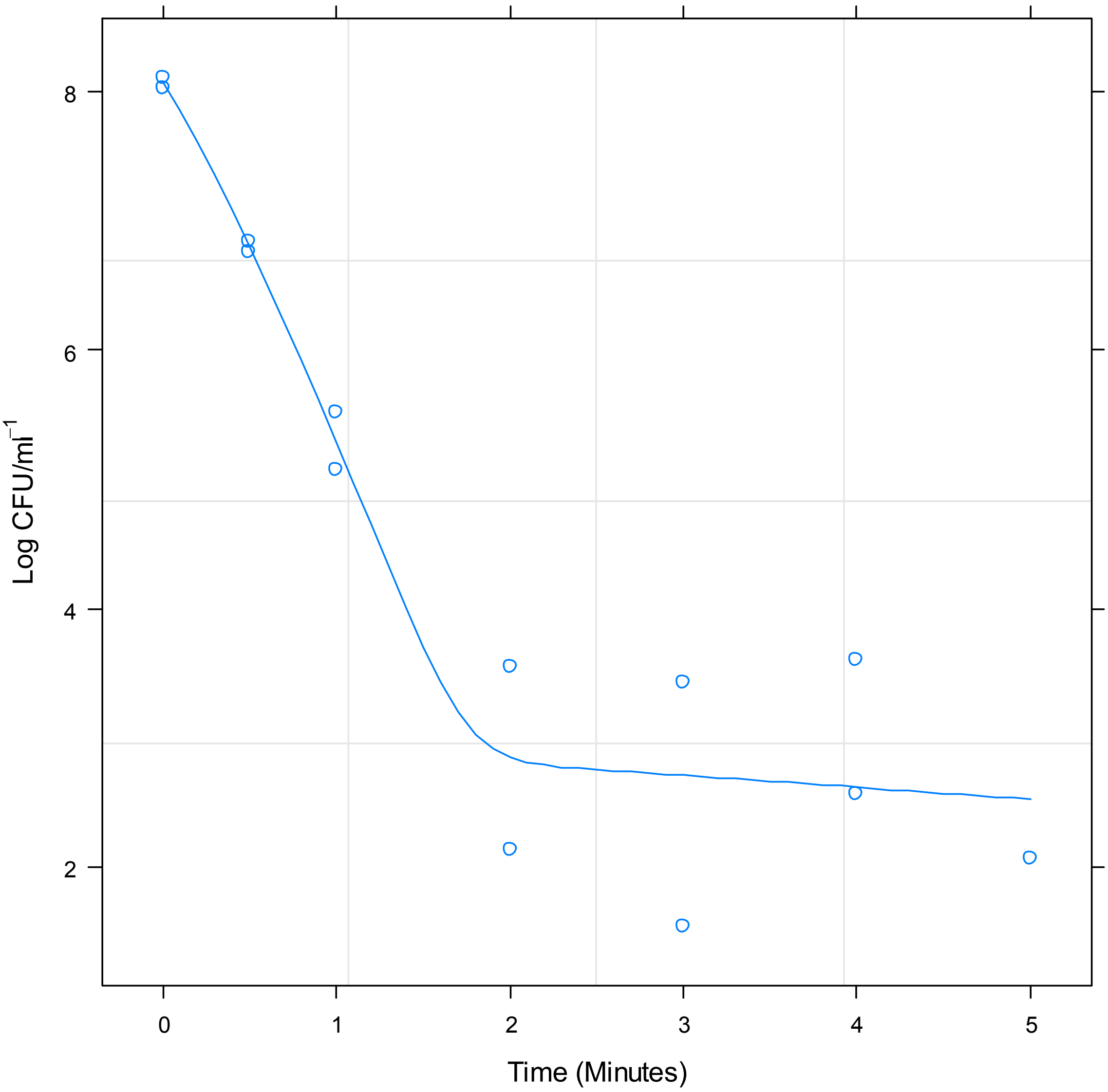

Figure 224. Predicted response curve using a mixed Weibull distribution model of strain 13136 (ST-45, CC-45) at pH 5.5 following heating at 64°C.

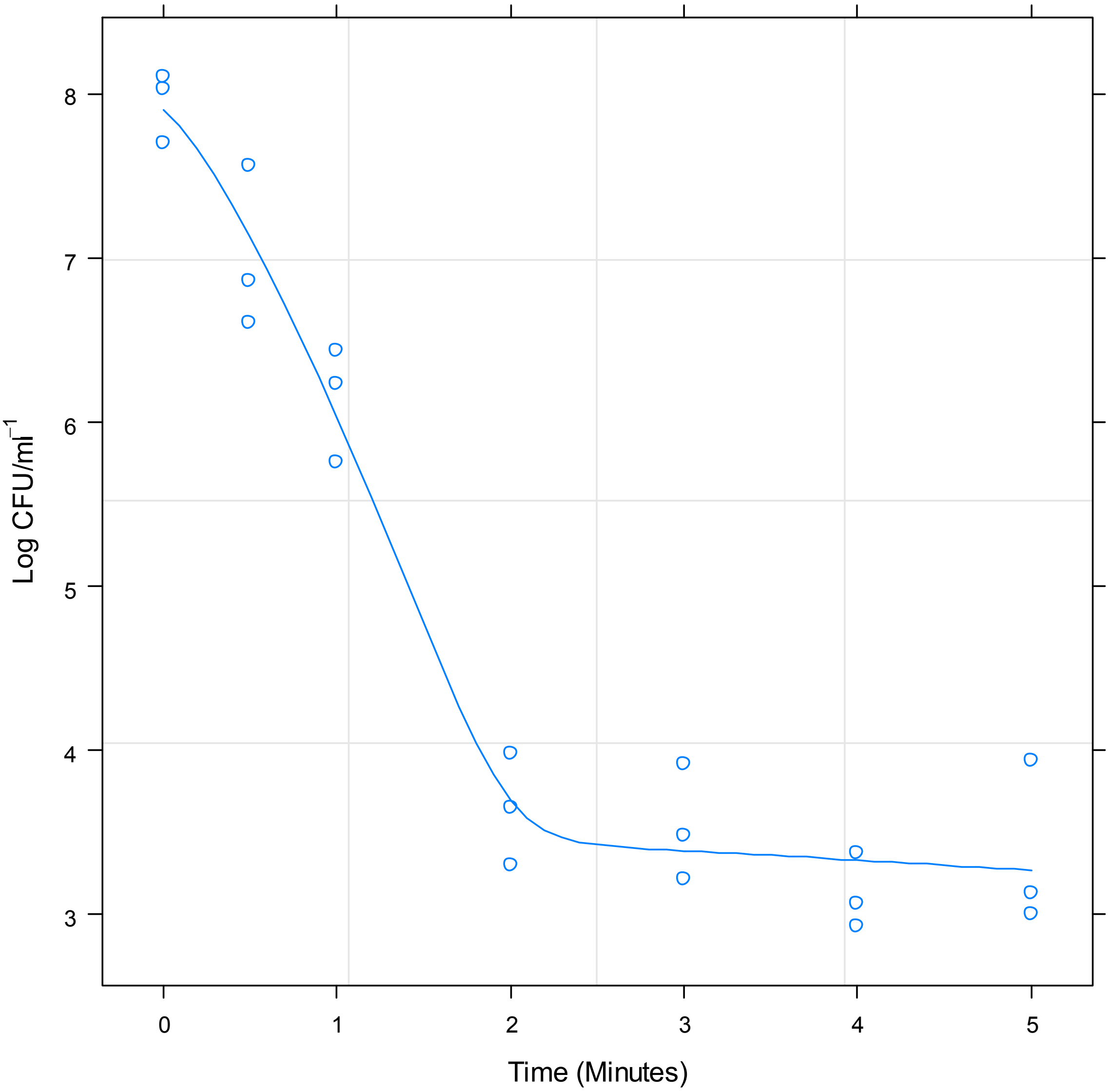

Figure 225. Predicted response curve using a mixed Weibull distribution model of strain 13136 (ST-45, CC-45) at pH 6.5 following heating at 64°C.

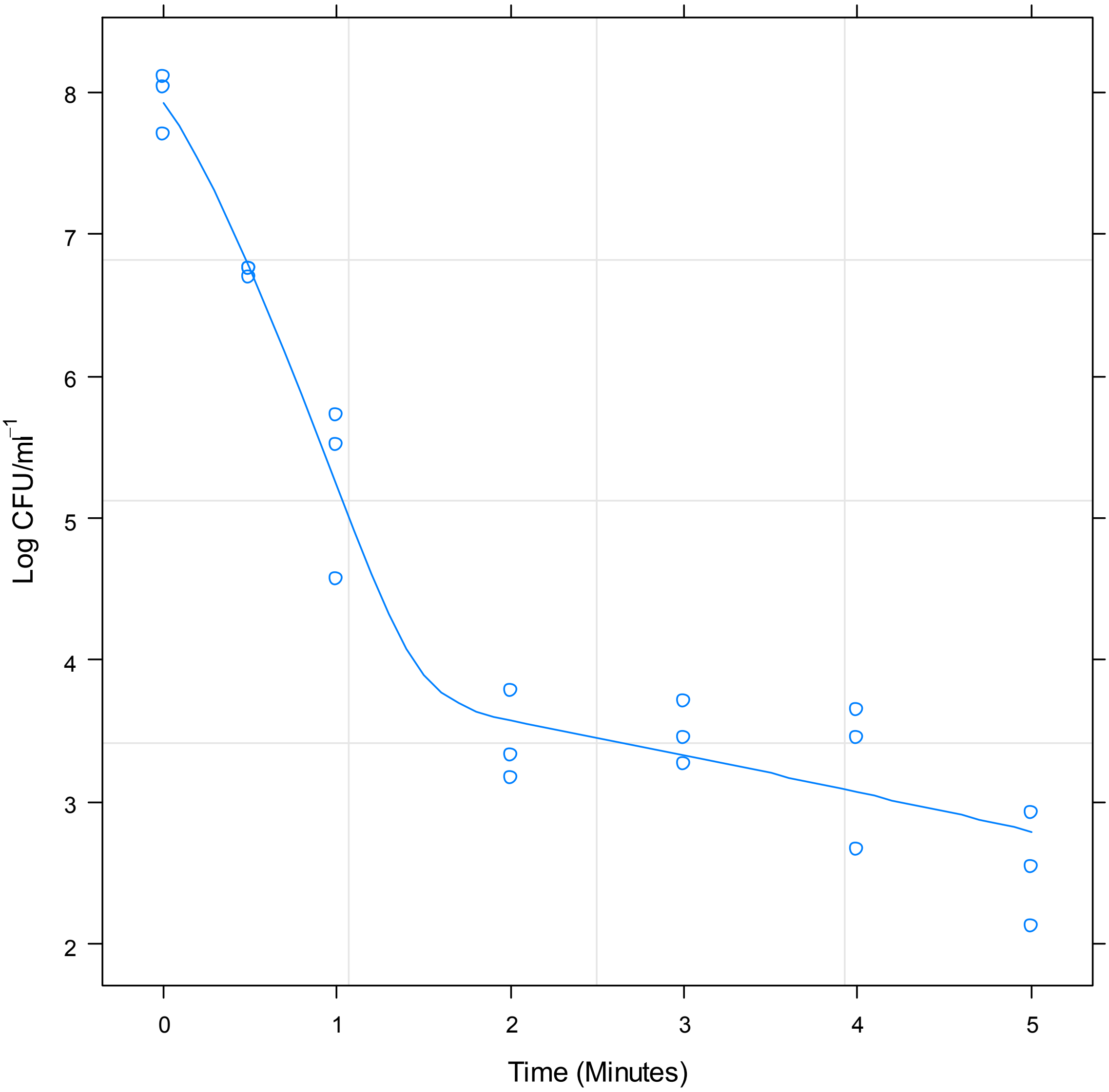

Figure 226. Predicted response curve using a mixed Weibull distribution model of strain 13136 (ST-45, CC-45) at pH 7.5 following heating at 64°C.

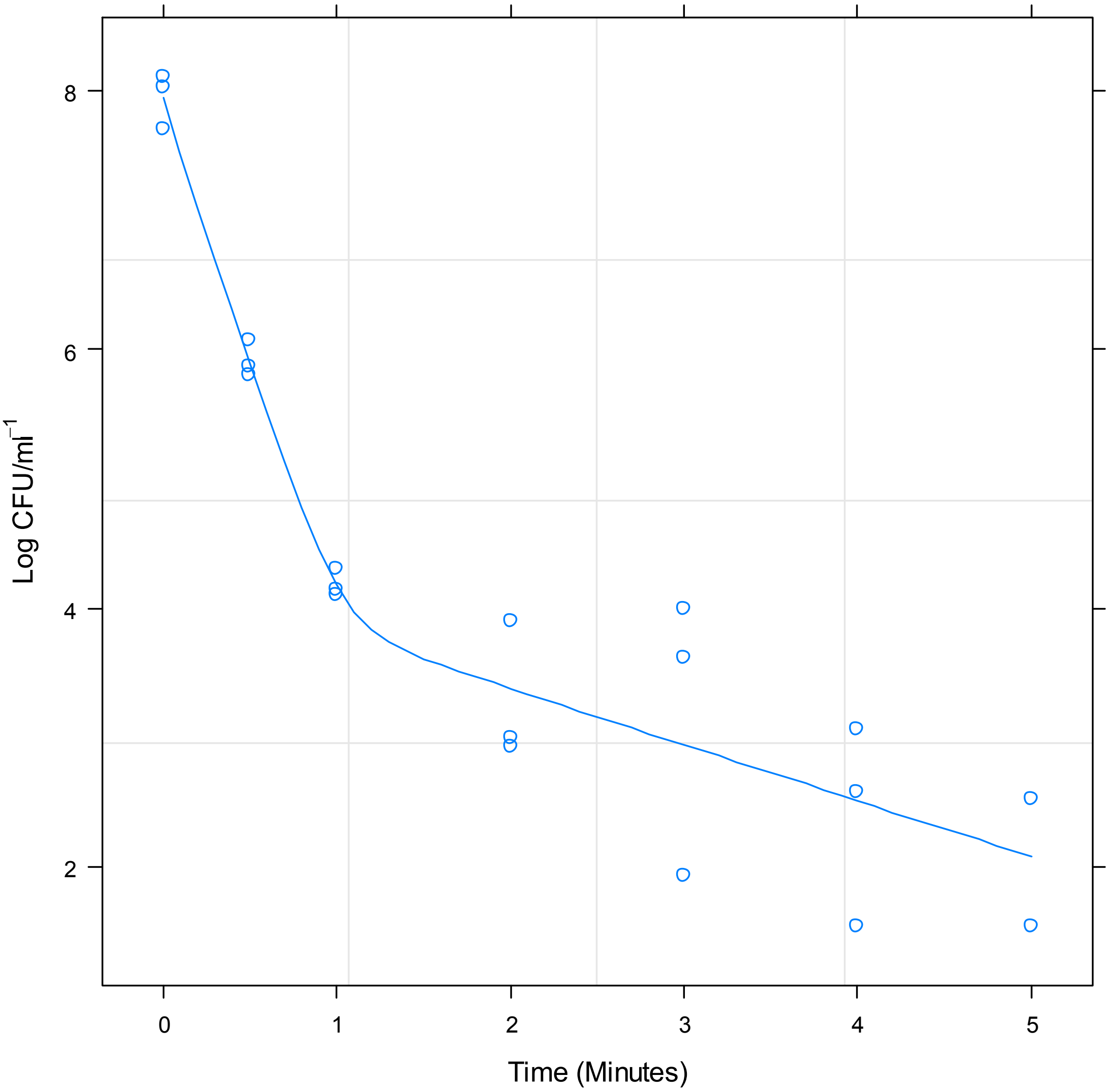

Figure 227. Predicted response curve using a mixed Weibull distribution model of strain 13136 (ST-45, CC-45) at pH 8.5 following heating at 64^{o}C.

1.8.29 Assessment of Model Parameters

Table 197. Assessment of model parameters generated by mixed Weibull distribution function for temperature simulations undertaken at 56^{o}C.

Strain	Parameter				
	N0	**δ1**	**δ2**	***p***	**α**
11253 (ST-825, CC-828)	8.225	2.598	9.791	1.758	4.078
11368 (ST-574, CC-574)					
11762 (ST-828, CC-829)	8.190	2.940	11.327	2.279	3.833
12610 (ST-828, CC-825)	8.151	2.653	13.274	1.569	3.972
12628 (ST-1773, CC-828)	8.230	2.430	16.952	1.606	4.651
12645 (ST-51, CC-443)		Table 99			
12662 (ST-257, CC257)					
12720 (ST-51, CC-443)	8.084	3.240	20.859	1.540	4.592
12745 (ST-257, CC-257)					
12783 (ST-574, CC-574)					
13121 (ST-45, CC-45)					
13126 (ST-21, CC-21)	8.047	2.462	8.684	1.682	3.623
13136 (ST-45, CC-45)	8.138	3.027	9.017	1.684	3.923
13163 (ST-21, CC-21)	7.992	2.971	10.933	1.514	3.704

Table 198. Assessment of model parameters generated by mixed Weibull distribution function for temperature simulations undertaken at 60^{o}C.

Strain	Parameter				
	N0	**δ1**	**δ2**	***p***	**α**
11253 (ST-825, CC-828)					
11368 (ST-574, CC-574)	7.971	1.466	29.098	1.799	4.728
11762 (ST-828, CC-829)					
12610 (ST-828, CC-825)					
12628 (ST-1773, CC-828)					
12645 (ST-51, CC-443)	8.001	1.340	11.084	1.736	4.404
12662 (ST-257, CC257)	8.090	1.076	4.847	1.343	3.567
12720 (ST-51, CC-443)	7.953	1.207	9.999	1.565	4.187
12745 (ST-257, CC-257)	8.134	1.403	6.718	3.536	3.982
12783 (ST-574, CC-574)	7.943	0.915	8.689	1.208	4.221
13121 (ST-45, CC-45)	7.931	0.066	6.256	0.365	3.690
13126 (ST-21, CC-21)	8.056	1.223	6.139	1.990	3.631
13136 (ST-45, CC-45)	8.012	1.017	5.621	1.423	3.671
13163 (ST-21, CC-21)					

Table 199. Assessment of model parameters generated by mixed Weibull distribution function for temperature simulations undertaken at 64^{o}C.

Strain	Parameter				
	N0	**δ1**	**δ2**	***p***	**α**
11253 (ST-825, CC-828)	8.011	0.535	4.657	2.238	5.101
11368 (ST-574, CC-574)					
11762 (ST-828, CC-829)	8.119	0.698	5.708	3.852	5.381
12610 (ST-828, CC-825)					
12628 (ST-1773, CC-828)					
12645 (ST-51, CC-443)					
12662 (ST-257, CC257)	8.173	0.288	2.296	1.102	3.550
12720 (ST-51, CC-443)					
12745 (ST-257, CC-257)					
12783 (ST-574, CC-574)	8.072	0.589	3.946	2.615	4.654
13121 (ST-45, CC-45)					
13126 (ST-21, CC-21)	8.056	0.251	2.671	1.001	3.677
13136 (ST-45, CC-45)	8.011	0.506	3.915	2.095	4.202
13163 (ST-21, CC-21)					

Table 200. Assessment of model parameters generated by mixed Weibull distribution function for combined pH and Temperature simulations undertaken at 56°C.

Strain	pH	Parameter				
		N0	**δ1**	**δ2**	**α**	***p***
12628 (ST-1773, CC-828)	4.5	7.990	1.217	14.249	5.390	2.894
12628 (ST-1773, CC-828)	5.5	8.104	3.881	10.928	3.796	3.058
12628 (ST-1773, CC-828)	6.5	8.100	3.192	10.385	3.574	1.664
12628 (ST-1773, CC-828)	7.5	8.118	2.270	5.619	3.120	1.179
12628 (ST-1773, CC-828)	8.5	8.098	1.946	6.449	2.806	1.509
12662 (ST-257, CC-257)	4.5	8.043	0.082	1403.846	5.539	0.405
12662 (ST-257, CC-257)	5.5					
12662 (ST-257, CC-257)	6.5					
12662 (ST-257, CC-257)	7.5					
12662 (ST-257, CC-257)	8.5	7.973	1.468	8.222	3.669	1.300
13126 (ST-21, CC-21)	4.5	7.490	0.065	2.680	5.120	0.310
13126 (ST-21, CC-21)	5.5	7.799	4.445	10.020	2.252	2.026
13126 (ST-21, CC-21)	6.5	7.794	4.136	16.001	3.596	1.807
13126 (ST-21, CC-21)	7.5	7.804	2.455	20.243	3.579	1.327
13126 (ST-21, CC-21)	8.5	7.799	1.835	9.898	3.438	3.247
13136 (ST-45, CC-45)	4.5	7.830	1.348	9.489	4.887	3.291
13136 (ST-45, CC-45)	5.5	7.905	4.559	9.645	2.955	2.267
13136 (ST-45, CC-45)	6.5	7.985	3.494	9.984	3.059	1.707
13136 (ST-45, CC-45)	7.5	7.981	3.056	8.146	3.324	1.772
13136 (ST-45, CC-45)	8.5	7.993	1.686	10.473	3.762	1.479

Table 201. Assessment of model parameters generated by mixed Weibull distribution function for combined pH and temperature simulations undertaken at 60°C

Strain	pH	Parameter				
		N0	**δ1**	**δ2**	**α**	***p***
12628 (ST-1773, CC-828)	4.5					
12628 (ST-1773, CC-828)	5.5	8.013	1.577	10.236	4.826	2.125
12628 (ST-1773, CC-828)	6.5	8.033	0.478	3.583	3.249	0.750
12628 (ST-1773, CC-828)	7.5	8.034	0.993	5.874	3.279	1.741
12628 (ST-1773, CC-828)	8.5	8.104	1.127	8.160	4.447	4.533
12662 (ST-257, CC-257)	4.5	8.091	0.120	5.452	0.537	3.968
12662 (ST-257, CC-257)	5.5	7.912	1.746	9.699	2.452	4.398
12662 (ST-257, CC-257)	6.5	7.966	1.494	8.523	1.548	3.892
12662 (ST-257, CC-257)	7.5	7.959	1.023	3.086	1.155	2.505
12662 (ST-257, CC-257)	8.5	7.986	0.350	2.824	0.802	3.334
13126 (ST-21, CC-21)	4.5	8.091	0.120	5.452	3.968	0.537
13126 (ST-21, CC-21)	5.5	7.865	1.628	6.510	2.382	3.628
13126 (ST-21, CC-21)	6.5	8.017	1.451	8.375	2.319	3.996
13126 (ST-21, CC-21)	7.5	8.016	1.305	20.651	1.683	4.501
13126 (ST-21, CC-21)	8.5	8.092	0.555	6.081	1.233	3.660
13136 (ST-45, CC-45)	4.5					
13136 (ST-45, CC-45)	5.5	7.969	1.605	28.006	4.142	1.676
13136 (ST-45, CC-45)	6.5	7.970	1.069	5.873	3.658	1.429
13136 (ST-45, CC-45)	7.5	7.966	0.589	5.143	3.579	0.827
13136 (ST-45, CC-45)	8.5					

Table 201. Assessment of model parameters generated by mixed Weibull distribution function for combined pH and temperature simulations undertaken at 64°C.

Strain	pH	Parameter				
		N0	**δ1**	**δ2**	**α**	***p***
12628 (ST-1773, CC-828)	4.5	8.162	0.010	0.077	2.990	0.309
12628 (ST-1773, CC-828)	5.5	7.987	0.369	4.877	4.442	1.180
12628 (ST-1773, CC-828)	6.5	7.986	0.415	3.248	3.582	1.289
12628 (ST-1773, CC-828)	7.5	7.982	0.307	3.767	3.818	1.129
12628 (ST-1773, CC-828)	8.5	7.988	0.178	2.191	3.211	1.004
12662 (ST-257, CC-257)	4.5	8.051	0.058	1.539	4.324	0.651
12662 (ST-257, CC-257)	5.5	8.026	0.942	5.719	3.938	1.899
12662 (ST-257, CC-257)	6.5	7.986	0.757	4.400	3.868	1.505
12662 (ST-257, CC-257)	7.5	8.033	0.432	4.127	4.361	1.070
12662 (ST-257, CC-257)	8.5	8.063	0.279	3.189	3.812	1.750
13126 (ST-21, CC-21)	4.5	7.870	0.013	0.465	3.633	0.390
13126 (ST-21, CC-21)	5.5	7.795	0.700	10.554	4.424	1.288
13126 (ST-21, CC-21)	6.5	7.838	0.504	85.295	5.105	1.038
13126 (ST-21, CC-21)	7.5	7.814	0.195	1.545	3.162	0.797
13126 (ST-21, CC-21)	8.5	7.814	0.399	4.956	3.956	4.886
13136 (ST-45, CC-45)	4.5	7.910	0.021	66.256	5.504	0.388
13136 (ST-45, CC-45)	5.5	8.061	0.412	10.768	5.123	1.150
13136 (ST-45, CC-45)	6.5	7.901	0.616	14.641	4.384	1.289
13136 (ST-45, CC-45)	7.5	7.918	0.452	4.039	3.893	1.247
13136 (ST-45, CC-45)	8.5	7.944	0.242	2.243	3.670	0.980

1.9 DISCUSSION

The underlying response of all *Campylobacter* strains following simulations undertaken at varying temperatures and pH values were modelled independently using generalised non-linear least-squares (Pinheiro and Bates, 2000). The non-linear functions used to describe the underlying response varied according to *Campylobacter* strain and the type and intensity of biochemical and biophysical stress used during experimental simulations. The evaluation of goodness-of-fit of models to the data was undertaken by calculating the concordance correlation coefficient (ρ_c) goodness-of-fit statistic (Lin 1989 and 2000).

1.9.1 Time-Temperature Simulations:

1.9.1.1 Predictive Model:

The asymptotic regression, logistic regression, four-parameter logistic regression and four-parameter Weibull non-linear functions were used to describe the response of *Campylobacter* during simulations undertaken at 56^{o}C (Table 1). The asymptotic regression and four-parameter logistic regression non-linear functions were used to describe the response during simulation undertaken at 60^{o}C (Table 32). By comparison, the asymptotic regression non-linear function was the mathematical model required to describe the underlying response of *Campylobacter* during simulations at 64^{o}C (Table 56).

The concordance correlation coefficient (ρ_c) was used as an absolute measure of goodness-of-fit of models to the data. Overall, high values of the goodness-of-fit statistic indicate that models generated for each type and intensity of biochemical and biophysical stress was a good fit to the data. There were, however, several exceptions. The goodness-of-fit statistic for the model used to describe the underlying response of strain 13163 (ST-21, CC-21) during simulation at 64^{o}C was ρ_c = 0.561 (Table 56). This is in direct contrast to the goodness-of-fit of models for other strains where values of the concordance correlation coefficient where observed to be in excess of $\rho_c \geq 0.881$ (Table 56). The comparatively low goodness-of-fit statistic may be attributed to greater variability in the response of this particular strain to higher temperature (Figure 44). Indeed, an increase in heterogeneity in the response of *Campylobacter* to increases in temperature as a function of time was observed during experimental simulations undertaken at 60^{o}C and 64^{o}C. During temperature simulations undertaken at 60^{o}C, increased heterogeneity in the underlying response was observed for strains 12628 (ST-1773, CC-828) (Figure 21), 12662 (ST-257, CC-257) (Figure 23), 12745 (ST-257, CC-257) (Figure 25) and 13163 (ST-21, CC-21) (Figure 29). However, in each case the goodness-of-fit statistic suggested that the model provided an adequate representation of the underlying response

(Table 56). This suggests that increased experimental heterogeneity did not always affect the magnitude of goodness-of-fit statistic from corresponding models (Tables 1, 17, 20, 32 and 56). It is important to consider, therefore, that while the goodness-of-fit statistic may provide an indication of absolute model fit it does not necessarily reflect the ability of a model to faithfully replicate the underlying biological mechanism. Increased heterogeneity in the observed response of *Campylobacter* was more pronounced throughout the simulations undertaken at 64^{o}C; for example 11253 (ST-825, CC-828) (Figure 31), 12610 (ST-828, CC-825) (Figure 34) and 13136 (ST-45, CC-45) (Figure 43). Findings for individual models for temperature simulations undertaken at 56^{o}C (Tables 2 - 15), 60^{o}C (Tables 33 - 46) and 64^{o}C (Tables 57 - 70) are provided. For example, the individual parameter estimates for all models for simulations undertaken at 56^{o}C and 60^{o}C were found to be significant at *P*-value ≤ 0.05. The four-parameter logistic regression non-linear function used to model the underlying response of strain 11253 (ST-825, CC-828) illustrates that the estimate of asymptote A to be 8.357 Log CFU/ml^{-1} (*P* ≤ 0.000) whereas the estimate for asymptote B is 3.119 Log CFU/ml^{-1} (*P*-value = 0.000) (Table 2). The estimate of the mid-point is 4.280 Log CFU/ml^{-1} (*P*-value = 0.000) whereas the estimate of the scale-parameter is 1.22 Log CFU/ml^{-1} (*P*-value = 0.000) (Table 2). The logistic regression non-linear function was used to describe the underlying response of strain 12745 (ST-257, CC-257) following simulations undertaken at 56^{o}C (Table 10). The estimate for the asymptote parameter is 8.698 Log CFU/ml^{-1}(*P*-value = 0.000) whereas the mid-point is 8.391 Log CFU/ml^{-1} (*P* ≤ 0.000) while the parameter estimate for the scale parameter is -3.697 (*P*-value = 0.000). The asymptotic regression non-linear function (Table A1.1) was used to describe the underlying response of strain 13121 (ST-45, CC-45). The estimate for the parameter R0 was 8.017 Log CFU/ml^{-1} (*P*-value = 0.000) whereas the estimate of the asymptote is 2.456 Log_{10}/ml^{-1} (*P*-value = 0.000). The estimate of the rate parameter LRC was -1.476 (*P*-value = 0.000) (Table 12).

1.9.1.2 Extended Simulations:

The four-parameter logistic regression non-linear function was used to examine effect of using different initial inocula on the underlying response of *Campylobacter* (Table 17) whereas asymptotic regression and four-parameter logistic regression non-linear functions were used to examine differences in the numbers of sub-lethally damaged cells of *Campylobacter* following use of different experimental media for recovery (Table 20). The overall goodness-of-fit for models generated during the extended analyses was high (Table 17 and 20) where models that compared the numbers of cells recovered from different initial inocula for strains 13121 (ST-45, CC-45) and 13136 (ST-45, CC-45) recorded ρ_c = 0.954 and ρ_c = 0.991 respectively (Table 17). Significant differences between initial inocula (6 Log CFU/ml^{-1} and 8 Log CFU/ml^{-1}) are shown for the parameter asymptote A for 13121 (ST-

45, CC-45) (7.113 +2.947 = 10.060 Log CFU/ml^{-1}, *P*-value = 0.014) (Table 18) and 13136 (ST-45, CC-45) (6.534 +1.972 = 8.506 Log CFU/ml^{-1}, $P \leq 0.014$) (Table 19). These differences were not unexpected and merely reflect the nature of experimental design. However, an assessment of differences between initial inocula for successive model parameters did not yield significant differences in the numbers of cells recovered for strain 13121 (ST-45, CC-45) (Table 18). Nevertheless, a significant difference in the numbers of cells recovered for the asymptote B parameter ($P \leq 0.000$) was found when using an inoculum of 8 Log CFU/ml^{-1} for strain 13136 (ST-45, CC-45) (Table 19) indicating that higher volumes of inocula may promote enhanced recovery of cells during the later stages of the observation period (Figure 63).

The absolute goodness-of-fit of models describing the underlying response for strains 11168 (ST-45, CC-21) and 13121 (ST-45, CC-45) following simulations using different experimental media was $\rho_c = 0.965$ and $\rho_c = 0.988$ respectively (Table 20). Analyses comparing experimental simulations of different enumeration media suggest that media type influenced the numbers of cells recovered for strain 11168 (ST-45, CC-21). Fewer numbers of sub-lethally damaged cells were recovered from media type mCCDA in comparison to CAB-FBP (Table 21). Differences in the numbers of sub-lethally damages cells recovered were found for model parameters representing the mid-point (4.782 – 1.470 = 3.042 Log CFU/ml^{-1}, *P*-value = 0.000) and the scale parameter (4.206 – 1.384 = 2.822, *P*-value = 0.006). No significant differences were found between model parameters, Asymptotes A and B. In addition, there were no significant differences in the numbers of sub-lethally damaged cells recovered between media types for strain 13121 (ST-45, CC-45) (Table 22). These findings may indicate that the use of experimental media supplemented with antimicrobial agents, such as mCCDA, may negatively affect the recovery of sub-lethally damaged cells (Tables 21 – 22).

1.9.1.3 Mixed Weibull Distribution Model:

The mixed Weibull distribution model proposed by Coroller *et al*. (2006) was also used to describe the underlying response of *Campylobacter* following experimental simulations undertaken at 56^{o}C (Table 23), 60^{o}C (Table 47) and 64^{o}C (Table 71). The overall goodness-of-fit for models generated during simulations undertaken at 56^{o}C was found to be high ($\rho_c = 0.988$) (Table 23). Correspondingly, the goodness-of-fit statistics for simulations undertaken at 60^{o}c (Table 47) and 64^{o}C (Table 71) were also found to be high and in excess of $\rho_c = 0.960$ and $\rho_c = 0.940$ respectively. The parameter estimates for each individual model were reviewed in order to improve understanding of the underlying biological mechanism. Each of the five parameters describes a specific aspect of the response of the organism following exposure to stress. Coroller *et al*. (2006) describe each parameter; N_0 represents the initial inoculum size at time zero. The parameters δ1 and δ2 describe the time taken to achieve one logarithmic reduction in the population size of each subpopulation. The parameter α determines the fraction of first subpopulation remaining within the primary population, while the shape of the inactivation curve is determined by the parameter *p*.

Estimates for parameters of each individual model are presented for each simulation; 56°C (Tables 24 – 31), 60°C (Table 33 – 46) and 64°C (Tables 72 – 77). It became evident throughout the model evaluation process, that estimates of parameters used by the mixed Weibull distribution function were sensitive to the underlying shape of the response curve. For instance, coefficient estimate representing the numbers of cells recovered the precision surround the estimate and significance of the δ2, *p* and *α* parameters were found to vary greatly. This was especially found to be the case when a horizontal asymptote was absent, or when there was strong evidence of a horizontal asymptote at later stages of experimental simulation.

For example, strain 12628 (ST-1773, CC-828) exhibits different characteristics with regards to the underlying response following simulations undertaken at different temperatures. At 56°C the mixed Weibull distribution model was unable to detect a statistical difference in the reduction in size of the second subpopulation as described by parameter δ2 (16.952, *P*-value = 0.198) (Table 28). Furthermore, the standard error surrounding the estimate ($SE_{\overline{x}}$ = 473.314) calls into question the underlying assumptions of this model with regard to predicting a reduction in size of a secondary subpopulation. The predicted response curve does not provide any evidence in favour of a second subpopulation (Figure 68). However, such reservations are almost certainly related to variation in the response under specific conditions. In contrast, the predicted response curve of strain 12720 (ST-51, CC-443) at 60°C provides evidence in favour of the presence of a second subpopulation as defined by Coroller *et al*. (2006). Nevertheless, the corresponding parameter estimate of δ2 is not significant (9.999, *P*-value = 0.110) and the standard error is greatly reduced ($SE_{\overline{x}}$ = 6.013) (Table 51). However, an attempt to describe the underlying response of this strain at 64°C using the mixed Weibull distribution function was unsuccessful due to an inability to identify suitable starting values for the initial optimisation process. It is possible that an underlying response of this kind (Figure 38) for strain 12628 (ST-1773, CC-828) may best be described using a combined biphasic non-linear function as advocated by Geeraerd *et al*. (2006a and 2006b).

A comparison of the estimates for the parameter representing decimal reduction time (δ1) shows a high degree of variability between strains and temperature (Tables 200 – 202). The highest values of δ1 corresponding to increased resistance at 56°C was observed for strains 12720 (ST-51, CC-443) (δ1 = 3.240) and 13136 (ST-45, CC-45) (δ1 = 3.027) (Table 200). For simulations undertaken at 60°C the highest δ1 were recorded for strains 11368 (ST-574, CC-574) (δ1 = 1.466), 12645 (ST-51, CC-443) (δ1 = 1.403) and 12745 (ST-257, CC-257) (δ1 = 1.403) (Table 201). In contrast, for simulations undertaken at 64°C, the highest δ1 were recorded for strains 11762 (ST-828, CC-829) (δ1 = 0.698), 12783 (ST-257, CC-574) (δ1 = 0.589) (Table 202). There was no discernible pattern between temperature simulations with regard to which strains were the most resistant. Overall, the decimal reduction time, and therefore the degree of resistance, declined with an increase in temperature (Tables 200 – 202).

1.9.2 pH and Time-Temperature Simulations:

1.9.2.1 Predictive Models:

The predicted response curves for combined simulations undertaken at 56°C are shown in Figures 115 – 134, whereas predicted response curves for simulations at undertaken 60°C and 64°C are shown in Figures 152 – 170 and 188 – 207 respectively. The asymptotic regression, four-parameter logistic regression and bi-exponential models were used to describe the response of *Campylobacter* during combined pH (4.5, 5.5, 6.5, 7.5 and 8.5) and temperature simulations undertaken at 56°C (Table 78), 60°C (Table 117) and 64°C (Table 155).

The goodness-of-fit of models to the data for combined pH and temperature simulations undertaken at 56°C was assessed (Table 78). The minimum and maximum values of the concordance correlation coefficient were recorded for strain 13136 (ST-45, CC-45) pH 4.5 (ρ_c = 0.883) and pH 5.5 ρ_c = 0.989. The goodness-of-fit of models to the data for combined simulations undertaken at 60°C are presented in Table 117. The minimum value of goodness-of-fit was recorded for strain 12628 (ST-1773, CC-828) pH 8.5 ρ_c = 0.922, whereas the maximum value was observed for strain 12662 (ST-257, CC-257) pH 6.5 ρ_c = 0.971. Overall, the goodness-of-fit for combined simulations conducted at 64°C, was also observed to be high (Table 155). The minimum and maximum values of concordance correlation coefficient were recorded for strains 12628 (ST-1773, CC-828) pH 4.5 (ρ_c = 0.915) and 13136 (ST-45, CC-45) pH 6.5 (ρ_c = 0.990) respectively (Table 155).

Individual parameter estimates of models for simulations undertaken at 56°C and 60°C were found to be significant at *P*-value = 0.05 in the majority of cases. The four-parameter logistic regression non-linear function used to model the underlying response of strain 12628 (ST-1773, CC-828) at pH 4.5 and 56°C (Table 79) shows that the estimate of asymptote A to be 8.151 Log CFU/ml^{-1} ($P \leq 0.000$) whereas the estimate for asymptote B is 3.044 Log CFU/ml^{-1} (*P*-value = 0.000). The estimate of the mid-point is 4.909 Log CFU/ml^{-1} (*P*-value = 0.000) whereas the estimate of the scale-parameter is 0.958 Log CFU/ml^{-1} (*P*-value = 0.008). In contrast, the asymptotic regression non-linear function was used to describe the underlying response of strain 12628 (ST-257, CC-257) at pH 8.5 and 56°C (Table 83). The estimate for the R0 parameter is 8.222 Log CFU/ml^{-1}(*P*-value = 0.000) whereas the estimate for the asymptote is 1.124 Log_{10}/ml^{-1} (*P*-value = 0.354) while the estimate for the scale parameter is -2.114 Log CFU/ml^{-1} (*P*-value = 0.000).

The four-parameter logistic regression non-linear function used to model the underlying response of strain 12628 (ST-1773, CC-828) at pH 5.5 at 60^{o}C (Table 118) illustrates that the estimate of the asymptote A to be 8.133 Log CFU/ml^{-1} (*P*-value = 0.000) whereas the estimate for asymptote B is 2.754 Log CFU/ml^{-1} (*P*-value = 0.000). The estimate of the mid-point is 2.246 Log CFU/ml^{-1} ($P \leq$ 0.000) whereas the estimate of the scale-parameter is 0.536 Log CFU/ml^{-1} (*P*-value = 0.000). The asymptotic regression non-linear function was used to describe the underlying response of strain 12628 (ST-257, CC-257) at pH 8.5 at 60^{o}C (Table 83) and In contrast to simulations undertaken at 56^{o}C, all parameter estimates were significant. The estimate for the R0 parameter is 7.954 Log CFU/ml^{-1}($P \leq$ 0.000) whereas the estimate for the asymptote is 2.781 Log CFU/ml^{-1} (*P*-value = 0.354) and the estimate for the scale parameter is -0.554 Log CFU/ml^{-1} (*P*-value = 0.006).

Combined pH and temperature simulations undertaken at 64^{o}C the majority parameter estimates of individual models were also found to be significant at $P \leq 0.050$ (Tables 156 – 175). For example, the asymptotic regression non-linear function was used to describe the underlying response of strain 12628 (ST-257, CC-257) at pH 5.5 (Table 157). Estimates for the parameters R0 and the asymptote were found to be significant; 8.139 Log CFU/ml^{-1} (*P*-value = 0.000) and 2.451 Log CFU/ml^{-1} (*P*-value = 0.000) respectively. However, the estimate of the LRC parameter was not significant -0.612 Log CFU/ml^{-1}(*P*-value = 0.422).

1.9.2.2 Mixed Weibull Distribution Model:

The mixed Weibull distribution model was also used to describe the underlying response of *Campylobacter* under conditions of combined simulations using pH and temperature. The predicted response curves for combined simulations undertaken at 56^{o}C are shown in Figures 135 – 151, whereas predicted response curves for simulations at undertaken 60^{o}C and 64^{o}C are shown in Figures 171 – 187 and 208 – 227 respectively. The goodness-of-fit of models to the data are presented for each combined pH and temperature simulation. For simulations undertaken at 56^{o}C, the minimum and maximum values of concordance correlation coefficient were recorded for strains was 13126 (ST-21, CC-21) pH 8.5 (ρ_c = 0.883) and 12628 (ST-1773, CC-828) pH 6.5 ρ_c = 0.992 (Table 99). The goodness-of-fit of models to the data for combined pH and temperature simulations undertaken at 60^{o}C are presented in Table 137. The minimum value of goodness-of-fit was recorded for strain 12628 (ST-1773, CC-828) pH 8.5 ρ_c = 0.950, whereas the maximum value was observed for strain 12662 (ST-257, CC-257) pH 6.5 ρ_c = 0.986. The goodness-of-fit of models to the data are presented for each combined pH and temperature simulation. For simulations undertaken at 64^{o}C, the minimum and maximum values of concordance correlation coefficient were recorded for strain 12628 (ST-1773, CC-828) pH 8.5 (ρ_c = 0.944) and pH 4.5 (ρ_c = 0.990) respectively (Table 176). The parameter estimates for individual models were also examined (Tables 177 – 196).

Estimates of parameters δ1, δ2 and α parameters was found to vary according to strain and the combined intensity of pH and temperature. Parameter estimates of simulations undertaken at 56°C for strain 12628 (ST-1773, CC-828) pH 4.5, show that δ1, δ2 and p parameters were not significant; δ1 (1.218, P = 0.377), δ2 (14.249, P = 0.112), and p (2.894, P = 0.657) (Table 100). In contrast, parameter estimates of simulations undertaken at 56°C for 12628 (ST-1773, CC-828) pH 5.5 was significant $P \leq 0.000$ (Table 101). Heterogeneity in observations influenced the performance of predictive models. For example, considerable variation in measurements was recorded for strain 12662 (ST-1773, CC-828) 56°C at pH 4.5 (Figure 140) and this variation had a pronounced effect on the estimate and corresponding precision of the δ2 parameter; 1403.846, P = 0.986 and standard error $SE_{\overline{x}}$ = 79238.880 (Table 105). Similarly, estimates of δ1, δ2 and α parameters for the combined simulations undertaken at 60°C and 64°C were observed not to be significantly different at pH 4.5 and 8.5. For example, parameter estimates of simulations undertaken at 60°C for strain 12662 (ST-257, CC-257) pH 4.5, shows δ1 (0.120, P = 0.831), δ2 (5.452, P = 0.707), and α (0.538, P = 0.591) (Table 142). In addition, simulations undertaken at 64°C for strain 12628 (ST-1773, CC-828) pH 4.5 and pH 8.5 show that estimates for δ1, δ2, p and α parameters are not significant at $P \leq 0.05$ (Tables 177, 181).

Direct comparisons between model parameters reveal variability in the decimal reduction time (δ1) according to strain and the type and intensity of stress (Tables 200 – 202). Higher values of δ1 were observed for strain 12628 (ST-1773, CC-828) at pH 5.5 (δ1 = 3.881) and pH 6.5 (δ1 = 3.192) for simulations undertaken at 56°C (Table 200). Values of δ1 were higher for remaining strains corresponding to increased resistance (Table 202). Higher values for strain 13126 (ST-21, CC-21) at pH 5.5 (δ1 = 4.445) and pH 6.5 (δ1 = 4.136) and strain 13136 (ST-45, CC-45) at pH 5.5 (δ1 = 4.559) and pH 6.5 (δ1 = 3.494) indicated increased resistance to combined stressors (Table 202).

In contrast, for combined simulations undertaken at 60°C, strains showed highest resistance at pH 5.5 (Table 201). Strain 12628 (ST-1773, CC-828) (δ1 = 1.577), strain 12662 (ST-257, CC-257) (δ1 = 1.746), strain 13126 (ST-21, CC-21) at pH 5.5 (δ1 = 1.628) and 13136 (ST-45, CC-45) at pH 5.5 (δ1 = 1.605). Surprisingly, strain 12628 (ST-1773, CC-828) also indicated that resistance was comparatively high for pH 8.5 (δ1 = 1.127) (Table 201). However, the predicted response curve for this strain and combined experimental simulation suggests an inappropriate fit of the model to data. Figure 174 illustrates that an initial shoulder effect has been enforced during the model fitting process. The validity of parameter estimates for this individual model is therefore open to question (Table 141).

The estimates for decimal reduction time for combined simulations undertaken at 64°C are shown in Table 202. A similar trend can be observed in that higher values of δ1 are estimated for all strains at pH 5.5 and/or pH 6.5. Strain 12628 (ST-1773, CC-828) pH 6.5 (δ1 = 0.415), strain 12662 (ST-257, CC-257) pH 6.5 (δ1 = 0.942), strain 13126 (ST-21, CC-21) at pH 5.5 (δ1 = 0.700) and 13136 (ST-45, CC-45) at pH 6.5 (δ1 = 0.616) (Table 201). Comparatively, it is interesting to note that estimates of δ1 are highest, and therefore resistance is at its greatest, for all strains at pH 5.5 and pH 6.5. However, the ability to resist combined stress decreases with an increase in temperature (Tables 200 – 202).

1.10 CONCLUSIONS:

We used a non-linear framework to describe the response of *Campylobacter* strains to experimental simulations undertaken at 56°C, 60°C and 64°C as a function of time. Simulations were also undertaken to examine differences in the underlying response of *Campylobacter* following the combined exposure to pH (4.5, 5.5, 6.5, 7.0 and 8.5) and temperature. *Campylobacter* was shown to respond to variation in the type and intensity of stress in a manner similar to other organisms such as *Listeria monocytogenes* and *Salmonella enterica* (Greenacre *et al*., 2003; Coroller *et al*., 2006).

1.10.1 Predictive Models:

Non-linear functions used during the model building exercise to describe the underlying response of *Campylobacter* to variation in biochemical and biophysical stress used between three and five parameters in order to fit particular types and shapes of response curves; namely, asymptotic regression, four-parameter logistic regression, logistic regression, four-parameter Weibull regression and the biexponential regression (Pinheiro and Bates, 2000; Pinheiro *et al.,* 2012). In addition, we used the non-linear function proposed by the Coroller *et al*. (2006) in order to describe variation in behaviour of *Campylobacter* in response to high intensity biophysical and biochemical stress. The predicted response curves generated for *Campylobacter* species was found to vary according to the type and intensity of the biophysical and biochemical stress. For example strain 13126 (ST-21, CC-21) at combined pH and temperature simulations shows a high degree of variability in shape of the underlying response. Three non-linear functions were used to describe the response of strain 13136 (ST-21, CC-21) to combined pH and temperature simulations. For simulations undertaken at 56°C (Table 78) the asymptotic regression function was used to generate a predicted response curve at pH 4.5 for strain 12628 (ST-1773, CC-828) (Figure 115) while the four-parameter logistic regression function was used to generate predicted response curves under simulation at pH 5.5 (Figure 116), pH 6.5 (Figure 117), pH 7.5 (Figure 118) and pH 8.5 (Figure 119). By implication, the use of four-parameter logistic regression functions suggests a greater degree of resistance at pH 5.5, pH 6.5, pH 7.5 and pH 8.5 than is the case at pH 4.5 when using an asymptotic regression function. A potential increase in resistance may also be present when examining the response of strains for simulations undertaken at 60^{o}C (Table 117) and 64^{o}C (Table 155).

For simulations undertaken at 60^{o}C, the four-parameter logistic regression function was used to generate the predicted response curve for strain 12628 (ST-1773, CC-828) at pH 5.5 (Figure 152) whereas asymptotic regression function was used to generate predicted response curves for pH 6.5 (Figure 153), pH 7.5 (Figure 154) and pH 8.5 (Figure 155).

In contrast, the biexponential regression function was used to generate the predicted response curve for strain 13126 (ST-21, CC-21) for simulations at pH 8.5 (Figure 165). Interpretation of the predicted response curves generated by the four-parameter logistic regression function suggests increased resistance at pH 4.5, pH 5.5 and pH 6.5. This is in contrast to the asymptotic regression and the biexponential functions used to generate the response curves at pH 4.5 (Figure 161) and pH 8.5 (Figure 165) where resistance is reduced.

A similar pattern in the application of non-linear regression functions was also observed for combined pH simulations undertaken at 64^{o}C (Table 155). The predicted response curves for strain 12628 (ST-1773, CC-828) at pH 4.5 (Figure 188), pH 5.5 (Figure 189), and pH 6.5 (190) and pH 7.5 (191) were generated using an asymptotic regression function. In contrast, the biexponential regression function was used also used to generate the predicted response curve for simulations at pH 8.5 (Figure 192). The differences between combined pH and temperature simulations using standard non-linear functions has been made comparatively using the predicted response curves. However, it is necessary to validate these quantitatively by calculating the decimal reduction time for each response curve.

1.10.2 Mixed Weibull Distribution Model:

The mixed Weibull distribution model advocated by Coroller *et al*. (2006) was used to address complex variation in the shape of underlying curves by organisms in response to variation in the type and intensity of stress. The general model assumes the presence of two bacterial subpopulations that differ in their ability to withstand stress (Coroller *et al*., 2006). The model is fit to the data using five parameters and can be used to predict the numbers of cells at any point in time during experimental simulation. However, this characteristic is shared by many linear and non-linear modelling approaches used within R and is not exclusive to the general modelling approach described by Coroller *et al*. (2006).

It was not possible to describe the underlying response of all *Campylobacter* strains to combined simulations using standard non-linear and general modelling approaches. This may, in part, be due to complexity in the response of *Campylobacter* to stress and also to increased heterogeneity encountered in recording the numbers of cells when the combined effects of higher temperatures interacting with low and high pH.

While the presence of heterogeneity was addressed formally within the model building process, by means of fitting variance functions, it was not always possible to generate models for all combined simulations; for example, for simulations undertaken at 60^{o}C see strain 12628 (ST-1773, CC-828) pH 4.5 (Tables 118 and 139). As such, models are sensitive to increased heterogeneity within and between experimental replicates, and in particular to outlying data points and missing values that may induce failure during the optimization process.

The importance of the optimization process cannot be overemphasised. Indeed, using the non-linear framework in conjunction with GlnaFiT was the only means available with which to generate the initial values required to the fit the general model to the data. Furthermore, access to mathematical solution that governs the optimization process is protected within software. Models were initially fit to data using GlnaFiT (1.6) whereby the integral optimization routine produced starting values for parameters that allow a predicted response curve to be generated. These values were exported and used within the R non-linear framework to generate more complex models that allow for the inclusion of experimental replicates.

In addition, we used variance functions to control for increasing and multiple sources of heterogeneity encountered during the experimental simulations. The use of variance functions improves the likelihood of achieving model fit while also simultaneously improving model accuracy. Nevertheless, in some instances, the magnitude of heterogeneity was such that even the use of combined variance functions, designed to control for the increase in multiple sources of heterogeneity with and between replicates simultaneously, did not improve the likelihood of success in achieving model fit.

In contrast, there are several advantages to using the GlnaFiT to generate predicted response curves. Primarily, this tool is freely available and can fit and evaluate ten different types of non-linear function capable of describing the response of micro-organisms to biophysical and biochemical stress. Secondly, models have been validated and published in peer reviewed literature. In addition, the software presents a simple user interface with Microsoft Excel that does not require direct intervention from the user in order to generate initial starting values. Finally, the software is regularly maintained and updated by the University of Leuven. However, there were also limitations identified while using GlnaFiT. The computational process is sensitive to heterogeneity insofar as missing and outlying values can induce a failure during the computational phase of model fitting. Furthermore, heterogeneity in data may also result in unrealistic parameter estimates that result in an inappropriate fit of the model to data. Currently, there are no technical means to control for heterogeneity within GlnaFit other than by removing individual observations. This is in direct contrast to models generated with R where the negative influence of moderate levels of heterogeneity can be suppressed by using variance functions devised by Pinheiro and Bates (2000). In addition, models generated within R may be compared directly using Information Theoretic approaches.

However, complexity associated with the development and use of non-linear models within the R framework, requires a high degree of intervention on behalf of the user in order to fit and evaluate models effectively. In addition to the unavailability of an integral optimization routine, these constraints may render the use of the general model within R (as well as the fitting of standard non-linear models) as inappropriate for wider use by industry. With this in mind, it is prudent to consider whether the needs of industry are better served by reducing the overall complexity of the modelling approach in favour of implementing the predictive modelling approach by the GlnaFiT (Geeraerd 2006a, 2006b).